UNIVERSITÄT
BAYREUTH

Pulsating Galaxies

Von der Universität Bayreuth
zur Erlangung des Grades eines
Doktors der Naturwissenschaften (Dr. rer. nat.)
genehmigte Abhandlung

von

Christopher Straub
aus Nürnberg

1. Gutachter: Prof. Dr. Gerhard Rein
2. Gutachter: Prof. Dr. Mahir Hadžić
3. Gutachter: Prof. Dr. Yan Guo

Tag der Einreichung: 15.12.2023
Tag des Kolloquiums: 13.03.2024

Acknowledgements

I am deeply thankful to Gerhard Rein for guiding me in the intricacies of analysis, igniting my enthusiasm for the field along the way. The freedom he granted me when I wished for it, and the help he offered me when I needed it, were invaluable. I will always be grateful for the opportunity to have pursued my doctorate under his excellent guidance.

I am profoundly grateful to Mahir Hadžić, whose relentless pursuit of new insights and expansive perspective on mathematics greatly influenced this thesis and me. I am thankful for each of our countless discussions and his numerous "TED Talks".

I thank Yan Guo for committing his time to referee this thesis.

I thank Sebastian Wolfschmidt, in whom I found a close friend over the last years. I am grateful for all of our collaborations, which would not have been possible without him repeatedly explaining the differences between the words "Poisson" and "Einstein" to me.

I thank Thomas Kriecherbauer, whose kindness and passion for mathematics greatly inspire me.

I thank all academic companions for making my time at the university enriching and fun.

Most importantly, I thank my family and friends for bringing joy and strength to my (doctoral) life. In particular, to my brother, for always providing a window to another world. To Johanna, for her encouragement and distraction. And to my parents, for their example of perseverance and endless support.

Abstract

In this thesis we investigate the existence of pulsating solutions of the spherically symmetric gravitational Vlasov-Poisson system on a linear level. To this end, we linearise the system around compactly supported steady states, which we first introduce in detail at the beginning of the thesis. In order to explain different aspects of oscillations on the non-linear level – in particular, the pulsating behaviour, where the support of the solution changes periodically – we employ three different linearisation methods. All of them lead to the same linear operator whose spectral properties determine the dynamics on the linear level.

The analysis of this operator forms the main part of this thesis. Firstly, we analyse the functional analytical properties of the operator and prove that it is self-adjoint if its domain of definition is chosen appropriately. Then we explicitly determine its essential spectrum. It is given by the radial particle periods within the underlying steady state, to which we devote a separate analysis in the appendix.

On a linear level, oscillating solutions correspond to positive eigenvalues of the operator. We investigate their existence by developing an adaptation of the Birman-Schwinger principle from quantum mechanics for our situation. We combine this with a reduction method discovered by Mathur. Overall, this allows us to characterise the existence and number of positive eigenvalues below the essential spectrum of the original operator by spectral properties of a simpler operator. Using this characterisation, we can explain the linear oscillations around some stationary solutions.

Afterwards, we consider the slightly modified setting of steady states surrounding a point mass. If the steady state is sufficiently small compared to the point mass, we show that perturbations are damped on a linear level. The main step towards this (non-quantitative) damping result is to exclude eigenvalues embedded in the essential spectrum of the operator. The absence of other eigenvalues can be ensured by applying the Birman-Schwinger-Mathur principle described above.

To conclude, we discuss how the techniques developed here can be applied in related situations and conduct a comprehensive numerical analysis. In particular, we investigate the dynamics near the most commonly used steady states and show in which cases undamped oscillatory behaviour occurs at the linear level. Moreover, we numerically show that the actual non-linear effects can be accurately described by the analysis on the linear level performed here.

Kurzfassung

In dieser Abhandlung untersuchen wir die Existenz pulsierender Lösungen des sphärisch symmetrischen gravitativen Vlasov-Poisson-Systems auf linearer Ebene. Dafür linearisieren wir das System um stationäre Lösungen mit kompaktem Träger, die wir zu Beginn der Arbeit zunächst ausführlich einführen. Um verschiedene Aspekte von Oszillationen auf der nicht-linearen Ebene – insbesondere das pulsierende Verhalten, bei dem sich der Träger der Lösung periodisch bewegt – erklären zu können, verwenden wir zur Linearisierung drei verschiedene Verfahren. Alle führen auf denselben linearen Operator, dessen spektrale Eigenschaften die Dynamik auf der linearen Ebene bestimmen.

Die Analyse dieses Operators bildet den Hauptteil dieser Abhandlung. Zuerst analysieren wir die funktionalanalytischen Eigenschaften des Operators und zeigen, dass er bei geeigneter Wahl seines Definitionsbereiches selbstadjungiert ist. Anschließend bestimmen wir sein wesentliches Spektrum explizit. Es ist gegeben durch die radialen Teilchenperioden in der zugrundeliegenden stationären Lösung, denen wir im Anhang eine gesonderte Analyse widmen.

Auf linearer Ebene entsprechen oszillierende Lösungen positiven Eigenwerten des Operators. Wir untersuchen deren Existenz durch Entwicklung einer Adaption des Birman-Schwinger-Prinzips aus der Quantenmechanik für unsere Situation. Wir kombinieren dies mit einer von Mathur entdeckten Reduktionsmethode. Insgesamt können wir so die Existenz und Anzahl der positiven Eigenwerte unterhalb des wesentlichen Spektrums des ursprünglichen Operators durch spektrale Eigenschaften eines einfacheren Operators charakterisieren. Mittels dieser Charakterisierung können wir die linearen Oszillationen um einige stationäre Lösungen erklären.

Im Anschluss betrachten wir die leicht modifizierte Situation von stationären Lösungen, welche eine Punktmasse umgeben. Wir zeigen, dass wenn die stationäre Lösung im Vergleich zur Punktmasse genügend klein ist, Störungen auf linearer Ebene gedämpft sind. Der Hauptschritt zu diesem (nichtquantitativen) Dämpfungsresultat besteht darin, im wesentlichen Spektrum eingebettete Eigenwerte des Operators auszuschließen. Die Abwesenheit anderer Eigenwerte kann durch Anwendung des oben beschriebenen Birman-Schwinger-Mathur-Prinzips sichergestellt werden.

Abschließend diskutieren wir einerseits, wie die hier entwickelten Techniken in verwandten Situationen angewendet werden können, und führen andererseits eine umfassende numerische Analyse durch. Insbesondere untersuchen wir die Dynamik nahe der populärsten stationären Lösungen und zeigen auf, in welchen Fällen auf linearer Ebene ein ungedämpftes oszillierendes Verhalten auftritt. Darüber hinaus stellen wir numerisch fest, dass die tatsächlichen nicht-linearen Effekte durch die hier durchgeführte Analyse auf linearer Ebene genau beschrieben werden können.

Contents

Chapter 1

Introduction

Consider a long-existing galaxy. We aim to investigate its evolution by analysing a mathematical model of it. Because a galaxy is frequently perturbed, e.g., by the gravitational forces of other nearby galaxies, only models that are resilient to slight perturbations can describe real galaxies. What these models are is quite well understood – this is the subject of stability theory which we will review below. Here we are interested in the less well comprehended question of how a galaxy (model) evolves qualitatively. A common hypothesis is that relaxation mechanisms drive galaxies towards an equilibrium state [19, 104] and that every slight perturbation gets *damped* away. However, observations suggest that certain real galaxies may not be in such equilibrium state, cf. [101]. Explanations for these behaviours have been extensively discussed in the (astro)physics literature [26, 33, 100, 101, 103, 104, 110, 111, 115, 124, 132, 148, 159, 161, 162, 163, 168, 171, 172, 174, 175, 176, 179, 180] and, more recently, also in the mathematics literature [61, 62, 85, 86, 117]. These investigations indicate that a non-damped galaxy exhibits an oscillatory behaviour of *pulsating* nature, i.e., the galaxy expands and contracts in a time-periodic way. The aim of this thesis is to study this phenomenon mathematically.

1.1 The Mathematical Set-Up

We describe the state of a galaxy at some fixed time $t \in \mathbb{R}$ by its phase space density function $f = f(t, x, v) \geq 0$. The phase space variables consist of the space variable $x \in \mathbb{R}^3$ and the velocity variable $v \in \mathbb{R}^3$. Integrating $f(t)$ over some part of phase space gives the mass of stars contained in this phase space region. The evolution of an individual star inside the galaxy is determined by Newton's equations of motion

$$\dot{x} = v, \qquad \dot{v} = -\partial_x U(t, x), \tag{1.1.1}$$

where $U = U(t, x)$ is the gravitational potential of the galaxy and $\partial_x U$ denotes its gradient with respect to (henceforth abbreviated as "w.r.t.") the space variable x. Here, we neglect close encounters between stars, and also potential collisions. The latter implies that the phase space density f is constant along the trajectories of stars, which leads to the *Vlasov equation*

$$\partial_t f + v \cdot \partial_x f - \partial_x U \cdot \partial_v f = 0, \tag{1.1.2}$$

see [67] for a review of the origins of this equation.[1] Middle dots $\cdot$ denote the Euclidean scalar product. By Newton's law for gravity, the gravitational potential solves the *Poisson*

[1] Although the conclusion of [67] is that *collisionless Boltzmann equation* would be the proper name of the equation (1.1.2), we will still use the more common name *Vlasov equation* here.

equation

$$\Delta U = 4\pi\rho, \tag{1.1.3}$$

where Δ denotes the Laplacian w.r.t. x, the gravitational constant is normalised to unity, and $\rho = \rho(t,x)$ is the (spatial) mass density of the galaxy given by

$$\rho(t,x) = \int_{\mathbb{R}^3} f(t,x,v)\,\mathrm{d}v. \tag{1.1.4}$$

Here, we assume that all stars have unit mass. We equip the Poisson equation with the usual boundary condition at spatial infinity

$$\lim_{|x|\to\infty} U(t,x) = 0, \tag{1.1.5}$$

corresponding to an isolated galaxy. The equations (1.1.2)–(1.1.5) form a closed system for the evolution of f, known as the three-dimensional gravitational *Vlasov-Poisson system*. For an extensive physical background to this system we refer to [19]. More mathematical aspects, like the global existence of classical solutions, are reviewed in [47, 143]. The Vlasov-Poisson system can also be used to model the evolution of particle ensembles other than galaxies, which is why we will below use the more general term "particles" when referring to the individual stars in a galaxy model.

We consider this system in *spherical symmetry* (or *radial symmetry*), i.e., we assume that the phase space density function f is invariant under simultaneous rotations of x and v. This means that the originally six-dimensional phase space can be parametrised by the variables

$$r = |x|, \qquad w = \frac{x\cdot v}{r}, \qquad L = |x\times v|^2, \tag{1.1.6}$$

which can be interpreted as the *spatial radius*, the *radial velocity*, and the *squared modulus of the angular momentum*. The space dependencies of the gravitational potential U and the mass density ρ reduce to a dependency on the spatial radius r. In Section 2.1, we discuss in detail the notion of spherical symmetry as well as the Vlasov-Poisson system in the radial variables (r,w,L); we refer to this system as the *radial Vlasov-Poisson system*. The main motivation for assuming spherical symmetry is that it simplifies the mathematical analysis. From a physics point of view [44, Ch. IX, Sc. 1], it means that our model describes spheroidal galaxies (and globular clusters).

We analyse solutions of the radial Vlasov-Poisson system close to *steady states*, i.e., close to time-independent solutions $f_0 = f_0(x,v)$ of the Vlasov-Poisson system. We will describe below the class of steady states considered here. They are all compactly supported, have finite mass, and are stable, which means that they are realistic models for galaxies in an equilibrium state. As motivated above, it is our intention to establish the presence of oscillating/pulsating solutions. It is natural to expect that such oscillations take place around an equilibrium state. Hence, our strategy is to obtain (undamped) oscillatory solutions as perturbations of steady states. It is, however, unclear whether such solutions exist. It is also possible that all solutions close to a steady state converge towards the steady state.

Numerical simulations [115, 124, 132, 159, 161, 162, 168] revealed that the occurrence of these qualitatively different behaviours depends on the steady state. In Figure 1.1.1, we depict two (numerically computed) solutions starting close to different steady states. The solution in the left panel shows an undamped oscillatory behaviour, and we can clearly see that the oscillation is of pulsating nature, i.e., the solution moves radially in and out in a time-periodic way. In contrast, the solution in the right panel is damped, i.e., after a brief period of time it is nearly a steady state. Our aim is to analyse which of these two cases

applies to which steady state. In particular, we want to understand the occurrence of the former one.

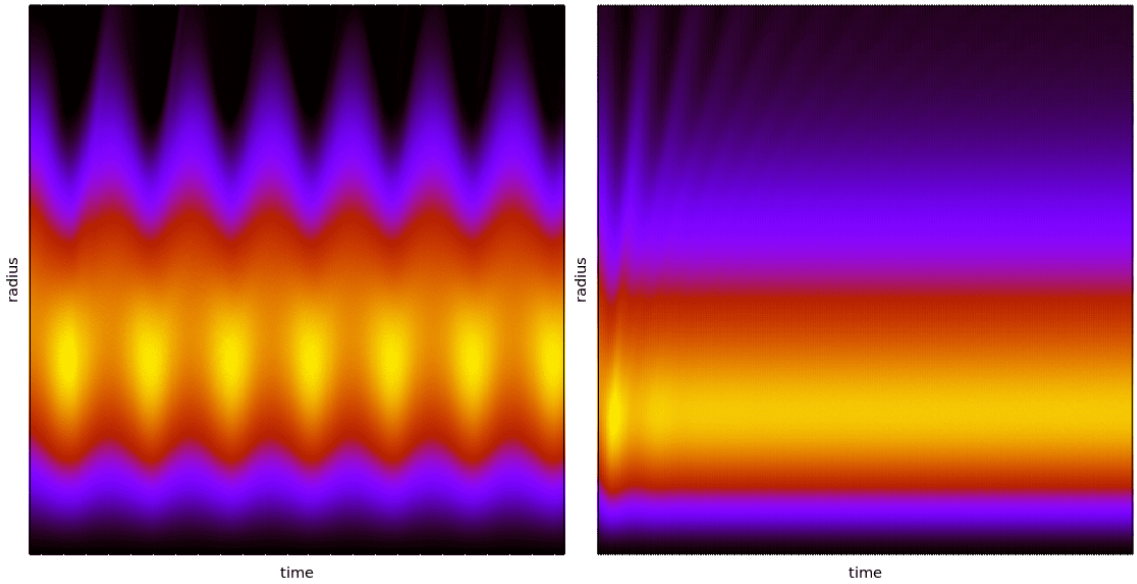

Figure 1.1.1: The time evolutions of the radial mass densities $(t, r) \mapsto 4\pi r^2 \rho(t, r)$ of two spherically symmetric solutions of the Vlasov-Poisson system. The colour gradients depict the values of these functions, increasing from black to yellow. Both solutions start close to different steady states. The initial data and the numerical method used to create these plots will be presented in Section 8.4.

1.2 Outline of the Thesis

Let us now outline the analysis conducted in this thesis and discuss the connections to previous research. The approaches and results presented here are primarily based on [62] and the subsequent works [49, 61]. There is some overlap between [62] and the monograph [85] by Kunze, which was developed simultaneously and independently of [62]. Hence, several of the results presented here (in particular, those from Chapters 4 and 5 and Appendices A and B) are also contained in [85]; we will consistently discuss the connections of our results and those of [85]. The key aspects of [85] are also presented in the lecture notes [86].

Steady States (Sections 2.2 and 4.1)

The starting point for our analysis is a thorough understanding of the steady states of the Vlasov-Poisson system. In Section 2.2, we review the well-established existence theory of spherically symmetric, compactly supported steady states of the Vlasov-Poisson system, cf. [14, 63, 130, 140, 146] and [19, Sc. 4.3]. We mainly follow [130] in this part.

The key idea is to search for time-independent solutions f_0 of the form

$$f_0(x, v) = \varphi(E(x, v), L(x, v)), \tag{1.2.1}$$

where $\varphi\colon \mathbb{R}^2 \to [0, \infty[$ is a prescribed *microscopic equation of state*, E is the *particle energy*

$$E(x, v) = \frac{1}{2}|v|^2 + U_0(x) \tag{1.2.2}$$

determined by the gravitational potential U_0 associated to f_0, and L is the squared modulus of the angular momentum given by (1.1.6). Obviously, E and L are conserved quantities of the characteristic system (1.1.1) if U_0 is spherically symmetric. Hence, (1.2.1) defines a time-independent solution of the Vlasov equation (1.1.2). If φ is sufficiently smooth, this solution is classical, but we do not require this to be the case, cf. Definition 2.2.2. The precise class of steady states which will be considered in (the main part of) this thesis is specified by the conditions (φ1)–(φ5) stated in Sections 2.2 and 4.1.[2] Let us present here the most "popular" steady states – i.e., the ones which are most commonly used in the literature – covered by our analysis. We will review the other works that have considered these steady states in Section 2.2. The first ones are the *isotropic polytropes*

$$f_0(x,v) = (E_0 - E(x,v))_+^k, \tag{1.2.3}$$

where $E_0 < 0$ is a negative *cut-off energy*, a subscript + denotes taking the positive part of an expression,[3] and k is the *polytropic exponent*. For the latter we require $0 < k < \frac{7}{2}$. The second important class of steady states are the *King models*

$$f_0(x,v) = (e^{E_0 - E(x,v)} - 1)_+, \tag{1.2.4}$$

with similar $E_0 < 0$ as above. Steady states of the form (1.2.3) or (1.2.4) are *isotropic*, which means that they depend only on the particle energy, but not explicitly on the angular momentum. Our analysis also covers steady states that do not have this property; such steady states are called *anisotropic*. The most important examples for this are *polytropes*[4]

$$f_0(x,v) = (E_0 - E(x,v))_+^k \, (L(x,v) - L_0)_+^\ell, \tag{1.2.5}$$

with $E_0 < 0$ as above, a parameter $L_0 > 0$, and polytropic exponents k and ℓ satisfying $\ell > -\frac{1}{2}$ and $0 < k < 3\ell + \frac{7}{2}$. These steady states are called *polytropic shells* because the positive lower bound $L_0 > 0$ on the L-values results in an inner vacuum region of the steady state, i.e., $R_{\min} \coloneqq \inf\{|x| \mid \rho_0(x) \neq 0\} > 0$, where ρ_0 denotes the mass density associated to the steady state f_0. For isotropic steady states, no such inner vacuum region exists, i.e., $R_{\min} = 0$. All of the steady states considered here have finite mass and finite extent, i.e., $M_0 \coloneqq \int_{\mathbb{R}^3} \rho_0(x)\,\mathrm{d}x < \infty$ and $R_{\max} \coloneqq \sup\{|x| \mid \rho_0(x) \neq 0\} < \infty$. These two properties are ensured by incorporating the negative cut-off energy E_0 into the ansatz, with $f_0(x,v) = 0$ for $E(x,v) \geq E_0$. We will see later that it is not convenient to prescribe E_0. Instead, it is implicitly determined by the parameter

$$\kappa = E_0 - U_0(0). \tag{1.2.6}$$

In the isotropic case, κ is in one-to-one correspondence with the central density $\rho_0(0) > 0$, cf. Remark 2.2.10 (a). For a polytropic shell (1.2.5), κ determines $R_{\min}$, i.e., the size of the inner vacuum region. In Proposition 2.2.9, we show that any prescribed $\kappa > 0$ and suitable microscopic equation of state φ lead to a spherically symmetric steady state with the properties described above. In Appendix B, we show that isotropic polytropes (1.2.3) (as well as polytropes (1.2.5) with $L_0 = 0$) with different values of κ satisfy a scaling law. It applies to all relevant quantities associated to the steady states, including the periods of

[2] Section 2.2 addresses the existence theory of steady states, while Section 4.1 separately presents further assumptions on the steady states which are important for the subsequent analysis.

[3] See (2.2.13) for a rigorous definition of expressions of the form b_+^α.

[4] From a physics point of view, the term *polytropic* is only meaningful in the case $L_0 = 0$ in (1.2.5). However, for the sake of convenience, we also use this name in the case $L_0 > 0$ here.

possible oscillatory modes. This is similar to the *Eddington-Ritter relation* [39] known from the context of gas spheres.

As mentioned previously, the steady states (1.2.3)–(1.2.5) (and all other steady states satisfying the assumptions imposed in Sections 2.2 and 4.1) are stable. This is due to the fact that they are all energy-decreasing, i.e.,

$$\varphi' \coloneqq \partial_E \varphi < 0 \tag{1.2.7}$$

inside the steady state support. This property is natural from a physics point of view [184]; it means that the concentration of ever more energetic particles is decreasing within the equilibrium configuration. It was first argued by Antonov [9, 10] that this property leads to stability, which is why (1.2.7) is also known as *Antonov's stability criterion*. However, Antonov's result addresses only the *linear* stability of (certain) such steady states, i.e., the stability after (formally) linearising the Vlasov-Poisson system around a fixed steady state. Further linear stability results were developed in [15, 36, 37, 77, 128, 169]. Afterwards, using techniques independent from the ones used to show linear stability, actual non-linear stability results for (suitable) steady states satisfying (1.2.7) were proven, cf. [51, 52, 53, 54, 55, 56, 57, 94, 96, 150, 181], culminating in the orbital stability established in [97]. A review of these stability results can be found in [119]. Stability ensures that a solution of the Vlasov-Poisson system starting close to a steady state remains close to it. As motivated above, we are interested in the qualitative behaviour of such solutions.

Linearisation (Chapter 3)

To study the qualitative behaviour of solutions close to some steady state f_0, we linearise the Vlasov-Poisson system around the steady state. In fact, the whole analysis in this thesis only concerns this linearised system. For studying the presence of oscillatory solutions close to steady states, it is convenient to first gain an in-depth understanding at the linear level before attempting to prove the corresponding results at the non-linear level. The same strategy already succeeded in the context of the Euler-Poisson system, which is somewhat related to the Vlasov-Poisson system, where the presence of oscillatory solutions was established first on the linear level [39, 107, 149] and afterwards transferred to the actual non-linear system [74].

In Section 3.1, we describe the linearisation process in detail. The main idea is to insert the formal expression $f_0+\varepsilon f+\mathcal{O}(\varepsilon^2)$ with $0 < \varepsilon \ll 1$ into the Vlasov-Poisson system (1.1.2)–(1.1.5) and dispense with terms of order $\mathcal{O}(\varepsilon^2)$. Here, $f(t)\colon \mathbb{R}^3 \times \mathbb{R}^3 \to \mathbb{R}$ gives the linear order of the perturbation of the steady state, which we require to be spherically symmetric and to vanish outside of the support of the steady state; see [15, App.] for a motivation of the latter property. This process leads to a linear(ised) version of the Vlasov equation (1.1.2) for f. Because the Vlasov equation is a first-order transport equation, so is its linearised version. However, the existence of oscillating solutions is more convenient for a second-order equation. Based on a calculation due to Antonov [8], the linearised Vlasov-Poisson system can be rewritten as a second-order equation for the odd-in-v part f_- of the linear perturbation f, i.e., $f_-(t,x,v) = -f_-(t,x,-v)$. The resulting *linearised Vlasov-Poisson system in second-order formulation* is of the form

$$\partial_t^2 f_- + \mathcal{L} f_- = 0, \tag{1.2.8}$$

where $\mathcal{L}$ is the *linearised operator* (or *Antonov operator*) associated to the underlying steady state f_0. This operator is given by

$$\mathcal{L} \coloneqq -\mathcal{T}^2 - \mathcal{R}. \tag{1.2.9}$$

The first term is the negative square of the *transport operator*

$$\mathcal{T} \coloneqq v \cdot \partial_x - \partial_x U_0(x) \cdot \partial_v. \tag{1.2.10}$$

This part of $\mathcal{L}$ describes how the linear perturbation evolves according to the characteristic flow of the steady state. The other part of the linearised operator describes the gravitational forces of the perturbation via the *gravitational response operator*

$$\mathcal{R}g(r, w, L) \coloneqq 4\pi \, |\varphi'(E, L)| \, w \, j_g(r), \tag{1.2.11}$$

which is defined for any suitable spherically symmetric function $g = g(x, v) = g(r, w, L)$. The function j_g denotes the radial velocity density induced by g, cf. Lemma 4.4.1.

The behaviour of solutions of (1.2.8) is determined by the spectral properties of the linearised operator $\mathcal{L}$. By the linear stability results mentioned above, the spectrum of $\mathcal{L}$ is positive. If $\lambda > 0$ is a positive eigenvalue of $\mathcal{L}$ with eigenfunction g, the function $t \mapsto \cos(\sqrt{\lambda}\, t)g$ is a time-periodic solution of (1.2.8) with period

$$p = \frac{2\pi}{\sqrt{\lambda}}. \tag{1.2.12}$$

In Section 3.1, we will see that this explains the oscillations of the kinetic and potential energies of solutions of the Vlasov-Poisson system close to f_0 to linear order. Hence, our primary objective of showing the presence of oscillatory solutions corresponds to proving the existence of positive eigenvalues of the linearised operator $\mathcal{L}$. If no such eigenvalue exists, it is expected that the solutions of (1.2.8) are damped; we will discuss this case in more detail below.

However, the above does not explain the pulsating nature of the oscillations. To address this issue, we offer two additional linearisation schemes in a *mass-Lagrangian picture* and a *Lagrangian picture* in Sections 3.2 and 3.3, respectively. These linearisation schemes are commonly used in related settings, cf. [75, 107, 109]; in the context of the Vlasov-Poisson system, they have first been derived in [62, Sc. 3] and [172]. Both of these approaches also lead to the equation (1.2.8) obtained from the *Eulerian* linearisation. To linear order, they indeed explain the oscillations of the phase space support of solutions of the Vlasov-Poisson system close to f_0.

The Operators (Chapter 4)

In Chapter 4, we establish the foundations for the spectral analysis of the linearised operator $\mathcal{L}$ for a fixed steady state f_0 by analysing its functional analytical properties. The natural Hilbert space for our analysis is a suitably weighted L^2-space H (cf. Definition 4.2.3) containing functions defined on the *steady state support*

$$\Omega_0 \coloneqq \{(x, v) \in \mathbb{R}^3 \times \mathbb{R}^3 \mid f_0(x, v) > 0\}. \tag{1.2.13}$$

Throughout this thesis, we will use the term *support* rather loosely; the support of some function f may refer to $\{f > 0\}$, $\overline{\{f > 0\}}$, or any set in between. Because $\mathcal{L}$ only covers the evolution of the odd-in-v part of the linearised perturbation, we further consider the odd-in-v subspace of H:

$$\mathcal{H} \coloneqq \{f \in H \mid f \text{ is odd in } v\}. \tag{1.2.14}$$

From a functional analysis point of view, the crucial part of $\mathcal{L}$ is the transport part because the transport operator (1.2.10) is a derivative operator and thus unbounded. The

properties of this operator were widely studied in the literature [53, 61, 62, 85, 96, 147, 148, 165]. We follow [147] to suitably define $\mathcal{T}$ in a weak sense on a subset $\mathrm{D}(\mathcal{T})$ of H, cf. Definition 4.2.5. This naturally leads to the weak definition of the squared transport operator $\mathcal{T}^2$ on a set $\mathrm{D}(\mathcal{T}^2)$; the sets $\mathrm{D}(\mathcal{T})$ and $\mathrm{D}(\mathcal{T}^2)$ are both dense subsets of H and contain smooth functions with compact support in Ω_0. The definitions are designed so that $\mathcal{T}\colon \mathrm{D}(\mathcal{T}) \to H$ is skew-adjoint, cf. Proposition 4.3.15, and $\mathcal{T}^2\colon \mathrm{D}(\mathcal{T}^2) \to H$ and $\mathcal{T}^2\big|_{\mathcal{H}}\colon \mathrm{D}(\mathcal{T}^2) \cap \mathcal{H} \to \mathcal{H}$ are self-adjoint, cf. Proposition 4.3.17; the latter operator is well-defined because $\mathcal{T}$ reverses v-parity. The results are based on [147, Thm. 2.2] and [62, Prop. 2], but they are proven here in a different way using the following tool.

The transport operator $\mathcal{T}$ can be interpreted as computing the derivative along the characteristic flow of the steady state. In radial variables, the characteristic system turns into the planar ODE

$$\dot{r} = w, \qquad \dot{w} = -\Psi_L'(r); \tag{1.2.15}$$

the variable L takes on the role of a parameter of this ODE. The characteristic flow is hence determined by the *effective potential*

$$\Psi_L(r) \coloneqq U_0(r) + \frac{L}{2r^2}, \qquad L, r > 0. \tag{1.2.16}$$

For any $L > 0$, it is straight-forward to verify that Ψ_L is of single-well structure, i.e., it attains a unique minimum $E_L^{\min} \coloneqq \min_{]0,\infty[} \Psi_L = \Psi_L(r_L)$ at some radius r_L, and for every $E_L^{\min} < E < 0$ there exist two unique radii $r_-(E,L) < r_+(E,L)$ such that (henceforth abbreviated as "s.t.") $\Psi_L(r_\pm(E,L)) = E$; see Lemma 2.2.12 for a rigorous proof and Figure 2.2.1 for a visualisation. Hence, as the particle energy $E(r,w,L) = \frac{1}{2}w^2 + \Psi_L(r)$ is conserved along the characteristic flow, every solution of (1.2.15) with $L > 0$ and energy value $E_L^{\min} < E < 0$ is periodic, cf. Section 2.2.2; for now, let us ignore the stationary point $(r_L, 0)$ corresponding to the energy $E = E_L^{\min}$. The periods are given by the *(radial) period function*

$$T(E,L) \coloneqq 2\int_{r_-(E,L)}^{r_+(E,L)} \frac{\mathrm{d}r}{\sqrt{2E - 2\Psi_L(r)}}, \qquad L > 0,\ E_L^{\min} < E < 0. \tag{1.2.17}$$

In order to study $\mathcal{T}$, it is convenient to introduce new variables which are adapted to the characteristic flow. For fixed $L > 0$, we parametrise a point in the (r,w)-plane by the energy value E of the characteristic orbit it lies on and an angle type variable $\theta \in \mathbb{S}^1 \cong [0,1[$ determining the position on the orbit; see Section 4.3.1 for details and Figure 4.3.1 for a visualisation. This leads to the new variables $(\theta, E, L) \in \mathbb{S}^1 \times \mathbb{D}_0$ on the steady state support, which we refer to as *action-angle type variables*.[5] Here, $\mathbb{D}_0 \coloneqq \{(E,L) \mid L > L_0,\ E_L^{\min} < E < E_0\}$ denotes the steady state support in (E,L)-variables; in the isotropic case we set $L_0 \coloneqq 0$. In these variables, the transport operator and its square simply correspond to suitably weighted derivatives w.r.t. θ:

$$\mathcal{T} = \frac{1}{T(E,L)}\,\partial_\theta, \qquad \mathcal{T}^2 = \frac{1}{T(E,L)^2}\,\partial_\theta^2. \tag{1.2.18}$$

These formulae are straight-forward to verify for smooth functions (cf. Lemma 4.3.8) and also hold in the weak sense (cf. Lemmas 4.3.9 and 4.3.10).

The formulae (1.2.18) show that the properties of $\mathcal{T}$ and $\mathcal{T}^2$ are intimately related to the ones of the period function T. The properties of T will be important for other parts of

[5] We will explain in Remark 4.3.2 why (θ, E, L) are not true action-angle variables.

this thesis as well, which is the reason why we thoroughly analyse the period function in Appendix A. This analysis is mainly based on [62, App. B] and [85, Ch. 3]; other analyses of the period function are conducted in [148, Apps. B and C] as well as, in different settings, in [49, Sc. 3.2] and [61, App. A.2]. The main properties of T are that it is smooth as well as bounded and bounded away from zero on the steady state support $\mathbb{D}_0$, cf. Proposition A.0.1.

Based on [62, Thm. 5.7], we use the action-angle type variables and apply Weyl's criterion [69, Thm. 7.2] to show that

$$\sigma(-\mathcal{T}^2\big|_{\mathcal{H}}) = \sigma_{\mathrm{ess}}(-\mathcal{T}^2\big|_{\mathcal{H}}) = \overline{\left(\frac{2\pi\mathbb{N}}{T(\mathbb{D}_0)}\right)^2}, \tag{1.2.19}$$

cf. Proposition 4.3.19; throughout this thesis we use the convention $\mathbb{N} = \mathbb{N} \setminus \{0\}$. Here, σ_{ess} denotes the essential spectrum, i.e., all elements of the spectrum that are not isolated eigenvalues of finite multiplicity.

In Section 4.4, we analyse the functional analytic properties of the second part of the linearised operator: The response operator $\mathcal{R}$ given by (1.2.11). It is straight-forward to verify that $\mathcal{R}\colon H \to H$ is bounded, symmetric, and non-negative, cf. Lemma 4.4.2; the same properties also hold for the restriction of $\mathcal{R}$ to $\mathcal{H}$. The symmetry of $\mathcal{R}$ is due to the weight incorporated into H and $\mathcal{H}$, cf. Remark 4.4.3.

By combining the properties of $\mathcal{T}^2$ and $\mathcal{R}$, we deduce that the linearised operator $\mathcal{L}\colon \mathrm{D}(\mathcal{L}) \to \mathcal{H}$ given by (1.2.9) is self-adjoint with the natural domain of definition $\mathrm{D}(\mathcal{L}) \coloneqq \mathrm{D}(\mathcal{T}^2) \cap \mathcal{H}$, cf. Lemma 4.5.2. In addition, in Proposition 4.5.4 we show that the essential spectrum of $\mathcal{L}$ is entirely determined by the transport part, i.e.,

$$\sigma_{\mathrm{ess}}(\mathcal{L}) = \sigma_{\mathrm{ess}}(-\mathcal{T}^2\big|_{\mathcal{H}}) = \overline{\left(\frac{2\pi\mathbb{N}}{T(\mathbb{D}_0)}\right)^2}. \tag{1.2.20}$$

This is due to the fact that the essential spectrum is stable under "relatively compact" perturbations by Weyl's theorem [69, Thm. 14.6]. In Lemma 4.5.3, we show that $\mathcal{R}$ is such a perturbation of $\mathcal{T}^2\big|_{\mathcal{H}}$. As observed in [117, Thm. 1.1], a similar result also holds for the absolutely continuous spectrum, cf. Remark 4.5.5. Because the period function T is bounded on the steady state support $\mathbb{D}_0$, (1.2.20) implies that $\sigma_{\mathrm{ess}}(\mathcal{L})$ is bounded away from 0. The gap between 0 and $\inf(\sigma_{\mathrm{ess}}(\mathcal{L})) = \min(\sigma_{\mathrm{ess}}(\mathcal{L}))$ is denoted by

$$\mathcal{G} \coloneqq]0, \inf(\sigma_{\mathrm{ess}}(\mathcal{L}))[. \tag{1.2.21}$$

We refer to $\mathcal{G}$ as the *essential gap*.[6] In Proposition 4.5.11, we derive a positive lower bound on the entire spectrum of $\mathcal{L}$, i.e., we show $\inf(\sigma(\mathcal{L})) > 0$. This is based on [62, Thm. 7.5], where $]0, \inf(\sigma(\mathcal{L}))[$ is called the *spectral gap*. The positivity of $\mathcal{L}$ is mainly due to *Antonov's coercivity bound* – a lower bound on the quadratic form $\langle \mathcal{L}f, f\rangle_H$ for odd-in-v functions f first derived in [9, 10] – and corresponds to the linear stability of the steady state. In Appendix C, we rigorously establish this linear stability result alongside a suitable well-posedness theory for the linearised system (1.2.8) based on (semi)group theory.

As discussed before, our main interest is to show the existence of eigenvalues of the linearised operator $\mathcal{L}$. We restrict our search for eigenvalues to the essential gap $\mathcal{G}$. The main reason for this is that the existence of eigenvalues in $\mathcal{G}$ can be characterised by variational principles. More precisely,

$$\mathcal{L} \text{ has an eigenvalue} \in \mathcal{G} \quad \Leftrightarrow \quad \exists f \in \mathrm{D}(\mathcal{L}) \setminus \{0\}\colon \frac{\langle \mathcal{L}f, f\rangle_H}{\|f\|_H^2} < \inf(\sigma_{\mathrm{ess}}(\mathcal{L})) = \frac{4\pi^2}{\sup^2_{\mathbb{D}_0}(T)}, \tag{1.2.22}$$

[6] In [62, Eqn. (1.34)], $\mathcal{G}$ is called the *principal gap*. This name is inspired by [111]. Here we prefer the name *essential gap*, as it emphasises that $\mathcal{G}$ is the gap between the essential spectrum of $\mathcal{L}$ and 0.

cf. Lemma 4.5.16. In Section 4.5.4, we also discuss further reasons why it is natural to search for eigenvalues of $\mathcal{L}$ in $\mathcal{G}$. By (1.2.22), a way to show the existence of such eigenvalues is to insert some function $f \in \mathrm{D}(\mathcal{L})$ into $\frac{\langle \mathcal{L}f, f\rangle_H}{\|f\|_H^2}$ and compare the result to $\inf(\sigma_{\mathrm{ess}}(\mathcal{L}))$. In [85, Ex. 2.1], it was observed that the quadratic form of $\mathcal{L}$ takes on a particularly simple form for $f = |\varphi'|\, rw$. This leads to *Kunze's criterion* for the existence of an oscillatory mode, cf. Lemma 4.5.19, which, however, could not yet be (rigorously) verified for any steady state.

Inspired by techniques originating from the context of plasma physics, some other approaches were pursued in the literature to study the presence of eigenvalues of $\mathcal{L}$. An adaptation of the Kalnajs matrix method [19, Sc. 5.3.2] was derived in [175, 180]. A related approach based on an expansion of the linear perturbation in the velocity variable was pursued in [161]. In [174], the theory of van Kampen modes [19, Box 5.1] was established in the context of the (gravitational) linearised Vlasov-Poisson system. Below we will present in detail a different approach.

The Birman-Schwinger-Mathur Principle (Chapter 5)

In order to establish the presence of oscillatory modes, we aim to further characterise the existence of eigenvalues of $\mathcal{L}$ in $\mathcal{G}$. A related problem in the context of quantum mechanics is to determine the negative eigenvalues of a Schrödinger operator $S \coloneqq -\Delta - V\colon H^2(\mathbb{R}^3) \to L^2(\mathbb{R}^3)$ for a given potential $V\colon \mathbb{R}^3 \to [0,\infty[$.[7] As first observed by Birman [21] and Schwinger [158], $\lambda < 0$ is an eigenvalue of S if and only if 1 is an eigenvalue of the *Birman-Schwinger operator*

$$B_\lambda \coloneqq \sqrt{V}\,(-\Delta - \lambda)^{-1}\sqrt{V}, \tag{1.2.23}$$

and the associated eigenfunctions can be explicitly transformed into one another. The reason why the eigenvalue problem for B_λ is more convenient to study than the original one for S is that B_λ has nicer properties from a functional analysis point of view: Under suitable assumptions on V, B_λ is a bounded integral operator.[8] This transformation of the eigenvalue problem became known as the *Birman-Schwinger principle* and provided numerous insights into the properties of the negative eigenvalues of Schrödinger operators. An extensive overview of the applications of the Birman-Schwinger principle in quantum mechanics (and proofs of the properties stated above) can, e.g., be found in [99, Sc. 4.3].

It was first observed by Mathur [111] that an adaption of the Birman-Schwinger principle can also be applied in the context of a linearised Vlasov-Poisson system. Subsequently, these methods were refined and extended in [62, 85] as well as, in related settings, in [49, 61]. The analogue of the Birman-Schwinger operator (1.2.23) in our setting is

$$Q_\lambda \coloneqq \sqrt{\mathcal{R}}\left(-\mathcal{T}^2|_{\mathcal{H}} - \lambda\right)^{-1}\sqrt{\mathcal{R}} \tag{1.2.24}$$

with $\lambda \in \mathcal{G}$. Here, $\sqrt{\mathcal{R}}$ is the square root of the response operator $\mathcal{R}$ in the sense of [136, Thm. VI.9]. It is explicitly given by

$$\sqrt{\mathcal{R}}g(r,w,L) = 2\sqrt{\pi}\,|\varphi'(E,L)|\,\frac{w}{\sqrt{\rho_0(r)}}\,j_g(r), \tag{1.2.25}$$

[7] Under suitable assumptions on V, $\sigma_{\mathrm{ess}}(S) = \sigma_{\mathrm{ess}}(-\Delta) = [0,\infty[$, cf. [69, Sc. 14.3]. This shows that the negative eigenvalues of S are precisely the ones below its essential spectrum, and thus correspond to the eigenvalues of $\mathcal{L}$ in $\mathcal{G}$.

[8] Another way to think of the Birman-Schwinger principle is that it transforms a differential equation (the eigenvalue problem for S) into an integral equation (the eigenvalue problem for B_λ).

i.e., it has a similar form to $\mathcal{R}$ itself and thus has similar properties to $\mathcal{R}$, cf. Lemma 4.4.4. In Proposition 5.1.13, we derive an analogue of the Birman-Schwinger principle: The existence of an eigenvalue $\lambda \in \mathcal{G}$ of $\mathcal{L}$ is equivalent to 1 being an eigenvalue of Q_λ. In addition, in Proposition 5.1.14 we show that the number of eigenvalues of $\mathcal{L}$ smaller than some $\lambda \in \mathcal{G}$ is identical to the number of eigenvalues of Q_λ larger than 1. This quantitative statement requires a careful treatment of the monotonicity of the eigenvalues of Q_λ in λ, cf. Section 5.1.1 and Remark 5.1.16. As in the context of quantum mechanics, the functional analytic properties of Q_λ are nicer than the ones of the unbounded operator $\mathcal{L}$. By Lemma 5.1.15, $Q_\lambda \colon \mathcal{H} \to \mathcal{H}$ is compact, symmetric, and non-negative for $\lambda \in \mathcal{G}$.

It is evident from (1.2.24) and (1.2.25) that any function in the range of Q_λ is of the separated form $|\varphi'(E,L)|\, w\, F(r)$ with some suitably integrable F, cf. Lemma 5.2.2. Hence, any eigenfunction of Q_λ to a non-zero eigenvalue is of this form, which allows us to restrict Q_λ to such functions. This leads to the operator

$$\mathcal{M}_\lambda \colon L^2([R_{\min}, R_{\max}]) \to L^2([R_{\min}, R_{\max}]), \tag{1.2.26}$$

which essentially describes how Q_λ acts on the radial part $F = F(r)$ of a function of the form $|\varphi'(E,L)|\, w\, F(r)$, cf. Definition 5.2.4. This reduction process is due to Mathur [111], which is why we refer to $\mathcal{M}_\lambda$ as the *Mathur operator*. The operator $\mathcal{M}_\lambda$ is reduced in the sense that it acts on functions of only one variable r. Nevertheless, the non-zero eigenvalues of Q_λ and $\mathcal{M}_\lambda$ are identical (cf. Lemma 5.2.5), so that the number of eigenvalues of $\mathcal{L}$ smaller than $\lambda \in \mathcal{G}$ is also given by the number of eigenvalues of $\mathcal{M}_\lambda$ larger than 1, cf. Proposition 5.2.7. We refer to this transformation of the original eigenvalue problem for $\mathcal{L}$ into the one for $\mathcal{M}_\lambda$ as the *Birman-Schwinger-Mathur principle*.

To make use of this principle, we need to compute the Mathur operator $\mathcal{M}_\lambda$ as explicitly as possible. By a Fourier expansion in the angle variable θ, it is possible to explicitly compute the resolvent operator $(-\mathcal{T}^2|_{\mathcal{H}} - \lambda)^{-1}$ in action-angle type variables, cf. Lemma 4.3.18. This leads to the following integral representation of the Mathur operator:

$$\mathcal{M}_\lambda F(r) = \int_{R_{\min}}^{R_{\max}} K_\lambda(r,s)\, F(s)\, \mathrm{d}s, \qquad F \in L^2([R_{\min}, R_{\max}]), \tag{1.2.27}$$

cf. Proposition 5.2.12. The integral kernel $K_\lambda \colon [R_{\min}, R_{\max}]^2 \to \mathbb{R}$ is explicitly known, although it is rather intricate. This is because $\sqrt{\mathcal{R}}$ is not convenient to analyse in action-angle type variables, which corresponds to the antagonism between transport and gravity discussed in [105]. Nonetheless, we can show that K_λ is continuous on $[R_{\min}, R_{\max}]^2$. Thus, $\mathcal{M}_\lambda$ is a Hilbert-Schmidt operator.

In Section 5.3, we collect the main results provided by the Birman-Schwinger-Mathur principle. Theorem 5.3.1 gives a sharp characterisation of the presence of eigenvalues of $\mathcal{L}$ in $\mathcal{G}$ in terms of the Mathur operator $\mathcal{M}_\lambda$. This characterisation is similar to [85, Thm. 4.13]. In Theorem 5.3.3, we derive explicit bounds on the number of eigenvalues of $\mathcal{L}$ in $\mathcal{G}$ inspired by the Birman-Schwinger bound(s) from quantum mechanics [99, Cor. 4.3]. A related bound is also contained in [117, Thm. 1.2], cf. Remark 5.3.4.

In Section 5.4, we then discuss (first) applications of the Birman-Schwinger-Mathur principle. The main finding, Theorem 5.4.1, is due to [62, Thm. 8.15]. It shows that there exits an oscillatory mode for polytropic shells (1.2.5) with $k + \ell \leq 0$ provided that the longest particle period within the steady state is attained by the particles with the largest orbit, i.e., $\sup_{\mathbb{D}_0}(T) = T(E_0, L_0)$. Although we cannot rigorously prove this property of the period function, we will numerically verify that it is indeed satisfied in many cases, cf. Observation 8.2.8. Other applications are that there exists an oscillatory mode if the

period function T attains its maximum on the interior of the steady state support $\mathbb{D}_0$ (cf. Corollary 5.4.3, which is due to [85, Cor. 4.16]) and that the number of eigenvalues of $\mathcal{L}$ in $\mathcal{G}$ is finite for certain isotropic polytropes (1.2.3), cf. Corollary 5.4.4. The latter result is inspired by [117, Cor. 1.3] and also requires some assumptions on the radial particle periods.

Damping (Chapter 6)

In Chapter 6, we study the opposite effect to (undamped) oscillations: Damping. The fact that solutions of the linearised Vlasov-Poisson system can be damped on the macroscopic level – despite the absence of dissipation – is well-explored in the context of plasma physics, where it is known as *Landau damping* [91]. It was shown to hold on the non-linear level in [120] and further developed in many directions; see [17] for a recent review. In the gravitational case, some results towards damping (on the linearised level) were derived in [103, 104, 110, 171]. Here, we study this issue by the spectral approach developed in [61].

The setting we consider here differs slightly from the previous one. We now add a point mass $M > 0$ fixed at the spatial origin $x = 0$ to our model. The Vlasov equation (1.1.2) becomes

$$\partial_t f + v \cdot \partial_x f - \left(\partial_x U + M \frac{x}{|x|^3} \right) \cdot \partial_v f = 0, \tag{1.2.28}$$

the other equations (1.1.3)–(1.1.5) of the system remain unchanged. From a physics point of view, the point mass can be interpreted as a simple model of a black hole, and we describe the evolution of a (spheroidal) galaxy surrounding it; see [44, Ch. IX, Sc. 8] for a motivation of this setting.

In Section 6.2, we extend the steady state existence theory to the system including a point mass. We focus on steady states which are *polytropic shells*, i.e., which are of the form

$$f_0(x,v) = \varepsilon \left(E_0 - E(x,v)\right)_+^k \left(L(x,v) - L_0\right)_+^\ell, \tag{1.2.29}$$

with polytropic exponents k and ℓ as above. The parameter $L_0 > 0$ ensures that the steady state is bounded away from the singular point mass. The cut-off energy $E_0 < 0$ is again implicitly determined by the parameter κ, recall (1.2.6). It is important here that κ is suitably chosen, cf. Remark 6.2.1; in particular, it now has to be negative. The factor ε on the right-hand side of (1.2.29) is a parameter which we use to control the size of the steady state. In Proposition 6.2.6, we study the limiting behaviour in the *perturbative regime* $\varepsilon \to 0$, i.e., we consider steady states which are small compared to the point mass. Unsurprisingly, all steady state quantities converge to the respective quantities in the pure point mass case $\varepsilon = 0$, and the radial supports have a non-trivial limiting configuration.

Linearising the Vlasov-Poisson system including a point mass around a fixed steady state leads to a system of the same form as (1.2.8), and the linearised operator $\mathcal{L}$ has similar properties to the case without a point mass, cf. Section 6.3. Furthermore, a Birman-Schwinger-Mathur principle can be established in the same way as before. In Section 6.4, we apply it to show that there is no eigenvalue of $\mathcal{L}$ in the essential gap $\mathcal{G}$ for a steady state of the form (1.2.29) with polytropic exponent $k > 1$ and $0 < \varepsilon \ll 1$, cf. Theorem 6.4.1.

In Theorem 6.5.5, we show for the same steady states that $\mathcal{L}$ also possesses no eigenvalues embedded into its essential spectrum $\sigma_{\mathrm{ess}}(\mathcal{L})$. This is the crucial part of Chapter 6 and is based on transforming the eigenvalue equation into a Fourier series w.r.t. the angle variable θ. In particular, our arguments require a careful treatment of the period function function $T(E,L)$ and the action-angle type variables (θ, E, L) in the near circular regime $E \approx E_L^{\min}$.

By choosing the parameter κ appropriately, we can ensure that any eigenvalue of $\mathcal{L}$ either lies in $\mathcal{G}$ or $\sigma_{\mathrm{ess}}(\mathcal{L})$, provided that ε is sufficiently small. Hence, the above implies that $\mathcal{L}$ does not possess any eigenvalues. By the RAGE theorem (cf. [135, Thm. XI.115] and Lemma C.0.7), we thus conclude that the linearised dynamics for a steady state of the form (1.2.29) with $k > 1$ and $0 < \varepsilon \ll 1$ are damped in the following (non-quantitative) way, cf. Theorem 6.6.1: For any solution $t \mapsto f(t)$ of (1.2.8) with $(f(0), \partial_t f(0)) \in \mathrm{D}(\mathcal{L}) \times (\mathrm{D}(\mathcal{T}) \cap \mathcal{H})$,

$$\lim_{T\to\infty} \frac{1}{T} \int_0^T \|\partial_x U_{\mathcal{T}f(t)}\|^2_{L^2(\mathbb{R}^3)} \,\mathrm{d}t = 0, \tag{1.2.30}$$

where $U_{\mathcal{T}f(t)}$ denotes the gravitational potential induced by $\mathcal{T}f(t)$, cf. Definition 4.4.5. This damping is similar to the one established in [61, Thm. 1.2 (b)]; here, we extended the results from [61] to the actual spherically symmetric setting. The assumption $k > 1$ ensures that the steady state is sufficiently smooth and leads to the finiteness of various integrals and the vanishing of some boundary terms. The consideration of a steady state in the perturbative regime $0 < \varepsilon \ll 1$ is essential for our arguments in two main aspects: Firstly, it ensures that several quantities, like the period function and its derivatives w.r.t. E, are close to the respective quantities in the explicitly known limiting case $\varepsilon = 0$. Secondly, it allows us to deduce that certain constants are sufficiently small. The latter could also be achieved in a non-perturbative regime if one had quantitative control on the sizes of several constants (cf. Remark 6.5.6) or if one only wants to show the absence of embedded eigenvalues at high frequencies (cf. Remark 6.5.7).

Let us emphasise that the damping result for steady states in the perturbative regime is not just a phase mixing effect. Although the gravitational response operator $\mathcal{R}$ tends to zero as $\varepsilon \to 0$ (and the transport part does not), [61, Thm. 1.2 (a)] shows that the linearised dynamics close to steady states with $0 < \varepsilon \ll 1$ can also be undamped oscillatory, albeit in a setting different from the one considered here. We expect the same behaviour here, cf. Remark 6.4.2, although we cannot quite prove it (yet).

Similar Results in Related Settings (Chapter 7)

In Chapter 7, we demonstrate the versatility of our methods by presenting four further settings in which they can be applied – we expect/hope that further fields of application will arise in the future. The first one, presented in Section 7.1 and based on [62], is the Vlasov-Poisson system in *plane symmetry*. It describes an ensemble of space-homogeneous, gravitating planes passing freely through each other. This setting (or a related/equivalent one) was considered in [43, 62, 84, 100, 108, 111, 179], although it is surely not as natural as the spherically symmetric setting. As derived in [62, Sc. 2.2], there exist compactly supported steady states of this system. The properties of the associated period functions are better understood than in the spherically symmetric setting. This is because in plane symmetry, gravity only acts (effectively) in one space dimension, simplifying certain arguments. In addition, linearising the Vlasov-Poisson system in plane symmetry around a fixed steady state again leads to a system of the form (1.2.8). The linearised operator $\mathcal{L}$ has similar properties to the spherically symmetric setting. In particular, there again exists a gap between 0 and the essential spectrum of $\mathcal{L}$. The existence of eigenvalues of $\mathcal{L}$ inside this gap can be characterised by an analogue of the Birman-Schwinger-Mathur principle. The resulting criterion can be verified (in a fully rigorous way) for certain steady states, cf. Theorem 7.1.3, proving the presence of oscillatory modes in plane symmetry.

In Section 7.2, we consider the radial Vlasov-Poisson system with a point mass fixed at the spatial origin and additionally require that all particles have the same (positive) L-

value, i.e., the same modulus of angular momentum. The latter assumption is not physically motivated and is mainly intended to simplify some aspects of the mathematical analysis. This setting was used in [61] to originally develop the methods from Chapter 6. In analogy to (1.2.29), we consider steady states of the polytropic form

$$f_0(r,w) = \varepsilon \left(E_0 - E(r,w)\right)_+^k \tag{1.2.31}$$

with polytropic exponent $k > \frac{1}{2}$ as well as a suitable choice of the parameter κ. In Theorem 7.2.1, we present the main result of [61] regarding the linearised dynamics around these steady states in the perturbative regime $0 < \varepsilon \ll 1$: If $\frac{1}{2} < k \leq 1$, there exists an oscillatory mode whose presence is shown after deriving an analogue of the Birman-Schwinger-Mathur principle. If $k > 1$, any solution of the linearised system is damped in a similar way to (1.2.30). This damping is verified by similar, but easier arguments than those used to prove Theorem 6.6.1.

So far, all of our models have been purely Newtonian, neglecting the influences of relativistic effects. In the third and fourth sections of Chapter 7, we outline how our methods can be applied in relativistic settings. In Section 7.3, we briefly introduce the *relativistic Vlasov-Poisson system* for which the adaption of our methods is currently in progress [102]. Section 7.4 concerns the *Einstein-Vlasov system*, where adaptations of our methods were used in [49] to characterise/prove linear stability. The techniques from [49] were further extended in [182] to show the existence of oscillatory modes. A recent review discussing these two relativistic settings and their connections to the Vlasov-Poisson system can be found in [144].

Numerical Experiments (Chapter 8)

In Chapter 8 we carry out an extensive numerical analysis of the steady states, their period functions, and the dynamics close to them in the setting of Chapters 2–5, i.e., in spherical symmetry without a point mass. The program used for this analysis is publicly available, cf. Chapter 8. In Section 8.1, we visualise the steady states (1.2.3)–(1.2.5) in different ways and study their dependence on the various parameters.

In Section 8.2, we numerically analyse the period functions associated to these steady states; to our knowledge, this is the first such analysis. The primary aim of this part is to numerically verify the assumptions we have made at some points in this thesis regarding the properties of T. For instance, for the isotropic steady states (1.2.3)–(1.2.4), we see that the maximal period $\sup_{\mathbb{D}_0}(T)$ is always attained at $(E_0, 0)$ and that the period function is increasing w.r.t. the particle energy E on the steady state support, cf. Observations 8.2.4–8.2.6. These observations further reveal a promising approach to verify the E-monotonicity of T rigorously. The same properties of T hold for polytropic shells (1.2.5) with $\ell < 0$, cf. Observation 8.2.8, which justifies the assumption on T in Theorem 5.4.1. For anisotropic polytropes with $k, \ell > 0$ and small values of $L_0 \gtrsim 0$, the period function can behave differently, cf. Observation 8.2.7.

After determining the maximal particle period of a steady state, we can numerically check the validity of Kunze's criterion (cf. Lemma 4.5.19). We find that the criterion is satisfied for isotropic polytropes (1.2.3) with very small polytropic exponents $0 < k \ll 1$, cf. Observation 8.2.11, as well as for polytropic shells (1.2.5) with not too small values of L_0, cf. Observation 8.2.12.

To gain a more detailed understanding of the presence of oscillatory modes, we numerically analyse solutions of the linearised Vlasov-Poisson system for different steady states in

Section 8.3. We do this by simulating the linearised Vlasov-Poisson system via a particle-in-cell method adapted from investigations in non-linear settings, cf. below. Related methods to simulate the linearised Vlasov-Poisson system were used in [93, 112, 173]. Our numerical investigation shows that there exist (partially) undamped oscillatory solutions of the linearised Vlasov-Poisson system for isotropic polytropes (1.2.3) with polytropic exponents $0 < k < 1.2$ (cf. Observation 8.3.3) and that the periods of the oscillations correspond to eigenvalues of $\mathcal{L}$ in the essential gap $\mathcal{G}$ (cf. Observation 8.3.4). For larger polytropic exponents $k > 1.3$, all solutions exhibit a (fully) damped oscillatory behaviour with an oscillation period which is in resonance with the periods of individual stars within the steady state. For the King models (1.2.4), the qualitative behaviour of solutions of the linearised Vlasov-Poisson system depends on the parameter $\kappa > 0$: For small values of κ, there exist undamped oscillatory solutions, whereas all solutions are damped for large values of κ, cf. Observation 8.3.7. In particular, this shows that the presence/absence of oscillatory solutions is not only a matter of steady state regularity, cf. Observation 8.3.6. For anisotropic polytropes (1.2.5) with $L_0 = 0$,[9] the existence of undamped oscillatory solutions of the linearised Vlasov-Poisson system depends linearly on the polytropic exponents k and ℓ, cf. Observation 8.3.8. A similar behaviour holds for polytropic shells (1.2.5) with very small values of $L_0 > 0$. For polytropic shells with larger values of L_0, there always exist undamped oscillatory solutions (as already suggested by Kunze's criterion), cf. Observation 8.3.9.

We also numerically analyse the solutions of the *pure transport equation* $\partial_t^2 f_- - \mathcal{T}^2 f_- = 0$, which arises when neglecting the gravitational response $\mathcal{R}$ in the linearised Vlasov-Poisson system (1.2.8). This equation was often studied as a first step towards damping results, cf. [27, 103, 116, 148]. However, we find that the solutions of the pure transport equation differ qualitatively from those of the linearised Vlasov-Poisson system, cf. Observation 8.3.5.

In Section 8.4, we then numerically analyse solutions of the (non-linearised) Vlasov-Poisson system close to steady states. Previous numerical studies of such solutions – using numerical methods different from the ones we are using here – were conducted in [13, 66, 100, 115, 124, 127, 159, 168, 177, 180]. The most recent numerical study of the Vlasov-Poisson system is [132], which is closely related to the issues considered here. Based on [132] and the numerical investigations [5, 48, 50] of the Einstein-Vlasov system, we employ a particle-in-cell scheme to simulate the system. Our code is based on the ones used in [5, 48, 50, 132], yet we have entirely rewritten it to adjust to the present situation. Our primary aim is to check whether solutions of the Vlasov-Poisson system close to steady states are indeed accurately described by solutions of the respective linearised Vlasov-Poisson system. Most fortunately, we find that they are, cf. Observation 8.4.4. More precisely, for any steady state for which we observed undamped oscillatory solutions of the linearised Vlasov-Poisson system, we see that the solutions of the non-linearised system close to the steady state oscillate undamped with the same period. In contrast, if all solutions of the linearised Vlasov-Poisson system were damped, the damping is also present for solutions of the non-linearised system close to the respective steady state. In particular, the damping rates on the linearised and non-linearised levels seem to be identical. This degree of consistency even exceeds our expectations – for other PDEs, there occur damping effects when transitioning from the linearised to the non-linearised level, cf. [164]. We thus confidently conclude that the observed/proven properties of the linearised Vlasov-Poisson system indeed correspond to the real effects on the non-linearised level.

[9] Above, we required $L_0 > 0$ for polytropes (1.2.5). In fact, polytropes with $L_0 = 0$ are not included in most of the theoretical parts of this thesis, but it is nevertheless enlightening to study them numerically.

Outlook (Chapter 9)

To conclude this thesis, Chapter 9 addresses several open questions that have remained unanswered by our theoretical analysis, but which the numerical observations suggest to be solvable in future work.

1.3 A Reader's Guide

Before starting, we would like to add some comments on how to read this, admittedly rather lengthy, thesis.

We will mostly refrain from giving references when using results from real analysis, ODE theory, Lebesgue integration theory, or Sobolev space theory. In contrast, we will usually provide references, mostly to [69] or [133, 134, 135, 136], when using results from functional analysis or spectral analysis. This is because the author is less experienced in the latter fields and thus more careful when dealing with them.

Some parts of our notation were already introduced above. In general, we will introduce new symbols when they first appear and will often recall definitions/notations to ensure clarity of the notation. Also, we try to choose the notation as intuitive as possible and in accordance with common conventions from the literature.

The (numerous) footnotes in this thesis contain additional comments by the author. These may be generalisations of proven statements, further explanations of arguments, clarifications of non-rigorous statements, further links to other works, or minor additional observations. The contents of the footnotes are, however, not essential.[10]

This thesis has three appendices which provide self-contained discussions, the inclusion of which in the main chapters would have disrupted the flow of argumentation. It should be emphasised that the appendices are not less important than the other chapters; in fact, they are necessary for some key arguments. If the reader is particularly faithful and aims to read this thesis in its entirety, we recommend the following order to ensure that the results are presented in a cohesive manner. Read the main chapters sequentially. After Section 4.1, read Appendix A, and then Appendices B and C after Chapter 5.

The presentation style of different parts of this thesis intentionally varies. Section 2.2 is a review of known results, Chapter 3 contains formal calculations only, Chapter 8 is a pure numerical analysis, and the other parts are mathematical analyses with different levels of elaborateness. In general, the style here differs from the one of research papers, which often resemble a sprint aiming to reach the destination as quickly as possible. This thesis instead resembles a leisurely walk, deliberately embracing detours to fully savour the beauty of the surrounding landscape. We will revisit this metaphor in Chapter 9, but for now, let us embark on our joint journey.

[10] In short: If this is the only footnote you read in this thesis, you will be fine.

Chapter 2

The Vlasov-Poisson System and its Steady States

As motivated in the introduction, throughout this thesis we consider the Vlasov-Poisson system under the assumption of spherical symmetry. The first part of this chapter, Section 2.1, is devoted to carefully introducing the relevant concepts of spherical symmetry in general and analysing the Vlasov-Poisson system within this setting.

Following this, Section 2.2 reviews the existence of time-independent solutions of the radial Vlasov-Poisson system. In addition, we introduce and analyse several quantities used in the succeeding stability analysis of these steady states.

2.1 The Radial Vlasov-Poisson System

Let us begin by introducing the concept(s) of spherical symmetry used here.

Definition 2.1.1 (Spherical Symmetry)**.** *Let $n \in \mathbb{N}$.*

(a) A function $f\colon \mathbb{R}^n \to \mathbb{R}$ is spherically symmetric (on $\mathbb{R}^n$) *if $f(x) = f(Ax)$ for $x \in \mathbb{R}^n$ and any rotation matrix $A \in \mathrm{SO}(n)$.*

(b) A function $f\colon \mathbb{R}^n \times \mathbb{R}^n \to \mathbb{R}$ is spherically symmetric (on $\mathbb{R}^n \times \mathbb{R}^n$) *if $f(x,v) = f(Ax,Av)$ for $x, v \in \mathbb{R}^n$ and any rotation matrix $A \in \mathrm{SO}(n)$.*

(c) A function $f\colon \Omega \to \mathbb{R}$ with $\Omega \subset \mathbb{R}^n$ or $\Omega \subset \mathbb{R}^n \times \mathbb{R}^n$ is spherically symmetric (on Ω) *if its extension by 0 is spherically symmetric in the sense of part (a) or part (b), respectively.*

Similar definitions are used for complex-valued functions. Later on, in Definition 4.2.1, we generalise the concept of spherical symmetry to functions which are only defined almost everywhere.

Note that spherical symmetry on $\mathbb{R}^n \times \mathbb{R}^n$ differs from spherical symmetry on $\mathbb{R}^{2n}$.[11,12] From a mathematical point of view, the main simplification in the spherically symmetric case results from the fact that any spherically symmetric function can be expressed in lower-dimensional variables. We discuss this feature as well as further properties of spherically symmetric functions in the relevant case $n = 3$ in the following remark.

[11] Spherical symmetry on $\mathbb{R}^n \times \mathbb{R}^n$ is strictly weaker than spherical symmetry on $\mathbb{R}^{2n}$.

[12] In order to be constantly reminded of this difference, we always denote the phase space of the Vlasov-Poisson system by $\mathbb{R}^3 \times \mathbb{R}^3$ instead of $\mathbb{R}^6$.

Remark 2.1.2. *(a) Let $f\colon \mathbb{R}^3 \to \mathbb{R},\ x \mapsto f(x)$ be spherically symmetric on $\mathbb{R}^3$. Writing*

$$r := |x|, \tag{2.1.1}$$

there exists a function $\tilde{f} = \tilde{f}(r)$ s.t.

$$f(x) = \tilde{f}(r). \tag{2.1.2}$$

Explicitly,[13] $\tilde{f}(r) := f(r\,\mathrm{e}_1)$ defines a function as required.

(b) Let $f\colon \mathbb{R}^3 \times \mathbb{R}^3 \to \mathbb{R},\ (x,v) \mapsto f(x,v)$ be spherically symmetric on $\mathbb{R}^3 \times \mathbb{R}^3$ and write[14]

$$r := |x|, \quad w := \frac{x \cdot v}{r}, \quad L := |x \times v|^2 \tag{2.1.3}$$

for $x, v \in \mathbb{R}^3$ where these expressions are well-defined. Then there exists a function $\tilde{f} = \tilde{f}(r, w, L)$ s.t.

$$f(x,v) = \tilde{f}(r, w, L). \tag{2.1.4}$$

Explicitly, $\tilde{f}(r, w, L) = f(r\,\mathrm{e}_1, w\,\mathrm{e}_1 + \frac{\sqrt{L}}{r}\,\mathrm{e}_2)$ yields a function as required; note that changing from (x,v) to (Ax, Av) for $A \in \mathrm{SO}(3)$ leaves the variables (r,w,L) defined in (2.1.3) *unchanged.*

(c) In parts (a) and (b) we deliberately state no domains of definition for the functions $\tilde{f}$. The reason for this is that in radial variables, one must handle the spatial origin $x = 0$ with caution due to the presence of an (artificial) singularity there. Concretely, it is unclear how/if $\tilde{f}$ must be defined at $r = 0$, in particular in part (b). Later, this discrepancy will not be significant as the values of all relevant functions will only be needed almost everywhere. Besides, it is usually more convenient to use the original Cartesian coordinates when dealing with the spatial origin anyway.

(d) In the situations of part (a) and part (b), $\tilde{f}$ is uniquely determined by f on suitable[15] domains of definition. In order to keep the notation concise, we identify $\tilde{f}$ with f and write

$$\tilde{f} = f \tag{2.1.5}$$

by slight abuse of notation.

(e) The variable r as defined in (2.1.1) *or* (2.1.3) *can be interpreted as the* spatial radius*, while w takes on the role of the* radial velocity *(or radial momentum) and L is the* squared modulus of the angular momentum*.*

(f) In the situation of part (b), it is possible – and sometimes more convenient – to choose different variables than (r,w,L). For example, the discrete approximation of the radial Vlasov-Poisson system in [153] is performed in the variables

$$r := |x|, \quad u := |v|, \quad \alpha := \sphericalangle(x,v) = \arccos\left(\frac{x \cdot v}{|x|\,|v|}\right), \tag{2.1.6}$$

[13] $\mathrm{e}_j \in \mathbb{R}^3$ denotes the j-th canonical unit vector for $j = 1,2,3$, e.g., $\mathrm{e}_1 := (1,0,0)^T$.

[14] In the physics literature, the symbol L typically denotes the angular momentum, i.e., the vector $x \times v \in \mathbb{R}^3$, instead of its squared modulus. Although the actual angular momentum vector will not appear in this work, we apologise to the reader for any confusion which might be caused by this deviation from the usual notational convention.

[15] For part (a) consider $\tilde{f}\colon [0,\infty[\to \mathbb{R}$, while a possible domain of definition for $\tilde{f}$ in the situation of part (b) is $]0,\infty[\times \mathbb{R} \times [0,\infty[$.

which we also use in our numerical analysis in Chapter 8. Similar as above, any spherically symmetric function $f\colon \mathbb{R}^3 \times \mathbb{R}^3 \to \mathbb{R}$ only depends on these variables, i.e., by slight abuse of notation,

$$f(x,v) = f(r,u,\alpha). \tag{2.1.7}$$

We now consider the Vlasov-Poisson system in spherical symmetry, i.e., a solution launched by spherically symmetric initial data. If this symmetry class is to be well suited for the analysis of the system, it must be preserved during the evolution. Indeed, it is:

Lemma 2.1.3. *Let $\mathring{f}\colon \mathbb{R}^3 \times \mathbb{R}^3 \to [0,\infty[$ be some initial phase space distribution which is continuously differentiable, compactly supported, and spherically symmetric on $\mathbb{R}^3 \times \mathbb{R}^3$. In addition, let $f\colon [0,\infty[\times \mathbb{R}^3 \times \mathbb{R}^3 \to [0,\infty[$ be the classical solution of the Vlasov-Poisson system satisfying $f(0) = \mathring{f}$, which exists by [143, Thm. 1.11]. Then $f(t)$ is spherically symmetric on $\mathbb{R}^3 \times \mathbb{R}^3$ at any time $t \geq 0$. Furthermore, the associated potential $U(t)$ and mass density $\rho(t)$ are both spherically symmetric on $\mathbb{R}^3$ for $t \geq 0$.*

Proof. The spherical symmetry of $f(t)$ follows by the uniqueness of classical solutions [143, Thm. 1.11] because $\mathbb{R}^3 \times \mathbb{R}^3 \ni (x,v) \mapsto \mathring{f}(Ax,Av)$ launches the classical solution $[0,\infty[\times \mathbb{R}^3 \times \mathbb{R}^3 \ni (t,x,v) \mapsto f(t,Ax,Av)$, but $\mathring{f}(A\cdot,A\cdot) = \mathring{f}$ for $A \in \mathrm{SO}(3)$ by spherical symmetry and the resulting solutions have to be identical. The spherical symmetries of $\rho(t)$ and $U(t)$ then follow immediately by (1.1.3)–(1.1.5). □

For more details on all parts of the above proof we refer to [143].

By a slight abuse of notation similar to Remark 2.1.2 (d), we hence write

$$f(t,x,v) = f(t,r,w,L), \quad U(t,x) = U(t,r), \quad \rho(t,x) = \rho(t,r), \tag{2.1.8}$$

for every such spherically symmetric solution. Expressing the derivatives w.r.t. the Cartesian coordinates (x,v) in terms of derivatives w.r.t. (r,w,L) and writing the Poisson equation in its radial form leads to the following system of equations:

$$\partial_t f + w\,\partial_r f - \left(U' - \frac{L}{r^3}\right)\partial_w f = 0, \tag{2.1.9}$$

$$U'(t,r) = \frac{4\pi}{r^2}\int_0^r s^2 \rho(t,s)\,\mathrm{d}s, \qquad \lim_{r\to\infty} U(t,r) = 0, \tag{2.1.10}$$

$$\rho(t,r) = \frac{\pi}{r^2}\int_0^\infty \int_{\mathbb{R}} f(t,r,w,L)\,\mathrm{d}w\,\mathrm{d}L. \tag{2.1.11}$$

Here, we use the shorthand

$$U' \coloneqq \partial_r U. \tag{2.1.12}$$

We refer to (2.1.9)–(2.1.11) as the *radial Vlasov-Poisson system* or *spherically symmetric Vlasov-Poisson system.*

2.2 Steady States

We now discuss the existence of stationary, i.e., time-independent, solutions of the radial Vlasov-Poisson system. Although most of the results presented in this section are well-known in the literature, we recall them here because a thorough understanding of the equilibrium states is essential for the upcoming analysis. We mainly follow the approach from [130].

To construct stationary solutions of the Vlasov-Poisson system, we first consider the characteristic system associated to the time-independent Vlasov equation.

Lemma 2.2.1. *For some prescribed potential $U \in C^1(\mathbb{R}^3)$ we consider the ODE*[16]

$$\ddot{x} = -\partial_x U(x), \tag{2.2.1}$$

or, equivalently,

$$\dot{x} = v, \tag{2.2.2a}$$
$$\dot{v} = -\partial_x U(x). \tag{2.2.2b}$$

The following assertions hold:

(a) The function

$$E\colon \mathbb{R}^3 \times \mathbb{R}^3 \to \mathbb{R},\ E(x,v) \coloneqq \frac{1}{2}|v|^2 + U(x) \tag{2.2.3}$$

is conserved along solutions of (2.2.2).[17] *We call E the* particle energy *or* local energy *because $E(x,v)$ can be interpreted as the energy of a particle with position $(x,v) \in \mathbb{R}^3 \times \mathbb{R}^3$ in phase space inside the potential U.*

(b) Let U be spherically symmetric. Then the squared modulus of the angular momentum given by

$$L(x,v) = |x \times v|^2, \qquad x, v \in \mathbb{R}^3, \tag{2.2.4}$$

is conserved along solutions of (2.2.2).[18]

Proof. Both statements are straight-forward to verify. For part (b) note that $\partial_x U(x) = \partial_r U(|x|)\,\frac{x}{|x|}$ for $x \in \mathbb{R}^3 \setminus \{0\}$ due to the spherical symmetry of U. □

The solutions $f = f(x,v)$ of the time-independent Vlasov equation

$$v \cdot \partial_x f - \partial_x U(x) \cdot \partial_v f = 0 \tag{2.2.5}$$

for a (suitably smooth[19]) prescribed potential $U = U(x)$ are given by functions f which are constant along solutions of the associated characteristic system (2.2.2), see, e.g., [143, Lemma 1.3]. Hence, if the potential is additionally spherically symmetric, any function which only depends on E and L is a solution of the time-independent Vlasov equation. This observation leads to the following ansatz for stationary solutions of the (radial) Vlasov-Poisson system.

Definition 2.2.2 (Steady State)**.** *Let $U_0 \in C^2(\mathbb{R}^3)$ be spherically symmetric in the sense of Definition 2.1.1 (a). For $\varphi\colon \mathbb{R} \times \mathbb{R} \to [0,\infty[$ consider the ansatz*

$$f_0\colon \mathbb{R}^3 \times \mathbb{R}^3 \to [0,\infty[,\ f_0(x,v) \coloneqq \varphi(E(x,v), L(x,v)) = \varphi\left(\frac{1}{2}|v|^2 + U_0(x), |x \times v|^2\right), \tag{2.2.6}$$

where E is the particle energy induced by the potential U_0 similar to (2.2.3)*, i.e.,*

$$E(x,v) \coloneqq \frac{1}{2}|v|^2 + U_0(x), \qquad (x,v) \in \mathbb{R}^3 \times \mathbb{R}^3. \tag{2.2.7}$$

[16] Later on, all relevant potentials U are twice continuously differentiable so that the standard existence and uniqueness results apply to the ODE (2.2.1).

[17] Indeed, E is the Hamiltonian function of the Hamiltonian system (2.2.2).

[18] Not only the squared modulus of the angular momentum is an integral of (2.2.2) in spherical symmetry, but also the angular momentum vector $x \times v$ itself.

[19] For this statement it suffices if U is twice continuously differentiable.

Then f_0 is called a steady state *or* equilibrium *or* stationary solution *of the Vlasov-Poisson system if U_0 is the gravitational potential induced by f_0 via the Poisson equation, i.e.,*

$$\Delta U_0 = 4\pi\rho_0, \qquad \lim_{|x|\to\infty} U_0(x) = 0, \tag{2.2.8}$$

where

$$\rho_0(x) \coloneqq \int_{\mathbb{R}^3} f_0(x,v)\,\mathrm{d}v = \int_{\mathbb{R}^3} \varphi(E(x,v), L(x,v))\,\mathrm{d}v, \qquad x \in \mathbb{R}^3. \tag{2.2.9}$$

In this case, φ is called the associated ansatz function *or* microscopic equation of state.

If φ does not depend on L, i.e., under slight abuse of notation,

$$f_0(x,v) = \varphi(E(x,v)), \qquad (x,v) \in \mathbb{R}^3 \times \mathbb{R}^3, \tag{2.2.10}$$

the steady state is called isotropic[20]*. Steady states which are not isotropic are called* anisotropic.

As mentioned before, a steady state is indeed a solution of the Vlasov-Poisson system (1.1.2)–(1.1.5) provided that it is sufficiently regular.

Lemma 2.2.3. *Let f_0 be a steady state of the Vlasov-Poisson system with differentiable ansatz function φ. Then f_0 is a solution of the Vlasov-Poisson system* (1.1.2)–(1.1.5) *with potential U_0 and mass density ρ_0 as specified in Definition 2.2.2.*

Proof. The fact that f_0 solves the Vlasov equation (1.1.2) follows by Lemma 2.2.1 and the chain rule. The validity of the remaining equations (1.1.3)–(1.1.5) is explicitly included into Definition 2.2.2. □

Before investigating the existence of steady states which are physically reasonable, we wish to add some more comments on the important Definition 2.2.2.

Remark 2.2.4. *(a) Although the Vlasov equation may not be solved in the classical way, we include non-smooth steady states in our analysis. Such equilibria still have the property that the phase space distribution function is constant along characteristics of the Vlasov equation. This is usually referred to as a* Lagrangian solution*; for recent discussions of this concept of solutions of the (time-dependent) Vlasov-Poisson system we refer to [1, 83].*

(b) In Definition 2.2.2 we explicitly require the potential to be spherically symmetric. This is mandatory in order for L to be conserved along the characteristic flow of the Vlasov equation. In particular, any steady state f_0 as defined above is obviously spherically symmetric in the sense of Definition 2.1.1 (b) and the associated stationary mass density ρ_0 is spherically symmetric in the sense of Definition 2.1.1 (a). Thus, the statement from Lemma 2.2.3 similarly applies to the radial Vlasov-Poisson system.

However, as previously noted in [142, Thm. 3], [130], and [19, Box 4.1], it is not necessary to explicitly require the spherical symmetry of U_0 in the case of an isotropic ansatz leading to a physically reasonable steady state. More precisely, [46, Thm. 4] implies that any solution $U_0 \in C^2(\mathbb{R}^3)$ of (2.2.8)–(2.2.10) *with f_0 having compact support and finite mass has to be spherically symmetric w.r.t. some point in $\mathbb{R}^3$. In other words, no such isotropic equilibria are lost by imposing the spherical symmetry of U_0 in Definition 2.2.2.*

[20] For a discussion of the term *isotropic* from a physics point of view we refer to [19, Sc. 4.2.1(a)].

(c) The majority of the mathematical literature regarding stationary solution of the Vlasov-Poisson system focuses on spherically symmetric equilibria. Less is known about the existence and further properties of non-radial steady states. We refer the interested reader to [19, Chapter 4] for an overview over general physical relevant equilibria and point out the mathematical investigations [139, 141, 145, 156, 167] of non-radial steady states. Furthermore, we briefly discuss the Vlasov-Poisson system and properties of its equilibria in a different symmetry class – plane symmetry – in Section 7.1 of this thesis.

(d) It was first stated by J. H. Jeans in [76] that the phase space distribution function of any stationary solution of the Vlasov-Poisson system can only depend on the phase space variables through the integrals of motion. This statement is usually referred to as Jeans' theorem. *In the radial setting, this means that every spherically symmetric, stationary solution can be obtained via the ansatz* (2.2.6). *A rigorous proof of the latter statement is given in [14].*

We emphasize that this is a particular feature of the Vlasov-Poisson system. In the case of the (somewhat related) Einstein-Vlasov system there are counterexamples to Jeans' theorem [154].

For some fixed microscopic equation of state φ, the construction of steady states of the Vlasov-Poisson system is reduced to solving the semi-linear Poisson equation (2.2.8) for U_0; note that ρ_0 depends on U_0 by inserting the ansatz (2.2.6) into (2.2.9). Hence, it remains to analyse which choices of φ lead to equilibria which are physically reasonable. This means that each steady state f_0 should have finite mass and compact support, i.e., the *total mass*

$$M_0 \coloneqq \int_{\mathbb{R}^3\times\mathbb{R}^3} f_0(x,v)\,\mathrm{d}(x,v) \tag{2.2.11}$$

has to be finite and $\operatorname{supp}(f_0)$ has to be bounded.

Both of these properties will be ensured by a microscopic equation of state φ of the form

$$\varphi(E,L) = \Phi(E_0 - E)\,(L - L_0)_+^{\ell} \tag{2.2.12}$$

for $E, L \in \mathbb{R}$, provided Φ, E_0, L_0, and ℓ are chosen suitably. Here, an index "+" denotes the positive part of a function. More precisely, for $b, \alpha \in \mathbb{R}$ we set[21]

$$b_+^{\alpha} \coloneqq \begin{cases} b^{\alpha}, & \text{if } b > 0, \\ 0, & \text{if } b \leq 0. \end{cases} \tag{2.2.13}$$

The parameter $L_0 \geq 0$ gives a lower bound on the L-values within the steady state support and ℓ is some prescribed exponent. We require that these parameters and the *energy dependency function* Φ satisfy the following properties:

(φ1) One of the following conditions is satisfied:

(i) $L_0 > 0$ and $\ell > -\frac{1}{2}$. In this case the resulting steady state is called a *shell*; the reason for this name will become apparent in Proposition 2.2.9 (c).

[21] The convention chosen in (2.2.13) for expressions of the form 0_+^{α} with $\alpha \leq 0$ has no significant influence on the properties of the resulting equilibria.

(ii) $L_0 = 0$ and $\ell \geq 0$.[22] In particular, in the case $L_0 = 0 = \ell$ we use the convention $0_+^0 = 1$ in (2.2.12) and arrive at an L-independent[23] ansatz function leading to an isotropic steady state.

(φ2) $\Phi\colon \mathbb{R} \to [0, \infty[$, $\Phi \in L^\infty_{\mathrm{loc}}(\mathbb{R})$, and

$$\Phi(\eta) = 0, \qquad \eta \leq 0. \tag{2.2.14}$$

(φ3) There exists $k \geq 0$ s.t. one of the following conditions is satisfied:

(i) There exist $c, \eta_0 > 0$ s.t.

$$\Phi(\eta) \geq c\,\eta^k, \qquad 0 < \eta < \eta_0. \tag{2.2.15}$$

In this case we require $0 \leq k < \ell + \frac{3}{2}$.

(ii) The function Φ is of the explicit form[24]

$$\Phi(\eta) = \eta_+^k, \qquad \eta \in \mathbb{R}, \tag{2.2.16}$$

with $0 \leq k < 3\ell + \frac{7}{2}$, where we again employ (2.2.13). In this case the ansatz function as well as the resulting steady state are called *polytropic*, k and ℓ are referred to as the *polytropic exponents*.[25]

The remaining parameter $E_0 < 0$ in (2.2.12) is referred to as the *cut-off energy* because $\varphi(E, L) = 0$ for $E \geq E_0$ by (2.2.14). We do not (directly) prescribe this parameter, but it is implicitly determined by the equations satisfied by the steady state; this will become more apparent later.

Let us now review some classes of ansatz functions of the form (2.2.12) which are commonly used in the literature. Polytropic equations of state

$$\varphi(E, L) = (E_0 - E)_+^k\,(L - L_0)_+^\ell \tag{2.2.17}$$

and the associated steady states are widely studied, see, e.g., [14, 52, 140, 155, 181]. Such polytropes with $L_0 = 0$ also enjoy a distinct scaling property which we discuss in Appendix B.

Choosing $L_0 = 0 = \ell$ in (2.2.17) yields the commonly studied *isotropic polytropes* with equations of state of the form

$$\varphi(E, L) = \varphi(E) = (E_0 - E)_+^k. \tag{2.2.18}$$

Another class of steady states which plays a prominent role in the literature are the *King models*[26] induced by an ansatz function of the form

$$\varphi(E, L) = \varphi(E) = \left(e^{E_0 - E} - 1\right)_+. \tag{2.2.19}$$

[22] The assumption $\ell \geq 0$ in the case $L_0 = 0$ is imposed for regularity reasons. More precisely, the computations below show that the mass density ρ_0 of an equilibrium with $L_0 = 0 > \ell$ necessarily has a singularity at the spatial origin, which is not desired.

[23] Obviously, only non-negative L-values are relevant in Definition 2.2.2.

[24] It is straight-forward to carry out the following analysis with (2.2.16) replaced by the more general condition $\Phi(\eta) = c\,\eta_+^k$ for $\eta \in \mathbb{R}$ and some $c > 0$. In general, multiplying the ansatz function φ by some factor merely results in a rescaling of the resulting steady state, cf., e.g., [35].

[25] For a discussion of the term *polytropic* from a physics point of view (in the isotropic case) we refer to [19, Sc. 4.3.3(a)]. It should be noted that, physically, the term "polytropic" is only meaningful in the case $L_0 = 0$. For the sake of convenience, we use it here for general $L_0 \geq 0$.

[26] At this point it is worth referring to the brief historical discussion of the origins of these models in [79, p. 232], which concludes that the name *King model* might be historically inadequate. To be consistent with the literature, we nevertheless use this name here.

Accordingly, this function is called the *King ansatz function*. Such equations of state were first proposed in [78, 113, 114] as adequate models for stationary star clusters, see [79] or [19, Sc. 4.3.3(c)] for physical derivations of this ansatz. In the mathematics literature, the associated steady states and their properties are explicitly studied in [53, 57, 131] among others. An ansatz function of the form (2.2.19) is obtained by setting $\Phi(\eta) = (e^\eta - 1)_+$ for $\eta \in \mathbb{R}$ in (2.2.12); obviously, this choice of Φ satisfies the above conditions by choosing $k = 1$ in (φ3) (i).

Before showing that ansatz functions of the form (2.2.12) indeed lead to physically reasonable steady states, we add some comments on the choice of φ.

Remark 2.2.5. *(a) In order to obtain physically reasonable steady states of the Vlasov-Poisson system, the conditions imposed above can be relaxed in various aspects. For example, energy dependencies Φ which are not locally bounded are also covered in [130]. However, the conditions imposed above – together with further assumptions stated in Section 4.1 – will become useful when analysing the dynamics close to steady states in the succeeding chapters of this thesis. Thus, we decided to refrain from reviewing the construction of steady states under weaker conditions here in order to keep the arguments in the present section more clear.*

(b) It is straight-forward to extend the following investigation to ansatz functions φ which are not separated in their variables (E, L) and with more general L-dependencies than the power law incorporated in (2.2.12).[27] *Both of these features are merely chosen for the sake of simplicity*[28] *and because equations of state of the form* (2.2.12) *are commonly used in the literature as reviewed above.*

(c) In [146, Thm. 2.1] it is shown that the existence of a cut-off energy, i.e., some suitable E_0 s.t. $\varphi(E, L) = 0$ for $E \geq E_0$, is mandatory for the resulting steady state to have finite mass and compact support.

(d) In this thesis the whole analysis is limited to steady states with finite mass and compact support, as those are the most physically relevant when modelling stationary galaxies. Nonetheless, other equilibria are also analysed in the physics literature, see [19, Sc. 4.3] for an overview. Prominent examples of steady states with unbounded support are the isochrone models *[18, 64, 65] or the* Plummer sphere *[19, Sc. 4.3.3(a)]; the latter corresponds to an isotropic polytropic ansatz* (2.2.18) *with exponent $k = \frac{7}{2}$. In particular, this shows that the upper bound on k in (φ3) (ii) is necessary in order to arrive at a compactly supported steady state.*

In order to construct steady states of the Vlasov-Poisson system as defined in Definition 2.2.2, we first compute how ρ_0 given by (2.2.9) depends on some spherically symmetric $U_0 \in C^2(\mathbb{R}^3)$ for φ as chosen above; the following calculation is similar to [130, p. 905]. Inserting (2.2.12) into (2.2.9) yields

$$\begin{aligned}\rho_0(x) &= \int_{\mathbb{R}^3} \Phi\left(E_0 - \frac{1}{2}|v|^2 - U_0(x)\right) \left(|x \times v|^2 - L_0\right)_+^\ell \,\mathrm{d}v = \\ &= \frac{\pi}{r^2} \int_0^\infty \int_{\mathbb{R}} \Phi\left(E_0 - \frac{1}{2}w^2 - U_0(r) - \frac{L}{2r^2}\right) (L - L_0)_+^\ell \,\mathrm{d}w \,\mathrm{d}L \end{aligned} \tag{2.2.20}$$

[27] Some examples of steady states corresponding to ansatz functions that are different from (2.2.12) are reviewed in [19, Section 4.3]. Let us only explicitly mention the *Camm type steady states* [25, 55] here, whose associated microscopic equations of state are canonical extensions of the polytropes (2.2.17).

[28] For example, the explicit structure of the L-dependency in (2.2.12) simplifies the relation between ρ_0 and U_0 encoded into the function g defined in (2.2.25).

for $x \in \mathbb{R}^3 \setminus \{0\}$ and $r = |x|$. Here, we changed variables $v \mapsto (w, L)$ (recall (2.1.3) for the definition of the new variables), used the relation

$$|v|^2 = w^2 + \frac{L}{r^2}, \tag{2.2.21}$$

and identified $U_0(x) = U_0(r)$ as in Remark 2.1.2 (d). Next, we apply the change of variables induced by $E = \frac{1}{2}w^2 + U_0(r) + \frac{L}{2r^2}$ in the inner integral; observe that the integrand in (2.2.20) is even in w. This leads to

$$\begin{aligned}\rho_0(x) &= \frac{2\pi}{r^2} \int_0^\infty \int_{U_0(r)+\frac{L}{2r^2}}^\infty \Phi(E_0 - E) \, \frac{(L - L_0)_+^\ell}{\sqrt{2E - 2U_0(r) - \frac{L}{r^2}}} \, \mathrm{d}E \, \mathrm{d}L = \\ &= \frac{2\pi}{r^2} \int_{U_0(r)+\frac{L_0}{2r^2}}^{E_0} \Phi(E_0 - E) \int_{L_0}^{2r^2E - 2r^2U_0(r)} \frac{(L - L_0)^\ell}{\sqrt{2E - 2U_0(r) - \frac{L}{r^2}}} \, \mathrm{d}L \, \mathrm{d}E; \end{aligned} \tag{2.2.22}$$

the whole integral is meant to vanish if $U_0(r) + \frac{L_0}{2r^2} \geq E_0$. For the second equality, we changed the order of integration and restricted the domain of integration to the set where the integrand does not vanish; recall (2.2.14). Inserting the standard integral identity

$$\int_a^b (s-a)^\alpha \, (b-s)^\beta \, \mathrm{d}s = \frac{\Gamma(\alpha+1)\,\Gamma(\beta+1)}{\Gamma(\alpha+\beta+2)} \, (b-a)^{\alpha+\beta+1}, \qquad \alpha, \beta > -1, \ a < b, \tag{2.2.23}$$

into the inner integral, recalling $\ell > -\frac{1}{2}$, and using the final change of variables $\eta = E_0 - E$ then yields

$$\begin{aligned}\rho_0(x) &= 2^{\ell+\frac{3}{2}} \pi^{\frac{3}{2}} \frac{\Gamma(\ell+1)}{\Gamma(\ell+\frac{3}{2})} \, r^{2\ell} \int_{U_0(r)+\frac{L_0}{2r^2}}^{E_0} \Phi(E_0 - E) \left(E - U_0(r) - \frac{L_0}{2r^2} \right)^{\ell+\frac{1}{2}} \mathrm{d}E = \\ &= 2^{\ell+\frac{3}{2}} \pi^{\frac{3}{2}} \frac{\Gamma(\ell+1)}{\Gamma(\ell+\frac{3}{2})} \, r^{2\ell} \int_0^{E_0 - U_0(r) - \frac{L_0}{2r^2}} \Phi(\eta) \left(E_0 - U_0(r) - \frac{L_0}{2r^2} - \eta \right)^{\ell+\frac{1}{2}} \mathrm{d}\eta \end{aligned} \tag{2.2.24}$$

for $x \in \mathbb{R}^3 \setminus \{0\}$. Hence, by introducing the function

$$g \colon \mathbb{R} \to \mathbb{R}, \ g(z) \coloneqq \begin{cases} c_\ell \int_0^z \Phi(\eta) \, (z - \eta)^{\ell+\frac{1}{2}} \, \mathrm{d}\eta, & \text{if } z > 0, \\ 0, & \text{if } z \leq 0, \end{cases} \tag{2.2.25}$$

with

$$c_\ell \coloneqq 2^{\ell+\frac{3}{2}} \, \pi^{\frac{3}{2}} \, \frac{\Gamma(\ell+1)}{\Gamma(\ell+\frac{3}{2})}, \tag{2.2.26}$$

the dependency of ρ_0 on U_0 can be written as

$$\rho_0(x) = r^{2\ell} \, g\left(E_0 - U_0(r) - \frac{L_0}{2r^2} \right), \qquad x \in \mathbb{R}^3 \setminus \{0\}, \ r = |x|. \tag{2.2.27}$$

We note that the above formula can also be suitably extended to $x = 0$. Concretely, in the case $L_0 = 0$ there holds $\rho_0(0) = 0$ if $\ell > 0$ and $\rho_0(0) = g(E_0 - U_0(0))$ if $\ell = 0$.

We thus analyse the function g, in particular, its regularity properties. The following result is also contained in [130, p. 905].

Lemma 2.2.6. *The function $g\colon \mathbb{R} \to \mathbb{R}$ is continuously differentiable with*

$$g'(z) = \begin{cases} c_\ell \left(\ell + \frac{1}{2}\right) \int_0^z \Phi(\eta)\,(z-\eta)^{\ell-\frac{1}{2}}\,\mathrm{d}\eta, & \text{if } z > 0, \\ 0, & \text{if } z \leq 0, \end{cases} \tag{2.2.28}$$

for $z \in \mathbb{R}$. Furthermore, g is strictly increasing on $[0, \infty[$.

Proof. The continuous differentiability of g with derivative given by (2.2.28) is straightforward to verify using Lebesgue's dominated convergence theorem; recall that we have chosen $\ell > -\frac{1}{2}$ and $\Phi \in L^\infty_{\mathrm{loc}}(\mathbb{R})$. The monotonicity of g on $[0, \infty[$ then follows by (2.2.28) since the condition (φ3) ensures that Φ is positive on $]0, \eta_0[$ for some $\eta_0 > 0$. □

In general, we cannot derive a more explicit form for g than (2.2.25). However, as, e.g., earlier noted in [14, Ex. 4.1], this is possible in the case of a polytropic ansatz.

Remark 2.2.7. *Let Φ be as specified in (φ3) (ii), i.e., the ansatz is polytropic. Then, using the integral identity* (2.2.23) *once again yields*

$$g(z) = c_{k,\ell}\, z_+^{k+\ell+\frac{3}{2}}, \qquad z \in \mathbb{R}, \tag{2.2.29}$$

with

$$c_{k,\ell} \coloneqq 2^{\ell+\frac{3}{2}}\, \pi^{\frac{3}{2}}\, \frac{\Gamma(k+1)\,\Gamma(\ell+1)}{\Gamma(k+\ell+\frac{5}{2})}. \tag{2.2.30}$$

After inserting (2.2.27) into the semi-linear Poisson equation (2.2.8) for U_0 and expressing the Laplacian in its radial form, we arrive at the integro-differential equation

$$U_0'(r) = \frac{4\pi}{r^2} \int_0^r s^{2\ell+2}\, g\left(E_0 - U_0(s) - \frac{L_0}{2s^2}\right) \mathrm{d}s, \qquad r > 0. \tag{2.2.31}$$

In a more concise way, the latter equation can be written as

$$U_0'(r) = \frac{m_0(r)}{r^2}, \qquad r > 0, \tag{2.2.32}$$

where

$$m_0(r) \coloneqq 4\pi \int_0^r s^2 \rho_0(s)\,\mathrm{d}s, \qquad r \geq 0, \tag{2.2.33}$$

defines the *local mass* induced by the mass density ρ_0. For $r > 0$, the value of $m_0(r)$ describes the mass contained inside the ball $B_r(0)$.

Since U_0 is smooth and spherically symmetric, we get $U_0'(0) = 0$ as one boundary condition for (2.2.31). As usual, we also require that U_0 vanishes at spatial infinity, i.e., $\lim_{r\to\infty} U_0(r) = 0$. However, the latter boundary condition does not fit well with equation (2.2.31): In order to evaluate the right-hand side of (2.2.31) at some radius $r > 0$, one has to know the values $U_0(s)$ for all smaller radii $s \in]0, r[$. Thus, one instead prefers to solve (2.2.31) by starting at the spatial origin $r = 0$ and then moving radially outwards. This strategy is basically pursued in [14, 140, 146], where the existence of solutions of (2.2.31) is shown[29] for some prescribed value of $U_0(0)$. Afterwards, one adjusts this solution suitably in order to satisfy the original boundary condition (1.1.5) at spatial infinity and verifies that the resulting steady state is indeed physically reasonable.

[29] In the aforementioned works the class of ansatz functions differs from our choice of φ, but the equations analysed there are still of the same type as in our situation.

An elegant way of realising this mathematically is introduced in [130], which we also follow here: The idea is to consider the function

$$y \coloneqq E_0 - U_0 \tag{2.2.34}$$

instead of U_0. In this way the cut-off energy $E_0 < 0$ – which was originally a prescribed parameter as part of the microscopic equation of state φ – becomes part of the unknowns and gets suitably adjusted later on. Inserting this definition into (2.2.31) yields the following integro-differential equation for y:[30]

$$y'(r) = -\frac{4\pi}{r^2} \int_0^r s^{2\ell+2}\, g\left(y(s) - \frac{L_0}{2s^2}\right) \mathrm{d}s, \qquad r > 0. \tag{2.2.35}$$

We equip this equation with the boundary/initial conditions[31]

$$y(0) = \kappa, \qquad y'(0) = 0, \tag{2.2.36}$$

for prescribed $\kappa > 0$. Once a suitably regular solution y of (2.2.35)–(2.2.36) with

$$y_\infty \coloneqq \lim_{r\to\infty} y(r) < 0 \tag{2.2.37}$$

is known, we set

$$E_0 \coloneqq y_\infty, \qquad U_0 \coloneqq E_0 - y \tag{2.2.38}$$

in order to arrive at a solution of the original equation (2.2.31) for U_0. Here, we simply solved (2.2.34) for U_0 and ensured that U_0 vanishes at spatial infinity by properly defining E_0. In fact, the negativity of y_∞ in (2.2.37) corresponds to the resulting steady state being physically reasonable, i.e., having compact support and finite mass.

Hence, the main step is to show the existence of a solution y as described above.

Lemma 2.2.8. *Let φ be an ansatz of the form (2.2.12) with ℓ, L_0, and Φ satisfying (φ1)–(φ3). Then, for every $\kappa > 0$ there exists a unique solution $y \in C^2([0,\infty[)$ of (2.2.35)–(2.2.36) s.t. $y_\infty = \lim_{r\to\infty} y(r) \in \,]-\infty, 0[$.*

Proof. Existence and uniqueness of a solution $y \in C^1([0,\infty[)$ follow by a standard contraction argument – recall $g \in C^1(\mathbb{R})$ by Lemma 2.2.6 – and by using the monotonicity of y. In the case $L_0 = 0$ this is described in [130, p. 906]. Similar arguments also apply in the case $L_0 > 0$, together with the observation

$$y(r) = \kappa, \qquad 0 \le r \le \sqrt{\frac{L_0}{2\kappa}}. \tag{2.2.39}$$

The regularity of g further implies $y \in C^2([0,\infty[)$ after differentiating (2.2.35); for the continuity of y'' at $r = 0$ in the case $L_0 = 0$ recall (2.2.27) and that we require ℓ to be non-negative in this case.

Furthermore, since $y' \le 0$, we know that y_∞ exists in $[-\infty, \infty[$. It is easily verified that $y_\infty > -\infty$ because once y has a zero at some radius, the solution can be explicitly extended to larger radii. For the proof that y_∞ is indeed negative, we distinguish between two cases.

[30] In [130], the integro-differential equation for y is called the "master equation" because obtaining steady states of related systems is also reduced to solving a similar equation. Here, we prefer the more modest name "equation (2.2.35)".

[31] Since (2.2.35) is a first-order equation, equipping it with two initial conditions could lead to an overdetermined system. However, we shall see that any (sufficiently smooth) solution y of (2.2.35) does automatically satisfy $y'(0) = 0$.

Firstly, in the situation where Φ satisfies (φ3) (i), we apply the "compact-support lemma" from [130, Lemma 3.1] to deduce $y_\infty < 0$; see [130, Sc. 4.1] for a proof that g satisfies the estimate required in the compact-support lemma. As noted in [130, Sc. 4.3], these arguments work in the case $L_0 > 0$ as well.[32]

Secondly, we consider the situation of a polytropic ansatz with Φ as specified in (φ3) (ii). In the case $L_0 = 0$, it is proven in [151], see also [14, Lemma 5.3], that y possesses a zero, which obviously leads to $y_\infty < 0$. This statement can then be extended to the case $L_0 > 0$ by a perturbation argument similar to [140, Thm. 1]. □

As described above, the existence of y as proven in Lemma 2.2.8 yields a physically reasonable steady state. We collect this result as well as various properties of the resulting equilibrium in the following statement.

Proposition 2.2.9 (Existence of Steady States)**.** *Let φ be an ansatz of the form* (2.2.12) *with ℓ, L_0, and Φ satisfying (φ1)–(φ3). Furthermore, for $\kappa > 0$ let y be the solution of* (2.2.35)–(2.2.36) *obtained in Lemma 2.2.8. Then, setting U_0 and E_0 according to* (2.2.38)*, i.e., $E_0 = y_\infty$ and $U_0 = E_0 - y$, yields a steady state of the Vlasov-Poisson system as defined in Definition 2.2.2. This steady state enjoys the following properties:*

(a) The total mass M_0 defined in (2.2.11) *is positive & finite.*

(b) The steady state is radially bounded, i.e.,

$$R_{\max} \coloneqq \sup\{r \geq 0 \mid \rho_0(r) > 0\} < \infty. \tag{2.2.40}$$

(c) It holds that

$$\{r > 0 \mid \rho_0(r) > 0\} =]R_{\min}, R_{\max}[, \tag{2.2.41}$$

where

$$R_{\min} \coloneqq \sqrt{\frac{L_0}{2\kappa}} \in [0, R_{\max}[. \tag{2.2.42}$$

In particular, the radial support of the steady state is of the form

$$\operatorname{supp}(\rho_0) = [R_{\min}, R_{\max}]. \tag{2.2.43}$$

(d) The support of the steady state is bounded, i.e., the sets

$$\Omega_0 \coloneqq \{(x,v) \in \mathbb{R}^3 \times \mathbb{R}^3 \mid f_0(x,v) > 0\} \tag{2.2.44}$$

and[33]

$$\Omega_0 \coloneqq \{(r,w,L) \in]0,\infty[\times \mathbb{R} \times [0,\infty[\mid f_0(r,w,L) > 0\} \tag{2.2.45}$$

are bounded. Similar to Remark 2.1.2 (d), we slightly abuse the notation and do not notationally distinguish between the set Ω_0 in (x,v)-coordinates and in (r,w,L)-coordinates. We refer to Ω_0, in either coordinates, as the phase space support *of the steady state.*

[32] One way to adapt the arguments from [130, Lemma 3.1] to the case $L_0 > 0$ is to consider $z(r) \coloneqq y(r) - \frac{L_0}{2r^2}$ instead of y; note that $\lim_{r\to\infty} z(r) = \lim_{r\to\infty} y(r)$.

[33] We restrict the set Ω_0 in (r,w,L)-coordinates to $r > 0$, although it is reasonable to include points $(0,w,0)$ with $\frac{1}{2}w^2 + U_0(0) < E_0$ in this set as well. However, as earlier noted in Remark 2.1.2 (c), we prefer to avoid the difficulties of the spatial origin in radial coordinates.

(e) It holds that $\rho_0 \in C^1(\mathbb{R}^3 \setminus \{0\})$ *and* $U_0 \in C^3(\mathbb{R}^3 \setminus \{0\})$. *If* $L_0 > 0$, *there further holds* $\rho_0 \in C^1(\mathbb{R}^3)$ *and* $U_0 \in C^3(\mathbb{R}^3)$. *The latter regularities are also present in the case* $L_0 = 0$ *provided that* $\ell = 0$ *or* $\ell > \frac{1}{2}$.

Proof. The fact that U_0 indeed defines a steady state is straight-forward to verify. In particular, note that $y \in C^2(\mathbb{R}^3)$ since $y \in C^2([0,\infty[)$ with $y'(0) = 0$ by (2.2.36).

Part (b) is a consequence of $y_\infty < 0$, which was shown in Lemma 2.2.8, and

$$\rho_0(r) > 0 \quad \Leftrightarrow \quad y(r) - \frac{L_0}{2r^2} > 0, \qquad\qquad r > 0; \tag{2.2.46}$$

this equivalence follows by (2.2.27). We then deduce part (a) since $M_0 = 4\pi \int_0^{R_{\max}} r^2 \rho_0(r)\,\mathrm{d}r$ and $r^2\rho_0(r)$ is bounded on compact radial intervals; the positivity of M_0 also follows by (2.2.46).

In order to show the precise form of the radial support claimed in part (c), first observe that $R_{\min} = \inf(\mathrm{supp}\,(\rho_0))$ follows by (2.2.39) and (2.2.46). What remains to be proven is that the steady state only consists of one connected radial shell. If $L_0 = 0$, this is due to the monotonicity of y together with (2.2.46). In the case $L_0 > 0$, first observe that $y'(r) + \frac{L_0}{r^3} = \frac{1}{r^2}\left(\frac{L_0}{r} - m_0(r)\right)$. Hence, the monotonicities of the two terms inside the latter bracket yield that there exists a unique radius $s_0 > 0$ s.t. $y'(s_0) + \frac{L_0}{s_0^3} = 0$. Therefore, the function $]0,\infty[\ni r \mapsto y(r) - \frac{L_0}{2r^2}$ is increasing on $]0, s_0]$ and decreasing on $[s_0, \infty[$. Together with (2.2.46) we thus obtain (2.2.41) and (2.2.43).

As to the phase space support, observe that the ansatz (2.2.6) for f_0 implies[34]

$$\Omega_0 \subset \{E < E_0\}, \tag{2.2.47}$$

where E is the particle energy induced by the stationary potential U_0 via (2.2.7). Hence, for $(x,v) \in \Omega_0$ we obtain the bounds $|x| < R_{\max}$ and $|v| < \sqrt{2E_0 - 2U_0(0)}$; for the latter estimate we used that $U_0(x) \geq U_0(0)$ for $x \in \mathbb{R}^3$. Thus, we also deduce that $r = |x|$ and $|w| \leq |v|$ are bounded for $(r, w, L) \in \Omega_0$. Lastly, the boundedness of the L-component can be seen by expressing the particle energy E in (r, w, L) coordinates and using (2.2.47), resulting in $L < 2R_{\max}^2(E_0 - U_0(0))$.

The regularity of ρ_0 stated in part (e) follows by differentiating (2.2.27) and using Lemma 2.2.6. The claimed regularity of U_0 is then due to (2.2.32). Finally, the regularities at the spatial origin can be obtained in a similar way after extending (2.2.27) to $x = 0$. □

Overall, we see that there indeed exits a plethora of physically reasonable steady states of the Vlasov-Poisson system: For each choice of ℓ, L_0 and Φ we obtain a one-parameter family of such equilibria with parameter $\kappa > 0$. Let us add some comments on the role of this parameter as well as its connection to the cut-off energy E_0.

Remark 2.2.10. *Let* f_0 *be a steady state as obtained in Proposition 2.2.9.*

(a) Consider the situation of an isotropic equilibrium, i.e., $\ell = 0 = L_0$. *Since* U_0 *is radially increasing and* g *is non-decreasing by Lemma 2.2.6, the relation* (2.2.27) *yields that* ρ_0 *is radially non-increasing on* $[0,\infty[$ *and strictly decreasing on* $[0, R_{\max}]$ *with*[35]

$$\rho_0(0) = g(\kappa) > 0. \tag{2.2.48}$$

[34] In Lemma 4.1.4, we study the relations between the sets Ω_0 and $\{E < E_0\}$ in more detail (for a further restricted class of steady states).

[35] In the case of an isotropic polytrope, the formula (2.2.48) can be further simplified by using the explicit representation of g derived in Remark 2.2.7.

Hence, the parameter $\kappa > 0$ is in one-to-one correspondence to the central density *$\rho_0(0)$ of the steady state; recall that g is injective on $[0,\infty[$ by Lemma 2.2.6.*[36]

(b) If $L_0 > 0$, the parameter $\kappa > 0$ determines the size of the inner radial vacuum region via (2.2.42)*.*

(c) The value of the cut-off energy $E_0 = y_\infty$ depends implicitly on the parameters ℓ, L_0, Φ, and κ through the behaviour of the solution y from Lemma 2.2.8. Since $y(R_{\max}) = \frac{L_0}{2R_{\max}^2}$ by (2.2.46) *and $y'(r) = -\frac{M_0}{r^2}$ for $r \geq R_{\max}$, the main theorem of calculus yields the representation*

$$E_0 = y_\infty = \frac{L_0}{2R_{\max}^2} - \frac{M_0}{R_{\max}}. \tag{2.2.49}$$

In fact, the dependency of E_0 on the steady state parameters is quite involved. For general ℓ, L_0, and Φ, a fixed cut-off energy $E_0 < 0$ can correspond to none, one, or multiple steady states with equation of state (2.2.12)*. It is hence not possible to prescribe the value of the cut-off energy E_0 when constructing a steady state. In the case of King's equation of state* (2.2.19)*, this follows from the results in [131]; see Figure 8.1.7 for a visualisation of this fact.*

A notable exception of this problem are polytropic ansatz functions (2.2.17) *with $L_0 = 0$, where the relation between E_0 and κ simplifies due to the scaling law analysed in Appendix B.*

In the later part of this thesis we will use numerical methods to study and illustrate further properties of steady states, see Section 8.1.

2.2.1 The Effective Potential

From now on let f_0 be a fixed steady state as constructed in Proposition 2.2.9. We next introduce a quantity which turns out to be crucial for the analysis of stationary solutions of the Vlasov-Poisson system in spherical symmetry.

Definition 2.2.11 (The Effective Potential)**.** *Let $L \geq 0$. The function*

$$\Psi_L \colon]0,\infty[\to \mathbb{R},\ \Psi_L(r) \coloneqq U_0(r) + \frac{L}{2r^2} \tag{2.2.50}$$

is called the effective potential *(of the steady state f_0).*

The additional term $\frac{L}{2r^2}$ added to the original potential U_0 plays the role of the squared tangential velocity. The main reason why it is important to understand the properties of the function Ψ_L is that it takes on the role of the potential when expressing the particle energy E in (r, w, L) coordinates. More precisely, inserting (2.2.21) into (2.2.7) yields

$$E(r, w, L) = \frac{1}{2}w^2 + U_0(r) + \frac{L}{2r^2} = \frac{1}{2}w^2 + \Psi_L(r) \tag{2.2.51}$$

for $(r, w, L) \in]0,\infty[\times \mathbb{R} \times [0,\infty[$.

The effective potential is, e.g., analysed in [14, p. 163f.], [57, Sc. 3.2], [62, Lemma 2.1], [85, App. A.1], [96, Lemma 2.1], [147, Lemma 4.1], and [165, Thm. 2.4]. Nonetheless, as the present class of steady states differs from the ones in the aforementioned works, we prefer to include the (rather simple) proofs of the following results here as well.

[36] In fact, the condition ($\varphi 3$) implies that $g \colon [0,\infty[\to [0,\infty[$ is one-to-one.

Lemma 2.2.12 (Structure of the Effective Potential)**.** *(a) For any $L > 0$ there exists a unique radius $r_L > 0$ s.t.*

$$\min_{]0,\infty[} \Psi_L = \Psi_L(r_L) < 0. \tag{2.2.52}$$

This radius is given as the unique zero of Ψ_L' on $]0,\infty[$ or, equivalently, as the unique solution of

$$r_L\, m_0(r_L) = L. \tag{2.2.53}$$

It holds that $\Psi_L' < 0$ on $]0, r_L[$ and $\Psi_L' > 0$ on $]r_L, \infty[$. We further introduce the abbreviation

$$E_L^{\min} := \Psi_L(r_L) = \min_{]0,\infty[} \Psi_L \tag{2.2.54}$$

for the minimal energy *for fixed $L > 0$.*[37]

(b) Let

$$\mathbb{A}_0 := \{(E, L) \in \,]-\infty, 0[\times]0,\infty[\mid E_L^{\min} < E\} \tag{2.2.55}$$

denote the set of all admissible (E, L)-pairs*. Then, for any $(E, L) \in \mathbb{A}_0$ there exist two unique radii $r_\pm(E, L)$ s.t.*

$$0 < r_-(E, L) < r_L < r_+(E, L) < \infty \tag{2.2.56}$$

and

$$\Psi_L(r_\pm(E, L)) = E. \tag{2.2.57}$$

Proof. Differentiating the effective potential radially yields

$$\Psi_L'(r) = U_0'(r) - \frac{L}{r^3} = \frac{1}{r^2}\left(m_0(r) - \frac{L}{r}\right) \tag{2.2.58}$$

for $r > 0$ by (2.2.32). Since $]0,\infty[\ni r \mapsto m_0(r) - \frac{L}{r}$ is increasing for $L > 0$ and

$$\lim_{r\to 0}\left(m_0(r) - \frac{L}{r}\right) = -\infty, \qquad \lim_{r\to\infty}\left(m_0(r) - \frac{L}{r}\right) = M_0 > 0, \tag{2.2.59}$$

there exists a unique $r_L > 0$ with $\Psi_L'(r_L) = 0$. Moreover, $\Psi_L' < 0$ on $]0, r_L[$ and $\Psi_L' > 0$ on $]r_L, \infty[$. Together with the limiting behaviour of the effective potential, which is given by

$$\lim_{r\to 0} \Psi_L(r) = \infty, \qquad \lim_{r\to\infty} \Psi_L(r) = \lim_{r\to\infty} U_0(r) = 0, \tag{2.2.60}$$

for $L > 0$, we deduce the claimed statements. □

We note that most of the notations employed in the context of the effective potential are based on [57]. The structure of the effective potential as well as the definitions of r_L and $r_\pm(E, L)$ are visualised in Figure 2.2.1; similar visualisations can be found in [85, Fig. A.1] and [96, Fig. 1]. An actual plot of the effective potential (based on a numerical computation) of an isotropic polytropic steady state is shown later in Figure 8.2.1.

[37] The name *minimal energy* is due to the obvious estimate $E(r, w, L) \geq E(r_L, 0, L) = E_L^{\min}$ for $(r, w, L) \in]0,\infty[\times \mathbb{R} \times [0,\infty[$.

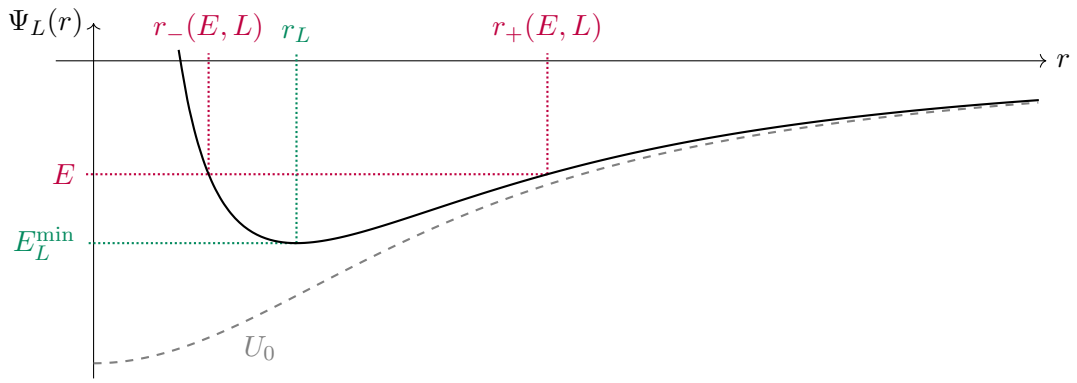

Figure 2.2.1: A schematic visualisation of the structure of the effective potential Ψ_L for $L > 0$.

Remark 2.2.13. *Due to the shape of the effective potential derived above, the steady states obtained in Proposition 2.2.9 are said to have* single-well structure. *We emphasize that it is a particular feature of the Vlasov-Poisson system that this property holds for all steady states constructed as above. In the context of the Einstein-Vlasov system, it is an open question for which steady states the analogous property is present. We refer to [49, Sc. 3.1] for a detailed discussion of this aspect.*

Before relating the effective potential to other important steady state quantities, we derive further properties of Ψ_L and the radii r_L and $r_\pm(E,L)$. Some parts of the following results originate from [57, 96] and are also stated in [62, 85, 147, 165].

Lemma 2.2.14 (Properties of Ψ_L, r_L, and $r_\pm$)**.** *(a) The mapping* $]0,\infty[\ni L \mapsto r_L$ *is continuously differentiable with*

$$\partial_L(r_L) = \frac{1}{4\pi\, r_L^3\, \rho_0(r_L) + m_0(r_L)}, \qquad L > 0. \tag{2.2.61}$$

Furthermore, r_L *is increasing in* L *with*

$$\lim_{L\to 0} r_L = R_{\min}, \qquad \lim_{L\to\infty} r_L = \infty. \tag{2.2.62}$$

(b) The mapping $]0,\infty[\ni L \mapsto E_L^{\min}$ *is continuously differentiable with*

$$\partial_L\big(E_L^{\min}\big) = \frac{1}{2r_L^2}, \qquad L > 0. \tag{2.2.63}$$

Furthermore, $E_L^{\min}$ *is increasing in* L *with*

$$\lim_{L\to 0} E_L^{\min} = U_0(R_{\min}) = U_0(0), \qquad \lim_{L\to\infty} E_L^{\min} = 0. \tag{2.2.64}$$

(c) The mappings $\mathbb{A}_0 \ni (E,L) \mapsto r_\pm(E,L)$ *are continuously differentiable with*

$$\partial_E r_\pm(E,L) = \frac{1}{\Psi_L'(r_\pm(E,L))}, \qquad \partial_L r_\pm(E,L) = -\frac{1}{2r_\pm^2(E,L)\,\Psi_L'(r_\pm(E,L))}, \tag{2.2.65}$$

for $(E, L) \in \mathbb{A}_0$. Furthermore, $r_-(E, L)$ is increasing in L and decreasing in E while $r_+(E, L)$ is decreasing in L and increasing in E, and there hold the following limiting statements for fixed $L^* > 0$ and $U_0(0) < E^* < 0$:

$$\lim_{\mathbb{A}_0 \ni (E,L) \to (E^{\min}_{L^*}, L^*)} r_\pm(E, L) = r_{L^*}, \tag{2.2.66}$$

$$\lim_{\mathbb{A}_0 \ni (E,L) \to (E^*, 0)} r_-(E, L) = 0, \tag{2.2.67}$$

$$\lim_{\mathbb{A}_0 \ni (E,L) \to (E^*, 0)} r_+(E, L) = r_+(E^*, 0) \in]R_{\min}, \infty[, \tag{2.2.68}$$

$$\lim_{\mathbb{A}_0 \ni (E,L) \to (U_0(0), 0)} r_+(E, L) = R_{\min}. \tag{2.2.69}$$

Here, $r_+(E^*, 0) \in]R_{\min}, \infty[$ is defined as the unique radius satisfying

$$U_0(r_+(E^*, 0)) = E^*. \tag{2.2.70}$$

(d) For any $L > 0$ there holds

$$E^{\min}_L \geq -\frac{M_0^2}{2L}. \tag{2.2.71}$$

(e) For any $(E, L) \in \mathbb{A}_0$ there holds

$$\frac{L}{2M_0} \leq r_-(E, L) < r_L < r_+(E, L) \leq -\frac{M_0}{E}. \tag{2.2.72}$$

(f) For any $(E, L) \in \mathbb{A}_0$ and $r \in [r_-(E, L), r_+(E, L)]$ the following concavity estimate holds:

$$E - \Psi_L(r) \geq L \, \frac{(r_+(E, L) - r)\,(r - r_-(E, L))}{2r^2\, r_-(E, L)\, r_+(E, L)}. \tag{2.2.73}$$

Proof. The continuous differentiability of r_L as well as (2.2.61) follow by (2.2.53) and the implicit function theorem; note that $m_0(r_L) > 0$ by (2.2.53). The limiting properties claimed in (2.2.62) also follow by (2.2.53) since $0 \leq m_0 \leq M_0 < \infty$ as well as $m_0 = 0$ on $]0, R_{\min}]$ and $m_0 > 0$ on $]R_{\min}, \infty[$ by (2.2.41).

Since $E^{\min}_L = \Psi_L(r_L)$, we then deduce the regularity of $L \mapsto E^{\min}_L$ claimed in (b) as well as (2.2.63). The fact that $E^{\min}_L$ tends to $U_0(0)$ as $L \to 0$ follows, e.g., by observing that $\Psi_L(L^{\frac{1}{4}}) \to U_0(0)$ as $L \to 0$; obviously, $E^{\min}_L \geq U_0(0)$. The limiting behaviour of $E^{\min}_L$ as $L \to \infty$ is a consequence of the estimate (2.2.71) which we will prove later; recall that $E^{\min}_L < 0$ by (2.2.52).

The differentiability of $r_\pm$ and the formulae (2.2.65) can be derived similar to part (a) by applying the implicit function theorem to (2.2.57) since $\Psi'_L(r_\pm(E, L)) \neq 0$. In order to prove (2.2.66) let $0 < \varepsilon < r_{L^*}$ and choose $\delta_1 > 0$ s.t. $\Psi_{L^*}(r_{L^*} \pm \varepsilon) \geq E^{\min}_{L^*} + 2\delta_1$. By part (a) as well as the continuous dependency of the effective potential on L, there exists $\delta_2 > 0$ s.t. for every $L > 0$ with $|L - L^*| < \delta_2$ it holds that $|r_{L^*} - r_L| < \varepsilon$ and $\Psi_L(r_{L^*} \pm \varepsilon) \geq E^{\min}_{L^*} + \delta_1$. Therefore, the monotonicity properties of the effective potential yield that for every $(E, L) \in \mathbb{A}_0$ with $|L - L^*| < \delta_2$ and $E \leq E^{\min}_{L^*} + \delta_1$ there holds $|r_\pm(E, L) - r_{L^*}| < \varepsilon$, which concludes the proof of (2.2.66). As to (2.2.67), first choose $\delta_1 > 0$ s.t. $E^* + \delta_1 < 0$ and $E^* - 2\delta_1 > U_0(0)$. Parts (a) and (b) imply the existence of some $\tilde{L} > 0$ s.t. $U_0(r_{\tilde{L}}) < U_0(0) + \delta_1$ and $E^{\min}_{\tilde{L}} < E^* - \delta_1$. For $0 < L \leq \tilde{L}$ and $|E - E^*| < \delta_1$ we thus obtain $(E, L) \in \mathbb{A}_0$ as well as the estimates $U_0(r_L) < U_0(0) + \delta_1$ and $r_-(E, L) \leq r_-(E^* - \delta_1, L)$ by the monotonicities of U_0, r_L, and r_-. In addition, for such L and $r \in]0, r_{\tilde{L}}[$ there holds

$\Psi_L(r) \leq U_0(r_{\tilde{L}}) + \frac{L}{2r^2} < U_0(0) + \delta_1 + \frac{L}{2r^2}$. Inserting $r = r_-(E^* - \delta_1, L) < r_L \leq r_{\tilde{L}}$ for $0 < L \leq \tilde{L}$ into the latter inequality yields $E^* - U_0(0) - 2\delta_1 < \frac{L}{2r_-^2(E^*-\delta_1,L)}$, which implies $r_-(E^* - \delta_1, L) \to 0$ as $L \to 0$ and thus concludes the proof of (2.2.67). The limit (2.2.68) with $r_+(E^*, 0)$ defined by (2.2.70) follows in a similar way as (2.2.66). For (2.2.69), observe that $r_+(E, 0) \to R_{\min}$ as $E \searrow U_0(0) = U_0(R_{\min})$. Together with the L-monotonicity of r_+ we then deduce (2.2.69).

For part (d) we make use of the structure of solutions of the radial Poisson equation to deduce

$$U_0(r) = -\frac{m_0(r)}{r} - 4\pi \int_r^\infty s\,\rho_0(s)\,\mathrm{d}s \geq -\frac{1}{r}\left(m_0(r) + 4\pi \int_r^\infty s^2\,\rho_0(s)\,\mathrm{d}s\right) = -\frac{M_0}{r} \quad (2.2.74)$$

for $r > 0$. Together with (2.2.53) we thus obtain

$$\begin{aligned} E_L^{\min} = \Psi_L(r_L) &\geq -\frac{M_0}{r_L} + \frac{L}{2r_L^2} = -m_0(r_L)\,\frac{M_0}{L} + \frac{m_0^2(r_L)}{2L} = \\ &= -\frac{M_0^2}{2L}\left(2\frac{m_0(r_L)}{M_0} - \frac{m_0^2(r_L)}{M_0^2}\right) \geq -\frac{M_0^2}{2L} \end{aligned} \quad (2.2.75)$$

for $L > 0$.

For $(E, L) \in \mathbb{A}_0$, the estimate (2.2.74) implies that every $r > 0$ with $\Psi_L(r) \leq E$ there holds $E + \frac{M_0}{r} - \frac{L}{2r^2} \geq 0$. Solving this quadratic inequality yields

$$\frac{L}{M_0 + \sqrt{M_0^2 + 2EL}} \leq r \leq \frac{L}{M_0 - \sqrt{M_0^2 + 2EL}}; \quad (2.2.76)$$

note that $M_0^2 + 2EL > 0$ by (2.2.71). Hence,

$$r_-(E, L) \geq \frac{L}{M_0 + \sqrt{M_0^2 + 2EL}} > \frac{L}{2M_0}, \quad (2.2.77)$$

$$r_+(E, L) \leq \frac{L}{M_0 - \sqrt{M_0^2 + 2EL}} = \frac{-M_0 - \sqrt{M_0^2 + 2EL}}{2E} < -\frac{M_0}{E}. \quad (2.2.78)$$

Lastly, in order to prove the concavity estimate (2.2.73) we consider the function $\xi\colon [r_-(E, L), r_+(E, L)] \to \mathbb{R}$ defined by

$$\xi(r) \coloneqq E - \Psi_L(r) - L\,\frac{(r_+(E, L) - r)\,(r - r_-(E, L))}{2r^2\,r_-(E, L)\,r_+(E, L)}, \qquad r \in [r_-(E, L), r_+(E, L)], \quad (2.2.79)$$

for fixed $(E, L) \in \mathbb{A}_0$. The radial Poisson equation then yields

$$\partial_r^2[r\,\xi(r)] = -2\Psi_L'(r) - r\,\Psi_L''(r) + \frac{L}{r^3} = -\frac{1}{r}\,\partial_r\big[r^2\,U_0'(r)\big] = -4\pi r\,\rho_0(r) \leq 0. \quad (2.2.80)$$

Thus, the mapping $[r_-(E, L), r_+(E, L)] \ni r \mapsto r\xi(r)$ is concave with $\xi(r_\pm(E, L)) = 0$, which implies $\xi \geq 0$ on $[r_-(E, L), r_+(E, L)]$ and concludes the proof of part (f). □

We refer to [85, App. A.1] for some additional properties of the effective potential, e.g., a more detailed analysis of some of the rates of convergence analysed in the above lemma.

A thorough understanding of the effective potential allows one to control the support of the steady state. Concretely, (2.2.46) implies

$$\{r > 0 \mid \rho_0(r) > 0\} = \{r > 0 \mid \Psi_{L_0}(r) < E_0\}. \quad (2.2.81)$$

Hence,

$$R_{\min} = r_-(E_0, L_0), \qquad R_{\max} = r_+(E_0, L_0), \tag{2.2.82}$$

where we use the convention $r_-(E_0, 0) \coloneqq 0$, which is consistent with Lemma 2.2.14 (c).

Furthermore, the *L-support* of the steady state, i.e., the set

$$\mathbb{L}_0 \coloneqq \{L(x,v) \mid (x,v) \in \Omega_0\}, \tag{2.2.83}$$

can be characterised explicitly:

Lemma 2.2.15. *Let $L_{\max} > L_0$ be defined as the unique solution of*[38]

$$E^{\min}_{L_{\max}} = E_0. \tag{2.2.84}$$

If $L_0 = 0 = \ell$,

$$\mathbb{L}_0 = [0, L_{\max}[. \tag{2.2.85}$$

Otherwise,

$$\mathbb{L}_0 =]L_0, L_{\max}[. \tag{2.2.86}$$

Proof. Changing to (r, w, L)-coordinates and using (2.2.12) yields

$$\mathbb{L}_0 = \{L \mid (r,w,L) \in]0,\infty[\times\mathbb{R}\times[0,\infty[: (L-L_0)^\ell_+ > 0 \ \&\ \Phi(E_0 - E(r,w,L)) > 0\}. \tag{2.2.87}$$

Observe that, for $L \geq 0$, $(L - L_0)^\ell_+ > 0$ is equivalent to $L > L_0$ or $L = L_0 = 0 = \ell$; recall the conventions employed for $(\ldots)^\ell_+$. The claimed statements are now a consequence of $E(r,w,L) \geq E^{\min}_L = E(r_L, 0, L)$ for $L > 0$ and $E(r,w,0) \geq U_0(0)$ for $(r,w) \in]0,\infty[\times \mathbb{R}$ combined with the monotonicity of $L \mapsto E^{\min}_L$ and the fact that $\Phi > 0$ on $]0, \eta_0[$ for some $\eta_0 > 0$ by (φ3). □

In order to analyse all (E, L)-pairs associated to the energy support of the steady state, we define

$$\mathbb{D}_0 \coloneqq \{(E,L) \in]-\infty, 0[\times]0,\infty[\mid L > L_0 \ \&\ E^{\min}_L < E < E_0\}, \tag{2.2.88}$$

where $E^{\min}_L$ is defined in Lemma 2.2.12. Equivalently,

$$\mathbb{D}_0 = \{(E,L) \in \mathbb{A}_0 \mid L > L_0 \ \&\ E < E_0\} \subset \mathbb{A}_0, \tag{2.2.89}$$

recall (2.2.55). Due to the regularity of $L \mapsto E^{\min}_L$ shown in Lemma 2.2.14 (b), the set $\mathbb{D}_0$ is open. Although the name is somewhat misleading[39], we sometimes refer to $\mathbb{D}_0$ as the (E, L)-*triangle* of the steady state; however, we usually refer to it as the (E, L)-*support* of the steady state. We illustrate the shape of this set in Figure 2.2.2, see also [85, Fig. 1.1] and [117, Fig. 1] for similar visualisations. Actual numerical plots of $\mathbb{D}_0$ for some selected steady states will be presented in Section 8.2.

If $L_0 > 0$ or $\ell > 0$, the set $\mathbb{D}_0$ is related to $\mathbb{L}_0$ via

$$\mathbb{L}_0 = \{L \mid (E,L) \in \mathbb{D}_0\}. \tag{2.2.90}$$

In the case $L_0 = 0 = \ell$, it holds that

$$\mathbb{L}_0 = \{L \mid (E,L) \in \mathbb{D}_0\} \cup \{0\}, \tag{2.2.91}$$

i.e., we generally exclude $L = 0$ from $\mathbb{D}_0$. The connection between $\mathbb{D}_0$ and the phase space support Ω_0 will be analysed in Lemma 4.1.5 after we have further restricted the class of steady states. For now, we note

$$\{(E(x,v), L(x,v)) \mid (x,v) \in \Omega_0\} \subset \overline{\mathbb{D}}_0. \tag{2.2.92}$$

[38] The existence of such $L_{\max}$ follows by Lemma 2.2.14 (b).

[39] The curve $\{(E,L) \in]-\infty, 0[\times]0,\infty[\mid E = E^{\min}_L\}$ is obviously not a straight line in general.

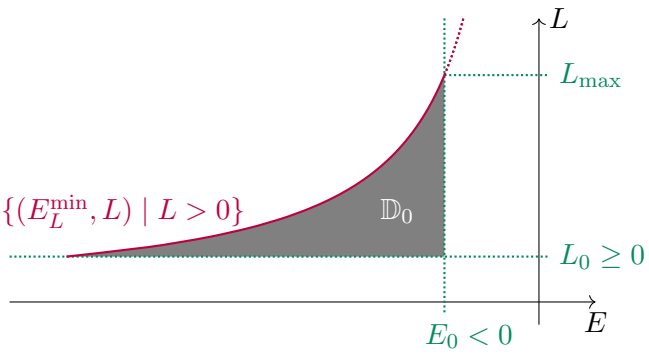

Figure 2.2.2: A schematic visualisation of the (E, L)-support $\mathbb{D}_0$ of a steady state.

2.2.2 The Radial Particle Motions

The most important feature of the effective potential is that it is the key quantity determining the particle motions in (r, w, L)-coordinates. In the original Cartesian (x, v)-coordinates, the particle motions within the fixed equilibrium are given by the characteristic system (2.2.2) with potential $U = U_0$. In (r, w, L)-coordinates, this systems transforms[40] to

$$\dot{r} = w, \tag{2.2.93a}$$
$$\dot{w} = -\Psi_L'(r), \tag{2.2.93b}$$

together with

$$\dot{L} = 0. \tag{2.2.94}$$

The latter equation allows us to interpret L as a parameter of the planar (i.e., two-dimensional) system (2.2.93). The particle energy E given by (2.2.51) takes on the role of the Hamiltonian function of (2.2.93). The term $\frac{L}{r^3}$ appearing on the right-hand side of (2.2.93b) is the centrifugal force. The aim of the present section is to analyse the behaviour of solutions of (2.2.93); a related discussion can, e.g., be found in [14, Sc. 2].

Let $(R, W)\colon I \to]0, \infty[\times \mathbb{R}$ be the unique maximal solution of (2.2.93) with parameter[41] $L > 0$ satisfying the initial condition $(R, W)(0) = (r, w)$ for fixed $(r, w) \in]0, \infty[\times \mathbb{R}$. We require that the conserved energy value $E = E(r, w, L)$ is negative; otherwise the solution is not of interest.[42] Now observe that the radial component R of the solution always stays in $[r_-(E, L), r_+(E, L)]$ by Lemma 2.2.12 since $E = E(R(s), W(s), L) \geq \Psi_L(R(s))$ for $s \in I$. Since the w-component is also bounded by $|W(s)| \leq \sqrt{2E - 2E_L^{\min}}$, the solution is global, i.e., $I = \mathbb{R}$. There are two qualitatively different cases for the behaviour of the solution, which are both visualised in Figure 2.2.3.

If $(r, w) = (r_L, 0)$, the solution is constant with energy-value $E = E_L^{\min}$. Such radially constant solutions are usually called *circular* [19, p. 145], as they correspond to circular motions in Cartesian (x, v)-coordinates.

[40] More precisely, let $(x, v)\colon I \to \mathbb{R}^3 \times \mathbb{R}^3$ be a solution of (2.2.2) and assume that $x(s) \neq 0$ for $s \in I$. Then, defining (r, w, L) according to (2.1.3) yields a solution $(r, w, L)\colon I \to]0, \infty[\times \mathbb{R} \times [0, \infty[$ of (2.2.93).

[41] For now, we omit the case $L = 0$ although most of the arguments can be extended to this situation as well, cf. Remark 2.2.17 (a).

[42] Later on, only the particle motions within the steady state support are relevant. The latter set, however, only contains points where the particle energy is smaller than the cut-off energy $E_0 < 0$.

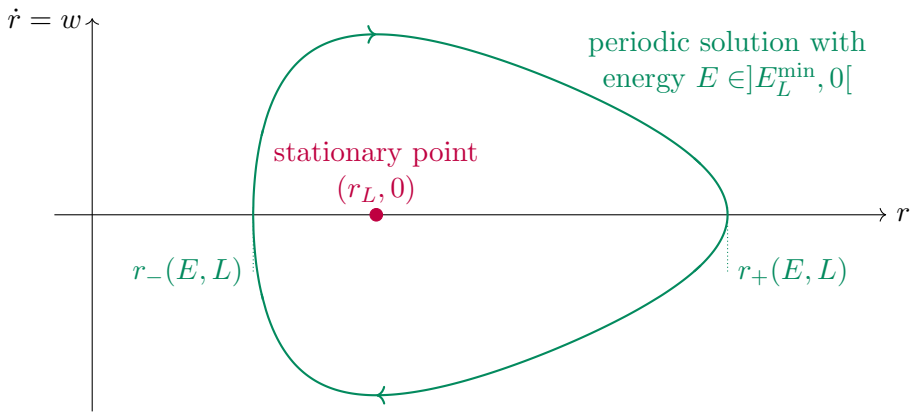

Figure 2.2.3: A schematic phase space diagram of the ODE (2.2.93) in the (r, w)-plane for fixed $L > 0$.

Otherwise, i.e., $E_L^{\min} < E < 0$, we solve for W to obtain

$$W(s) = \pm\sqrt{2E - 2\Psi_L(R(s))} \tag{2.2.95}$$

for $s \in \mathbb{R}$. Thus, basic ODE theory yields that the solution is time-periodic and covers the orbit $(R, W)(\mathbb{R}) = \{(\tilde{r}, \tilde{w}) \in]0, \infty[\times \mathbb{R} \mid E(\tilde{r}, \tilde{w}, L) = E\}$; note that this set is connected and does not contain any stationary points of (2.2.93) due to the structure of the effective potential derived in Lemma 2.2.12. More precisely, R oscillates between the radii $r_-(E, L)$ and $r_+(E, L)$, where $\dot{R}(s) = 0$ is equivalent to $R(s) = r_\pm(E, L)$ and $\dot{R}$ always switches its sign when reaching $r_\pm(E, L)$.[43] Applying the inverse function theorem and integrating equation (2.2.95) as described in [19, Sc. 3.1] allows us to determine the oscillation period – i.e., the time needed for R to travel from $r_-(E, L)$ to $r_+(E, L)$ and back – more explicitly. This important quantity is defined below, where we also introduce a more suitable parametrisation of the solutions of the characteristic system (2.2.93) based on the conserved quantities (E, L) similar to [49, Def. 3.5].

Definition & Lemma 2.2.16 (The Period Function)**.** *Let $(E, L) \in \mathbb{A}_0$, where $\mathbb{A}_0$ is the set of admissible (E, L)-pairs defined in* (2.2.55)*. Let $(R, W)(\cdot, E, L) \colon \mathbb{R} \to]0, \infty[\times \mathbb{R}$ be the maximal solution of the characteristic system* (2.2.93) *with parameter L satisfying the initial condition*

$$(R, W)(0, E, L) = (r_-(E, L), 0). \tag{2.2.96}$$

Then the solution $(R, W)(\cdot, E, L)$ is time-periodic with period given by

$$T(E, L) \coloneqq 2 \int_{r_-(E,L)}^{r_+(E,L)} \frac{\mathrm{d}r}{\sqrt{2E - 2\Psi_L(r)}}. \tag{2.2.97}$$

The induced function $T \colon \mathbb{A}_0 \to]0, \infty[$ is called the (radial) period function *of the steady state.*

Proof. The properties of the solution $(R, W)(\cdot, E, L)$ are shown above. The integral (2.2.97) is well-defined and finite since $\Psi_L < E$ on $]r_-(E, L), r_+(E, L)[$ and $\Psi_L'(r_\pm(E, L)) \neq 0$ by Lemma 2.2.12. □

[43] In an astrophysical context, the radii $r_-(E, L)$ and $r_+(E, L)$ are usually referred to as the *pericenter* and *apocenter* of the particle motion, respectively, cf. [19, p. 145].

In the course of this thesis we shall discover that the dynamical behaviour of solutions of the Vlasov-Poisson system close to the fixed steady state f_0 is crucially influenced by the properties of the period function T. This is why we devote the entire Appendix A to a thorough analysis of this function, including its regularity and boundedness for suitable[44] equilibria. Similar analyses are conducted in [62, App. B] and [85, Ch. 3]. In Section 8.2, we numerically investigate relevant properties the period function. In particular, we present numerical plots of T on the (E, L)-triangle $\mathbb{D}_0$, recall (2.2.88), for some selected steady states in Figures 8.2.2, 8.2.5, 8.2.9, and 8.2.10.

Let us add some concluding remarks on the particle motions within the fixed equilibrium.

Remark 2.2.17. *(a) It is straight-forward to extend the above discussion to the case $L = 0$. In this situation, the radial characteristic system* (2.2.93) *becomes*

$$\dot{r} = w, \tag{2.2.98a}$$
$$\dot{w} = -U_0'(r), \tag{2.2.98b}$$

with Hamiltonian $E(r, w, 0) = \frac{1}{2}w^2 + U_0(r)$. After extending U_0 via $U_0(r) \coloneqq U_0(-r)$ for $r < 0$ – note that this defines a smooth[45] extension of U_0 since $U_0 \in C^2(\mathbb{R}^3)$ – it becomes apparent that the solutions of the system (2.2.98) *behave similarly to the case of non-zero angular momentum: For $U_0(0) \leq E < 0$ let $(R, W)\colon I \to \mathbb{R}^2$ be the unique maximal solution of* (2.2.98) *satisfying the initial condition $(R, W)(0) = (-r_+(E, 0), 0)$. Here, $r_+(E, 0)$ is defined in Lemma 2.2.14 (c) for $U_0(0) < E < 0$ and we set $r_+(U_0(0), 0) \coloneqq R_{\min}$ according to* (2.2.69). *The minimal energy value $E = U_0(0)$ again corresponds to the circular case, i.e., (R, W) is constant. Otherwise, i.e., $U_0(0) < E < 0$, the solution is global, bounded, and time-periodic with period given by*

$$T(E, 0) \coloneqq 2\int_0^{r_+(E,0)} \frac{\mathrm{d}r}{\sqrt{2E - 2U_0(r)}}. \tag{2.2.99}$$

In light of Lemma 2.2.14 (c), the formula (2.2.99) *is a natural extension of* (2.2.97). *However, a rigorous proof that this indeed defines a continuous extension of the period function for suitable equilibria is technically quite involved, see [85, Lemma 3.12].*

We further note that in the case $L = 0$, the motion of a particle (in Cartesian (x, v)-coordinates) is purely radial. More precisely, the particle moves on a fixed line through the spatial origin and has no angular speed, cf. [19, Sc. 3.1].

(b) In the case $L > 0$ and $E \geq 0$, the associated solution of the characteristic system is no longer bounded. More precisely, let $(R, W)\colon I \to]0, \infty[\times \mathbb{R}$ be the maximal solution of (2.2.93) *with parameter $L > 0$ satisfying the initial condition $(R, W)(0) = (r_-(E, L), 0)$ for some $E \geq 0$.[46] Here, $r_-(E, 0)$ is defined as the unique solution of $\Psi_L(r_-(E, L)) = E$; the existence of this radius follows by the structure of the effective potential established in Lemma 2.2.12. It is then straight-forward to verify that the solution exhibits the following limiting behaviour: $\lim_{s\to\inf(I)} R(s) = \infty = \lim_{s\to\sup(I)} R(s)$ as well as $\lim_{s\to\inf(I)} W(s) = -\sqrt{2E}$ and $\lim_{s\to\sup(I)} W(s) = \sqrt{2E}$.*

[44] In Appendix A, we further restrict the class of steady states. This is in particular necessary to show that T is bounded on $\mathbb{D}_0$, cf. Remark A.4.5.

[45] Here, "smooth" means that the right-hand side of the system (2.2.98) is, in particular, locally Lipschitz-continuous.

[46] It follows by [143, Lemma 1.2] that any maximal solution of (2.2.93) exists for all times, i.e., $I = \mathbb{R}$, even in the case $E \geq 0$, but this is not relevant here.

(c) Although the solution of (2.2.93) *is time-periodic in the case* $(E, L) \in \mathbb{A}_0$*, we emphasise that the associated solution of the characteristic system* (2.2.2) *in the Cartesian* (x, v)*-coordinates is not time-periodic in general. This is due to the additional angular motion in Cartesian coordinates, cf. [19, Sc. 3.1].*

Chapter 3

Linearising the Vlasov-Poisson System

In this chapter, which is entirely based on [62, Sc. 3],[47] we linearise the Vlasov-Poisson system around a fixed equilibrium. The resulting system governs the dynamics of small perturbations of the equilibrium up to first order and is widely studied in the astrophysics literature [8, 19, 36, 37, 43, 71, 77, 111, 161] as well as in the mathematics literature [15, 53, 95] among others.

Let f_0 be a fixed steady state of the Vlasov-Poisson system as constructed in Proposition 2.2.9 with associated potential U_0, mass density ρ_0, and equation of state φ. In fact, in order to justify the following calculations we have to make further assumptions on the equilibrium state, especially concerning the regularity of the equation of state φ. However, we deliberately dispense with rigour and refrain from specifying these conditions here[48] to emphasise that the following arguments should be regarded only as the formal derivation of a new system. One would have to make these calculations rigorous if one wants to deduce properties of the non-linearised Vlasov-Poisson system, which is beyond the scope of the present thesis.

We present three different methods to linearise the Vlasov-Poisson system, which each allows for a different physical interpretation. Each approach leads to a linear operator whose (spectral) properties determine the behaviour of solutions to the linearised system. Fortunately[49], these operators are (essentially) identical for the different linearisation schemes used here. A rigorous analysis of the (spectral) properties of the operator will then be conducted in the remainder of this work.

3.1 The Eulerian Picture

The most common way [8, 15, 53, 71, 77, 111] to linearise the Vlasov-Poisson system is in Eulerian variables. The idea is to plug the (formal) expression $f_0 + \varepsilon f + \mathcal{O}(\varepsilon^2)$ for

[47] The contents forming the basis of Section 3.3 are not included in the published version of [62], but can be found in its preprint version arXiv:2102.11672v2.

[48] In Section 4.1, we explicitly state the class of equilibria for which we (rigorously) analyse the associated linearised system. We note that the calculations in the present chapter can also be performed rigorously for these equilibria.

[49] When linearising a system of differential equations in different coordinates, it is not to be expected to arrive at the same linearisation. Even in a finite dimensional context, linearising in different coordinates can lead to different system; nonetheless, such systems are always equivalent. In an infinite dimensional context, this equivalence is also unclear.

$0 < \varepsilon \ll 1$ into the Vlasov-Poisson system (1.1.2)–(1.1.5) and dispense with terms of order $\mathcal{O}(\varepsilon^2)$. For every time t, we require $f(t)\colon \mathbb{R}^3 \times \mathbb{R}^3 \to \mathbb{R}$ to be spherically symmetric – recall Definition 2.1.1 (b) – and to vanish outside of the support of the steady state. The latter condition ensures that $|\varepsilon f(t)| \ll f_0$ on $\mathbb{R}^3 \times \mathbb{R}^3$ for $0 < \varepsilon \ll 1$ and is a natural one, see [15, App.] for a detailed discussion of this aspect. Using that the steady state f_0 is a solution of the Vlasov-Poisson system then leads to the *linearised Vlasov equation*

$$\partial_t f + \mathcal{T} f - \partial_v f_0 \cdot \partial_x U_f = 0, \tag{3.1.1}$$

where $\mathcal{T}$ is the transport operator associated to the (characteristic flow of the) steady state f_0 defined in (1.2.10) and $U_f = U_{f(t)}$ is the gravitational potential induced by the linear perturbation f via the Poisson equation, i.e.,

$$\Delta U_f = 4\pi\rho_f, \qquad \lim_{|x|\to\infty} U_f(t,x) = 0, \tag{3.1.2}$$

$$\rho_f(t,x) = \int_{\mathbb{R}^3} f(t,x,v)\,\mathrm{d}v, \tag{3.1.3}$$

similar definitions for ρ_g and U_g are employed for general $g\colon \mathbb{R}^3 \times \mathbb{R}^3 \to \mathbb{R}$. We refer to (3.1.1)–(3.1.3) as the *linearised Vlasov-Poisson system*. A detailed (and mathematically rigorous) analysis of this system can be found in [15], including an appropriate global existence result in the case of suitable isotropic steady states.

Notice that (3.1.1) is a first-order transport-type equation for the linear perturbation f. The presence of oscillatory solutions is, however, more convenient to analyse (and also more "physically intuitive" [71, Sc. IIId)]) for a second-order equation. As a matter of fact, V. A. Antonov [8] developed a method – typically referred to as the *Antonov trick* – to rewrite the linearised Vlasov-Poisson system as a second-order system, see also [71, Sc. IIId)]: We split f into its even and odd part in the velocity variable v, i.e.,

$$f_\pm(t,x,v) \coloneqq \frac{1}{2}(f(t,x,v) \pm f(t,x,-v)). \tag{3.1.4}$$

Obviously, $f = f_+ + f_-$ as well as $f_+(t,x,-v) = f_+(t,x,v)$ and $f_-(t,x,-v) = -f_-(t,x,v)$, i.e., f_+ and f_- are even in v and odd in v, respectively. The key observation is that the linearised Vlasov-Poisson system (3.1.1)–(3.1.3) can also be decomposed into its even and odd parts in v quite naturally. The reason for this is that the transport operator $\mathcal{T}$ reverses v-parity[50] and that the mass density is only determined by the even-in-v part, i.e., $\rho_f = \rho_{f_+}$. Hence, splitting the linearised Vlasov equation (3.1.1) into its even-in-v and odd-in-v parts leads to the identities

$$\partial_t f_+ + \mathcal{T}(f_-) = 0, \tag{3.1.5a}$$

$$\partial_t f_- + \mathcal{T}(f_+) - \partial_v f_0 \cdot \partial_x U_{f_+} = 0. \tag{3.1.5b}$$

The next step is to differentiate the odd-in-v equation (3.1.5b) w.r.t. t and to insert the even-in-v equation (3.1.5a). We then arrive at the following second-order identity for the odd-in-v part of the linear perturbation:

$$\partial_t^2 f_- - \mathcal{T}^2(f_-) + \partial_v f_0 \cdot \partial_x U_{\mathcal{T}(f_-)} = 0. \tag{3.1.6}$$

We refer to this equation (coupled with (3.1.2)–(3.1.3)) as the *linearised Vlasov-Poisson system in second-order formulation*. Its well-posedness is established in Appendix C (for a

[50] More precisely, $\mathcal{T}(f_\pm) = (\mathcal{T} f)_\pm$ for sufficiently regular f, see Lemma 4.3.16 for a rigorous statement.

suitable class of solutions). It is straight-forward to verify that the latter system is indeed equivalent to (3.1.1)–(3.1.3): If f_- solves (3.1.6), taking f_+ as a solution of (3.1.5a) yields a solution $f \coloneqq f_+ + f_-$ of (3.1.1). We will not discuss here how initial data $f(0)$ for (3.1.1) can be transformed into equivalent initial data $f(0)$, $\partial_t f(0)$ for (3.1.6) and vice versa, as this aspect is somewhat involved. The important point here is that any solution of one system can be converted into a solution of the other, so that for the general study of solution behaviour it is equivalent whether one considers (3.1.1) or (3.1.6).

We rewrite (3.1.6) as

$$\partial_t^2 f_- + \mathcal{L}(f_-) = 0 \tag{3.1.7}$$

by introducing the operator $\mathcal{L} = -\mathcal{T}^2 - \mathcal{R}$. The first addend of this operator contains the influence of the steady state flow onto the perturbation, while the second addend corresponds to the gravitational response of the perturbation and is given by

$$\mathcal{R}g \coloneqq -\partial_v f_0 \cdot \partial_x U_{\mathcal{T}g} \tag{3.1.8}$$

for suitable $g = g(x, v)$.

So far we have not used the assumption of spherical symmetry on the linear perturbation f; obviously, f being spherically symmetric implies that $f_\pm$ are too. We do this now to rewrite (3.1.7) in the radial coordinates (r, w, L) introduced in Remark 2.1.2 (b). It is straight-forward to verify that the transport operator can be written as

$$\mathcal{T} = w\,\partial_r - \left(U_0' - \frac{L}{r^3}\right)\partial_w; \tag{3.1.9}$$

in particular, $\mathcal{T}$ preserves spherical symmetry.[51] In order to rewrite the response operator, we change to (w, L)-coordinates in the velocity integral of the mass density $\rho_{\mathcal{T}g}$ and insert (3.1.9) to obtain

$$\rho_{\mathcal{T}g}(r) = \frac{\pi}{r^2}\int_0^\infty \int_{\mathbb{R}} \mathcal{T}g(r, w, L)\,\mathrm{d}w\,\mathrm{d}L = \frac{\pi}{r^2}\,\partial_r\left[\int_0^\infty \int_{\mathbb{R}} w\, g(r, w, L)\,\mathrm{d}w\,\mathrm{d}L\right] \tag{3.1.10}$$

for suitable, spherically symmetric $g\colon \mathbb{R}^3 \times \mathbb{R}^3 \to \mathbb{R}$, which then leads to[52]

$$U_{\mathcal{T}g}'(r) = \frac{4\pi}{r^2}\int_0^r s^2 \rho_{\mathcal{T}g}(s)\,\mathrm{d}s = \frac{4\pi^2}{r^2}\int_0^\infty \int_{\mathbb{R}} w\, g(r, w, L)\,\mathrm{d}w\,\mathrm{d}L. \tag{3.1.11}$$

In addition, differentiating the ansatz (2.2.6) for the steady state f_0 yields

$$\partial_v f_0(x, v) = \partial_E \varphi(E(x, v), L(x, v))\, v + \partial_L \varphi(E(x, v), L(x, v))\,\big(2r^2 v - 2x \cdot v\, x\big). \tag{3.1.12}$$

Since $\partial_x U = U' \frac{x}{r}$ for any spherically symmetric function $U\colon \mathbb{R}^3 \to \mathbb{R}$ and $\big(2r^2 v - 2x \cdot v\, x\big) \cdot \frac{x}{r} = 0$, we deduce that the response operator $\mathcal{R}$ applied to some suitable, spherically symmetric function $g\colon \mathbb{R}^3 \times \mathbb{R}^3 \to \mathbb{R}$ can be written as

$$(\mathcal{R}g)(r, w, L) = -4\pi\, w\, \partial_E \varphi(E, L)\, j_g(r), \tag{3.1.13}$$

where use the abbreviations $E = E(r, w, L)$ and

$$j_g(r) \coloneqq \frac{\pi}{r^2}\int_0^\infty \int_{\mathbb{R}} w\, g(r, w, L)\,\mathrm{d}w\,\mathrm{d}L. \tag{3.1.14}$$

[51] See Remark 4.2.6 (g) for more rigorous statements.

[52] We will later verify the identity (3.1.11) rigorously for suitable g, see Lemma 4.4.6.

The function j_g can be interpreted as the (radial) velocity density induced by g.

Let us now discuss the relation between the spectral properties of the linearised operator $\mathcal{L}$ and the behaviour of solutions of the linearised Vlasov-Poisson system in the second-order formulation (3.1.7). We will later[53] show that $\mathcal{L}$ is a symmetric operator when defined on (a proper dense subset of) a suitable Hilbert space $\mathcal{H}$. We hence only have to consider real-valued elements of the spectrum of $\mathcal{L}$.

Suppose that $\lambda < 0$ is a negative eigenvalue of $\mathcal{L}$ with eigenfunction $g = g(x,v) = g_-(x,v)$. Then

$$f_-(t,x,v) \coloneqq e^{\sqrt{-\lambda}\,t} g(x,v) \tag{3.1.15}$$

defines a growing mode solution of (3.1.7), i.e., a solution which grows exponentially in time. Hence, the steady state f_0 is *linearly unstable* in this situation.

For the implications of the existence of the eigenvalue 0 of $\mathcal{L}$ as well as its physical interpretation, we refer to [71, Sc. IIIf)].

However, as first observed in [9, 10], these two situations do not arise for a large class of natural steady states[54]. More precisely, the whole spectrum of the linearised operator $\mathcal{L}$ is positive; a rigorous proof of this statement is given in Proposition 4.5.11. Due to the absence of zero mode solutions and growing mode solutions, it is reasonable to call such equilibria *linearly stable*. A rigorous stability result for the linearised Vlasov-Poisson system (3.1.7) is established in Lemma C.0.3.

Now suppose that $\lambda > 0$ is a positive eigenvalue of $\mathcal{L}$ with eigenfunction $g = g(x,v) = g_-(x,v)$. Then

$$f_-(t,x,v) \coloneqq \cos(\sqrt{\lambda}\,t)\, g(x,v) \tag{3.1.16}$$

defines an *oscillatory mode*, i.e., a time-periodic solution of (3.1.7) with period p given by

$$p = \frac{2\pi}{\sqrt{\lambda}}. \tag{3.1.17}$$

As discussed above, setting

$$f_+(t,x,v) \coloneqq -\frac{1}{\sqrt{\lambda}} \sin(\sqrt{\lambda}\,t)\, (\mathcal{T} g)(x,v), \tag{3.1.18}$$

and $f \coloneqq f_+ + f_-$ then defines an oscillatory solution of (3.1.1)–(3.1.3).

At the level of the non-linearised Vlasov-Poisson system, such oscillation can be observed, e.g., in the kinetic and potential energies. These energies are given by

$$E_{\mathrm{kin}}(h) \coloneqq \frac{1}{2} \int_{\mathbb{R}^3 \times \mathbb{R}^3} |v|^2\, h(x,v)\, \mathrm{d}(x,v), \tag{3.1.19}$$

$$E_{\mathrm{pot}}(h) \coloneqq -\frac{1}{8\pi} \int_{\mathbb{R}^3} |\partial_x U_h(x)|^2\, \mathrm{d}x = \frac{1}{2} \int_{\mathbb{R}^3} U_h(x)\, \rho_h(x)\, \mathrm{d}x \tag{3.1.20}$$

for suitable $h = h(x,v)$. For f as defined above, integrating by parts yields

$$\begin{aligned} E_{\mathrm{kin}}(f_0 + \varepsilon f(t) + \mathcal{O}(\varepsilon^2)) &= E_{\mathrm{kin}}(f_0) - \varepsilon\, \frac{\sin(\sqrt{\lambda}\,t)}{2\sqrt{\lambda}} \int_{\mathbb{R}^3 \times \mathbb{R}^3} |v|^2\, (\mathcal{T} g)(x,v)\, \mathrm{d}(x,v) + \mathcal{O}(\varepsilon^2) = \\ &= E_{\mathrm{kin}}(f_0) - 4\pi\, \varepsilon\, \frac{\sin(\sqrt{\lambda}\,t)}{\sqrt{\lambda}} \int_0^\infty r^2\, U_0'(r)\, j_g(r)\, \mathrm{d}r + \mathcal{O}(\varepsilon^2), \end{aligned} \tag{3.1.21}$$

[53] It is proven in Lemma 4.5.2 that the linearised operator is indeed self-adjoint when defined properly. The symmetry of $\mathcal{L}$ is also formally explained in [8, 71].

[54] A precise definition of this class of equilibria is given in Section 4.1.

and, by using (3.1.11),

$$E_{\mathrm{pot}}(f_0 + \varepsilon f(t) + \mathcal{O}(\varepsilon^2)) = E_{\mathrm{pot}}(f_0) + 4\pi\,\varepsilon\,\frac{\sin(\sqrt{\lambda}\,t)}{\sqrt{\lambda}} \int_0^\infty r^2\,U_0'(r)\,j_g(r)\,\mathrm{d}r + \mathcal{O}(\varepsilon^2). \tag{3.1.22}$$

This shows that the kinetic and potential energies of the formal expression $f_0 + \varepsilon f + \mathcal{O}(\varepsilon^2)$ oscillate about the respective energies of the steady state f_0 up to higher-order terms in $\varepsilon \ll 1$. In Section 8.4, we will conduct a numerical analysis to investigate whether such oscillations of E_{kin} and E_{pot} can indeed be observed for solutions of the (non-linearised) Vlasov-Poisson system.

However, as discussed in the introduction, the expansion and contraction of the spatial support of solutions of the non-linearised system cannot be explained with the present, Eulerian linearisation; observe that the phase space support of $f_\pm(t)$ defined by (3.1.16) and (3.1.18) is time-independent. This is the reason why we present two additional linearisation schemes in the following sections, aiming to explain this phenomenon.

3.2 The Mass-Lagrangian Picture

The following derivation is based on the so-called mass-Lagrange coordinates which are often used in the context of the radial Euler-Poisson system, cf. [75, 107]. We restrict ourselves from the start to the spherically symmetric situation, recall Definition 2.1.1 and Remark 2.1.2. In contrast to the linearisation schemes from Sections 3.1 and 3.3, it is essential in the present context to assume spherical symmetry from the beginning.

We first derive the radial Vlasov-Poisson system in mass coordinates before developing a suitable Lagrangian linearisation scheme.

The Radial Vlasov-Poisson System in Mass Coordinates

Let $f = f(t, r, w, L) \geq 0$ be a solution of the radial Vlasov-Poisson system (2.1.9)–(2.1.11) with finite mass and compact support (in phase space). As usual, let $\rho = \rho(t, r)$ denote the associated mass density.

We assume that the solution consists of one connected radial region, i.e., there exist non-negative functions $R_\pm = R_\pm(t)$ s.t.

$$\{r > 0 \mid \rho(t, r) > 0\} =]R_-(t), R_+(t)[. \tag{3.2.1}$$

This assumption simplifies much of the following calculations, but we expect that it can be weakened. Notice, however, that this assumption is reasonable for solutions close to the steady state f_0, because the latter satisfies (3.2.1) by Proposition 2.2.9 (c). Further note that choosing $R_-(t) \equiv 0$ yields the natural situation of a solution with no inner radial vacuum region; this case is covered in [62, Sc. 3.2].

We consider the *local mass* function m defined by

$$m(t, r) \coloneqq 4\pi \int_0^r s^2 \rho(t, s)\,\mathrm{d}s, \qquad r > 0; \tag{3.2.2}$$

the value $m(t, r)$ gives the amount of mass within the ball of radius $r > 0$ centred around the spatial origin at time t. Accordingly, the *total mass* is

$$M \coloneqq \lim_{r\to\infty} m(t, r) = 4\pi \int_0^\infty s^2 \rho(t, s)\,\mathrm{d}s = m(t, R_+(t)) < \infty; \tag{3.2.3}$$

note that M is time-independent since the total mass is a conserved quantity of the Vlasov-Poisson system, cf. [143, Sc. 1.5]. Differentiating (3.2.2) radially yields

$$\partial_r m(t,r) = 4\pi r^2 \rho(t,r), \tag{3.2.4}$$

i.e., $\partial_r m(t,r) > 0$ for $R_-(t) < r < R_+(t)$ by (3.2.1). Hence, $m(t)\colon]R_-(t), R_+(t)[\to]0, M[$ is strictly increasing and possesses an inverse

$$\tilde{r}(t)\colon]0, M[\to]R_-(t), R_+(t)[,\ m \mapsto \tilde{r}(t,m). \tag{3.2.5}$$

The (physical) interpretation of $\tilde{r}(t,m)$ is that it gives the radius of the ball around the origin in which the mass $m \in]0, M[$ of the solution $f(t)$ is contained; in the physics literature, $\tilde{r}(t,m)$ is occasionally referred to as a *Lagrangian radius* [168]. This defines a change of variables which we use to express the unknowns in the *mass coordinates* (m, w, L), i.e., we consider

$$\tilde{f}(t,m,w,L) = f(t,\tilde{r},w,L), \qquad \tilde{\rho}(t,m) = \rho(t,\tilde{r}), \tag{3.2.6}$$

where $\tilde{r} = \tilde{r}(t,m)$. Furthermore, for a function $g = g(\cdot, w, L)$ we introduce the abbreviations

$$\mathcal{Q}(g) \coloneqq \int_0^\infty \int_{\mathbb{R}} g(\cdot,w,L)\,\mathrm{d}w\,\mathrm{d}L, \qquad \mathcal{J}(g) \coloneqq \int_0^\infty \int_{\mathbb{R}} w\, g(\cdot,w,L)\,\mathrm{d}w\,\mathrm{d}L, \tag{3.2.7}$$

so that

$$\rho(t) = \frac{\pi}{r^2}\,\mathcal{Q}(f(t)), \qquad \tilde{\rho}(t) = \frac{\pi}{\tilde{r}^2}\mathcal{Q}(\tilde{f}(t)). \tag{3.2.8}$$

In order to express the Vlasov equation in mass coordinates, we use (2.1.9) and (2.1.11) to compute

$$\partial_t m(t,r) = 4\pi \int_0^r s^2 \partial_t \rho(t,s)\,\mathrm{d}s = -4\pi^2 \int_0^r \partial_r \mathcal{J}(f(t))(s)\,\mathrm{d}s = -4\pi^2 \mathcal{J}(f(t))(r); \tag{3.2.9}$$

note that there are no boundary terms when integrating by parts in the second identity because $f(t)$ is assumed to be compactly supported. Furthermore, in the last identity we used that $\mathcal{J}(f(t))(0) = 0$, which can, e.g., be verified by repeating the calculation (3.2.9) with $r = R_+(t)$. Hence, applying the chain rule yields

$$\partial_t f = \partial_t \tilde{f} + \partial_m \tilde{f}\,\partial_t m = \partial_t \tilde{f} - 4\pi^2 \mathcal{J}(\tilde{f}(t))\,\partial_m \tilde{f}, \tag{3.2.10}$$

$$\partial_r f = \partial_m \tilde{f}\,\partial_r m = 4\pi^2 \mathcal{Q}(\tilde{f}(t))\,\partial_m \tilde{f}, \tag{3.2.11}$$

and the radial Vlasov equation (2.1.9) takes the form

$$\partial_t \tilde{f} + 4\pi^2 \Big(w\,\mathcal{Q}(\tilde{f}(t)) - \mathcal{J}(\tilde{f}(t)) \Big)\,\partial_m \tilde{f} + \left(\frac{L}{\tilde{r}^3} - \frac{m}{\tilde{r}^2} \right) \partial_w \tilde{f} = 0. \tag{3.2.12}$$

In order to derive a relation between the functions $\tilde{r}$ and $\tilde{f}$, observe that

$$\partial_m \tilde{r}(t,m) = \frac{1}{4\pi^2 \mathcal{Q}(\tilde{f}(t))(m)} \tag{3.2.13}$$

for $0 < m < M$ by (3.2.4), (3.2.8), and the inverse function theorem. Integrating this equation yields

$$\tilde{r}(t,m) = R_-(t) + \frac{1}{4\pi^2} \int_0^m \frac{\mathrm{d}\mu}{\mathcal{Q}(\tilde{f}(t))(\mu)} \tag{3.2.14}$$

for $0 < m < M$; note that, by (3.2.1), $\tilde{r}(t,0) = R_-(t)$ extends $\tilde{r}$ suitably.

We refer to the equations (3.2.12) and (3.2.14) as the *(radial) Vlasov-Poisson system in mass coordinates*, where we recall the abbreviations introduced in (3.2.7). Note that the function $R_- = R_-(t)$ is now a prescribed parameter of the system which determines the inner boundary of the radial support of the solution.[55] Another parameter is the total mass $M > 0$ determining the range of the mass variable m. To the author's knowledge, the Vlasov-Poisson system has never been written down in these coordinates before (except of [62, Sc. 3.2]). In particular, there are no existence results known for this system. In the present thesis, we do not go into the existence theory of the Vlasov-Poisson system in mass coordinates because we only use this system to formally derive an alternative linearisation scheme. Nonetheless, analysing which choices of $R_-(t)$ and M (and initial conditions $\tilde{r}(0)$ and $\tilde{f}(0)$) yield suitable solutions of this system is an interesting question for future work.

Before proceeding, we derive a further identity for $\tilde{r}$ which will be useful below. The first step is to observe that $\tilde{r}(t, m(t,r)) = r$ for $r \in]R_-(t), R_+(t)[$, which implies

$$\begin{aligned} 0 = \partial_t[\tilde{r}(t,m(t,r))] &= \partial_t\tilde{r}(t,m(t,r)) + \partial_m\tilde{r}(t,m(t,r))\,\partial_t m(t,r) = \\ &= \partial_t\tilde{r}(t,m(t,r)) - \frac{\mathcal{J}(f(t))(r)}{\mathcal{Q}(\tilde{f}(t))(m(t,r))} \end{aligned} \tag{3.2.15}$$

by (3.2.9) and (3.2.13). Hence, inserting $r = \tilde{r}(t,m)$ into this equation yields the identity

$$\partial_t\tilde{r}(t,m) = \frac{\mathcal{J}(\tilde{f}(t))(m)}{\mathcal{Q}(\tilde{f}(t))(m)} \tag{3.2.16}$$

for $0 < m < M$.

The Radial Vlasov-Poisson System in Mass-Lagrange Coordinates

Now let $f_0 = f_0(r,w,L)$ be a steady state of the Vlasov-Poisson system as stated at the start of this chapter and let $f = f(t,r,w,L)$ be as above. In addition, we assume that f has the same mass as the steady state f_0, i.e., $M = M_0$; recall the definitions of M_0 and M in (2.2.11) and (3.2.3), respectively. We note that this condition is rather natural from a physics point of view because it is, e.g., satisfied by so-called dynamically accessible perturbations, see [118, Sc. VI.C] for a detailed discussion of this concept.

Therefore, the mapping

$$m_0\colon [R_{\min}, R_{\max}] \to [0,M],\ m_0(r) = 4\pi\int_0^r s^2\rho_0(s)\,\mathrm{d}s \tag{3.2.17}$$

is one-to-one by Proposition 2.2.9. Let

$$\bar{r}\colon [0,M] \to [R_{\min}, R_{\max}],\ m \mapsto \bar{r}(m) \tag{3.2.18}$$

denote the inverse of m_0. We now express the unknowns in this new radial variable:

$$\hat{f}(t,\bar{r},w,L) = \tilde{f}(t,m,w,L) = f(t,\tilde{r},w,L), \qquad \hat{\rho}(t,\bar{r}) = \tilde{\rho}(t,m) = \rho(t,\tilde{r}), \tag{3.2.19}$$

[55] Alternatively, one could prescribe the outer radius $R_+(t)$ instead of $R_-(t)$ by replacing (3.2.14) with

$$\tilde{r}(t,m) = R_+(t) - \frac{1}{4\pi^2}\int_m^M \frac{\mathrm{d}\mu}{\mathcal{Q}(\tilde{f}(t))(\mu)};$$

this identity follows by integrating (3.2.13) and using the extension $\tilde{r}(t,M) = R_+(t)$.

where $m = m_0(\bar{r})$ and $\tilde{r} = \tilde{r}(t, m) = \tilde{r}(t, m_0(\bar{r}))$. If we further set

$$\hat{r}(t)\colon]R_{\min}, R_{\max}[\to]R_-(t), R_+(t)[,\ \hat{r}(t,\bar{r}) \coloneqq \tilde{r}(t, m_0(\bar{r})), \tag{3.2.20}$$

the equations (3.2.12) and (3.2.14) become

$$\partial_t \hat{f} + \left(w\, \frac{\mathcal{Q}(\hat{f}(t))}{\mathcal{Q}(f_0)} - \frac{\mathcal{J}(\hat{f}(t))}{\mathcal{Q}(f_0)} \right) \partial_{\bar{r}} \hat{f} + \left(\frac{L}{\hat{r}^3} - \frac{m_0(\bar{r})}{\hat{r}^2} \right) \partial_w \hat{f} = 0, \tag{3.2.21}$$

$$\hat{r}(t,\bar{r}) = R_-(t) + \int_{R_{\min}}^{\bar{r}} \frac{\mathcal{Q}(f_0)(s)}{\mathcal{Q}(\hat{f}(t))(s)}\, \mathrm{d}s; \tag{3.2.22}$$

where we used that $\partial_{\bar{r}} m = 4\pi^2 \mathcal{Q}(f_0)$ and (3.2.22) is obtained from (3.2.14) via the change of variables $s \mapsto \mu = m_0(s)$. The ball of radius $\hat{r}(t,\bar{r})$ around the origin contains for the time dependent solution $f(t)$ the same amount of mass as the ball of radius $\bar{r}$ does for the steady state f_0, i.e., $m(t, \hat{r}(t,\bar{r})) = m_0(\bar{r})$. In this way the steady state's mass distribution is used as the reference frame for describing the mass distribution of the time dependent solution. We hence refer to the system (3.2.21)–(3.2.22) as the *(radial) Vlasov-Poisson system in mass-Lagrange coordinates*.

Moreover, observe that the identity (3.2.16) translates to

$$\partial_t \hat{r}(t,\bar{r}) = \frac{\mathcal{J}(\hat{f}(t))(\bar{r})}{\mathcal{Q}(\hat{f}(t))(\bar{r})} \tag{3.2.23}$$

for $R_{\min} < \bar{r} < R_{\max}$.

Linearisation in Mass-Lagrange Coordinates

In order to linearise the Vlasov-Poisson system in mass-Lagrange coordinates (3.2.21)–(3.2.22) around the steady state f_0, we again consider the formal expressions

$$\hat{f} = f_0 + \varepsilon\, \delta\hat{f} + \mathcal{O}(\varepsilon^2), \qquad \hat{\rho} = \rho_0 + \varepsilon\, \delta\hat{\rho} + \mathcal{O}(\varepsilon^2), \tag{3.2.24}$$

as well as

$$\hat{r}(t,\bar{r}) = \bar{r} + \varepsilon\, \delta\hat{r}(t,\bar{r}) + \mathcal{O}(\varepsilon^2) \tag{3.2.25}$$

with $0 < \varepsilon \ll 1$. In particular, inserting $\bar{r} = R_{\min}$ and $\bar{r} = R_{\max}$ into the latter expression implies that $R_\pm(t)$ possess the expansions

$$R_-(t) = R_{\min} + \varepsilon\, \delta R_-(t) + \mathcal{O}(\varepsilon^2), \qquad R_+(t) = R_{\max} + \varepsilon\, \delta R_+(t) + \mathcal{O}(\varepsilon^2) \tag{3.2.26}$$

with $\delta R_-(t) = \delta\hat{r}(t, R_{\min})$ and $\delta R_+(t) = \delta\hat{r}(t, R_{\max})$; it is straight-forward to extend the definition (3.2.20) of $\hat{r}$ to $\bar{r} = R_{\min}$ and $\bar{r} = R_{\max}$.

We now expand (3.2.21)–(3.2.22) to first order in $0 < \varepsilon \ll 1$, i.e., we insert the formal expressions (3.2.24)–(3.2.26) into the system, use that the steady state solves the system, and dispense with higher-order terms in ε. With the transport operator now being of the form

$$\mathcal{T} = w\, \partial_{\bar{r}} - \left(\frac{m_0(\bar{r})}{\bar{r}^2} - \frac{L}{\bar{r}^3} \right) \partial_w, \tag{3.2.27}$$

we arrive at the system

$$\partial_t \delta\hat{f} + \mathcal{T}\delta\hat{f} + \left(w\,\frac{\mathcal{Q}(\delta\hat{f})}{\mathcal{Q}(f_0)} - \frac{\mathcal{J}(\delta\hat{f})}{\mathcal{Q}(f_0)} \right) \partial_{\bar{r}} f_0 + \left(\frac{2m_0(\bar{r})}{\bar{r}^3} - \frac{3L}{\bar{r}^4} \right) \delta\hat{r}\,\partial_w f_0 = 0, \tag{3.2.28}$$

$$\delta\hat{r}(t,\bar{r}) = \delta R_-(t) - \int_{R_{\min}}^{\bar{r}} \frac{\mathcal{Q}(\delta\hat{f}(t))(s)}{\mathcal{Q}(f_0)(s)}\,\mathrm{d}s; \tag{3.2.29}$$

note that $\mathcal{J}(f_0) = 0$ because f_0 is even in w. Furthermore, linearising the identity (3.2.23) yields

$$\partial_t \delta\hat{r}(t,\bar{r}) = \frac{\mathcal{J}(\delta\hat{f}(t))(\bar{r})}{\mathcal{Q}(f_0)(\bar{r})}. \tag{3.2.30}$$

The next step is to transform the linearised system (3.2.28)–(3.2.29) into a second-order system. This is achieved similarly to the Eulerian picture, i.e., we apply the Antonov trick and split the linear perturbation $\delta\hat{f}$ into its even and odd part in the (radial) velocity w:

$$\delta\hat{f} = \delta\hat{f}_+ + \delta\hat{f}_-, \tag{3.2.31}$$

where

$$\delta\hat{f}_\pm(t,\bar{r},w,L) = \frac{1}{2}\Big(\delta\hat{f}(t,\bar{r},w,L) \pm \delta\hat{f}(t,\bar{r},-w,L)\Big). \tag{3.2.32}$$

Before deriving suitable identities for these functions, note that $\mathcal{Q}(\delta\hat{f}(t)) = \mathcal{Q}(\delta\hat{f}_+(t))$, $\mathcal{J}(\delta\hat{f}(t)) = \mathcal{J}(\delta\hat{f}_-(t))$, and that the transport operator (3.2.27) reverses w-parity, i.e., $\mathcal{T}(\delta\hat{f}_\pm) = (\mathcal{T}\delta\hat{f})_\mp$. Moreover, the ansatz (2.2.6) for f_0 implies that f_0 and $\partial_{\bar{r}} f_0$ are even in w while $\partial_w f_0$ is odd in w. Hence, (3.2.28)–(3.2.29) decomposes into even and odd parts in w as follows:

$$\partial_t \delta\hat{f}_+ + \mathcal{T}(\delta\hat{f}_-) - \frac{\mathcal{J}(\delta\hat{f}_-)}{\mathcal{Q}(f_0)}\,\partial_{\bar{r}} f_0 = 0, \tag{3.2.33}$$

$$\partial_t \delta\hat{f}_- + \mathcal{T}(\delta\hat{f}_+) + w\,\frac{\mathcal{Q}(\delta\hat{f}_+)}{\mathcal{Q}(f_0)}\,\partial_{\bar{r}} f_0 + \left(\frac{2m_0(\bar{r})}{\bar{r}^3} - \frac{3L}{\bar{r}^4} \right) \delta\hat{r}\,\partial_w f_0 = 0, \tag{3.2.34}$$

$$\delta\hat{r}(t,\bar{r}) = \delta R_-(t) - \int_{R_{\min}}^{\bar{r}} \frac{\mathcal{Q}(\delta\hat{f}_+(t))(s)}{\mathcal{Q}(f_0)(s)}\,\mathrm{d}s. \tag{3.2.35}$$

In order to calculate the t-derivative of (3.2.34), we first use (3.2.27) and (3.2.33) to infer

$$\begin{aligned} \partial_t \mathcal{Q}(\delta\hat{f}_+(t)) &= -\mathcal{Q}(\mathcal{T}(\delta\hat{f}_-)) + \frac{\mathcal{J}(\delta\hat{f}_-)}{\mathcal{Q}(f_0)}\,\mathcal{Q}(\partial_{\bar{r}} f_0) = \\ &= -\partial_{\bar{r}}\mathcal{J}(\delta\hat{f}_-) + \frac{\mathcal{J}(\delta\hat{f}_-)}{\mathcal{Q}(f_0)}\,\partial_{\bar{r}}\mathcal{Q}(f_0) = -\mathcal{Q}(f_0)\,\partial_{\bar{r}}\left[\frac{\mathcal{J}(\delta\hat{f}_-)}{\mathcal{Q}(f_0)} \right]. \end{aligned} \tag{3.2.36}$$

Then, differentiating (3.2.34) w.r.t. t and inserting (3.2.30), (3.2.33), and (3.2.36) leads to

$$\begin{aligned} 0 = \partial_t^2 \delta\hat{f}_- - \mathcal{T}^2\delta\hat{f}_- + \mathcal{T}\left(\frac{\mathcal{J}(\delta\hat{f}_-)}{\mathcal{Q}(f_0)}\,\partial_{\bar{r}} f_0 \right) - w\,\partial_{\bar{r}}\left[\frac{\mathcal{J}(\delta\hat{f}_-)}{\mathcal{Q}(f_0)} \right] \partial_{\bar{r}} f_0 + \\ + \left(\frac{2m_0(\bar{r})}{\bar{r}^3} - \frac{3L}{\bar{r}^4} \right) \frac{\mathcal{J}(\delta\hat{f}_-)}{\mathcal{Q}(f_0)}\,\partial_w f_0 = \\ = \partial_t^2 \delta\hat{f}_- - \mathcal{T}^2\delta\hat{f}_- - \mathcal{R}\delta\hat{f}_-, \end{aligned} \tag{3.2.37}$$

where

$$\mathcal{R}g \coloneqq -\mathcal{T}\left(\frac{\mathcal{J}(g)}{\mathcal{Q}(f_0)}\,\partial_{\bar r} f_0\right) + w\,\partial_{\bar r}\left[\frac{\mathcal{J}(g)}{\mathcal{Q}(f_0)}\right]\partial_{\bar r} f_0 - \left(\frac{2m_0(\bar r)}{\bar r^3} - \frac{3L}{\bar r^4}\right)\frac{\mathcal{J}(g)}{\mathcal{Q}(f_0)}\,\partial_w f_0 \tag{3.2.38}$$

for suitable odd-in-w functions $g = g(\bar r, w, L)$. Using the ansatz (2.2.6) for f_0 and the structure of the transport operator (3.2.27) allows us to simplify the latter expression:

$$\begin{aligned}\mathcal{R}g &= \partial_E\varphi(E,L)\left[-\mathcal{T}\left(\frac{\mathcal{J}(g)}{\mathcal{Q}(f_0)}\,\partial_{\bar r}E\right) + w\,\partial_{\bar r}\left[\frac{\mathcal{J}(g)}{\mathcal{Q}(f_0)}\right]\partial_{\bar r}E - w\left(\frac{2m_0(\bar r)}{\bar r^3} - \frac{3L}{\bar r^4}\right)\frac{\mathcal{J}(g)}{\mathcal{Q}(f_0)}\right] = \\ &= \partial_E\varphi(E,L)\left[-w\,\frac{\mathcal{J}(g)}{\mathcal{Q}(f_0)}\,\partial_{\bar r}^2 E - w\,\frac{\mathcal{J}(g)}{\mathcal{Q}(f_0)}\left(\frac{2m_0(\bar r)}{\bar r^3} - \frac{3L}{\bar r^4}\right)\right] = \\ &= -4\pi^2\partial_E\varphi(E,L)\,\frac{w}{\bar r^2}\,\mathcal{J}(g),\end{aligned} \tag{3.2.39}$$

where we used the fact that $\mathcal{T}(\partial_E\varphi(E,L)) = 0$ in the first equation and

$$\partial_{\bar r}^2 E = \partial_{\bar r}^2\left[\frac{1}{2}w^2 + U_0 + \frac{L}{2\bar r^2}\right] = -\frac{2m_0}{\bar r^3} + \frac{4\pi^2}{\bar r^2}\,\mathcal{Q}(f_0) + \frac{3L}{\bar r^4} \tag{3.2.40}$$

in the last equation of (3.2.39).

We have therefore shown that the linearised dynamics in mass-Lagrange coordinates is governed by the equation

$$\partial_t^2\delta\hat f_- + \mathcal{L}\delta\hat f_- = 0, \tag{3.2.41}$$

where the linearised operator $\mathcal{L}$ is again of the form (1.2.9). In particular, comparing (3.2.39) to (3.1.13) shows that $\mathcal{R}$ is indeed identical to the response operator in the Eulerian picture.

Assume now that $\lambda > 0$ is an eigenvalue of $\mathcal{L} = -\mathcal{T}^2 - \mathcal{R}$ with corresponding odd-in-w eigenfunction $g = g(r, w, L)$. Then $\delta\hat f_-(t) = \cos(\sqrt{\lambda}\,t)g$ solves the linearized system (3.2.37). If we impose the initial condition $\delta\hat r(0) = 0$, (3.2.25) and (3.2.30) yield

$$\hat r(t,\bar r) = \bar r + \varepsilon\,\frac{\sin(\sqrt{\lambda}\,t)}{\sqrt{\lambda}}\,\frac{\mathcal{J}(g)}{\mathcal{Q}(f_0)}(\bar r) + \mathcal{O}(\varepsilon^2). \tag{3.2.42}$$

Hence, to linear order, the radius of the ball containing a certain mass oscillates around the corresponding radius $\bar r$ for the steady state. Note that the period of this oscillation is $\frac{2\pi}{\sqrt{\lambda}}$, which is the same as in the Eulerian picture. Of course, the details of the oscillation – like which portions of the configuration take part in it – depend on the actual eigenfunction g, but, to linear order, (3.2.42) still nicely explains the pulsating behaviour of the solution in the case of a positive eigenvalue of $\mathcal{L}$.

3.3 The Lagrangian Picture

The main concept in this section is to interpret a solution of the Vlasov-Poisson system as redistributing the particles in phase space. We first derive the system for the mapping which describes this redistribution process before linearising it.

The Lagrangian Formulation of the Vlasov-Poisson System

We study the initial value problem for the Vlasov-Poisson system (1.1.2)–(1.1.5) with initial data

$$\mathring f = f_0 \circ \mathring Z^{-1}, \tag{3.3.1}$$

where f_0 is the fixed steady state and

$$\mathring{Z}\colon \Omega_0 \to \Omega^0 \tag{3.3.2}$$

is a diffeomorphism onto some open set $\Omega^0 \subset \mathbb{R}^3 \times \mathbb{R}^3$; recall the definition (2.2.44) of Ω_0. We further assume that $\mathring{Z}$ is measure-preserving, i.e., $\det \partial_z \mathring{Z} = 1$ on Ω_0, where we use the notation $z = (x, v)$. Initial data of the form (3.3.1) are said to be *dynamically accessible* from the steady state f_0, cf. [118, Sc. VI.C], and are particularly natural from a physics point of view as, e.g., an external force acting on the equilibrium leads to such perturbations.

We describe the solution of the Vlasov-Poisson system induced by the initial value $\mathring{f}$ using the time-dependent family

$$Z(t) = (X(t), V(t))\colon \Omega_0 \to \Omega^t \tag{3.3.3}$$

of measure-preserving diffeomorphisms onto open sets $\Omega^t \subset \mathbb{R}^3 \times \mathbb{R}^3$ s.t.

$$\dot{X} = V, \qquad \dot{V} = -\partial_x U_{Z(t)}(X), \tag{3.3.4}$$

where

$$U_{Z(t)}(x) = -\int_{\mathbb{R}^3\times\mathbb{R}^3} \frac{f_0(\tilde{z})}{|x - X(t,\tilde{z})|}\,\mathrm{d}\tilde{z}, \quad \partial_x U_{Z(t)}(x) = \int_{\mathbb{R}^3\times\mathbb{R}^3} \frac{x - X(t,\tilde{z})}{|x - X(t,\tilde{z})|^3}\, f_0(\tilde{z})\,\mathrm{d}\tilde{z}. \tag{3.3.5}$$

We refer to (3.3.4)–(3.3.5) as the *Lagrangian formulation of the Vlasov-Poisson system*. The basic unknown of this system is the *flow map* $Z(t)$ and the configuration space is the set of measure-preserving diffeomorphisms. The mathematical structure of this configuration space is studied in [38, Sc. 4], see also [109]. The initial condition becomes

$$Z(0) = \mathring{Z}. \tag{3.3.6}$$

If $Z(t)$ is a solution of this initial value problem, $f(t,z) = f_0(Z(t)^{-1}(z))$, extended by 0 outside $\Omega^t = Z(t, \Omega_0)$, defines a solution of the corresponding initial value problem for the original Vlasov-Poisson system (provided that the steady state f_0 is sufficiently regular) with $\operatorname{supp}(f(t)) = \overline{\Omega^t}$. This can be verified by using the relation between the Vlasov equation and the characteristic flow $Z(t) \circ \mathring{Z}^{-1}$, cf. [143, Lemma 1.3].

Conversely, let f be a sufficiently regular solution[56] of the Vlasov-Poisson system (1.1.2)–(1.1.5) satisfying the initial condition $f(0) = \mathring{f}$. We then define $Z(t) = (X, V)(t)\colon \Omega_0 \to \mathbb{R}^3 \times \mathbb{R}^3$ as the solution of

$$\dot{X} = V, \qquad \dot{V} = -\partial_x U(t, X), \qquad (X, V)(0, x, v) = \mathring{Z}(x, v), \tag{3.3.7}$$

where $U = U(t,x)$ is the gravitational potential associated to f. Since $f(t,z) = f_0(Z(t)^{-1}(z))$ by (3.3.1) and [143, Lemma 1.3(b)], it is straight-forward to verify that Z indeed solves (3.3.4)–(3.3.6).

Linearisation in the Lagrangian Formulation

We now linearise the Vlasov-Poisson system in the Lagrangian formulation (3.3.4)–(3.3.5) around the steady state f_0; see [172, Sc. III] for a related approach. In the Lagrangian

[56] The regularity of f is required for the regularity of Z. For example, if f is a classical solution in the sense of [143, Sc. 1.2], $Z(t)\colon \Omega_0 \to Z(t, \Omega_0)$ defined by (3.3.7) is indeed a measure-preserving diffeomorphism, cf. [143, Lemma 1.2].

formulation, the equilibrium state corresponds to the initial condition $\mathring{Z} = \mathrm{id}$. We denote the solution of (3.3.4)–(3.3.5) with $Z(0) = \mathrm{id}$ by $Z_0(t)$, which is the characteristic flow of the steady state.

For small perturbations of the steady state it is expected that $Z(t) \circ Z_0(t)^{-1}$ remains close to the identity. Hence, the natural definition of the linear perturbation δZ is given through the (formal) expansion

$$Z(t) \circ Z_0(t)^{-1} = \mathrm{id} + \varepsilon\, \delta Z(t) + \mathcal{O}(\varepsilon^2), \tag{3.3.8}$$

or equivalently,

$$Z(t) = Z_0(t) + \varepsilon\, \delta Z(t) \circ Z_0(t) + \mathcal{O}(\varepsilon^2), \tag{3.3.9}$$

for $0 < \varepsilon \ll 1$. Differentiating (3.3.9) w.r.t. t and linearising, i.e., dropping higher-order terms in ε, leads to

$$\dot{Z} = \dot{Z}_0 + \varepsilon\, [(\partial_t + \mathcal{T})\delta Z] \circ Z_0, \tag{3.3.10}$$

where $\mathcal{T} = v \cdot \partial_x - \partial_x U_0 \cdot \partial_v$ is again the transport operator of the steady state. In order to derive a system governing the evolution of $\delta Z(t)$ we expand the right-hand side of (3.3.4), in particular, the force term $\partial_x U_{Z(t)}$ defined in (3.3.5): First observe

$$\partial_x U_{Z_0(t)+\varepsilon\, \delta Z(t,Z_0(t))}(X_0(t) + \varepsilon\, \delta X(t, Z_0(t))) = \partial_x U_{Z_0(t)}(X_0(t)) + \varepsilon\, I_1 + \varepsilon\, I_2, \tag{3.3.11}$$

where we again dropped the higher-order terms in ε and introduce the abbreviations

$$I_1 = I_1(t,z) \coloneqq \partial_\varepsilon\big|_{\varepsilon=0} \partial_x U_{Z_0(t)}(X_0(t,z) + \varepsilon\, \delta X(t, Z_0(t,z))), \tag{3.3.12}$$

$$I_2 = I_2(t,z) \coloneqq \partial_\varepsilon\big|_{\varepsilon=0} \partial_x U_{Z_0(t)+\varepsilon\, \delta Z(t,Z_0(t))}(X_0(t,z)). \tag{3.3.13}$$

Since $U_{Z_0(t)} = U_0$ is the gravitational potential of the steady state and thus smooth, we deduce

$$I_1 = D^2 U_0(X_0(t,z))\, \delta X(t, Z_0(t,z)), \tag{3.3.14}$$

where $D^2 U_0$ denotes the Hessian matrix of U_0. Computing I_2 is harder because ε is part of the function generating the potential. We resolve this problem by rewriting I_2 s.t. the ε-dependence is again contained in the argument of a suitable potential. Multiplying I_2 with a test function $\psi \in C_c^\infty(\Omega_0)$ and integrating w.r.t. $z \in \Omega_0$ leads to

$$\begin{aligned}
&\int_{\mathbb{R}^3\times\mathbb{R}^3} I_2(z)\, \psi(z)\, \mathrm{d}z = \\
&= \int_{\mathbb{R}^3\times\mathbb{R}^3} f_0(\tilde{z})\, \partial_\varepsilon\big|_{\varepsilon=0} \left[\int_{\mathbb{R}^3\times\mathbb{R}^3} \frac{X_0(t,z) - (X_0(t,\tilde{z}) + \varepsilon\, \delta X(t, Z_0(t,\tilde{z})))}{|X_0(t,z) - (X_0(t,\tilde{z}) + \varepsilon\, \delta X(t, Z_0(t,\tilde{z})))|^3}\, \psi(z)\, \mathrm{d}z \right] \mathrm{d}\tilde{z} = \\
&= \int_{\mathbb{R}^3\times\mathbb{R}^3} f_0(\tilde{z})\, \partial_\varepsilon\big|_{\varepsilon=0} \left[- \int_{\mathbb{R}^3\times\mathbb{R}^3} \frac{X_0(t,\tilde{z}) + \varepsilon\, \delta X(t, Z_0(t,\tilde{z})) - \bar{x}}{|X_0(t,\tilde{z}) + \varepsilon\, \delta X(t, Z_0(t,\tilde{z})) - \bar{x}|^3}\, \psi(Z_0(t)^{-1}(\bar{z}))\, \mathrm{d}\bar{z} \right] \mathrm{d}\tilde{z}
\end{aligned} \tag{3.3.15}$$

by inserting (3.3.5) and using the measure-preserving change of variables $\bar{z} = Z_0(t,z)$. In order to rewrite the latter expression, we introduce the notation

$$U^\psi_{Z_0(t)}(x) \coloneqq - \int_{\mathbb{R}^3\times\mathbb{R}^3} \frac{\psi(\bar{z})}{|x - X_0(t,\bar{x})|}\, \mathrm{d}\bar{z} = - \int_{\mathbb{R}^3\times\mathbb{R}^3} \frac{\psi(Z_0(t)^{-1}(\bar{z}))}{|x - \bar{x}|}\, \mathrm{d}\bar{z}, \qquad x \in \mathbb{R}^3, \tag{3.3.16}$$

for the gravitational potential generated by $\psi \circ Z_0(t)^{-1}$. This potential is again smooth and, continuing the calculation (3.3.15), we arrive at

$$\begin{aligned}\int_{\mathbb{R}^3\times\mathbb{R}^3} I_2(z)\,\psi(z)\,\mathrm{d}z &= \\ &= -\int_{\mathbb{R}^3\times\mathbb{R}^3} f_0(\tilde{z})\,\partial_\varepsilon\big|_{\varepsilon=0}\Big[\partial_x U^\psi_{Z_0(t)}(X_0(t,\tilde{z})+\varepsilon\,\delta X(t,Z_0(t,\tilde{z})))\Big]\,\mathrm{d}\tilde{z} = \\ &= -\int_{\mathbb{R}^3\times\mathbb{R}^3} f_0(\tilde{z})\,D^2U^\psi_{Z_0(t)}(X_0(t,\tilde{z}))\,\delta X(t,Z_0(t,\tilde{z}))\,\mathrm{d}\tilde{z}. \end{aligned} \tag{3.3.17}$$

Reversing the change of variables performed in (3.3.15) and changing the order of integration then yields

$$\int_{\mathbb{R}^3\times\mathbb{R}^3} I_2(z)\,\psi(z)\,\mathrm{d}z = -\int_{\mathbb{R}^3\times\mathbb{R}^3} \psi(z)\,\partial_x \mathrm{div}_x \tilde{U}_{\delta X(t)}(X_0(t,z))\,\mathrm{d}z, \tag{3.3.18}$$

where

$$\tilde{U}_{\delta X(t)}(x) \coloneqq -\int_{\mathbb{R}^3\times\mathbb{R}^3} \frac{f_0(\tilde{z})}{|x-\tilde{x}|}\,\delta X(t,\tilde{z})\,\mathrm{d}\tilde{z}, \qquad x\in\mathbb{R}^3, \tag{3.3.19}$$

is the gravitational potential generated by $f_0\,\delta X(t)$. Since ψ is arbitrary we hence conclude

$$I_2 = -\partial_x \mathrm{div}_x \tilde{U}_{\delta X(t)}(X_0(t,z)). \tag{3.3.20}$$

Inserting (3.3.10), (3.3.11), (3.3.14), and (3.3.20) into (3.3.4) and comparing terms linear in ε then results in

$$(\partial_t + \mathcal{T})\delta X = \delta V, \tag{3.3.21a}$$

$$(\partial_t + \mathcal{T})\delta V = -D^2U_0\,\delta X + \partial_x \mathrm{div}_x \tilde{U}_{\delta X}, \tag{3.3.21b}$$

where we again used that $Z_0(t)\colon \Omega_0 \to \Omega_0$ is a diffeomorphism. The system (3.3.21) is the *Lagrangian linearisation of the Vlasov-Poisson system*, which was previously stated in [172, Eqn. (6)].

In order to further analyse this system we use certain commutator relations between the transport operator $\mathcal{T}$ and derivatives w.r.t. x and v. For smooth functions $f\colon \mathbb{R}^3\times\mathbb{R}^3 \to \mathbb{R}$ and vector fields $F\colon \mathbb{R}^3\times\mathbb{R}^3 \to \mathbb{R}^3$ direct computation yields[57]

$$\mathcal{T}\partial_x f = \partial_x \mathcal{T} f + D^2U_0\,\partial_v f, \tag{3.3.22}$$

$$\mathcal{T}\partial_v f = \partial_v \mathcal{T} f - \partial_x f, \tag{3.3.23}$$

$$\mathcal{T}\mathrm{div}_x F = \mathrm{div}_x \mathcal{T} F + D^2U_0 \cdot D_v F, \tag{3.3.24}$$

$$\mathcal{T}\mathrm{div}_v F = \mathrm{div}_v \mathcal{T} F - \mathrm{div}_x F, \tag{3.3.25}$$

where the dot in (3.3.24) denotes the Frobenius inner product. Using (3.3.24) and (3.3.25) implies that every solution $\delta Z = (\delta X, \delta V)$ of the system (3.3.21) satisfies

$$\begin{aligned}(\partial_t + \mathcal{T})(\mathrm{div}_z \delta Z) &= (\partial_t + \mathcal{T})(\mathrm{div}_x \delta X + \mathrm{div}_v \delta V) = \\ &= D^2U_0 \cdot D_v \delta X + \mathrm{div}_x(\partial_t + \mathcal{T})\delta X - \mathrm{div}_x \delta V + \mathrm{div}_v(\partial_t + \mathcal{T})\delta V = \\ &= D^2U_0 \cdot D_v \delta X + \mathrm{div}_x \delta V - \mathrm{div}_x \delta V + \mathrm{div}_v(-D^2U_0 \delta X + \partial_x \mathrm{div}_x \tilde{U}_{\delta X(t)}) = 0. \end{aligned} \tag{3.3.26}$$

[57] Obviously, the same identities also hold when f or F are only defined on a subset of $\mathbb{R}^3\times\mathbb{R}^3$.

Because the unique solution of the initial value problem $(\partial_t + \mathcal{T})g = 0$, $g\big|_{t=0} = 0$ is given by $g(t,z) \equiv 0$, cf. [143, Lemma 1.3], the calculation (3.3.26) shows that $\mathrm{div}_z \delta Z(t) = 0$ for all t provided this is true for $t = 0$. In this situation, the flow δZ is measure preserving, i.e., phase space volume is preserved at the linear level. This property is required for the solution Z given by (3.3.9) to be in the configuration space of the (non-linearised) Lagrangian formulation of the Vlasov-Poisson system (3.3.4)–(3.3.5).

In what follows, we restrict δZ to a particular form which guarantees this preservation of phase space volume. Concretely, we assume that there exists a smooth function $h\colon \mathbb{R}\times\Omega_0 \to \mathbb{R}$, $(t,z) \mapsto h(t,z)$ s.t. δZ is the skew-gradient of h, i.e.,

$$\delta X = \partial_v h, \qquad \delta V = -\partial_x h. \tag{3.3.27}$$

We call h the *generating function* of the linear perturbation δZ. Inserting the ansatz (3.3.27) into (3.3.21) leads to the following system for the generating function:

$$(\partial_t + \mathcal{T})\partial_v h = -\partial_x h, \tag{3.3.28a}$$
$$(\partial_t + \mathcal{T})\partial_x h = D^2 U_0\, \partial_v h - \partial_x \mathrm{div}_x \tilde{U}_{\partial_v h}. \tag{3.3.28b}$$

Using the commutator identities (3.3.22) and (3.3.23) transforms this system into

$$\partial_v(\partial_t + \mathcal{T})h = 0, \tag{3.3.29a}$$
$$\partial_x(\partial_t + \mathcal{T})h = -\partial_x \mathrm{div}_x \tilde{U}_{\partial_v h}. \tag{3.3.29b}$$

Integrating (3.3.29a) in v using that $\{v \in \mathbb{R}^3 \mid (x,v) \in \Omega_0\}$ is connected for fixed $x \in \mathbb{R}^3$ then shows that (3.3.29) is equivalent to

$$(\partial_t + \mathcal{T})h = f(t,x) \tag{3.3.30}$$

for some $f\colon \mathbb{R}\times\mathbb{R}^3 \to \mathbb{R}$ with

$$\partial_x f = -\partial_x \mathrm{div}_x \tilde{U}_{\partial_v h}. \tag{3.3.31}$$

We next apply the Antonov trick similar to Section 3.1, i.e., we split the generating function $h = h(t,x,v)$ into its even-in-v and odd-in-v parts $h_\pm$. Decomposing (3.3.30) in a similar way leads to the system

$$\partial_t h_+ + \mathcal{T}(h_-) = f, \tag{3.3.32a}$$
$$\partial_t h_- + \mathcal{T}(h_+) = 0. \tag{3.3.32b}$$

After differentiating (3.3.32b) w.r.t. t, inserting (3.3.31) and (3.3.32a), and observing that $\partial_v h_+$ is odd in v and thus does not contribute to $\tilde{U}_{\partial_v h} = \tilde{U}_{\partial_v h_-}$ since f_0 is even in v, we arrive at

$$\partial_t^2 h_- - \mathcal{T}^2(h_-) - v \cdot \partial_x \mathrm{div}_x \tilde{U}_{\partial_v h_-} = 0. \tag{3.3.33}$$

This equation is the *second-order formulation of the Lagrangian linearisation of the Vlasov-Poisson system* for the ansatz (3.3.27) for δZ; recall that $\mathcal{T}$ is given by (1.2.10) and $\tilde{U}$ is defined in (3.3.19).

We again restrict the discussion to radial perturbations, i.e., we assume that the generating function h is spherically symmetric in the sense of Definition 2.1.1. By Remark 2.1.2 (b),

we may thus write $h = h(t,x,v) = h(t,r,w,L)$; analogous representations in (r,w,L)-coordinates also hold for $h_\pm$. Changing to radial variables allows us to rewrite the potential $\tilde{U}_{\partial_v h_-}$: First, we integrate by parts in v and insert (3.1.12) to obtain

$$\begin{aligned}\tilde{U}_{\partial_v h_-(t)}(x) &= -\int_{\mathbb{R}^3\times\mathbb{R}^3} \frac{f_0(\tilde{z})}{|x-\tilde{x}|}\,\partial_v h_-(t,\tilde{z})\,\mathrm{d}\tilde{z} = \int_{\mathbb{R}^3\times\mathbb{R}^3} \frac{h_-(t,\tilde{z})}{|x-\tilde{x}|}\,\partial_v f_0(\tilde{z})\,\mathrm{d}\tilde{z} = \\ &= \int_{\mathbb{R}^3} \frac{1}{|x-\tilde{x}|} \int_{\mathbb{R}^3} h_-(t,\tilde{z}) \Big[\partial_E\varphi(\tilde{E},\tilde{L})\,\tilde{v} + \partial_L\varphi(\tilde{E},\tilde{L})\,\big(2|\tilde{x}|^2\tilde{v} - 2\tilde{x}\cdot\tilde{v}\,\tilde{x}\big)\Big]\,\mathrm{d}\tilde{v}\,\mathrm{d}\tilde{x}\end{aligned} \tag{3.3.34}$$

for $x\in\mathbb{R}^3$, where we use the abbreviation $(\tilde{E},\tilde{L}) = (E(\tilde{z}),L(\tilde{z}))$. Next, we use the spherical symmetry of $h_-(t)$, E, and L and apply the change of variables $\tilde{v}\mapsto(w(\tilde{z}),L(\tilde{z})) = (\tilde{w},\tilde{L})$ defined by (2.1.3) to derive the following identity for the inner integral in (3.3.34):

$$\begin{aligned}&\int_{\mathbb{R}^3} h_-(t,\tilde{z}) \Big[\partial_E\varphi(\tilde{E},\tilde{L})\,\tilde{v} + \partial_L\varphi(\tilde{E},\tilde{L})\,\big(2|\tilde{x}|^2\tilde{v} - 2\tilde{x}\cdot\tilde{v}\,\tilde{x}\big)\Big]\,\mathrm{d}\tilde{v} = \\ &\qquad = \frac{\pi}{|\tilde{x}|^3}\,\tilde{x} \int_0^\infty \int_{\mathbb{R}} \tilde{w}\,h_-(t,|\tilde{x}|,\tilde{w},\tilde{L})\,\partial_E\varphi(E(|\tilde{x}|,\tilde{w},\tilde{L}),\tilde{L})\,\mathrm{d}\tilde{w}\,\mathrm{d}\tilde{L}\end{aligned} \tag{3.3.35}$$

for $\tilde{x}\in\mathbb{R}^3\setminus\{0\}$.[58] In particular, the two terms containing $\partial_L\varphi$ cancel each other out.[59] Inserting (3.3.35) into (3.3.34) shows, after a straight-forward calculation[60], that $\tilde{U}_{\partial_v h_-}$ is a radial vector field, i.e., there exists $\tilde{V}_{h_-(t)}\colon]0,\infty[\to\mathbb{R}$ s.t. $\tilde{U}_{\partial_v h_-}$ is of the form

$$\tilde{U}_{\partial_v h_-(t)}(x) = \frac{x}{|x|}\,\tilde{V}_{h_-(t)}(|x|), \qquad x\in\mathbb{R}^3\setminus\{0\}. \tag{3.3.36}$$

For such radial vector fields there holds the identity

$$\partial_x \mathrm{div}_x \tilde{U}_{\partial_v h_-} = \Delta\tilde{U}_{\partial_v h_-}, \tag{3.3.37}$$

which, together with (3.3.34) and (3.3.35), implies

$$\partial_x \mathrm{div}_x \tilde{U}_{\partial_v h_-(t)}(x) = -4\pi^2\,\frac{x}{|x|^3} \int_0^\infty \int_{\mathbb{R}} w\,\partial_E\varphi(E(|x|,w,L),L)\,h_-(t,|x|,w,L)\,\mathrm{d}w\,\mathrm{d}L \tag{3.3.38}$$

for $x\in\mathbb{R}^3\setminus\{0\}$. We have thus shown that the second-order formulation of the Lagrangian linearisation of the Vlasov-Poisson system (3.3.33) takes on the following form in radial coordinates (r,w,L):

$$\partial_t^2 h_- + \tilde{\mathcal{L}}(h_-) = 0, \tag{3.3.39}$$

where

$$(\tilde{\mathcal{L}}g)(r,w,L) \coloneqq -(\mathcal{T}^2 g)(r,w,L) + \frac{4\pi^2}{r^2}\,w \int_0^\infty \int_{\mathbb{R}} \tilde{w}\,\partial_E\varphi(E(r,\tilde{w},\tilde{L}),\tilde{L})\,g(r,\tilde{w},\tilde{L})\,\mathrm{d}\tilde{w}\,\mathrm{d}\tilde{L} \tag{3.3.40}$$

for suitable odd-in-w functions $g = g(r,w,L)$.

[58] One way to establish (3.3.35) is as follows: Pick $A\in\mathrm{SO}(3)$ s.t. $A\tilde{x} = |\tilde{x}|\,\mathrm{e}_3$ and apply the change of variables given by $A\tilde{v} = (\frac{\sqrt{\tilde{L}}}{|\tilde{x}|}\cos(\phi), \frac{\sqrt{\tilde{L}}}{|\tilde{x}|}\sin(\phi), \tilde{w})^T$ with $0<\phi<2\pi$, $\tilde{L}>0$, and $\tilde{w}\in\mathbb{R}$.

[59] Recall that a similar effect also occurred when linearising in Eulerian coordinates (cf. Section 3.1), i.e., all terms which contain the L-derivative of φ cancel out when considering spherically symmetric perturbations.

[60] Choose $A\in\mathrm{SO}(3)$ s.t. $Ax = |x|\,\mathrm{e}_3$ and express $A\tilde{x}$ in standard spherical coordinates.

Observe that $\tilde{\mathcal{L}}$ differs from the operator $\mathcal{L}$ defined in (1.2.9) which occurs when using the linearisation schemes from Sections 3.1 and 3.2.[61] Nonetheless, the following equivalence holds:

$$\mathcal{L}(g\,\partial_E\varphi) = \partial_E\varphi\,\tilde{\mathcal{L}}g \tag{3.3.41}$$

for g as above, which is due to $\mathcal{T}(g\,\partial_E\varphi) = \partial_E\varphi\,\mathcal{T}g$. In particular, on a formal level, the point spectra of $\mathcal{L}$ and $\tilde{\mathcal{L}}$ are identical since any eigenfunction $\tilde{g}$ of $\tilde{\mathcal{L}}$ gives an eigenfunction $g \coloneqq \partial_E\varphi\,\tilde{g}$ of $\mathcal{L}$ to the same eigenvalue and vice versa.[62]

Now assume that $\lambda > 0$ is an eigenvalue of the linearised operator $\mathcal{L}$ and thus, by the above discussion, also an eigenvalue of $\tilde{\mathcal{L}}$. Let $g = g(r, w, L)$ be an odd-in-w eigenfunction associated to the eigenvalue λ of $\tilde{\mathcal{L}}$. Then

$$h_-(t, r, w, L) \coloneqq \cos(\sqrt{\lambda}\,t)\,g(r, w, L) \tag{3.3.42}$$

defines a solution of (3.3.39) which is $\frac{2\pi}{\sqrt{\lambda}}$-periodic in time. Integrating (3.3.32a) in t then yields an associated even-in-w part h_+ which is also time-periodic. Overall, we arrive at a $\frac{2\pi}{\sqrt{\lambda}}$-periodic solution δZ of the Lagrangian linearisation of the Vlasov-Poisson system (3.3.21) generated by $h = h_+ + h_-$ via (3.3.27). By the above discussion, the solution f of the Vlasov-Poisson system in Eulerian coordinates associated to the flow map Z given by (3.3.9) then satisfies

$$\operatorname{supp}(f(t)) = Z(t, \overline{\Omega}_0) = \{z + \varepsilon\,\delta Z(t, z) \mid z \in \overline{\Omega}_0\} \tag{3.3.43}$$

to linear order. Hence, on the linear level, the eigenvalue λ leads to a perturbed solution f whose phase space support oscillates (or pulsates) around the respective support of the steady state f_0 with period $\frac{2\pi}{\sqrt{\lambda}}$. Recall that the linearisation in mass-Lagrange coordinates could only explain the pulsations of the radial support of the solution, while the present linearisation scheme shows that the entire phase space support of the solution indeed pulsates.

[61] We would arrive at the operator $\frac{1}{\partial_E\varphi}\mathcal{L}$ instead of $\tilde{\mathcal{L}}$ if we replaced h with $\frac{h}{\partial_E\varphi}$ in the ansatz (3.3.27) for the linearised perturbation.

[62] Later we limit the discussion to steady states where $\partial_E\varphi$ does not vanish on the steady state support. This is why we do not worry about possible zeros of $\partial_E\varphi$ when relating $\mathcal{L}$ to $\tilde{\mathcal{L}}$.

Chapter 4

Properties of the Operators

In this chapter we analyse the operators which describe the linearised dynamics around a fixed steady state f_0. The class of equilibria for which we (can) conduct this analysis is further restricted compared to Section 2.2. We collect all assumptions on the underlying steady state f_0 in Section 4.1 and prove some technical properties of the equilibrium.

As derived in Chapter 3, the linearised dynamics around this steady state are governed by the linearised operator $\mathcal{L} = -\mathcal{T}^2 - \mathcal{R}$ via the equation (1.2.8). In order to study the properties of $\mathcal{L}$, we have to define it on a suitable domain $\mathrm{D}(\mathcal{L})$ of a fitting Hilbert space. In particular, defining the derivative operator $\mathcal{T}$ (and its square) in a suitable weak sense is important in order for the resulting operators to behave well from a functional analysis point of view. All these definitions are provided in Section 4.2.

In Sections 4.3 and 4.4, we then separately analyse the two parts $\mathcal{T}^2$ and $\mathcal{R}$ of the linearised operator. Afterwards, we combine these properties in a suitable way to study the whole linearised operator $\mathcal{L}$ in Section 4.5. With the discussion from Chapter 3 in mind, it is of particular interest to investigate the existence of positive eigenvalues of $\mathcal{L}$, which we start doing in Section 4.5.4. Further techniques to analyse the presence of such eigenvalues will then be developed in Chapter 5.

Most of the definitions and results from this chapter originate from [62, 147]. Related discussions can also be found in [49, 61, 85, 165].

4.1 The Steady States Under Consideration

We consider a steady state f_0 as constructed in Proposition 2.2.9. Recall that f_0 is spherically symmetric in the sense of Definition 2.1.1 (a), solves the Vlasov-Poisson system in the sense of Definition 2.2.2, and is of the form

$$f_0(x,v) = \varphi(E(x,v), L(x,v)) = \Phi(E_0 - E(x,v))\,(L(x,v) - L_0)_+^\ell \tag{4.1.1}$$

for $x, v \in \mathbb{R}^3$. Here, L is the squared modulus of the angular momentum given by (2.2.4) and E is the particle energy defined as

$$E(x,v) = \frac{1}{2}|v|^2 + U_0(x), \qquad E(r,w,L) = \frac{1}{2}w^2 + \Psi_L(r), \tag{4.1.2}$$

where U_0 and Ψ_L are the potential and the effective potential (recall Definition 2.2.11) associated to the steady state, respectively. In order to establish the existence of the steady state, we made the assumptions (φ1)–(φ3). For the upcoming analysis, we additionally

require that the parameters ℓ, L_0, and Φ of the microscopic equation of state φ satisfy the following conditions:[63]

(φ4) If $L_0 = 0$, then $\ell = 0$, i.e., the steady state is isotropic.

(φ5) The function Φ is continuous on $\mathbb{R}$ and continuously differentiable on $]0,\infty[$ with

$$\Phi'(\eta) > 0, \qquad \eta > 0. \tag{4.1.3}$$

Hence, φ given by (2.2.12) is continuously differentiable w.r.t. E on $]-\infty, E_0[\times \mathbb{R}$.[64] We extend $\partial_E \varphi$ with 0 onto $\mathbb{R}^2$ and use the abbreviation

$$\varphi' \coloneqq \partial_E \varphi \tag{4.1.4}$$

for this extension.

Some comments on these additional assumptions are in order.

Remark 4.1.1. *(a) The condition (φ4) implies that we consider either an isotropic steady state ($L_0 = 0 = \ell$) or a shell ($L_0 > 0$). Compared to (φ1), we now exclude ansatz functions with $L_0 = 0 < \ell$ by assuming (φ4). The reason for this is the following: For any steady state of the form* (4.1.1) *with $L_0 = 0 < \ell$, there hold $0 \in \operatorname{supp}(\rho_0)$ and $\rho_0(0) = 0$, recall* (2.2.27) *and Proposition 2.2.9 (c). These two properties, however, result in the period function T being unbounded on the (E,L)-triangle $\mathbb{D}_0$, cf. Remark A.4.5, which is undesirable for the following analysis.*[65]

(b) We shall see later that the monotonicity condition (φ5) is crucial to the mathematical basis of our analysis, cf. Remark 4.4.3. This condition is, however, also natural from a physics point of view [184]: It implies $\varphi' < 0$ inside the steady state support, i.e., the concentration of ever more energetic particles is decreasing within the equilibrium configuration. We further note that the dynamics close to the steady state might be qualitatively different for steady states which do not satisfy (φ5), see [53, 178].

(c) One could weaken the monotonicity condition (φ5) by only requiring $\Phi'(\eta) > 0$ for $0 < \eta \le \kappa$, where $\kappa = E_0 - U_0(0) > 0$ is the parameter used for the construction of the steady state in Proposition 2.2.9. The reason for this is that we only need $\varphi' < 0$ inside the steady state support and $E_0 - E(x,v) \in]0,\kappa]$ for $(x,v) \in \Omega_0$. Anyway, the values of Φ on $]\kappa,\infty[$ do not affect the associated steady state, which is why we stick to (φ5).

(d) Together with (φ2), the continuity of Φ on $\mathbb{R}$ implies $\lim_{\eta \searrow 0} \Phi(\eta) = 0$, which ensures that several boundary terms will vanish in what follows. From a physics point of view, it makes sure that the steady state passes continuously from its phase space support into the vacuum, at least at the part of the boundary given by $\{E = E_0\}$.

(e) The continuity of Φ' on $]0,\infty[$ is included into (φ5) to make sure that integrals involving φ' are well-defined.[66] *It is possible to relax this assumption.*

[63] Recall that the cut-off energy $E_0 < 0$ is only implicitly determined by the parameter $\kappa = E_0 - U_0(0) > 0$ and the equations satisfied by the steady state, cf. Proposition 2.2.9.

[64] By (φ2), φ is obviously differentiable on $]E_0,\infty[\times \mathbb{R}$ as well with $\partial_E \varphi = 0$ on $]E_0,\infty[\times \mathbb{R}$.

[65] Most of the results proven in this chapter can also be obtained in the case of an unbounded period function (and steady state support) by refining the arguments suitably. In the specific situation of an isochrone steady state [18, 64, 65], this will be part of [7].

[66] More precisely, we use the continuity of φ' to make sure that various integrands are measurable.

(f) The monotonicity condition ($\varphi 5$) implies that we necessarily have to choose $k > 0$ in the polytropic case ($\varphi 3$) (ii).

Further observe that the conditions ($\varphi 1$)–($\varphi 5$) are satisfied by the prominent examples of ansatz functions (2.2.17)–(2.2.19), at least after suitably adjusting the parameters. Concretely, the anisotropic polytropes

$$\varphi(E,L) = (E_0 - E)_+^k \, (L - L_0)_+^\ell \qquad \text{with} \qquad L_0 > 0,\ \ell > -\frac{1}{2},\ 0 < k < 3\ell + \frac{7}{2}, \tag{4.1.5}$$

the isotropic polytropes

$$\varphi(E,L) = \varphi(E) = (E_0 - E)_+^k \qquad \text{with} \qquad 0 < k < \frac{7}{2}, \tag{4.1.6}$$

and the (isotropic) King models

$$\varphi(E,L) = \varphi(E) = \left(e^{E_0 - E} - 1\right)_+ \tag{4.1.7}$$

are all part of the admissible class of steady states.

Before actually analysing the linearised system associated to the steady state f_0, we derive some technical statements involving the equilibrium. The first result is an important integration-by-parts identity which will be frequently used in the remainder of this thesis. The same identity is established in [57, p. 507], [62, Eqn. (4.5)], [96, Eqn. (B.3)], and [85, Lemma 2.5] among others, see also [58, Lemma 4.4] for more general such formulae in a different context. Recall (2.2.9) for the definition of the stationary mass density ρ_0.

Lemma 4.1.2. *For $r > 0$ it holds that*

$$\int_0^\infty \int_{\mathbb{R}} w^2 \, |\varphi'(E(r,w,L),L)| \, \mathrm{d}w \, \mathrm{d}L = \frac{r^2}{\pi} \, \rho_0(r). \tag{4.1.8}$$

Proof. We use ($\varphi 5$) to obtain

$$\int_0^\infty \int_{\mathbb{R}} w^2 \, |\varphi'(E(r,w,L),L)| \, \mathrm{d}w \, \mathrm{d}L = -\int_0^\infty \int_{-\sqrt{2E_0 - 2\Psi_L(r)}}^{\sqrt{2E_0 - 2\Psi_L(r)}} w^2 \, \varphi'(E(r,w,L),L) \, \mathrm{d}w \, \mathrm{d}L \tag{4.1.9}$$

for $r > 0$; the inner integral is meant to vanish if $E_0 - \Psi_L(r) \leq 0$. By (4.1.1) and (4.1.2), there holds

$$w \, \varphi'(E(r,w,L),L) = \partial_w[\varphi(E(r,w,L),L)] = \partial_w f_0(r,w,L) \tag{4.1.10}$$

for $(r,w,L) \in \Omega_0$, recall (2.2.47). Hence, for all $(L,r) \in \,]0,\infty[\times [0,\infty[$ where the w-integral in (4.1.9) does not vanish, integrating by parts yields

$$\begin{aligned} -\int_{-\sqrt{2E_0 - 2\Psi_L(r)}}^{\sqrt{2E_0 - 2\Psi_L(r)}} w^2 \, \varphi'(E(r,w,L),L) \, \mathrm{d}w &= \int_{-\sqrt{2E_0 - 2\Psi_L(r)}}^{\sqrt{2E_0 - 2\Psi_L(r)}} f_0(r,w,L) \, \mathrm{d}w = \\ &= \int_{\mathbb{R}} f_0(r,w,L) \, \mathrm{d}w; \end{aligned} \tag{4.1.11}$$

in particular, the boundary terms vanish due to ($\varphi 5$)[67] and the last identity follows by ($\varphi 2$). Inserting (4.1.11) into (4.1.9) then implies

$$\int_0^\infty \int_{\mathbb{R}} w^2 \, |\varphi'(E(r,w,L),L)| \, \mathrm{d}w \, \mathrm{d}L = \int_0^\infty \int_{\mathbb{R}} f_0(r,w,L) \, \mathrm{d}w \, \mathrm{d}L = \frac{r^2}{\pi} \, \rho_0(r) \tag{4.1.12}$$

[67] In fact, we impose the continuity of Φ on $\mathbb{R}$ mainly so that the boundary term disappear here. If we would not do this, $\lim_{\eta \searrow 0} \Phi(\eta)$ could be positive, resulting in the presence of boundary terms in (4.1.11).

for $r > 0$ by changing variables from (w, L) to v. In the above arguments we have focused on the case where the integrals do not vanish. Notice, however, that the sets where φ and φ' vanish are identical by (φ2) and (φ5). □

The second result gives an estimate on the velocity integral of φ' and will be used to bound various integrals later. This estimate originates from [62, Eqn. (2.5)], see also [15, p. 166] for a similar bound in the isotropic case and [49, Sc. 4.1] for related arguments in a different context.

Lemma 4.1.3. *There exists a constant $C > 0$ s.t. for all $x \in \mathbb{R}^3$ there holds*

$$\int_{\mathbb{R}^3} |\varphi'(E(x,v), L(x,v))| \,\mathrm{d}v \leq C. \tag{4.1.13}$$

Proof. For $x \in \mathbb{R}^3 \setminus \{0\}$ and $r = |x|$, we perform a calculation similar to (2.2.20)–(2.2.27) to rewrite the integral on the left-hand side of (4.1.13) as follows:

$$\begin{aligned}
&\int_{\mathbb{R}^3} |\varphi'(E(x,v), L(x,v))| \,\mathrm{d}v \\
&\quad = \frac{\pi}{r^2} \int_{L_0}^{\infty} \int_{-\sqrt{2E_0 - 2\Psi_L(r)}}^{\sqrt{2E_0 - 2\Psi_L(r)}} \Phi'\left(E_0 - \frac{1}{2}w^2 - \Psi_L(r)\right) (L - L_0)_+^{\ell} \,\mathrm{d}w \,\mathrm{d}L = \\
&\quad = \frac{2\pi}{r^2} \int_{\Psi_{L_0}(r)}^{E_0} \Phi'(E_0 - E) \int_{L_0}^{2r^2 E - 2r^2 U_0(r)} \frac{(L - L_0)^{\ell}}{\sqrt{2E - 2\Psi_L(r)}} \,\mathrm{d}L \,\mathrm{d}E = \\
&\quad = c_\ell \, r^{2\ell} \int_0^{E_0 - \Psi_{L_0}(r)} \Phi'(\eta) \, (E_0 - \Psi_{L_0}(r) - \eta)^{\ell + \frac{1}{2}} \,\mathrm{d}\eta
\end{aligned} \tag{4.1.14}$$

with constant $c_\ell > 0$ again given by (2.2.26); the integral is meant to vanish if $E_0 - \Psi_{L_0}(r) \leq 0$.[68] Since $\ell > -\frac{1}{2}$, integrating by parts yields

$$\int_{\mathbb{R}^3} |\varphi'(E(x,v), L(x,v))| \,\mathrm{d}v = r^{2\ell} g'(E_0 - \Psi_{L_0}(r)), \tag{4.1.15}$$

where g' is defined in (2.2.28). This estimate also extends to $x = 0$ using the convention $0^0 = 1$ in the isotropic case $L_0 = 0 = \ell$. We thus conclude (4.1.13) because g' is continuous by Lemma 2.2.6, $E_0 - \Psi_{L_0}(r) \leq \kappa$ for $r > 0$, and $\sup\{r^{2\ell} \mid \rho_0(r) > 0\} < \infty$. □

Next, we use the further assumptions (φ4) and (φ5) on the steady state to derive useful representations of the (interior of the) steady state support Ω_0.[69] Recall (2.2.44) and (2.2.45) for the definition of Ω_0 in (x, v)-variables and (r, w, L)-variables, respectively.

Lemma 4.1.4 (The Structure of Ω_0)**.** *(a) In the isotropic case $L_0 = 0 = \ell$ it holds that*

$$\Omega_0 = \{(x,v) \in \mathbb{R}^3 \times \mathbb{R}^3 \mid E(x,v) < E_0\}, \tag{4.1.16}$$

$$\Omega_0 = \{(r,w,L) \in \,]0,\infty[\,\times \mathbb{R} \times [0,\infty[\mid E(r,w,L) < E_0\}. \tag{4.1.17}$$

Otherwise, $L_0 > 0$ and it holds that

$$\Omega_0 = \{(x,v) \in \mathbb{R}^3 \times \mathbb{R}^3 \mid E(x,v) < E_0 \ \&\ L(x,v) > L_0\}, \tag{4.1.18}$$

$$\Omega_0 = \{(r,w,L) \in \,]0,\infty[\,\times \mathbb{R} \times [0,\infty[\mid E(r,w,L) < E_0 \ \&\ L > L_0\}. \tag{4.1.19}$$

[68] In the polytropic case $\Phi(\eta) = \eta_+^k$, one could, in fact, explicitly compute the integral (4.1.14) by applying the integral identity (2.2.23).

[69] Notice that the statements of Lemma 4.1.4 (a)–(c) are, in general, not true if the steady state satisfies only (φ1)–(φ3) because it could then be possible that $\Phi(\eta) = 0$ for some $\eta > 0$.

(b) In (x,v)-coordinates as well as in (r,w,L)-coordinates it holds that

$$\Omega_0 \overset{a.e.}{=} \{E < E_0 \ \&\ L > L_0\}, \tag{4.1.20}$$

i.e., the sets are identical up to sets of measure zero.

(c) In Cartesian (x,v)-coordinates, the set $\Omega_0 \subset \mathbb{R}^3 \times \mathbb{R}^3$ is open.[70]

(d) The relation between the representations of Ω_0 in (x,v)-coordinates and (r,w,L)-coordinates is

$$\Omega_0 = \{(x,v) \in \mathbb{R}^3 \times \mathbb{R}^3 \mid x \neq 0 \ \&\ (|x|, \frac{x \cdot v}{|x|}, |x \times v|^2) \in \Omega_0\}. \tag{4.1.21}$$

Proof. The representations of Ω_0 claimed in part (a) follow directly by the ansatz (4.1.1) because $\Phi(\eta) > 0$ is equivalent to $\eta > 0$ by $(\varphi 2)$ and $(\varphi 5)$; recall the convention (2.2.13).

Part (a) together with the fact[71] that $\{(x,v) \in \mathbb{R}^3 \times \mathbb{R}^3 \mid L(x,v) = 0\}$ forms a set of measure zero in $\mathbb{R}^3 \times \mathbb{R}^3$ then yields the relation (4.1.20).

Ω_0 being open in $\mathbb{R}^3 \times \mathbb{R}^3$ is due to the regularity of U_0, while part (d) follows directly by the definitions of the different representations of Ω_0. □

Lastly, we study the connection between Ω_0 and the (E,L)-support $\mathbb{D}_0$ of the steady state; recall (2.2.88) for the definition of the latter set.

Lemma 4.1.5. *In the isotropic case $L_0 = 0 = \ell$ it holds that*

$$\mathbb{D}_0 = \{(E(x,v), L(x,v)) \mid (x,v) \in \Omega_0 \text{ with } L(x,v) > 0 \ \&\ E(x,v) \neq E^{\min}_{L(x,v)}\}; \tag{4.1.22}$$

recall Lemma 2.2.12 for the definition of $E^{\min}_L$. In the anisotropic case $L_0 > 0$ it holds that

$$\mathbb{D}_0 = \{(E(x,v), L(x,v)) \mid (x,v) \in \Omega_0 \text{ with } E(x,v) \neq E^{\min}_{L(x,v)}\}; \tag{4.1.23}$$

In both cases,

$$\mathbb{D}_0 \overset{a.e.}{=} (E,L)(\Omega_0) = \{(E(x,v), L(x,v)) \mid (x,v) \in \Omega_0\}. \tag{4.1.24}$$

The analogues of these statements in (r,w,L)-coordinates hold true as well.

Proof. For $(x,v) \in \mathbb{R}^3 \times \mathbb{R}^3$ with $L(x,v) > 0$, changing to (r,w,L)-coordinates yields

$$E(x,v) \geq \Psi_{L(x,v)}(|x|) \geq E^{\min}_{L(x,v)}, \tag{4.1.25}$$

with

$$E(x,v) = E^{\min}_{L(x,v)} \qquad \Leftrightarrow \qquad x \cdot v = 0 \ \&\ |x| = r_{L(x,v)} \tag{4.1.26}$$

by Lemma 2.2.12. Together with Lemma 4.1.4 this shows (4.1.22) and (4.1.23). In order to deduce (4.1.24) we further note that $\{(x,v) \in \mathbb{R}^3 \times \mathbb{R}^3 \mid x \cdot v = 0 \vee x \times v = 0\}$ is a set of measure zero. □

[70] Ω_0 is also open in (r,w,L)-coordinates when considering it in the topology of $]0,\infty[\times \mathbb{R} \times [0,\infty[$.

[71] Note that $L(x,v) = 0$ is equivalent to $x = 0 \vee v \in \operatorname{span}(x)$.

4.2 Definition of the Operators & Function Spaces

For a fixed steady state f_0 as specified in the previous section, we now lay the mathematical foundations for the upcoming analysis by defining the function spaces and operators in a suitable way. The definitions provided here originate from [62, 147, 165].

We start by generalising the concept of spherical symmetry introduced in Definition 2.1.1 to functions which are only defined almost everywhere (henceforth abbreviated as "a.e.").

Definition 4.2.1 (Spherical Symmetry Almost Everywhere)**.** *Let $n \in \mathbb{N}$.*

(a) A function $f\colon \mathbb{R}^n \to \mathbb{R}$ is spherically symmetric almost everywhere (on $\mathbb{R}^n$) *if for any rotation matrix $A \in \mathrm{SO}(n)$ there holds $f(x) = f(Ax)$ for a.e.[72] $x \in \mathbb{R}^n$.*

(b) A function $f\colon \mathbb{R}^n \times \mathbb{R}^n \to \mathbb{R}$ is spherically symmetric almost everywhere (on $\mathbb{R}^n \times \mathbb{R}^n$) *if for any rotation matrix $A \in \mathrm{SO}(n)$ there holds $f(x,v) = f(Ax,Av)$ for a.e.[73] $(x,v) \in \mathbb{R}^n \times \mathbb{R}^n$.*

(c) A function $f\colon \Omega \to \mathbb{R}$ with $\Omega \subset \mathbb{R}^n$ or $\Omega \subset \mathbb{R}^n \times \mathbb{R}^n$ is spherically symmetric almost everywhere (on Ω) *if its extension by 0 is spherically symmetric a.e. in the sense of part (a) or part (b), respectively.*

(d) We add a subscript "r" to function spaces to indicate that we are restricting them to their spherically symmetric (a.e.) subspace, e.g.,

$$C^1_r(\Omega_0) = \{f \in C^1(\Omega_0) \mid f \text{ is spherically symmetric on } \Omega_0 \subset \mathbb{R}^3 \times \mathbb{R}^3\}, \tag{4.2.1}$$

$$L^2_r(\Omega_0) = \{f \in L^2(\Omega_0) \mid f \text{ is spherically symmetric a.e. on } \Omega_0 \subset \mathbb{R}^3 \times \mathbb{R}^3\}. \tag{4.2.2}$$

Similar to Remark 2.1.2, spherical symmetry a.e. again allows us to express a function in lower-dimensional variables adapted to the symmetry. We state this property in the relevant case $n = 3$ in the following remark without giving any proofs but refer the interested reader to [165, Sc. 2.4] for a more detailed discussion.

Remark 4.2.2. *(a) Let $f \in L^1_{\mathrm{loc}}(\mathbb{R}^3)$ be spherically symmetric a.e.[74] Then there exists a measurable function $\tilde{f}\colon [0,\infty[\to \mathbb{R}$ s.t. $f(x) = \tilde{f}(|x|)$ for a.e. $x \in \mathbb{R}^3$. Moreover, $\tilde{f}$ is uniquely determined a.e. on $[0,\infty[$ by this property.*

(b) Let $f \in L^1_{\mathrm{loc}}(\mathbb{R}^3 \times \mathbb{R}^3)$ be spherically symmetric a.e. Then there exists a measurable function $\tilde{f}\colon]0,\infty[\times \mathbb{R} \times [0,\infty[\to \mathbb{R}$ s.t. $f(x,v) = \tilde{f}(|x|, \frac{x\cdot v}{|x|}, |x \times v|^2)$ for a.e. $(x,v) \in \mathbb{R}^3 \times \mathbb{R}^3$. Moreover, $\tilde{f}$ is uniquely determined a.e. on $]0,\infty[\times \mathbb{R} \times [0,\infty[$ by this property.

(c) In the situation of part (b), f being odd in v a.e., i.e., $f(x,-v) = -f(x,v)$ for a.e. $(x,v) \in \mathbb{R}^3 \times \mathbb{R}^3$, is equivalent to $\tilde{f}$ being odd in w a.e., i.e., $\tilde{f}(r,-w,L) = -\tilde{f}(r,w,L)$ for a.e. $(r,w,L) \in]0,\infty[\times \mathbb{R} \times [0,\infty[$.

(d) In the situations of part (a) and part (b), we again identify $\tilde{f}$ with f and write $\tilde{f} = f$ by slight abuse of notation.

We next define the underlying function spaces for our analysis. Similar spaces are used in [49, 61, 62, 85, 96, 111, 147, 165] among others.

[72] The set of measure zero may depend on the rotation matrix.

[73] The set of measure zero may depend on the rotation matrix.

[74] As usual when dealing with elements from an L^p-space, this means that one representative of the equivalence class defined by f is spherically symmetric a.e.

Definition 4.2.3 (The Spaces H and $\mathcal{H}$). *(a) Let*

$$H := \{f\colon \Omega_0 \to \mathbb{R} \text{ measurable \& spherically symmetric a.e. } | \, \|f\|_H < \infty\}, \quad (4.2.3)$$

where

$$\|f\|_H^2 := \int_{\Omega_0} \frac{1}{|\varphi'(E,L)|} \, |f(x,v)|^2 \, \mathrm{d}(x,v) \quad (4.2.4)$$

and we use the abbreviation $(E,L) = (E,L)(x,v)$. Recall $\varphi'(E,L) < 0$ on Ω_0 by (φ5) and by the properties of Ω_0 derived in Lemma 4.1.4 (a). As usual, we identify objects in H which are identical almost everywhere. The inner product on H associated to the norm (4.2.4) *is given by*

$$\langle f, g\rangle_H := \int_{\Omega_0} \frac{1}{|\varphi'(E,L)|} \, f(x,v)\, g(x,v) \, \mathrm{d}(x,v), \qquad f, g \in H. \quad (4.2.5)$$

(b) Let

$$\mathcal{H} := \{f \in H \mid f \text{ is odd in } v \text{ a.e.}\}. \quad (4.2.6)$$

Let us add some comments on these function spaces.

Remark 4.2.4. *(a) The space H is (the spherically symmetric subspace of) a weighted L^2-space. As such, it has the usual properties of L^2-spaces, in particular, $(H, \langle\cdot,\cdot\rangle_H)$ is a real-valued separable Hilbert space with dual space $H^* \cong H$.*

Similar statements also hold for $\mathcal{H}$, i.e., $(\mathcal{H}, \langle\cdot,\cdot\rangle_H)$ is a separable Hilbert space as well.

(b) The reason why we include the weight $\frac{1}{|\varphi'|}$ in the function space H will become apparent when studying the response operator $\mathcal{R}$ in Section 4.4, see Remark 4.4.3. During the analysis of the transport operator $\mathcal{T}$ in Section 4.3 we thus have to include the weight in various integrals, but we shall see that the weight does not cause any issues there.

(c) Because any element of H is spherically symmetric a.e. on Ω_0, we can express it in (r,w,L)-variables a.e. by Remark 4.2.2 (b).[75] *Changing to these variables in the integrals* (4.2.4) *and* (4.2.5) *yields*

$$\|f\|_H^2 = 4\pi^2 \int_{\Omega_0} \frac{1}{|\varphi'(E,L)|} \, |f(r,w,L)|^2 \, \mathrm{d}(r,w,L), \quad (4.2.7)$$

$$\langle f, g\rangle_H = 4\pi^2 \int_{\Omega_0} \frac{1}{|\varphi'(E,L)|} \, f(r,w,L)\, g(r,w,L) \, \mathrm{d}(r,w,L), \quad (4.2.8)$$

for $f, g \in H$, where we use the abbreviation $E = E(r,w,L)$.

(d) On any compact subset K of Ω_0, the weight $|\varphi'(E,L)|^{-1}$ is bounded. In the isotropic case $L_0 = 0 = \ell$ this follows by (φ5) and the structure of Ω_0 derived in Lemma 4.1.4 (a). Otherwise, $L(x,v)$ is bounded by $L_{\max} < \infty$ and bounded away from $L_0 > 0$ for $(x,v) \in K$.

Thus, any measurable, bounded, and spherically symmetric function with compact support in Ω_0 lies in H. In particular, $C_{c,r}(\Omega_0) \subset H$.

[75] Due to the weight included in H, extending $f \in H$ with 0 onto $\mathbb{R}^3 \times \mathbb{R}^3$ does not necessarily lead to $f \in L^1_{\mathrm{loc}}(\mathbb{R}^3 \times \mathbb{R}^3)$. Nonetheless, extending $|\varphi'(E,L)|^{-1/2} f$ with 0 gives an element of $L^1(\mathbb{R}^3 \times \mathbb{R}^3)$ and applying Remark 4.2.2 (b) to this function then yields that f can indeed be written in (r,w,L)-coordinates a.e.

(e) Similar to part (d), $|\varphi'(E,L)|$ is bounded on compact subsets of Ω_0. In particular, $H \subset L^2_{\mathrm{loc},r}(\Omega_0)$.

(f) Later on, it is sometimes convenient to also include complex-valued functions in our analysis. A function $f\colon \Omega_0 \to \mathbb{C}$ is said to be in H if $\mathrm{Re}(f) \in H$ and $\mathrm{Im}(f) \in H$. The canonical extension of the inner product on H to complex-valued $f, g \in H$ is given by

$$\langle f, g\rangle_H \coloneqq \int_{\Omega_0} \frac{1}{|\varphi'(E,L)|}\, f(x,v)\, \overline{g(x,v)}\, \mathrm{d}(x,v). \tag{4.2.9}$$

The same convention is also used for general sets: A complex-valued function is meant to lie in a set that is initially defined only for real-valued functions if both its real and imaginary parts do. In the same way, one obtains the real or imaginary part of a (linear) operator applied to a complex-valued function by applying the operator to the real or imaginary part of the function, respectively. By slight abuse of notation, we will not notationally distinguish between objects and their complex-valued analogues.

In fact, including complex-valued functions everywhere in our analysis would not make a conceptual difference. However, since the Vlasov-Poisson system is naturally real-valued, we try as far as possible to carry out all arguments with real-valued functions only.

We now consider the first part of the linearised operator $\mathcal{L}$, the transport operator $\mathcal{T}$; recall (1.2.10) for an informal definition. The aim is to define $\mathcal{T}$ as a linear operator on a subset of H which is as large as possible. Due to the derivatives contained in $\mathcal{T}$, we cannot define $\mathcal{T}$ (in a meaningful way) on the whole space H – choosing the "right" domain is a non-trivial task. The following definition originates[76] from [147, Def. 2.1], which in turn is based on the author's master thesis [165]. The same definition is used [62] and variations of it can be found in [49, 58, 61].

Definition 4.2.5 (The Transport Operator $\mathcal{T}$)**.** *For $f \in L^1_{\mathrm{loc},r}(\Omega_0)$, the* transport term $\mathcal{T}f$ exists weakly *if there exists some $\mu \in L^1_{\mathrm{loc},r}(\Omega_0)$ s.t. for any test function[77] $\xi \in C^1_{c,r}(\Omega_0)$ there holds*

$$\int_{\Omega_0} \frac{1}{|\varphi'(E,L)|}\, f\, \mathcal{T}\xi\, \mathrm{d}(x,v) = -\int_{\Omega_0} \frac{1}{|\varphi'(E,L)|}\, \mu\, \xi\, \mathrm{d}(x,v), \tag{4.2.10}$$

where $\mathcal{T}\xi$ is defined classically via

$$\mathcal{T}\xi(x,v) \coloneqq v \cdot \partial_x \xi(x,v) - \partial_x U_0(x) \cdot \partial_v \xi(x,v), \qquad (x,v) \in \Omega_0. \tag{4.2.11}$$

In this case $\mathcal{T}f \coloneqq \mu$ weakly*. The domains of $\mathcal{T}$ and $\mathcal{T}^2$ are defined as*

$$\mathrm{D}(\mathcal{T}) \coloneqq \{f \in H \mid \mathcal{T}f \text{ exists weakly } \&\ \mathcal{T}f \in H\}, \tag{4.2.12}$$

$$\mathrm{D}(\mathcal{T}^2) \coloneqq \{f \in \mathrm{D}(\mathcal{T}) \mid \mathcal{T}f \in \mathrm{D}(\mathcal{T})\}. \tag{4.2.13}$$

The resulting operator $\mathcal{T}\colon \mathrm{D}(\mathcal{T}) \to H$ is called the transport operator*, $\mathcal{T}^2\colon \mathrm{D}(\mathcal{T}^2) \to H$ is the* squared transport operator*.*

Although we wanted to restrict ourselves here only to the definition of the operators, we cannot resist from discussing some properties of the weak definition of $\mathcal{T}$ similar to [147, Rem. 2] and [165, p. 23].

[76] Compared to [147, Def. 2.1], we choose a different class of test functions here. However, as noted in Remark 4.2.6 (e) and [147, Rem. 2 (c)], this results in an equivalent definition.

[77] Recall that Ω_0 is open by Lemma 4.1.4 (c).

Remark 4.2.6. *(a) If $\mathcal{T}f$ exists weakly for some $f \in L^1_{\mathrm{loc},r}(\Omega_0)$, it is uniquely determined a.e. on Ω_0. This can be seen by applying the fundamental lemma of the calculus of variations [98, Thm. 6.5] in (r, w, L)-coordinates.*

(b) It holds that $C^1_{c,r}(\Omega_0) \subset \mathrm{D}(\mathcal{T})$. In addition, for $f \in C^1_{c,r}(\Omega_0)$, the weak definition of $\mathcal{T}f$ coincides with the classical definition (4.2.11)*.*

We verify this statement similarly to [147, Prop. 1] and [165, Lemma 3.2].[78] *First observe that $\mathcal{T}$ (defined classically by* (4.2.11)*) preserves the spherical symmetry of $f \in C^1_{c,r}(\Omega_0)$ because U_0 is spherically symmetric.*[79] *Hence, $\mathcal{T}f \in C_{c,r}(\Omega_0) \subset H$. For $(x,v) \in \Omega_0$ let $(X,V)\colon \mathbb{R} \to \mathbb{R}^3 \times \mathbb{R}^3$ denote the maximal solution of the characteristic system* (2.2.2) *associated to the steady state satisfying the initial condition $(X,V)(0,x,v) = (x,v)$; this solution is global-in-time by [143, Lemma 1.2].*[80] *Applying the chain rule yields the following alternative expression of the transport operator:*

$$\mathcal{T}f(x,v) = \partial_s\big|_{s=0}[f((X,V)(s,x,v))], \qquad (x,v) \in \Omega_0; \tag{4.2.14}$$

note that $(X,V)(s,x,v) \in \Omega_0$ for $s \in \mathbb{R}$, $(x,v) \in \Omega_0$ by Lemmas 2.2.1 and 4.1.4. Furthermore, for any $s \in \mathbb{R}$, the mapping $(X,V)(s)\colon \Omega_0 \to \Omega_0$ is a measure-preserving C^1-diffeomorphism because the right-hand side of the characteristic system (2.2.2) *is divergence-free [143, Lemma 1.2]. Hence, using this diffeomorphism to change variables yields*

$$\begin{aligned}\int_{\Omega_0} \frac{1}{|\varphi'(E(x,v),L(x,v))|}\, f((X,V)(s,x,v))\, \xi((X,V)(s,x,v))\, \mathrm{d}(x,v) = \\ = \int_{\Omega_0} \frac{1}{|\varphi'(E(x,v),L(x,v))|}\, f(x,v)\, \xi(x,v)\, \mathrm{d}(x,v)\end{aligned} \tag{4.2.15}$$

for every test function $\xi \in C^1_{c,r}(\Omega_0)$ and $s \in \mathbb{R}$, where we have again used that E and L are conserved along characteristics by Lemma 2.2.1. Differentiating this equation w.r.t. s,[81] *inserting $s = 0$, and using* (4.2.14) *then shows*

$$\langle f, \mathcal{T}\xi\rangle_H = -\langle \mathcal{T}f, \xi\rangle_H. \tag{4.2.16}$$

(c) If $\mathcal{T}f$ and $\mathcal{T}g$ exist weakly for $f, g \in L^1_{\mathrm{loc},r}(\Omega_0)$, it is straight-forward to verify that $\mathcal{T}(\alpha f + g)$ exists weakly for $\alpha \in \mathbb{R}$ with $\mathcal{T}(\alpha f + g) = \alpha\mathcal{T}f + \mathcal{T}g$. Hence, $\mathrm{D}(\mathcal{T})$ is a linear subspace of H and $\mathcal{T}\colon \mathrm{D}(\mathcal{T}) \to H$ is a linear operator.

(d) In part (b) we have proven $C^1_{c,r}(\Omega_0) \subset \mathrm{D}(\mathcal{T})$. Moreover, standard approximation arguments show that $C^1_{c,r}(\Omega_0)$ is a dense subspace of H. Hence, $\mathrm{D}(\mathcal{T})$ is a dense subspace of H and the linear operator $\mathcal{T}\colon \mathrm{D}(\mathcal{T}) \to H$ is densely defined on H.

(e) Choosing $C^\infty_{c,r}(\Omega_0)$ instead of $C^1_{c,r}(\Omega_0)$ as the class of test functions in Definition 4.2.5 results in an equivalent weak definition of the transport term. This can be verified by

[78] If further regularity of φ were to be assumed, this property would become easier to prove as one could simply integrate by parts in (4.2.10). In general, however, we cannot apply (the classical definition (4.2.11) of) $\mathcal{T}$ on the integral weight $|\varphi'|^{-1}$.

[79] A detailed proof of this statement is provided in [165, Lemma 3.3 a)].

[80] In the case where the conserved energy value is negative, this also follows by the arguments from Section 2.2.2.

[81] Note that we can switch the order of differentiation and integration due to Remark 4.2.4 (d) and the compact supports of f and ξ.

standard mollifier arguments, see [147, Rem. 2 (c)], and it also follows by the more general approximation result which we will establish in Lemma 4.3.31. We prefer to use this larger class of test functions in order to be able to, e.g., insert functions depending on the particle energy E as test functions in (4.2.10)*; notice that E is, in general, not infinitely differentiable.*

(f) One might be tempted to weakly define the transport term $\mathcal{T} = v\cdot\partial_v - \partial_x U_0(x)\cdot\partial_x$ by just requiring that the derivatives ∂_v and ∂_x both exist weakly. However, Definition 4.2.5 defines the transport term in a weak sense on a larger set of functions compared to this naïve approach.[82] It is hence crucial to weakly define the transport term as a whole via an integration by parts identity like (4.2.10) *to arrive at a domain of definition which is as large as possible.*

(g) As discussed in part (b), $\mathcal{T}$ preserves spherical symmetry of smooth functions. For $f \in C^1_r(\Omega_0)$, the transport term $\mathcal{T}f$ takes on the following form in radial variables:

$$\mathcal{T}f(r,w,L) = w\,\partial_r f(r,w,L) - \Psi_L'(r)\,\partial_w f(r,w,L), \qquad (r,w,L)\in\Omega_0. \tag{4.2.17}$$

Further properties of the transport operator will be studied in Section 4.3.

We also feel obliged to briefly review two alternative ways to define the transport operator in a weak sense which are used in the literature.

Remark 4.2.7. *The transport operator $\mathcal{T}$ can be interpreted as computing the derivative along characteristics of the steady state flow. Mathematically, this corresponds to the representation* (4.2.14) *of $\mathcal{T}$. This interpretation can be used to define the transport operator in alternative ways:*

(a) In [53, Proof of Lemma 2.4], the transport operator is defined as the generator of a suitable C^0-group, see also [165, Rem. 3.10]. More precisely, let $(X,V)\colon \mathbb{R}\times\Omega_0\to\Omega_0$ be defined as in Remark 4.2.6 (b), i.e., (X,V) denotes the characteristic flow of the steady state. For $s\in\mathbb{R}$ and[83] $f\in H$ we define $(\mathcal{U}(s)f)\colon\Omega_0\to\mathbb{R}$ via

$$(\mathcal{U}(s)f)(x,v) \coloneqq f((X,V)(s,x,v)), \qquad (x,v)\in\Omega_0. \tag{4.2.18}$$

Using the properties of the characteristic flow (X,V) from [143, Lemma 1.2], it is straight-forward to verify that $(\mathcal{U}(s))_{s\in\mathbb{R}}$ is a unitary C^0-group [40, Def. I.5.1] on the Hilbert space H. Hence, by Stone's theorem [40, Thm. II.3.24], the group possesses a skew-adjoint generator $\tilde{\mathcal{T}}\colon \mathrm{D}(\tilde{\mathcal{T}})\to H$ defined by

$$\tilde{\mathcal{T}}f \coloneqq \lim_{s\to 0}\frac{\mathcal{U}(s)f - f}{s}, \qquad f\in\mathrm{D}(\tilde{\mathcal{T}}), \tag{4.2.19}$$

where

$$\mathrm{D}(\tilde{\mathcal{T}}) \coloneqq \{f\in H \mid \lim_{s\to 0}\frac{\mathcal{U}(s)f - f}{s} \text{ exists as a limit in } H\}. \tag{4.2.20}$$

As earlier noted in [165, Rem. 3.10], one can in fact show that this definition is equivalent to the one from Definition 4.2.5. This is due to the skew-adjointness of

[82] We shall see in Lemma 4.3.9 that the transport term exists weakly for (suitably integrable) functions which depend on E and L only. For instance, $\mathbb{1}_{\{E<E_0-\frac{1}{k}\}}\in\mathrm{D}(\mathcal{T})$ for $k\in\mathbb{N}$, but partial derivatives of $\mathbb{1}_{\{E<E_0-\frac{1}{k}\}}$ contain distributional terms (for sufficiently large k).

[83] In [53], these arguments are actually carried out on the unweighted space $L^2(\mathbb{R}^3\times\mathbb{R}^3)$ and without the restriction to spherical symmetry.

$\mathcal{T}\colon \mathrm{D}(\mathcal{T}) \to H$ which will be shown in Proposition 4.3.15 combined with the observation that $\mathcal{T}$ and $\tilde{\mathcal{T}}$ coincide on the dense subspace $C^1_{c,r}(\Omega_0)$ of H, which is due to (4.2.14).[84]

(b) We will present the methods used to define the transport operator in [85, Lemma B.8] in more detail in Section 4.3.1. The basic idea is as follows: Use the (suitably normalised) proper time along steady state characteristics as a periodic variable on the phase space support Ω_0. The transport operator $\mathcal{T}$ corresponds to a partial derivative w.r.t. this new variable (up to the multiplication with suitable constants); see Lemma 4.3.9. The weak existence and suitable integrability of the transport term $\mathcal{T}f$ can then be characterised via the convergence of (suitably weighted) Fourier series w.r.t. the proper time variable. It will be shown in Remark 4.3.13 that this way of defining $\mathcal{T}$ is equivalent to Definition 4.2.5.

We next define the second part of the linearised operator $\mathcal{L}$, the response operator $\mathcal{R}$; recall (1.2.11) for an informal definition. The following definition is based on [62, Eqn. (4.4)] and is also used in [61, Eqn. (1.15)].

Definition 4.2.8 (The Response Operator $\mathcal{R}$)**.** *For $f \in H$ define the a.e. spherically symmetric function $\mathcal{R}f\colon \Omega_0 \to \mathbb{R}$ by*

$$\mathcal{R}f(r,w,L) \coloneqq 4\pi\,|\varphi'(E,L)|\,w\,j_f(r), \qquad \text{a.e. } (r,w,L) \in \Omega_0, \tag{4.2.21}$$

where we use the abbreviation $E = E(r,w,L)$ and recall that the a.e. spherically symmetric velocity density $j_f\colon \mathbb{R}^3 \to \mathbb{R}$ associated to f is given by

$$j_f(r) \coloneqq \frac{\pi}{r^2}\int_0^\infty \int_{\mathbb{R}} w\, f(r,w,L)\,\mathrm{d}w\,\mathrm{d}L, \qquad \text{a.e. } r > 0. \tag{4.2.22}$$

Here, f is extended by 0 to $\mathbb{R}^3 \times \mathbb{R}^3$.

The properties of the response operator will be studied in detail in Section 4.4. In particular, we will show that $\mathcal{R}$ is indeed well-defined on H, cf. Lemma 4.4.2. Moreover, in Corollary 4.4.7 we will derive an alternative representation for $\mathcal{R}f$ under the assumption that f is suitably smooth.

We have now collected all tools to rigorously define the whole linearised operator $\mathcal{L}$ as in [62, Def. 4.4]; see also [61, p. 20] and [49, Def. 4.2 (d)] for similar definitions.

Definition 4.2.9 (The Linearised Operator $\mathcal{L}$)**.** *Let*

$$\mathrm{D}(\mathcal{L}) \coloneqq \mathrm{D}(\mathcal{T}^2) \cap \mathcal{H}, \tag{4.2.23}$$

where $\mathcal{H}$ and $\mathrm{D}(\mathcal{T}^2)$ are introduced in Definitions 4.2.3 and 4.2.5, respectively. Then the linearised operator *or* Antonov operator *is defined by*

$$\mathcal{L}f \coloneqq -\mathcal{T}^2 f - \mathcal{R}f, \qquad f \in \mathrm{D}(\mathcal{L}). \tag{4.2.24}$$

Functional analytic and spectral properties of the linearised operator $\mathcal{L}$ will be studied in Section 4.5. Let us conclude the present section with a short remark regarding the domain of definition $\mathrm{D}(\mathcal{L})$ of the linearised operator.

[84] It follows similarly to [136, p. 256] that two skew-adjoint operators which coincide on a dense subspace are identical.

Remark 4.2.10. *As derived in Chapter 3, the linearised operator $\mathcal{L}$ describes the evolution of the odd-in-v part of the linear perturbation only. This is why we restrict the domain $\mathrm{D}(\mathcal{L})$ of the linearised operator $\mathcal{L}$ to the odd-in-v subspace $\mathcal{H}$ of H. From a purely mathematical point of view, however, one could also consider $\mathcal{L}$ on the domain $\mathrm{D}(\mathcal{T}^2)$, i.e., include the even-in-v parts of all functions. This is done in [62], but we shall see that the analysis of the linearised operator is not significantly affected by the differing domains.*[85]

4.3 The Transport Operator $\mathcal{T}$

In this section we analyse the transport operator[86] $\mathcal{T}$ introduced in Definition 4.2.5. The results presented here mainly originate from [62, Scs. 4.1 and 5.1] and [147, 165]. Related analyses are also contained in [85, App. B] as well as, in different settings, in [49, Sc. 5.1] and [61, Lemma 3.7].

We first introduce a crucial tool for studying the transport operator: action-angle type variables. This tool is then used in Sections 4.3.2–4.3.4 to analyse functional analytical properties and spectral properties of the transport operator $\mathcal{T}$ and its square $\mathcal{T}^2$. In Section 4.3.5 we then prove a useful approximation result.

4.3.1 Action-Angle Type Variables

In order to study the transport operator $\mathcal{T}$, it is useful to work in new variables on the steady state support Ω_0, recall Proposition 2.2.9 (d) for the definition of this set, which are adapted to the characteristic flow of the steady state. These variables are introduced in the following definition; the underlying intuition will be discussed afterwards. In order to study the (linearised) Vlasov-Poisson system and related systems, these variables and variations of it are used in [49, 53, 61, 62, 85, 105, 126, 147, 148] among others.

Definition & Lemma 4.3.1 (Action-Angle Type Variables)**.** *Let*

$$\Omega_0^* \coloneqq \{(r,w,L) \in \Omega_0 \mid L > 0 \ \&\ (r,w) \neq (r_L, 0)\}, \tag{4.3.1}$$

i.e., Ω_0^* contains all elements of Ω_0 with $L > 0$ except for $(r,w,L) \in \Omega_0$ with minimal energy $E(r,w,L) = E_L^{\min}$. For fixed $(r,w,L) \in \Omega_0^*$, we thus have $E \coloneqq E(r,w,L) \in \,]E_L^{\min}, E_0[$, which means $(E,L) \in \mathbb{D}_0$ by Lemma 4.1.5. Now let $(R,W)(\cdot,E,L)$ be as specified in Definition 2.2.16, i.e., it is the $T(E,L)$-periodic solution of the characteristic system (2.2.93) *associated to the steady state satisfying the initial condition $(R,W)(0,E,L) = (r_-(E,L),0)$. Then there exists a unique $\theta \in \mathbb{S}^1$ on the* circle[87,88]

$$\mathbb{S}^1 \coloneqq \mathbb{R}/\mathbb{Z} \tag{4.3.2}$$

s.t.

$$(R,W)(\theta\, T(E,L), E, L) = (r,w). \tag{4.3.3}$$

[85] The only noteworthy difference is that the nullspace of $\mathcal{L}$ with domain $\mathrm{D}(\mathcal{T}^2)$ is non-trivial, cf. [62, Cor. 7.3], while the nullspace of $\mathcal{L}$ with domain $\mathrm{D}(\mathcal{L}) = \mathrm{D}(\mathcal{T}^2) \cap \mathcal{H}$ is trivial, cf. Corollary 4.5.10. However, considering $\mathcal{L}$ on $\mathrm{D}(\mathcal{T}^2) \cap (\ker(\mathcal{L})^\perp)$ results in similar properties of the operator as for the domain $\mathrm{D}(\mathcal{L})$.

[86] We use the term *transport operator* rather loosely here. For example, we also use it to refer to (weakly defined) transport terms $\mathcal{T}f$ with $f \in L^1_{\mathrm{loc},r}(\Omega_0)$.

[87] We always identity $\mathbb{R}/\mathbb{Z}$ with the unit circle $\{z \in \mathbb{C} \mid |z| = 1\}$ in the complex plane using the standard homeomorphism $\mathbb{S}^1 \ni \theta \mapsto e^{2\pi i\theta}$.

[88] It is sometimes convenient to think of $\mathbb{S}^1$ as the interval $[0,1]$ where the endpoints are identified.

This defines the mapping

$$\Omega_0^* \ni (r, w, L) \mapsto (\theta, E, L) \in \mathbb{S}^1 \times \mathbb{D}_0, \tag{4.3.4}$$

which is one-to-one. We refer to the new variables (θ, E, L) *as* action-angle type variables. *The variable* $\theta \in \mathbb{S}^1$ *is the* angle variable, *while* $(E, L) \in \mathbb{D}_0$ *are the* action variables.[89]

Proof. All statements claimed above are due to the properties of the characteristic flow $(R, W)(\cdot, E, L)$ derived in Section 2.2.2. In particular, recall that the orbit of the $T(E, L)$-periodic solution $(R, W)(\cdot, E, L)$ is of the form

$$(R, W)(\mathbb{R}, E, L) = \{(r, w) \in]0, \infty[\times \mathbb{R} \mid E(r, w, L) = E\} \tag{4.3.5}$$

for $(E, L) \in \mathbb{D}_0$. □

As an aside, we note that one could as well define this change of variables on the larger domain

$$\{(\tilde{r}, \tilde{w}, \tilde{L}) \in]0, \infty[\times \mathbb{R} \times]0, \infty[\mid\ E_{\tilde{L}}^{\min} < E(\tilde{r}, \tilde{w}, \tilde{L}) < 0\} \ni (r, w, L) \mapsto (\theta, E, L) \in \mathbb{S}^1 \times \mathbb{A}_0. \tag{4.3.6}$$

However, for the analysis of the linearised Vlasov-Poisson system, it suffices to work on the support of the underlying steady state.

Illustratively, changing to action-angle type variables works as follows: In order to represent some $(r, w, L) \in \Omega_0^*$, one first chooses the actions $(E, L) \in \mathbb{D}_0$ s.t. (r, w, L) lies on the associated characteristic orbit. Next, the angle $\theta \in \mathbb{S}^1$, which corresponds to the normalised proper time of the characteristic solution starting at the minimal radius $r_-(E, L)$, determines the position on the orbit. This procedure is visualised in Figure 4.3.1.

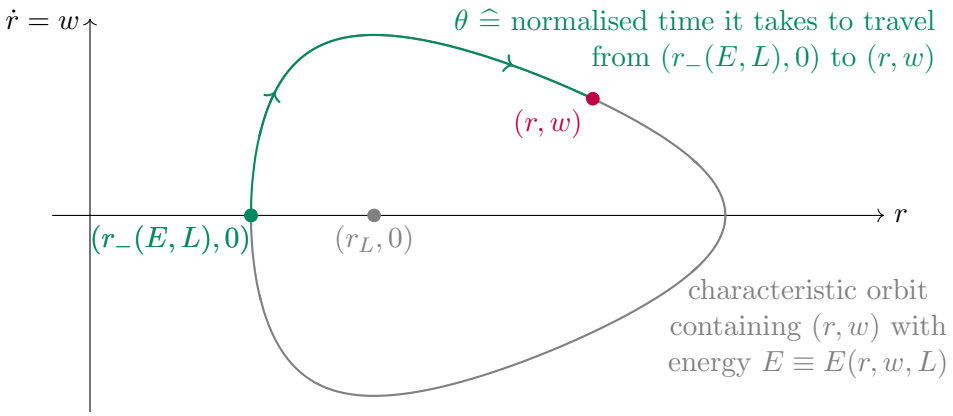

Figure 4.3.1: A schematic visualisation of the relation between $(r, w, L) \in \Omega_0^*$ and the associated action-angle type variables $(\theta, E, L) \in \mathbb{S}^1 \times \mathbb{D}_0$ for fixed $L > 0$.

In the context of general Hamiltonian systems, changing to such variables is a well-known technique. Under some additional assumptions, they are called *action-angle variables*. We refer to [11, 19, 92, 105] for a detailed background and discuss the relation to our variables (θ, E, L) next.

[89] Given the name *action-angle type variables*, one could argue that it is more natural to write these variables in the order (E, L, θ) instead of (θ, E, L). However, from a mathematics point of view, we think that (θ, E, L) is the most natural order of these variables. Moreover, as the terminology *action-angle variables* is commonly used in the literature, we choose not to use the name *angle-action type variables* for (θ, E, L) here. We apologise to the reader for any confusion that might be caused by this convention of ours.

Remark 4.3.2 ("True" Action-Angle Variables)**.** *We will see in Remark 4.3.5 that the change of variables $(r, w, L) \mapsto (\theta, E, L)$ is not measure-preserving. Hence, (θ, E, L) cannot be action-angle variables as defined in the above references. However, because the interpretation of the variables (θ, E, L) is similar to the one of action-angle variables, we use the terminology action-angle* type *variables here.*

A derivation of "true" action-angle variables in our setting can be found, e.g., in [85, App. A.1]. We do not include this derivation here, but still briefly state that "true" action-angle variables are given by

$$(\theta, A, L), \tag{4.3.7}$$

where $A = A(E, L)$ is the area function introduced in Definition A.3.6. Because $\partial_E A = T > 0$ by (A.3.31)*, the mapping $]E_L^{\min}, 0[\ni E \mapsto A(E, L)$ is injective for fixed $L > 0$. Hence, the relation between A and E is one-to-one. Since the meaning of the "true" action variable A, cf. Remark A.3.7, is, however, not as intuitive as the physical interpretation of the particle energy E, we stick to the variables (θ, E, L) here.*

Let us next show that changing to action-angle type variables or back is smooth.

Lemma 4.3.3. *The change to action-angle type variables given by* (4.3.4) *is a C^1-diffeomorphism.*

Proof. By the regularities of (R, W) and T established in Lemmas A.3.2 and A.3.3, the dependence of (r, w) on (θ, E, L) is (even twice) continuously differentiable. In addition, a straight-forward computation shows

$$\det(D(r, w, L)(\theta, E, L)) = T(E, L) \det\begin{pmatrix} W(\theta\, T(E, L), E, L) & \partial_E R(\theta\, T(E, L), E, L) \\ \dot{W}(\theta\, T(E, L), E, L) & \partial_E \dot{R}(\theta\, T(E, L), E, L) \end{pmatrix} \tag{4.3.8}$$

for $(\theta, E, L) \in \mathbb{S}^1 \times \mathbb{D}_0$. By the discussion from Remark A.3.4, the latter determinant equals 1. The claimed regularity of (4.3.4) hence follows by the inverse function theorem. □

In Definition 4.3.1, the angle variable θ is only implicitly determined by $(r, w, L) \in \Omega_0^*$ through (4.3.3). The next lemma, which is based on [62, Eqn. (5.3)], provides a more explicit way of calculating the angle.

Lemma 4.3.4. *For $(E, L) \in \mathbb{A}_0$ let*

$$\theta(\cdot, E, L) \colon [r_-(E, L), r_+(E, L)] \to [0, \frac{1}{2}],\ \theta(r, E, L) \coloneqq \frac{1}{T(E, L)} \int_{r_-(E,L)}^{r} \frac{\mathrm{d}s}{\sqrt{2E - 2\Psi_L(s)}}. \tag{4.3.9}$$

This mapping is continuous and one-to-one. In addition, it is continuously differentiable on $]r_-(E, L), r_+(E, L)[$ with

$$\partial_r \theta(r, E, L) = \frac{1}{T(E, L)} \frac{1}{\sqrt{2E - 2\Psi_L(r)}}, \qquad r \in]r_-(E, L), r_+(E, L)[. \tag{4.3.10}$$

Furthermore, for $(r, w, L) \in \Omega_0^*$, the associated angle $\theta \in \mathbb{S}^1$ defined by Definition 4.3.1 is explicitly given by[90]

$$\begin{cases} \theta(r, E, L), & w \geq 0, \\ 1 - \theta(r, E, L), & w \leq 0. \end{cases} \tag{4.3.11}$$

[90] Observe that $w = 0$ corresponds to $r = r_\pm(E, L)$, where the two expressions $\theta(r, E, L)$ and $1 - \theta(r, E, L)$ are equal.

Proof. All statements concerning the mapping $\theta(\cdot, E, L)$ are straight-forward to verify; recall the integral representation (2.2.97) of the period function T. The relation between $\theta(\cdot, E, L)$ and the angle θ from Definition 4.3.1 follows by applying the inverse function theorem similarly to Section 2.2.2. □

Throughout this thesis we use the action-angle type variables to represent spherically symmetric (a.e.) functions on the steady state support. We next introduce the notational framework for this and further analyse the change of variables. These results and notational conventions are based on [62, Sc. 5.1] as well as [49, Sc. 3.3] and [61, Sc. 3.2].

Remark 4.3.5. *For $f\colon \Omega_0^* \to \mathbb{R}$ we write, by slight abuse of notation,*

$$f(r, w, L) = f(\theta, E, L), \tag{4.3.12}$$

where $(r, w, L) \in \Omega_0^*$ and $(\theta, E, L) \in \mathbb{S}^1 \times \mathbb{D}_0$ are related as specified in Definition 4.3.1. By Lemmas 4.1.4 and 4.1.5, there holds

$$\Omega_0 \overset{a.e.}{=} \Omega_0^*, \tag{4.3.13}$$

which is why we also write (4.3.12) *a.e. for functions $f\colon \Omega_0 \to \mathbb{R}$ which are spherically symmetric a.e.*

Furthermore, for any spherically symmetric a.e. and integrable function $f\colon \Omega_0 \to \mathbb{R}$ it holds that

$$\int_{\Omega_0} f(x, v)\,\mathrm{d}(x, v) = 4\pi^2 \int_{\Omega_0} f(r, w, L)\,\mathrm{d}(r, w, L) = 4\pi^2 \int_{\mathbb{S}^1\times\mathbb{D}_0} T(E, L)\, f(\theta, E, L)\,\mathrm{d}(\theta, E, L). \tag{4.3.14}$$

While the first identity can be verified similarly to Remark 4.2.4 (c), the second identity can be obtained as follows: Applying Fubini's theorem and changing variables via $E = E(r, w, L)$ yields

$$\begin{aligned}\int_{\Omega_0} f(r, w, L)\,\mathrm{d}(r, w, L) &= \left(\int_{\Omega_0\cap\{w>0\}} + \int_{\Omega_0\cap\{w<0\}}\right) f(r, w, L)\,\mathrm{d}(r, w, L) = \\ &= \int_{]0,\infty[^2} \int_{\Psi_L(r)}^{\infty} \Big(f(r, \sqrt{2E - 2\Psi_L(r)}, L) + f(r, -\sqrt{2E - 2\Psi_L(r)}, L)\Big) \frac{\mathrm{d}E\,\mathrm{d}(r, L)}{\sqrt{2E - 2\Psi_L(r)}},\end{aligned} \tag{4.3.15}$$

where $f = f(r, w, L)$ is extended by 0 to the whole space $]0, \infty[\times \mathbb{R} \times]0, \infty[$. Again switching the order of integration and using Lemmas 2.2.12 and 4.1.5 to adjust the domain of integration yields

$$\begin{aligned}&\int_{\Omega_0} f(r, w, L)\,\mathrm{d}(r, w, L) = \\ &= \int_{\mathbb{D}_0} \int_{r_-(E,L)}^{r_+(E,L)} \Big(f(r, \sqrt{2E - 2\Psi_L(r)}, L) + f(r, -\sqrt{2E - 2\Psi_L(r)}, L)\Big) \frac{\mathrm{d}r\,\mathrm{d}(E, L)}{\sqrt{2E - 2\Psi_L(r)}}.\end{aligned} \tag{4.3.16}$$

For the first addend on the right-hand side, we apply the change of variables $\theta = \theta(r, E, L)$ given by Lemma 4.3.4. A similar change of variables for the second addend, recall (4.3.11)*, and another application of Fubini's theorem then shows* (4.3.14)*.*

Later on we will frequently work with weak derivatives w.r.t. the angle variable $\theta \in \mathbb{S}^1$. As the concepts of weak derivatives and Sobolev spaces are usually studied on open subsets of $\mathbb{R}^n$, we introduce the analogous concepts on the circle $\mathbb{S}^1$ next; recall (4.3.2) for the definition of $\mathbb{S}^1$.[91]

Remark 4.3.6 (Sobolev Spaces on the Circle)**.** *Let*

$$L^2(\mathbb{S}^1) \coloneqq \{y\colon \mathbb{S}^1 \to \mathbb{R} \mid y \text{ measurable with } \|y\|_{L^2(\mathbb{S}^1)} < \infty\}, \tag{4.3.17}$$

where $\|\cdot\|_{L^2(\mathbb{S}^1)}$ *is the norm induced by the canonical scalar product*

$$\langle y, z\rangle_2 \coloneqq \int_{\mathbb{S}^1} y(\theta)\, z(\theta)\,\mathrm{d}\theta = \int_0^1 y(\theta)\, z(\theta)\,\mathrm{d}\theta, \qquad y, z \in L^2(\mathbb{S}^1), \tag{4.3.18}$$

and we identify elements of $L^2(\mathbb{S}^1)$ *which are identical a.e. Obviously,* $L^2(\mathbb{S}^1)$ *is a Hilbert space and*

$$L^2(\mathbb{S}^1) \cong L^2(]0,1[). \tag{4.3.19}$$

Furthermore, for $j \in \mathbb{N}$*, a function* $y \in L^2(\mathbb{S}^1)$ *is* j times weakly differentiable on $\mathbb{S}^1$ *with* $y^{(j)} = z \in L^2(\mathbb{S}^1)$ weakly *if*

$$\int_{\mathbb{S}^1} y(\theta)\, \xi^{(j)}(\theta)\,\mathrm{d}\theta = (-1)^j \int_{\mathbb{S}^1} z(\theta)\, \xi(\theta)\,\mathrm{d}\theta \tag{4.3.20}$$

for any test function[92] $\xi \in C^\infty(\mathbb{S}^1) \cong \{\zeta \in C^\infty(\mathbb{R}) \mid \zeta \text{ is 1-periodic}\}$*. Accordingly, for* $m \in \mathbb{N}$*, let*

$$H^m(\mathbb{S}^1) \coloneqq \{y \in L^2(\mathbb{S}^1) \mid \forall j \in \{1,\dots,m\}\colon \\ y \text{ is } j \text{ times weakly differentiable with } y^{(j)} \in L^2(\mathbb{S}^1)\}. \tag{4.3.21}$$

If – like the author – one prefers to work with "classical" Sobolev spaces on open subsets of $\mathbb{R}^n$*, we note the relation*

$$H^m(\mathbb{S}^1) \cong \{y \in H^m(]0,1[) \mid \forall j \in \{0,\dots,m-1\}\colon y^{(j)}(0) = y^{(j)}(1)\} \tag{4.3.22}$$

for $m \in \mathbb{N}$*; observe that* $H^m(]0,1[) \hookrightarrow C^{m-1}([0,1])$*, i.e., the boundary conditions in the latter set are imposed for the continuous representatives of the respective functions.*

As discussed earlier, cf. Remark 4.2.10, it is of particular interest to analyse (spherically symmetric a.e.) functions on Ω_0 which are odd in v. The following remark, which is based on [62, Rem. 5.3], shows how this parity translates into action-angle type variables.

Remark 4.3.7. *Let*

$$L^{2,\mathrm{odd}}(\mathbb{S}^1) \coloneqq \{y \in L^2(\mathbb{S}^1) \mid y(\theta) = -y(1-\theta) \text{ for a.e. } \theta \in \mathbb{S}^1\}. \tag{4.3.23}$$

Using the properties of the characteristic flow of the steady state derived in Section 2.2.2, it is easy to verify that for every $f \in H$*,*[93,94]

$$f \in \mathcal{H} \quad \Leftrightarrow \quad \text{for a.e. } (E,L) \in \mathbb{D}_0\colon f(\cdot,E,L) \in L^{2,\mathrm{odd}}(\mathbb{S}^1). \tag{4.3.24}$$

[91] We deliberately omit here giving references to the rich literature regarding Sobolev spaces on general manifolds because we think that these are overly complex for our specific situation of a circle.

[92] Because $\mathbb{S}^1$ is a closed manifold, the support of any such test function is compact.

[93] A similar characterisation of oddness in v also holds for general spherically symmetric a.e. functions which are not necessarily contained in H.

[94] Note that $f(\cdot,E,L) \in L^2(\mathbb{S}^1)$ for a.e. $(E,L) \in \mathbb{D}_0$ by Remark 4.3.5 and Fubini's theorem.

As stated at the start of the present section, action-angle type variables are particularly useful when studying the transport operator because $\mathcal{T}$ simply corresponds to a partial derivative in (θ, E, L)-variables. We first derive this property for smooth functions. The following lemma is based on [62, Lemma 5.1].

Lemma 4.3.8. *For $m \in \mathbb{N}$ and[95] $f \in C_r^m(\Omega_0)$ it holds that $f(\cdot, E, L) \in C^m(\mathbb{S}^1)$ for $(E, L) \in \mathbb{D}_0$ with*

$$\mathcal{T}^m f(\theta, E, L) = \frac{1}{T(E,L)^m}\, \partial_\theta^m f(\theta, E, L), \qquad (\theta, E, L) \in \mathbb{S}^1 \times \mathbb{D}_0. \tag{4.3.25}$$

Proof. The statements follow by the chain rule; recall the representation (4.2.17) of the transport operator in (r, w, L)-coordinates. □

The analogous representation of $\mathcal{T}$ in action-angle type variables also holds for the weak definition of the transport operator. This will be a fundamental ingredient for the analysis of the operator $\mathcal{T}\colon \mathrm{D}(\mathcal{T}) \to H$. The following lemma originates from [62, Lemma 5.2]; variations of it can also be found in [49, Prop. 5.1 (b)] and [61, Lemma 3.7 (b)].

Lemma 4.3.9 (The Transport Operator in Action-Angle Type Variables)**.** *It holds that*[96]

$$\begin{aligned}\mathrm{D}(\mathcal{T}) = \Big\{ f \in H \mid \text{for a.e. } (E,L) \in \mathbb{D}_0 \colon f(\cdot, E, L) \in H^1(\mathbb{S}^1) \\ \text{with } \int_{\mathbb{D}_0} \frac{T(E,L)^{-1}}{|\varphi'(E,L)|} \int_{\mathbb{S}^1} |\partial_\theta f(\theta, E, L)|^2 \,\mathrm{d}\theta \,\mathrm{d}(E,L) < \infty \Big\}.\end{aligned} \tag{4.3.26}$$

If $f \in \mathrm{D}(\mathcal{T})$,

$$\mathcal{T} f(\theta, E, L) = \frac{1}{T(E,L)}\, \partial_\theta f(\theta, E, L) \qquad \text{for a.e. } (\theta, E, L) \in \mathbb{S}^1 \times \mathbb{D}_0. \tag{4.3.27}$$

Proof. We follow the proof of [62, Lemma 5.2] and start by considering $f \in \mathrm{D}(\mathcal{T})$. By Lemma 4.3.8, a change of variables as in Remark 4.3.5, and the weak definition of $\mathcal{T}$ we obtain the following equations for every test function $\xi \in C_{c,r}^1(\Omega_0)$:

$$\begin{aligned} 4\pi^2 &\int_{\mathbb{D}_0} \frac{1}{|\varphi'(E,L)|} \int_{\mathbb{S}^1} f(\theta, E, L)\, \partial_\theta \xi(\theta, E, L) \,\mathrm{d}\theta \,\mathrm{d}(E,L) = \\ &= \int_{\Omega_0} \frac{1}{|\varphi'(E,L)|}\, f(x,v)\, \mathcal{T}\xi(x,v) \,\mathrm{d}(x,v) = -\int_{\Omega_0} \frac{1}{|\varphi'(E,L)|}\, \mathcal{T} f(x,v)\, \xi(x,v) \,\mathrm{d}(x,v) = \\ &= -4\pi^2 \int_{\mathbb{D}_0} \frac{T(E,L)}{|\varphi'(E,L)|} \int_{\mathbb{S}^1} \mathcal{T} f(\theta, E, L)\, \xi(\theta, E, L) \,\mathrm{d}\theta \,\mathrm{d}(E,L). \end{aligned} \tag{4.3.28}$$

We now choose the test function ξ to be factorised in θ and (E, L), i.e.,

$$\xi(\theta, E, L) = \zeta(\theta)\, \chi(E, L), \qquad (\theta, E, L) \in \mathbb{S}^1 \times \mathbb{D}_0, \tag{4.3.29}$$

where $\zeta \in C^\infty(\mathbb{S}^1)$ and $\chi \in C_c^\infty(\mathbb{D}_0)$. In particular, every such choice of ζ and χ induces a valid test function $\xi \in C_{c,r}^1(\Omega_0)$ by Lemmas 4.1.5 and 4.3.3. Inserting the ansatz (4.3.29)

[95] It would actually suffice to impose the regularity of f on Ω_0^* in order to show (4.3.25).

[96] Since the period function T is bounded and bounded away from 0 on $\mathbb{D}_0$ by Proposition A.0.1 (a), one could also leave out the factor $T(E,L)^{-1}$ in the integral contained in (4.3.26).

into (4.3.28) yields

$$\int_{\mathbb{D}_0} \chi(E,L)\,\frac{1}{|\varphi'(E,L)|}\int_{\mathbb{S}^1} f(\theta,E,L)\,\dot\zeta(\theta)\,\mathrm{d}\theta\,\mathrm{d}(E,L) = \\ = -\int_{\mathbb{D}_0}\chi(E,L)\,\frac{T(E,L)}{|\varphi'(E,L)|}\int_{\mathbb{S}^1}\mathcal{T}f(\theta,E,L)\,\zeta(\theta)\,\mathrm{d}\theta\,\mathrm{d}(E,L). \quad (4.3.30)$$

Since this holds true for every $\chi\in C_c^\infty(\mathbb{D}_0)$, it follows

$$\int_{\mathbb{S}^1} f(\theta,E,L)\,\dot\zeta(\theta)\,\mathrm{d}\theta = -T(E,L)\int_{\mathbb{S}^1}\mathcal{T}f(\theta,E,L)\,\zeta(\theta)\,\mathrm{d}\theta \qquad \text{for a.e. } (E,L)\in\mathbb{D}_0 \quad (4.3.31)$$

and $\zeta\in C^\infty(\mathbb{S}^1)$. In particular, the set of measure zero in (4.3.31) can be chosen independently of ζ by considering a countable subset of $C^\infty(\mathbb{S}^1)$ which is dense in $H^1(\mathbb{S}^1)$.[97] Since $\zeta\in C^\infty(\mathbb{S}^1)$ is arbitrary, this means that $f(\cdot,E,L)$ is weakly differentiable on $\mathbb{S}^1$ for a.e. $(E,L)\in\mathbb{D}_0$ with

$$\partial_\theta f(\cdot,E,L) = T(E,L)\,\mathcal{T}f(\cdot,E,L) \qquad \text{weakly;} \quad (4.3.32)$$

recall Remark 4.3.6. In particular, by Remark 4.3.5,

$$4\pi^2\int_{\mathbb{D}_0}\frac{T(E,L)^{-1}}{|\varphi'(E,L)|}\int_{\mathbb{S}^1}|\partial_\theta f(\theta,E,L)|^2\,\mathrm{d}\theta\,\mathrm{d}(E,L) = \|\mathcal{T}f\|_H^2<\infty, \quad (4.3.33)$$

and hence $\partial_\theta f(\cdot,E,L)\in L^2(\mathbb{S}^1)$ for a.e. $(E,L)\in\mathbb{D}_0$ by Fubini's theorem. We have thus proven that f is indeed contained in the set on the right-hand side of (4.3.26).

Conversely, consider f in the set on the right-hand side of (4.3.26), i.e., $f\in H$ and $f(\cdot,E,L)\in H^1(\mathbb{S}^1)$ for a.e. $(E,L)\in\mathbb{D}_0$ with

$$\int_{\mathbb{D}_0}\frac{T(E,L)^{-1}}{|\varphi'(E,L)|}\int_{\mathbb{S}^1}|\partial_\theta f(\theta,E,L)|^2\,\mathrm{d}\theta\,\mathrm{d}(E,L)<\infty. \quad (4.3.34)$$

For any test function $\xi\in C^1_{c,r}(\Omega_0)$, we change variables via (4.3.14), apply Lemma 4.3.8, and integrate by parts on $\mathbb{S}^1$ in the weak sense to obtain

$$\int_{\Omega_0}\frac{1}{|\varphi'(E,L)|}\,f\,\mathcal{T}\xi\,\mathrm{d}(x,v) = 4\pi^2\int_{\mathbb{D}_0}\frac{1}{|\varphi'(E,L)|}\int_{\mathbb{S}^1} f(\theta,E,L)\,\partial_\theta\xi(\theta,E,L)\,\mathrm{d}\theta\,\mathrm{d}(E,L) = \\ = -4\pi^2\int_{\mathbb{D}_0}\frac{1}{|\varphi'(E,L)|}\int_{\mathbb{S}^1}\partial_\theta f(\theta,E,L)\,\xi(\theta,E,L)\,\mathrm{d}\theta\,\mathrm{d}(E,L) = \\ = -\int_{\Omega_0}\frac{T(E,L)^{-1}}{|\varphi'(E,L)|}\,\partial_\theta f\,\xi\,\mathrm{d}(x,v). \quad (4.3.35)$$

By Definition 4.2.5, this means that $\mathcal{T}f$ exists weakly and is given by

$$\mathcal{T}f = \frac{1}{T(E,L)}\,\partial_\theta f. \quad (4.3.36)$$

In particular,

$$\|\mathcal{T}f\|_H^2 = 4\pi^2\int_{\mathbb{D}_0}\frac{T(E,L)^{-1}}{|\varphi'(E,L)|}\int_{\mathbb{S}^1}|\partial_\theta f(\theta,E,L)|^2\,\mathrm{d}\theta\,\mathrm{d}(E,L)<\infty \quad (4.3.37)$$

by (4.3.34), which shows $f\in\mathrm{D}(\mathcal{T})$. □

[97] One way to construct such a dense subset is as follows: Let $A\subset C_c^\infty(]0,1[)$ be countable and dense in $H_0^1(]0,1[)$; such a set exists since $H_0^1(]0,1[)$ is separable and $C_c^\infty(]0,1[)$ is dense in $H_0^1(]0,1[)$. Then, $\{q+y\mid q\in\mathbb{Q},\,y\in A\}\subset C^\infty(\mathbb{S}^1)$ is dense in $H^1(\mathbb{S}^1)$; recall Remark 4.3.6.

The analogous result is also true for the squared transport operator.[98] This is based on [62, Cor. 5.4]; variations of this result can be found in [49, Prop. 5.1 (b)] and [61, Lemma 3.7 (b)].

Lemma 4.3.10. *It holds that*

$$\begin{aligned}\mathrm{D}(\mathcal{T}^2) = \Big\{ f \in H \mid \text{for a.e. } (E,L) \in \mathbb{D}_0 \colon f(\cdot,E,L) \in H^2(\mathbb{S}^1) \\ \text{with } \int_{\mathbb{D}_0} \frac{T(E,L)^{-1}}{|\varphi'(E,L)|} \int_{\mathbb{S}^1} |\partial_\theta f(\theta,E,L)|^2 \,\mathrm{d}\theta \,\mathrm{d}(E,L) < \infty \\ \text{and } \int_{\mathbb{D}_0} \frac{T(E,L)^{-3}}{|\varphi'(E,L)|} \int_{\mathbb{S}^1} |\partial_\theta^2 f(\theta,E,L)|^2 \,\mathrm{d}\theta \,\mathrm{d}(E,L) < \infty \Big\}. \quad (4.3.38)\end{aligned}$$

If $f \in \mathrm{D}(\mathcal{T}^2)$,

$$\mathcal{T}^2 f(\theta,E,L) = \frac{1}{T(E,L)^2}\, \partial_\theta^2 f(\theta,E,L) \qquad \text{for a.e. } (\theta,E,L) \in \mathbb{S}^1 \times \mathbb{D}_0. \quad (4.3.39)$$

Proof. The statements follow by applying Lemma 4.3.9. □

We have thus shown that the action-angle type variables introduced in Definition 4.3.1 provide simple characterisations of the transport operator and its domain of definition. Before applying these characterisations to analyse $\mathcal{T}$, we discuss another useful feature of the action-angle type variables (θ, E, L). The discussion is based on [61, Sc. 2] and [62, Rem. 5.18], where similar techniques are used in slightly different contexts. We also refer to [85, App. B.1] for similar arguments.

Remark 4.3.11 (Fourier Expansion in the Angle Variable)**.** *Let $f \in H$ be fixed. For $j \in \mathbb{Z}$ and a.e. $(E,L) \in \mathbb{D}_0$ let*

$$\hat{f}(j,E,L) \coloneqq \int_{\mathbb{S}^1} f(\theta,E,L)\, e^{-2\pi i j\,\theta} \,\mathrm{d}\theta \in \mathbb{C} \quad (4.3.40)$$

be the j-th Fourier coefficient of $f(\cdot,E,L) \in L^2(\mathbb{S}^1)$. Since $(\mathbb{S}^1 \ni \theta \mapsto e^{2\pi i j\,\theta})_{j\in\mathbb{Z}}$ is an orthonormal basis of[99] $L^2(\mathbb{S}^1)$, Lebesgue's dominated convergence theorem yields[100]

$$\sum_{j\in\mathbb{Z}} \hat{f}(j,E,L)\, e^{2\pi i j\,\theta} \coloneqq \lim_{n\to\infty} \sum_{j=-n}^{n} \hat{f}(j,E,L)\, e^{2\pi i j\,\theta} = f(\theta,E,L) \qquad \text{as a limit in } H. \quad (4.3.41)$$

Although the Fourier coefficients and the basis functions are both complex-valued, the Fourier partial series can be written as a real-valued trigonometric polynomial:

$$\sum_{j=-n}^{n} \hat{f}(j,E,L)\, e^{2\pi i j\,\theta} = a_0(E,L) + \sum_{j=1}^{n} a_j(E,L)\cos(2\pi j\,\theta) + \sum_{j=1}^{n} b_j(E,L)\sin(2\pi j\,\theta) \quad (4.3.42)$$

[98] One can also represent higher powers of the weakly defined transport operator in action-angle type variables in a similar way, but this is not relevant here.

[99] In order for $(e^{2\pi i j\,\theta})_{j\in\mathbb{Z}}$ to define an orthonormal basis of $L^2(\mathbb{S}^1)$, recall (4.3.17), we have to include complex-valued functions into $L^2(\mathbb{S}^1)$ as well. This is to be understood in the sense of Remark 4.2.4 (f).

[100] Since orthonormal bases are invariant under reordering, one could also use different denumerations of $\mathbb{Z}$ to define the limit $\sum_{j\in\mathbb{Z}} \ldots$ and arrive at an equivalent definition.

for $n \in \mathbb{N}$, $\theta \in \mathbb{S}^1$, and a.e. $(E, L) \in \mathbb{D}_0$, where

$$a_0(E,L) \coloneqq \hat{f}(0,E,L) = \int_{\mathbb{S}^1} f(\theta,E,L)\,\mathrm{d}\theta, \tag{4.3.43}$$

$$a_j(E,L) \coloneqq \hat{f}(j,E,L) + \hat{f}(-j,E,L) = 2\int_{\mathbb{S}^1} f(\theta,E,L)\,\cos(2\pi j\,\theta)\,\mathrm{d}\theta, \tag{4.3.44}$$

$$b_j(E,L) \coloneqq i\Big(\hat{f}(j,E,L) - \hat{f}(-j,E,L)\Big) = 2\int_{\mathbb{S}^1} f(\theta,E,L)\,\sin(2\pi j\,\theta)\,\mathrm{d}\theta, \tag{4.3.45}$$

for $j \in \mathbb{N}$.

If $f \in \mathcal{H}$, i.e., f is odd in v a.e., it follows that $a_j = 0$ for $j \in \mathbb{N}_0$ by Remark 4.3.7. Hence, the above implies

$$\sum_{j=1}^{\infty} b_j(E,L)\sin(2\pi j\,\theta) = f(\theta,E,L) \qquad \text{as a limit in } H \text{ for } f \in \mathcal{H}. \tag{4.3.46}$$

Since the transport operator simply corresponds to a partial derivative w.r.t. to the angle variable $\theta \in \mathbb{S}^1$, Fourier expansion in θ provides further useful representations of $\mathcal{T}$ and $\mathcal{T}^2$. This is based on [62, Rem. 5.18].

Lemma 4.3.12 (Fourier Expansion of the Transport Operator)**.** *The following identities hold as limits in H:*

$$\mathcal{T}f(\theta,E,L) = \frac{2\pi i}{T(E,L)}\sum_{j\in\mathbb{Z}} \hat{f}(j,E,L)\,j\,e^{2\pi i j\,\theta}, \qquad f \in \mathrm{D}(\mathcal{T}), \tag{4.3.47}$$

$$\mathcal{T}^2 f(\theta,E,L) = -\frac{4\pi^2}{T(E,L)^2}\sum_{j\in\mathbb{Z}} \hat{f}(j,E,L)\,j^2\,e^{2\pi i j\,\theta}, \qquad f \in \mathrm{D}(\mathcal{T}^2), \tag{4.3.48}$$

$$\mathcal{T}^2 f(\theta,E,L) = -\frac{4\pi^2}{T(E,L)^2}\sum_{j=1}^{\infty} b_j(E,L)\,j^2\,\sin(2\pi j\,\theta), \qquad f \in \mathrm{D}(\mathcal{T}^2)\cap\mathcal{H}, \tag{4.3.49}$$

where $\hat{f}$ and b_j are defined in (4.3.40) *and* (4.3.45)*, respectively.*

Proof. Applying the Fourier expansion introduced in Remark 4.3.11 to the representations of $\mathcal{T}f$ and $\mathcal{T}^2 f$ from Lemmas 4.3.9 and 4.3.10 and using

$$\widehat{\partial_\theta f}(j,E,L) = 2\pi i j\,\hat{f}(j,E,L), \qquad f \in \mathrm{D}(\mathcal{T}),\ j \in \mathbb{Z},\ \text{a.e. } (E,L) \in \mathbb{D}_0, \tag{4.3.50}$$

which follows by integrating by parts, yields the claimed statements. □

We further note that the Fourier expansion can also be used to characterise the domains of definition of $\mathcal{T}$ and $\mathcal{T}^2$.

Remark 4.3.13. *For the Sobolev spaces on the circle introduced in Remark 4.3.6, there holds*

$$H^m(\mathbb{S}^1) = \Big\{\mathbb{S}^1 \ni \theta \mapsto \sum_{j\in\mathbb{Z}} c_j\,e^{2\pi i j\,\theta} \in \mathbb{R} \mid (c_j)_{j\in\mathbb{Z}} \subset \mathbb{C} \text{ with } \sum_{j\in\mathbb{Z}} (1+j^2)^m\,|c_j|^2 < \infty\Big\} \tag{4.3.51}$$

for $m \in \mathbb{N}$, where the sum is meant to converge in $L^2(\mathbb{S}^1)$.[101] *Hence, by using Lemmas 4.3.9 and 4.3.10 as well as the boundedness of T on $\mathbb{D}_0$ established in Proposition A.0.1, we obtain*

$$\mathrm{D}(\mathcal{T}^m) = \Big\{ \mathbb{S}^1 \times \mathbb{D}_0 \ni (\theta, E, L) \mapsto \sum_{j\in\mathbb{Z}} c_j(E,L)\, e^{2\pi i j\,\theta} \in \mathbb{R} \mid c_j \colon \mathbb{D}_0 \to \mathbb{C} \text{ measurable, } j \in \mathbb{Z}, \text{ with } \sum_{j\in\mathbb{Z}} (1+j^2)^m \, \|c_j\|_H^2 < \infty \Big\} \tag{4.3.52}$$

for $m \in \{1, 2\}$, where the sum is meant to converge in H.

In [85, App. B], the characterisations (4.3.52) *of* $\mathrm{D}(\mathcal{T})$ *and* $\mathrm{D}(\mathcal{T}^2)$ *are used to define these sets. The transport operator $\mathcal{T} \colon \mathrm{D}(\mathcal{T}) \to H$ and its square $\mathcal{T}^2 \colon \mathrm{D}(\mathcal{T}^2) \to H$ are then defined via* (4.3.47) *and* (4.3.48)*, respectively, cf. [85, Lemma B.8].*

4.3.2 Self-Adjointness of the Squared Transport Operator

In this section we establish first functional analytic properties of the transport operator $\mathcal{T} \colon \mathrm{D}(\mathcal{T}) \to H$ and its square $\mathcal{T}^2 \colon \mathrm{D}(\mathcal{T}^2) \to H$. The main results are that these operators are skew-adjoint[102] and self-adjoint, respectively. This means that $\mathcal{T}^* = -\mathcal{T}$ and $(\mathcal{T}^2)^* =: \mathcal{T}^{2*} = \mathcal{T}^2$, where A^* denotes the adjoint of a suitable operator A; for background on the functional analytical concepts used in this section, we refer to [136, Ch. VIII] and [69, Chs. 4 and 5].

We first prove that the transport operator is skew-adjoint, and then use this result to afterwards study the squared transport operator. The skew-adjointness of the transport operator is a crucial property for the analysis of the (linearised) Vlasov-Poisson system. It has previously been stated in this context in [53, p. 805], [61, Lemma 3.7 (a)], [62, Prop. 4.2 (a)], and [96, Prop. 4.1 (i)] among others. For $\mathcal{T} \colon \mathrm{D}(\mathcal{T}) \to H$ defined as in Definition 4.2.5, the skew-adjointness was first proven in [147, Thm. 2.2] and [165, Thm. 3.18]. Here, however, we pursue a strategy different from [147, 165] and make use of the representation of $\mathcal{T}$ in action-angle type variables.

Remark 4.3.14. *In [147, 165], the skew-adjointness of $\mathcal{T} \colon \mathrm{D}(\mathcal{T}) \to H$ is proven without using action-angle type variables. This proof has, in fact, conceptual advantages as it can be generalised to related system more directly. For instance, it is unknown whether (the analogue of) the effective potential associated to relevant steady states of the Einstein-Vlasov system has the same structure as Ψ_L does here, cf. the discussion in [49, Sc. 3.1]. This structure is, however, crucial in order to introduce action-angle type variables. Hence, one cannot use action-angle type variables in the context of the Einstein-Vlasov system in general. Nonetheless, in [147], the skew-adjointness of the transport operator is also proven for suitable steady states of the Einstein-Vlasov system.*

The proofs in [147, 165] mainly rely on a suitable approximation result for the transport operator, cf. [147, Prop. 2] and [165, Thm. 3.15], whose proof is, however, quite technical. We will also need this approximation result later, see Section 4.3.5, but not yet to obtain the results of the present section.

[101] More precisely, we require that the limit $\lim_{n\to\infty} \sum_{j=-n}^{n} c_j\, e^{2\pi i j\,\theta}$ exists in $L^2(\mathbb{S}^1)$ and that it is real-valued a.e. on $\mathbb{S}^1$.

[102] The terminology *skew-adjoint* is inspired by the finite-dimensional setting, where a matrix $A \in \mathbb{R}^{n\times n}$ satisfying $A^T = -A$ is usually called skew-symmetric. Skew-adjoint operators are also often called *anti-self-adjoint*, but we do not like this name very much and will hence not use it here.

The main idea of our proof, which is also outlined in [62, Prop. 5.15 (a)] in a different context, is that Lemma 4.3.9 allows us to reduce the application of the transport operator $\mathcal{T}$ to the calculation of the partial derivative w.r.t. the angle variable θ; recall Definition 4.2.5 for the definition of the transport operator and its domain of definition.

Proposition 4.3.15 (Skew-Adjointness of the Transport Operator)**.** *The transport operator $\mathcal{T}\colon \mathrm{D}(\mathcal{T}) \to H$ is skew-adjoint as a densely defined operator on H, i.e., $\mathcal{T}^* = -\mathcal{T}$. In particular, $\mathcal{T}$ is skew-symmetric, i.e.,*

$$\langle \mathcal{T} f, g\rangle_H = -\langle f, \mathcal{T} g, \rangle_H, \qquad f, g \in \mathrm{D}(\mathcal{T}). \tag{4.3.53}$$

Proof. Recall that the transport operator $\mathcal{T}\colon \mathrm{D}(\mathcal{T}) \to H$ is linear and densely defined on the Hilbert space H by Remark 4.2.6. The domain of definition of its adjoint $\mathcal{T}^*$ is given by

$$\mathrm{D}(\mathcal{T}^*) = \{f \in H \mid \exists_1 \mathcal{T}^* f \in H \,\forall \xi \in \mathrm{D}(\mathcal{T})\colon \langle \mathcal{T}\xi, f\rangle_H = \langle \xi, \mathcal{T}^* f\rangle_H\}. \tag{4.3.54}$$

If $f \in \mathrm{D}(\mathcal{T}^*)$, there thus holds

$$\langle \mathcal{T}\xi, f\rangle_H = \langle \xi, \mathcal{T}^* f\rangle_H \tag{4.3.55}$$

for any test function $\xi \in C^1_{c,r}(\Omega_0)$; recall $C^1_{c,r}(\Omega_0) \subset \mathrm{D}(\mathcal{T})$ by Remark 4.2.6 (b). By Definition 4.2.5, this means that the transport term $\mathcal{T} f$ exists weakly with $\mathcal{T} f = -\mathcal{T}^* f \in H$.

Conversely, if $f \in \mathrm{D}(\mathcal{T})$, changing variables via (4.3.14) and using Lemma 4.3.9 yields

$$\langle \mathcal{T}\xi, f\rangle_H = 4\pi^2 \int_{\mathbb{D}_0} \frac{1}{|\varphi'(E,L)|} \int_{\mathbb{S}^1} \partial_\theta \xi(\theta, E, L)\, f(\theta, E, L)\, \mathrm{d}\theta\, \mathrm{d}(E, L) \tag{4.3.56}$$

for $\xi \in \mathrm{D}(\mathcal{T})$. Integrating by parts (in the weak sense) in the inner integral – notice that $\xi(\cdot, E, L) \in H^1(\mathbb{S}^1)$ and $f(\cdot, E, L) \in H^1(\mathbb{S}^1)$ for a.e. $(E, L) \in \mathbb{D}_0$ by Lemma 4.3.9 – and reversing the change of variables hence implies

$$\langle \mathcal{T}\xi, f\rangle_H = -\langle \xi, \mathcal{T} f\rangle_H, \tag{4.3.57}$$

i.e., $f \in \mathrm{D}(\mathcal{T}^*)$ with $\mathcal{T}^* f = -\mathcal{T} f \in H$. □

The next step is to deduce an analogous result for the squared transport operator $\mathcal{T}^2\colon \mathrm{D}(\mathcal{T}^2) \to H$ as well as for its restriction to odd-in-v functions $\mathcal{T}^2\colon \mathrm{D}(\mathcal{T}^2) \cap \mathcal{H} \to \mathcal{H}$. We first verify that the restriction of $\mathcal{T}^2$ to odd-in-v functions is indeed well-defined by studying how applying the transport operator affects the v-parity of a function; a similar discussion is contained in [85, Rem. B.18] and [165, Lemma 3.3 and Cor. 3.17] as well as in [49, Prop. 5.1 (f)] in a different context.

Lemma 4.3.16. *The transport operator $\mathcal{T}\colon \mathrm{D}(\mathcal{T}) \to H$ reverses v-parity, i.e.,*

$$(\mathcal{T} f)_\pm = \mathcal{T}(f_\mp) =: \mathcal{T} f_\mp, \qquad f \in \mathrm{D}(\mathcal{T}); \tag{4.3.58}$$

in particular, $f \in \mathrm{D}(\mathcal{T})$ is equivalent to $f_\pm \in \mathrm{D}(\mathcal{T})$. As in Chapter 3, a subscript $+$ or $-$ denotes the even-in-v or odd-in-v part of a function, respectively, i.e.,[103]

$$f_\pm(x, v) \coloneqq \frac{1}{2}(f(x, v) \pm f(x, -v)), \qquad \text{a.e. } (x, v) \in \Omega_0,\ f \in H. \tag{4.3.59}$$

Accordingly, the squared transport operator $\mathcal{T}^2$ preserves v-parity, i.e.,

$$(\mathcal{T}^2 f)_\pm = \mathcal{T}^2 f_\pm, \qquad f \in \mathrm{D}(\mathcal{T}^2), \tag{4.3.60}$$

and $f \in \mathrm{D}(\mathcal{T}^2)$ is equivalent to $f_\pm \in \mathrm{D}(\mathcal{T}^2)$. In particular, $\mathcal{T}^2 f \in \mathcal{H}$ for $f \in \mathrm{D}(\mathcal{T}^2) \cap \mathcal{H}$.

[103] Note that the set Ω_0 is even-in-v, in the sense that $(x, v) \in \Omega_0$ is equivalent to $(x, -v) \in \Omega_0$.

Proof. The identity (4.3.58) is straight-forward to verify in the case of a smooth function $f \in C^1_{c,r}(\Omega_0)$ using the chain rule, cf. [165, Lemma 3.3]. Then, by using that even-in-v and odd-in-v functions are orthogonal w.r.t. $\langle \cdot, \cdot \rangle_H$, we deduce

$$\langle (\mathcal{T} f)_\pm, \xi \rangle_H = \langle \mathcal{T} f, \xi_\pm \rangle_H = -\langle f, \mathcal{T} \xi_\pm \rangle_H = -\langle f, (\mathcal{T}\xi)_\mp \rangle_H = -\langle f_\mp, \mathcal{T}\xi \rangle_H \tag{4.3.61}$$

for $f \in \mathrm{D}(\mathcal{T})$ and any test function $\xi \in C^1_{c,r}(\Omega_0)$, which shows (4.3.58). The claims regarding the squared transport operator follow from the results for $\mathcal{T}$. □

Using Proposition 4.3.15, we now show that $\mathcal{T}^2 \colon \mathrm{D}(\mathcal{T}^2) \to H$ and $\mathcal{T}^2 \colon \mathrm{D}(\mathcal{T}^2) \cap \mathcal{H} \to \mathcal{H}$ are self-adjoint; recall Definitions 4.2.3 and 4.2.5 for the definitions of $\mathcal{H}$ and $\mathrm{D}(\mathcal{T}^2)$. This result is crucial when studying the operator associated to linearised Vlasov-Poisson system in the second-order formulation. Similar results are contained in [62, Prop. 4.2] and [85, Lemma B.8 (b)] as well as in [49, Prop. 5.1 (a)] and [61, Lemma 3.7] in different settings.

Proposition 4.3.17 (Self-Adjointness of the Squared Transport Operator)**.** *The following assertions hold.*

(a) The squared transport operator $\mathcal{T}^2 \colon \mathrm{D}(\mathcal{T}^2) \to H$ is self-adjoint as a densely defined operator on H.

(b) The operator $\mathcal{T}^2\big|_{\mathcal{H}} \colon \mathrm{D}(\mathcal{T}^2) \cap \mathcal{H} \to \mathcal{H}$ is self-adjoint as a densely defined operator on $\mathcal{H}$.

Proof. First observe that $C^2_{c,r}(\Omega_0) \subset \mathrm{D}(\mathcal{T}^2)$ by Remark 4.2.6 (b), which shows that $\mathcal{T}^2 \colon \mathrm{D}(\mathcal{T}^2) \to H$ is indeed densely defined on H. In order to obtain the self-adjointness of $\mathcal{T}^2$, we proceed as in [62, Proof of Prop. 4.2 (c)]: By Proposition 4.3.15, the transport operator $\mathcal{T} \colon (\mathcal{T}) \to H$ is closed[104] and it holds that $\mathcal{T}^2 = -\mathcal{T}^*\mathcal{T}$ as well as $\mathrm{D}(\mathcal{T}^2) = \{f \in \mathrm{D}(\mathcal{T}) \mid \mathcal{T} f \in \mathrm{D}(\mathcal{T}^*)\}$. It hence follows by von Neumann's theorem [133, Thm. X.25] that $\mathcal{T}^2 \colon \mathrm{D}(\mathcal{T}^2) \to H$ is self-adjoint.

For part (b), first note that $\mathcal{T}^2 \colon \mathrm{D}(\mathcal{T}^2) \cap \mathcal{H} \to \mathcal{H}$ is well-defined by Lemma 4.3.16. The same arguments as above further show that it is densely defined since $C^2_{c,r}(\Omega_0) \cap \mathcal{H}$ is dense in $\mathcal{H}$. Similar to [62, Proof of Prop. 4.2 (d)], the self-adjointness of the restricted operator $\mathcal{T}^2\big|_{\mathcal{H}}$ follows by part (a) by splitting all functions into their even and odd parts in v. More precisely, the adjoint $\mathcal{T}^2\big|^*_{\mathcal{H}}$ of the operator in part (b) is defined on

$$\mathrm{D}(\mathcal{T}^2\big|^*_{\mathcal{H}}) = \{f \in \mathcal{H} \mid \exists_1 \mathcal{T}^2\big|^*_{\mathcal{H}} f \in \mathcal{H} \; \forall \xi \in \mathrm{D}(\mathcal{T}^2) \cap \mathcal{H} \colon \langle \mathcal{T}^2 \xi, f \rangle_H = \langle \xi, \mathcal{T}^2\big|^*_{\mathcal{H}} f \rangle_H\}. \tag{4.3.62}$$

For $f \in \mathrm{D}(\mathcal{T}^2\big|^*_{\mathcal{H}})$, Lemma 4.3.16 implies the following for all $\xi \in \mathrm{D}(\mathcal{T}^2)$:

$$\langle \mathcal{T}^2 \xi, f \rangle_H = \langle (\mathcal{T}^2 \xi)_-, f \rangle_H = \langle \mathcal{T}^2 \xi_-, f \rangle_H = \langle \xi_-, \mathcal{T}^2\big|^*_{\mathcal{H}} f \rangle_H = \langle \xi, \mathcal{T}^2\big|^*_{\mathcal{H}} f \rangle_H. \tag{4.3.63}$$

Hence, by part (a), $f \in \mathrm{D}(\mathcal{T}^2)$ with $\mathcal{T}^2 f = \mathcal{T}^2\big|^*_{\mathcal{H}} f$. Conversely, if $f \in \mathrm{D}(\mathcal{T}^2) \cap \mathcal{H}$, the symmetry of $\mathcal{T}^2$ from part (a) yields

$$\langle \mathcal{T}^2 \xi, f \rangle_H = \langle \xi, \mathcal{T}^2 f \rangle_H, \qquad \xi \in \mathrm{D}(\mathcal{T}^2) \cap \mathcal{H}, \tag{4.3.64}$$

which means $f \in \mathrm{D}(\mathcal{T}^2\big|^*_{\mathcal{H}})$ with $\mathcal{T}^2\big|^*_{\mathcal{H}} f = \mathcal{T}^2 f \in \mathcal{H}$. □

A more direct proof of the self-adjointness of $\mathcal{T}^2 \colon \mathrm{D}(\mathcal{T}^2) \to H$ based on the Fourier expansion in the angle variable, cf. Remark 4.3.13, can be found in [85, Lemma B.8 (b)].

[104] By [136, Thm. VIII.1], the adjoint of a densely defined operator on a Hilbert space is always closed. Thus, any skew-adjoint operator is closed.

4.3.3 The Spectrum of the Squared Transport Operator

The aim of this section is to analyse the spectrum of the squared transport operator restricted to odd-in-v functions $-\mathcal{T}^2\big|_{\mathcal{H}}\colon \mathrm{D}(\mathcal{T}^2)\cap\mathcal{H}\to\mathcal{H}$ as thoroughly as possible; recall Definition 4.2.5 for the definition of this operator. The reason for this is that certain parts of the spectrum of the linearised operator $\mathcal{L}$ are determined by the spectrum of $-\mathcal{T}^2\big|_{\mathcal{H}}$, cf. Section 4.5.2. Recall that $\mathcal{T}^2\big|_{\mathcal{H}}$ is self-adjoint by Proposition 4.3.17. For general background on the concepts of spectral theory for self-adjoint operators that we use in this section, we refer to [69, 133, 136].

Of particular help for the analysis of the spectrum of $-\mathcal{T}^2\big|_{\mathcal{H}}$ are the action-angle type variables introduced in Section 4.3.1. The Fourier series expansion from Lemma 4.3.12 allows us to explicitly derive resolvent operators for $-\mathcal{T}^2\big|_{\mathcal{H}}$. This is based on [62, Eqn. (8.15)], see also [85, Cor. B.10].

Lemma 4.3.18. *For the spectrum of the operator $-\mathcal{T}^2\big|_{\mathcal{H}}\colon \mathrm{D}(\mathcal{T}^2)\cap\mathcal{H}\to\mathcal{H}$ it holds that*

$$\sigma(-\mathcal{T}^2\big|_{\mathcal{H}})\subset\overline{\left(\frac{2\pi\mathbb{N}}{T(\mathbb{D}_0)}\right)^2}, \tag{4.3.65}$$

where

$$\left(\frac{2\pi\mathbb{N}}{T(\mathbb{D}_0)}\right)^2 := \left\{\frac{4\pi^2 j^2}{T(E,L)^2}\mid (E,L)\in\mathbb{D}_0,\, j\in\mathbb{N}=\mathbb{N}\setminus\{0\}\right\}, \tag{4.3.66}$$

T is the period function, and $\mathbb{D}_0$ denotes the (E,L)-triangle defined in (2.2.88). *For*[105] *$\lambda\in\mathbb{R}\setminus\overline{\left(\frac{2\pi\mathbb{N}}{T(\mathbb{D}_0)}\right)^2}$, the resolvent operator*[106]

$$\left(-\mathcal{T}^2\big|_{\mathcal{H}}-\lambda\right)^{-1}\colon\mathcal{H}\to\mathcal{H} \tag{4.3.67}$$

is given by

$$\left(-\mathcal{T}^2|_{\mathcal{H}}-\lambda\right)^{-1}f(\theta,E,L)=\sum_{j=1}^{\infty}\frac{b_j(E,L)}{\frac{4\pi^2j^2}{T(E,L)^2}-\lambda}\sin(2\pi j\,\theta),\qquad f\in\mathcal{H},\,(\theta,E,L)\in\mathbb{S}^1\times\mathbb{D}_0, \tag{4.3.68}$$

which is meant to hold as a limit in H with b_j determined by f via (4.3.45).

Proof. Using the Fourier series expansion (4.3.46) of $f\in\mathcal{H}$ yields

$$\|f\|_H^2=\frac{1}{2}\sum_{j=1}^{\infty}\|b_j\|_H^2. \tag{4.3.69}$$

Hence,

$$\begin{aligned}\left\|\sum_{j=1}^{\infty}\frac{b_j}{\frac{4\pi^2j^2}{T^2}-\lambda}\sin(2\pi j\,\cdot)\right\|_H^2&=\sum_{j=1}^{\infty}\left\|\frac{b_j}{\frac{4\pi^2j^2}{T^2}-\lambda}\right\|_H^2\|\sin(2\pi j\,\cdot)\|_{L^2(\mathbb{S}^1)}^2\le\\&\le\operatorname{dist}\left(\lambda,\left(\frac{2\pi\mathbb{N}}{T(\mathbb{D}_0)}\right)^2\right)^{-2}\frac{1}{2}\sum_{j=1}^{\infty}\|b_j\|_H^2=\operatorname{dist}\left(\lambda,\left(\frac{2\pi\mathbb{N}}{T(\mathbb{D}_0)}\right)^2\right)^{-2}\|f\|_H^2,\end{aligned} \tag{4.3.70}$$

[105] A similar statement also holds for complex-valued $\lambda\in\mathbb{C}\setminus\overline{\left(\frac{2\pi\mathbb{N}}{T(\mathbb{D}_0)}\right)^2}$.

[106] We always identify λ with the operator $\lambda\,\mathrm{id}$.

which shows that (4.3.68) indeed defines a bounded operator for $\lambda \in \mathbb{R} \setminus \overline{\left(\frac{2\pi\mathbb{N}}{T(\mathbb{D}_0)}\right)^2}$; note that the limit (4.3.68) is odd-in-v a.e. by Remark 4.3.7 since $\mathcal{H}$ is closed and $\sin(2\pi j\cdot) \in L^{2,\mathrm{odd}}(\mathbb{S}^1)$ for $j \in \mathbb{N}$.

The fact that (4.3.68) defines the inverse of $(-\mathcal{T}^2\big|_{\mathcal{H}} - \lambda)\colon \mathrm{D}(\mathcal{T}^2) \cap \mathcal{H} \to \mathcal{H}$ is straightforward to verify using the Fourier series expansions (4.3.46) and (4.3.49) as well as the Fourier characterisation of $\mathrm{D}(\mathcal{T}^2)$ derived in Remark 4.3.13.

Lastly, note that the entire spectrum of $-\mathcal{T}^2\big|_{\mathcal{H}}$ has to be real-valued because the operator is self-adjoint, cf. [69, Thm. 5.5]. □

The lemma above bounds the size of the spectrum of $-\mathcal{T}^2\big|_{\mathcal{H}}$, but leaves it open which elements are actually contained in this set. The following result shows that $\sigma(-\mathcal{T}^2\big|_{\mathcal{H}})$ is indeed as large as the lemma above allows it to be. Furthermore, we can explicitly determine the *essential spectrum* σ_{ess} of the operator, i.e., all elements of the spectrum which are not isolated eigenvalues of finite multiplicity, cf. [69, Ch. 7] or [136, p. 236] and recall that the operator under consideration is self-adjoint. This result forms the basis for all further spectral statements about $-\mathcal{T}^2\big|_{\mathcal{H}}$ and the whole linearised operator $\mathcal{L}$. It is based on [62, Thm. 5.7]; see also [85, Lemma B.12] for a slightly different proof as well as [61, Lemma 3.7 (e)] for an adaption of the result.

Proposition 4.3.19 (The Spectrum of the Squared Transport Operator on $\mathcal{H}$)**.** *The spectrum of the operator* $-\mathcal{T}^2\big|_{\mathcal{H}}\colon \mathrm{D}(\mathcal{T}^2) \cap \mathcal{H} \to \mathcal{H}$ *is given by*

$$\sigma(-\mathcal{T}^2\big|_{\mathcal{H}}) = \overline{\left(\frac{2\pi\mathbb{N}}{T(\mathbb{D}_0)}\right)^2}, \tag{4.3.71}$$

recall (4.3.66) *for the definition of the set on the right-hand side. Furthermore, the spectrum is purely essential, i.e.,*

$$\sigma_{\mathrm{ess}}(-\mathcal{T}^2\big|_{\mathcal{H}}) = \sigma(-\mathcal{T}^2\big|_{\mathcal{H}}). \tag{4.3.72}$$

Proof. We first show $\lambda^* \coloneqq 4\pi^2 n^2\, T(E^*, L^*)^{-2} \in \sigma_{\mathrm{ess}}(-\mathcal{T}^2\big|_{\mathcal{H}})$ for fixed $n \in \mathbb{N}$ and $(E^*, L^*) \in \mathbb{D}_0$. The idea is that

$$\mathbb{S}^1 \times \mathbb{D}_0 \ni (\theta, E, L) \mapsto \delta_{(E^*,L^*)}(E, L)\, \sin(2\pi n\, \theta) \tag{4.3.73}$$

is an "eigendistribution" of $-\mathcal{T}^2\big|_{\mathcal{H}}$, where δ denotes Dirac's delta distribution.[107] Hence, λ^* is an "approximate eigenvalue", and suitably approximating the eigendistribution shows that it belongs to the essential spectrum.

This idea can be turned into a rigorous proof by applying *Weyl's criterion*, see [69, Thm. 7.2] or, in the case of a bounded operator, [136, Thm. VII.12]. In our situation, it states that $\lambda^* \in \sigma_{\mathrm{ess}}(-\mathcal{T}^2\big|_{\mathcal{H}})$ iff there exists a sequence $(f_j)_{j\in\mathbb{N}} \subset \mathrm{D}(\mathcal{T}^2) \cap \mathcal{H}$ with the following three properties:

(i) $\|f_j\|_H = 1$ for $j \in \mathbb{N}$.

(ii) $\| - \mathcal{T}^2 f_j - \lambda^* f_j\|_H \to 0$ as $j \to \infty$.

(iii) $f_j \rightharpoonup 0$ in $\mathcal{H}$ as $j \to \infty$.

[107] More precisely, (4.3.73) formally solves $-\mathcal{T}^2 f = \lambda^* f$ if one takes (4.3.39) as the definition of the squared transport operator. Furthermore, in the light of Remark 4.3.7, the expression (4.3.73) is formally odd in v.

In order to construct such a sequence, which is then usually called a *Weyl sequence*, we approximate the Dirac delta distribution contained in (4.3.73) as follows:[108] For $j \in \mathbb{N}$ let $\chi_j \colon \mathbb{R}^2 \to \mathbb{R}$ be measurable and s.t.

$$\operatorname{supp}(\chi_j) \subset \mathbb{D}_0 \cap B_{\frac{1}{j}}(E^*, L^*) \tag{4.3.74}$$

as well as

$$\int_{\mathbb{D}_0} \chi_j^2(E,L)\,\mathrm{d}(E,L) = \frac{1}{2\pi^2}. \tag{4.3.75}$$

It is straight-forward to explicitly define such χ_j by a rescaling scheme. We then define the a.e. spherically symmetric function $f_j \colon \Omega_0 \to \mathbb{R}$ for $j \in \mathbb{N}$ by

$$f_j(\theta,E,L) \coloneqq \sqrt{\frac{|\varphi'(E,L)|}{T(E,L)}}\,\chi_j(E,L)\,\sin(2\pi n\,\theta), \qquad (\theta,E,L) \in \mathbb{S}^1 \times \mathbb{D}_0. \tag{4.3.76}$$

In order to verify that $(f_j)_{j\in\mathbb{N}}$ indeed forms a Weyl sequence, first note that $f_j \in \mathrm{D}(\mathcal{T}^2)$ for $j \in \mathbb{N}$ by Lemma 4.3.10 and since T is bounded and bounded away from zero on the compact support of χ_j by Proposition A.0.1. Furthermore, $f_j \in \mathcal{H}$ by Remark 4.3.7 since $\sin(2\pi n\cdot) \in L^{2,\mathrm{odd}}(\mathbb{S}^1)$. Let us now verify the properties (i)–(iii):

(i) For $j \in \mathbb{N}$, changing variables via (4.3.14) and using (4.3.75) yields

$$\begin{aligned}\|f_j\|_H^2 &= 4\pi^2 \int_{\mathbb{D}_0} \frac{T(E,L)}{|\varphi'(E,L)|} \int_{\mathbb{S}^1} |f_j(\theta,E,L)|^2\,\mathrm{d}\theta\,\mathrm{d}(E,L) = \\ &= 4\pi^2 \int_{\mathbb{D}_0} \chi_j^2(E,L) \int_{\mathbb{S}^1} \sin^2(2\pi n\,\theta)\,\mathrm{d}\theta\,\mathrm{d}(E,L) = 1.\end{aligned} \tag{4.3.77}$$

(ii) Lemma 4.3.10 implies

$$-\mathcal{T}^2 f_j(\theta,E,L) = \frac{4\pi^2 n^2}{T(E,L)^2}\,f_j(\theta,E,L), \qquad \text{a.e. } (\theta,E,L) \in \mathbb{S}^1 \times \mathbb{D}_0, \tag{4.3.78}$$

for $j \in \mathbb{N}$. Hence,

$$\begin{aligned}&\|-\mathcal{T}^2 f_j - \lambda^* f_j\|_H^2 = \\ &= 4\pi^2 \int_{\mathbb{D}_0} \frac{T(E,L)}{|\varphi'(E,L)|} \left| \frac{4\pi^2 n^2}{T(E,L)^2} - \lambda^* \right|^2 \int_{\mathbb{S}^1} |f_j(\theta,E,L)|^2\,\mathrm{d}\theta\,\mathrm{d}(E,L) = \\ &= (2\pi)^6 n^4 \int_{\mathbb{D}_0} \chi_j^2(E,L) \left| \frac{1}{T(E,L)^2} - \frac{1}{T(E^*,L^*)^2} \right|^2 \int_{\mathbb{S}^1} \sin^2(2\pi n\,\theta)\,\mathrm{d}\theta\,\mathrm{d}(E,L) = \\ &= 2^5 \pi^6 n^4 \int_{\mathbb{D}_0} \chi_j^2(E,L) \left| \frac{1}{T(E,L)^2} - \frac{1}{T(E^*,L^*)^2} \right|^2 \mathrm{d}(E,L).\end{aligned} \tag{4.3.79}$$

Because the period function T is positive and continuous on $\mathbb{D}_0$ by Proposition A.0.1 (b), the integrand of the latter integral converges pointwise to zero as $j \to \infty$ by (4.3.74). Together with (4.3.75), Lebesgue's dominated convergence theorem implies $\left\|-\mathcal{T}^2 f_j - \lambda^* f_j\right\|_H \to 0$ as $j \to \infty$.

[108] Although $(\chi_j)_{j\in\mathbb{N}}$ is used to approximate the Dirac delta distribution, we note that χ_j does not convergence to $\delta_{(E^*,L^*)}$ as $j \to \infty$ in the sense of distributional convergence [98, Sc. 6.3].

(iii) First note that $\mathcal{H}^* \cong \mathcal{H}$ by the Riesz representation theorem. For every $h \in \mathcal{H}$ and $j \in \mathbb{N}$, applying the Cauchy-Schwarz inequality yields

$$|\langle f_j, h\rangle_H| \leq \|f_j\|_H \left(4\pi^2 \int_{\operatorname{supp}(\chi_j)} \frac{T(E,L)}{|\varphi'(E,L)|} \int_{\mathbb{S}^1} |h(\theta,E,L)|^2 \,\mathrm{d}\theta \,\mathrm{d}(E,L)\right)^{\frac{1}{2}}. \quad (4.3.80)$$

Since $\|f_j\|_H = 1$ by (i), the integral on the right-hand side tends to zero as $j \to \infty$ by (4.3.74) and Lebesgue's dominated convergence theorem. Hence, $f_j \rightharpoonup 0$ in $\mathcal{H}$ as $j \to \infty$.

We have thus proven

$$\left(\frac{2\pi\mathbb{N}}{T(\mathbb{D}_0)}\right)^2 \subset \sigma_{\mathrm{ess}}(-\mathcal{T}^2\big|_{\mathcal{H}}). \quad (4.3.81)$$

Since the essential spectrum is always closed,[109] we deduce

$$\overline{\left(\frac{2\pi\mathbb{N}}{T(\mathbb{D}_0)}\right)^2} \subset \sigma_{\mathrm{ess}}(-\mathcal{T}^2\big|_{\mathcal{H}}) \subset \sigma(-\mathcal{T}^2\big|_{\mathcal{H}}). \quad (4.3.82)$$

Combining this statement with Lemma 4.3.18 concludes the proof. □

The proposition above hence shows that the spectrum of $-\mathcal{T}^2\big|_{\mathcal{H}}$ is entirely determined by the period function T, or, to be more precise, by the values which T attains on $\mathbb{D}_0$. Let us briefly discuss the possible shapes of the set $\sigma(-\mathcal{T}^2\big|_{\mathcal{H}})$. This is based on [62, Rem. 5.10].

Remark 4.3.20 (The Structure of the Spectrum of the Squared Transport Operator)**.** *Inspired by [61, Eqn. (3.11)], let*

$$T_{\min} \coloneqq \inf_{\mathbb{D}_0} T, \qquad T_{\max} \coloneqq \sup_{\mathbb{D}_0} T; \quad (4.3.83)$$

it follows by Proposition A.0.1 (a) that both of these values are positive and finite. Since $\mathbb{D}_0$ is connected and T is continuous by Proposition A.0.1 (b), there holds

$$\overline{T(\mathbb{D}_0)} = [T_{\min}, T_{\max}], \quad (4.3.84)$$

and, accordingly,

$$\sigma(-\mathcal{T}^2\big|_{\mathcal{H}}) = \bigcup_{j\in\mathbb{N}} \left[\frac{4\pi^2 j^2}{T_{\max}^2}, \frac{4\pi^2 j^2}{T_{\min}^2}\right]; \quad (4.3.85)$$

see also [85, Lemma B.12], where the spectrum is written down in the same way. The qualitative structure of this set depends on the ratio of $T_{\min}$ and $T_{\max}$:

If $T_{\max} \geq 2T_{\min}$,

$$\sigma(-\mathcal{T}^2\big|_{\mathcal{H}}) = \left[\frac{4\pi^2}{T_{\max}^2}, \infty\right[. \quad (4.3.86)$$

In [61], one solely works in this setting, cf. [61, Lemma 3.10 (b) and Cor. 3.11]. Since the spectrum is connected, it is referred to be of a single gap structure *due to the "gap" between 0 and $\min\sigma(-\mathcal{T}^2\big|_{\mathcal{H}})$.*

[109] In order to see that the essential spectrum is closed, observe that the whole spectrum is always closed, cf. [69, Thm. 1.2], and that, by definition, σ_{ess} contains all non-isolated elements of the spectrum. In the case of a bounded and self-adjoint operator, the fact that σ_{ess} is closed is proven in [136, Thm. VII.9].

In contrast, if $T_{\max} < 2T_{\min}$*, there are also gaps inside* $\sigma(-\mathcal{T}^2\big|_{\mathcal{H}})$*. For instance, if* $\frac{3}{2} \leq \frac{T_{\max}}{T_{\min}} < 2$*,*

$$\sigma(-\mathcal{T}^2\big|_{\mathcal{H}}) = \left[\frac{4\pi^2}{T_{\max}^2}, \frac{4\pi^2}{T_{\min}^2}\right] \dot{\cup} \left[\frac{16\pi^2}{T_{\max}^2}, \infty\right[. \tag{4.3.87}$$

In general, the number of gaps inside $\sigma(-\mathcal{T}^2\big|_{\mathcal{H}})$*, not counting the one between* 0 *and* $\min \sigma(-\mathcal{T}^2\big|_{\mathcal{H}})$*, is given by*

$$\sup\{j \in \mathbb{N}_0 \mid (j+1)\, T_{\min} > j\, T_{\max}\}. \tag{4.3.88}$$

In particular, the spectrum has infinitely many gaps iff T *is constant on* $\mathbb{D}_0$*.*

In the situations (4.3.86) *and* (4.3.87)*, the set* $\sigma(-\mathcal{T}^2\big|_{\mathcal{H}})$ *is visualised in Figure 4.3.2.*

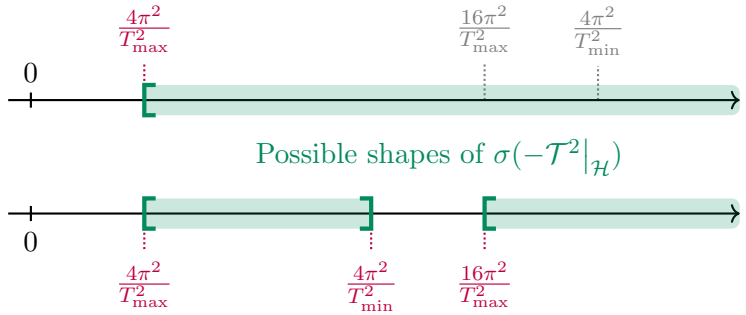

Figure 4.3.2: A schematic visualisation of the spectrum of $-\mathcal{T}^2\big|_{\mathcal{H}}$ in the two situations (4.3.86) and (4.3.87).

So far we have only studied the spectrum of the squared transport operator when it is restricted to odd-in-v functions. With regard to the analysis of the linearised operator $\mathcal{L}$, this is the relevant case, cf. Remark 4.2.10. However, with the same methods as above, one can also determine the spectrum of the non-restricted squared transport operator $\mathcal{T}^2 \colon \mathrm{D}(\mathcal{T}^2) \to H$. This is done in [62, Sc. 5.1] and mentioned in [85, Rem. B.11], and we also state the results here.

Remark 4.3.21. *The spectrum of* $-\mathcal{T}^2 \colon \mathrm{D}(\mathcal{T}^2) \to H$ *is of the form*

$$\sigma(-\mathcal{T}^2) = \sigma_{\mathrm{ess}}(-\mathcal{T}^2) = \overline{\left(\frac{2\pi\mathbb{N}_0}{T(\mathbb{D}_0)}\right)^2}, \tag{4.3.89}$$

where the set on the right-hand side is defined similarly to (4.3.66)*. Compared to the restricted operator* $-\mathcal{T}^2\big|_{\mathcal{H}} \colon \mathrm{D}(\mathcal{T}^2) \cap \mathcal{H} \to \mathcal{H}$*, cf. Proposition 4.3.19,* 0 *is now part of the (essential) spectrum. This can be seen by replacing the* θ*-dependency in the eigendistribution in the proof of Proposition 4.3.19 by a non-vanishing, constant-in-*θ *function. Note that such* θ*-dependence does not correspond to an odd-in-*v *expression, cf. Remark 4.3.7. The fact that no further elements besides* 0 *are contained in* $\sigma(-\mathcal{T}^2) \setminus \sigma(-\mathcal{T}^2\big|_{\mathcal{H}})$ *can be verified similarly to Lemma 4.3.18 by explicitly deriving the resolvent operator* $(-\mathcal{T}^2 - \lambda)^{-1}$ *using the Fourier expansions* (4.3.41) *and* (4.3.48)*.*

Although Proposition 4.3.19 determines the spectrum of $-\mathcal{T}^2\big|_{\mathcal{H}}$ explicitly, and even shows that the spectrum is purely essential, it still remains unclear whether $-\mathcal{T}^2\big|_{\mathcal{H}}$ possesses eigenvalues. Note that the elements of the essential spectrum might be eigenvalues

of infinite multiplicity, embedded eigenvalues, or just "approximate eigenvalues", cf. [69, Ch. 7]. Understanding whether $-\mathcal{T}^2\big|_{\mathcal{H}}$ possesses eigenvalues is important when studying the behaviour of solutions of the so-called "pure transport equation" $\partial_t + \mathcal{T} f = 0$, which is studied in [27, 103, 116, 148] among others, but on which we will not further elaborate at this point. The following lemma shows that the presence of eigenvalues of $-\mathcal{T}^2\big|_{\mathcal{H}}$ is determined by the level sets of the period function T defined in Definition 2.2.16.

Lemma 4.3.22 (Eigenvalues of the Squared Transport Operator on $\mathcal{H}$)**.** *If there exists $t > 0$ s.t. the level set*

$$T\big|_{\mathbb{D}_0}^{-1}(\{t\}) = \{(E, L) \in \mathbb{D}_0 \mid T(E, L) = t\} \tag{4.3.90}$$

has positive (Lebesgue) measure, then, for every $j \in \mathbb{N}$,

$$\frac{4\pi^2 j^2}{t^2} \tag{4.3.91}$$

is an eigenvalue of $-\mathcal{T}^2\big|_{\mathcal{H}} \colon \mathrm{D}(\mathcal{T}^2) \cap \mathcal{H} \to \mathcal{H}$ with eigenfunction[110]

$$\mathbb{S}^1 \times \mathbb{D}_0 \ni (\theta, E, L) \mapsto \sqrt{|\varphi'(E, L)|}\, \mathbb{1}_{T|_{\mathbb{D}_0}^{-1}(\{t\})}(E, L)\, \sin(2\pi j\, \theta). \tag{4.3.92}$$

Conversely, if $T\big|_{\mathbb{D}_0}^{-1}(\{t\})$ has measure zero for every $t > 0$, no eigenvalues of $-\mathcal{T}^2\big|_{\mathcal{H}} \colon \mathrm{D}(\mathcal{T}^2) \cap \mathcal{H} \to \mathcal{H}$ exist.

Proof. If $T\big|_{\mathbb{D}_0}^{-1}(\{t\})$ has positive measure for some $t > 0$, it is straight-forward to verify that (4.3.92) indeed defines an eigenfunction to the eigenvalue (4.3.91) using Lemma 4.3.10. In particular, the eigenfunction is an element of $\mathrm{D}(\mathcal{T}^2) \cap \mathcal{H}$ by Remark 4.3.7.

In the case where no such t exists, suppose that $\lambda \in \mathbb{R}$ is an eigenvalue of $-\mathcal{T}^2\big|_{\mathcal{H}}$ with associated eigenfunction $f \in \mathrm{D}(\mathcal{T}^2) \cap \mathcal{H}$, i.e., $-\mathcal{T}^2 f = \lambda f$. Recall that $-\mathcal{T}^2\big|_{\mathcal{H}}$ is self-adjoint by Proposition 4.3.17, which is why every eigenvalue of the operator is necessarily real-valued. Inserting the Fourier expansions (4.3.46) and (4.3.49) into the eigenvalue equation yields

$$\lambda \sum_{j=1}^{\infty} b_j(E, L)\, \sin(2\pi j\, \theta) = \frac{4\pi^2}{T(E, L)^2} \sum_{j=1}^{\infty} b_j(E, L)\, j^2\, \sin(2\pi j\, \theta), \qquad (\theta, E, L) \in \mathbb{S}^1 \times \mathbb{D}_0, \tag{4.3.93}$$

where both sides hold as limits in H and the Fourier coefficients b_j are determined by f via (4.3.45). Equating the coefficients hence implies

$$\lambda\, b_j(E, L) = \frac{4\pi^2}{T(E, L)^2}\, b_j(E, L)\, j^2, \qquad j \in \mathbb{N},\ (E, L) \in \mathbb{D}_0. \tag{4.3.94}$$

Since f is an eigenfunction, it cannot vanish identically, which means that there exist $j^* \in \mathbb{N}$ and a set $A^* \subset \mathbb{D}_0$ with positive measure s.t. $b_{j^*} \neq 0$ a.e. on A^*. By (4.3.94), we thus deduce

$$\lambda = \frac{4\pi^2}{T(E, L)^2} (j^*)^2 \qquad \text{for a.e. } (E, L) \in A^*, \tag{4.3.95}$$

which contradicts the assumption that every level set of $T\big|_{\mathbb{D}_0}$ has measure zero. □

In Section 8.2, numerical simulations will indicate that the level sets of the period function on $\mathbb{D}_0$ have measure zero, cf. Observation 8.2.10.

[110] For every $A \subset T\big|_{\mathbb{D}_0}^{-1}(\{t\})$ with positive measure, $\mathbb{S}^1 \times \mathbb{D}_0 \ni (\theta, E, L) \mapsto \sqrt{|\varphi'(E, L)|}\, \mathbb{1}_A(E, L)\, \sin(2\pi j\, \theta)$ defines an eigenfunction as well. Hence, the eigenvalue (4.3.91) has infinite multiplicity.

4.3.4 Spectral Properties of the Transport Operator

The aim of this section is to study further, spectral type properties of the transport operator $\mathcal{T}\colon \mathrm{D}(\mathcal{T}) \to H$; recall that this operator is skew-adjoint by Proposition 4.3.15. Of particular interest is to characterise the nullspace (or *kernel*) of $\mathcal{T}$, i.e., the eigenspace associated to the eigenvalue zero. The first mathematically rigorous result in this direction was [14, Thm. 2.2]. For the weak definition of the transport operator as in Definition 4.2.5, the nullspace was first determined in [147, Thm. 2.3] and [165, Thm. 3.21], see also [49, Prop. 5.1 (c)], [53, p. 805f.], [61, Lemma 3.7 (c)], [62, Prop. 4.2 (b)], [85, Lemma B.9], and [96, Prop. 4.1 (i)] for related statements. Here, we follow an easier and more direct strategy than in [147, 165], which is based on the use of the action-angle type variables introduced in Section 4.3.1.

Proposition 4.3.23 (The Nullspace of the Transport Operator)**.** *The nullspace of the transport operator $\mathcal{T}\colon \mathrm{D}(\mathcal{T}) \to H$ is given by*

$$\ker(\mathcal{T}) = \{f \in H \mid \exists g\colon \mathbb{R}^2 \to \mathbb{R} \text{ s.t. } f(x,v) = g(E(x,v), L(x,v)) \text{ for a.e. } (x,v) \in \Omega_0\}. \tag{4.3.96}$$

Proof. Reformulating the claimed statement in action-angle type variables, we have to show that the nullspace of $\mathcal{T}$ is given by the functions in H which are a.e. independent from the angle variable $\theta \in \mathbb{S}^1$. This is, however, evident from Lemma 4.3.9 since

$$\ker\big(\partial_\theta\colon H^1(\mathbb{S}^1) \to L^2(\mathbb{S}^1)\big) = \{\mathbb{S}^1 \ni \theta \mapsto c \mid c \in \mathbb{R}\}. \tag{4.3.97}$$

□

The above proposition is closely related to *Jeans' theorem*, i.e., the statement that every spherically symmetric steady state of the Vlasov-Poisson system depends on E and L only, cf. Remark 2.2.4 (d). We discuss this connection in the following remark.

Remark 4.3.24. *Imagine that f_0 is a general spherically symmetric stationary solution of the Vlasov-Poisson system, not necessarily of the form* (2.2.6).[111] *The fact that f_0 solves the stationary Vlasov equation, potentially in a weak sense, can be interpreted as f_0 lying in the nullspace of its associated transport operator. If the latter is of the form as in the above proposition, the stationary solution can only depend on the phase space variables (x,v) through E and L, which is precisely the statement of Jeans' theorem.*

Due to this connection, the results in [147, 165] determining the nullspace of the transport operator are also referred to as Jeans' theorem.

In the context of general Hilbert space theory, the situation where $\ker(\mathcal{T})$ consists of functions depending only on the conserved quantities E and L of the associated characteristic flow is also called *ergodic*, cf. [136, Sc. II.5].[112]

As an aside, we note that the orthogonal projection onto the closed subspace $\ker(\mathcal{T})$ of H has been studied several times in the literature, cf. [53, Eqn. (29)], [96, Lemma 4.2], [147, Eqn. (17)], and [165, Def. and Rem. 3.20]. For $f \in H$, it is given by the zeroth Fourier coefficient $\hat{f}(0)$ defined in (4.3.40). This projection occurs naturally when transforming the linearised operator into a reduced operator for the potential as done in [53, Thm. 1.1]. However, we do not need this projection here.

An important consequence of Proposition 4.3.23 is that non-trivial odd-in-v functions are not in the nullspace of the transport operator. We even obtain the following useful result.

[111] This, more general, concept of a stationary solution of the Vlasov-Poisson system is not covered in Definition 2.2.2. We simply mean, analogously to before, that f_0 is constant along solutions of the characteristic system. This corresponds to f_0 solving the stationary Vlasov equation in an appropriate sense.

[112] More precisely, the characteristic flow of (2.2.93) is called ergodic in our situation.

Corollary 4.3.25. *It holds that*

$$\mathcal{H} \subset \ker(\mathcal{T})^{\perp}, \tag{4.3.98}$$

where the latter set denotes the orthogonal complement of $\ker(\mathcal{T})$ *w.r.t. the inner product on* H*, i.e.,*

$$\ker(\mathcal{T})^{\perp} \coloneqq \{f \in H \mid \forall g \in \ker(\mathcal{T})\colon f \perp g, \ \textit{i.e.,}\ \langle f, g\rangle_H = 0\}. \tag{4.3.99}$$

Proof. For $f \in \mathcal{H}$ and $g \in \ker(\mathcal{T})$, changing to action-angle type variables via (4.3.14) and using Proposition 4.3.23 yields

$$\langle f, g\rangle_H = 4\pi^2 \int_{\mathbb{D}_0} \frac{T(E,L)}{|\varphi'(E,L)|}\, g(E,L) \int_{\mathbb{S}^1} f(\theta, E, L)\,\mathrm{d}\theta\,\mathrm{d}(E,L) = 0, \tag{4.3.100}$$

where the latter equality is due to Remark 4.3.7. □

Besides characterising the nullspace of the transport operator, it is also important to understand the structure of the range (or *image*) of $\mathcal{T}$. In particular, the range has a natural connection to the orthogonal complement of $\ker(\mathcal{T})$: Since the transport operator is skew-adjoint by Proposition 4.3.15, it holds that

$$\ker(\mathcal{T})^{\perp} = \overline{\mathrm{im}(\mathcal{T})}, \tag{4.3.101}$$

cf. [24, Cor. 2.18]. Using the representation of $\mathcal{T}$ in action-angle type variables, we next show that $\mathrm{im}(\mathcal{T})$ is closed[113] and derive a useful characterisation of this set. This is based on [62, Lemma 5.5], see also [49, Prop. 5.1 (d)] for an adaptation of this result. We further note that similar ideas are already presented in [57, Sc. 3.2]. However, no action-angle type variables are used there, which makes the arguments more technical.[114]

Lemma 4.3.26 (The Range of the Transport Operator)**.** *The range and the nullspace of the transport operator* $\mathcal{T}\colon \mathrm{D}(\mathcal{T}) \to H$ *are related as follows:*

$$\mathrm{im}(\mathcal{T}) = \ker(\mathcal{T})^{\perp} = \{f \in H \mid \textit{for a.e. } (E,L) \in \mathbb{D}_0\colon \int_{\mathbb{S}^1} f(\theta, E, L)\,\mathrm{d}\theta = 0\}; \tag{4.3.102}$$

recall (4.3.99) *for the definition of the set* $\ker(\mathcal{T})^{\perp}$*.*

Proof. We start by proving the second identity in (4.3.102). The claim that any $f \in H$ with $\int_{\mathbb{S}^1} f(\theta, E, L)\,\mathrm{d}\theta = 0$ for a.e. $(E,L) \in \mathbb{D}_0$ is an element of $\ker(\mathcal{T})^{\perp}$ follows by the same arguments as the ones used the prove Corollary 4.3.25. Conversely, let $f \in \ker(\mathcal{T})^{\perp}$. By Proposition 4.3.23, every $\chi \in C_c^{\infty}(\mathbb{D}_0)$ corresponds to the element $\mathbb{S}^1 \times \mathbb{D}_0 \ni (\theta, E, L) \mapsto \chi(E,L)$ of $\ker(\mathcal{T})$. Hence, changing variables via (4.3.14) shows

$$\int_{\mathbb{D}_0} \frac{T(E,L)}{|\varphi'(E,L)|}\, \chi(E,L) \int_{\mathbb{S}^1} f(\theta, E, L)\,\mathrm{d}\theta\,\mathrm{d}(E,L) = 0 \tag{4.3.103}$$

for every such χ, which implies $\int_{\mathbb{S}^1} f(\theta, E, L)\,\mathrm{d}\theta = 0$ for a.e. $(E,L) \in \mathbb{D}_0$.

As to the first identity in (4.3.102), observe that the skew-symmetry of $\mathcal{T}$ derived in Proposition 4.3.15 immediately yields $\mathrm{im}(\mathcal{T}) \subset \ker(\mathcal{T})^{\perp}$. In order to verify the converse

[113] We will not explicitly state that $\mathrm{im}(\mathcal{T})$ is closed below, but this statement will follow from the fact that $\ker(\mathcal{T})^{\perp}$ is closed.

[114] In fact, the relation (4.3.104) corresponds to [57, Eqn. (3.13)] after rewriting the θ-integral in (r, w, L) variables.

inclusion, consider $f \in \ker(\mathcal{T})^\perp$ and define the spherically symmetric a.e. function $g\colon \Omega_0 \to \mathbb{R}$ via

$$g(\theta, E, L) \coloneqq T(E, L) \int_0^\theta f(\tau, E, L)\,\mathrm{d}\tau, \qquad \text{a.e. } (\theta, E, L) \in \mathbb{S}^1 \times \mathbb{D}_0. \tag{4.3.104}$$

Since $\int_0^1 f(\theta, E, L)\,\mathrm{d}\theta = \int_{\mathbb{S}^1} f(\theta, E, L)\,\mathrm{d}\theta = 0$ for a.e. $(E, L) \in \mathbb{D}_0$ by the arguments from above, $g(\cdot, E, L)$ is indeed well-defined on $\mathbb{S}^1$ for a.e. $(E, L) \in \mathbb{D}_0$. Moreover, $g(\cdot, E, L)$ is weakly differentiable on $\mathbb{S}^1$ for a.e. $(E, L) \in \mathbb{D}_0$ with

$$\partial_\theta g(\cdot, E, L) = T(E, L)\, f(\cdot, E, L) \qquad \text{weakly on } \mathbb{S}^1 \text{ for a.e. } (E, L) \in \mathbb{D}_0; \tag{4.3.105}$$

recall Remark 4.3.6 for the definition of weak derivatives on the circle $\mathbb{S}^1$. Furthermore, by the Cauchy-Schwarz inequality,

$$|g(\theta, E, L)|^2 \le T(E, L)^2 \int_{\mathbb{S}^1} |f(\tau, E, L)|^2\,\mathrm{d}\tau \qquad \text{for a.e. } (\theta, E, L) \in \mathbb{S}^1 \times \mathbb{D}_0, \tag{4.3.106}$$

which implies

$$\|g\|_H^2 \le 4\pi^2 \int_{\mathbb{D}_0} \frac{T(E, L)^3}{|\varphi'(E, L)|} \int_{\mathbb{S}^1} |f(\tau, E, L)|^2\,\mathrm{d}\tau\,\mathrm{d}(E, L) \le \sup_{\mathbb{D}_0}{}^2(T)\, \|f\|_H^2 < \infty \tag{4.3.107}$$

since the period function T is bounded by Proposition A.0.1 (a). Hence, $g \in H$, and together with

$$4\pi^2 \int_{\mathbb{D}_0} \frac{T(E, L)^{-1}}{|\varphi'(E, L)|} \int_{\mathbb{S}^1} |\partial_\theta g(\theta, E, L)|^2\,\mathrm{d}\theta\,\mathrm{d}(E, L) = \|f\|_H^2, \tag{4.3.108}$$

we conclude $g \in \mathrm{D}(\mathcal{T})$ with $\mathcal{T}g = f$ by Lemma 4.3.9, which means $f \in \mathrm{im}(\mathcal{T})$. □

In fact, the proof not only implies that $\mathrm{im}(\mathcal{T})$ and $\ker(\mathcal{T})^\perp$ are identical, but also shows how to explicitly construct $g \in \mathrm{D}(\mathcal{T})$ s.t. $\mathcal{T}g = f$ for prescribed $f \in \ker(\mathcal{T})^\perp$. Refining these arguments further provides a way of explicitly determining the inverse of the transport operator on the set $\ker(\mathcal{T})^\perp$. Since this representation of the inverse of $\mathcal{T}$ is also useful in other contexts, we state it next. This result is based on [49, Prop. 5.1 (g)].

Lemma 4.3.27 (The Inverse of the Transport Operator)**.** *The mapping $\mathcal{T}\colon \mathrm{D}(\mathcal{T}) \cap \ker(\mathcal{T})^\perp \to \mathrm{im}(\mathcal{T})$ is bijective, with inverse $\mathcal{T}^{-1}\colon \mathrm{im}(\mathcal{T}) \to \mathrm{D}(\mathcal{T}) \cap \ker(\mathcal{T})^\perp$ given by*

$$\mathcal{T}^{-1} f(\theta, E, L) = T(E, L) \left(\int_0^\theta f(\tau, E, L)\,\mathrm{d}\tau - \int_{\mathbb{S}^1} \int_0^\sigma f(\tau, E, L)\,\mathrm{d}\tau\,\mathrm{d}\sigma \right) \tag{4.3.109}$$

for $f \in \mathrm{im}(\mathcal{T})$ and a.e. $(\theta, E, L) \in \mathbb{S}^1 \times \mathbb{D}_0$.

Proof. Similar arguments as in the proof of Lemma 4.3.26 show that (4.3.109) indeed defines a function in $\mathrm{D}(\mathcal{T})$ satisfying $\mathcal{T}(\mathcal{T}^{-1} f) = f$ for $f \in \mathrm{im}(\mathcal{T}) = \ker(\mathcal{T})^\perp$; note that the additional term on the right-hand side of (4.3.109) compared to (4.3.104) is independent of θ and does thus not contribute to $\mathcal{T}(\mathcal{T}^{-1} f)$. However, the additional term obviously has the effect that $\int_{\mathbb{S}^1} \mathcal{T}^{-1} f(\theta, E, L)\,\mathrm{d}\theta = 0$ for a.e. $(E, L) \in \mathbb{D}_0$, which implies $\mathcal{T}^{-1} f \in \ker(\mathcal{T})^\perp$ by Lemma 4.3.26. Hence, $\mathcal{T}^{-1}\colon \mathrm{im}(\mathcal{T}) \to \mathrm{D}(\mathcal{T}) \cap \ker(\mathcal{T})^\perp$ given by (4.3.109) is indeed well-defined. Furthermore, for $f \in \mathrm{D}(\mathcal{T}) \cap \ker(\mathcal{T})^\perp$, using Lemma 4.3.9 and the main theorem of calculus yields

$$\begin{aligned} \mathcal{T}^{-1}(\mathcal{T} f)(\theta, E, L) &= \int_0^\theta \partial_\theta f(\tau, E, L)\,\mathrm{d}\tau - \int_{\mathbb{S}^1} \int_0^\sigma \partial_\theta f(\tau, E, L)\,\mathrm{d}\tau\,\mathrm{d}\sigma = \\ &= f(\theta, E, L) - f(0, E, L) - \int_{\mathbb{S}^1} (f(\sigma, E, L) - f(0, E, L))\,\mathrm{d}\sigma = f(\theta, E, L) \end{aligned} \tag{4.3.110}$$

for a.e. $(\theta, E, L) \in \mathbb{S}^1 \times \mathbb{D}_0$, where we again used $\int_{\mathbb{S}^1} f(\sigma, E, L)\,\mathrm{d}\sigma = 0$. □

A different way of deriving the inverse of the transport operator is by using the Fourier series expansion (4.3.47) similarly to Lemma 4.3.18, see [85, Lemma B.13]. Observe that (4.3.102) characterises $f \in \ker(\mathcal{T})^\perp$ by the property that the zeroth Fourier coefficient of f vanishes, i.e., $\hat{f}(0,E,L) = 0$ for a.e. $(E,L) \in \mathbb{D}_0$; recall Remark 4.3.11 for the definition of the Fourier coefficients.

Another statement which can be obtained by a Fourier series expansion is the following useful Poincaré type inequality for the transport operator. It is based on [62, Cor. 5.8]; see also [85, Lemma B.13 (a)], where a similar estimate is derived using the inverse of $\mathcal{T}$.[115]

Lemma 4.3.28 (A Poincaré Type Inequality for the Transport Operator)**.** *For all $f \in \mathrm{D}(\mathcal{T}) \cap \ker(\mathcal{T})^\perp$ it holds that*

$$\|\mathcal{T} f\|_H \geq \frac{2\pi}{\sup_{\mathbb{D}_0} T} \|f\|_H; \tag{4.3.111}$$

note that T is bounded on $\mathbb{D}_0$ by Proposition A.0.1 (a).

Proof. Lemma 4.3.26 implies $\hat{f}(0,E,L) = 0$ for a.e. $(E,L) \in \mathbb{D}_0$. Hence, Fourier expanding f and $\mathcal{T}f$, see (4.3.41) and (4.3.47), respectively, yields

$$\|\mathcal{T} f\|_H^2 = \sum_{j\in\mathbb{Z}\setminus\{0\}} \left\| \frac{2\pi}{T}\, j\, \hat{f}(j) \right\|_H^2 \geq \frac{4\pi^2}{\sup_{\mathbb{D}_0}^2(T)} \sum_{j\in\mathbb{Z}\setminus\{0\}} \|\hat{f}(j)\|_H^2 = \frac{4\pi^2}{\sup_{\mathbb{D}_0}^2(T)} \|f\|_H^2. \tag{4.3.112}$$

□

We have actually chosen a more direct proof here than in [62, Cor. 5.8], where the estimate (4.3.111) is proven by variational principles for the operator $-\mathcal{T}^2$. Nevertheless, we briefly discuss this alternative proof, as it provides further insights into the Poincaré type inequality from above.

Remark 4.3.29. *Recall that the spectrum of $-\mathcal{T}^2 \colon \mathrm{D}(\mathcal{T}^2) \to H$ is given by* (4.3.89)*. In particular, since the period function T is bounded on $\mathbb{D}_0$ by Proposition A.0.1, 0 is an isolated eigenvalue of $-\mathcal{T}^2$ with eigenspace $\ker(\mathcal{T})$. The latter is due to the observation that for any $f \in \mathrm{D}(\mathcal{T}^2)$ with $\mathcal{T}^2 f = 0$ it holds that $0 = \langle -\mathcal{T}^2 f, f\rangle_H = \|\mathcal{T} f\|_H^2$ by the skew-symmetry of $\mathcal{T}$ from Proposition 4.3.15. If one excludes this eigenspace and considers the restriction of $-\mathcal{T}^2$ onto the orthogonal complement of $\ker(\mathcal{T})$, the eigenvalue 0 vanishes from the spectrum, i.e.,*

$$\sigma(-\mathcal{T}^2\big|_{\ker(\mathcal{T})^\perp}) = \overline{\left(\frac{2\pi\mathbb{N}}{T(\mathbb{D}_0)}\right)^2}, \tag{4.3.113}$$

cf. [69, Prop. 6.6]. Using standard variational principles, see, e.g., [69, Prop. 5.12] or [134, Thm. XIII.1], it hence follows that

$$\langle -\mathcal{T}^2 f, f\rangle_H \geq \left(\frac{2\pi}{\sup_{\mathbb{D}_0} T}\right)^2 \|f\|_H^2, \qquad f \in \mathrm{D}(\mathcal{T}^2) \cap \ker(\mathcal{T})^\perp. \tag{4.3.114}$$

By the skew-symmetry of $\mathcal{T}$, we thus deduce the estimate (4.3.111) *for $f \in \mathrm{D}(\mathcal{T}^2) \cap \ker(\mathcal{T})^\perp$. One can then extend this inequality to $f \in \mathrm{D}(\mathcal{T}) \cap \ker(\mathcal{T})^\perp$ by approximating f by its Fourier partial series, cf.* (4.3.41)*. Notice that the property $f \perp \ker(\mathcal{T})$ is preserved by this approximation scheme since it is equivalent to $\hat{f}(0,E,L) = 0$ for a.e. $(E,L) \in \mathbb{D}_0$ by Lemma 4.3.26.*

[115] The reason why we do not derive an inequality of the form (4.3.111) by estimating the operator norm of $\mathcal{T}^{-1}$ is that it is harder to get the optimal constant in this way; cf. Remark 4.3.29 for a discussion that the estimate (4.3.111) is, in fact, sharp.

In particular, this alternative proof shows that the Poincaré type estimate (4.3.111) *is sharp.*[116] *For instance, one can explicitly construct a normalised sequence of functions s.t. both sides of* (4.3.111) *tend to each other by proceeding as in the proof of Proposition 4.3.19 and approximating the eigendistribution* $\mathbb{S}^1 \times \mathbb{D}_0 \ni (\theta, E, L) \mapsto \delta_{(E^*,L^*)}(E, L) \sin(2\pi\,\theta)$ *for* $(E^*, L^*) \in \mathbb{D}_0$ *with* $T(E^*, L^*)$ *close to* $\sup_{\mathbb{D}_0} T$.

To conclude this section we state the spectrum of the transport operator $\mathcal{T}\colon \mathrm{D}(\mathcal{T}) \to H$. We will not need this result for the subsequent analysis, which is why we keep the arguments rather short. However, we think that this result ought to be part of a complete presentation of the properties of the transport operator. We follow the same strategy as in Proposition 4.3.19 to derive the spectrum $\mathcal{T}$. This strategy is, essentially, also described in [111, Sc. 2.2].

Remark 4.3.30. *If one extends the function spaces to complex-valued functions, the spectrum of the transport operator* $\mathcal{T}\colon \mathrm{D}(\mathcal{T}) \to H$ *is given by*

$$\sigma(\mathcal{T}) = \sigma_{\mathrm{ess}}(\mathcal{T}) = \overline{\left(\frac{2\pi i\mathbb{Z}}{T(\mathbb{D}_0)}\right)}, \tag{4.3.115}$$

where the set on the right-hand side is defined similarly to (4.3.66)*. This can be shown by explicitly deriving the resolvent operators using the Fourier expansion* (4.3.47) *as in Lemma 4.3.18, and then applying the Weyl criterion similarly to the proof of Proposition 4.3.19 to deduce that the eigendistribution*

$$\mathbb{S}^1 \times \mathbb{D}_0 \ni (\theta, E, L) \mapsto \delta_{(E^*,L^*)}(E, L)\, e^{2\pi i n\,\theta} \tag{4.3.116}$$

corresponds to the element $\frac{2\pi i n}{T(E^*,L^*)}$ *of* $\sigma_{\mathrm{ess}}(\mathcal{T})$ *for any* $n \in \mathbb{Z}$ *and* $(E^*, L^*) \in \mathbb{D}_0$.

By Proposition 4.3.23, 0 *is, in fact, an eigenvalue of* $\mathcal{T}$ *with the (infinite dimensional) eigenspace* $\ker(\mathcal{T})$*. The presence of further eigenvalues of the transport operator* $\mathcal{T}$ *is, similar to Lemma 4.3.22, equivalent to the period function* $T\big|_{\mathbb{D}_0}$ *possessing level sets with positive measure. More precisely, if* $T\big|_{\mathbb{D}_0}^{-1}(\{t\})$ *has positive measure for some* $t > 0$, $\frac{2\pi i n}{t}$ *is an eigenvalue of* $\mathcal{T}$ *for any* $n \in \mathbb{Z}$.

4.3.5 An Approximation Result

The last part of the analysis of the transport operator is to establish an approximation result which will later allow us to extend some statements from smooth functions to elements of $\mathrm{D}(\mathcal{T})$. The approximation result is based on [147, Prop. 2] and [165, Thm. 3.15], where it is mainly used to derive the skew-symmetry of the transport operator $\mathcal{T}$. Due to a careful treatment of the transport operator in action-angle type variables, we did not need the approximation result for this purpose, cf. Remark 4.3.14. The result is, however, useful for other tasks. Related arguments are also used in [57, p. 504ff.]. An adaptation of the approximation result is included in [49, Prop. 5.1 (e)].

Lemma 4.3.31. *Let* $f \in \mathrm{D}(\mathcal{T})$*. Then there exists a sequence of smooth functions* $(f_j)_{j\in\mathbb{N}} \subset C^\infty_{c,r}(\Omega_0)$ *s.t.*

$$f_j \to f \quad \text{and} \quad \mathcal{T} f_j \to \mathcal{T} f \qquad \text{in } H \text{ as } j \to \infty. \tag{4.3.117}$$

[116] The estimate (4.3.111) being sharp means that the constant $\frac{2\pi}{\sup_{\mathbb{D}_0} T}$ cannot be replaced by any larger value, although we are not certain whether there exists a function $f \in \mathrm{D}(\mathcal{T}) \cap \ker(\mathcal{T})^\perp$ s.t. there holds equality in (4.3.111).

In addition to $\operatorname{supp}(f_j)$ *being compact in* Ω_0 *in Cartesian* (x,v)*-coordinates, the support of* f_j *in radial* (r,w,L)*-coordinates is also compactly contained in* Ω_0.[117] *Moreover, if* $f \in \mathcal{H}$*, one can choose* $f_j \in \mathcal{H}$ *for* $j \in \mathbb{N}$.

Proof. We follow [147, Prop. 2] and [165, Thm. 3.15] and split the proof into several steps.
Step 1: Reduction to a Compact Support. For $j \in \mathbb{N}$ let $\chi_j \in C^\infty(\mathbb{R})$ be an increasing cut-off function s.t.

$$\chi_j(s) = 0 \text{ for } s \le \frac{1}{2j} \quad \text{and} \quad \chi_j(s) = 1 \text{ for } s \ge \frac{1}{j}. \tag{4.3.118}$$

We then set

$$f_j(x,v) \coloneqq \chi_j(L(x,v) - L_0)\, \chi_j(E_0 - E(x,v))\, f(x,v), \qquad \text{a.e. } (x,v) \in \Omega_0. \tag{4.3.119}$$

Lemma 4.3.9 shows $f_j \in \mathrm{D}(\mathcal{T})$ with $\mathcal{T} f_j = (\chi_j \circ (L - L_0))\,(\chi_j \circ (E_0 - E))\,\mathcal{T} f$ for $j \in \mathbb{N}$. Hence, by Lebesgue's dominated convergence theorem,

$$f_j \to f \quad \text{and} \quad \mathcal{T} f_j \to \mathcal{T} f \qquad \text{in } H \text{ as } j \to \infty. \tag{4.3.120}$$

By applying the following arguments to f_j with $j \in \mathbb{N}$ sufficiently large instead of to f, we may assume that f has compact support[118] in Ω_0. More precisely, we assume that there exists some $m \in \mathbb{N}$ s.t.

$$f(x,v) = 0 \text{ for a.e. } (x,v) \in \Omega_0 \text{ with } |x| \le \frac{1}{m} \vee L(x,v) \le L_0 + \frac{1}{m} \vee E(x,v) \ge E_0 - \frac{1}{m}. \tag{4.3.121}$$

In particular, since the integral weight $|\varphi'(E,L)|$ is bounded on compact subsets of Ω_0, cf. Remark 4.2.4 (e), there holds $f, \mathcal{T} f \in L^2(\Omega_0)$.
Step 2: The Approximation Sequence. We mollify f in (r,w,L)-variables in order to construct the desired approximating sequence. Let $J \in C_c^\infty(B_1^3(0))$ be a standard three-dimensional mollifier, i.e., $B_1^3(0) = B_1(0) \subset \mathbb{R}^3$, $\int_{\mathbb{R}^3} J = 1$, and $J \ge 0$. We further define $J_n \coloneqq n^3 J(n\cdot)$ as well as

$$f_n \coloneqq J_n * f, \qquad g_n \coloneqq J_n * \mathcal{T} f \tag{4.3.122}$$

for $n \in \mathbb{N}$, where the convolution is to be interpreted in (r,w,L)-variables. Due to the compact supports of f and $\mathcal{T} f$, we deduce that f_n and g_n have compact supports in Ω_0 for sufficiently large $n \in \mathbb{N}$. In addition, after possibly increasing the number $m \in \mathbb{N}$ from above, we may assume $\bar{B}_{\frac{1}{m}}(\operatorname{supp}(f_n)) \subset \Omega_0$ and that (4.3.121) holds with f replaced by f_n for sufficiently large n. We further deduce $f_n \in C_{c,r}^\infty(\Omega_0)$ for sufficiently large $n \in \mathbb{N}$ since changing from (r,w,L)-variables to (x,v)-variables is smooth away from $\{x = 0\}$. Using standard mollifying arguments as well as the fact that the integral weight $|\varphi'(E,L)|^{-1}$ is bounded on compact subsets of Ω_0, cf. Remark 4.2.4 (d), yields

$$f_n \to f \quad \text{and} \quad g_n \to \mathcal{T} f \qquad \text{in } H \text{ and } L^2(\Omega_0) \text{ as } n \to \infty. \tag{4.3.123}$$

Moreover, by choosing a mollifier $J = J(r,w,L)$ which is even in w, the property that f is odd in v carries over to the approximating functions $(f_n)_{n\in\mathbb{N}}$.

[117] More precisely, this means that $\operatorname{supp}(f_j) \Subset \mathring{\Omega}_0$ in (r,w,L)-coordinates. In particular, $\operatorname{supp}(f_j)$ is bounded away from $\{r = 0\}$ and $\{L = 0\}$.
[118] The support of f is compact in Ω_0 both in Cartesian (x,v)-variables as well as in the radial (r,w,L)-variables; notice that the lower bound on $|x| = r$ is due to the lower bound on L.

Step 3: Boundedness. We next show that $(\mathcal{T}f_n)_{n\in\mathbb{N}}$ is bounded in $L^2(\Omega_0)$. In order to do so, we use the representation (4.2.17) of the transport operator in (r,w,L)-variables to rewrite $\mathcal{T}f_n(z)$ for $z=(r,w,L)\in\operatorname{supp}(f_n)\Subset\Omega_0$ and sufficiently large $n\in\mathbb{N}$ as follows:

$$\begin{aligned}\mathcal{T}f_n(z) &= w\,[(\partial_r J_n)*f](z) - \Psi_L'(r)\,[(\partial_w J_n)*f](z) = \\ &= \int_{B_{\frac{1}{n}}(z)} \Big[(w-\tilde{w})\,\partial_r J_n(z-\tilde{z}) - \Big(\Psi_L'(r) - \Psi_{\tilde{L}}'(\tilde{r})\Big)\,\partial_w J_n(z-\tilde{z})\Big] f(\tilde{z})\,\mathrm{d}\tilde{z} + \\ &\quad + \int_{\Omega_0} \Big[\tilde{w}\,\partial_r J_n(z-\tilde{z}) - \Psi_{\tilde{L}}'(\tilde{r})\,\partial_w J_n(z-\tilde{z})\Big] f(\tilde{z})\,\mathrm{d}\tilde{z}, \end{aligned} \tag{4.3.124}$$

where $\tilde{z}=(\tilde{r},\tilde{w},\tilde{L})$. Since $\overline{B_{\frac{1}{m}}(\operatorname{supp}(f))}\ni\tilde{z}\mapsto\Psi_{\tilde{L}}'(\tilde{r})$ is Lipschitz continuous, we obtain the following estimate:

$$\begin{aligned}&\left|\int_{B_{\frac{1}{n}}(z)} \Big[(w-\tilde{w})\,\partial_r J_n(z-\tilde{z}) - \Big(\Psi_L'(r) - \Psi_{\tilde{L}}'(\tilde{r})\Big)\,\partial_w J_n(z-\tilde{z})\Big] f(\tilde{z})\,\mathrm{d}\tilde{z}\right| \leq \\ &\qquad \leq \frac{C}{n}\int_{B_{\frac{1}{n}}(z)} |DJ_n(z-\tilde{z})|\,|f(\tilde{z})|\,\mathrm{d}\tilde{z} = Cn^3\,(|DJ(n\cdot)|*|f|)(z) \end{aligned} \tag{4.3.125}$$

for $z=(r,w,L)\in\operatorname{supp}(f_n)\Subset\Omega_0$ and all sufficiently large $n\in\mathbb{N}$, where the constant $C>0$ depends on the support of f but is independent from n; the constant is allowed to change its value from line to line. In order to bound the second term on the right-hand side of (4.3.124), observe that $|\varphi'(E,L)|\,f\in\mathrm{D}(\mathcal{T})$ with $\mathcal{T}(|\varphi'(E,L)|\,f)=|\varphi'(E,L)|\,\mathcal{T}f$ by Lemma 4.3.9 and the compact support of f. Hence,

$$\begin{aligned}&4\pi^2\int_{\Omega_0}\Big[\tilde{w}\,\partial_r J_n(z-\tilde{z}) - \Psi_{\tilde{L}}'(\tilde{r})\,\partial_w J_n(z-\tilde{z})\Big] f(\tilde{z})\,\mathrm{d}\tilde{z} = -\langle\mathcal{T}(J_n(z-\cdot)), f\rangle_{L^2(\Omega_0)} = \\ &\quad = -\langle\mathcal{T}(J_n(z-\cdot)), |\varphi'(E,L)|\,f\rangle_H = \langle J_n(z-\cdot), |\varphi'(E,L)|\,\mathcal{T}f\rangle_H = 4\pi^2 g_n(z) \end{aligned} \tag{4.3.126}$$

for sufficiently large $n\in\mathbb{N}$, where the second to last equation is due to Definition 4.2.5. Inserting (4.3.125) and (4.3.126) into (4.3.124) then yields

$$\|\mathcal{T}f_n\|_2 \leq Cn^3\,\||DJ(n\cdot)|*|f|\|_2 + \|g_n\|_2 \tag{4.3.127}$$

for sufficiently large $n\in\mathbb{N}$, where the L^p-norms are interpreted in (r,w,L)-variables here. Applying Young's inequality shows

$$Cn^3\,\||DJ(n\cdot)|*|f|\|_2 \leq Cn^3\,\||DJ(n\cdot)\|_1\,\|f\|_2 = C\|DJ\|_1\,\|f\|_2, \tag{4.3.128}$$

which, together with the fact that $(g_n)_{n\in\mathbb{N}}$ converges in $L^2(\Omega_0)$, implies that $(\mathcal{T}f_n)_{n\in\mathbb{N}}$ is indeed bounded in $L^2(\Omega_0)$.

Step 4: Weak Convergence. Due to the previous step there exists a subsequence of $(f_n)_{n\in\mathbb{N}}$ – which, by slight abuse of notation, we again denote by $(f_n)_{n\in\mathbb{N}}$ – and a spherically symmetric a.e. limiting function $g\in L^2(\Omega_0)$ s.t.

$$\mathcal{T}f_n \rightharpoonup g \qquad \text{in } L^2(\Omega_0) \text{ as } n\to\infty. \tag{4.3.129}$$

In particular, the compact supports of f_n carry over to g, which implies $g\in H$. We need to show $g=\mathcal{T}f$. In order to verify this equality, let $\xi\in C^1_{c,r}(\Omega_0)$ be a test function as

required in Definition 4.2.5. Since $\langle \cdot, \xi \rangle_H \in \left[L^2(\Omega_0)\right]'$ by the compact support of ξ, the weak convergence (4.3.129) and (4.3.123) imply

$$\langle g, \xi \rangle_H = \lim_{n\to\infty} \langle \mathcal{T} f_n, \xi \rangle_H = -\lim_{n\to\infty} \langle f_n, \mathcal{T}\xi \rangle_H = -\langle f, \mathcal{T}\xi \rangle_H. \tag{4.3.130}$$

Step 5: Strong Convergence. Due to the previous step there holds $\mathcal{T} f_n \rightharpoonup \mathcal{T} f$ in $L^2(\Omega_0)$ as $n \to \infty$. We upgrade this limiting behaviour to actual strong convergence in H by passing to convex combinations of f_n. More precisely, Mazur's lemma implies that for every $n \in \mathbb{N}$ there exists $N_n \geq n$ and weights $c_n^n, \ldots, c_{N_n}^n \in [0,1]$ with $\sum_{j=n}^{N_n} c_j^n = 1$ s.t.

$$\mathcal{T}\left[\sum_{j=n}^{N_n} c_j^n \, f_j\right] = \sum_{j=n}^{N_n} c_j^n \, \mathcal{T} f_j \to \mathcal{T} f \qquad \text{in } L^2(\Omega_0) \text{ as } n \to \infty. \tag{4.3.131}$$

Letting $F_n \coloneqq \sum_{j=n}^{N_n} c_j^n \, f_j$ for $n \in \mathbb{N}$ then defines the desired approximating sequence because, by the compact supports of f_n, the limit (4.3.131) also holds in H. □

4.4 The Response Operator $\mathcal{R}$

In this section we analyse the response operator $\mathcal{R}$ given by Definition 4.2.8. The results presented here mainly originate from [62, Lemma 4.3 and App. A.1] and [49, Lemma 5.15]; see also [61, Lemmas 3.8 and 3.9] and [85, Lemma B.15] for related results.

We first show that the mass density ρ_f and the radial velocity density j_f induced by a function $f \in H$ are well-defined; recall that $\mathcal{R} f$ contains the factor j_f.

Lemma 4.4.1. *Let $f \in H$. Then the associated mass density*[119]

$$\rho_f \colon \mathbb{R}^3 \to \mathbb{R}, \; \rho_f(x) \coloneqq \int_{\mathbb{R}^3} f(x,v) \, \mathrm{d}v \tag{4.4.1}$$

and the associated radial velocity density

$$j_f \colon \mathbb{R}^3 \to \mathbb{R}, \; j_f(x) \coloneqq \int_{\mathbb{R}^3} \frac{x \cdot v}{|x|} \, f(x,v) \, \mathrm{d}v \tag{4.4.2}$$

are well-defined a.e., where we extend f by 0 onto the whole space $\mathbb{R}^3 \times \mathbb{R}^3$. In addition, $\rho_f, j_f \in L^2(\mathbb{R}^3)$ with

$$\|\rho_f\|_2 + \|j_f\|_2 \leq C \|f\|_H, \tag{4.4.3}$$

where the constant $C > 0$ depends only on the fixed steady state. Furthermore, ρ_f and j_f are spherically symmetric a.e. in the sense of Definition 4.2.1 (a) and, in radial variables, there hold the representations

$$\rho_f(r) = \frac{\pi}{r^2} \int_0^\infty \int_{\mathbb{R}} f(r, w, L) \, \mathrm{d}w \, \mathrm{d}L, \qquad \text{a.e. } r > 0, \tag{4.4.4}$$

and (4.2.22).

[119] It will always be clear from the context whether we refer to the (trivial) mass density ρ_f with $f = 0$ or to the mass density $\rho_0 = \rho_{f_0}$ of the steady state when writing ρ_0.

Proof. Using the Cauchy-Schwarz inequality and Lemma 4.1.3 yields

$$\|\rho_f\|_2^2 \leq \int_{\mathbb{R}^3} \left(\int_{\mathbb{R}^3} |\varphi'(E,L)| \,\mathrm{d}v \right) \left(\int_{\mathbb{R}^3} \frac{1}{|\varphi'(E,L)|} \, |f(x,v)|^2 \,\mathrm{d}v \right) \mathrm{d}x \leq C \|f\|_H^2, \tag{4.4.5}$$

which shows that ρ_f is indeed well-defined and square-integrable. Since $\frac{x \cdot v}{|x|}$ is bounded for $(x,v) \in \Omega_0$, similar arguments yield the respective statements for j_f as well as the estimate (4.4.3).[120] The fact that the a.e. spherical symmetry of f implies that ρ_f and j_f are spherically symmetric a.e. is easy to verify using Definition 4.2.1. The representations (4.2.22) and (4.4.4) then follow by the usual change of variables $v \mapsto (w, L)$. □

In particular, the above lemma shows that the expression (4.2.21) defining $\mathcal{R}$ is indeed well-defined. We next show that the response operator defines a bounded operator $\mathcal{R} \colon H \to H$. This is based on [62, Lemma 4.3] and [49, Lemma 5.15].

Lemma 4.4.2 (Main Properties of the Response Operator)**.** *The response operator $\mathcal{R} \colon H \to H$ is well-defined, linear, bounded, symmetric, and non-negative. The latter means $\langle \mathcal{R} f, f \rangle_H \geq 0$ for $f \in H$ and we write $\mathcal{R} \geq 0$, cf. [69, Def. 5.11] or [136, Sc. VI.4].*[121] *Moreover, $\mathcal{R} f \in \mathcal{H}$ for $f \in H$.*

Proof. For $f \in H$, we express $\| \cdot \|_H$ in radial variables via (4.2.7) and apply Lemma 4.1.2 to obtain

$$\|\mathcal{R} f\|_H^2 = 2^6 \pi^4 \int_0^\infty j_f^2(r) \int_0^\infty \int_{\mathbb{R}} w^2 \, |\varphi'(E,L)| \,\mathrm{d}w \,\mathrm{d}L \,\mathrm{d}r = (4\pi)^3 \int_0^\infty r^2 \, \rho_0(r) \, j_f^2(r) \,\mathrm{d}r. \tag{4.4.6}$$

Inserting the representation (4.2.22) of j_f and using that ρ_0 is bounded by Proposition 2.2.9 then yields

$$\begin{aligned} \|\mathcal{R} f\|_H^2 &\leq C \int_0^\infty \frac{1}{r^2} \left(\int_0^\infty \int_{\mathbb{R}} w \, f(r,w,L) \,\mathrm{d}w \,\mathrm{d}L \right)^2 \mathrm{d}r \leq \\ &\leq C \int_0^\infty \frac{1}{r^2} \left(\int_0^\infty \int_{\mathbb{R}} w^2 \, |\varphi'(E,L)| \,\mathrm{d}w \,\mathrm{d}L \right) \left(\int_0^\infty \int_{\mathbb{R}} \frac{|f(r,w,L)|^2}{|\varphi'(E,L)|} \,\mathrm{d}w \,\mathrm{d}L \right) \mathrm{d}r \leq \\ &\leq C \int_0^\infty \int_0^\infty \int_{\mathbb{R}} \frac{|f(r,w,L)|^2}{|\varphi'(E,L)|} \,\mathrm{d}w \,\mathrm{d}L \,\mathrm{d}r = C \|f\|_H^2, \end{aligned} \tag{4.4.7}$$

where used the Cauchy-Schwarz inequality and, once again, Lemma 4.1.2. The constant $C > 0$ in this calculation depends only on the fixed steady state and is allowed to change from line to line. We have thus shown that $\mathcal{R} \colon H \to H$ is indeed well-defined and bounded; $\mathcal{R}$ is obviously linear since j_f depends linearly on f. In addition, it is evident that $\mathcal{R} f$ is odd in w for $f \in H$ since the particle energy E is even in w. Thus, $\mathcal{R} f$ is odd in v, recall Remark 4.2.2 (c), and $\mathcal{R} f \in \mathcal{H}$.

In order to verify the remaining properties, let $f, g \in H$. Expressing the inner product $\langle \cdot, \cdot \rangle_H$ in radial variables via (4.2.8) shows

$$\langle \mathcal{R} f, g \rangle_H = 2^4 \pi^3 \int_{\Omega_0} w \, j_f(r) \, g(r,w,L) \,\mathrm{d}(r,w,L) = (4\pi)^2 \int_0^\infty r^2 \, j_f(r) \, j_g(r) \,\mathrm{d}r. \tag{4.4.8}$$

Because the latter expression is symmetric in f and g, we deduce that $\mathcal{R}$ is symmetric. Furthermore, by inserting $g = f$ into (4.4.8), we conclude that $\mathcal{R}$ is non-negative. □

[120] The proof of Lemma 4.4.2 will illustrate a different strategy to establish $j_f \in L^2(\mathbb{R}^3)$, which will be based on Lemma 4.1.2 and the boundedness of ρ_0 instead of Lemma 4.1.3.

[121] Different from the cited literature, we call an operator with this property *non-negative* instead of *positive*.

The proof above uses the fact that we have included the weight $\frac{1}{|\varphi'|}$ into the L^2-space H in an essential way. Let us elaborate on this point.

Remark 4.4.3 (On the Weight $\frac{1}{|\varphi'|}$)**.** *For the response operator $\mathcal{R}\colon H \to H$ to be symmetric, it is crucial that we have included the weight $\frac{1}{|\varphi'|}$ into the L^2-space H; recall Definition 4.2.3 for the definition of H. This can be seen in* (4.4.8)*, where the factor $|\varphi'(E,L)|$ contained in $\mathcal{R}f$ cancels out with the integral weight. Without this cancellation, the response operator $\mathcal{R}$ would not be symmetric in general. The symmetry of $\mathcal{R}$ is, however, used in Section 4.5 to show that the whole linearised operator $\mathcal{L} = -\mathcal{T}^2 - \mathcal{R}$ is symmetric, which in turn is important to analyse the spectrum of $\mathcal{L}$.*

This further shows that it is essential for our arguments that φ' does not change its sign, at least on the support of the steady state. If φ' would change its sign, one would have to replace the factor $|\varphi'|$ in $\mathcal{R}f$ with $-\varphi'$. In order to preserve the cancellation effect described above, one would then have to include the weight $\frac{1}{\varphi'}$ (or $-\frac{1}{\varphi'}$) into the underlying L^2-space. This would lead to an indefinite inner product space, cf. [22], instead of the Hilbert space H and thus make all arguments significantly more complicated.[122] *To prove statements about solutions of the linearised Vlasov-Poisson system in this setting, it is probably more convenient not to work with such spaces but to analyse the system more directly; this is, e.g., done in [53, Sc. 2].*

This is the reason why we impose the condition (φ5) on the steady state, which ensures $\varphi' < 0$ on the steady state support. In order to obtain the symmetry of the response operator, one could, in principle, also consider steady states with $\varphi' > 0$. We do, however, restrict the analysis here to steady states with $\varphi' < 0$, since these equilibria are more natural from a physics point of view, recall the discussion in Remark 4.1.1 (b), and are thus mainly considered in the literature.

Next, we determine the square root of the response operator $\mathcal{R}\colon H \to H$, i.e., we derive a linear and bounded operator $\sqrt{\mathcal{R}}\colon H \to H$ with $\sqrt{\mathcal{R}} \geq 0$ and $(\sqrt{\mathcal{R}})^2 = \mathcal{R}$. This square root operator will play an important role in Chapter 5, cf. Remark 5.1.12. Since $\mathcal{R}\colon H \to H$ is bounded and non-negative by Lemma 4.4.2, such a square root operator exists, cf. [136, Thm. VI.9]. Fortunately, by taking $\sqrt{\mathcal{R}}f$ to be of a similar form as $\mathcal{R}f$, we can derive the square root operator explicitly. This is based on [49, Lemma 5.15] and [61, Lemma 3.8].

Lemma 4.4.4 (The Square Root of the Response Operator)**.** *The square root $\sqrt{\mathcal{R}}\colon H \to H$ of the response operator $\mathcal{R}\colon H \to H$ is given by*

$$\sqrt{\mathcal{R}}f(r,w,L) \coloneqq 2\sqrt{\pi}\,|\varphi'(E,L)|\,\frac{w}{\sqrt{\rho_0(r)}}\,j_f(r), \qquad f \in H,\ \text{a.e. } (r,w,L) \in \Omega_0. \tag{4.4.9}$$

Moreover, $\sqrt{\mathcal{R}}$ is a symmetric operator and $\sqrt{\mathcal{R}}f \in \mathcal{H}$ for $f \in H$.

Proof. Using the representation (4.2.22) of j_f and Lemma 4.1.2 yields

$$\begin{aligned}\sqrt{\mathcal{R}}\,\sqrt{\mathcal{R}}f(r,w,L) &= 2\sqrt{\pi}\,|\varphi'(E,L)|\,\frac{w}{\sqrt{\rho_0(r)}}\,j_{\sqrt{\mathcal{R}}f}(r) = 4\pi\,|\varphi'(E,L)|\,\frac{w}{\rho_0(r)}\,j_f(r)\,j_{w\,|\varphi'|}(r) = \\ &= 4\pi\,|\varphi'(E,L)|\,w\,j_f(r) = \mathcal{R}f(r,w,L)\end{aligned} \tag{4.4.10}$$

[122] Another way to ensure that the linearised operator is symmetric is to consider $\frac{1}{\varphi'}\mathcal{L}$ on the unweighted L^2-space $L^2(\Omega_0)$. This is, e.g., done in [8, 71, 77]. However, if φ' changes its sign on the steady state support, the associated kinetic energy $\int_{\Omega_0} \frac{1}{-\varphi'}|f(x,v)|^2\,\mathrm{d}(x,v)$ can be negative, which essentially leads to similar problems as the ones described above.

for $f \in H$ and a.e. $(r, w, L) \in \Omega_0$. The remaining properties of $\sqrt{\mathcal{R}}$ can be verified similarly to the proof of Lemma 4.4.2. Concretely, for $f \in H$, applying Lemma 4.1.2 and the Cauchy-Schwarz inequality yields

$$\begin{aligned}\|\sqrt{\mathcal{R}}f\|_H^2 &= 2^4\pi^3 \int_{\Omega_0} |\varphi'(E,L)|\, w^2\, \frac{1}{\rho_0(r)}\, j_f^2(r)\, \mathrm{d}(r,w,L) = (4\pi)^2 \int_0^\infty r^2\, j_f^2(r)\, \mathrm{d}r = \\ &= (2\pi)^4 \int_0^\infty \frac{1}{r^2} \left(\int_0^\infty \int_{\mathbb{R}} w\, f(r,w,L)\, \mathrm{d}w\, \mathrm{d}L \right)^2 \mathrm{d}r \leq \\ &= (2\pi)^4 \int_0^\infty \frac{1}{r^2} \left(\int_0^\infty \int_{\mathbb{R}} w^2\, |\varphi'(E,L)|\, \mathrm{d}w\, \mathrm{d}L \right) \left(\int_0^\infty \int_{\mathbb{R}} \frac{f(r,w,L)^2}{|\varphi'(E,L)|}\, \mathrm{d}w\, \mathrm{d}L \right) \mathrm{d}r \leq \\ &\leq C\|f\|_H^2. \end{aligned} \tag{4.4.11}$$

Moreover, $\sqrt{\mathcal{R}}f$ is obviously odd in v, i.e., $\sqrt{\mathcal{R}}f \in \mathcal{H}$. There further holds

$$\langle \sqrt{\mathcal{R}}f, g\rangle_H = 2^3\pi^{\frac{5}{2}} \int_{\Omega_0} \frac{w}{\sqrt{\rho_0(r)}}\, j_f(r)\, g(r,w,L)\, \mathrm{d}(r,w,L) = 2^3\pi^{\frac{3}{2}} \int_0^\infty \frac{r^2}{\sqrt{\rho_0(r)}}\, j_f(r)\, j_g(r)\, \mathrm{d}r \tag{4.4.12}$$

for $f, g \in H$, which shows that (4.4.9) indeed defines a symmetric, non-negative operator. □

The last part of this section is concerned with deriving an alternative representation of the response operator $\mathcal{R}f$ (and its square root) provided that f is sufficiently smooth. More precisely, the aim is to rigorously establish a representation like (3.1.8) for $\mathcal{R}f$ if the transport term $\mathcal{T}f$ exists in the weak sense, cf. Definition 4.2.5. As a preparation for this, we first introduce and analyse gravitational potentials induced by functions in H.

Definition & Lemma 4.4.5 (Gravitational Potentials)**.** *For $f \in H$ let $U_f \colon \mathbb{R}^3 \to \mathbb{R}$ be the gravitational potential induced by ρ_f, i.e.,*

$$U_f \coloneqq -\frac{1}{|\cdot|} * \rho_f; \tag{4.4.13}$$

recall Lemma 4.4.1 for the properties of ρ_f. It then holds that $U_f \in C(\mathbb{R}^3)$ with $\lim_{|x|\to\infty} U_f(x) = 0$ as well as $U_f \in L^p \cap L^\infty(\mathbb{R}^3)$ for every $p > 3$. Furthermore, U_f is differentiable in the distributional sense with $\partial_x U_f \in L^p(\mathbb{R}^3;\mathbb{R}^3)$ for $\frac{3}{2} < p \leq 6$, and there holds the estimate[123]

$$\|U_f\|_\infty + \|\partial_x U_f\|_2 \leq C\|\rho_f\|_2, \tag{4.4.14}$$

where the constant $C > 0$ depends only on the fixed steady state. There further holds

$$\Delta U_f = 4\pi\rho_f \tag{4.4.15}$$

in the distributional sense. Moreover, U_f is spherically symmetric with

$$U_f'(r) = \frac{4\pi}{r^2} \int_0^r s^2 \rho_f(s)\, \mathrm{d}s, \qquad r > 0, \tag{4.4.16}$$

in the weak sense.

[123] Similar estimates also hold for other L^p-norms of U_f and $\partial_x U_f$.

Proof. Lemma 4.4.1 yields $\rho_f \in L^2(\mathbb{R}^3)$, and the support of ρ_f is bounded by the compact radial support of the steady state. Thus, $\rho_f \in L^1 \cap L^2(\mathbb{R}^3)$ with

$$\|\rho_f\|_p \leq C\|\rho_f\|_2, \qquad 1 \leq p \leq 2, \tag{4.4.17}$$

for some constant $C > 0$ as specified above. Basic potential theory [98, Thm. 6.21 and Ch. 10] hence yields the claimed regularity and integrability of U_f and $\partial_x U_f$ as well as (4.4.14) and (4.4.15). The spherical symmetry of U_f together with (4.4.16) follows by a straight-forward calculation using the a.e. spherical symmetry of ρ_f. □

We obtain further information about U_f when we know more about f. Concretely, we consider the situation $f \in \mathrm{im}(\mathcal{T})$ in the following lemma. The additional properties of U_f in this case will then allow us to deduce alternative representations of the response operator and its square root. This is based on [62, App. A.1], see also [61, Lemma 3.9] and [85, Lemma B.15 and Cor. B.16] for related results. Some of the following arguments were also used earlier in [53, Proof of Thm. 1.1].

Lemma 4.4.6. *Let $f \in \mathrm{D}(\mathcal{T})$. In addition to the properties of $U_{\mathcal{T}f}$ which follow from Lemma 4.4.5, it holds that $U_{\mathcal{T}f} \in C \cap H^2(\mathbb{R}^3)$ with*

$$\|U_{\mathcal{T}f}\|_\infty + \|U_{\mathcal{T}f}\|_{H^2} \leq C\|\mathcal{T}f\|_H \tag{4.4.18}$$

for some constant $C > 0$ which depends only on the underlying steady state. Moreover,

$$U'_{\mathcal{T}f}(r) = 4\pi j_f(r), \qquad \text{a.e. } r > 0. \tag{4.4.19}$$

Proof. The key observation on which the proof is mainly based is

$$\int_{\mathbb{R}^3} \rho_{\mathcal{T}f}(x)\,\mathrm{d}x = \langle |\varphi'|, \mathcal{T}f\rangle_H = -\langle \mathcal{T}|\varphi'|, f\rangle_H = 0, \tag{4.4.20}$$

which is due to $|\varphi'| \in H$ by Lemma 4.1.3 with $|\varphi'| \in \ker(\mathcal{T})$ by Proposition 4.3.23 and the skew-symmetry of the transport operator $\mathcal{T}$, cf. Proposition 4.3.15. Since $\mathrm{supp}\,(\rho_{\mathcal{T}f}) \subset \bar{B}_{R_{\max}}(0)$, we hence obtain the following estimate for $x \in \mathbb{R}^3$ with $|x| \geq 2R_{\max}$:

$$|U_{\mathcal{T}f}(x)| = \left| \int_{B_{R_{\max}}(0)} \frac{\rho_{\mathcal{T}f}(y)}{|x-y|}\,\mathrm{d}y - \int_{B_{R_{\max}}(0)} \frac{\rho_{\mathcal{T}f}(y)}{|x|}\,\mathrm{d}y \right| \leq \frac{2R_{\max}}{|x|^2}\,\|\rho_{\mathcal{T}f}\|_1. \tag{4.4.21}$$

Since $U_{\mathcal{T}f}$ is continuous by Lemma 4.4.5, this shows $U_{\mathcal{T}f} \in L^2(\mathbb{R}^3)$. Together with (4.4.15) and the estimates (4.4.3), (4.4.14), and (4.4.17) we hence conclude $U_{\mathcal{T}f} \in H^2(\mathbb{R}^3)$ with (4.4.18).

In order to prove (4.4.19), we first consider the case $f \in C^\infty_{c,r}(\Omega_0)$ and further assume that the support of f is bounded away from $\{x = 0\}$.[124] In this situation, (4.4.19) follows by integrating the radial Poisson equation as in [57, App.] or [96, Eqn. (B.1)]. Concretely, by (4.4.16),

$$\begin{aligned} U'_{\mathcal{T}f}(r) &= \frac{4\pi^2}{r^2} \int_0^r \int_0^\infty \int_{\mathbb{R}} \mathcal{T}f(s,w,L)\,\mathrm{d}w\,\mathrm{d}L\,\mathrm{d}s = \\ &= \frac{4\pi^2}{r^2} \int_0^\infty \int_{\mathbb{R}} w \int_0^r \partial_r f(s,w,L)\,\mathrm{d}s\,\mathrm{d}w\,\mathrm{d}L = 4\pi j_f(r) \end{aligned} \tag{4.4.22}$$

[124] The calculation (4.4.22) is true without assuming that the support of f is bounded away from $\{x = 0\}$. However, imposing this additional assumptions makes it easier to see that the boundary term arising from the radial origin vanishes.

for $r > 0$, where we inserted the representation (4.2.17) of $\mathcal{T}f$. Applying the approximation result from Lemma 4.3.31 as well as the estimates (4.4.3) and (4.4.18) then allow us to conclude that (4.4.19) indeed holds for every $f \in \mathrm{D}(\mathcal{T})$. □

Inserting (4.4.19) into the response operator and its square root, cf. (4.2.21) and (4.4.9), respectively, then yields the desired alternative representations of these operators.

Corollary 4.4.7. *For $f \in \mathrm{D}(\mathcal{T})$ it holds that*

$$\mathcal{R}f(r,w,L) = |\varphi'(E,L)|\, w\, U'_{\mathcal{T}f}(r), \tag{4.4.23}$$

$$\sqrt{\mathcal{R}}f(r,w,L) = \frac{1}{2\sqrt{\pi}}\, |\varphi'(E,L)|\, \frac{w}{\sqrt{\rho_0(r)}}\, U'_{\mathcal{T}f}(r), \tag{4.4.24}$$

for a.e. $(r,w,L) \in \Omega_0$.

4.5 The Linearised Operator $\mathcal{L}$

In this section we analyse the linearised operator $\mathcal{L} = -\mathcal{T}^2\big|_{\mathcal{H}} - \mathcal{R}\big|_{\mathcal{H}}$ defined in Definition 4.2.9. We first combine suitable properties of the squared transport operator and the response operator derived in Sections 4.3 and 4.4 to obtain functional analytic properties of $\mathcal{L}$ and to determine the essential spectrum of $\mathcal{L}$. The remaining part of this section is then concerned with studying the entire spectrum of $\mathcal{L}$. We mainly follow [62] here.

Before we get to the statements described above, we first state that the linearised operator is indeed a well-defined linear operator.

Lemma 4.5.1. *The linearised operator $\mathcal{L}\colon \mathrm{D}(\mathcal{L}) \to \mathcal{H}$ is a well-defined linear operator which is densely defined on $\mathcal{H}$.*

Proof. Lemma 4.3.16 shows that the squared transport operator preserves v-parity, which implies $\mathcal{T}^2 f \in \mathcal{H}$ for $f \in \mathrm{D}(\mathcal{L}) = \mathrm{D}(\mathcal{T}^2) \cap \mathcal{H}$. In addition, $\mathrm{D}(\mathcal{L})$ is dense in $\mathcal{H}$ by Proposition 4.3.17 (b). Since the response operator is defined on the whole space $\mathcal{H}$ with $\mathcal{R}f \in \mathcal{H}$ for $f \in \mathcal{H}$ by Lemma 4.4.2, we conclude the claimed statements regarding $\mathcal{L} = -\mathcal{T}^2\big|_{\mathcal{H}} - \mathcal{R}\big|_{\mathcal{H}}\colon \mathrm{D}(\mathcal{L}) \to \mathcal{H}$. □

4.5.1 Self-Adjointness of the Linearised Operator

The aim of this section is to show that the linearised operator $\mathcal{L}\colon \mathrm{D}(\mathcal{L}) \to \mathcal{H}$ is self-adjoint. This seems plausible since both of the addends of $\mathcal{L} = \mathcal{T}^2\big|_{\mathcal{H}} - \mathcal{R}\big|_{\mathcal{H}}$ have this property, cf. Proposition 4.3.17 (b) and Lemma 4.4.2.[125] However, in general, even if the sum of two self-adjoint operators is densely defined, it need not be self-adjoint again.[126] Fortunately, in our specific situation, the self-adjointness of $\mathcal{L}$ is rather easy to deduce since the response operator $\mathcal{R}$ is bounded. This is based on [62, Lemma 4.5], see also [61, Lemma 3.10 (a)] and [85, Lemma B.17] for similar results.

Lemma 4.5.2 (Self-Adjointness of the Linearised Operator)**.** *The linearised operator $\mathcal{L}\colon \mathrm{D}(\mathcal{L}) \to \mathcal{H}$ is self-adjoint as a densely defined operator on $\mathcal{H}$.*

[125] Note that any bounded and symmetric operator is self-adjoint, which means that $\mathcal{R}\big|_{\mathcal{H}}$ is indeed self-adjoint by Lemma 4.4.2.

[126] An easy example for this is the following: Let $A\colon \mathrm{D}(A) \to H$ be a self-adjoint operator on some general Hilbert space H. In addition, assume that A is unbounded, i.e., $\mathrm{D}(A) \subsetneq H$. Then the sum of A and $-A\colon \mathrm{D}(A) \to H$ is $\mathrm{D}(A) \ni x \mapsto 0$, which is not self-adjoint since $\mathrm{D}(A) \subsetneq H$.

Proof. The claim follows by the Kato-Rellich theorem, cf. [69, Thm. 13.5] or [133, Thm. X.12], since $\mathcal{T}^2\big|_{\mathcal{H}}\colon \mathrm{D}(\mathcal{L}) \to \mathcal{H}$ is self-adjoint by Proposition 4.3.17 (b) and $\mathcal{R}\big|_{\mathcal{H}}\colon \mathcal{H} \to \mathcal{H}$ is bounded and symmetric by Lemma 4.4.2. □

4.5.2 The Essential Spectrum of the Linearised Operator

The aim of this section is to explicitly determine the essential spectrum of the linearised operator $\mathcal{L}\colon \mathrm{D}(\mathcal{L}) \to \mathcal{H}$. Loosely speaking, the reason why this succeeds is the following: Recall that we have explicitly determined the essential spectrum of $-\mathcal{T}^2\big|_{\mathcal{H}}$ in Proposition 4.3.19 using Weyl's criterion. The latter criterion also illustrates that every element in the essential spectrum is generated by infinitely many approximate eigenfunctions. Hence, finite dimensional perturbations of $-\mathcal{T}^2\big|_{\mathcal{H}}$ do not affect the essential spectrum. The same is also true for compact perturbations, i.e., adding some compact operator to $-\mathcal{T}^2\big|_{\mathcal{H}}$, since compact operators are "almost finite dimensional", see [69, Thm. 9.15] or [136, Thm. VI.13] for precise statements. Although the response operator might not be compact, the next lemma shows that it is relatively $(\mathcal{T}^2\big|_{\mathcal{H}})$-compact, and this property suffices for the above arguments. The lemma is based on [62, Thm. 5.9], see also [49, Lemma 5.16], [61, Lemma 3.10 (b)], or [85, Cor. B.19] for related results.

Lemma 4.5.3 (Relative $(\mathcal{T}^2\big|_{\mathcal{H}})$-Compactness of the Response Operator)**.** *The response operator $\mathcal{R}\big|_{\mathcal{H}}\colon \mathcal{H} \to \mathcal{H}$ and its square root $\sqrt{\mathcal{R}}\big|_{\mathcal{H}}\colon \mathcal{H} \to \mathcal{H}$ are both relatively $(\mathcal{T}^2\big|_{\mathcal{H}})$-compact in the sense of [69, Def. 14.1]. This means that the operators $\mathcal{R}\left(-\mathcal{T}^2|_{\mathcal{H}} - \lambda\right)^{-1}\colon \mathcal{H} \to \mathcal{H}$ and $\sqrt{\mathcal{R}}\left(-\mathcal{T}^2|_{\mathcal{H}} - \lambda\right)^{-1}\colon \mathcal{H} \to \mathcal{H}$ are both compact for every $\lambda \in \rho(-\mathcal{T}^2\big|_{\mathcal{H}})$.*

Proof. Because $\mathcal{R} = (\sqrt{\mathcal{R}})^2$ and $\sqrt{\mathcal{R}}$ is bounded by Lemma 4.4.4, it suffices to show that $\sqrt{\mathcal{R}}\big|_{\mathcal{H}}$ is relatively $(\mathcal{T}^2\big|_{\mathcal{H}})$-compact.[127]

By [40, III Def. 2.15 and Ex. 2.18(1)], this is equivalent to

$$\sqrt{\mathcal{R}}\colon \left(\mathrm{D}(\mathcal{L}), \|\mathcal{T}^2 \cdot\|_H + \|\cdot\|_H\right) \to \mathcal{H} \tag{4.5.1}$$

being compact; the domain of $\sqrt{\mathcal{R}}$ in (4.5.1) is $\mathrm{D}(\mathcal{L}) = \mathrm{D}(\mathcal{T}^2) \cap \mathcal{H}$ equipped with the graph norm of $\mathcal{T}^2$.[128] To prove this statement, consider a sequence $(f_n)_{n\in\mathbb{N}} \subset \mathrm{D}(\mathcal{L})$ s.t. $(f_n)_{n\in\mathbb{N}}$ and $(\mathcal{T}^2 f_n)_{n\in\mathbb{N}}$ are bounded in H. Applying the Poincaré type inequality from Lemma 4.3.28 to $\mathcal{T} f_n \in \mathrm{im}(\mathcal{T}) = \ker(\mathcal{T})^\perp$, recall Lemma 4.3.26 for the latter identity, shows that $(\mathcal{T} f_n)_{n\in\mathbb{N}}$ is also bounded in H. By Lemma 4.4.6, $(U_{\mathcal{T}f_n})_{n\in\mathbb{N}} \subset C \cap H^2(\mathbb{R}^3)$ is thus bounded in $H^2(\mathbb{R}^3)$. Moreover, the identity (4.4.19) implies $\mathrm{supp}\,(\partial_x U_{\mathcal{T}f_n}) \subset \bar{B}_{R_{\max}}(0)$ for $n \in \mathbb{N}$. Hence, using the compact embedding $H^2(B_{R_{\max}}(0)) \Subset H^1(B_{R_{\max}}(0))$, we obtain that $(\partial_x U_{\mathcal{T}f_n})_{n\in\mathbb{N}}$ is (strongly) convergent in $L^2(\mathbb{R}^3;\mathbb{R}^3)$ after extracting a subsequence – by slight abuse of notation, we do not notationally distinguish between this subsequence and the original sequence. Then, using Lemma 4.1.2 and the representation (4.4.24) of $\sqrt{\mathcal{R}}$ yields

$$\begin{aligned}\|\sqrt{\mathcal{R}} f_n - \sqrt{\mathcal{R}} f_m\|_H^2 &= \pi \int_{\Omega_0} |\varphi'(E,L)| \frac{w^2}{\rho_0(r)} \left|U'_{\mathcal{T}f_n}(r) - U'_{\mathcal{T}f_m}(r)\right|^2 \mathrm{d}(r,w,L) = \\ &= \int_0^\infty r^2 \left|U'_{\mathcal{T}f_n}(r) - U'_{\mathcal{T}f_m}(r)\right|^2 \mathrm{d}r = \frac{1}{4\pi} \|\partial_x U_{\mathcal{T}f_n} - \partial_x U_{\mathcal{T}f_m}\|_2^2 \to 0\end{aligned} \tag{4.5.2}$$

[127] Since $\mathcal{R}$ and $\sqrt{\mathcal{R}}$ are essentially of the same form, straight-forward modifications of the arguments below also yield a more direct proof that $\mathcal{R}\big|_{\mathcal{H}}$ is relatively $(\mathcal{T}^2\big|_{\mathcal{H}})$-compact.

[128] Alternatively, one could show that $\sqrt{\mathcal{R}}\left(-\mathcal{T}^2|_{\mathcal{H}} - \lambda\right)^{-1}$ is compact by using the Fourier series representation (4.3.68) of $\left(-\mathcal{T}^2|_{\mathcal{H}} - \lambda\right)^{-1}$. This, more direct, approach is pursued in [85, Proof of Cor. B.19].

as $n, m \to \infty$. This means that $(\sqrt{\mathcal{R}} f_n)_{n\in\mathbb{N}}$ is a Cauchy sequence in $\mathcal{H}$ and thus, since $\mathcal{H}$ is complete, (strongly) convergent in $\mathcal{H}$. □

As motivated before, the lemma above can be used to derive a connection between the essential spectra of $-\mathcal{T}^2\big|_{\mathcal{H}}$ and $\mathcal{L}$.

Proposition 4.5.4 (The Essential Spectrum of the Linearised Operator)**.** *The essential spectrum of the linearised operator $\mathcal{L}\colon \mathrm{D}(\mathcal{L}) \to \mathcal{H}$ is given by*

$$\sigma_{\mathrm{ess}}(\mathcal{L}) = \sigma_{\mathrm{ess}}(-\mathcal{T}^2\big|_{\mathcal{H}}) = \overline{\left(\frac{2\pi\mathbb{N}}{T(\mathbb{D}_0)}\right)^2}, \tag{4.5.3}$$

where the latter set is defined in (4.3.66)*.*

Proof. Since $\mathcal{L} = -\mathcal{T}^2\big|_{\mathcal{H}} - \mathcal{R}\big|_{\mathcal{H}}$ and $\mathcal{R}\big|_{\mathcal{H}}$ is relatively $(\mathcal{T}^2\big|_{\mathcal{H}})$-compact by Lemma 4.5.3, Weyl's theorem [69, Thm. 14.6] implies that the essential spectra of $-\mathcal{T}^2\big|_{\mathcal{H}}$ and $\mathcal{L}$ are identical. The explicit form of $\sigma_{\mathrm{ess}}(-\mathcal{T}^2\big|_{\mathcal{H}})$ is due to Proposition 4.3.19. □

We refer to Remark 4.3.20 for a discussion about the structure of $\sigma_{\mathrm{ess}}(\mathcal{L}) = \sigma_{\mathrm{ess}}(-\mathcal{T}^2\big|_{\mathcal{H}})$ including schematic visualisations of this set.

As observed in [117, Thm. 1.1], not only the essential spectrum of $\mathcal{L}$ is determined by the one of $-\mathcal{T}^2\big|_{\mathcal{H}}$, but also further/different parts of the spectrum. Let us discuss this matter in the following remark.

Remark 4.5.5. *The equation* (4.4.23) *can be rewritten as*

$$\mathcal{R} f = \mathcal{T}\mathcal{K}\mathcal{T} f, \qquad f \in \mathrm{D}(\mathcal{T}), \tag{4.5.4}$$

where $\mathcal{K}\colon H \to H$ is given by

$$\mathcal{K} f \coloneqq |\varphi'|\, U_f, \qquad f \in H; \tag{4.5.5}$$

recall Definition 4.4.5 or the definition of U_f. Note that $\mathcal{K}\mathcal{T} f \in \mathrm{D}(\mathcal{T})$ for $f \in \mathrm{D}(\mathcal{T})$ by Lemma 4.4.6. The integrability of $|\varphi'|$, cf. Lemma 4.1.3, together with the estimates (4.4.3) *and* (4.4.14) *shows that $\mathcal{K}$ is a bounded operator. Moreover, $\mathcal{K}$ is symmetric and non-positive with quadratic form given by*

$$\langle \mathcal{K} f, g\rangle_H = -\frac{1}{4\pi}\int_{\mathbb{R}^3} \partial_x U_f(x) \cdot \partial_x U_g(x)\,\mathrm{d}x, \qquad f, g \in H. \tag{4.5.6}$$

In order to derive further properties of $\mathcal{K}$, note that by the spherical symmetry a.e. of $f \in H$ and ρ_f, (4.4.13) *can be rewritten as*

$$U_f(r) = -4\pi^2 \int_{\Omega_0} \frac{f(s, w, L)}{\max\{r, s\}}\,\mathrm{d}(s, w, L), \qquad r > 0. \tag{4.5.7}$$

Hence, $\mathcal{K}$ is an integral operator of the form

$$\mathcal{K} f(r, w, L) = 4\pi^2 \int_{\Omega_0} \frac{1}{|\varphi'(E(\tilde r, \tilde w, \tilde L), \tilde L)|}\, K(r, w, L, \tilde r, \tilde w, \tilde L)\, f(\tilde r, \tilde w, \tilde L)\,\mathrm{d}(\tilde r, \tilde w, \tilde L), \qquad f \in H, \tag{4.5.8}$$

with integral kernel $K\colon \Omega_0 \times \Omega_0 \to \mathbb{R}$ given by

$$K(r, w, L, \tilde r, \tilde w, \tilde L) \coloneqq -\frac{|\varphi'(E(r, w, L), L)|\,|\varphi'(E(\tilde r, \tilde w, \tilde L), \tilde L)|}{\max\{r, \tilde r\}} \tag{4.5.9}$$

for a.e. $(r, w, L), (\tilde{r}, \tilde{w}, \tilde{L}) \in \Omega_0$. *By condition* ($\varphi 5$), *the integral kernel* K *is continuous on* $\Omega_0 \times \Omega_0$. *Thus, by Mercer's Theorem (see [32, III §5] and, for a more general version of the theorem, [42, Thm. 2.4]),* $\mathcal{K}$ *is a trace class operator [136, Sc. VI.6] with trace given by*

$$\operatorname{Tr}(\mathcal{K}) = 4\pi^2 \int_{\Omega_0} \frac{|K(r, w, L, r, w, L)|}{|\varphi'(E, L)|} \,\mathrm{d}(r, w, L) = 4\pi^2 \int_{\Omega_0} \frac{|\varphi'(E, L)|}{r} \,\mathrm{d}(r, w, L); \quad (4.5.10)$$

the latter integral is finite by Lemma 4.1.3.

Kato-Birman theory [135, Sc. XI.3] then reveals further connections between the linearised operator $\mathcal{L}$ *and the squared transport operator* $-\mathcal{T}^2\big|_{\mathcal{H}}$. *For instance, as shown in [117, Thm. 1.1], the absolutely continuous spectra of* $\mathcal{L}$ *and* $-\mathcal{T}^2\big|_{\mathcal{H}}$ *are identical; see [136, Sc. VII.2] for the definition of this part of the spectrum. This statement can be proven as follows: By [34, 88, 89], it suffices to show that* $(\mathcal{L} - z)^{-1} - (-\mathcal{T}^2\big|_{\mathcal{H}} - z)^{-1}$ *is a trace class operator for one/any* $z \in \mathbb{C} \setminus \mathbb{R}$. *Using the second resolvent identity [69, Prop. 1.9] and* (4.5.4), *this operator can be written as*

$$(\mathcal{L} - z)^{-1} - (-\mathcal{T}^2\big|_{\mathcal{H}} - z)^{-1} = (-\mathcal{T}^2\big|_{\mathcal{H}} - z)^{-1} \mathcal{T} \mathcal{K} \mathcal{T} (\mathcal{L} - z)^{-1}. \quad (4.5.11)$$

The Fourier series representation of $(-\mathcal{T}^2\big|_{\mathcal{H}} - z)^{-1}$ *derived in Lemma 4.3.18 shows that* $(-\mathcal{T}^2\big|_{\mathcal{H}} - z)^{-1}\mathcal{T}$ *is a bounded operator on* $\mathcal{H}$. *Moreover,* $\mathcal{T}(\mathcal{L} - i)^{-1} = \mathcal{T}^{-1}\mathcal{T}^2(\mathcal{L} - i)^{-1}$ *is bounded by [69, Lemma 13.6];*[129] *notice that* $\mathcal{T}^{-1} \colon \mathcal{H} \to H$ *is bounded by Corollary 4.3.25 and Lemma 4.3.27. Hence, as the composition of a trace class operator and bounded operators is again in the trace class, cf. [136, Thm. VI.19], we conclude that the absolutely continuous spectra of* $\mathcal{L}$ *and* $-\mathcal{T}^2\big|_{\mathcal{H}}$ *are indeed identical.*

4.5.3 Positivity of the Linearised Operator

It follows by Propositions 4.5.4 and A.0.1 that the essential spectrum of the linearised operator $\mathcal{L} \colon \mathrm{D}(\mathcal{L}) \to \mathcal{H}$ is positive, i.e.,

$$\inf(\sigma_{\mathrm{ess}}(\mathcal{L})) > 0. \quad (4.5.12)$$

The aim of this section is to show that the same is also true for the entire spectrum of $\mathcal{L}$. As discussed in Chapter 3 and proven in Lemma C.0.3, this property corresponds to the linear stability of the underlying steady state. We mainly follow [62, Sc. 7.1] here.

The basis for the results of this section forms the *Antonov coercivity bound*. This classical estimate gives a positive lower bound on the quadratic form of the linearised operator $\langle \mathcal{L} f, f \rangle_H$ for suitably regular, spherically symmetric, odd-in-v functions $f \colon \Omega_0 \to \mathbb{R}$. It was first proven in [9, 10] for isotropic polytropic steady states (1.2.3). Simplified proofs and extensions of the original result covering a larger class of steady states were then developed in [36, 37, 57, 77, 96, 128, 169]. Further adaptions and applications of the estimate are contained in [53, Lemma 3.1], [61, Lemma 3.10 (c)], [62, Prop. 7.1], [85, Thm. 1.2], and [119, Prop. 3.5] among others. In fact, it is mainly the monotonicity condition ($\varphi 5$) which is needed to establish such estimate; due to this reason, the condition ($\varphi 5$) is sometimes called the *Antonov (linear) stability condition*. We first present a simplified version[130] of

[129] One can apply the first resolvent identity [69, Prop. 1.6 (2)] to deduce that $\mathcal{T}(\mathcal{L} - z)^{-1}$ is, in fact, bounded for any $z \in \mathbb{C} \setminus \mathbb{R}$.

[130] In Lemma 4.5.6, we require that the supports of the functions under consideration are bounded away from the spatial origin. This assumption allows us to avoid several technical arguments in the proof of the lemma. Nonetheless, due to Lemma 4.3.31, establishing the estimate for such functions still suffices to extend the estimate to more general functions afterwards.

the estimate for smooth functions before extending it to more general functions. Since the present class of steady states differs from the ones used in the literature, we also include a proof here which is based on [57, App.].

Lemma 4.5.6 (Antonov's Coercivity Bound for Smooth Functions)**.** *Let $f \in C^2_{c,r}(\Omega_0)$ be odd in v and s.t. the support of f is bounded away from $\{x = 0\}$. Then there holds the estimate*

$$\langle \mathcal{L}f, f\rangle_H \geq \int_{\Omega_0} \frac{1}{|\varphi'(E,L)|}\,\frac{U_0'(r)}{r}\,|f(x,v)|^2\,\mathrm{d}(x,v), \tag{4.5.13}$$

where, as usual, $r = |x|$.

Proof. By the skew-symmetry of the transport operator derived in Proposition 4.3.15, the quadratic form of $\mathcal{L}$ is of the form

$$\langle \mathcal{L}f, f\rangle_H = \|\mathcal{T}f\|_H^2 - \langle \mathcal{R}f, f\rangle_H. \tag{4.5.14}$$

Using the Cauchy-Schwarz inequality and Lemma 4.1.2 gives the following estimate for the second term on the right-hand side:

$$\begin{aligned}\langle \mathcal{R}f, f\rangle_H &= 2^4\pi^3 \int_{\Omega_0} w\, f(r,w,L)\, j_f(r)\,\mathrm{d}(r,w,L) = \\ &= (2\pi)^4 \int_0^\infty \frac{1}{r^2}\left(\int_0^\infty \int_{\mathbb{R}} w\, f(r,w,L)\,\mathrm{d}w\,\mathrm{d}L\right)^2 \mathrm{d}r \leq \\ &\leq 2^4\pi^3 \int_{\Omega_0} \frac{1}{|\varphi'(E,L)|}\,\rho_0(r)\,|f(r,w,L)|^2\,\mathrm{d}(r,w,L).\end{aligned} \tag{4.5.15}$$

In order to estimate the first term on the right-hand side of (4.5.14), we consider the spherically symmetric function $g\colon \Omega_0 \to \mathbb{R}$ defined by

$$g(r,w,L) \coloneqq \frac{1}{rw}\,f(r,w,L). \tag{4.5.16}$$

Since f is odd in v and vanishes at $r = 0$, (4.5.16) indeed defines a continuously differentiable function on Ω_0. Applying the product rule to the representation (4.2.17) of the transport operator yields

$$\mathcal{T}f = \mathcal{T}(rw\,g) = g\,\mathcal{T}(rw) + rw\,\mathcal{T}g \tag{4.5.17}$$

as well as

$$(\mathcal{T}f)^2 = r^2w^2\,(\mathcal{T}g)^2 + \mathcal{T}\big(rw\,g^2\,\mathcal{T}(rw)\big) - rw\,g^2\,\mathcal{T}^2(rw). \tag{4.5.18}$$

Hence, the first term on the right-hand side of (4.5.14) can be rewritten as follows:

$$\begin{aligned}\frac{1}{4\pi^2}\,\|\mathcal{T}f\|_H^2 = &\int_{\Omega_0} \frac{1}{|\varphi'(E,L)|}\,r^2w^2\,(\mathcal{T}g(r,w,L))^2\,\mathrm{d}(r,w,L) + \\ &+ \int_{\Omega_0} \frac{1}{|\varphi'(E,L)|}\,\mathcal{T}\big(rw\,g^2\,\mathcal{T}(rw)\big)\,\mathrm{d}(r,w,L) + \\ &- \int_{\Omega_0} \frac{1}{|\varphi'(E,L)|}\,rw\,g(r,w,L)^2\,\mathcal{T}^2(rw)\,\mathrm{d}(r,w,L).\end{aligned} \tag{4.5.19}$$

The first term on the right-hand side of this equation is obviously non-negative.[131] The second term vanishes by the skew-symmetry of the transport operator; note that

[131] In the literature, this term is often included in the right-hand side of the Antonov bound, which then gives a "sharper" estimate than (4.5.13). Here, we just drop this term since it is not helpful for our applications.

$rw\, g(r,w,L)^2\, \mathcal{T}(rw)$ defines a smooth function on Ω_0. In order to rewrite the third term, we use the radial Poisson equation to deduce

$$\mathcal{T}^2(rw) = \mathcal{T}\big(w^2 - r\,\Psi_L'(r)\big) = -rw\left(\Psi_L''(r) + \frac{3}{r}\,\Psi_L'(r)\right) = -rw\left(4\pi\rho_0(r) + \frac{U_0'(r)}{r}\right) \tag{4.5.20}$$

for $r > 0$ and $w \in \mathbb{R}$. Hence,

$$\begin{aligned}\|\mathcal{T}f\|_H^2 &\geq 4\pi^2 \int_{\Omega_0} \frac{1}{|\varphi'(E,L)|}\left(4\pi\rho_0(r) + \frac{U_0'(r)}{r}\right) r^2 w^2\, g(r,w,L)^2\,\mathrm{d}(r,w,L) = \\ &= 4\pi^2 \int_{\Omega_0} \frac{1}{|\varphi'(E,L)|}\left(4\pi\rho_0(r) + \frac{U_0'(r)}{r}\right) f(r,w,L)^2\,\mathrm{d}(r,w,L). \end{aligned} \tag{4.5.21}$$

Inserting (4.5.15) and (4.5.21) into (4.5.14) then shows (4.5.13). □

In order to extend the above estimate to a larger set of functions, we first introduce an extension of the quadratic form of the linearised operator similar to [62, Def. 4.4], see also [85, Cor. B.19].

Definition & Lemma 4.5.7 (The Quadratic Form of the Linearised Operator)**.** *For $f \in \mathrm{D}(\mathcal{T}) \cap \mathcal{H}$ let*

$$\langle \mathcal{L}f, f\rangle_H \coloneqq \|\mathcal{T}f\|_H^2 - \frac{1}{4\pi}\|\partial_x U_{\mathcal{T}f}\|_2^2; \tag{4.5.22}$$

this expression is well-defined by Lemma 4.4.6.[132] *Furthermore, for $f \in \mathrm{D}(\mathcal{L})$, this definition is consistent with the usual definition of the quadratic form of $\mathcal{L}$.*

Proof. Let $f \in \mathrm{D}(\mathcal{L})$. Using the skew-symmetry of the transport operator, cf. Proposition 4.3.15, and the identity (4.4.19) from Lemma 4.4.6 yields

$$\begin{aligned} -\langle \mathcal{T}^2 f, f\rangle_H - \langle \mathcal{R}f, f\rangle_H &= \|\mathcal{T}f\|_H^2 - (4\pi)^2 \int_0^\infty r^2\, j_f^2(r)\,\mathrm{d}r = \\ &= \|\mathcal{T}f\|_H^2 - \int_0^\infty r^2\, U_{\mathcal{T}f}'(r)^2\,\mathrm{d}r = \|\mathcal{T}f\|_H^2 - \frac{1}{4\pi}\,\|\partial_x U_{\mathcal{T}f}\|_2^2, \end{aligned} \tag{4.5.23}$$

which shows that (4.5.22) is indeed consistent with the usual definition of $\langle \mathcal{L}f, f\rangle_H$. □

By applying the approximation result from Section 4.3.5, we obtain that the Antonov coercivity bound from Lemma 4.5.6 can be extended to $\mathrm{D}(\mathcal{T}) \cap \mathcal{H}$.

Lemma 4.5.8 (Antonov's Coercivity Bound on $\mathrm{D}(\mathcal{T}) \cap \mathcal{H}$)**.** *For $f \in \mathrm{D}(\mathcal{T}) \cap \mathcal{H}$ there holds the estimate* (4.5.13)*, where the left-hand side is to be interpreted in the sense of Definition 4.5.7.*

Proof. Let $(f_j)_{j\in\mathbb{N}} \subset C_{c,r}^\infty(\Omega_0) \cap \mathcal{H}$ be an approximation sequence as constructed in Lemma 4.3.31, i.e., $f_j \to f$ and $\mathcal{T}f_j \to \mathcal{T}f$ in H as $j \to \infty$. By Lemma 4.5.6, the estimate (4.5.13) holds after replacing f with f_j for $j \in \mathbb{N}$; in particular, the support of f_j is bounded away from $\{x = 0\}$ for $j \in \mathbb{N}$ by Lemma 4.3.31. Furthermore, Lemma 4.4.6 implies $\langle \mathcal{L}f_j, f_j\rangle_H \to \langle \mathcal{L}f, f\rangle_H$ as $j \to \infty$. The same convergence as $j \to \infty$ also holds for the right-hand side of (4.5.13) because $\frac{U_0'(r)}{r}$ is bounded on the radial support of the steady

[132] From a mathematics point of view, one could further extend this definition to $f \in \mathrm{D}(\mathcal{T})$ which are not necessarily odd in v. However, as discussed in Remark 4.2.10, the linearised operator is only meaningful for odd in v functions.

state. In the case $L_0 > 0$, this is obvious since $R_{\min} > 0$. Otherwise, the steady state is isotropic by (φ5) and, by the radial Poisson equation (2.2.32),

$$\frac{U_0'(r)}{r} = \frac{m_0(r)}{r^3} = \frac{4\pi}{r^3}\int_0^r s^2\,\rho_0(s)\,\mathrm{d}s \to \frac{4\pi}{3}\,\rho_0(0) \qquad \text{as } r \to 0, \tag{4.5.24}$$

which also shows the boundedness of $\frac{U_0'(r)}{r}$. □

An immediate consequence of the above lemma is that $\mathcal{L}$ is a non-negative operator.[133] The same observation is stated in [62, Cor. 7.2].

Corollary 4.5.9. *The linearised operator $\mathcal{L}\colon \mathrm{D}(\mathcal{L}) \to \mathcal{H}$ is non-negative, i.e., $\sigma(\mathcal{L}) \subset [0,\infty[$.*

Proof. Lemma 4.5.8 shows that the quadratic form of $\mathcal{L}$ is non-negative on $\mathrm{D}(\mathcal{L})$. By standard variational principles, cf. [69, Prop. 5.12] or [134, Thm. XIII.1], we then conclude the non-negativity of the spectrum of $\mathcal{L}$. □

As motivated at the start of this section, we aim to show not only that $\mathcal{L}$ is non-negative, but even that it is positive, which means $\sigma(\mathcal{L}) \subset]0,\infty[$.[134] A key observation in this direction is that 0 is not an eigenvalue of $\mathcal{L}$. As the previous corollary, this result follows directly from the Antonov coercivity bound and is based on [62, Cor. 7.3].[135]

Corollary 4.5.10. *The nullspace of the linearised operator $\mathcal{L}\colon \mathrm{D}(\mathcal{L}) \to \mathcal{H}$ is trivial, i.e., $\ker(\mathcal{L}) = \{0\}$.*

Proof. Since the radial weight $\frac{U_0'(r)}{r} = \frac{m_0(r)}{r^3}$ in the integral on the right-hand side of (4.5.13) is positive for $r \in]R_{\min}, R_{\max}]$, the claim follows by Lemma 4.5.8. □

Together with the characterisation of the essential spectrum of $\mathcal{L}$ from Proposition 4.5.4, the above two corollaries already yield the desired positivity of $\mathcal{L}$.

Proposition 4.5.11 (Positivity of the Linearised Operator)**.** *There exists a constant $c > 0$ depending on the underlying steady state s.t. for all $f \in \mathrm{D}(\mathcal{T}) \cap \mathcal{H}$ there holds the estimate*

$$\langle \mathcal{L}f, f\rangle_H \geq c\|f\|_H^2, \tag{4.5.25}$$

where the left-hand side is given by Definition 4.5.7. This means that the linearised operator is positive, i.e.,

$$\inf(\sigma(\mathcal{L})) \geq c > 0. \tag{4.5.26}$$

Proof. By the approximation result from Lemma 4.3.31 and standard variational principles, cf. [69, Prop. 5.12] or [134, Thm. XIII.1], the validity of the estimate (4.5.25) is equivalent to (4.5.26). Let us suppose that the latter is false, i.e., by Corollary 4.5.9, $\inf(\sigma(\mathcal{L})) = 0$. Since the spectrum of an operator is always closed [69, Thm. 1.2], 0 has to lie inside the spectrum of $\mathcal{L}$. By Proposition 4.5.4 and the boundedness of the period function T on $\mathbb{D}_0$, 0 is not in the essential spectrum of $\mathcal{L}$, so it must be an eigenvalue. But this contradicts Corollary 4.5.10. □

[133] The non-negativity of the linearised operator is defined similarly to the response operator, cf. Lemma 4.4.2.

[134] Since the spectrum of an operator is always closed, $\sigma(\mathcal{L}) \subset]0,\infty[$ is equivalent to $\inf(\sigma(\mathcal{L})) > 0$.

[135] Note that the domain of definition of the linearised operator in [62, Sc. 7.1] is $\mathrm{D}(\mathcal{T}^2)$, which is larger then the domain of definition $\mathrm{D}(\mathcal{L})$ chosen here. This leads to the fact that the nullspace of the linearised operator in [62, Cor. 7.3] is larger than the nullspace of $\mathcal{L}$ here.

Although the above proposition already shows the desired positivity of (the spectrum of) $\mathcal{L}$, we will now provide alternative proofs for this statement. On the one hand, this will illustrate how the positivity of $\mathcal{L}$ could be proven without prior knowledge of its essential spectrum, which may be helpful in other situations. On the other hand, this will show how to obtain more explicit lower bounds on $\mathcal{L}$.

The following result is based on the observation that the radial weight $\frac{U_0'(r)}{r}$ contained in the right-hand side of Antonov's coercivity bound (4.5.13) is bounded away from 0 for certain steady states. The analogous observation is used in [62, Thm. 7.9] and [85, Thm. 1.2].

Lemma 4.5.12. *Assume that the underlying steady state is isotropic, i.e., $L_0 = 0 = \ell$. Then, for all $f \in \mathrm{D}(\mathcal{T}) \cap \mathcal{H}$,*

$$\langle \mathcal{L}f, f\rangle_H \geq \frac{M_0}{R_{\max}^3} \|f\|_H^2, \tag{4.5.27}$$

where the left-hand side is to be interpreted in the sense of Definition 4.5.7 and $M_0 > 0$ is the total mass of the steady state, recall (2.2.11).

Proof. As observed in [85, Lemma A.6 (a)], the function $]0,\infty[\ni r \mapsto \frac{U_0'(r)}{r}$ is non-increasing in the case of an isotropic steady state since

$$\partial_r\left[\frac{U_0'(r)}{r}\right] = \frac{U_0''(r) - \frac{1}{r}U_0'(r)}{r} = \frac{4\pi\rho_0(r) - \frac{3}{r}U_0'(r)}{r} = \frac{4\pi}{r}\left(\rho_0(r) - \frac{3}{r^3}\int_0^r s^2\rho_0(s)\,\mathrm{d}s\right) \leq 0 \tag{4.5.28}$$

for $r > 0$, where we used that ρ_0 is non-increasing by Remark 2.2.10 (a). Hence,

$$\frac{U_0'(r)}{r} \geq \frac{U_0'(R_{\max})}{R_{\max}} = \frac{M_0}{R_{\max}^3}, \qquad r \in]0, R_{\max}]. \tag{4.5.29}$$

Inserting this estimate into the coercivity bound from Lemma 4.5.8 yields (4.5.27). □

Unfortunately, the radial weight $\frac{U_0'(r)}{r}$ is not bounded away from 0 if the steady state is anisotropic. Recall that $L_0 > 0$ in this case by assumption (φ4), and thus $R_{\min} > 0$ by (2.2.42). Hence, $\frac{U_0'(r)}{r} = \frac{m_0(r)}{r^3}$ vanishes at the boundary of Ω_0 since $m_0(R_{\min}) = 0$.

Before considering the case of a general, not necessarily isotropic, equilibrium, we illustrate that the arguments from above can also be used to derive an explicit upper bound on the period function T on $\mathbb{D}_0$ for isotropic steady states. In particular, the proof of the lemma below does not use the boundedness of T established in Section A.1, which means that it provides an alternative way of establishing $\sup_{\mathbb{D}_0}(T) < \infty$. The lemma is inspired by [85, Cor. 2.2].

Lemma 4.5.13. *Assume that the underlying steady state is isotropic, i.e., $L_0 = 0 = \ell$. Then*

$$\sup_{\mathbb{D}_0}{}^2(T) \leq 4\pi^2 \frac{R_{\max}^3}{M_0}. \tag{4.5.30}$$

Proof. Using the non-negativity of the response operator $\mathcal{R}$ proven in Lemma 4.4.2 and the bound (4.5.27) from the lemma above yield

$$\langle -\mathcal{T}^2 f, f\rangle_H \geq \langle \mathcal{L}f, f\rangle_H \geq \frac{M_0}{R_{\max}^3}\|f\|_H^2, \qquad f \in \mathrm{D}(\mathcal{T}^2) \cap \mathcal{H}. \tag{4.5.31}$$

By standard variational principles, cf. [69, Prop. 5.12] or [134, Thm. XIII.1], we thus deduce

$$\inf\big(\sigma(-\mathcal{T}^2|_{\mathcal{H}})\big) \geq \frac{M_0}{R_{\max}^3}. \tag{4.5.32}$$

Using the explicit structure of the spectrum of $-\mathcal{T}^2\big|_{\mathcal{H}}$ derived in Proposition 4.3.19, we hence conclude (4.5.30). □

The remaining part of this section is devoted to finding an alternative way to prove the positivity of $\mathcal{L}$ in the case of a general steady state, including the situation of an anisotropic equilibrium. We proceed as in [62, Sc. 7.1] and first consider an intermediate variational problem based on [62, Prop. 7.4]. The techniques used in the proof of this result are inspired by related arguments for Schrödinger operators [98, Ch. 11] as well as, in the context of the linearised Vlasov-Poisson system, by variational principles for the so-called "Guo-Lin operator", see [53, Lemma 3.1] and [165, Prop. 4.8]. A related estimate is shown in [95, Thm. 1.3] in the case of an isotropic polytropic steady state (1.2.3); see [119, Sc. 3.6] for a review of these arguments.

Lemma 4.5.14. *Let*

$$\tilde{\lambda} \coloneqq \inf_{\substack{f\in \mathrm{D}(\mathcal{T})\cap\mathcal{H}\\ f\neq 0}} \frac{\langle \mathcal{L}f, f\rangle_H}{\|\mathcal{T}f\|_H^2} = \inf_{\substack{f\in \mathrm{D}(\mathcal{T})\cap\mathcal{H}\\ f\neq 0}} 1 - \frac{\|\partial_x U_{\mathcal{T}f}\|_2^2}{4\pi\|\mathcal{T}f\|_H^2}; \tag{4.5.33}$$

see Definition 4.5.7 for the latter identity and recall $f \perp \ker(\mathcal{T})$ for $f \in \mathcal{H}$ by Corollary 4.3.25. Then

$$\tilde{\lambda} \in]0,1[\tag{4.5.34}$$

and the infimum (4.5.33) *is attained by a minimiser.*

Proof. Let $(f_j)_{j\in\mathbb{N}} \subset \mathrm{D}(\mathcal{T}) \cap \mathcal{H}$ be a normalised minimising sequence, i.e., $\|\mathcal{T}f_j\|_H = 1$ for $j \in \mathbb{N}$ and $\langle \mathcal{L}f_j, f_j\rangle_H \to \tilde{\lambda}$. Our aim is to obtain a minimising function of the variational problem (4.5.33) as a suitable limit of $(f_j)_{j\in\mathbb{N}}$. Following [62, Prop. 7.4], we split the proof into several steps.

Step 1: Convergence of the Potentials. Lemma 4.4.6 implies $U_{\mathcal{T}f_j} \in C_r \cap H^2(\mathbb{R}^3)$ for $j \in \mathbb{N}$ and that $(U_{\mathcal{T}f_j})_{j\in\mathbb{N}}$ is bounded in $H^2(\mathbb{R}^3)$. Hence, there exists a spherically symmetric a.e. function $\psi \in H^2(\mathbb{R}^3)$ s.t.

$$U_{\mathcal{T}f_j} \rightharpoonup \psi \quad \text{and} \quad \Delta U_{\mathcal{T}f_j} \rightharpoonup \Delta\psi \qquad \text{in } L^2(\mathbb{R}^3) \text{ as } j \to \infty \tag{4.5.35}$$

and

$$\partial_x U_{\mathcal{T}f_j} \rightharpoonup \partial_x \psi \qquad \text{in } L^2(\mathbb{R}^3;\mathbb{R}^3) \text{ as } j \to \infty \tag{4.5.36}$$

after extracting a subsequence – by slight abuse of notation, we do not change the name of the minimal sequence when passing to a subsequence of the original sequence throughout this proof. The identity (4.4.19) yields $\operatorname{supp}(\partial_x U_{\mathcal{T}f_j}) \subset \bar{B}_{R_{\max}}(0)$ for $j \in \mathbb{N}$, and thus $\operatorname{supp}(\partial_x\psi) \subset \bar{B}_{R_{\max}}(0)$. Together with the compact embedding $H^2(B_{R_{\max}}(0)) \Subset H^1(B_{R_{\max}}(0))$ we therefore obtain

$$\partial_x U_{\mathcal{T}f_j} \to \partial_x \psi \qquad \text{in } L^2(\mathbb{R}^3;\mathbb{R}^3) \text{ as } j \to \infty. \tag{4.5.37}$$

Step 2: Weak Convergence of $(\mathcal{T}f_j)_{j\in\mathbb{N}}$. Since $(\mathcal{T}f_j)_{j\in\mathbb{N}}$ is bounded in H, there exists $g \in H$ s.t. $\mathcal{T}f_j \rightharpoonup g$ in H as $j \to \infty$ after extracting a subsequence. Moreover, by Lemma 4.3.16, $\mathcal{T}f_j$ is even in v a.e. for $j \in \mathbb{N}$ and this property carries over to the weak limit g.

Step 3: The Connection Between the Above Limits. For every $h \in L^2_r(\mathbb{R}^3) \cong \big[L^2_r(\mathbb{R}^3)\big]'$, $\Omega_0 \ni (x,v) \mapsto |\varphi'(E,L)|\, h(x)$ is an element of $H \cong H'$ by Lemma 4.1.3. Hence, by the previous step it follows that

$$\rho_{\mathcal{T}f_j} = \int_{\mathbb{R}^3} \mathcal{T}f_j(\cdot,v)\,\mathrm{d}v \rightharpoonup \int_{\mathbb{R}^3} g(\cdot,v)\,\mathrm{d}v = \rho_g \qquad \text{in } L^2_r(\mathbb{R}^3) \text{ as } j \to \infty; \tag{4.5.38}$$

as before, functions defined on Ω_0 are extended by 0 to the entire space $\mathbb{R}^3 \times \mathbb{R}^3$. On the other hand, $4\pi\rho_{\mathcal{T}f_j} = \Delta U_{\mathcal{T}f_j} \rightharpoonup \Delta\psi$ in $L^2(\mathbb{R}^3)$ as $j \to \infty$ by (4.4.15) and (4.5.35). Hence, by the uniqueness of weak limits in $L^2_r(\mathbb{R}^3)$ we deduce[136]

$$\Delta\psi = 4\pi\rho_g \qquad \text{a.e. on } \mathbb{R}^3. \tag{4.5.39}$$

From this identity we conclude

$$\psi = U_g \qquad \text{a.e. on } \mathbb{R}^3. \tag{4.5.40}$$

because solutions of the Poisson equation are unique in $L^p(\mathbb{R}^3)$. More precisely, the latter can be obtained as follows: The embedding $H^1(\mathbb{R}^3) \hookrightarrow L^6(\mathbb{R}^3)$ yields $\psi \in L^6(\mathbb{R}^3)$, while Lemma 4.4.5 shows $U_g \in L^6(\mathbb{R}^3)$. Thus, $u \coloneqq \psi - U_g \in L^6(\mathbb{R}^3)$ and u is harmonic by (4.5.39). The mean value property of harmonic functions then implies $u \equiv 0$, i.e., (4.5.40).

Step 4: The Minimiser. Since $\mathcal{T}f_j \in \ker(\mathcal{T})^\perp$ for $j \in \mathbb{N}$ by Lemma 4.3.26, there holds $g \in \ker(\mathcal{T})^\perp$. The same lemma thus implies that there exists $f \in \mathrm{D}(\mathcal{T})$ s.t. $\mathcal{T}f = g$. In addition, we can choose f to be odd in v a.e. because g is even in v a.e. and $\mathcal{T}f_+ = g_- = 0$ by Lemma 4.3.16. Using the convergence (4.5.37), we deduce

$$1 - \frac{1}{4\pi}\|\partial_x U_{\mathcal{T}f}\|_2^2 = 1 - \frac{1}{4\pi}\|\partial_x\psi\|_2^2 = \lim_{j\to\infty} 1 - \frac{1}{4\pi}\|\partial_x U_{\mathcal{T}f_j}\|_2^2 = \lim_{j\to\infty}\langle \mathcal{L}f_j, f_j\rangle_H = \tilde{\lambda}. \tag{4.5.41}$$

Thus, if $\|\partial_x U_{\mathcal{T}f}\|_2 = 0$, the above would imply $\tilde{\lambda} = 1$. However, this would contradict the fact that inserting $f \in \mathrm{D}(\mathcal{T}) \cap \mathcal{H} \setminus \{0\}$ with $\partial_x U_{\mathcal{T}f} \not\equiv 0$ into the infimum (4.5.33) directly yields $\tilde{\lambda} < 1$.

Therefore, $\|\partial_x U_{\mathcal{T}f}\|_2 > 0$, and thus $f \not\equiv 0$. This means that we can take f as a test function in the infimum (4.5.33), which, together with (4.5.41), leads to

$$1 - \frac{1}{4\pi}\|\partial_x U_{\mathcal{T}f}\|_2^2 = \tilde{\lambda} \leq 1 - \frac{\|\partial_x U_{\mathcal{T}f}\|_2^2}{4\pi\|\mathcal{T}f\|_H^2}, \tag{4.5.42}$$

i.e., $\|\mathcal{T}f\|_H \geq 1$. On the other hand, the weak lower semicontinuity of the weighted L^2-norm $\|\cdot\|_H$ yields

$$\|\mathcal{T}f\|_H \leq \liminf_{j\to\infty} \|\mathcal{T}f_j\|_H = 1. \tag{4.5.43}$$

Overall, $\|\mathcal{T}f\|_H = 1$ and therefore

$$\tilde{\lambda} = 1 - \frac{1}{4\pi}\|\partial_x U_{\mathcal{T}f}\|_2^2 = \langle \mathcal{L}f, f\rangle_H = \frac{\langle \mathcal{L}f, f\rangle_H}{\|\mathcal{T}f\|_H^2}, \tag{4.5.44}$$

which shows that f is indeed the desired minimiser.

Step 5: Positivity of $\tilde{\lambda}$. It follows by the previous step that $f \in \mathrm{D}(\mathcal{T}) \cap \mathcal{H}$ with $\|f\|_H > 0$. Hence, the Antonov coercivity bound from Lemma 4.5.8 implies $\langle \mathcal{L}f, f\rangle_H > 0$ since the radial weight $\frac{U_0'(r)}{r}$ is positive on $]R_{\min}, R_{\max}]$. By (4.5.44), we thus conclude $\tilde{\lambda} > 0$. □

Before using this result to deduce the positivity of $\mathcal{L}$, we discuss an interpretation of the variational problem (4.5.33).

[136] Notice that $\tilde{f}_j \rightharpoonup \tilde{f}$ in $L^2(\mathbb{R}^3)$ is equivalent to $\tilde{f}_j \rightharpoonup \tilde{f}$ in $L^2_r(\mathbb{R}^3)$ for $(\tilde{f}_j)_{j\in\mathbb{N}} \subset L^2_r(\mathbb{R}^3)$ and $\tilde{f} \in L^2_r(\mathbb{R}^3)$.

Remark 4.5.15. *For $\gamma > 0$ let $\mathcal{L}_\gamma := -\mathcal{T}^2 - \frac{1}{\gamma}\mathcal{R}\colon \mathrm{D}(\mathcal{L}) \to \mathcal{H}$. This family of operators will be studied in detail in Section 5.1.1. Compared to the linearised operator $\mathcal{L}$, the gravitational response term $\mathcal{R}$ gets "amplified" in $\mathcal{L}_\gamma$ by choosing smaller values of $\gamma > 0$. After extending the quadratic form associated to $\mathcal{L}_\gamma$ onto $\mathrm{D}(\mathcal{T}) \cap \mathcal{H}$ similarly to Definition 4.5.7, we obtain*

$$\gamma \langle \mathcal{L}_\gamma f, f\rangle_H = \gamma \|\mathcal{T} f\|_H^2 - \langle \mathcal{R} f, f\rangle_H = \langle \mathcal{L} f, f\rangle_H - (1-\gamma)\|\mathcal{T} f\|_H^2 \tag{4.5.45}$$

for $f \in \mathrm{D}(\mathcal{T}) \cap \mathcal{H}$ and $\gamma > 0$. This reveals a connection between $\mathcal{L}_\gamma$ and the variational problem (4.5.33)*: For the minimiser $f^* \in \mathrm{D}(\mathcal{T}) \cap \mathcal{H}$ obtained in Lemma 4.5.14, there holds $\langle \mathcal{L}_{(1-\tilde{\lambda})} f^*, f^*\rangle_H = 0$. Moreover, $\mathcal{L}_\gamma \geq 0$ is equivalent to $\gamma \geq 1 - \tilde{\lambda}$.*

This shows that for the non-negativity of the linearised operator $\mathcal{L} = \mathcal{L}_1$, cf. Corollary 4.5.9, it is crucial that the gravitational response term is not weighted too strongly.

Combined with the Poincaré type inequality from Lemma 4.3.28, the above lemma yields

$$\langle \mathcal{L} f, f\rangle_H \geq \tilde{\lambda}\|\mathcal{T} f\|_H^2 \geq \frac{4\pi^2}{\sup_{\mathbb{D}_0}^2(T)}\tilde{\lambda}\|f\|_H^2, \qquad f \in \mathrm{D}(\mathcal{T}) \cap \mathcal{H}. \tag{4.5.46}$$

This shows that $\frac{4\pi^2\tilde{\lambda}}{\sup_{\mathbb{D}_0}^2(T)} > 0$ is a lower bound on $\mathcal{L}$, which was used in [62, Thm. 7.5] as well as in [61, Lemma 3.10 (c)].

4.5.4 Eigenvalues of the Linearised Operator ?

As motivated in Chapter 3, our key interest regarding the linearised operator $\mathcal{L}\colon \mathrm{D}(\mathcal{L}) \to \mathcal{H}$ is whether it possesses eigenvalues. By the results from the previous section, every eigenvalue of $\mathcal{L}$ has to be positive and thus corresponds to a pulsating mode of the linearised Vlasov-Poisson system. In this section we (start to) discuss whether such eigenvalues exist.

We restrict the discussion to the presence of eigenvalues of $\mathcal{L}$ inside the essential gap $\mathcal{G}$, recall (1.2.21) for the definition of this set. In the case of such an eigenvalue, the oscillation period of the perturbed equilibrium is larger than the radial period of every single particle in the steady state – a property which seems quite intuitive. There are, however, also more profound reasons for restricting the search for eigenvalues of $\mathcal{L}$ to $\mathcal{G}$:

1. We shall see in Chapter 6 that it is quite natural that there are no eigenvalues of $\mathcal{L}$ embedded into its essential spectrum. This can be proven for some equilibria, cf. Section 6.5, but is expected to hold for a larger class of steady states as well. The latter claim will be supported by the numerical simulations in Section 8.3, which will show that, for a large class of steady states, the behaviour of solutions of the linearised Vlasov-Poisson system is determined by whether an eigenvalue of $\mathcal{L}$ exists in $\mathcal{G}$, see Observations 8.3.4 and 8.3.7.

2. The discussion in Section 6.5 will show that the question of whether there exist eigenvalues of $\mathcal{L}$ inside its essential spectrum is rather difficult to answer. Similar difficulties also arise in the study of Schrödinger operators, cf. [134, Sc. XIII.13].

3. Eigenvalues in $\mathcal{G}$ can be characterised using variational principles, which is not possible for other eigenvalues (without further effort).

The application of variational methods was already suggested in [71, p. 258] and is our main tool for analysing the presence of eigenvalues.

Lemma 4.5.16 (Variational Characterisation of Eigenvalues in the Essential Gap)**.** *The bottom of the spectrum of the linearised operator* $\mathcal{L}\colon \mathrm{D}(\mathcal{L}) \to \mathcal{H}$ *is given by*[137]

$$\inf(\sigma(\mathcal{L})) = \inf_{\substack{f\in \mathrm{D}(\mathcal{L})\\ f\neq 0}} \frac{\langle \mathcal{L}f, f\rangle_H}{\|f\|_H^2}. \tag{4.5.47}$$

In addition, the linearised operator $\mathcal{L}\colon \mathrm{D}(\mathcal{L}) \to \mathcal{H}$ *possesses an eigenvalue*[138] *in the essential gap* $\mathcal{G}$ *if and only if*

$$\inf(\sigma(\mathcal{L})) < \inf(\sigma_{\mathrm{ess}}(\mathcal{L})) = \frac{4\pi^2}{\sup^2_{\mathbb{D}_0}(T)}. \tag{4.5.48}$$

In this case, the infimum (4.5.47) *is attained by an eigenfunction to the eigenvalue* $\inf(\sigma(\mathcal{L}))$ *of* $\mathcal{L}$*.*

Proof. The characterisation (4.5.47) of $\inf(\sigma(\mathcal{L}))$ follows by standard variational principles, cf. [69, Prop. 5.12] or [134, Thm. XIII.1]. If (4.5.48) holds true, $\inf(\sigma(\mathcal{L}))$ is an eigenvalue of $\mathcal{L}$ with finite multiplicity by the definition of the essential spectrum. In this situation, it is straight-forward to verify that any eigenfunction is a minimiser of (4.5.47). Moreover, $\inf(\sigma(\mathcal{L})) > 0$ by Proposition 4.5.11, i.e., $\inf(\sigma(\mathcal{L})) \in \mathcal{G}$. Conversely, if (4.5.48) does not hold true, there cannot be an element of $\sigma(\mathcal{L})$ inside $\mathcal{G}$. □

Using similar arguments, one can also characterise the presence of multiple eigenvalues of $\mathcal{L}$ inside the essential gap $\mathcal{G}$ variationally, see Lemma 5.1.3 (with $\gamma = 1$).

In [85, Sc. 1.6], obtaining the infimum (4.5.47) is interpreted as finding the best constant $c > 0$ in the estimate (4.5.25).[139]

Inspired by (4.5.46), a naïve approach to obtain a small value of the quadratic form $\langle \mathcal{L}f, f\rangle_H$ is to insert the minimiser $f \in \mathrm{D}(\mathcal{T}) \cap \mathcal{H}$ of the variational problem from Lemma 4.5.14. Unfortunately, this strategy does not seem to be very helpful because the minimiser f is not known explicitly and because f is not necessarily a minimiser of $\inf_{g\in \mathrm{D}(\mathcal{T})\cap\mathcal{H}\setminus\{0\}} \frac{\|\mathcal{T}g\|_H^2}{\|g\|_H^2}$, cf. Remark 4.3.29.

A more promising approach to estimate $\inf(\sigma(\mathcal{L}))$ is to insert a function into the quadratic form for which the linearised operator can be easily computed. The following lemma gives an example of such a function. It is based on [85, Ex. 2.1]; related arguments are also used in the proof of Lemma 4.5.6.

Lemma 4.5.17. *Consider the spherically symmetric a.e. function* $f\colon \Omega_0 \to \mathbb{R}$ *defined via*

$$f(r, w, L) \coloneqq |\varphi'(E, L)|\, rw, \qquad \text{a.e. } (r, w, L) \in \Omega_0. \tag{4.5.49}$$

Then $f \in \mathrm{D}(\mathcal{L})$ *with*

$$\mathcal{L}f(r, w, L) = \frac{U_0'(r)}{r}\, f(r, w, L), \qquad \text{a.e. } (r, w, L) \in \Omega_0. \tag{4.5.50}$$

[137] Since the spectrum of an operator is always closed and $\mathcal{L} \geq 0$ by Corollary 4.5.9, there actually holds $\inf(\sigma(\mathcal{L})) = \min(\sigma(\mathcal{L}))$.

[138] $\mathcal{L}$ possessing *an* eigenvalue in $\mathcal{G}$ always means that $\mathcal{L}$ possesses *at least one* eigenvalue in $\mathcal{G}$.

[139] The infimum (4.5.47) indeed defines the best constant in (4.5.25) because, by the approximation result from Lemma 4.3.31, $\inf\limits_{\substack{f\in \mathrm{D}(\mathcal{T})\cap\mathcal{H}\\ f\neq 0}} \frac{\langle \mathcal{L}f, f\rangle_H}{\|f\|_H^2} = \inf\limits_{\substack{f\in C^\infty_{c,r}(\Omega_0)\cap\mathcal{H}\\ f\neq 0}} \frac{\langle \mathcal{L}f, f\rangle_H}{\|f\|_H^2} = \inf\limits_{\substack{f\in \mathrm{D}(\mathcal{L})\\ f\neq 0}} \frac{\langle \mathcal{L}f, f\rangle_H}{\|f\|_H^2}$.

Proof. By Lemma 4.1.3, there obviously holds $f \in \mathcal{H}$. Lemma 4.1.2 yields

$$\mathcal{R}f(r,w,L) = 4\pi|\varphi'(E,L)|\, rw\, j_{w\,|\varphi'|}(r) = 4\pi\rho_0(r)\, f(r,w,L), \qquad \text{a.e. } (r,w,L) \in \Omega_0. \tag{4.5.51}$$

Furthermore, $\mathcal{T}^2 f = |\varphi'(E,L)|\, \mathcal{T}^2(rw)$ by Lemma 4.3.10, which implies $f \in \mathrm{D}(\mathcal{T}^2)$ by a similar discussion as in Remark 4.2.6 (b). Recalling the calculation (4.5.20) from the proof of Lemma 4.5.6, we thus deduce

$$\mathcal{T}^2 f(r,w,L) = -\left(4\pi\rho_0(r) + \frac{U_0'(r)}{r}\right) f(r,w,L), \qquad \text{a.e. } (r,w,L) \in \Omega_0. \tag{4.5.52}$$

Combining (4.5.51) and (4.5.52) then shows (4.5.50). □

Remark 4.5.18. *The above lemma shows that* (4.5.49) *would define an eigenfunction of* $\mathcal{L}$ *if* $\frac{U_0'(r)}{r}$ *were constant on the steady state support. This is the case for the* Kurth steady state *introduced in [90], see also [62, Sc. 6.1], [87], and [143, Sc. 1.3] for further analyses. This steady state has been developed so that a suitable rescaling of it leads to an oscillatory solution (on the non-linearised level). However, the Kurth steady state does not satisfy the assumptions (φ1)–(φ5) imposed here; it is rather irregular at the boundary of its phase space support.*

Inserting the function from the above lemma into the quadratic form of $\mathcal{L}$, along with Lemma 4.5.16, yields a criterion for the existence of an eigenvalue of $\mathcal{L}$ into the essential gap $\mathcal{G}$. This observation is due to [85, Cor. 2.2], which is why we refer to the following result as *Kunze's criterion.*

Lemma 4.5.19 (Kunze's Criterion for the Existence of Eigenvalues)**.** *If*

$$\sup_{r\in]R_{\min},R_{\max}]} \frac{U_0'(r)}{r} < \frac{4\pi^2}{\sup^2_{\mathbb{D}_0}(T)}, \tag{4.5.53}$$

the linearised operator $\mathcal{L}\colon \mathrm{D}(\mathcal{L}) \to \mathcal{H}$ *possesses an eigenvalue inside the essential gap* $\mathcal{G}$.[140]

In the case of an isotropic steady state, i.e., $L_0 = 0 = \ell$*, the supremum on the left-hand side of* (4.5.53) *is explicitly given by*

$$\sup_{r\in]R_{\min},R_{\max}]} \frac{U_0'(r)}{r} = \frac{4\pi}{3}\,\rho_0(0), \tag{4.5.54}$$

recall Remark 2.2.10 (a) for an explicit representation of $\rho_0(0)$*.*

Proof. Let $f \in \mathrm{D}(\mathcal{L})$ be defined via (4.5.49). By (4.5.47) and (4.5.50) we obtain

$$\inf(\sigma(\mathcal{L})) \le \frac{\langle \mathcal{L}f, f\rangle_H}{\|f\|_H^2} = \frac{1}{\|f\|_H^2}\int_{\Omega_0} \frac{1}{|\varphi'(E,L)|}\,\frac{U_0'(r)}{r}\, f(x,v)^2\,\mathrm{d}(x,v) \le \sup_{r\in]R_{\min},R_{\max}]} \frac{U_0'(r)}{r}. \tag{4.5.55}$$

Lemma 4.5.16 thus yields the claimed criterion for the existence of eigenvalues of $\mathcal{L}$.

The identity (4.5.54) in the case of an isotropic steady state is due to the fact that $]0,\infty[\ni r \mapsto \frac{U_0'(r)}{r}$ is non-increasing – which follows by the calculation (4.5.28), see also [85, Lemma A.6 (a)] – and because of $\lim_{r\to 0}\frac{U_0'(r)}{r} = \frac{4\pi}{3}\,\rho_0(0)$, cf. (4.5.24). □

[140] It seems tempting to use the explicit bound on $\sup^2_{\mathbb{D}_0}(T)$ from Lemma 4.5.13 to estimate the right-hand side of (4.5.53) in the case of an isotropic steady state and thus arrive at a more explicit criterion which does not require knowledge on the period function. However, since $\frac{M_0}{R_{\max}^3} = \frac{U_0'(R_{\max})}{R_{\max}}$, the bound from Lemma 4.5.13 is not helpful for this purpose.

In Section 8.2, we will numerically check this criterion and see that it is indeed satisfied for some steady state, cf. Observations 8.2.11 and 8.2.12. The strength of the criterion from Lemma 4.5.19 is that it is rather easy to check, since only the gravitational potential of the steady state and the (maximum of the) period function need to be known. However, given that we used several estimates to derive the criterion, we cannot expect it to be particularly sharp. This is meant in the sense that we cannot expect the criterion to be satisfied in every situation in which there exists an eigenvalue of $\mathcal{L}$ inside $\mathcal{G}$.

For this reason, we will develop an additional, sharp criterion for the existence of eigenvalues of the linearised operator $\mathcal{L}$ inside the essential gap $\mathcal{G}$ in Chapter 5.

Chapter 5

The Birman-Schwinger-Mathur Principle

In this chapter we derive a sharp criterion for the existence of eigenvalues of the linearised operator $\mathcal{L}\colon \mathrm{D}(\mathcal{L}) \to \mathcal{H}$ in the essential gap $\mathcal{G}$; recall Section 4.2 for the definition of the operator and the function spaces and recall (1.2.21) for the definition of $\mathcal{G}$. Throughout this chapter, we assume that the underlying steady state f_0 satisfies the conditions (φ1)–(φ5) stated in Sections 2.2 and 4.1.

As discussed in the introduction, our approach is motivated by the classical Birman-Schwinger principle used to characterise negative eigenvalues of Schrödinger operators, see, e.g., [99, Sc. 4.3]. It was first observed by Mathur [111] that similar techniques are also useful in the context of the linearised Vlasov-Poisson system. In addition, Mathur showed that all relevant information contained in the Birman-Schwinger operator are also contained in a reduced operator. Extensions of this method were then developed in [62, 85] for the linearised Vlasov-Poisson system, in [49] for the linearised Einstein-Vlasov system, and in [61] for a slightly modified version of the linearised Vlasov-Poisson system. Here, we follow [62, Sc. 8] and [49, Sc. 6]. More precisely, the general concepts are based on [62], but we include several improvements developed in [49]. For instance, we derive a quantitative bound on the number of eigenvalues of $\mathcal{L}$ in $\mathcal{G}$ which is not included in [62]. The connections between our results and the ones from [85, Ch. 4] will be discussed in Remark 5.2.16.

We begin by adapting the Birman-Schwinger principle to our specific situation in Section 5.1, followed by the application of Mathur's reduction method in Section 5.2. The resulting criteria for the existence of eigenvalues of $\mathcal{L}$ in $\mathcal{G}$ are then collected in Section 5.3. Lastly, in Section 5.4, we discuss first applications of these criteria.

5.1 A Birman-Schwinger Principle

The aim of this section is to develop a Birman-Schwinger principle for the linearised operator $\mathcal{L}$. Our strategy is inspired by [98, Step 1 in Proof of Thm. 12.4].

As a preparation, we first consider the following auxiliary family of operators. The definition is based on [49, Def. 6.1]; the same operators also appear in [62, Sc. 8.1].

Definition 5.1.1 (The Operators $\mathcal{L}_\gamma$)**.** *For $\gamma > 0$ let*

$$\mathcal{L}_\gamma \coloneqq -\mathcal{T}^2 - \frac{1}{\gamma}\mathcal{R}\colon \mathrm{D}(\mathcal{L}) \to \mathcal{H}. \tag{5.1.1}$$

The parameter $\gamma > 0$ controls the weight of the gravitational response term in $\mathcal{L}_\gamma$: The smaller $\gamma > 0$, the stronger the gravitational response term is weighted. In the case $\gamma = 1$ we recover the linearised operator, i.e.,

$$\mathcal{L}_1 = \mathcal{L}. \tag{5.1.2}$$

5.1.1 Analysis of the Operators $\mathcal{L}_\gamma$

The first part of Section 5.1 is devoted to an analysis of the functional analytic and spectral properties of the operators $\mathcal{L}_\gamma$ introduced in Definition 5.1.1. This is based on [49, Sc. 6.1]. The reasons why it is useful to analyse these operators will become apparent at the close of this section, cf. Remark 5.1.10.

We first show that the operators $\mathcal{L}_\gamma$ are self-adjoint and that their essential spectra do not dependent on γ. This is due to the reason that the essential spectrum is determined by the transport part $-\mathcal{T}^2\big|_{\mathcal{H}}$, which carries no γ-weight. The lemma is based on [49, Lemma 6.2].

Lemma 5.1.2. *For $\gamma > 0$, the operator $\mathcal{L}_\gamma \colon \mathrm{D}(\mathcal{L}) \to \mathcal{H}$ is self-adjoint as a densely defined operator on $\mathcal{H}$. Its essential spectrum is given by*

$$\sigma_{\mathrm{ess}}(\mathcal{L}_\gamma) = \sigma_{\mathrm{ess}}(\mathcal{L}) = \sigma(-\mathcal{T}^2\big|_{\mathcal{H}}); \tag{5.1.3}$$

the latter set is explicitly determined in Proposition 4.3.19.

Proof. The claims follow by the same arguments as the respective statements for $\mathcal{L}$ in Sections 4.5.1 and 4.5.2 because $-\mathcal{T}^2\big|_{\mathcal{H}}$ is self-adjoint by Proposition 4.3.17 and $\mathcal{R}$ is bounded and symmetric by Lemma 4.4.2 as well as relatively $(\mathcal{T}^2\big|_{\mathcal{H}})$-compact by Lemma 4.5.3. □

In particular, the above lemma shows $\inf(\sigma_{\mathrm{ess}}(\mathcal{L}_\gamma)) = \inf(\sigma_{\mathrm{ess}}(\mathcal{L})) > 0$ and that the essential gap $\mathcal{G}$ is disjoint with $\sigma_{\mathrm{ess}}(\mathcal{L}_\gamma)$ for $\gamma > 0$.

Although the essential spectrum of $\mathcal{L}_\gamma$ is independent of $\gamma > 0$, the entire spectrum of $\mathcal{L}_\gamma$ does depend on γ. We have already noted this in Remark 4.5.15, where we have seen that the non-negativity of $\mathcal{L}_\gamma$, i.e., $\sigma(\mathcal{L}_\gamma) \subset [0, \infty[$, is equivalent to $\gamma \geq 1 - \tilde{\lambda}$. In order to characterise the elements of $\sigma(\mathcal{L}_\gamma) \setminus \sigma_{\mathrm{ess}}(\mathcal{L}_\gamma)$ inside the essential gap $\mathcal{G}$, we extend the variational principle from Lemma 4.5.16. A similar statement can be found in [49, Def. & Prop. 6.4].

Definition & Lemma 5.1.3 (The Values $\mu_n(\gamma)$)**.** *For $\gamma > 0$ and $n \in \mathbb{N}$ let*[141,142]

$$\mu_n(\gamma) \coloneqq \sup_{g_1,\dots,g_{n-1} \in \mathcal{H}} \left(\inf_{\substack{h \in \mathrm{D}(\mathcal{L}),\, \|h\|_H = 1, \\ h \perp g_1,\dots,g_{n-1}}} \langle \mathcal{L}_\gamma h, h \rangle_H \right). \tag{5.1.4}$$

Then $\mu_n(\gamma)$ is finite, and either

(i) $\mu_n(\gamma) < \inf(\sigma(-\mathcal{T}^2|_{\mathcal{H}}))$. In this case there exist at least n eigenvalues (counting multiplicities) of $\mathcal{L}_\gamma$ below $\inf(\sigma(-\mathcal{T}^2|_{\mathcal{H}}))$, and $\mu_n(\gamma)$ is the n-th smallest eigenvalue (counting multiplicities) of $\mathcal{L}_\gamma$.

or

[141] As usual, the orthogonality in (5.1.4) is meant w.r.t. the inner product $\langle \cdot, \cdot \rangle_H$.

[142] In the case $n = 1$, the supremum in (5.1.4) is dropped and one takes the infimum over all $h \in \mathrm{D}(\mathcal{L})$ with $\|h\|_H = 1$. This notational convention is used throughout this section.

(ii) $\mu_n(\gamma) = \inf(\sigma(-\mathcal{T}^2|_{\mathcal{H}}))$. *In this case there exist at most* $n-1$ *eigenvalues (counting multiplicities) of* $\mathcal{L}_\gamma$ *below* $\inf(\sigma(-\mathcal{T}^2|_{\mathcal{H}}))$, *and* $\mu_{n+j}(\gamma) = \inf(\sigma(-\mathcal{T}^2|_{\mathcal{H}}))$ *for* $j \in \mathbb{N}$.

Proof. For $h \in \mathrm{D}(\mathcal{L})$ with $\|h\|_H = 1$ there holds

$$\langle \mathcal{L}_\gamma h, h\rangle_H = \|\mathcal{T}h\|_H^2 - \frac{1}{\gamma}\langle \mathcal{R}h, h\rangle_H \geq -\frac{\|\mathcal{R}\|_{H\to H}}{\gamma} \tag{5.1.5}$$

by the skew-symmetry of the transport operator, cf. Proposition 4.3.15. Here, $\|\mathcal{R}\|_{H\to H}$ denotes the operator norm of $\mathcal{R}\colon H \to H$, which is finite by Lemma 4.4.2. This shows that the operator $\mathcal{L}_\gamma$ is bounded from below. Then the statement is just the min-max principle for semi-bounded, self-adjoint operators, see [134, Thm. XIII.1] or [160, Prop. II.32]. □

In the above statement – and everywhere else in this thesis – the multiplicity of an eigenvalue λ of $\mathcal{L}_\gamma$ refers to the dimension of the associated eigenspace $\ker(\mathcal{L}_\gamma - \lambda\,\mathrm{id}) = \{f \in \mathrm{D}(\mathcal{L}) \mid \mathcal{L}_\gamma f = \lambda f\}$. In general, this dimension can be infinite. In the case $\lambda \notin \sigma_{\mathrm{ess}}(\mathcal{L}_\gamma)$, the eigenspace is finite dimensional by the definition of the essential spectrum.

Our aim is to analyse the properties of the mappings $]0,\infty[\ni \gamma \mapsto \mu_n(\gamma)$ for $n \in \mathbb{N}$ as thoroughly as possible. The following lemma is a regularity statement for these mappings. It is based on [49, Lemma 6.6], which is in turn inspired by [134, XIII Problem 2] and [160, Thm. II.33].

Lemma 5.1.4. *For fixed* $n \in \mathbb{N}$, *the mapping* $]0,\infty[\ni \gamma \mapsto \mu_n(\gamma)$ *is non-decreasing and*

$$|\mu_n(\gamma) - \mu_n(\beta)| \leq \left|\frac{1}{\gamma} - \frac{1}{\beta}\right| \|\mathcal{R}\|_{H\to H}, \qquad \gamma, \beta > 0. \tag{5.1.6}$$

In particular, $]0,\infty[\ni \gamma \mapsto \mu_n(\gamma)$ *is continuous.*

Proof. For $\gamma > 0$ and $h \in \mathrm{D}(\mathcal{L})$ with $\|h\|_H = 1$ let

$$f_h(\gamma) \coloneqq \langle \mathcal{L}_\gamma h, h\rangle_H, \qquad \gamma > 0. \tag{5.1.7}$$

We first prove the claimed properties for f_h instead of μ_n. For $0 < \gamma < \beta$, the non-negativity of $\mathcal{R}$, cf. Lemma 4.4.2, implies

$$f_h(\gamma) = \|\mathcal{T}h\|_H^2 - \frac{1}{\gamma}\langle \mathcal{R}h, h\rangle_H \leq \|\mathcal{T}h\|_H^2 - \frac{1}{\beta}\langle \mathcal{R}h, h\rangle_H = f_h(\beta). \tag{5.1.8}$$

Furthermore, by the Cauchy-Schwarz inequality,

$$|f_h(\gamma) - f_h(\beta)| = \left|\frac{1}{\gamma} - \frac{1}{\beta}\right| \langle \mathcal{R}h, h\rangle_H \leq \left|\frac{1}{\gamma} - \frac{1}{\beta}\right| \|\mathcal{R}\|_{H\to H} \tag{5.1.9}$$

for any $\gamma, \beta > 0$.

The next step is to show that the monotonicity (5.1.8) and the estimate (5.1.9) carry over from f_h to the sup-inf μ_n. For this purpose, let

$$I_\gamma(g_1, \ldots, g_{n-1}) \coloneqq \inf_{\substack{h \in \mathrm{D}(\mathcal{L}),\, \|h\|_H = 1,\\ h \perp g_1, \ldots, g_{n-1}}} f_h(\gamma) \tag{5.1.10}$$

for $\gamma > 0$ and $g_1, \ldots, g_{n-1} \in \mathcal{H}$. For fixed $g_1, \ldots, g_{n-1} \in \mathcal{H}$, $\gamma, \beta > 0$, and $h \in \mathrm{D}(\mathcal{L})$ with $\|h\|_H = 1$ and $h \perp g_1, \ldots g_{n-1}$, we obtain

$$I_\gamma(g_1, \ldots, g_{n-1}) \leq f_h(\gamma) \leq f_h(\beta) + \left|\frac{1}{\gamma} - \frac{1}{\beta}\right| \|\mathcal{R}\|_{H\to H} \tag{5.1.11}$$

by (5.1.9). Taking the infimum over all such h and switching the roles of γ and β hence yields

$$|I_\gamma(g_1,\dots,g_{n-1}) - I_\beta(g_1,\dots,g_{n-1})| \leq \left|\frac{1}{\gamma} - \frac{1}{\beta}\right| \|\mathcal{R}\|_{H\to H}. \tag{5.1.12}$$

For fixed $g_1,\dots,g_{n-1} \in \mathcal{H}$, this implies

$$\mu_n(\gamma) \geq I_\gamma(g_1,\dots,g_{n-1}) \geq I_\beta(g_1,\dots,g_{n-1}) - \left|\frac{1}{\gamma} - \frac{1}{\beta}\right| \|\mathcal{R}\|_{H\to H} \tag{5.1.13}$$

for $\gamma,\beta > 0$. Taking the supremum over all $g_1,\dots,g_{n-1} \in \mathcal{H}$ thus yields

$$\mu_n(\beta) - \mu_n(\gamma) \leq \left|\frac{1}{\gamma} - \frac{1}{\beta}\right| \|\mathcal{R}\|_{H\to H}, \qquad \gamma,\beta > 0, \tag{5.1.14}$$

which shows (5.1.6) after switching the roles of γ and β.

Furthermore, (5.1.8) implies $I_\gamma(g_1,\dots,g_{n-1}) \leq I_\beta(g_1,\dots,g_{n-1})$ for $0 < \gamma < \beta$ and $g_1,\dots,g_{n-1} \in \mathcal{H}$. Taking the supremum over all $g_1,\dots,g_{n-1} \in \mathcal{H}$ yields the claimed monotonicity of μ_n. □

The monotonicity of μ_n corresponds to the fact that decreasing $\gamma > 0$ means that we assign more weight to the non-positive term $-\frac{1}{\gamma}\mathcal{R}$ in the operator $\mathcal{L}_\gamma$, which leads to the spectrum of $\mathcal{L}_\gamma$ to be shifted towards more negative values. In fact, the monotonicity from the previous lemma is even strict if μ_n departs from $\inf(\sigma(-\mathcal{T}^2|_{\mathcal{H}})) > 0$. The lemma is based on [49, Lemma 6.7], which is in turn inspired by [98, Proof of Thm. 12.1].

Lemma 5.1.5. *Fix $n \in \mathbb{N}$ and suppose that there exists $\gamma_0 > 0$ s.t. $\mu_n(\gamma_0) < \inf(\sigma(-\mathcal{T}^2|_{\mathcal{H}}))$. Then $]0,\gamma_0] \ni \gamma \mapsto \mu_n(\gamma)$ is strictly increasing.*

Proof. First observe that Lemmas 5.1.3 and 5.1.4 imply $\mu_i(\gamma) < \inf(\sigma(-\mathcal{T}^2|_{\mathcal{H}}))$ for $1 \leq i \leq n$ and $0 < \gamma \leq \gamma_0$. In particular, $\mu_i(\gamma)$ is an eigenvalue of $\mathcal{L}_\gamma$ for all such i and γ. Choosing orthonormal eigenfunctions to these eigenvalues of $\mathcal{L}_\gamma$, we deduce that for every $0 < \gamma \leq \gamma_0$ and $1 \leq i \leq n$ there exists $h_i^\gamma \in \mathrm{D}(\mathcal{L})$ s.t. $\mathcal{L}_\gamma h_i^\gamma = \mu_i(\gamma)\, h_i^\gamma$, $\|h_i^\gamma\|_H = 1$, and $h_j^\gamma \perp h_i^\gamma$ for $i \neq j \in \{1,\dots,n\}$.

Now fix $0 < \gamma < \beta \leq \gamma_0$ and let $c_1,\dots,c_n \in \mathbb{R}$ be s.t. $h^* \coloneqq \sum_{i=1}^n c_i h_i^\beta \in \mathrm{D}(\mathcal{L})$ satisfies $1 = \|h^*\|_H^2 = \sum_{i=1}^n c_i^2$ and $h^* \perp h_1^\gamma,\dots,h_{n-1}^\gamma$.[143] Then

$$\langle \mathcal{L}_\beta h^*, h^*\rangle_H = \sum_{i=1}^n c_i^2\, \mu_i(\beta) \leq \mu_n(\beta) \sum_{i=1}^n c_i^2 = \mu_n(\beta) < \inf(\sigma(-\mathcal{T}^2|_{\mathcal{H}})), \tag{5.1.15}$$

which implies $\langle \mathcal{R}h^*, h^*\rangle_H > 0$ since $\|\mathcal{T}h^*\|_H^2 \geq \inf(\sigma(-\mathcal{T}^2|_{\mathcal{H}}))$, recall Remark 4.3.29. Thus,

$$\langle \mathcal{L}_\gamma h^*, h^*\rangle_H = \|\mathcal{T}h^*\|_H^2 - \frac{1}{\gamma}\langle \mathcal{R}h^*, h^*\rangle_H < \|\mathcal{T}h^*\|_H^2 - \frac{1}{\beta}\langle \mathcal{R}h^*, h^*\rangle_H = \langle \mathcal{L}_\beta h^*, h^*\rangle_H. \tag{5.1.16}$$

The last step is to observe that the supremum in $\mu_n(\gamma)$, see Definition 5.1.3, is attained when choosing $g_1,\dots,g_{n-1} = h_1^\gamma,\dots,h_{n-1}^\gamma$. This is due to the fact that the spectrum of $\mathcal{L}_\gamma$ restricted to the orthogonal complement of $\mathrm{span}\{h_1^\gamma,\dots,h_{n-1}^\gamma\}$ is given by

[143] The existence of such $c_1,\dots,c_n \in \mathbb{R}$ can be obtained as follows: For $\tilde{h} = \sum_{i=1}^n c_i h_i^\beta$ with arbitrary $c = (c_1,\dots,c_n) \in \mathbb{R}^n$, $\tilde{h} \perp h_1^\gamma,\dots,h_{n-1}^\gamma$ is equivalent to $\sum_{i=1}^n c_i z_i = 0$, where $z_i \coloneqq (\langle h_i^\beta, h_1^\gamma\rangle_H,\dots,\langle h_i^\beta, h_{n-1}^\gamma\rangle_H) \in \mathbb{R}^{n-1}$ for $i = 1,\dots,n$. Since the n vectors $z_1,\dots,z_n \in \mathbb{R}^{n-1}$ have to be linearly dependent, we conclude the existence of c as claimed.

$\sigma(\mathcal{L}_\gamma\big|_{\mathrm{span}\{h_1^\gamma,\dots,h_{n-1}^\gamma\}^\perp}) = (\sigma(\mathcal{L}_\gamma)\setminus\{\mu_1(\gamma),\dots,\mu_{n-1}(\gamma)\})\cup\{\mu_n(\gamma)\}$, cf. [69, Prop. 6.6]. In particular, $\inf(\sigma(\mathcal{L}_\gamma\big|_{\mathrm{span}\{h_1^\gamma,\dots,h_{n-1}^\gamma\}^\perp})) = \mu_n(\gamma)$ and thus, by standard variational principles,[144] $\mu_n(\gamma) = \inf\{\langle\mathcal{L}_\gamma h,h\rangle_H \mid h\in\mathrm{D}(\mathcal{L})\cap\mathrm{span}\{h_1^\gamma,\dots,h_{n-1}^\gamma\}^\perp,\ \|h\|_H=1\}$.

Together with (5.1.15) and (5.1.16) we hence conclude

$$\mu_n(\gamma) = \inf_{\substack{h\in\mathrm{D}(\mathcal{L}),\ \|h\|_H=1,\\ h\perp h_1^\gamma,\dots,h_{n-1}^\gamma}} \langle\mathcal{L}_\gamma h,h\rangle_H \le \langle\mathcal{L}_\gamma h^*,h^*\rangle_H < \langle\mathcal{L}_\beta h^*,h^*\rangle_H \le \mu_n(\beta). \tag{5.1.17}$$

□

The above lemma shows that once the n-th eigenvalue of $\mathcal{L}_\gamma$ departs from the essential spectrum $\sigma_{\mathrm{ess}}(\mathcal{L}_\gamma) = \sigma(-\mathcal{T}^2\big|_{\mathcal{H}})$, the mapping μ_n is strictly monotone for smaller values of γ. However, for $n\ge 2$, we are not certain whether the n-th eigenvalue μ_n actually departs from the essential spectrum. For the first eigenvalue, it follows by Remark 4.5.15 that this is the case since

$$\mu_1(1-\tilde\lambda) = 0, \tag{5.1.18}$$

where $\tilde\lambda\in\,]0,1[$ is the infimum from Lemma 4.5.14. We even get the following limiting behaviour of μ_1, which is based on [49, Lemma 6.8].

Lemma 5.1.6. *It holds that* $\lim_{\gamma\searrow 0}\mu_1(\gamma) = -\infty$.

Proof. Since

$$\mu_1(\gamma) = \inf_{\substack{h\in\mathrm{D}(\mathcal{L}),\\ \|h\|_H=1}} \langle\mathcal{L}_\gamma h,h\rangle_H = \inf_{\substack{h\in\mathrm{D}(\mathcal{L}),\\ \|h\|_H=1}} \left(\|\mathcal{T}h\|_H^2 - \frac{1}{\gamma}\langle\mathcal{R}h,h\rangle_H\right) \tag{5.1.19}$$

for $\gamma>0$, we just choose some $\tilde h\in\mathrm{D}(\mathcal{L})$ with $\|\tilde h\|_H=1$ and[145] $\langle\mathcal{R}\tilde h,\tilde h\rangle_H>0$ to conclude

$$\mu_1(\gamma) \le \|\mathcal{T}\tilde h\|_H^2 - \frac{1}{\gamma}\langle\mathcal{R}\tilde h,\tilde h\rangle_H \to -\infty,\quad \gamma\to 0. \tag{5.1.20}$$

□

On the other hand, the limiting behaviour of all eigenvalues $\mu_n(\gamma)$ as γ tends to infinity is rather clear. This is based on [49, Lemma 6.9].

Lemma 5.1.7. *For every* $n\in\mathbb{N}$ *there holds* $\lim_{\gamma\to\infty}\mu_n(\gamma) = \inf(\sigma(-\mathcal{T}^2|_{\mathcal{H}})) > 0$.

Proof. First note that the limit $\lim_{\gamma\to\infty}\mu_n(\gamma)$ exists in $]-\infty,\inf(\sigma(-\mathcal{T}^2|_{\mathcal{H}}))]$ by Lemmas 5.1.3 and 5.1.4. The claim then follows by the observation that for any $\gamma>0$ and $h\in\mathrm{D}(\mathcal{L})$ with $\|h\|_H=1$ there holds the estimate

$$\langle\mathcal{L}_\gamma h,h\rangle_H = \|\mathcal{T}h\|_H^2 - \frac{1}{\gamma}\langle\mathcal{R}h,h\rangle_H \ge \inf(\sigma(-\mathcal{T}^2|_{\mathcal{H}})) - \frac{\|\mathcal{R}\|_{H\to H}}{\gamma}, \tag{5.1.21}$$

where we used the variational identity $\inf(\sigma(-\mathcal{T}^2|_{\mathcal{H}})) = \inf_{g\in\mathrm{D}(\mathcal{L})\setminus\{0\}}\frac{\|\mathcal{T}g\|_H^2}{\|g\|_H^2}$ once again. □

The monotonicity of $\mu_n(\gamma)$ in n and γ allows us to translate the number of eigenvalues of $\mathcal{L}=\mathcal{L}_1$ below some prescribed $\lambda<\inf(\sigma(-\mathcal{T}^2|_{\mathcal{H}}))$ into the position of the zeros of the mappings $]0,\infty[\ \ni\ \gamma\mapsto\mu_n(\gamma)-\lambda$ for $n\in\mathbb{N}$. For this purpose, we define the following quantities similar to [49, Def. & Rem. 6.10].

[144] In particular, $\mathcal{L}_\gamma\big|_{\mathrm{span}\{h_1^\gamma,\dots,h_{n-1}^\gamma\}^\perp}\colon \mathrm{D}(\mathcal{L})\cap\mathrm{span}\{h_1^\gamma,\dots,h_{n-1}^\gamma\}^\perp\to\mathrm{span}\{h_1^\gamma,\dots,h_{n-1}^\gamma\}^\perp$ is self-adjoint. This can be verified by using similar arguments as in [69, Lemma 7.3].

[145] $\langle\mathcal{R}h,h\rangle_H>0$ follows if $j_h\not\equiv 0$ a.e., recall (4.4.8).

Definition & Lemma 5.1.8 (The Values $\gamma_n(\lambda)$)**.** *For $n \in \mathbb{N}$ and $\lambda < \inf(\sigma(-\mathcal{T}^2|_{\mathcal{H}}))$ we define $\gamma_n(\lambda) \in [0, \infty[$ as follows:*

(i) If $\mu_n(\gamma) > \lambda$ for every $\gamma > 0$, let $\gamma_n(\lambda) \coloneqq 0$.

(ii) Otherwise, define $\gamma_n(\lambda) > 0$ via $\mu_n(\gamma_n(\lambda)) = \lambda$.

Then $\gamma_n(\lambda)$ is well-defined. In the case (ii), λ is an eigenvalue of $\mathcal{L}_{\gamma_n(\lambda)}$. In addition, $\gamma_{n+1}(\lambda) \leq \gamma_n(\lambda)$ for $n \in \mathbb{N}$.

Proof. Lemmas 5.1.4, 5.1.5, and 5.1.7 show that (i) and (ii) uniquely define $\gamma_n(\lambda) \geq 0$. The additional claims follow by Lemma 5.1.3. □

The properties of $\mu_n(\lambda)$ from Lemmas 5.1.3–5.1.7 as well as the definition of $\gamma_n(\lambda)$ are illustrated in Figure 5.1.1.

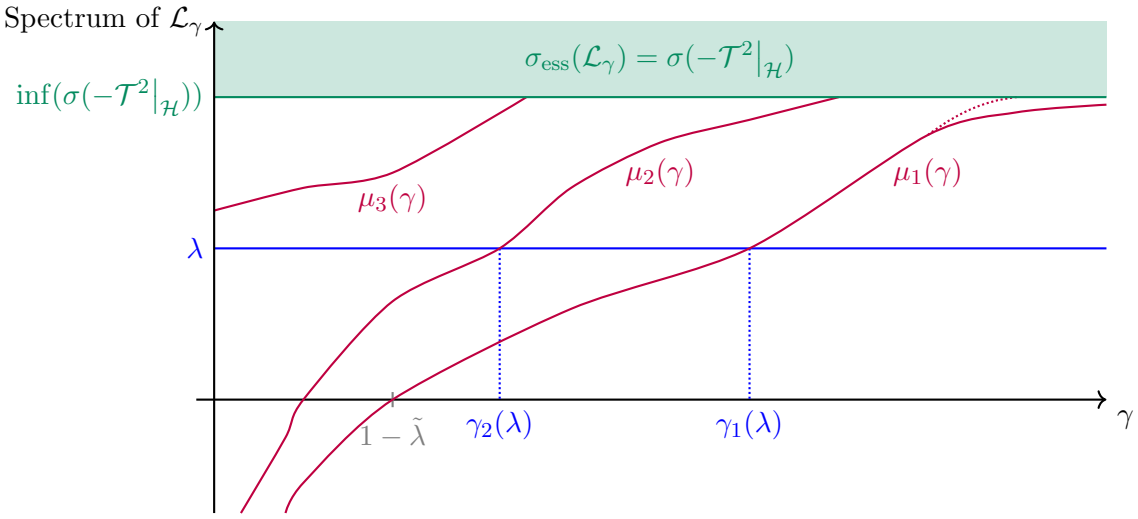

Figure 5.1.1: Possible behaviour of $\mu_n(\gamma)$ and the definition of $\gamma_n(\lambda)$. The dotted curve departing from $\mu_1(\gamma)$ illustrates that it is possible that $\mu_1(\gamma_0) = \inf(\sigma(-\mathcal{T}^2|_{\mathcal{H}}))$ for some $\gamma_0 > 0$.

An interpretation of the values $\gamma_n(\lambda)$ will be discussed in Remark 5.1.16.

As motivated before, the positions of $\gamma_n(\lambda)$ reveal the number of eigenvalues of the linearised operator $\mathcal{L} = \mathcal{L}_1$ below $\lambda < \inf(\sigma(-\mathcal{T}^2|_{\mathcal{H}}))$. This is the key result regarding the operators $\mathcal{L}_\gamma$. It is based on [49, Prop. 6.11].

Lemma 5.1.9. *For $\lambda < \inf(\sigma(-\mathcal{T}^2|_{\mathcal{H}}))$ the following identities hold:*

$$\#\{\textit{eigenvalues} < \lambda \textit{ of } \mathcal{L} \textit{ (counting multiplicities)}\} = \#\{n \in \mathbb{N} \mid \gamma_n(\lambda) > 1\}, \tag{5.1.22}$$

$$\#\{\textit{eigenvalues} \leq \lambda \textit{ of } \mathcal{L} \textit{ (counting multiplicities)}\} = \#\{n \in \mathbb{N} \mid \gamma_n(\lambda) \geq 1\}. \tag{5.1.23}$$

When referring to both (5.1.22) *and* (5.1.23)*, we write*

$$\#\{\textit{eigenvalues} \leqq \lambda \textit{ of } \mathcal{L} \textit{ (counting multiplicities)}\} = \#\{n \in \mathbb{N} \mid \gamma_n(\lambda) \geqq 1\}. \tag{5.1.24}$$

Proof. By Lemma 5.1.3,

$$\#\{\text{eigenvalues} \leqq \lambda \text{ of } \mathcal{L} \text{ (counting multiplicities)}\} = \#\{n \in \mathbb{N} \mid \mu_n(1) \leqq \lambda\}. \tag{5.1.25}$$

Since $\mu_n(1) \leqq \lambda$ for some $n \in \mathbb{N}$ is equivalent to $\gamma_n(\lambda) \geqq 1$ by the above lemmas, we thus conclude (5.1.24). □

We note that the number of eigenvalues $\leq \lambda$ of the linearised operator $\mathcal{L}$ (counting multiplicities) is finite for $\lambda < \inf(\sigma(-\mathcal{T}^2|_{\mathcal{H}}))$ because $\mathcal{L} \geq 0$ by Corollary 4.5.9 and $\inf(\sigma_{\mathrm{ess}}(\mathcal{L})) = \inf(\sigma(-\mathcal{T}^2|_{\mathcal{H}})) > \lambda$.

To conclude the analysis of the operators $\mathcal{L}_\gamma$, let us explain our motivation for conducting this analysis.

Remark 5.1.10. *The lemma above shows that the properties of $\mathcal{L}_\gamma$ – in particular, the properties of the eigenvalues $\mu_n(\gamma)$ – allow us to characterise the amount of eigenvalues of $\mathcal{L}$ below some $\lambda < \inf(\sigma(-\mathcal{T}^2|_{\mathcal{H}}))$. We will further develop this result to arrive at a characterisation of the amount of eigenvalues of $\mathcal{L}$ in the essential gap $\mathcal{G}$. If one is not interested in the precise number of eigenvalues of $\mathcal{L}$ in $\mathcal{G}$, but only in whether $\mathcal{L}$ possesses an eigenvalue in $\mathcal{G}$ or not, such a detailed analysis of $\mathcal{L}_\gamma$ is not necessary. This is why such an analysis is not included in [62].*

5.1.2 The Birman-Schwinger Operator

Armed with the tools collected in Section 5.1.1, we are now in the position to establish a connection between the spectra of the linearised operator $\mathcal{L}$ and the following operator. We will comment on the definition afterwards.

Definition 5.1.11 (The Birman-Schwinger Operator Q_λ)**.** *For $\lambda < \inf(\sigma(-\mathcal{T}^2|_{\mathcal{H}}))$ let*

$$Q_\lambda \coloneqq \sqrt{\mathcal{R}}\left(-\mathcal{T}^2|_{\mathcal{H}} - \lambda\right)^{-1}\sqrt{\mathcal{R}}\colon \mathcal{H} \to \mathcal{H}, \tag{5.1.26}$$

recall Lemma 4.4.4 for the definition of $\sqrt{\mathcal{R}}$. This operator is called the Birman-Schwinger operator *associated to $\mathcal{L}$ with parameter λ.*

Remark 5.1.12. *The form of the Birman-Schwinger operator Q_λ in Definition 5.1.11 differs from the ones in [62, Eqn. (8.1)] and [111, Eqn. (3.3)]. In our notation, the Birman-Schwinger operator in [62, 111] is $\mathcal{R}\left(-\mathcal{T}^2|_{\mathcal{H}} - \lambda\right)^{-1}\colon \mathcal{H} \to \mathcal{H}$. The definition* (5.1.26) *is based on [49, Def. 6.12], see also [61, Eqn. (5.1)] for an adaption in the context of a linearised Vlasov-Poisson system. As discussed in the introduction, the use of the square root operator $\sqrt{\mathcal{R}}$ is motivated by the analysis of Schrödinger operators. In this way, the operator Q_λ is symmetric, cf. Lemma 5.1.15, which is not the case in [62, 111]. This property will simplify the analysis later on, see Remark 5.2.9.*

Before studying the properties of Q_λ, we derive the connection between the eigenvalues of $\mathcal{L}_\gamma$ and Q_λ. This is based on [49, Prop. 6.13] and [61, Lemma 5.1].

Proposition 5.1.13 (A Birman-Schwinger Principle)**.** *Let $\gamma > 0$ and $\lambda < \inf(\sigma(-\mathcal{T}^2|_{\mathcal{H}}))$. Then λ is an eigenvalue of $\mathcal{L}_\gamma$ if and only if γ is an eigenvalue of Q_λ. In this case, the multiplicities of these eigenvalues are equal and the associated eigenfunctions can be transformed explicitly into one another:*

(a) If $f \in \mathrm{D}(\mathcal{L})$ is an eigenfunction of $\mathcal{L}_\gamma$ to the eigenvalue λ,

$$g \coloneqq \sqrt{\mathcal{R}}\, f \in \mathcal{H} \tag{5.1.27}$$

is an eigenfunction of Q_λ to the eigenvalue γ.

(b) If $g \in \mathcal{H}$ is an eigenfunction of Q_λ to the eigenvalue γ,

$$f \coloneqq \left(-\mathcal{T}^2|_{\mathcal{H}} - \lambda\right)^{-1}\sqrt{\mathcal{R}}\, g \in \mathrm{D}(\mathcal{L}) \tag{5.1.28}$$

is an eigenfunction of $\mathcal{L}_\gamma$ to the eigenvalue λ.

Proof. If $f \in \mathrm{D}(\mathcal{L})$ is a solution of $\mathcal{L}_\gamma f = \lambda f$, there also holds $\gamma\left(-\mathcal{T}^2 - \lambda\right)f = \mathcal{R}f$. Applying $\sqrt{\mathcal{R}}\left(-\mathcal{T}^2|_{\mathcal{H}} - \lambda\right)^{-1}$ to this equation and writing $\mathcal{R} = \sqrt{\mathcal{R}}\sqrt{\mathcal{R}}$ yields

$$\gamma g = \gamma\sqrt{\mathcal{R}}f = Q_\lambda\sqrt{\mathcal{R}}f = Q_\lambda g, \tag{5.1.29}$$

where g is defined via (5.1.27).

Conversely, if $g \in \mathcal{H}$ solves the eigenvalue equation $Q_\lambda g = \gamma g$ and $f \in \mathrm{D}(\mathcal{L})$ is defined via (5.1.28), it follows that

$$\mathcal{L}_\gamma f - \lambda f = \left(-\mathcal{T}^2 - \lambda\right)f - \frac{1}{\gamma}\,\mathcal{R}f = \sqrt{\mathcal{R}}\,g - \frac{1}{\gamma}\,\sqrt{\mathcal{R}}\,Q_\lambda g = 0. \tag{5.1.30}$$

What remains to be proven is that linear independence of eigenfunctions is preserved by (5.1.27) and (5.1.28). In particular, this will show that $f = 0$ is equivalent to $g = 0$ under the transformation (5.1.27) or (5.1.28).

First, let $f_1, \dots, f_n \in \ker(\mathcal{L}_\gamma - \lambda)$ be linearly independent and define $g_i \coloneqq \sqrt{\mathcal{R}}\,f_i \in \mathcal{H}$ for $1 \leq i \leq n$. Suppose that there exist $c_1, \dots, c_n \in \mathbb{R}$ s.t. $0 = \sum_{i=1}^n c_i\,g_i = \sqrt{\mathcal{R}}(\sum_{i=1}^n c_i f_i)$. We then apply $\frac{1}{\gamma}\left(-\mathcal{T}^2 - \lambda\right)^{-1}\sqrt{\mathcal{R}}$ to the latter equation and use that $\mathcal{L}_\gamma f = \lambda f$ is equivalent to $\frac{1}{\gamma}\left(-\mathcal{T}^2 - \lambda\right)^{-1}\mathcal{R}f = f$ for some $f \in \mathrm{D}(\mathcal{L})$. This implies $0 = \sum_{i=1}^n c_i f_i$, and thus $c_1 = \ldots = c_n = 0$ since $f_1, \dots, f_n$ are linearly independent.

Conversely, for linearly independent $g_1, \dots, g_n \in \ker(Q_\lambda - \gamma)$ let $f_1, \dots, f_n \in \mathrm{D}(\mathcal{L})$ be given by $f_i \coloneqq \left(-\mathcal{T}^2|_{\mathcal{H}} - \lambda\right)^{-1}\sqrt{\mathcal{R}}\,g_i$ for $1 \leq i \leq n$. Suppose that there exist $c_1, \dots, c_n \in \mathbb{R}$ s.t. $0 = \sum_{i=1}^n c_i f_i = \left(-\mathcal{T}^2|_{\mathcal{H}} - \lambda\right)^{-1}\sqrt{\mathcal{R}}(\sum_{i=1}^n c_i\,g_i)$. Applying $\sqrt{\mathcal{R}}$ to this equation yields $0 = Q_\lambda(\sum_{i=1}^n c_i\,g_i) = \gamma\sum_{i=1}^n c_i\,g_i$, which shows $c_1 = \ldots = c_n = 0$. □

Together with the relation between the eigenvalues of $\mathcal{L}$ and the ones of $\mathcal{L}_\gamma$ established in Lemma 5.1.9, the above proposition yields the following quantitative relation between the spectra of the linearised operator $\mathcal{L}$ and the Birman-Schwinger operator Q_λ. It is based on [49, Prop. 6.14], see [61, Lemma 5.1] and [62, Lemma 8.2] for non-quantitative versions of this result.

Proposition 5.1.14 (Quantitative Relation Between the Eigenvalues of $\mathcal{L}$ and Q_λ)**.** *For $\lambda < \inf(\sigma(-\mathcal{T}^2|_{\mathcal{H}}))$ it holds that*

$$\begin{aligned}\#\{\textit{eigenvalues} \leq_{(=)} \lambda \textit{ of } \mathcal{L} \textit{ (counting multiplicities)}\} = \\ = \#\{\textit{eigenvalues} \geq_{(=)} 1 \textit{ of } Q_\lambda \textit{ (counting multiplicities)}\},\end{aligned} \tag{5.1.31}$$

where we use the same notational convention as in Lemma 5.1.9.

Proof. Using the notation introduced in Definition 5.1.3 and the properties of the eigenvalues of $\mathcal{L}_\gamma$ – in particular, Lemma 5.1.5 – together with Proposition 5.1.13 implies

$$\#\{n \in \mathbb{N} \mid \exists \gamma \geq_{(=)} 1\colon \mu_n(\gamma) = \lambda\} = \#\{\text{eigenvalues} \geq_{(=)} 1 \text{ of } Q_\lambda \text{ (counting multiplicities)}\}. \tag{5.1.32}$$

By Lemma 5.1.9, the number on the left-hand side equals the amount of eigenvalues $\leq_{(=)} \lambda$ of $\mathcal{L}$ counting multiplicities. □

At first glance, it may not be clear what benefit Proposition 5.1.14 provides us, since it merely transforms the original eigenvalue problem for $\mathcal{L}$ into another eigenvalue problem. The reason why the latter is more convenient to analyse is because the Birman-Schwinger operator Q_λ possesses nicer properties from a functional analytic perspective than the (unbounded) operator $\mathcal{L}$. We derive these properties of Q_λ in the following lemma. It is based on [49, Lemma 6.15], [61, Lemma 5.1], and [62, Lemma 8.3].

Lemma 5.1.15 (Properties of the Birman-Schwinger Operator)**.** *For $\lambda < \inf(\sigma(-\mathcal{T}^2|_{\mathcal{H}}))$ the operator $Q_\lambda \colon \mathcal{H} \to \mathcal{H}$ introduced in Definition 5.1.11 is linear, bounded, symmetric, non-negative, and compact.*

Proof. The proof relies on the properties of $-\mathcal{T}^2\big|_{\mathcal{H}}$ and $\sqrt{\mathcal{R}}$ established in Section 4.3 and Lemma 4.4.4: Q_λ is linear, bounded, and symmetric because $\left(-\mathcal{T}^2|_{\mathcal{H}} - \lambda\right)^{-1}$ and $\sqrt{\mathcal{R}}$ both have these properties; the symmetry of $\left(-\mathcal{T}^2|_{\mathcal{H}} - \lambda\right)^{-1}$ follows from the symmetry of $\mathcal{T}^2$, cf. Proposition 4.3.17, and

$$\begin{aligned}\langle f, \left(-\mathcal{T}^2|_{\mathcal{H}} - \lambda\right)^{-1} g\rangle_H &= \langle \left(-\mathcal{T}^2|_{\mathcal{H}} - \lambda\right)\left(-\mathcal{T}^2|_{\mathcal{H}} - \lambda\right)^{-1} f, \left(-\mathcal{T}^2|_{\mathcal{H}} - \lambda\right)^{-1} g\rangle_H = \\ &= \langle \left(-\mathcal{T}^2|_{\mathcal{H}} - \lambda\right)^{-1} f, g\rangle_H \end{aligned} \tag{5.1.33}$$

for $f, g \in \mathcal{H}$. In addition, $\sqrt{\mathcal{R}}$ being relatively $(\mathcal{T}^2\big|_{\mathcal{H}})$-compact by Lemma 4.5.3 means that $\sqrt{\mathcal{R}}\left(-\mathcal{T}^2|_{\mathcal{H}} - \lambda\right)^{-1}$ is a compact operator. Hence, since $\sqrt{\mathcal{R}}$ is bounded, Q_λ is compact as well. In order to show the non-negativity of Q_λ, first observe that $\left(-\mathcal{T}^2|_{\mathcal{H}} - \lambda\right) \geq 0$ implies $\left(-\mathcal{T}^2|_{\mathcal{H}} - \lambda\right)^{-1} \geq 0$, i.e.,

$$\langle \left(-\mathcal{T}^2|_{\mathcal{H}} - \lambda\right)^{-1} g, g\rangle_H \geq 0, \qquad g \in \mathcal{H}. \tag{5.1.34}$$

Inserting $g = \sqrt{\mathcal{R}}\, f$ for $f \in \mathcal{H}$ into (5.1.34) and using the symmetry of $\sqrt{\mathcal{R}}$ then implies $Q_\lambda \geq 0$. □

Furthermore, there is a connection between the quantities from Section 5.1.1 and the spectrum of the Birman-Schwinger operator:

Remark 5.1.16 (The Spectrum of the Birman-Schwinger Operator)**.** *For $\lambda < \inf(\sigma(-\mathcal{T}^2|_{\mathcal{H}}))$, Proposition 5.1.13 shows that the values $\gamma_n(\lambda) > 0$ introduced in Definition 5.1.8 are precisely the non-zero eigenvalues of Q_λ. Moreover, each value is repeated according to the multiplicity of the associated eigenvalue, i.e., if $\gamma > 0$ is an eigenvalue of Q_λ of multiplicity $j \in \mathbb{N}$, $\#\{n \in \mathbb{N} \mid \gamma_n(\lambda) = \gamma\} = j$. Using the properties of Q_λ from Lemma 5.1.15 further yields*

$$\sigma(Q_\lambda) \setminus \{0\} = \{\gamma_n(\lambda) \mid n \in \mathbb{N},\, \gamma_n(\lambda) > 0\}. \tag{5.1.35}$$

The usual variational principles[146] *hence provide the following variational characterisation of $\gamma_n(\lambda)$ for $n \in \mathbb{N}$:*[147]

$$\gamma_n(\lambda) = \inf_{g_1,\ldots,g_{n-1} \in \mathcal{H}} \left(\sup_{\substack{h \in \mathcal{H},\, \|h\|_H = 1, \\ h \perp g_1,\ldots,g_{n-1}}} \langle Q_\lambda h, h\rangle_H \right). \tag{5.1.36}$$

In addition to the properties of Q_λ for fixed λ proven above, we now derive the monotonicity of Q_λ in the parameter λ. This is inspired by [99, p. 77].

Lemma 5.1.17. *For $\mu \leq \lambda < \inf(\sigma(-\mathcal{T}^2|_{\mathcal{H}}))$ there holds*

$$Q_\mu \leq Q_\lambda \tag{5.1.37}$$

in the sense of operators.

[146] The characterisation (5.1.36) follows, e.g., by applying [134, Thm. XIII.1] to $-Q_\lambda$.
[147] The identity (5.1.36) also holds in the case $\gamma_n(\lambda) = 0$.

Proof. By the first resolvent identity [69, Prop. 1.6(2)] we obtain

$$Q_\lambda - Q_\mu = \sqrt{\mathcal{R}}\left[(\lambda-\mu)\left(-\mathcal{T}^2|_{\mathcal{H}}-\lambda\right)^{-1}\left(-\mathcal{T}^2|_{\mathcal{H}}-\mu\right)^{-1}\right]\sqrt{\mathcal{R}}. \tag{5.1.38}$$

We thus conclude (5.1.37) since every term on the right-hand side of (5.1.38) is non-negative. More precisely, $(-\mathcal{T}^2|_{\mathcal{H}}-\lambda)^{-1}(-\mathcal{T}^2|_{\mathcal{H}}-\mu)^{-1} \geq 0$ can be verified using (5.1.34) and the square root lemma [136, Thm. VI.9]. □

In particular, the above lemma shows that the eigenvalues of Q_λ are non-decreasing in λ, i.e., by Remark 5.1.16, $\gamma_n(\mu) \leq \gamma_n(\lambda)$ for $n \in \mathbb{N}$ and $\mu \leq \lambda < \inf(\sigma(-\mathcal{T}^2|_{\mathcal{H}}))$. This follows by the variational characterisation (5.1.36) of the eigenvalues. This observation is consistent with Proposition 5.1.14 since the left-hand side of (5.1.31) is evidently non-decreasing in λ.

5.2 Mathur's Reduction Method

In this section we use the specific structure of the Birman-Schwinger operator $Q_\lambda = \sqrt{\mathcal{R}}\left(-\mathcal{T}^2|_{\mathcal{H}}-\lambda\right)^{-1}\sqrt{\mathcal{R}}$ to limit the search of eigenvalues ≥ 1 of Q_λ to a reduced setting. This method goes back to Mathur [111, Sc. 3.2] and was then developed further in [49, 61, 62, 85]. We follow [49, Sc. 6.3] and [62, Sc. 8.1] here.

The reduction is based on the following simple observation which originates from [111, Sc. 3.1]; see also [49, Rem. 6.16], [61, Eqn. (5.4)], and [62, p. 672].

Remark 5.2.1. *Let $\lambda < \inf(\sigma(-\mathcal{T}^2|_{\mathcal{H}}))$. Then $\operatorname{im}(Q_\lambda) \subset \operatorname{im}(\sqrt{\mathcal{R}})$, which shows that any eigenfunction $f \in \mathcal{H}$ of Q_λ corresponding to a non-zero eigenvalue lies in $\operatorname{im}(\sqrt{\mathcal{R}})$.*

We next show that the range of $\sqrt{\mathcal{R}}$ – recall Lemma 4.4.4 for the properties of this operator – is the subspace of a function space which is isometric to $L^2([R_{\min}, R_{\max}])$. This is based on [49, p. 46f.], [61, p. 29], and [62, Lemma 8.4].

Lemma 5.2.2 (The Range of $\sqrt{\mathcal{R}}$)**.** *Any $f \in \operatorname{im}(\sqrt{\mathcal{R}})$ is of the form*

$$f(r,w,L) = |\varphi'(E,L)|\,\frac{w}{r\sqrt{\rho_0(r)}}\,F(r), \qquad \text{a.e. } (r,w,L) \in \Omega_0, \tag{5.2.1}$$

for some $F \in L^2([R_{\min}, R_{\max}])$. Moreover, for any $f\colon \Omega_0 \to \mathbb{R}$ spherically symmetric a.e. of the form (5.2.1) with $F\colon [R_{\min}, R_{\max}] \to \mathbb{R}$, there holds

$$f \in H \quad \Leftrightarrow \quad F \in L^2([R_{\min}, R_{\max}]). \tag{5.2.2}$$

If, in addition, $g \in H$ is of the form $g(r,w,L) = |\varphi'(E,L)|\,\frac{w}{r\sqrt{\rho_0(r)}}\,G(r)$ for a.e. $(r,w,L) \in \Omega_0$,

$$\langle f, g\rangle_H = 4\pi\,\langle F, G\rangle_{L^2([R_{\min},R_{\max}])}. \tag{5.2.3}$$

Proof. For $f\colon \Omega_0 \to \mathbb{R}$ of the form (5.2.1), Lemma 4.1.2 yields

$$\|f\|_H^2 = 4\pi^2 \int_{\Omega_0} |\varphi'(E,L)|\,\frac{w^2}{r^2\rho_0(r)}\,F(r)^2\,\mathrm{d}(r,w,L) = 4\pi \int_{R_{\min}}^{R_{\max}} F(r)^2\,\mathrm{d}r. \tag{5.2.4}$$

This shows (5.2.2), and a similar calculation also yields (5.2.3). Recalling the properties of $\sqrt{\mathcal{R}}$ established in Lemma 4.4.4, we further conclude that any $f \in \operatorname{im}(\sqrt{\mathcal{R}})$ is of the form (5.2.1) for some $F \in L^2([R_{\min}, R_{\max}])$. □

Remark 5.2.3. *The above lemma states*

$$\operatorname{im}(\sqrt{\mathcal{R}}) \subset \Big\{ f(r,w,L) = |\varphi'(E,L)| \, \frac{w}{r\sqrt{\rho_0(r)}} \, F(r) \mid F \in L^2([R_{\min}, R_{\max}]) \Big\}. \tag{5.2.5}$$

This inclusion is, in fact, strict. A sharp characterisation of the range of $\sqrt{\mathcal{R}}$ *is given by*

$$\operatorname{im}(\sqrt{\mathcal{R}}) = \Big\{ f(r,w,L) = |\varphi'(E,L)| \, \frac{w}{r\sqrt{\rho_0(r)}} \, F(r) \mid \frac{F}{\sqrt{\rho_0}} \in L^2([R_{\min}, R_{\max}]) \Big\}. \tag{5.2.6}$$

Notice that the smooth function ρ_0 *vanishes at* $r = R_{\max}$*, which is why the set on the right-hand side of* (5.2.6) *is a strict subset of the set on the right-hand side of* (5.2.5)*.*

The identity (5.2.6) *can be verified by refining the proof of Lemma 4.4.1. More precisely, for any* $f \in H$*, the Cauchy-Schwarz inequality and Lemma 4.1.2 yield*

$$\begin{aligned} \| \frac{r}{\sqrt{\rho_0}} \, j_f \|^2_{L^2([R_{\min},R_{\max}])} &= \int_{R_{\min}}^{R_{\max}} \frac{r^2}{\rho_0(r)} \Big(\frac{\pi}{r^2} \int_0^\infty \int_{\mathbb{R}} w \, f(r,w,L) \, \mathrm{d}w \, \mathrm{d}L \Big)^2 \mathrm{d}r \leq \\ &\leq \pi^2 \int_{R_{\min}}^{R_{\max}} \frac{1}{r^2 \rho_0(r)} \Big(\int_0^\infty \int_{\mathbb{R}} w^2 |\varphi'(E,L)| \, \mathrm{d}w \, \mathrm{d}L \Big) \Big(\int_0^\infty \int_{\mathbb{R}} \frac{f(r,w,L)^2}{|\varphi'(E,L)|} \, \mathrm{d}w \, \mathrm{d}L \Big) \mathrm{d}r = \\ &= \pi \int_{R_{\min}}^{R_{\max}} \int_0^\infty \int_{\mathbb{R}} \frac{1}{|\varphi'(E,L)|} f(r,w,L)^2 \, \mathrm{d}w \, \mathrm{d}L \, \mathrm{d}r = \frac{1}{4\pi} \, \|f\|_H^2 < \infty, \end{aligned} \tag{5.2.7}$$

where j_f *is given by* (4.2.22)*. This shows that* $\sqrt{\mathcal{R}} f$ *is contained in the set on the right-hand side of* (5.2.6)*. Conversely, for fixed* $F \colon [R_{\min}, R_{\max}] \to \mathbb{R}$ *with* $\frac{F}{\sqrt{\rho_0}} \in L^2([R_{\min}, R_{\max}])$ *consider the spherically symmetric a.e. function* $f \colon \Omega_0 \to \mathbb{R}$ *defined via* $f(r,w,L) = \frac{1}{2\sqrt{\pi}} \, |\varphi'(E,L)| \, \frac{w}{r\rho_0(r)} \, F(r)$ *for a.e.* $(r,w,L) \in \Omega_0$*. Then* $f \in H$ *by* (5.2.2) *and* $\sqrt{\mathcal{R}} f(r,w,L) = |\varphi'(E,L)| \, \frac{w}{r\sqrt{\rho_0(r)}} \, F(r)$ *for a.e.* $(r,w,L) \in \Omega_0$ *by Lemma 4.1.2.*

The above observations suggest the definition of the following "reduced" operator describing the effect of the Birman-Schwinger operator Q_λ on the "radial part" F of a function of the form (5.2.1). Similar definitions can be found in [49, Def. 6.17], [61, Lemma 5.2], and [62, Def. 8.5].

Definition 5.2.4 (The Mathur Operator $\mathcal{M}_\lambda$)**.** *Let* $\lambda < \inf(\sigma(-\mathcal{T}^2|_{\mathcal{H}}))$*. For* $F \in L^2([R_{\min}, R_{\max}])$ *define* $f \in \mathcal{H}$ *via* (5.2.1)*. Since* $Q_\lambda f \in \operatorname{im}(\sqrt{\mathcal{R}})$ *by Remark 5.2.1, there exists a unique* $\mathcal{M}_\lambda F \in L^2([R_{\min}, R_{\max}])$ *s.t.*

$$Q_\lambda f(r,w,L) = |\varphi'(E,L)| \, \frac{w}{r\sqrt{\rho_0(r)}} \, \mathcal{M}_\lambda F(r), \qquad \text{a.e. } (r,w,L) \in \Omega_0, \tag{5.2.8}$$

cf. Lemma 5.2.2. The resulting mapping

$$\mathcal{M}_\lambda \colon L^2([R_{\min}, R_{\max}]) \to L^2([R_{\min}, R_{\max}]), \; F \mapsto \mathcal{M}_\lambda F \tag{5.2.9}$$

is called the Mathur operator *with parameter* λ*.*

As explained in the introduction, the Mathur operator is *reduced* in the sense that it acts on functions of one variable, compared to functions of three variables in the case of Q_λ.

As already indicated by Remark 5.2.1, non-zero eigenvalues of Q_λ and $\mathcal{M}_\lambda$ are equivalent to each other. This is shown in the following lemma which is based on [49, Lemma 6.18], [61, p. 31], and [62, Lemma 8.10(a)].

Lemma 5.2.5. *Let $\lambda < \inf(\sigma(-\mathcal{T}^2|_{\mathcal{H}}))$ and $\gamma \in \mathbb{R} \setminus \{0\}$. Then γ is an eigenvalue of Q_λ if and only if γ is an eigenvalue of $\mathcal{M}_\lambda$. In this case, the multiplicities of these eigenvalues are equal.*

Proof. Suppose that γ is an eigenvalue of Q_λ with multiplicity[148] $n \in \mathbb{N}$, which means that there exist orthogonal eigenfunctions $f_1, \dots, f_n \in \mathcal{H}$. By Remark 5.2.1, $f_i \in \mathrm{im}(\sqrt{\mathcal{R}})$ for $1 \leq i \leq n$, which, by Lemma 5.2.2, implies that there exist $F_1, \dots, F_n \in L^2([R_{\min}, R_{\max}])$ s.t.

$$f_i(r, w, L) = |\varphi'(E, L)| \frac{w}{r\sqrt{\rho_0(r)}} F_i(r), \qquad \text{a.e. } (r, w, L) \in \Omega_0, \tag{5.2.10}$$

for $1 \leq i \leq n$. By Definition 5.2.4, there holds $\mathcal{M}_\lambda F_i = \gamma F_i$ for $1 \leq i \leq n$. Moreover, by (5.2.3), the functions $F_1, \dots, F_n$ are non-trivial and pairwise orthogonal, which shows that the multiplicity of the eigenvalue γ of $\mathcal{M}_\lambda$ is at least n.

Conversely, suppose that γ is an eigenvalue of $\mathcal{M}_\lambda$ with multiplicity $m \in \mathbb{N} \cup \{\infty\}$ and let $(F_i)_{i=1,\dots,m}$ be a set of associated orthogonal eigenfunctions. Defining f_i for $1 \leq i \leq m$ via (5.2.10) then yields $f_i \in \mathcal{H}$ with $Q_\lambda f_i = \gamma f_i$. By (5.2.3), the functions $(f_i)_{i=1,\dots,m}$ are non-trivial and pairwise orthogonal, which shows that the multiplicity of the eigenvalue γ of Q_λ is at least m. □

A characterisation of the non-zero eigenvalues of the Birman-Schwinger operator Q_λ is provided in Remark 5.1.16. Together with the lemma above, we obtain the same characterisation for the eigenvalues of the Mathur operator $\mathcal{M}_\lambda$.

Remark 5.2.6. *For $\lambda < \inf(\sigma(-\mathcal{T}^2|_{\mathcal{H}}))$, the non-zero eigenvalues of the Mathur operator $\mathcal{M}_\lambda$ are given by the values $\gamma_n(\lambda) > 0$ introduced in Definition 5.1.8. Moreover, these values are sorted in descending order and each eigenvalue is repeated according to its (finite) multiplicity.*

Combining Proposition 5.1.14 and Lemma 5.2.5 yields the following relation between the spectra of the linearised operator $\mathcal{L}$ and the Mathur operator $\mathcal{M}_\lambda$. This is based on [49, p. 52], see also [61, Prop. 5.3] and [62, Thm. 8.11(a)] for non-quantitative versions.

Proposition 5.2.7 (Quantitative Relation Between the Eigenvalues of $\mathcal{L}$ and $\mathcal{M}_\lambda$)**.** *For $\lambda < \inf(\sigma(-\mathcal{T}^2|_{\mathcal{H}}))$ it holds that*

$$\begin{aligned}\#\{\textit{eigenvalues} \lesseqgtr \lambda \textit{ of } \mathcal{L} \textit{ (counting multiplicities)}\} = \\ = \#\{\textit{eigenvalues} \gtreqless 1 \textit{ of } \mathcal{M}_\lambda \textit{ (counting multiplicities)}\},\end{aligned} \tag{5.2.11}$$

where we use the same notational convention as in Lemma 5.1.9.

This result basically contains the desired criteria for the existence of eigenvalues of $\mathcal{L}$ in the essential gap $\mathcal{G}$. Before deriving these criteria in Section 5.3, we analyse the properties of the Mathur operator $\mathcal{M}_\lambda$. The first observation is that $\mathcal{M}_\lambda$ inherits the functional analytical properties of the Birman-Schwinger operator from Lemma 5.1.15. This is based on [49, Prop. 6.19], [61, Lemma 5.2], and [62, Lemma 8.8].

Lemma 5.2.8 (Properties of the Mathur Operator)**.** *For $\lambda < \inf(\sigma(-\mathcal{T}^2|_{\mathcal{H}}))$ the operator $\mathcal{M}_\lambda \colon L^2([R_{\min}, R_{\max}]) \to L^2([R_{\min}, R_{\max}])$ introduced in Definition 5.2.4 is linear, bounded, symmetric, non-negative, and compact.*

[148] Since Q_λ is compact by Lemma 5.1.15, the multiplicity of any non-zero eigenvalue of Q_λ is finite.

Proof. $\mathcal{M}_\lambda$ being linear, bounded, symmetric, and non-negative follows readily from the respective properties of Q_λ together with (5.2.3). For instance, for $F \in L^2([R_{\min}, R_{\max}])$,

$$\|\mathcal{M}_\lambda F\|^2_{L^2([R_{\min},R_{\max}])} = \frac{1}{4\pi} \|Q_\lambda f\|^2_H \leq C \|f\|^2_H = 4\pi C \|F\|^2_{L^2([R_{\min},R_{\max}])}, \tag{5.2.12}$$

with $f \in \mathcal{H}$ given by (5.2.1).

In order to see that $\mathcal{M}_\lambda$ is compact, let $(F_i)_{i\in\mathbb{N}} \subset L^2([R_{\min}, R_{\max}])$ be bounded. For $i \in \mathbb{N}$ define $f_i \in \mathcal{H}$ via (5.2.10). Then, by (5.2.3), $(f_i)_{i\in\mathbb{N}}$ is bounded in $\mathcal{H}$. Since Q_λ is compact, there exists a subsequence $(f_{i_j})_{j\in\mathbb{N}} \subset (f_i)_{i\in\mathbb{N}}$ s.t. $(Q_\lambda f_{i_j})_{j\in\mathbb{N}}$ is (strongly) convergent in $\mathcal{H}$. In particular, $(Q_\lambda f_{i_j})_{j\in\mathbb{N}}$ is a Cauchy sequence in $\mathcal{H}$. By (5.2.3) and (5.2.8), $(\mathcal{M}_\lambda F_{i_j})_{j\in\mathbb{N}}$ is thus a Cauchy sequence in $L^2([R_{\min}, R_{\max}])$, and hence (strongly) convergent in $L^2([R_{\min}, R_{\max}])$. □

Remark 5.2.9. *As discussed in Remark 5.1.12, the form of the Birman-Schwinger operator chosen in Definition 5.1.11 yields the symmetry of Q_λ. As seen above, this directly leads to the Mathur operator to be symmetric as well on the natural function space $L^2([R_{\min}, R_{\max}])$.*

In [62, 111], where Q_λ is non-symmetric, the symmetry of the associated Mathur operator instead has to be achieved by suitably modifying the function space.

In addition to the above properties of the Mathur operator $\mathcal{M}_\lambda$, in the light of Proposition 5.2.7, it is important to understand what the largest eigenvalue of $\mathcal{M}_\lambda$ is. This is analysed in the following lemma which is based on [49, p. 51], [61, p. 31], and [62, p. 680].[149]

Lemma 5.2.10. *Let $\lambda < \inf(\sigma(-\mathcal{T}^2|_{\mathcal{H}}))$. Then*

$$\sup(\sigma(\mathcal{M}_\lambda)) = \max(\sigma(\mathcal{M}_\lambda)) = \|\mathcal{M}_\lambda\|, \tag{5.2.13}$$

where $\|\cdot\|$ denotes the operator norm on $L^2([R_{\min}, R_{\max}])$ given by

$$\begin{aligned} \|\mathcal{M}_\lambda\| &= \sup\{\|\mathcal{M}_\lambda F\|_2 \mid F \in L^2([R_{\min}, R_{\max}]),\, \|F\|_2 = 1\} = \\ &= \sup\{\langle \mathcal{M}_\lambda F, F\rangle_2 \mid F \in L^2([R_{\min}, R_{\max}]),\, \|F\|_2 = 1\}. \end{aligned} \tag{5.2.14}$$

Proof. Since $\mathcal{M}_\lambda$ is bounded, symmetric, and non-negative by Lemma 5.2.8, the relation (5.2.13) follows by [136, Thm. VI.6]. Furthermore, by the usual variational principles, $\sup(\sigma(\mathcal{M}_\lambda))$ is given by the expression in the second line of (5.2.14), which proves the identity (5.2.14). □

The monotonicity of the Birman-Schwinger operator Q_λ in the parameter λ also carries over to the Mathur operator $\mathcal{M}_\lambda$.

Lemma 5.2.11. *For $\mu \leq \lambda < \inf(\sigma(-\mathcal{T}^2|_{\mathcal{H}}))$ there holds*

$$\mathcal{M}_\mu \leq \mathcal{M}_\lambda \tag{5.2.15}$$

in the sense of operators.

Proof. The assertion follows by Lemma 5.1.17 and (5.2.3). □

[149] The statement analogous to Lemma 5.2.10 is also true for the Birman-Schwinger operator instead of the Mathur operator.

We will see later that this monotonicity is, in fact, strict, cf. Lemma 5.2.15.

The most important property of the Mathur operator is that it is an integral operator with an explicit integral kernel. This was first observed in [111, Eqn. (3.19)]. The following result is based on [61, Lemma 5.2] and [62, Prop. 8.6]. Related, but more complicated calculations can be found in [49, Sc. 6.3.2].

Proposition 5.2.12 (Integral Representation of the Mathur Operator)**.** *For* $\lambda < \inf(\sigma(-\mathcal{T}^2|_{\mathcal{H}}))$ *and* $F \in L^2([R_{\min}, R_{\max}])$ *there holds*

$$\mathcal{M}_\lambda F(r) = \int_{R_{\min}}^{R_{\max}} K_\lambda(r,s)\, F(s)\, \mathrm{d}s, \qquad \text{a.e. } r \in [R_{\min}, R_{\max}], \tag{5.2.16}$$

with integral kernel $K_\lambda \in L^2([R_{\min}, R_{\max}]^2)$ *given by*[150]

$$K_\lambda(r,s) \coloneqq \frac{32\pi^2}{rs} \sum_{n=1}^{\infty} \int_{\mathbb{D}_0(r)\cap\mathbb{D}_0(s)} \frac{|\varphi'(E,L)|}{T(E,L)} \frac{\sin(2\pi n\, \theta(r,E,L))\, \sin(2\pi n\, \theta(s,E,L))}{\frac{4\pi^2 n^2}{T(E,L)^2} - \lambda}\, \mathrm{d}(E,L) \tag{5.2.17}$$

for $r, s \in [R_{\min}, R_{\max}]$*, where the function* θ *is defined in Lemma 4.3.4 and*

$$\mathbb{D}_0(r) \coloneqq \{(E,L) \in \mathbb{D}_0 \mid r_-(E,L) < r < r_+(E,L)\}, \qquad r \in [R_{\min}, R_{\max}]. \tag{5.2.18}$$

In the case $R_{\min} = 0$*,* (5.2.17) *is to be interpreted as*

$$K_\lambda(r,0) \coloneqq 0 =: K_\lambda(0,r), \qquad r \in [0, R_{\max}]. \tag{5.2.19}$$

In particular, $\mathcal{M}_\lambda$ *is a Hilbert-Schmidt operator, cf. [136, Sc. VI.6]. Moreover,* K_λ *is continuous on* $[R_{\min}, R_{\max}]^2$*.*

Proof. The proof relies on the explicit characterisations of $\left(-\mathcal{T}^2\big|_{\mathcal{H}} - \lambda\right)^{-1}$ and $\sqrt{\mathcal{R}}$ derived in Lemmas 4.3.18 and 4.4.4, respectively. Let $F \in L^2([R_{\min}, R_{\max}])$ be fixed and consider the associated function $f \in \mathcal{H}$ induced by (5.2.1). Fourier expanding f in the angle variable θ, cf. Remark 4.3.11, yields the Fourier expansion (4.3.46), where the Fourier coefficients $b_n \colon \mathbb{D}_0 \to \mathbb{R}$ for $n \in \mathbb{N}$ are given by (4.3.45). Using the explicit form (5.2.1) of f, they can be rewritten as

$$\begin{aligned} b_n(E,L) &= 4 \int_0^{\frac{1}{2}} f(\theta,E,L)\, \sin(2\pi n\, \theta)\, \mathrm{d}\theta = \\ &= 4 \frac{|\varphi'(E,L)|}{T(E,L)} \int_{r_-(E,L)}^{r_+(E,L)} \frac{F(r)}{r\sqrt{\rho_0(r)}}\, \sin(2\pi n\, \theta(r,E,L))\, \mathrm{d}r \end{aligned} \tag{5.2.20}$$

for $n \in \mathbb{N}$ and a.e. $(E,L) \in \mathbb{D}_0$, where we used Lemma 4.3.4 to change variables. Hence, by Lemma 4.3.18,

$$\begin{aligned} &\left(-\mathcal{T}^2\big|_{\mathcal{H}} - \lambda\right)^{-1} f(\theta,E,L) = \\ &\quad = 4 \frac{|\varphi'(E,L)|}{T(E,L)} \sum_{n=1}^{\infty} \int_{r_-(E,L)}^{r_+(E,L)} \frac{F(r)}{r\sqrt{\rho_0(r)}}\, \sin(2\pi n\, \theta(r,E,L))\, \mathrm{d}r\, \frac{\sin(2\pi n\, \theta)}{\frac{4\pi^2 n^2}{T(E,L)^2} - \lambda} \end{aligned} \tag{5.2.21}$$

[150] The series in the definition of K_λ is meant to convergence pointwise. In the proof, however, we shall see that it also converges uniformly and that switching the order of summation and integration yields the same function.

for a.e. $(\theta, E, L) \in \mathbb{S}^1 \times \mathbb{D}_0$ as a limit in H. In addition, by Lemmas 4.4.4 and 4.1.2,

$$\sqrt{\mathcal{R}} f(r, w, L) = 2\sqrt{\pi}\,|\varphi'(E, L)|\,\frac{w}{\sqrt{\rho_0(r)}}\,\frac{F(r)}{r\sqrt{\rho_0(r)}}\,j_{w\,|\varphi'|}(r) = 2\sqrt{\pi}\,|\varphi'(E, L)|\,\frac{w}{r}\,F(r) \tag{5.2.22}$$

for a.e. $(r, w, L) \in \Omega_0$. Hence, replacing f with $\sqrt{\mathcal{R}} f$ in (5.2.21) yields

$$\begin{aligned}\big(-\mathcal{T}^2\big|_{\mathcal{H}} - \lambda\big)^{-1}\sqrt{\mathcal{R}} f(\theta, E, L) = \\ = 8\sqrt{\pi}\,\frac{|\varphi'(E, L)|}{T(E, L)}\sum_{n=1}^{\infty}\int_{r_-(E,L)}^{r_+(E,L)}\frac{F(r)}{r}\,\sin(2\pi n\,\theta(r, E, L))\,\mathrm{d}r\,\frac{\sin(2\pi n\,\theta)}{\frac{4\pi^2 n^2}{T(E,L)^2} - \lambda}\end{aligned} \tag{5.2.23}$$

for a.e. $(\theta, E, L) \in \mathbb{S}^1 \times \mathbb{D}_0$ as a limit in H. In order to apply $\sqrt{\mathcal{R}}$ on the latter expression, we first note that the radial velocity density induced by some $g \in \mathcal{H}$ via (4.2.22) can be rewritten as

$$\begin{aligned}j_g(r) = \frac{2\pi}{r^2}\int_0^\infty\int_0^\infty w\,g(r, w, L)\,\mathrm{d}w\,\mathrm{d}L = \frac{2\pi}{r^2}\int_{\mathbb{D}_0(r)} g(r, \sqrt{2E - 2\Psi_L(r)}, L)\,\mathrm{d}(E, L) = \\ = \frac{2\pi}{r^2}\int_{\mathbb{D}_0(r)} g(\theta(r, E, L), E, L)\,\mathrm{d}(E, L)\end{aligned} \tag{5.2.24}$$

for a.e. $r \in [R_{\min}, R_{\max}]$. Inserting $g = \big(-\mathcal{T}^2\big|_{\mathcal{H}} - \lambda\big)^{-1}\sqrt{\mathcal{R}} f$ into this calculation then shows

$$\begin{aligned}Q_\lambda f(r, w, L) = \sqrt{\mathcal{R}}\big(-\mathcal{T}^2\big|_{\mathcal{H}} - \lambda\big)^{-1}\sqrt{\mathcal{R}} f(r, w, L) = \\ = 32\pi^2|\varphi'(E, L)|\,\frac{w}{r^2\sqrt{\rho_0(r)}}\int_{\mathbb{D}_0(r)}\frac{|\varphi'(\tilde{E}, \tilde{L})|}{T(\tilde{E}, \tilde{L})}\sum_{n=1}^{\infty}\int_{r_-(\tilde{E},\tilde{L})}^{r_+(\tilde{E},\tilde{L})}\frac{F(s)}{s}\,\sin(2\pi n\,\theta(s, \tilde{E}, \tilde{L}))\,\mathrm{d}s \\ \cdot\,\frac{\sin(2\pi n\,\theta(r, \tilde{E}, \tilde{L}))}{\frac{4\pi^2 n^2}{T(\tilde{E},\tilde{L})^2} - \lambda}\,\mathrm{d}(\tilde{E}, \tilde{L})\end{aligned} \tag{5.2.25}$$

for a.e. $(r, w, L) \in \Omega_0$. Hence, by Definition 5.2.4,

$$\begin{aligned}\mathcal{M}_\lambda F(r) = \frac{32\pi^2}{r}\int_{R_{\min}}^{R_{\max}}\frac{F(s)}{s}\int_{\mathbb{D}_0(r)\cap\mathbb{D}_0(s)}\frac{|\varphi'(E, L)|}{T(E, L)} \\ \cdot\sum_{n=1}^{\infty}\frac{\sin(2\pi n\,\theta(r, E, L))\,\sin(2\pi n\,\theta(s, E, L))}{\frac{4\pi^2 n^2}{T(E,L)^2} - \lambda}\,\mathrm{d}(E, L)\,\mathrm{d}s.\end{aligned} \tag{5.2.26}$$

In order to derive this identity, we switched the integration and summation and then applied Fubini's theorem to switch the order of integration. The former step can be verified by using the integrability of F and the positivity of $r_-(E, L)$ for $(E, L) \in \mathbb{D}_0$.

What is missing to deduce (5.2.16) is that we can switch the summation with the (E, L)-integral on the right-hand side of (5.2.26). To verify this operation, we first extend the mapping θ from Lemma 4.3.4 as follows:

$$\theta(r, E, L) \coloneqq 0 \qquad \text{for } (E, L) \in \mathbb{D}_0,\ r \in\,]0, \infty[\,\setminus\,[r_-(E, L), r_+(E, L)]. \tag{5.2.27}$$

Although this extension of $\theta(\cdot, E, L)$ has a jump discontinuity at $r = r_+(E, L)$, the mapping

$$]0, \infty[^2 \ni (r, s) \mapsto \sin(2\pi n\,\theta(r, E, L))\,\sin(2\pi n\,\theta(s, E, L)) \tag{5.2.28}$$

is continuous for every $n \in \mathbb{N}$ and $(E,L) \in \mathbb{D}_0$. Furthermore, there exists a constant $C > 0$ s.t.

$$\left| \sum_{n=1}^{m} \frac{\sin(2\pi n\, \theta(r,E,L))\, \sin(2\pi n\, \theta(s,E,L))}{\frac{4\pi^2 n^2}{T(E,L)^2} - \lambda} \right| \leq C \sum_{n=1}^{m} \frac{1}{n^2} \leq C\, \frac{\pi^2}{6} \tag{5.2.29}$$

for $r,s > 0$, $(E,L) \in \mathbb{D}_0$, and $m \in \mathbb{N}$; recall $\lambda < \inf(\sigma(-\mathcal{T}^2|_{\mathcal{H}})) = \frac{4\pi^2}{\sup^2_{\mathbb{D}_0}(T)}$. Hence, for fixed $(E,L) \in \mathbb{D}_0$, the mapping

$$]0,\infty[^2 \ni (r,s) \mapsto \sum_{n=1}^{\infty} \frac{\sin(2\pi n\, \theta(r,E,L))\, \sin(2\pi n\, \theta(s,E,L))}{\frac{4\pi^2 n^2}{T(E,L)^2} - \lambda} \tag{5.2.30}$$

is continuous and the series converges uniformly in $r,s > 0$. Since $|\varphi'|$ is integrable on $\mathbb{D}_0$ by Lemma 4.1.3[151] and $\inf_{\mathbb{D}_0}(T) > 0$ by Proposition A.0.1 (a), the estimate (5.2.29) further shows

$$\begin{aligned} &\int_{\mathbb{D}_0(r)\cap\mathbb{D}_0(s)} \frac{|\varphi'(E,L)|}{T(E,L)} \sum_{n=1}^{\infty} \frac{\sin(2\pi n\, \theta(r,E,L))\, \sin(2\pi n\, \theta(s,E,L))}{\frac{4\pi^2 n^2}{T(E,L)^2} - \lambda}\, \mathrm{d}(E,L) = \\ &\quad = \sum_{n=1}^{\infty} \int_{\mathbb{D}_0(r)\cap\mathbb{D}_0(s)} \frac{|\varphi'(E,L)|}{T(E,L)}\, \frac{\sin(2\pi n\, \theta(r,E,L))\, \sin(2\pi n\, \theta(s,E,L))}{\frac{4\pi^2 n^2}{T(E,L)^2} - \lambda}\, \mathrm{d}(E,L) \end{aligned} \tag{5.2.31}$$

for $r,s > 0$ and that (5.2.31) defines a function which is continuous in $(r,s) \in]0,\infty[^2$. We have thus proven (5.2.16) and that K_λ is continuous on $([R_{\min}, R_{\max}] \setminus \{0\})^2$.

It remains to show that K_λ is also continuous on $\{(r,s) \in [0,R_{\max}] \mid r = 0 \vee s = 0\}$ in the case $R_{\min} = 0$; recall that K_λ is given by (5.2.19) on this set. Due to the assumption (φ4), $R_{\min} = 0$ only occurs when the steady state is isotropic. The estimate (5.2.29) yields

$$\begin{aligned} |K_\lambda(r,s)| &\leq \frac{C}{rs} \int_{\mathbb{D}_0(r)\cap\mathbb{D}_0(s)} |\varphi'(E)|\, \mathrm{d}(E,L) \leq \\ &\leq \frac{C}{rs}\, \min\left\{ \int_{\mathbb{D}_0(r)} |\varphi'(E)|\, \mathrm{d}(E,L), \int_{\mathbb{D}_0(s)} |\varphi'(E)|\, \mathrm{d}(E,L) \right\} \end{aligned} \tag{5.2.32}$$

for $r,s \in]0,R_{\max}]$. In order to show that this expression tends to zero as r or s tend to zero, we consider

$$L_{\max}(r) \coloneqq \sup\{L > 0 \mid L \in \mathbb{L}_0 \ \&\ r_-(E_0,L) < r < r_+(E_0,L)\}, \qquad r \in]0,R_{\max}[; \tag{5.2.33}$$

recall that $\mathbb{L}_0 = [0, L_{\max}[$ by (2.2.85). By (2.2.82) and the monotonicities of $r_\pm$, cf. Lemma 2.2.14, we obtain $\{L > 0 \mid L \in \mathbb{D}_0(r)\} =]0, L_{\max}(r)[$ for $r \in]0,R_{\max}[$. Hence, for $r \in]0,R_{\max}[$ there holds the estimate

$$\int_{\mathbb{D}_0(r)} |\varphi'(E)|\, \mathrm{d}(E,L) \leq \int_0^{L_{\max}(r)} \int_{U_0(0)}^{E_0} |\varphi'(E)|\, \mathrm{d}E\, \mathrm{d}L = L_{\max}(r)\, \Phi(\kappa); \tag{5.2.34}$$

recall that $\Phi(0) = 0$ by the assumptions (φ2) and (φ5). Furthermore, from the identity

$$E_0 = \Psi_{L_{\max}(r)}(r_-(E_0, L_{\max}(r))) = U_0(r_-(E_0, L_{\max}(r))) + \frac{L_{\max}(r)}{2r_-(E_0, L_{\max}(r))^2}, \tag{5.2.35}$$

[151] Notice that $\int_{\mathbb{D}_0} |\varphi'(E,L)|\, \mathrm{d}(E,L) \leq C \int_{\Omega_0} |\varphi'(E,L)|\, \mathrm{d}(x,v)$ by Remark 4.3.5 and Proposition A.0.1 (a).

which is simply the definition of r_-, we deduce

$$L_{\max}(r) = 2r_-(E_0, L_{\max}(r))^2[E_0 - U_0(r_-(E_0, L_{\max}(r)))] \leq 2r^2\kappa \tag{5.2.36}$$

for $r \in]0, R_{\max}[$. Combining (5.2.32), (5.2.34), and (5.2.36) then proves the claimed continuity. □

Remark 5.2.13. *The above proof shows that one could continuously extend K_λ by 0 onto $[0,\infty[^2$. In particular, K_λ vanishes on $\partial\big([R_{\min}, R_{\max}]^2\big)$. One could hence also equivalently define the Mathur operator $\mathcal{M}_\lambda$ on the space $L^2([0,\infty[)$ by extending all functions by 0 as usual.*

Since the spectrum of the Birman-Schwinger operator Q_λ is related to the one of the Mathur operator $\mathcal{M}_\lambda$, the above proposition also yields further properties for the former operator.

Remark 5.2.14. *Since the Birman-Schwinger operator $Q_\lambda\colon \mathcal{H} \to \mathcal{H}$ is non-negative and compact by Lemma 5.1.15 and its non-zero eigenvalues are identical to the ones of $\mathcal{M}_\lambda$ (respecting multiplicities) by Lemma 5.2.5, the above proposition and [136, Thm. VI.22] imply that Q_λ is a Hilbert-Schmidt operator as well.*

As a first, rather trivial application of the integral representation of the Mathur operator, we show that the monotonicity of $\mathcal{M}_\lambda$ derived in Lemma 5.2.11 is strict. This is based on [62, Rem. 8.12].

Lemma 5.2.15. *The mapping*

$$\big]-\infty, \inf(\sigma(-\mathcal{T}^2|_{\mathcal{H}}))\big[\ni \lambda \mapsto \|\mathcal{M}_\lambda\| \tag{5.2.37}$$

is positive and strictly increasing. Here, $\|\mathcal{M}_\lambda\|$ denotes the operator norm of the (bounded) Mathur operator $\mathcal{M}_\lambda\colon L^2([R_{\min}, R_{\max}]) \to L^2([R_{\min}, R_{\max}])$.

Proof. Proposition 5.2.12 shows that for any $F \in L^2([R_{\min}, R_{\max}])$ there holds

$$\begin{aligned}\langle \mathcal{M}_\lambda F, F\rangle_{L^2([R_{\min},R_{\max}])} &= \int_{R_{\min}}^{R_{\max}} \int_{R_{\min}}^{R_{\max}} K_\lambda(r,s)\, F(r)\, F(s)\, \mathrm{d}s\, \mathrm{d}r = \\ &= 32\pi^2 \sum_{n=1}^{\infty} \int_{\mathbb{D}_0} \frac{|\varphi'(E,L)|}{T(E,L)} \frac{1}{\frac{4\pi^2 n^2}{T(E,L)^2} - \lambda} \left(\int_{r_-(E,L)}^{r_+(E,L)} \frac{F(r)}{r} \sin(2\pi n\, \theta(r,E,L))\, \mathrm{d}r \right)^2 \mathrm{d}(E,L).\end{aligned} \tag{5.2.38}$$

Note that we switched the order of the summation and the integrals in the last step of this calculation – similar arguments as in the proof of Proposition 5.2.12 can be used to justify these operations.

Now fix some F s.t. $\langle \mathcal{M}_\lambda F, F\rangle_2$ does not vanish. This means that the r-integral on the right-hand side of (5.2.38) does not vanish for every $n \in \mathbb{N}$ and a.e. $(E,L) \in \mathbb{D}_0$.[152] Obviously,

$$0 < \langle \mathcal{M}_\mu F, F\rangle_{L^2([R_{\min},R_{\max}])} < \langle \mathcal{M}_\lambda F, F\rangle_{L^2([R_{\min},R_{\max}])}, \qquad \mu < \lambda < \inf(\sigma(-\mathcal{T}^2|_{\mathcal{H}})). \tag{5.2.39}$$

Since the suprema on the right-hand side of (5.2.14) are attained by eigenfunctions to the eigenvalue $\|\mathcal{M}_\lambda\|$ of $\mathcal{M}_\lambda$, we hence conclude that $\|\mathcal{M}_\lambda\|$ is indeed positive and strictly increasing in λ. □

[152] An explicit example of such a function will be constructed in the proof of Theorem 5.4.1.

As mentioned before, the properties of the Mathur operator are analysed in [85, Ch. 4] as well, see also [86, Sc. 9]. To conclude the present section, we compare the results in [85] to the ones above and state some additional properties of the Mathur operator proven in [85].

Remark 5.2.16. *Proposition 5.2.12 shows that the operator defined in [85, Def. 4.1] corresponds to the Mathur operator $\mathcal{M}_\lambda$; note that the angle variable θ ranges in $[0, 2\pi]$ in [85], which leads to different factors at several places of the analysis. The main properties of $\mathcal{M}_\lambda$ from Lemmas 5.2.8, 5.2.10, and 5.2.11 and Proposition 5.2.12 are proven in [85, Lemma 4.3]. In addition, it is shown that the mapping $]-\infty, \inf(\sigma(-\mathcal{T}^2|_{\mathcal{H}}))[\ni \lambda \mapsto \mathcal{M}_\lambda$ is continuous w.r.t. the Hilbert-Schmidt norm as well as that the mapping*[153] *$\mathbb{C} \setminus [\inf(\sigma(-\mathcal{T}^2|_{\mathcal{H}})), \infty[\ni \lambda \mapsto \mathcal{M}_\lambda$ is analytic w.r.t. to the operator norm and that the derivatives of the latter mapping possess an integral representation similar to $\mathcal{M}_\lambda$ itself. The relations between the Mathur operator, the Birman-Schwinger operator (in a similar form as in [62, 111]), and the eigenvalues of the linearised operator in the essential gap are established in [85, Lemmas 4.4 and 4.6 and Thm. 4.5].*

The limiting behaviour of the Mathur operator $\mathcal{M}_\lambda$ and its eigenvalues in the limit $\lambda \nearrow \inf(\sigma(-\mathcal{T}^2|_{\mathcal{H}}))$ is then analysed in [85, Lemmas 4.7–4.12]. For instance, it is shown in [85, Lemma 4.9] that $\lim_{\lambda \nearrow \inf(\sigma(-\mathcal{T}^2|_{\mathcal{H}}))} \mathcal{M}_\lambda$ exists in the Hilbert-Schmidt norm under suitable assumptions on the period function T. We will also discuss some aspects of this limiting behaviour in the succeeding section, but not as comprehensively as in [85].

In [85, Scs. 4.2 and 4.3], the properties of the Mathur operator are used to derive criteria for the (non-)existence of eigenvalues of $\mathcal{L}$ below its essential spectrum and applications of these criteria are discussed. We will present some of these results (or adaptations of them) in the succeeding sections.

A particular emphasis in [85] is placed on characterising whether the bottom of the essential spectrum of the linearised operator $\mathcal{L}$, given by $\inf(\sigma_{\text{ess}}(\mathcal{L})) = \inf(\sigma(-\mathcal{T}^2|_{\mathcal{H}})) = \sup(\mathcal{G})$, is an eigenvalue or not. Concretely, characterisations for $\inf(\sigma(-\mathcal{T}^2|_{\mathcal{H}}))$ being an eigenvalue of $\mathcal{L}$ are derived in [85, Lemma 4.12, Thms. 4.14 and 4.15, and Cor. 4.17] under a variety of assumptions on the underlying steady state and its period function. Here, we do not analyse much the question whether $\inf(\sigma_{\text{ess}}(\mathcal{L})) = \inf(\sigma(-\mathcal{T}^2|_{\mathcal{H}})) = \sup(\mathcal{G})$ is an eigenvalue of $\mathcal{L}$ because we believe that it is more promising to show the existence of an eigenvalue of $\mathcal{L}$ in $\mathcal{G}$ than to show that $\sup(\mathcal{G})$ is an eigenvalue. In addition, in Section 6.5 we will present different arguments which prove the absence of eigenvalues of $\mathcal{L}$ in $\sigma_{\text{ess}}(\mathcal{L})$, including $\inf(\sigma_{\text{ess}}(\mathcal{L})) = \min(\sigma_{\text{ess}}(\mathcal{L})) = \sup(\mathcal{G})$. However, we will consider a different setting there. Our focus on the existence of eigenvalues of $\mathcal{L}$ in $\mathcal{G}$ is also motivated by the numerical observations from Section 8.3. For instance, for all isotropic polytropes (except the transitional cases), the numerics indicate that eigenvalues are always located in $\mathcal{G}$, cf. Observation 8.3.4. For anisotropic polytropes, we have also numerically observed the presence of eigenvalues of $\mathcal{L}$ embedded into its essential spectrum, but not necessarily located at the bottom of the essential spectrum, cf. Observation 8.3.9. Nonetheless, for a large range of King models, the smallest eigenvalue of $\mathcal{L}$ is in fact equal (or at least, close) to $\inf(\sigma_{\text{ess}}(\mathcal{L}))$, cf. Observation 8.3.7. Hence, the results from [85] could be valuable in proving the existence (or absence) of eigenvalues for such steady states.

In addition, in [85, Ch. 5], the Mathur operator $\mathcal{M}_\lambda$ with $\lambda = 0$ is studied. In particular, a connection between $\mathcal{M}_0$ and the "Guo-Lin operator" [53, Lemma 3.1], see also [165, Ch. 4], is established. Note that the largest eigenvalue of $\mathcal{M}_0$ equals $1 - \tilde{\lambda} \in]0, 1[$ by (5.1.18),

[153] It is straight-forward to extend the definitions of the Birman-Schwinger operator Q_λ and the Mathur operator $\mathcal{M}_\lambda$ to $\lambda \in \mathbb{C} \setminus \sigma(-\mathcal{T}^2|_{\mathcal{H}})$. It will, however, be sufficient for the proofs of the criteria in Section 5.3 to consider real-valued λ.

which is consistent with the fact that the linearised operator $\mathcal{L}$ is positive by Proposition 4.5.11. Further note that in the case $\lambda = 0$, an alternative representation of the Mathur operator without the θ-Fourier series can be derived by using Lemma 4.3.27 to compute $\mathcal{T}^{-2}$ instead of Lemma 4.3.18.

5.3 Criteria for the (Non-)Existence of Oscillatory Modes

In this section we use the properties of the Mathur operator $\mathcal{M}_\lambda$ established above to characterise the existence and estimate the amount of eigenvalues of the linearised operator $\mathcal{L}$ in the essential gap $\mathcal{G}$. This is based on [49, Sc. 6.4], [61, Sc. 5.1], and [62, Sc. 8.1]. As discussed in Remark 5.2.16, related results are also contained in [85, Ch. 4].

The main result of this entire thesis is the following sharp characterisation of the existence of eigenvalues of $\mathcal{L}$ in $\mathcal{G}$. It originates from [62, Thm. 8.11(a) and Rem. 8.12]; see [61, Prop. 5.3] and [85, Thm. 4.13] for similar results.

Theorem 5.3.1 (A Sharp Criterion for the Existence of Oscillatory Modes in $\mathcal{G}$)**.** *Let*

$$\mathfrak{M} := \lim_{\lambda \nearrow \inf(\sigma(-\mathcal{T}^2|_{\mathcal{H}}))} \|\mathcal{M}_\lambda\| \in]0, \infty], \tag{5.3.1}$$

where $\|\mathcal{M}_\lambda\|$ denotes the operator norm of the Mathur operator $\mathcal{M}_\lambda$ analysed in Lemmas 5.2.10 and 5.2.15. Then,

$$\mathfrak{M} > 1 \qquad \Leftrightarrow \qquad \mathcal{L} \text{ possesses an eigenvalue in } \mathcal{G}. \tag{5.3.2}$$

Proof. If $\mathfrak{M} > 1$, there exists $\lambda \in \mathcal{G}$ s.t. $\|\mathcal{M}_\lambda\| > 1$. By Lemma 5.2.10, the Mathur operator $\mathcal{M}_\lambda$ thus possesses an eigenvalue > 1. Hence, by Proposition 5.2.7, $\mathcal{L}$ possesses an eigenvalue $< \lambda$ which, by the positivity of $\mathcal{L}$ shown in Proposition 4.5.11, lies in $\mathcal{G}$.

Conversely, if $\mathfrak{M} \leq 1$, the strict monotonicity of $\lambda \mapsto \|\mathcal{M}_\lambda\|$ established in Lemma 5.2.15 yields $\|\mathcal{M}_\lambda\| < 1$ for every $\lambda < \inf(\sigma(-\mathcal{T}^2|_{\mathcal{H}}))$. Hence, $\mathcal{M}_\lambda$ possesses no eigenvalues ≥ 1 and, by Proposition 5.2.7, $\mathcal{L}$ has no eigenvalues $\leq \lambda$. As this holds for any $\lambda < \inf(\sigma(-\mathcal{T}^2|_{\mathcal{H}}))$, we conclude that $\mathcal{L}$ cannot possess an eigenvalue in $\mathcal{G}$. □

Although the above criterion is mainly used to characterise the existence of eigenvalues of $\mathcal{L}$ in $\mathcal{G}$, the methods from the previous sections also yield some information regarding the associated eigenfunctions.

Remark 5.3.2. *Suppose that we are in the situation $\mathfrak{M} > 1$ in the above theorem, i.e., there exists an eigenvalue $\lambda \in \mathcal{G}$ of $\mathcal{L}$. By Proposition 5.1.13 and Lemma 5.2.5, 1 is an eigenvalue of $\mathcal{M}_\lambda$. Let $F \in L^2([R_{\min}, R_{\max}])$ be an associated eigenfunction of $\mathcal{M}_\lambda$ to the eigenvalue 1. The proof of Lemma 5.2.5 shows that $f \in \mathcal{H}$ given by (5.2.1) is an eigenfunction of Q_λ to the eigenvalue 1. Proposition 5.1.13 thus implies that $(-\mathcal{T}^2\big|_{\mathcal{H}} - \lambda)^{-1}\sqrt{\mathcal{R}}f$ is an eigenfunction of $\mathcal{L}$ to the eigenvalue λ. Furthermore, the calculations in the proof of Proposition 5.2.12, cf. (5.2.23), show that this eigenfunction of $\mathcal{L}$ is of the form*

$$8\sqrt{\pi}\,\frac{|\varphi'(E,L)|}{T(E,L)} \sum_{n=1}^{\infty} \int_{r_-(E,L)}^{r_+(E,L)} \frac{F(r)}{r}\, \sin(2\pi n\, \theta(r,E,L))\, \mathrm{d}r\, \frac{\sin(2\pi n\, \theta)}{\frac{4\pi^2 n^2}{T(E,L)^2} - \lambda} \tag{5.3.3}$$

for a.e. $(\theta, E, L) \in \mathbb{S}^1 \times \mathbb{D}_0$; the series is to interpreted as a limit in H.

Since the multiplicity of eigenvalues is preserved in the statements of Proposition 5.1.13 and Lemma 5.2.5, we actually obtain that every eigenfunction of $\mathcal{L}$ associated to an eigenvalue in $\mathcal{G}$ is of the form (5.3.3) for some $\lambda \in \mathcal{G}$ and an eigenfunction $F \in L^2([R_{\min}, R_{\max}])$ of $\mathcal{M}_\lambda$ to the eigenvalue 1.

The second main result of this chapter is that the integral representation of the Mathur operator can also be used to bound the number of eigenvalues of the linearised operator $\mathcal{L}$ in the essential gap $\mathcal{G}$ in terms of a suitable integral. In the context of Schrödinger operators, such bounds are due to [21, 158] and are usually called "Birman-Schwinger bounds", see, e.g., [99, Cor. 4.3].[154] The result is inspired by [49, Thm. 6.24]; some of the calculations in the proof are based on [62, p. 678].

Theorem 5.3.3 (A Birman-Schwinger Bound on the Number of Oscillatory Modes in $\mathcal{G}$)**.** *It holds that*

$$\#\{\textit{eigenvalues} \in \mathcal{G} \textit{ of } \mathcal{L} \textit{ (counting multiplicities)}\} \leq \sup_{\lambda\in\mathcal{G}} \|K_\lambda\|^2_{L^2([R_{\min},R_{\max}]^2)}, \tag{5.3.4}$$

where K_λ is the integral kernel of the Mathur operator $\mathcal{M}_\lambda$ introduced in Proposition 5.2.12. Moreover, for the square root of the supremum on the right-hand side of (5.3.4) *there holds the estimate*

$$\begin{aligned}&\sup_{\lambda\in\mathcal{G}} \|K_\lambda\|_{L^2([R_{\min},R_{\max}]^2)} \leq \\ &\quad\leq 32\pi^2 \sum_{n=1}^{\infty} \int_{\mathbb{D}_0} \frac{|\varphi'(E,L)|}{T(E,L)} \frac{1}{\frac{4\pi^2 n^2}{T(E,L)^2} - \frac{4\pi^2}{\sup^2_{\mathbb{D}_0}(T)}} \int_{r_-(E,L)}^{r_+(E,L)} \frac{\sin^2(2\pi n\,\theta(r,E,L))}{r^2}\,\mathrm{d}r\,\mathrm{d}(E,L),\end{aligned} \tag{5.3.5}$$

where $\mathbb{D}_0$ is the (E,L)-support of the steady state given by (2.2.88)*, T is the period function introduced in Definition 2.2.16, and the function θ is defined in Lemma 4.3.4. In addition, since K_λ is continuous on $[R_{\min},R_{\max}]^2$, there holds the alternative estimate*

$$\begin{aligned}&\sup_{\lambda\in\mathcal{G}} \|K_\lambda\|_{L^2([R_{\min},R_{\max}]^2)} \leq (R_{\max}-R_{\min}) \sup_{\lambda\in\mathcal{G}} \|K_\lambda\|_{L^\infty([R_{\min},R_{\max}]^2)} \leq \\ &(R_{\max}-R_{\min}) \sup_{r,s\in]R_{\min},R_{\max}]} \frac{32\pi^2}{rs} \sum_{n=1}^{\infty} \int_{\mathbb{D}_0(r)\cap\mathbb{D}_0(s)} \frac{|\varphi'(E,L)|}{T(E,L)} \frac{1}{\frac{4\pi^2 n^2}{T(E,L)^2} - \frac{4\pi^2}{\sup^2_{\mathbb{D}_0}(T)}}\,\mathrm{d}(E,L),\end{aligned} \tag{5.3.6}$$

where $\mathbb{D}_0(r)$ is defined in (5.2.18) *Notice that all of the expressions in* (5.3.4)*,* (5.3.5)*, and* (5.3.6) *– including the number of eigenvalues of $\mathcal{L}$ in $\mathcal{G}$ – can be infinite.*

Proof. For fixed $\lambda \in \mathcal{G}$, Remark 5.2.6 shows that the positive eigenvalues of $\mathcal{M}_\lambda$ are given by the values $\gamma_n(\lambda) > 0$ introduced in Definition 5.1.8. Recall that each of these value is repeated according to the multiplicity of the respective eigenvalue of $\mathcal{M}_\lambda$ and that they are sorted in descending order, i.e., $\gamma_n(\lambda) \geq \gamma_{n+1}(\lambda)$. Let $m := \#\{n \in \mathbb{N} \mid \gamma_n(\lambda) > 0\} \in \mathbb{N} \cup \{\infty\}$ denote the amount of such positive eigenvalues counting multiplicities. Notice that Lemmas 5.2.10 and 5.2.15 show $m \geq 1$ since the largest eigenvalue of $\mathcal{M}_\lambda$ is given by $\gamma_1(\lambda) = \|\mathcal{M}_\lambda\| > 0$. Proposition 5.2.7 thus yields

$$\begin{aligned}&\#\{\text{eigenvalues} \leq \lambda \text{ of } \mathcal{L} \text{ (counting multiplicities)}\} = \\ &\qquad = \#\{1 \leq n \leq m \mid \gamma_n(\lambda) \geq 1\} \leq \sum_{\substack{n=1\\ \gamma_n(\lambda)\geq 1}}^{m} \gamma_n(\lambda)^2 \leq \sum_{n=1}^{m} \gamma_n(\lambda)^2.\end{aligned} \tag{5.3.7}$$

[154] More precisely, the Birman-Schwinger bound in quantum mechanics is derived by estimating the Hilbert-Schmidt norm of a suitable operator. This is also our strategy in Theorem 5.3.3.

Since $\mathcal{M}_\lambda$ is a Hilbert-Schmidt operator by Proposition 5.2.12, there holds, by [136, Thms. VI.16 and VI.22(b)],

$$\sum_{n=1}^{m} \gamma_n(\lambda)^2 = \|\mathcal{M}_\lambda\|_{\mathrm{HS}}^2. \tag{5.3.8}$$

Here $\|\mathcal{M}_\lambda\|_{\mathrm{HS}}$ denotes the Hilbert-Schmidt norm of $\mathcal{M}_\lambda$ which, by [136, Thm. VI.23], is given by

$$\|\mathcal{M}_\lambda\|_{\mathrm{HS}} = \|K_\lambda\|_{L^2([R_{\min},R_{\max}]^2)}. \tag{5.3.9}$$

Altogether, we thus conclude

$$\#\{\text{eigenvalues} \leq \lambda \text{ of } \mathcal{L} \text{ (counting multiplicities)}\} \leq \|K_\lambda\|^2_{L^2([R_{\min},R_{\max}]^2)} \tag{5.3.10}$$

for every $\lambda \in \mathcal{G}$, which proves (5.3.4).

In order to establish the estimate (5.3.5), we again fix $\lambda \in \mathcal{G}$. For any $f \in L^2([R_{\min}, R_{\max}]^2)$ there holds

$$\begin{aligned}
&|\langle K_\lambda, f\rangle_{L^2([R_{\min},R_{\max}]^2)}| \leq \\
&\leq 32\pi^2 \sum_{n=1}^{\infty} \int_{\mathbb{D}_0} \frac{|\varphi'(E,L)|}{T(E,L)} \frac{1}{\frac{4\pi^2 n^2}{T(E,L)^2} - \lambda} \cdot \\
&\qquad \cdot \int_{r_-(E,L)}^{r_+(E,L)} \int_{r_-(E,L)}^{r_+(E,L)} \left| \frac{\sin(2\pi n\, \theta(r,E,L))\, \sin(2\pi n\, \theta(s,E,L))}{rs} f(r,s) \right| \mathrm{d}r\, \mathrm{d}s\, \mathrm{d}(E,L) \leq \\
&\leq 32\pi^2 \|f\|_2 \sum_{n=1}^{\infty} \int_{\mathbb{D}_0} \frac{|\varphi'(E,L)|}{T(E,L)} \frac{1}{\frac{4\pi^2 n^2}{T(E,L)^2} - \lambda} \int_{r_-(E,L)}^{r_+(E,L)} \frac{\sin^2(2\pi n\, \theta(r,E,L))}{r^2}\, \mathrm{d}r\, \mathrm{d}(E,L)
\end{aligned} \tag{5.3.11}$$

by the Cauchy-Schwarz inequality. Similar arguments as in the proof of Proposition 5.2.12 justify interchanging the integrals and the series during this calculation. By Riesz's representation theorem we thus obtain

$$\begin{aligned}
&\|K_\lambda\|_{L^2([R_{\min},R_{\max}]^2)} \leq \\
&\leq 32\pi^2 \sum_{n=1}^{\infty} \int_{\mathbb{D}_0} \frac{|\varphi'(E,L)|}{T(E,L)} \frac{1}{\frac{4\pi^2 n^2}{T(E,L)^2} - \lambda} \int_{r_-(E,L)}^{r_+(E,L)} \frac{\sin^2(2\pi n\, \theta(r,E,L))}{r^2}\, \mathrm{d}r\, \mathrm{d}(E,L).
\end{aligned} \tag{5.3.12}$$

Although it is not necessary for this proof, we note that the integral on the right-hand side is finite. This can be shown analogously as in the proof of Proposition 5.2.12 by using the integrability of $|\varphi'|$ on $\mathbb{D}_0$ and the inequality $r_-(E,L) \geq \frac{\sqrt{L}}{\sqrt{2E_0 - 2U_0(0)}}$ for $(E,L) \in \mathbb{D}_0$. Anyway, inserting the estimate $\lambda < \inf(\sigma(-\mathcal{T}^2|_{\mathcal{H}})) = \frac{4\pi^2}{\sup^2_{\mathbb{D}_0}(T)}$ into the right-hand side of (5.3.12) yields (5.3.5).

The additional estimate (5.3.6) follows trivially from Proposition 5.2.12. □

An important special case of the above theorem is that the right-hand side of (5.3.5) or (5.3.6) being strictly smaller than one implies that there are no eigenvalues of $\mathcal{L}$ in $\mathcal{G}$.

Moreover, observe that the finiteness of the integral on the right-hand side of (5.3.5) or (5.3.6) is only unclear for the $n = 1$ addend. For this term, the integrability depends on where the period function T "attains" its supremum on $\mathbb{D}_0$ and how T behaves close to these points. For example, [85, Lemma 4.9] provides a criterion on the period function which

guarantees that the right-hand side of (5.3.5) is finite. We will derive a similar criterion below, cf. Corollary 5.4.4. A related result is also contained in [117, Cor. 1.3].

A bound on the number of eigenvalues of $\mathcal{L}$ inside the essential gap which is related to Theorem 5.3.3 is proven in [117, Thm. 1.2]. Let us briefly discuss the relation of these bounds.

Remark 5.3.4. *In [117, Sc. 4], a bound on the number of eigenvalues is derived by estimating the trace of a different Birman-Schwinger type operator $\tilde{Q}_\lambda$. In our notation, it is of the form $\tilde{Q}_\lambda = (-\mathcal{T}^2\big|_{\mathcal{H}} - \lambda)^{-\frac{1}{2}} \mathcal{R} (-\mathcal{T}^2\big|_{\mathcal{H}} - \lambda)^{-\frac{1}{2}}$, where $(-\mathcal{T}^2\big|_{\mathcal{H}} - \lambda)^{-\frac{1}{2}} \coloneqq \sqrt{-\mathcal{T}^2\big|_{\mathcal{H}} - \lambda}^{-1}$ can be shown to exist and written down explicitly using the Fourier series expansion in the angle variable θ. The functional analytical properties of $\tilde{Q}_\lambda$ are similar to the ones of Q_λ, in particular, $\tilde{Q}_\lambda$ is symmetric, non-negative, and compact. Moreover, similar arguments as in the proof of Proposition 5.1.13 show that the non-zero eigenvalues of $\tilde{Q}_\lambda$ are identical to the ones of Q_λ (respecting multiplicities), which are in turn the same as for the Mathur operator $\mathcal{M}_\lambda$, cf. Lemma 5.2.5. Hence, the three operators $\tilde{Q}_\lambda$, Q_λ, and $\mathcal{M}_\lambda$ share the same trace [136, Thm. VI.18]. The same statement is also true for the Hilbert-Schmidt norm [136, Thm. VI.22] of these operators.*

Evidently, both the trace and the squared Hilbert-Schmidt norm give an upper bound on the number of eigenvalues ≥ 1. The latter is used to derive the bound from Theorem 5.3.3, the former is used in [117, Prop. 4.1]. For the Mathur operator, such a trace-based bound can be established by modifying the proof of Theorem 5.3.3 as follows:

$$\begin{aligned} &\#\{\textit{eigenvalues} \leq \lambda \textit{ of } \mathcal{L} \textit{ (counting multiplicities)}\} = \\ &\qquad = \#\{n \in \mathbb{N} \mid \gamma_n(\lambda) \geq 1\} \leq \sum_{n \in \mathbb{N}} \gamma_n(\lambda) = \operatorname{Tr}(\mathcal{M}_\lambda) = \int_{R_{\min}}^{R_{\max}} K_\lambda(r,r)\,\mathrm{d}r, \end{aligned} \tag{5.3.13}$$

where the latter equality is due to Mercer's Theorem [42, Thm. 2.4]. The expression on the right-hand side of (5.3.13) *can then be estimated independently of λ in a similar way as $\|K_\lambda\|_2$.*

It is not possible to say in general whether the bound relying on the squared Hilbert-Schmidt norm or the trace-based bounds are sharper. There may be situations (especially when there are many eigenvalues < 1 of $\mathcal{M}_\lambda$) where the Birman-Schwinger bound from Theorem 5.3.3 is superior, and other situations (especially when there are many eigenvalues > 1 of $\mathcal{M}_\lambda$) where the trace-based bounds from (5.3.13) *and [117, Thm. 1.2] are superior. In any case, it should be acknowledged that the bound from [117, Thm. 1.2] looks cleaner than the bounds derived here.*

5.4 Applications of the Criteria

In this section we present (first) applications of the criteria for the existence of oscillatory modes derived in the previous section. Further applications will then be discussed in the succeeding chapter.

The first application originates from [62, Thm. 8.15] and shows the existence of an oscillatory mode for certain anisotropic polytropic steady states under a suitable assumption on the radial period function T. We will comment on the validity of this assumption as well as on the class of steady states after the proof.

Theorem 5.4.1 (Existence of an Oscillatory Mode for Some Polytropes)**.** *Consider the situation of a polytropic steady state* (1.2.5) *with parameters k, ℓ, and L_0 satisfying*

$$L_0 > 0, \qquad \ell > -\frac{1}{2}, \qquad 0 < k < 3\ell + \frac{7}{2}, \qquad k + \ell \leq 0. \tag{5.4.1}$$

Assume that the period function T "attains" its supremum on $\mathbb{D}_0$ at (E_0, L_0), i.e.,

$$\sup_{\mathbb{D}_0} T = T(E_0, L_0). \tag{5.4.2}$$

Then the linearised operator $\mathcal{L}$ possesses an eigenvalue in the essential gap $\mathcal{G}$.

Proof. Let $\lambda \in \mathcal{G}$ and $F \in L^2([R_{\min}, R_{\max}])$ with $\|F\|_2 = 1$. Using Lemma 5.2.10 and the integral representation of the Mathur operator from Proposition 5.2.12, the same calculation as in the proof of Lemma 5.2.15 yields

$$\begin{aligned}
&\|\mathcal{M}_\lambda\| \geq \langle \mathcal{M}_\lambda F, F\rangle_2 = \\
&= 32\pi^2 \sum_{n=1}^{\infty} \int_{\mathbb{D}_0} \frac{|\varphi'(E,L)|}{T(E,L)} \frac{1}{\frac{4\pi^2 n^2}{T(E,L)^2} - \lambda} \left(\int_{r_-(E,L)}^{r_+(E,L)} \frac{F(r)}{r} \sin(2\pi n\, \theta(r,E,L))\, \mathrm{d}r \right)^2 \mathrm{d}(E,L) \geq \\
&\geq 32\pi^2 \int_{\mathbb{D}_0} \frac{|\varphi'(E,L)|}{T(E,L)} \frac{1}{\frac{4\pi^2}{T(E,L)^2} - \lambda} \left(\int_{r_-(E,L)}^{r_+(E,L)} \frac{F(r)}{r} \sin(2\pi\, \theta(r,E,L))\, \mathrm{d}r \right)^2 \mathrm{d}(E,L).
\end{aligned} \tag{5.4.3}$$

Fixing F and considering the limit $\lambda \nearrow \inf(\sigma(-\mathcal{T}^2|_{\mathcal{H}})) = \frac{4\pi^2}{\sup^2_{\mathbb{D}_0}(T)}$, we obtain

$$\begin{aligned}
&\mathfrak{M} = \lim_{\lambda \nearrow \inf(\sigma(-\mathcal{T}^2|_{\mathcal{H}}))} \|\mathcal{M}_\lambda\| \geq \\
&\geq 32\pi^2 \int_{\mathbb{D}_0} \frac{|\varphi'(E,L)|}{T(E,L)} \frac{1}{\frac{4\pi^2}{T(E,L)^2} - \frac{4\pi^2}{\sup^2_{\mathbb{D}_0}(T)}} \left(\int_{r_-(E,L)}^{r_+(E,L)} \frac{F(r)}{r} \sin(2\pi\, \theta(r,E,L))\, \mathrm{d}r \right)^2 \mathrm{d}(E,L) \geq \\
&\geq c \int_{\mathbb{D}_0} \frac{|\varphi'(E,L)|}{T(E_0,L_0) - T(E,L)} \left(\int_{r_-(E,L)}^{r_+(E,L)} \frac{F(r)}{r} \sin(2\pi\, \theta(r,E,L))\, \mathrm{d}r \right)^2 \mathrm{d}(E,L),
\end{aligned} \tag{5.4.4}$$

where we used the monotone convergence theorem, the assumption (5.4.2), the bound $\inf_{\mathbb{D}_0} T > 0$ from Proposition A.0.1 (a), and

$$\frac{1}{T(E,L)^2} - \frac{1}{T(E_0,L_0)^2} \leq 2\, \frac{T(E_0,L_0) - T(E,L)}{\inf^3_{\mathbb{D}_0}(T)}, \qquad (E,L) \in \mathbb{D}_0, \tag{5.4.5}$$

Here, $c > 0$ is some constant depending on the fixed steady state and is allowed to change its value throughout this proof.

Our aim is to construct a function F s.t. the r-integral on the right-hand side of (5.4.4) is bounded away from zero for (E, L) close to (E_0, L_0). For this purpose let $\varepsilon > 0$ be chosen s.t. the interior of the set

$$N_\varepsilon \coloneqq [E_0 - \varepsilon, E_0] \times [L_0, L_0 + \varepsilon] \tag{5.4.6}$$

is contained in $\mathbb{D}_0$; recall (2.2.88) for the definition of $\mathbb{D}_0$. Such ε exists since $L \mapsto E^{\min}_L$ is continuous by Lemma 2.2.14 (b) and $E^{\min}_{L_0} < E_0$. Next, let

$$r_{\frac{1}{2}}(E,L) \coloneqq R(\frac{1}{4}\, T(E,L), E, L), \qquad (E,L) \in \mathbb{A}_0, \tag{5.4.7}$$

where R is defined as in Definition 2.2.16. By Proposition A.0.1 (b) and Lemma A.3.2, $r_{\frac{1}{2}}$ is continuous on $\mathbb{A}_0$. Moreover, by Lemma 4.3.4,

$$\theta(r_{\frac{1}{2}}(E,L),E,L)=\frac{1}{4}. \tag{5.4.8}$$

Hence, after possibly reducing $\varepsilon>0$, there exists an open interval $I\subset[R_{\min},R_{\max}]$ containing $r_{\frac{1}{2}}(E_0,L_0)$ s.t.

$$\sin(2\pi\,\theta(r,E,L))\geq\frac{1}{2},\qquad (E,L)\in N_\varepsilon,\ r\in I; \tag{5.4.9}$$

note that the mapping θ is continuous by Lemma 4.3.3. Now let $F:=|I|^{-\frac{1}{2}}\,\mathbb{1}_I$. Obviously, $\|F\|_{L^2([R_{\min},R_{\min}])}=1$. Inserting this choice of F into (5.4.4) and using $R_{\min}>0$ and (5.4.9) thus yields

$$\mathfrak{M}\geq c\int_{L_0}^{L_0+\varepsilon}\int_{E_0-\varepsilon}^{E_0}\frac{|\varphi'(E,L)|}{T(E_0,L_0)-T(E,L)}\,\mathrm{d}E\,\mathrm{d}L. \tag{5.4.10}$$

The final step is to show that the latter integral is infinite for the steady states under consideration. Taylor expanding the denominator of the integrand results in

$$T(E_0,L_0)-T(E,L)=\partial_E T(E_0,L_0)\,(E_0-E)-\partial_L T(E_0,L_0)\,(L-L_0)+ \\ +o(|(E,L)-(E_0,L_0)|) \tag{5.4.11}$$

as $(E,L)\to(E_0,L_0)$, note that T is continuously differentiable on a neighbourhood of $(E_0,L_0)\in\mathbb{A}_0$ by Proposition A.0.1 (b). Thus, after possibly reducing $\varepsilon>0$, there exists a constant $C>0$ s.t.

$$0\leq T(E_0,L_0)-T(E,L)\leq C\,(E_0-E+L-L_0),\qquad (E,L)\in N_\varepsilon. \tag{5.4.12}$$

Inserting this estimate together with the polytropic structure of φ into (5.4.10) hence yields

$$\mathfrak{M}\geq c\int_{L_0}^{L_0+\varepsilon}\int_{E_0-\varepsilon}^{E_0}\frac{(E_0-E)^{k-1}(L-L_0)^\ell}{E_0-E+L-L_0}\,\mathrm{d}E\,\mathrm{d}L=c\int_0^\varepsilon\int_0^\varepsilon\frac{\eta^{k-1}\nu^\ell}{\eta+\nu}\,\mathrm{d}\eta\,\mathrm{d}\nu, \tag{5.4.13}$$

where we used the obvious changes of variables $\eta=E_0-E$ and $\nu=L-L_0$. Since $k+\ell\leq 0$ by (5.4.1), the latter integral is indeed infinite.[155] This can be seen by the following simple calculation:

$$\int_0^\varepsilon\int_0^\varepsilon\frac{\eta^{k-1}\nu^\ell}{\eta+\nu}\,\mathrm{d}\eta\,\mathrm{d}\nu\geq\int_0^\varepsilon\int_0^\nu\frac{\eta^{k-1}\nu^\ell}{2\nu}\,\mathrm{d}\eta\,\mathrm{d}\nu=\frac{1}{2k}\int_0^\varepsilon\nu^{k+\ell-1}\,\mathrm{d}\eta=\infty. \tag{5.4.14}$$

We thus conclude $\mathfrak{M}=\infty$, which, by Theorem 5.3.1, proves the claimed statement. □

Remark 5.4.2. *(a) The assumption* (5.4.2) *on the period function is rather natural: It means that the particles in the steady state configuration with the longest radial period are those with the largest energy $E=E_0$ and the smallest L-value $L=L_0$. Notice that, by the monotonicities of $r_\pm$, these particles correspond to the largest radial orbits in the steady state configuration. For instance,* (5.4.2) *would be true if the radial period function would be non-decreasing in E and non-increasing in L, i.e.,*

$$\partial_E T\geq 0\quad\&\quad\partial_L T\leq 0\qquad\text{on }\mathbb{D}_0. \tag{5.4.15}$$

[155] It can, in fact, be shown that the integral on the right-hand side of (5.4.13) is infinite if, and only if, $k+\ell\leq 0$.

Unfortunately, we are not able to prove (5.4.2) *for any steady state, and even less so for the anisotropic steady states considered in the theorem above. Some mathematical evidence why* (5.4.15) *should be true and ideas towards a proof of it are discussed in Section A.3.3.*

Nonetheless, the numerical simulations in Section 8.2 indicate that (5.4.2) *is true for a large class of steady states including polytropes with parameters satisfying* (5.4.1)*, see Observation 8.2.8.*

(b) *In the above proof, we verify the criterion from Theorem 5.3.1 by showing that* $\mathfrak{M}$ *is infinite, although it would suffice to prove* $\mathfrak{M} > 1$*. This is achieved by assuming that* T *attains its supremum at* (E_0, L_0) *and that* φ *is not too regular at* (E_0, L_0)*. In Section 6.4, we shall see in a different situation that sufficiently high regularity of the steady state at* (E_0, L_0) *leads to the absence of eigenvalues of* $\mathcal{L}$ *in* $\mathcal{G}$*. However, the numerical simulations from Section 8.3 indicate that the regularity of the steady state (at* (E_0, L_0)*) alone does not determine whether there exists an eigenvalue, cf. Observation 8.3.6.*

(c) *The first three conditions from* (5.4.1) *make sure that the associated steady state satisfies the general assumptions (*φ*1)–(*φ*5). The fourth condition from* (5.4.1) *guarantees that (the microscopic equation of state* φ *associated to) the steady state is not too regular at* (E_0, L_0)*. As only the behaviour of* φ *close to* (E_0, L_0) *is relevant for the above proof, one could obtain the existence of an oscillatory mode for a non-polytropic steady state in an analogous way as long as*

$$\Phi(\eta) \gtrsim \eta^k, \qquad 0 < \eta \ll 1, \tag{5.4.16}$$

for k *satisfying* (5.4.1)*.*

As an aside, we note that in the polytropic case (1.2.5)*, the whole analysis of Chapters 2–5 can also be carried out with parameters* $L_0 > 0$*,* $k > 0$*, and* $\ell > -1$ *satisfying* $k < 3\ell + \frac{7}{2}$ *and* $k + \ell + \frac{1}{2} > 0$*. This is done in [62] and then leads to a slightly more general version of the above theorem, cf. [62, Thm. 8.15]. Here, we prefer to include the assumption* $\ell > -\frac{1}{2}$ *in the polytropic situation in order to be able to present the arguments in the polytropic and non-polytropic cases in a more unified way.*

The second application of the criteria from Section 5.3 originates from [85, Cor. 4.16]. It shows that if the supremum of the radial period function T on $\mathbb{D}_0$ is attained as a maximum on this set, there exists an oscillatory mode in the essential gap. Recall that the set $\mathbb{D}_0$ is open and $(E_0, L_0) \in \partial\mathbb{D}_0$. However, we note in advance that it is not to be expected that this assumption on T is satisfied by many steady states. On the contrary, during the numerical study in Section 8.2, we have not seen a single steady state where it is satisfied, cf. Observation 8.2.9.

Corollary 5.4.3 (Existence of Oscillatory Modes if T Attains Maximum on $\mathbb{D}_0$)**.** *Assume that there exists* $(E^*, L^*) \in \mathbb{D}_0$ *s.t.*

$$T(E^*, L^*) = \sup_{\mathbb{D}_0} T. \tag{5.4.17}$$

Then the linearised operator $\mathcal{L}$ *possesses an eigenvalue in the essential gap* $\mathcal{G}$*.*

Proof. We start by proceeding as in the proof of Theorem 5.4.1: For any $F \in L^2([R_{\min}, R_{\max}])$ with $\|F\|_2 = 1$ there holds the estimate (5.4.4) with $T(E_0, L_0)$ replaced by

$T(E^*, L^*)$. The same arguments as above again yield that $r_{\frac{1}{2}} = r_{\frac{1}{2}}(E, L)$ and $\theta = \theta(r, E, L)$ are continuous with $\theta(r_{\frac{1}{2}}(E^*, L^*), E^*, L^*) = \frac{1}{4}$, recall (5.4.7) and Lemma 4.3.4 for the definitions of these quantities, respectively. Hence, there exist an open interval $I \subset [R_{\min}, R_{\max}]$ which contains $r_{\frac{1}{2}}(E^*, L^*) > 0$ and which is bounded away from $r = 0$ as well as some $\varepsilon > 0$ with $\overline{B}_\varepsilon(E^*, L^*) \subset \mathbb{D}_0$ s.t.

$$\sin(2\pi\,\theta(r, E, L)) \geq \frac{1}{2}, \qquad (E, L) \in B_\varepsilon(E^*, L^*),\, r \in I. \tag{5.4.18}$$

Similar to (5.4.10), choosing $F \coloneqq |I|^{-\frac{1}{2}}\, \mathbb{1}_I$ in (5.4.4) yields

$$\mathfrak{M} \geq c \int_{B_\varepsilon(E^*, L^*)} \frac{|\varphi'(E, L)|}{T(E^*, L^*) - T(E, L)}\, \mathrm{d}(E, L), \tag{5.4.19}$$

where $c > 0$ is some constant depending on the steady state. By Remark 4.2.4 (d), $|\varphi'|$ is bounded away from zero on $B_\varepsilon(E^*, L^*)$. Moreover, since T is twice continuously differentiable on $\mathbb{D}_0$ by Lemma A.3.3, the assumption (5.4.17) implies $\partial_E T(E^*, L^*) = 0 = \partial_L T(E^*, L^*)$ and thus, by Taylor's theorem,

$$0 \leq T(E^*, L^*) - T(E, L) \leq C|(E^*, L^*) - (E, L)|^2, \qquad (E, L) \in B_\varepsilon(E^*, L^*), \tag{5.4.20}$$

for some constant $C > 0$. Inserting these findings into (5.4.19) hence shows

$$\mathfrak{M} \geq c \int_{B_\varepsilon(E^*, L^*)} \frac{\mathrm{d}(E, L)}{|(E^*, L^*) - (E, L)|^2} = \infty, \tag{5.4.21}$$

from which we conclude the claimed statement by Theorem 5.3.1. □

The last application we present here shows that for certain steady states, the amount of eigenvalues of the linearised operator $\mathcal{L}$ in the essential gap $\mathcal{G}$ is finite, i.e., there is no accumulation of eigenvalues at $\sup(\mathcal{G}) = \inf(\sigma_{\mathrm{ess}}(\mathcal{L}))$. This result will again require suitable assumptions on the behaviour of the radial period function T. The result is inspired by [117, Cor. 1.3], where a similar statement is shown for a larger class of steady states, but under more assumptions on T.[156] As discussed in Remark 5.3.4, the results in [117] rely on a bound on the amount of eigenvalues of $\mathcal{L}$ in $\mathcal{G}$ which is qualitatively different from Theorem 5.3.3. Furthermore, the following result is related to [85, Lemma 4.9]; the class of steady states and some calculations in the proof are also similar to [85, Cor. 4.17].

Corollary 5.4.4 (Finitely Many Eigenvalues in $\mathcal{G}$ for Some Isotropic Polytropes)**.** *Consider an isotropic polytropic steady state* (1.2.3) *with polytropic exponent* $1 < k < \frac{7}{2}$*. Assume that the period function* T *"attains" its supremum on the* (E, L)*-support* $\mathbb{D}_0$ *(given by* (2.2.88)*) only at* $(E_0, L_0) = (E_0, 0)$*, i.e.,*

$$\sup_{\mathbb{D}_0} T = T(E_0, 0) \qquad \textit{and} \qquad T < T(E_0, 0) \text{ on } \overline{\mathbb{D}}_0 \setminus \{(E_0, 0)\}. \tag{5.4.22}$$

[156] In our notation, [117, Cor. 1.3] shows that there are finitely many eigenvalues of $\mathcal{L}$ in $\mathcal{G}$ for all isotropic polytropes with polytropic exponents $0 < k < \frac{7}{2}$ provided $T(E_0, 0) = \sup_{\mathbb{D}_0}(T)$ with $\partial_L^2(\frac{1}{T})(E_0, 0) > 0$ and $\partial_E T(E_0, 0) > 0$. Notice that the latter property is rigorously established for all isotropic steady states in Lemma A.3.23, which originates from [85, Lemma 3.15]. Although not explicitly stated in [117, Cor. 1.3], the first line of the calculations in [117, Sc. 5] shows that it is additionally assumed that the maximum of T on $\overline{\mathbb{D}}_0$ is attained *only* at $(E_0, 0)$.

Here, $T(\cdot,0)$ denotes the continuous extension of T to $L = 0$ mentioned in Remark 2.2.17 (a), and we assume that this extension is continuously differentiable, so that[157]

$$T \in C^1(\overline{\mathbb{D}}_0). \tag{5.4.23}$$

Then the amount of eigenvalues of the linearised operator $\mathcal{L}$ in the essential gap $\mathcal{G}$ is finite.

Proof. By Theorem 5.3.3, it remains to show that the right-hand side of (5.3.5) is finite. A straight-forward to derive estimate of this expression is

$$C \int_{\mathbb{D}_0} \frac{|\varphi'(E)|}{\sup_{\mathbb{D}_0} T - T(E,L)} \int_{r_-(E,L)}^{r_+(E,L)} \frac{\mathrm{d}r}{r^2}\, \mathrm{d}(E,L) \leq C \int_{\mathbb{D}_0} \frac{|\varphi'(E)|}{T(E_0,0) - T(E,L)} \frac{\mathrm{d}(E,L)}{r_-(E,L)}, \tag{5.4.24}$$

where $C > 0$ is some constant depending on the steady state. To estimate the $\frac{1}{r_-(E,L)}$-factor, note that $\Psi_L(r_-(E,L)) = E$ implies

$$\frac{1}{r_-(E,L)} = \frac{\sqrt{2E - 2U_0(r_-(E,L))}}{\sqrt{L}} \leq \frac{\sqrt{2E_0 - 2U_0(0)}}{\sqrt{L}} = \frac{\sqrt{2\kappa}}{\sqrt{L}}. \tag{5.4.25}$$

This shows that the integral on the right-hand side of (5.4.24) is finite if one bounds the domain of integration away from $(E_0,0) \in \partial\mathbb{D}_0$, i.e., away from the only point where the denominator vanishes. To see that the integral also remains finite in the region around $(E_0,0)$, let $\varepsilon > 0$ be s.t.

$$\partial_E T > 0 \qquad \text{on } N_\varepsilon \coloneqq [E_0 - \varepsilon, E_0] \times [0,\varepsilon] \subset \overline{\mathbb{D}}_0; \tag{5.4.26}$$

such ε exists by (5.4.23) and Lemma A.3.23. Hence, by the mean value theorem,

$$T(E_0,0) - T(E,L) \geq T(E_0,L) - T(E,L) \geq \frac{1}{C}\,(E_0 - E) \tag{5.4.27}$$

for $(E,L) \in N_\varepsilon$. Restricting the integral on the right-hand side of (5.4.24) to N_ε and using this estimate as well as (5.4.25) yields

$$\int_{N_\varepsilon} \frac{|\varphi'(E)|}{T(E_0,0) - T(E,L)} \frac{\mathrm{d}(E,L)}{r_-(E,L)} \leq C \int_{N_\varepsilon} \frac{(E_0 - E)^{k-1}}{E_0 - E} \frac{\mathrm{d}(E,L)}{\sqrt{L}}. \tag{5.4.28}$$

The latter integral is finite since $k > 1$. □

We emphasise that the numerical simulations from Section 8.2 indicate that the assumption (5.4.22) holds for all isotropic polytropes, cf. Observation 8.2.4.

[157] Notice that T can be extended in a continuously differentiable way on $\partial\mathbb{D}_0 \setminus \{L = 0\}$ by the results from Section A.4, see Lemmas A.4.6 and A.4.8 and Remark A.4.7. Showing that T can be extended to $L = 0$ in a continuously differentiable way should be possible by applying the arguments from [85, Thm. 3.13] to the integral representations of $\partial_E T$ and $\partial_L T$ derived in Lemmas A.3.9 and A.3.16.

Chapter 6

Damping

The primary focus of this thesis so far has been to show the existence of oscillatory modes around as many steady states as possible. The goal of this chapter is to prove the opposite statement: the linearised dynamics around (other) steady states are damped.

To achieve this, we deviate from the previous setting and add a point mass fixed at the spatial origin to the Vlasov-Poisson system. This new system will be introduced in Section 6.1, the existence of steady states will be discussed in Section 6.2. The advantage of the point mass is that all crucial properties of a steady state – like the behaviour of its radial particle periods – are known as long as the steady state is "small" compared to the point mass. The precise meaning of the steady state being "small" and the corresponding limiting behaviour will be discussed in Section 6.2.1. Subsequently, we will analyse the linearised Vlasov-Poisson system as well as the linearised operators associated to such steady states. We shall see that all occurring operators behave similarly to the case without a point mass, so that we can apply the methods from Chapters 4 and 5 once again. In Section 6.4, we will then prove that for a small and sufficiently regular steady state, no eigenvalues of the linearised operator exist in the essential gap of its spectrum. The other part is to establish the absence of eigenvalues embedded into the essential spectrum of the linearised operator. This will be done in Section 6.5 and is the crucial part of this chapter. In the final section, all these results are combined with the analysis from Appendix C to conclude that solutions of the linearised system associated to such steady states are indeed damped in a suitable way.

This whole chapter is mainly based on [61], where the same questions are studied in a slightly different (and easier) setting.

6.1 The Radial Vlasov-Poisson System Around a Point Mass

Throughout this chapter, we consider the radial Vlasov-Poisson system with a point mass $M > 0$ fixed at the radial origin $r = 0$. The point mass resembles a compact, static object, and our aim is to model the matter surrounding it. This is a simple (i.e., Newtonian) model for a galaxy surrounding a black hole. Including the gravitational force of the point mass into the radial Vlasov-Poisson system (2.1.9)–(2.1.11) leads to the system

$$\partial_t f + w\,\partial_r f - \left(U' + \frac{M}{r^2} - \frac{L}{r^3}\right)\partial_w f = 0, \tag{6.1.1}$$

$$U'(t,r) = \frac{4\pi}{r^2}\int_0^r s^2\rho(t,s)\,\mathrm{d}s, \qquad \lim_{r\to\infty} U(t,r) = 0, \tag{6.1.2}$$

$$\rho(t,r) = \frac{\pi}{r^2}\int_0^\infty \int_{\mathbb{R}} f(t,r,w,L)\,\mathrm{d}w\,\mathrm{d}L, \tag{6.1.3}$$

for the spherically symmetric phase space density $f = f(t,r,w,L)$. Recall Section 2.1 for the definition of spherical symmetry and the radial variables (r,w,L). Notice that the gravitational potential $U = U(t,r)$ does not include the gravitational force of the point mass, but only the one of the matter surrounding it. We refer to the system (6.1.1)–(6.1.3) as the *radial Vlasov-Poisson system around a point mass*. In Cartesian coordinates $(x,v) \in \mathbb{R}^3 \times \mathbb{R}^3$, the system is given by (1.1.3)–(1.1.5) and (1.2.28).

In [157], the existence of classical solutions of (6.1.1)–(6.1.3) is studied. Due to the (singular) point mass located at the radial origin $r = 0$, any smooth solution has to vanish at $r = 0$. In [157, Thm. 2.1], it is proven that any spherically symmetric, compactly supported, smooth initial distribution $\mathring{f}$ which possesses an L-vacuum at the centre, i.e., $\mathring{f}(r,w,L) = 0$ for $L \leq L_1$ for some $L_1 > 0$, launches a unique classical solution of (6.1.1)–(6.1.3).

6.2 Steady States Around a Point Mass

In this section we construct and analyse stationary solutions of the radial Vlasov-Poisson system around a point mass. The approach is very similar to the case without a point mass, cf. Section 2.2, which is why we will present the arguments here rather concisely.

For the stationary phase space density f_0 we make the ansatz

$$f_0(x,v) = \varphi(E(x,v), L(x,v)), \qquad (x,v) \in (\mathbb{R}^3 \setminus \{0\}) \times \mathbb{R}^3, \tag{6.2.1}$$

where, as before, $L(x,v) = |x \times v|^2$ is the squared modulus of the angular momentum and

$$E(x,v) = \frac{1}{2}|v|^2 + U_0(x) - \frac{M}{|x|}, \qquad (x,v) \in (\mathbb{R}^3 \setminus \{0\}) \times \mathbb{R}^3, \tag{6.2.2}$$

is the particle energy. Similar to Definition 2.2.2, f_0 is a *steady state* of the system (6.1.1)–(6.1.3) if U_0 is the gravitational potential induced by f_0 via the radial Poisson equation

$$U_0'(r) = \frac{m_0(r)}{r^2}, \quad r > 0, \qquad \lim_{r\to\infty} U_0(r) = 0, \tag{6.2.3}$$

where m_0 is the local mass of the steady state, i.e.,

$$m_0(r) \coloneqq 4\pi \int_0^r s^2 \rho_0(s)\,\mathrm{d}s, \qquad r > 0, \tag{6.2.4}$$

induced by the stationary mass density

$$\rho_0(r) \coloneqq \frac{\pi}{r^2}\int_0^\infty \int_{\mathbb{R}} f_0(r,w,L)\,\mathrm{d}w\,\mathrm{d}L, \qquad r > 0. \tag{6.2.5}$$

We choose an ansatz function of the polytropic form

$$\varphi(E,L) \coloneqq \varepsilon\,\tilde{\varphi}(E,L) \coloneqq \varepsilon\,(E_0 - E)_+^k\,(L - L_0)_+^\ell, \qquad E, L \in \mathbb{R}, \tag{6.2.6}$$

where $\varepsilon > 0$ is a parameter which we will use later to control the size of the steady state. We again employ the convention (2.2.13) regarding $(\ldots)_+^\alpha$. To ensure that the steady state is

bounded away from the (singular) point mass, we take $L_0 > 0$. For the polytropic exponents $k, \ell \in \mathbb{R}$ we require[158]

$$k > 0, \qquad \ell > -1, \qquad k + \ell > -\frac{1}{2}, \tag{6.2.7}$$

for now. The cut-off energy $E_0 < 0$ is determined implicitly through the other parameters, cf. below. We note that it is straight-forward to extend the following analysis to a more general class of ansatz functions, more precisely, to all sufficiently smooth $\tilde{\varphi}$ which satisfy the conditions (φ1)–(φ5) from the case without a point mass with $L_0 > 0$. However, we believe that the findings of this chapter can be presented more clearly when considering only polytropic equations of states.

In order to construct a steady state of the form (6.2.1), we repeat the calculations (2.2.20)–(2.2.27) to deduce that the relation (6.2.5) can be rewritten as

$$\rho_0(r) = \varepsilon\, r^{2\ell} g\bigg(E_0 - U_0(r) + \frac{M}{r} - \frac{L_0}{2r^2}\bigg), \qquad r > 0, \tag{6.2.8}$$

with $g\colon \mathbb{R} \to [0, \infty[$ being determined by the polytropic exponents k and ℓ. Concretely, analogous to Remark 2.2.7, the function g is of the explicit form

$$g(z) = c_{k,\ell}\, z_+^{k+\ell+\frac{3}{2}}, \qquad z \in \mathbb{R}, \tag{6.2.9}$$

where the constant $c_{k,\ell} > 0$ is given by (2.2.30). By the assumption (6.2.7) on the range of the polytropic exponents,

$$g \in C^1(\mathbb{R}) \cap C^\infty(\mathbb{R} \setminus \{0\}). \tag{6.2.10}$$

With ρ_0 given by (6.2.8), the search for a steady state is reduced to solving the integro-differential equation (6.2.3) for U_0. Inspired by [130], we again solve this equation by considering the function

$$y \coloneqq E_0 - U_0 \tag{6.2.11}$$

instead of U_0. The resulting equation for y is

$$y'(r) = -\frac{4\pi}{r^2} \int_0^r s^{2\ell+2} g\bigg(y(s) + \frac{M}{s} - \frac{L_0}{2s^2}\bigg)\, \mathrm{d}s, \qquad r > 0. \tag{6.2.12}$$

We again equip this equation with the boundary/initial conditions

$$y(0) = \kappa, \qquad y'(0) = 0, \tag{6.2.13}$$

for some prescribed $\kappa \in \mathbb{R}$; below we will derive the suitable range for the parameter κ. We note that the whole steady state including the function y need not be defined at $r = 0$. For solving the y-equation (6.2.12) it is, however, convenient to extend y to $r = 0$; we shall see next that this can be done without any difficulties. The same arguments as in Lemma 2.2.8 show that for every $\kappa \in \mathbb{R}$ there exists a unique solution $y \in C^2([0, \infty[)$ of (6.2.12)–(6.2.13). This solution possesses a vacuum region around the spatial origin, i.e., there exists $R_{\min} > 0$ s.t.

$$y(r) = \kappa, \quad y'(r) = 0, \quad \rho_0(r) = 0, \qquad 0 \le r \le R_{\min}. \tag{6.2.14}$$

[158] Note that the range of these parameters is larger than in the anisotropic polytropic case without a point mass, recall (4.1.5). As already noted before, cf. Remark 5.4.2 (c), the analysis in the case without a point mass could, in fact, also be carried out with a polytropic ansatz (2.2.17) with parameters satisfying (6.2.7), $k < 3\ell + \frac{7}{2}$, and $L_0 > 0$.

The maximal radius $R_{\min}$ with this property is explicitly given by

$$R_{\min} \coloneqq \begin{cases} \frac{-M+\sqrt{M^2+2\kappa L_0}}{2\kappa}, & \text{if } \kappa > 0 \text{ or } -\frac{M^2}{2L_0} < \kappa < 0, \\ \frac{L_0}{2M}, & \text{if } \kappa = 0, \\ \infty, & \text{if } \kappa \leq -\frac{M^2}{2L_0}. \end{cases} \tag{6.2.15}$$

In particular, choosing $\kappa \leq -\frac{M^2}{2L_0}$ results in the trivial solution $y \equiv \kappa$, $\rho_0 \equiv 0 \equiv U_0$. For this reason, we always assume $\kappa > -\frac{M^2}{2L_0}$. For the later analysis, we further restrict the range of κ to

$$-\frac{M^2}{2L_0} < \kappa < 0. \tag{6.2.16}$$

Let us briefly motivate this choice of the κ-range:

Remark 6.2.1. *The crucial part of Section 2.2 is to show that the steady state is compactly supported, i.e., to show that* $\operatorname{supp}(\rho_0)$ *is compact. In the present setting, however, it is trivial to see that the support of* ρ_0 *is compact in the case* $\kappa \leq 0$*: any solution* y *of* (6.2.12) *is non-increasing, and thus the initial condition* (6.2.13) *with* $\kappa \leq 0$ *leads to* $\lim_{r\to\infty} y(r) < 0$*, which implies that* $\operatorname{supp}(\rho_0)$ *is indeed bounded. Due to this reason, the associated steady states in the case* $\kappa \leq 0$ *are called* trivially bounded*. Similarly, in the case* $\kappa < 0$*, using the estimate* $y(r) \leq y(0) = \kappa < 0$ *yields the following bound on the support of* ρ_0*:*

$$\rho_0(r) = 0 \qquad \text{for } r \geq \frac{-M-\sqrt{M^2+2\kappa L_0}}{2\kappa}. \tag{6.2.17}$$

In particular, this bound is uniform in the parameter $\varepsilon > 0$ *and will turn out to be essential when considering the limit* $\varepsilon \to 0$ *later on. Notice that for this argument, no further restrictions on the polytropic exponents* k *and* ℓ *need to be imposed (besides* (6.2.7)*). In particular,* k *can be chosen arbitrarily large, which was not possible in the case without a point mass, cf. Remark 2.2.5 (d).*

Nonetheless, we note that choosing $\kappa > 0$ *also leads to a compactly supported steady state around the point mass. This can be shown similarly to Lemma 2.2.8. However, for* $\kappa \geq 0$*, the support need not be uniformly bounded in* ε*.*

Once a solution y of (6.2.12)–(6.2.13) with κ satisfying (6.2.16) is known, the cut-off energy E_0 and the stationary potential U_0 can be obtained via

$$E_0 \coloneqq \lim_{r\to\infty} y(r) \in \left]-\infty, 0\right[, \qquad U_0 \coloneqq E_0 - y. \tag{6.2.18}$$

The resulting steady state f_0 is then given by (6.2.1). Let us collect the properties of this steady state.

Proposition 6.2.2 (Existence of Steady States Around a Point Mass)**.** *Let* φ *be an ansatz function of the form* (6.2.6) *with parameters* $\varepsilon > 0$*,* $L_0 > 0$*, and polytropic exponents* k*,* ℓ *satisfying* (6.2.7)*. In addition, let* κ *be in the range specified in* (6.2.16)*. Then there exists a steady state* f_0 *of the radial Vlasov-Poisson system around a point mass* (6.1.1)–(6.1.3) *of the form* (6.2.1) *with* E_0 *and* U_0 *given by* (6.2.18)*. This steady state enjoys the following properties:*

(a) The total mass

$$M_0 \coloneqq \lim_{r\to\infty} m_0(r) = 4\pi \int_0^\infty r^2 \rho_0(r)\,\mathrm{d}r \tag{6.2.19}$$

of the steady state is positive & finite. Notice that M_0 *gives the mass of the steady state only; it does not contain the fixed point mass* $M > 0$*.*

(b) The steady state is radially bounded, i.e.,

$$R_{\max} \coloneqq \sup\{r \geq 0 \mid \rho_0(r) > 0\} < \infty. \tag{6.2.20}$$

(c) The radial support of the steady state is given by

$$\operatorname{supp}(\rho_0) = [R_{\min}, R_{\max}], \tag{6.2.21}$$

where

$$R_{\min} \coloneqq \frac{-M + \sqrt{M^2 + 2\kappa L_0}}{2\kappa} =: R^0_{\min} > 0, \tag{6.2.22}$$

$$R_{\min} < R_{\max} < \frac{-M - \sqrt{M^2 + 2\kappa L_0}}{2\kappa} =: R^0_{\max}. \tag{6.2.23}$$

Due to (6.2.21)*, we sometimes refer to the steady state as a stationary* shell *surrounding the point mass.*

(d) The (phase space) support of the steady state is bounded, i.e., the set Ω_0 defined as in (2.2.44) *or* (2.2.45) *is bounded.*

(e) It holds that $\rho_0 \in C^1([0,\infty[)$ and $U_0 \in C^3([0,\infty[)$. In addition, $U_0, \rho_0 \in C^\infty([0,\infty[\setminus\{R_{\min}, R_{\max}\})$.

Proof. All statements were either proven above or follow in the same way as in Proposition 2.2.9. □

Before introducing and analysing further quantities associated to a steady state, let us briefly review alternative approaches to construct steady states around a point mass.

Remark 6.2.3. *In [157], the existence of polytropic steady states (with fixed ε and a smaller range for the polytropic exponents k and ℓ compared to* (6.2.7)*) is shown via the variational approach developed in [55]. In this way, one also obtains the non-linear stability of these steady states. We shall see later that the steady states constructed in Proposition 6.2.2 are linearly stable, cf. Section 6.3. We note that, after suitably adjusting the range* (6.2.7) *of the polytropic exponents, the present steady states can also be shown to be non-linearly stable by applying the methods from [57, 59], cf. [121].*

Another approach to construct "small" steady states is to interpret them as a perturbation of the trivial solution. Mathematically, the existence of such perturbations which solve the (stationary) Vlasov-Poisson system with a point mass can be derived by applying the implicit function theorem. In the case of the Einstein-Vlasov system with a black hole at the centre – which is the general relativistic analogue of the present setting – this strategy is pursued in [72, 73]. In this general relativistic setting, the existence of steady states surrounding a black hole is also proven in [49, 137] using similar methods as those presented above.

An important quantity associated to a fixed steady state f_0 as constructed above is its effective potential. In the case without a point mass, this function is analysed in detail in Section 2.2.1. In the present setting, we obtain similar results.

Definition & Lemma 6.2.4 (The Effective Potential)**.** *For $L > 0$ let*

$$\Psi_L \colon]0,\infty[\to \mathbb{R},\ \Psi_L(r) \coloneqq U_0(r) - \frac{M}{r} + \frac{L}{2r^2}. \tag{6.2.24}$$

This function is called the effective potential *of the underlying steady state. It has the same properties as those derived in Lemma 2.2.12, i.e., there exists a unique minimising radius* $r_L > 0$ *s.t.*

$$\Psi_L(r_L) = \min_{]0,\infty[} \Psi_L =: E_L^{\min} \in]-\infty, 0[, \tag{6.2.25}$$

and for every $E \in]E_L^{\min}, 0[$ *there exist two unique radii* $0 < r_-(E,L) < r_L < r_+(E,L) < \infty$ *s.t.*

$$\Psi_L(r_\pm(E,L)) = E. \tag{6.2.26}$$

In addition, the regularity and limiting statements from Lemma 2.2.14 hold, where $m_0(r)$ *and* M_0 *have to be replaced with* $m_0(r) + M$ *and* $M_0 + M$*, respectively.*

Proof. The assertions can be proven similarly to the case without a point mass. □

We note that the radii $r_\pm$ are related to $R_{\min}$ and $R_{\max}$ as follows:

$$R_{\min} = r_-(E_0, L_0), \qquad R_{\max} = r_+(E_0, L_0). \tag{6.2.27}$$

The effective potential appears naturally when expressing the particle energy E, cf. (6.2.2), in radial variables. Concretely,

$$E(r, w, L) = \frac{1}{2}w^2 + \Psi_L(r), \qquad (r, w, L) \in]0, \infty[\times \mathbb{R} \times]0, \infty[. \tag{6.2.28}$$

This shows that the (E, L)-support of the steady state is

$$\mathbb{D}_0 := \{(E, L) \mid L > L_0,\ E_L^{\min} < E < E_0\}. \tag{6.2.29}$$

The shape of this set is visualised in Figure 2.2.2; it is similar to the case without a point mass. In analogy to (2.2.86) and (2.2.90), the L-support of the steady state is of the form

$$\mathbb{L}_0 := \{L \mid (E, L) \in \mathbb{D}_0\} =]L_0, L_{\max}[, \tag{6.2.30}$$

where $L_{\max} \in]L_0, \infty[$ is given as the unique solution of

$$E_{L_{\max}}^{\min} = E_0. \tag{6.2.31}$$

The set $\mathbb{D}_0$ is a subset of the set of all admissible (E, L)-pairs

$$\mathbb{A}_0 := \{(E, L) \mid L > 0,\ E_L^{\min} < E < 0\}. \tag{6.2.32}$$

By the regularity of $]0, \infty[\ni L \mapsto E_L^{\min}$, the sets $\mathbb{D}_0$ and $\mathbb{A}_0$ are both open subsets of $\mathbb{R}^2$. Similar to Section 2.2.2, being "admissible" means that any solution of the radial characteristic system

$$\dot{r} = w, \qquad \dot{w} = -\Psi_L'(r), \tag{6.2.33}$$

with parameter L and conserved energy value E is time-periodic provided $(E, L) \in \mathbb{A}_0$. In analogy to Definition 2.2.16, the periods of these solutions are given by the (radial) period function

$$T\colon \mathbb{A}_0 \to]0, \infty[,\ T(E, L) := 2 \int_{r_-(E,L)}^{r_+(E,L)} \frac{\mathrm{d}r}{\sqrt{2E - 2\Psi_L(r)}}. \tag{6.2.34}$$

Most of the properties of T are similar to the case without a point mass, cf. Appendix A. We will study further properties of this function within the analysis below.

6.2.1 Limiting Behaviour as $\varepsilon \to 0$

As motivated above, we are interested in steady states of the form (6.2.1) with $0 < \varepsilon \ll 1$. The reason for this is that all steady state quantities converge to explicitly known objects in the limit $\varepsilon \to 0$. Let us first collect these limiting quantities.

Lemma 6.2.5 (The Pure Point Mass Case)**.** *The pure point mass case corresponds to the situation where the gravity is solely determined by the point mass. The effective potential in this situation is*

$$\Psi_L^0 \colon]0,\infty[\to \mathbb{R},\ \Psi_L^0(r) \coloneqq -\frac{M}{r} + \frac{L}{2r^2} \tag{6.2.35}$$

for $L > 0$. This function has similar properties as the ones derived in Lemma 6.2.4: For $L > 0$, the minimum of Ψ_L^0 is attained at the radius

$$r_L^0 \coloneqq \frac{L}{M}; \tag{6.2.36}$$

the minimal value is given by

$$E_L^{\min 0} \coloneqq \Psi_L^0(r_L^0) = -\frac{M^2}{2L}. \tag{6.2.37}$$

Similar to (6.2.32) *let*

$$\mathbb{A}_0^0 \coloneqq \{(E,L) \mid L > 0,\ E_L^{\min 0} < E < 0\} \tag{6.2.38}$$

denote the set of admissible (E,L)-pairs in the pure point mass case. Setting

$$r_\pm^0(E,L) \coloneqq \frac{-M \mp \sqrt{M^2 + 2EL}}{2E}, \qquad (E,L) \in \mathbb{A}_0^0, \tag{6.2.39}$$

defines the two unique radii $0 < r_-^0(E,L) < r_L^0 < r_+^0(E,L)$ which solve $\Psi_L^0(r_\pm^0(E,L)) = E$. These radii are related to $R_{\min}^0$ and $R_{\max}^0$ defined in (6.2.22) *and* (6.2.23)*, respectively, via*

$$R_{\min}^0 = r_-^0(\kappa, L_0), \qquad R_{\max}^0 = r_+^0(\kappa, L_0). \tag{6.2.40}$$

The particle motions within the gravitational field of the point mass are described by $\dot r = w$, $\dot w = -(\Psi_L^0)'(r)$. Solutions of this ODE with parameter L and conserved energy value E are time-periodic provided $(E,L) \in \mathbb{A}_0$, and their periods are given by

$$T^0 \colon \mathbb{A}_0^0 \to]0,\infty[,\ T^0(E,L) \coloneqq 2\int_{r_-^0(E,L)}^{r_+^0(E,L)} \frac{\mathrm{d}r}{\sqrt{2E - 2\Psi_L^0(r)}} = \frac{\pi}{\sqrt{2}}\,\frac{M}{(-E)^{\frac{3}{2}}}. \tag{6.2.41}$$

Moreover, similar to (6.2.29)*, we set*

$$\mathbb{D}_0^0 \coloneqq \{(E,L) \mid L > L_0,\ E_L^{\min 0} < E < \kappa\} \tag{6.2.42}$$

for L_0 and κ as specified in Proposition 6.2.2. The L-values in this set are

$$\mathbb{L}_0^0 \coloneqq]L_0, L_{\max}^0[, \tag{6.2.43}$$

with maximal L-value given by

$$L_{\max}^0 = -\frac{M^2}{2\kappa}. \tag{6.2.44}$$

Proof. The only non-trivial part is the second equality in (6.2.41). To verify it, first observe

$$T^0(E,L) = 2\int_{r_-^0(E,L)}^{r_+^0(E,L)} \frac{\mathrm{d}r}{\sqrt{2E - 2\Psi_L^0(r)}} = \sqrt{2}\int_{r_-^0(E,L)}^{r_+^0(E,L)} \frac{\mathrm{d}r}{\sqrt{E + \frac{M}{r} - \frac{L}{2r^2}}} =$$
$$= \frac{\sqrt{2}}{\sqrt{-E}}\int_{r_-^0(E,L)}^{r_+^0(E,L)} \frac{r}{\sqrt{(r_+^0(E,L) - r)\,(r - r_-^0(E,L))}}\,\mathrm{d}r. \tag{6.2.45}$$

In order to compute this integral, we make the usual affine change of variables $s = \frac{r-r_-^0}{r_+^0 - r_-^0}$, where $r_\pm^0 \coloneqq r_\pm^0(E,L)$. We thus arrive at

$$T^0(E,L) = \frac{\sqrt{2}}{\sqrt{-E}}(r_+^0 - r_-^0)\int_0^1 \frac{\sqrt{s}}{\sqrt{1-s}}\,\mathrm{d}s + \frac{\sqrt{2}}{\sqrt{-E}}\,r_-^0\int_0^1 \frac{\mathrm{d}s}{\sqrt{s\,(1-s)}} =$$
$$= \frac{\pi}{\sqrt{-2E}}\big(r_+^0(E,L) + r_-^0(E,L)\big). \tag{6.2.46}$$

Inserting (6.2.39) into the latter expression then implies the claimed identity. □

We now fix the parameters L_0, k, ℓ, and κ as specified in Proposition 6.2.2 and study the limiting behaviour of the steady states as $\varepsilon \to 0$. In order to make the ε-dependency more visible, we add a superscript ε to all quantities associated to the steady state $f_0 = f_0^\varepsilon$ when analysing this limit – this is consistent with the notation chosen in Lemma 6.2.5 for the quantities in the pure point mass case corresponding to $\varepsilon = 0$. The following result is partially based on [61, Lemma 3.6].

Proposition 6.2.6 (Limiting Behaviour as $\varepsilon \to 0$)**.** *The following assertions hold:*

(a) The functions ρ_0^ε, $(\rho_0^\varepsilon)'$, m_0^ε, U_0^ε, $(U_0^\varepsilon)'$, $(U_0^\varepsilon)''$, and $(U_0^\varepsilon)'''$ converge to zero uniformly on $[0,\infty[$ as $\varepsilon \to 0$.

(b) $E_0^\varepsilon \to \kappa$ as well as $r_L^\varepsilon \to r_L^0$ and $E_L^{\min\varepsilon} \to E_L^{\min 0}$ locally uniformly in $L > 0$ as $\varepsilon \to 0$.

(c) $L_{\max}^\varepsilon \to L_{\max}^0$ as $\varepsilon \to 0$.

(d) $R_{\min}^\varepsilon = R_{\min}^0$ and $R_{\max}^\varepsilon \to R_{\max}^0$ as $\varepsilon \to 0$.

(e) For $\varepsilon \geq 0$ let

$$T_{\min}^\varepsilon \coloneqq \inf_{\mathbb{D}_0^\varepsilon} T^\varepsilon, \qquad \partial_E T_{\min}^\varepsilon \coloneqq \inf_{\mathbb{D}_0^\varepsilon} \partial_E T^\varepsilon, \qquad \partial_E^2 T_{\min}^\varepsilon \coloneqq \inf_{\mathbb{D}_0^\varepsilon} \partial_E^2 T^\varepsilon, \tag{6.2.47}$$
$$T_{\max}^\varepsilon \coloneqq \sup_{\mathbb{D}_0^\varepsilon} T^\varepsilon, \qquad \partial_E T_{\max}^\varepsilon \coloneqq \sup_{\mathbb{D}_0^\varepsilon} \partial_E T^\varepsilon, \qquad \partial_E^2 T_{\max}^\varepsilon \coloneqq \sup_{\mathbb{D}_0^\varepsilon} \partial_E^2 T^\varepsilon; \tag{6.2.48}$$

in particular, $T^\varepsilon \in C^2(\mathbb{A}_0^\varepsilon)$. Then $T_{\min}^\varepsilon \to T_{\min}^0$, $T_{\max}^\varepsilon \to T_{\max}^0$, $\partial_E T_{\min}^\varepsilon \to \partial_E T_{\min}^0$, $\partial_E T_{\max}^\varepsilon \to \partial_E T_{\max}^0$, $\partial_E^2 T_{\min}^\varepsilon \to \partial_E^2 T_{\min}^0$, and $\partial_E^2 T_{\max}^\varepsilon \to \partial_E^2 T_{\max}^0$ as $\varepsilon \to 0$. In particular, since $\partial_E T_{\min}^0 > 0$, there exist $c > 0$ and $\varepsilon_0 > 0$ s.t.

$$\partial_E T^\varepsilon \geq c \text{ on } \mathbb{D}_0^\varepsilon, \qquad 0 < \varepsilon < \varepsilon_0. \tag{6.2.49}$$

Before proving the above proposition let us briefly comment on the limiting behaviour.

Remark 6.2.7. *When we previously mentioned in vague terms that the steady state "gets small", we mainly meant the convergences stated in part (a), in particular, the total mass M_0^ε of the steady state tending to zero. However, it is crucial for the subsequent arguments to understand how precisely this "getting small" is realised. For instance, an alternative approach would be to keep $\varepsilon > 0$ fixed and instead let the parameter κ tend to $-\frac{M^2}{2L_0}$. This would also yield the convergences in part (a). However, as $\kappa \searrow -\frac{M^2}{2L_0}$, the steady state support would contract to a single point, more precisely, $R_{\min} \to r_{L_0}^0$ and $R_{\max} \to r_{L_0}^0$. This is qualitatively different from the limiting behaviour as $\varepsilon \to 0$, where the supports of "small" steady states do not contract but instead converge to a non-trivial limiting configuration. For the radial support, this is evident from part (d). We shall see later that it is crucial to realise the steady states "getting small" in this way.*

The proof of Proposition 6.2.6 is the subject of the remaining part of this section, and it is no fun. Part (a) will be proven in Lemma 6.2.8, part (b) follows by Lemmas 6.2.8 and 6.2.9, part (c) is due to Lemma 6.2.13, part (d) will be shown in Lemma 6.2.11, and part (e) follows by Lemmas 6.2.21, 6.2.22, and 6.2.26. Although one gains a lot of insights into the properties of steady states through the following arguments, we advise the reader to omit this part on a first reading and proceed with Sections 6.3–6.6. There, the applications of the results from Proposition 6.2.6 will become clear.

Convergence of the Potential, Mass Density, and Cut-Off Energy

The first step is to show that the mass density ρ_0^ε and the gravitational potential U_0^ε converges to zero as $\varepsilon \to 0$ in a suitable way. This forms the basis for all further convergence results. The lemma is based on [61, Lemma A.1], which is in turn inspired by [49, Lemma 3.3].

Lemma 6.2.8. *As $\varepsilon \to 0$ it holds that $\rho_0^\varepsilon, (\rho_0^\varepsilon)', m_0^\varepsilon \to 0$ uniformly on $[0,\infty[$, $M_0^\varepsilon \to 0$, $E_0^\varepsilon \to \kappa$, and $(U_0^\varepsilon)^{(n)} \to 0$ uniformly on $[0,\infty[$ for $n \in \{0,1,2,3\}$.*

Proof. By Proposition 6.2.2 (c) there holds $\operatorname{supp}(\rho_0^\varepsilon) \subset [R_{\min}^0, R_{\max}^0]$, and for $r \in [R_{\min}^0, R_{\max}^0]$ we obtain

$$\rho_0^\varepsilon(r) = \varepsilon\, r^{2\ell} g(E_0^\varepsilon - \Psi_L^\varepsilon(r)) \le \varepsilon\, c_{k,\ell} \max\{(R_{\min}^0)^{2\ell}, (R_{\max}^0)^{2\ell}\} \left(\kappa + \frac{M}{R_{\min}^0}\right)^{k+\ell+\frac{3}{2}} \tag{6.2.50}$$

by (6.2.7)–(6.2.9) since $E_0^\varepsilon - \Psi_L^\varepsilon(r) = y^\varepsilon(r) + \frac{M}{r} - \frac{L}{2r^2} \le \kappa + \frac{M}{R_{\min}^0}$. We hence conclude $\rho_0^\varepsilon \to 0$ uniformly on $[0,\infty[$. This also implies the uniform convergence of the local mass m_0^ε to 0 as $\varepsilon \to 0$. In particular, the total mass $M_0^\varepsilon = m_0^\varepsilon(R_{\max}^0)$ tends to 0 as $\varepsilon \to 0$. Because $(y^\varepsilon)'(r) = -\frac{m_0^\varepsilon(r)}{r^2}$ for $r > 0$ with $m_0^\varepsilon(r) = 0$ for $0 \le r \le R_{\min}^\varepsilon = R_{\min}^0$, cf. (6.2.12) and (6.2.14), we deduce $(y^\varepsilon)' \to 0$ as $\varepsilon \to 0$ uniformly on $[0,\infty[$. Next observe

$$y^\varepsilon(r) = \kappa + \int_0^r (y^\varepsilon)'(s)\,\mathrm{d}s, \qquad r \ge 0, \tag{6.2.51}$$

and thus

$$y^\varepsilon(r) = \kappa + \int_{R_{\min}^0}^{R_{\max}^0} (y^\varepsilon)'(s)\,\mathrm{d}s + \left(\frac{M_0^\varepsilon}{r} - \frac{M_0^\varepsilon}{R_{\max}^0}\right), \qquad r \ge R_{\max}^0. \tag{6.2.52}$$

This shows $y^\varepsilon \to \kappa$ uniformly on $[0,\infty[$ as well as $E_0^\varepsilon = \lim_{r\to\infty} y^\varepsilon(r) \to \kappa$ as $\varepsilon \to 0$. We have hence proven $(U_0^\varepsilon)^{(n)} \to 0$ uniformly on $[0,\infty[$ for $n \in \{0,1\}$, recall (6.2.18). The uniform

convergence of $(\rho_0^\varepsilon)'$ to 0 follows by the same arguments as above by differentiating (6.2.8); recall (6.2.7). Further differentiating (6.2.3) w.r.t. $r > 0$ yields

$$(U_0^\varepsilon)''(r) = 4\pi\rho_0^\varepsilon(r) - 2\frac{m_0^\varepsilon(r)}{r^3}, \tag{6.2.53}$$

$$(U_0^\varepsilon)'''(r) = 4\pi(\rho_0^\varepsilon)'(r) - 8\pi\frac{\rho_0^\varepsilon(r)}{r} + 6\frac{m_0^\varepsilon(r)}{r^4}, \tag{6.2.54}$$

from which we conclude the claimed uniform convergences of the second-order and third-order derivatives of U_0^ε. □

We note that in the case of a more regular steady state, corresponding to $k + \ell$ being larger, it is straight-forward to extend the above result to higher-order derivatives of ρ_0^ε and U_0^ε.

Convergence of the Radii r_L^ε and $r_\pm^\varepsilon$

The next step is to show the convergences of the radii r_L^ε and $r_\pm^\varepsilon = r_\pm^\varepsilon(E, L)$ defined by the effective potential Ψ_L^ε, cf. Definition 6.2.4, to the respective quantities introduced in Lemma 6.2.5. We start with the minimising radius r_L^ε and the associated minimal energy value $E_L^{\min\varepsilon}$. This is based on [61, Lemma A.2], but the proof is significantly simplified here.

Lemma 6.2.9. *The mappings* $[0,\infty[\,\times\,]0,\infty[\ni(\varepsilon,L)\mapsto r_L^\varepsilon$ *and* $[0,\infty[\,\times\,]0,\infty[\ni(\varepsilon,L)\mapsto E_L^{\min\varepsilon}$ *are both continuous at* $\varepsilon = 0$ *locally uniformly in* L. *More precisely, for any* $\delta > 0$ *and* $L_2 > L_1 > 0$ *there exists* $\varepsilon_0 > 0$ *s.t. for all* $0 \le \varepsilon < \varepsilon_0$, $L_1 \le L^* \le L_2$, *and* $L > 0$ *with* $|L - L^*| < \varepsilon_0$ *there holds* $|r_L^\varepsilon - r_{L^*}^0| < \delta$ *and* $|E_L^{\min\varepsilon} - E_{L^*}^{\min 0}| < \delta$.

Proof. For $\varepsilon \ge 0$ and $L > 0$, the radius r_L^ε is given as the unique critical point of Ψ_L^ε, i.e., it solves the equation

$$m_0^\varepsilon(r_L^\varepsilon) + M - \frac{L}{r_L^\varepsilon} = 0; \tag{6.2.55}$$

here we set $m_0^0 \equiv 0$. Solving this equation for r_L^ε and using (6.2.36) yields

$$|r_L^\varepsilon - r_{L^*}^0| = \left|\frac{L^*}{M} - \frac{L}{m_0^\varepsilon(r_L^\varepsilon) + M}\right| \le \frac{|L^* - L|}{M} + \frac{|L|}{M^2}\sup_{[0,\infty[}(m_0^\varepsilon). \tag{6.2.56}$$

The uniform convergence $m_0^\varepsilon \to 0$ as $\varepsilon \to 0$ proven in Lemma 6.2.8 hence shows the claimed continuity of r_L^ε.

Together with the uniform convergence $U_0^\varepsilon \to 0$ established in Lemma 6.2.8 we then deduce $E_L^{\min\varepsilon} = \Psi_L^\varepsilon(r_L^\varepsilon) \to \Psi_L^0(r_{L^*}^0) = E_{L^*}^{\min 0}$ locally uniformly in L^* as $\varepsilon \to 0$. More precisely, for δ, L_1, and L_2 as above we choose $0 < \varepsilon_0 < \min\{\frac{\delta}{8}(r^0_{\frac12 L_1})^2, \frac12 L_1, 1\}$ s.t. $|U_0^\varepsilon| \le \frac{\delta}{4}$ on $[0,\infty[$ and $|r_L^\varepsilon - r_L^0| < \min\{\frac12 r^0_{\frac12 L_1}, 1\}$ for $0 \le \varepsilon < \varepsilon_0$ and $\frac12 L_1 \le L \le L_2 + 1$. For ε, L^*, and L as in the statement of the lemma we then have $\frac12 r^0_{\frac12 L_1} \le r_L^\varepsilon, r_{L^*}^0 \le r^0_{L_2+1} + 1$, from which we obtain

$$|\Psi_L^\varepsilon(r_L^\varepsilon) - \Psi_{L^*}^0(r_L^\varepsilon)| \le |U_0^\varepsilon(r_L^\varepsilon)| + \frac{|L - L^*|}{2(r_L^\varepsilon)^2} \le \frac{\delta}{4} + 2\frac{|L - L^*|}{(r^0_{\frac12 L_1})^2} \le \frac{\delta}{2}. \tag{6.2.57}$$

We hence deduce

$$\begin{aligned}|E_L^{\min\varepsilon} - E_{L^*}^{\min 0}| &\le |\Psi_L^\varepsilon(r_L^\varepsilon) - \Psi_{L^*}^0(r_L^\varepsilon)| + |\Psi_{L^*}^0(r_L^\varepsilon) - \Psi_{L^*}^0(r_{L^*}^0)| \le \\ &\le \frac{\delta}{2} + \left|\frac{M}{r_L^\varepsilon} - \frac{M}{r_{L^*}^0}\right| + \left|\frac{L^*}{2(r_L^\varepsilon)^2} - \frac{L^*}{2(r_L^0)^2}\right|.\end{aligned} \tag{6.2.58}$$

Using the convergence of r_L^ε established above thus allows us to conclude $|E_L^{\min\varepsilon} - E_{L^*}^{\min 0}| < \delta$ after potentially shrinking $\varepsilon_0 > 0$. □

The next step is to establish the analogous convergence result for the radii $r_\pm^\varepsilon(E, L)$. For this sake let

$$\mathcal{A}_0 \coloneqq \{(\varepsilon, E, L) \mid \varepsilon \geq 0,\, (E, L) \in \mathbb{A}_0^\varepsilon\} \tag{6.2.59}$$

denote the set of all *admissible* (ε, E, L)*-triplets*; this notation is similar to [61, Eqn. (A.10)]. The following lemma is based on [61, Lemma A.3 (a)].

Lemma 6.2.10. *The mappings $\mathcal{A}_0 \ni (\varepsilon, E, L) \mapsto r_\pm^\varepsilon(E, L)$ are continuous at $\varepsilon = 0$ uniformly on suitably bounded (E, L)-sets. More precisely, for any $\delta > 0$, $L_2 > L_1 > 0$, and $E_1 < 0$ there exists $\varepsilon_0 > 0$ s.t. for all $0 \leq \varepsilon < \varepsilon_0$, $L_1 \leq L^* \leq L_2$, and $E_{L^*}^{\min 0} < E^* < E_1$ as well as $L > 0$ and $E_L^{\min\varepsilon} < E < E_1$ with $|(E, L) - (E^*, L^*)| < \varepsilon_0$ there holds $|r_\pm^\varepsilon(E, L) - r_\pm^0(E^*, L^*)| < \delta$.*

Proof. For $\varepsilon \geq 0$ and $(E, L) \in \mathbb{A}_0^\varepsilon$, the radii $r_\pm^\varepsilon(E, L)$ are the unique solutions of

$$E = \Psi_L^\varepsilon(r_\pm^\varepsilon(E, L)) = U_0^\varepsilon(r_\pm^\varepsilon(E, L)) + \Psi_L^0(r_\pm^\varepsilon(E, L)). \tag{6.2.60}$$

Hence, similar to (6.2.39), there holds the identity

$$r_\pm^\varepsilon(E, L) = \frac{-M \mp \sqrt{M^2 + 2L(E - U_0^\varepsilon(r_\pm^\varepsilon(E, L)))}}{2E - 2U_0^\varepsilon(r_\pm^\varepsilon(E, L))}. \tag{6.2.61}$$

Since $U_0^\varepsilon \to 0$ uniformly as $\varepsilon \to 0$ by Lemma 6.2.8, it is straight-forward to verify that the difference between this expression and $r_\pm^0(E^*, L^*)$ given by (6.2.39) can be estimated as follows provided that $\varepsilon_0 > 0$ is sufficiently small:

$$|r_\pm^\varepsilon(E, L) - r_\pm^0(E^*, L^*)| \leq C(|E - E^*| + |L - L^*| + \sup_{[0,\infty[} |U_0^\varepsilon|), \tag{6.2.62}$$

where $C > 0$ depends on E_1, L_1, and L_2, but is uniform in (E, L), (E^*, L^*), and ε. This estimate together with Lemma 6.2.8 readily implies the claimed continuity. □

An immediate consequence of the above lemmas is the convergence of $R_{\max}^\varepsilon$. This is based on [61, Eqn. (A.11)].

Lemma 6.2.11. $R_{\max}^\varepsilon \to R_{\max}^0$ *as* $\varepsilon \to 0$.

Proof. Since $R_{\max}^0 = r_+^0(\kappa, L_0)$ and $R_{\max}^\varepsilon = r_+^\varepsilon(E_0^\varepsilon, L_0)$ for $\varepsilon > 0$, cf. (6.2.40) and (6.2.27), respectively, the claim follows by Lemmas 6.2.8 and 6.2.10. □

Next, we show that the convergence (2.2.66) of $r_\pm^\varepsilon$ in the near circular regime is "uniform" in ε. The lemma is based on [61, Lemma A.3 (b)].

Lemma 6.2.12. *The radii $r_\pm^\varepsilon(E, L)$ converge to $r_{L^*}^0$ as $(\varepsilon, E, L) \to (0, E_{L^*}^{\min 0}, L^*)$ locally uniformly in $L^* > 0$. More precisely, for any $\delta > 0$ and $L_2 > L_1 > 0$ there exist $\varepsilon_0 > 0$ and $\eta > 0$ s.t. for all $0 \leq \varepsilon < \varepsilon_0$, $L_1 \leq L^* \leq L_2$, and $L > 0$ with $|L - L^*| < \varepsilon_0$ as well as $E_L^{\min\varepsilon} < E < E_L^{\min\varepsilon} + \eta$ there holds $|r_\pm^\varepsilon(E, L) - r_{L^*}^0| < \delta$.*

Proof. The convergence can be proven in a way similar to Lemma 6.2.10. More precisely, inserting $E^* = E_{L^*}^{\min 0}$ into (6.2.62) yields

$$|r_\pm^\varepsilon(E, L) - r_{L^*}^0| \leq C(|E - E_{L^*}^{\min 0}| + |L - L^*| + \sup_{[0,\infty[} |U_0^\varepsilon|) \tag{6.2.63}$$

for $C > 0$ as before provided that $\varepsilon_0 > 0$ and $\eta > 0$ are sufficiently small. Together with the uniform convergence $U_0^\varepsilon \to 0$ as $\varepsilon \to 0$ proven in Lemma 6.2.8 and the locally uniform convergence $E_L^{\min\varepsilon} \to E_{L^*}^{\min 0}$ as $(\varepsilon, L) \to (0, L^*)$ shown in Lemma 6.2.9, we conclude the claimed convergence. □

"Convergence" of $\mathbb{D}_0^\varepsilon$

The next step is to establish the convergence of the (E,L)-support $\mathbb{D}_0^\varepsilon$ to $\mathbb{D}_0^0$ as $\varepsilon \to 0$ in a suitable sense; recall (6.2.29) and (6.2.42) for the definitions of these sets. The first step in this direction is the convergence of the L-support, i.e., the convergence of $L_{\max}^\varepsilon$ to $L_{\max}^0$ as $\varepsilon \to 0$; recall (6.2.31) and (6.2.44) for the definitions of the latter two quantities.

Lemma 6.2.13. *$L_{\max}^\varepsilon \to L_{\max}^0$ as $\varepsilon \to 0$.*

Proof. For any $\delta > 0$ with $\delta < L_{\max}^0$ there holds $E^{\min 0}_{L_{\max}^0-\delta} - \kappa < 0 < E^{\min 0}_{L_{\max}^0+\delta} - \kappa$; note that $L_{\max}^0$ satisfies $E^{\min 0}_{L_{\max}^0} = \kappa$. By Lemmas 6.2.8 and 6.2.9, there exists $\varepsilon_0 > 0$ s.t. for all $0 \le \varepsilon < \varepsilon_0$ there holds $E^{\min \varepsilon}_{L_{\max}^0-\delta} - E_0^\varepsilon < 0 < E^{\min \varepsilon}_{L_{\max}^0+\delta} - E_0^\varepsilon$. Hence, $L_{\max}^0 - \delta < L_{\max}^\varepsilon < L_{\max}^0 + \delta$, which concludes the proof. □

A direct consequence of the convergence of the L-support is that the (E,L)-support $\mathbb{D}_0^\varepsilon$ is uniformly bounded for $\varepsilon \ll 1$.

Lemma 6.2.14. *There exist $\varepsilon_0 > 0$ and $L_1 > L_0$ s.t. the following assertions hold:*

(a) For every $0 \le \varepsilon < \varepsilon_0$ there holds $\mathbb{L}_0^\varepsilon \subset]L_0, L_1[$.

(b) For every $0 \le \varepsilon < \varepsilon_0$ there holds

$$\mathbb{D}_0^\varepsilon \subset \{(E,L) \mid L_0 < L < L_1,\, E_L^{\min \varepsilon} < E < \frac{\kappa}{2}\} \subset \left]-\frac{M^2}{2L_0} - 1, \frac{\kappa}{2}\right[\times]L_0, L_1[. \quad (6.2.64)$$

Proof. Part (a) follows by Lemma 6.2.13. The first inclusion in (6.2.64) is due to Lemma 6.2.8. For the second one, we apply Lemma 6.2.9 to infer $E_{L_0}^{\min \varepsilon} > E_{L_0}^{\min 0} - 1 = -\frac{M^2}{2L_0} - 1$ for $0 \le \varepsilon < \varepsilon_0$ after potentially shrinking $\varepsilon_0 > 0$. □

The next result establishes the desired convergence $\mathbb{D}_0^\varepsilon \to \mathbb{D}_0^0$ as $\varepsilon \to 0$ in a suitable way. Due to $\mathbb{D}_0^\varepsilon$ being two-dimensional, this is more complex than the convergence $\mathbb{L}_0^\varepsilon \to \mathbb{L}_0^0$.

Lemma 6.2.15. *For every $\delta > 0$ there exists $\varepsilon_0 > 0$ s.t. the following statements hold:*

(a) For every $(E^*, L^*) \in \mathbb{D}_0^0$ and $0 \le \varepsilon < \varepsilon_0$ there exists $(E,L) \in \mathbb{D}_0^\varepsilon$ s.t. $|(E,L) - (E^*,L^*)| < \delta$.

(b) For every $0 \le \varepsilon < \varepsilon_0$ and $(E,L) \in \mathbb{D}_0^\varepsilon$ there exists $(E^*,L^*) \in \mathbb{D}_0^0$ s.t. $|(E,L) - (E^*,L^*)| < \delta$.

Proof. Let $\delta > 0$ be arbitrary and choose $\varepsilon_0 > 0$ and $L_1 > L_0 > 0$ according to Lemma 6.2.14. In addition, we require $\varepsilon_0 < \frac{\delta}{2}$ and $\varepsilon_0 < L_{\max}^0 - L_0$ as well as $d := \kappa - E^{\min 0}_{L_{\max}^0-\varepsilon_0} < \delta$; the latter is possible since $L \mapsto E_L^{\min 0}$ is continuous. By Lemmas 6.2.8 and 6.2.9, there exists $\varepsilon_1 \in]0, \varepsilon_0[$ s.t. $|E_0^\varepsilon - \kappa| < \frac{d}{3}$ and $|E_L^{\min \varepsilon} - E_{L^*}^{\min 0}| < \frac{d}{3}$ for $0 \le \varepsilon < \varepsilon_1$, $L_0 \le L^* \le L_1$, and $L > 0$ with $|L - L^*| < \varepsilon_1$.

Now let $(E^*, L^*) \in \mathbb{D}_0^0$ and $0 \le \varepsilon < \varepsilon_1$. If $L^* \ge L_{\max}^0 - \varepsilon_0$, we set $L := L_{\max}^0 - \varepsilon_0 > L_0$ and $E := \kappa - \frac{d}{2} = E_L^{\min 0} + \frac{d}{2}$. Since $E = \kappa - \frac{d}{2} < E_0^\varepsilon - \frac{d}{6}$ and $E = E_L^{\min 0} + \frac{d}{2} > E_L^{\min \varepsilon} + \frac{d}{6}$, there holds $(E,L) \in \mathbb{D}_0^\varepsilon$. Furthermore, $|L - L^*| \le \varepsilon_0 < \frac{\delta}{2}$ and $|E - E^*| \le \frac{d}{2} < \frac{\delta}{2}$ since $E^* < \kappa = E + \frac{d}{2}$ and $E^* > E_{L^*}^{\min 0} \ge E_L^{\min 0} = E - \frac{d}{2}$. Hence, $|(E^*,L^*) - (E,L)| < \delta$. Otherwise, i.e., if $L^* < L_{\max}^0 - \varepsilon_0$, we just set $L := L^*$ and obtain $E_L^{\min \varepsilon} < E_L^{\min 0} + \frac{d}{3} < E^{\min 0}_{L_{\max}^0-\varepsilon_0} + \frac{d}{3} = \kappa - \frac{2}{3}d < E_0^\varepsilon - \frac{d}{3}$. In order to choose E, we distinguish between three cases:

Firstly, if $E_L^{\min\varepsilon} < E^* < E_0^\varepsilon$, we just keep $E \coloneqq E^*$. Secondly, if $E^* \leq E_L^{\min\varepsilon}$, observe that $E^* > E_L^{\min 0} > E_L^{\min\varepsilon} - \frac{d}{3}$ and $E^* \leq E_L^{\min\varepsilon} < E_0^\varepsilon - \frac{d}{3}$. Hence, for $E \coloneqq E^* + \frac{d}{3}$ there holds $(E, L) \in \mathbb{D}_0^\varepsilon$ with $|E - E^*| = \frac{d}{3} < \frac{\delta}{3}$. Thirdly, if $E^* \geq E_0^\varepsilon$, there holds $E^* < \kappa < E_0^\varepsilon + \frac{d}{3}$ and $E^* \geq E_0^\varepsilon > E_L^{\min\varepsilon} + \frac{d}{3}$. Thus, setting $E \coloneqq E^* - \frac{d}{3}$ yields $(E, L) \in \mathbb{D}_0^\varepsilon$ with $|E - E^*| = \frac{d}{3} < \frac{\delta}{3}$. In all cases we have hence shown the existence of $(E, L) \in \mathbb{D}_0^\varepsilon$ with $|(E, L) - (E^*, L^*)| < \delta$, which concludes the proof of part (a).

For part (b), we first shrink $\varepsilon_0 > 0$, if necessary, according to Lemmas 6.2.8 and 6.2.9 s.t. $|E_0^\varepsilon - \kappa| < \frac{\delta}{2}$ and $|E_L^{\min\varepsilon} - E_{L^*}^{\min 0}| < \frac{\delta}{2}$ for $0 \leq \varepsilon < \varepsilon_0$ as well as $L_0 \leq L^* \leq L_1$ and $L > 0$ with $|L - L^*| < \varepsilon_0$. By Lemma 6.2.13, there exists $0 < \varepsilon_2 < \varepsilon_0$ s.t. $|L_{\max}^\varepsilon - L_{\max}^0| < \varepsilon_0$ for $0 \leq \varepsilon < \varepsilon_2$. Now let $0 \leq \varepsilon < \varepsilon_2$ and $(E, L) \in \mathbb{D}_0^\varepsilon$ be arbitrary. If $L \geq L_{\max}^0$, we set $L^* \coloneqq L_{\max}^0$. Then, $L^* \leq L < L_{\max}^\varepsilon < L^* + \varepsilon_0$, and thus $|L - L^*| < \varepsilon_0 < \frac{\delta}{2}$. Furthermore, setting $E^* \coloneqq \kappa = E_{L^*}^{\min 0}$ yields $E < E_0^\varepsilon < \kappa + \frac{\delta}{2} = E^* + \frac{\delta}{2}$ and $E > E_L^{\min\varepsilon} > E_{L^*}^{\min 0} - \frac{\delta}{2} = E^* - \frac{\delta}{2}$. Thus, $|(E, L) - (E^*, L^*)| < \delta$ and $(E^*, L^*) \in \overline{\mathbb{D}_0^0}$. Otherwise, i.e., if $L < L_{\max}^0$, we just set $L^* \coloneqq L$. In order to choose E^* we distinguish between three cases: Firstly, if $E_L^{\min 0} < E < \kappa$, we keep $E^* \coloneqq E$. Secondly, if $E \leq E_L^{\min 0}$, observe that $E > E_L^{\min\varepsilon} > E_L^{\min 0} - \frac{\delta}{2}$. Setting $E^* \coloneqq E_L^{\min 0}$ hence gives $|E - E^*| < \frac{\delta}{2}$. Thirdly, if $E \geq \kappa$, there holds $E < E_0^\varepsilon < \kappa + \frac{\delta}{2}$. Thus, setting $E^* \coloneqq \kappa$ yields $|E - E^*| < \frac{\delta}{2}$. In all cases we have hence shown the existence of $(E^*, L^*) \in \overline{\mathbb{D}_0^0}$ with $|(E, L) - (E^*, L^*)| < \delta$, which concludes the proof of part (b). □

Convergence of the Period Function

We next show the convergence of the period function T^ε to T^0 as $\varepsilon \to 0$ on the respective domains of definition $\mathbb{D}_0^\varepsilon$ and $\mathbb{D}_0^0$ in a suitable sense. This requires a particularly careful treatment of the near circular regime $E \approx E_L^{\min\varepsilon}$. By the analysis from Section A.4, the period function is given by derivatives of the effective potential Ψ_L^ε evaluated at r_L^ε in this regime. The following lemma analyses the convergence of derivatives of Ψ_L^ε in this region. It is based on [61, Lemma A.4].

Lemma 6.2.16. *Let $n \in \mathbb{N}_0$ and $0 < L_1 < L_2$. In the case $n \geq 4$, we require $R_{\min}^0 < r_{L_1}^0 < r_{L_2}^0 < R_{\max}^0$.*[159] *Then $(\Psi_L^\varepsilon)^{(n)}(s)$ converges to $(\Psi_{L^*}^0)^{(n)}(r_{L^*}^0)$ as $E \to E_L^{\min\varepsilon}$, $L \to L^*$, and $\varepsilon \to 0$ uniformly in $L^* \in [L_1, L_2]$ and $s \in [r_-^\varepsilon(E, L), r_+^\varepsilon(E, L)]$. More precisely, for any $\delta > 0$ there exist $\varepsilon_0 > 0$ and $\eta > 0$ s.t. for all $0 \leq \varepsilon < \varepsilon_0$, $L_1 \leq L^* \leq L_2$, and $L > 0$ with $|L - L^*| < \varepsilon_0$ as well as $E_L^{\min\varepsilon} < E < E_L^{\min\varepsilon} + \eta < 0$ there holds $|(\Psi_L^\varepsilon)^{(n)}(s) - (\Psi_{L^*}^0)^{(n)}(r_{L^*}^0)| < \delta$ for $s \in [r_-^\varepsilon(E, L), r_+^\varepsilon(E, L)]$.*

Proof. Let $L_2 > L_1 > 0$ be fixed. By Lemma 6.2.12, there exist $0 < R_- < R_+$ s.t. $[r_-^\varepsilon(E, L), r_+^\varepsilon(E, L)] \subset [R_-, R_+]$ for (ε, E, L) as above with sufficiently small $\varepsilon_0 > 0$ and $\eta > 0$. In the case $n \leq 3$, the claim follows easily by Lemmas 6.2.8 and 6.2.12. The additional assumption in the case $n \geq 4$ ensures that we can further achieve $[R_-, R_+] \subset [R_{\min}^0 + 2d, R_{\max}^0 - 2d] \subset [R_{\min}^\varepsilon + 2d, R_{\max}^\varepsilon - d]$ for some (ε, E, L)-independent $d > 0$ by shrinking $\varepsilon_0 > 0$ and $\eta > 0$ if necessary; this is possible by Lemmas 6.2.11 and 6.2.12. Hence, $(\Psi_L^\varepsilon)^{(n)}$ exists on $[r_-^\varepsilon(E, L), r_+^\varepsilon(E, L)]$ by Proposition 6.2.2 (e). After showing $(U_0^\varepsilon)^{(n)} \to 0$ uniformly on $[R_{\min}^0 + 2d, R_{\max}^0 - 2d]$ as $\varepsilon \to 0$ by iterating the arguments from Lemma 6.2.8, the claimed statement follows in the same way as above. □

The above lemma is the key tool to prove the convergence of $T^\varepsilon(E, L)$ in the near-circular regime. Essentially, we add the limit $\varepsilon \to 0$ to the result from Corollary A.4.2. The following lemma is based on [61, Lemma A.5].

[159] In the case $n \geq 4$ one could alternatively require $r_{L_1}^0 > R_{\max}^0$ or $r_{L_2}^0 < R_{\min}^0$.

Lemma 6.2.17. *The period function $T^\varepsilon(E,L)$ converges to $T^0(E^{\min 0}_{L^*},L^*)$ as $E\to E^{\min\varepsilon}_L$, $L\to L^*$, and $\varepsilon\to 0$ locally uniformly in $L^*>0$. More precisely, for any $\delta>0$ and $L_2>L_1>0$ there exist $\varepsilon_0>0$ and $\eta>0$ s.t. for all $0\le\varepsilon<\varepsilon_0$, $L_1\le L^*\le L_2$, and $L>0$ with $|L-L^*|<\varepsilon_0$ as well as $E^{\min\varepsilon}_L<E<E^{\min\varepsilon}_L+\eta$ there holds $|T^\varepsilon(E,L)-T^0(E^{\min 0}_{L^*},L^*)|<\delta$.*

Here, $T^0(E^{\min 0}_{L^*},L^*)$ denotes the continuous extension of T^0 onto $(E^{\min 0}_{L^*},L^*)$ for $L^*>0$. By Lemma 6.2.5, this extension is given by

$$T^0(E^{\min 0}_{L^*},L^*)=2\pi\frac{(L^*)^{\frac32}}{M^2}=\frac{2\pi}{\sqrt{(\Psi^0_{L^*})''(r^0_{L^*})}},\qquad L^*>0. \tag{6.2.65}$$

Proof. The proof proceeds in the same way as the one of Lemma A.4.1 (with $F_L(r)\equiv 1$). It relies on the bound $|[(\Psi^\varepsilon_L)''(s)]^{-\frac12}-[(\Psi^0_{L^*})''(r^0_{L^*})]^{-\frac12}|<\frac{\delta}{\pi}$ for $0\le\varepsilon<\varepsilon_0$, $L_1\le L^*\le L_2$, and $L>0$ with $|L-L^*|<\varepsilon_0$ as well as $E^{\min\varepsilon}_L<E<E^{\min\varepsilon}_L+\eta$ and $s\in[r^\varepsilon_-(E,L),r^\varepsilon_+(E,L)]$; this holds by Lemma 6.2.16 for sufficiently small $\varepsilon_0>0$ and $\eta>0$, note that $(\Psi^0_{L^*})''(r^0_{L^*})=\frac{M^4}{(L^*)^3}>0$. □

In order to establish the uniform convergence of T^ε on $\mathbb{D}^\varepsilon_0$, we next prove the pointwise convergence of $T^\varepsilon(E,L)$. This is based on [61, Lemma A.7] and is very much similar to Lemma A.3.1.

Lemma 6.2.18. *The mapping $\mathcal{A}_0\ni(\varepsilon,E,L)\mapsto T^\varepsilon(E,L)$ is continuous at $\varepsilon=0$. More precisely, for any $\delta>0$ and $(E^*,L^*)\in\mathbb{A}^0_0$ there exists $\varepsilon_0>0$ s.t. for all $0\le\varepsilon<\varepsilon_0$ and $(E,L)\in\mathbb{A}^\varepsilon_0$ with $|(E,L)-(E^*,L^*)|<\varepsilon_0$ there holds $|T^\varepsilon(E,L)-T^0(E^*,L^*)|<\delta$.*

Proof. The proof proceeds in the same way as the one of Lemma A.3.1 (with $F_L(r)\equiv 1$ and $m=\frac12$): We apply Lebesgue's dominated convergence theorem to the integral $T^\varepsilon(E,L)$ after the affine change of variables $r\mapsto s=\frac{r-r^\varepsilon_-(E,L)}{r^\varepsilon_+(E,L)-r^\varepsilon_-(E,L)}$. The dominating, integrable function is derived using the concavity bound (2.2.73). The pointwise convergence of the integrand follows by the continuities of $[0,\infty[\times]0,\infty[^2\ni(\varepsilon,L,r)\mapsto\Psi^\varepsilon_L(r)$ and $\mathcal{A}_0\ni(\varepsilon,E,L)\mapsto r^\varepsilon_\pm(E,L)$ at $\varepsilon=0$, cf. Lemmas 6.2.8 and 6.2.10. □

Unsurprisingly, the above continuity is uniform on compact (E,L)-sets, where compact means, in particular, that the set is bounded away from minimal energies.

Lemma 6.2.19. *The continuity of $\mathcal{A}_0\ni(\varepsilon,E,L)\mapsto T^\varepsilon(E,L)$ at $\varepsilon=0$ from Lemma 6.2.18 is uniform on compact (E,L)-sets. More precisely, for any $L_2>L_1>0$, $E_1<0$, $\eta>0$, and $\delta>0$ there exists $\varepsilon_0>0$ s.t. for all $0\le\varepsilon<\varepsilon_0$, $L_1\le L^*\le L_2$, and $E^{\min 0}_{L^*}+\eta\le E^*<E_1$ as well as $L>0$ and $E^{\min\varepsilon}_L<E<0$ with $|(E,L)-(E^*,L^*)|<\varepsilon_0$ there holds $|T^\varepsilon(E,L)-T^0(E^*,L^*)|<\delta$.*

Proof. This is a standard proof in calculus. Suppose that the statement is not true for some $L_2>L_1>0$, $E_1<0$, and $\eta>0$. This means that there exists $\delta>0$ s.t. for all $j\in\mathbb{N}$ with $j\ge 3$ there exist $\varepsilon_j\in[0,\frac1j[$, $L_1\le L^*_j\le L_2$, and $E^{\min 0}_{L^*_j}+\eta\le E^*_j<E_1$ as well as $L_j>0$ and $E^{\min\varepsilon_j}_{L_j}<E_j<0$ with $|(E_j,L_j)-(E^*_j,L^*_j)|<\frac1j$ and $|T^{\varepsilon_j}(E_j,L_j)-T^0(E^*_j,L^*_j)|\ge\delta$. Then, for every sufficiently large j, $E_j\ge E^*_j-\frac{\eta}{4}\ge E^{\min 0}_{L^*_j}+\frac34\eta\ge E^{\min 0}_{L_j}+\frac12\eta$ and $E_j\le\frac12E_1$ as well as $\frac12L_1\le L_j\le L_2+1$ by Lemma 6.2.9. For these j there hence holds $(E_j,L_j),(E^*_j,L^*_j)\in\{(E,L)\mid\frac12L_1\le L\le L_2+1,\,E^{\min 0}_L+\frac12\eta\le E\le E_1\}$. Since the latter set is compact, there exists $(\bar E,\bar L)$ within this set s.t. $(E_j,L_j)\to(\bar E,\bar L)$ and $(E^*_j,L^*_j)\to(\bar E,\bar L)$ as $j\to\infty$ after passing to subsequences. By Lemma 6.2.18, this implies $T^{\varepsilon_j}(E_j,L_j)\to T^0(\bar E,\bar L)$ and $T^0(E^*_j,L^*_j)\to T^0(\bar E,\bar L)$ as $j\to\infty$, which is the desired contradiction. □

Combining Lemmas 6.2.17 and 6.2.19 yields the desired uniform convergence of the period function. This is based on [61, Lemma A.8].

Lemma 6.2.20. *The mapping $\mathcal{A}_0 \ni (\varepsilon, E, L) \mapsto T^\varepsilon(E,L)$ is continuous at $\varepsilon = 0$ uniformly on suitably bounded (E,L)-sets. More precisely, for any $\delta > 0$, $L_2 > L_1 > 0$, and $E_1 < 0$ there exists $\varepsilon_0 > 0$ s.t. for all $0 \le \varepsilon < \varepsilon_0$, $L_1 \le L^* \le L_2$, and $E^{\min 0}_{L^*} < E^* < E_1$ as well as $L > 0$ and $E^{\min\varepsilon}_L < E < E_1$ with $|(E,L) - (E^*,L^*)| < \varepsilon_0$ there holds $|T^\varepsilon(E,L) - T^0(E^*,L^*)| < \delta$.*

Proof. Let $\delta > 0$, $L_2 > L_1 > 0$, and $E_1 < 0$ be arbitrary. We choose $\varepsilon_0 > 0$ and $\eta > 0$ according to Lemma 6.2.17 s.t. for all $0 \le \varepsilon < \varepsilon_0$, $L_1 \le L^* \le L_2$, and $L > 0$ with $|L - L^*| < \varepsilon_0$ as well as $E^{\min\varepsilon}_L < E < E^{\min\varepsilon}_L + 2\eta < 0$ there holds $|T^\varepsilon(E,L) - T^0(E^{\min 0}_{L^*}, L^*)| < \frac{\delta}{2}$. In addition, after potentially shrinking $\eta > 0$, there holds $|T^0(E^*,L^*) - T^0(E^{\min 0}_{L^*}, L^*)| < \frac{\delta}{2}$ for $L_1 \le L^* \le L_2$ and $E^{\min 0}_{L^*} < E^* < E^{\min 0}_{L^*} + \eta$ by the explicitly formulae from Lemma 6.2.5 and (6.2.65). For this fixed $\eta > 0$, we now shrink $\varepsilon_0 > 0$, if necessary, according to Lemma 6.2.19 s.t. for all $0 \le \varepsilon < \varepsilon_0$, $L_1 \le L^* \le L_2$, and $E^{\min 0}_{L^*} + \eta \le E^* < E_1$ as well as $L > 0$ and $E^{\min\varepsilon}_L < E < 0$ with $|(E,L) - (E^*,L^*)| < \varepsilon_0$ there holds $|T^\varepsilon(E,L) - T^0(E^*,L^*)| < \delta$. In addition, we choose $\varepsilon_0 > 0$ to be sufficiently small s.t. $\varepsilon_0 < \frac{\eta}{2}$ and $|E^{\min\varepsilon}_L - E^{\min 0}_{L^*}| < \frac{\eta}{2}$ for $0 \le \varepsilon < \varepsilon_0$, $L_1 \le L^* \le L_2$, and $L > 0$ with $|L - L^*| < \varepsilon_0$; this is possible by Lemma 6.2.9.

Now let $0 \le \varepsilon < \varepsilon_0$, $L_1 \le L^* \le L_2$, and $E^{\min 0}_{L^*} < E^* < E_1$ as well as $L > 0$ and $E^{\min\varepsilon}_L < E < E_1$ with $|(E,L) - (E^*,L^*)| < \varepsilon_0$. If $E^* \ge E^{\min 0}_{L^*} + \eta$, the above immediately shows $|T^\varepsilon(E,L) - T^0(E^*,L^*)| < \delta$. Otherwise, i.e., $E^* < E^{\min 0}_{L^*} + \eta$, we obtain $E < E^* + \varepsilon_0 < E^{\min 0}_{L^*} + \frac{3}{2}\eta < E^{\min\varepsilon}_L + 2\eta$. By our choice of $\eta > 0$, we again conclude $|T^\varepsilon(E,L) - T^0(E^*,L^*)| < \delta$. □

Together with Lemma 6.2.14, the above lemma implies the uniform convergence of T^ε to T^0 as $\varepsilon \to 0$ on the (E,L)-support $\mathbb{D}^\varepsilon_0$. Combining this with the convergence "$\mathbb{D}^\varepsilon_0 \to \mathbb{D}^0_0$" as $\varepsilon \to 0$ established in Lemma 6.2.15, we thus deduce the convergence of $T^\varepsilon_{\min}$ and $T^\varepsilon_{\max}$. This is based on [61, Lemma A.9].

Lemma 6.2.21. *There holds $\lim_{\varepsilon\to 0} T^\varepsilon_{\min} = T^0_{\min}$ and $\lim_{\varepsilon\to 0} T^\varepsilon_{\max} = T^0_{\max}$, where*

$$0 < T^0_{\min} = T^0(E^{\min 0}_{L_0}, L_0) = 2\pi \frac{L_0^{\frac{3}{2}}}{M^2} < \frac{\pi}{\sqrt{2}} \frac{M}{(-\kappa)^{\frac{3}{2}}} = T^0(\kappa, L_0) = T^0_{\max} < \infty \tag{6.2.66}$$

by (6.2.16)*, Lemma 6.2.5, and* (6.2.65)*.*

Proof. For fixed $\delta > 0$ we choose $\varepsilon_0 > 0$ s.t. for all $0 \le \varepsilon < \varepsilon_0$, $(E^*,L^*) \in \mathbb{D}^0_0$, and $(E,L) \in \mathbb{D}^\varepsilon_0$ with $|(E,L) - (E^*,L^*)| < \varepsilon_0$ there holds $|T^\varepsilon(E,L) - T^0(E^*,L^*)| < \delta$; as discussed above, this is possible by Lemmas 6.2.14 and 6.2.20. By Lemma 6.2.15 (b), there further exists $\varepsilon_1 > 0$ s.t. for all $0 \le \varepsilon < \varepsilon_1$ and $(E,L) \in \mathbb{D}^\varepsilon_0$ there exists $(E^*,L^*) \in \mathbb{D}^0_0$ s.t. $|(E,L) - (E^*,L^*)| < \varepsilon_0$. This implies $T^\varepsilon(E,L) \le T^0(E^*,L^*) + \delta \le T^0_{\max} + \delta$. Thus, for any $0 \le \varepsilon < \varepsilon_1$ there holds $T^\varepsilon_{\max} \le T^0_{\max} + \delta$, in particular, $T^\varepsilon_{\max} < \infty$. By Lemma 6.2.15 (a), we can shrink $\varepsilon_1 > 0$ s.t. for all $0 \le \varepsilon < \varepsilon_1$ and $(E^*,L^*) \in \mathbb{D}^0_0$ there exists $(E,L) \in \mathbb{D}^\varepsilon_0$ s.t. $|(E,L) - (E^*,L^*)| < \varepsilon_0$, which yields $T^0(E^*,L^*) \le T^\varepsilon(E,L) + \delta \le T^\varepsilon_{\max} + \delta$. We hence conclude $T^0_{\max} \le T^\varepsilon_{\max} + \delta$. Similar arguments show $|T^\varepsilon_{\min} - T^0_{\min}| < \delta$ for $0 \le \varepsilon < \varepsilon_1$ after potentially shrinking $\varepsilon_1 > 0$. □

Convergence of the Derivatives of the Period Function

We also need the analogous results for the partial derivatives $\partial_E T^\varepsilon$ and $\partial^2_E T^\varepsilon$ of the period function. We shall see that the arguments are similar, but more technically involved than

for T^ε itself. Mainly due to the former reason, but also due to the latter one, we keep the presentation here shorter than above.

Let us first analyse the regularity of T^ε.

Lemma 6.2.22. *For $\varepsilon \geq 0$ there holds $T^\varepsilon \in C^2(\mathbb{A}_0^\varepsilon)$. Moreover, the partial derivatives $\partial_E T^\varepsilon$ and $\partial_E^2 T^\varepsilon$ possess the integral representations* (A.3.32) *and* (A.3.84)*. The former holds for all $(E,L) \in \mathbb{A}_0^\varepsilon$, the latter holds for all $(E,L) \in \mathbb{A}_0^\varepsilon$ with $r_L^\varepsilon \notin \{R_{\min}^\varepsilon, R_{\max}^\varepsilon\}$.*

Proof. The regularity of T^ε follows in the same way as in Lemma A.3.3; it relies on the regularity of U_0^ε established in Proposition 6.2.2 (e). The integral representations of $\partial_E T^\varepsilon$ and $\partial_E^2 T^\varepsilon$ can also be derived similarly to the case without a point mass; recall $U_0^\varepsilon \in C^\infty([0,\infty[\setminus\{R_{\min}^\varepsilon, R_{\max}^\varepsilon\})$. □

Using the integral representations of the partial derivatives, we derive their limiting behaviour as $\varepsilon \to 0$ in the same way as for T^ε. We start by establishing a suitable analogue of Lemma 6.2.17. This is based on [61, Lemmas A.12 and A.15].

Lemma 6.2.23. *Let $L_2 > L_1 > 0$ be s.t. $R_{\min}^0 < r_{L_1}^0 < r_{L_2}^0 < R_{\max}^0$.*[160] *Then the partial derivatives $\partial_E T^\varepsilon(E,L)$ and $\partial_E^2 T^\varepsilon(E,L)$ of the period function converge to $\partial_E T^0(E_{L^*}^{\min 0}, L^*)$ and $\partial_E^2 T^0(E_{L^*}^{\min 0}, L^*)$, respectively, as $E \to E_L^{\min\varepsilon}$, $L \to L^*$, and $\varepsilon \to 0$ uniformly in $L^* \in [L_1, L_2]$. More precisely, for any $\delta > 0$ there exist $\varepsilon_0 > 0$ and $\eta > 0$ s.t. for all $0 \leq \varepsilon < \varepsilon_0$, $L_1 \leq L^* \leq L_2$, and $L > 0$ with $|L - L^*| < \varepsilon_0$ as well as $E_L^{\min\varepsilon} < E < E_L^{\min\varepsilon} + \eta$ there holds $|\partial_E T^\varepsilon(E,L) - \partial_E T^0(E_{L^*}^{\min 0}, L^*)| < \delta$ and $|\partial_E^2 T^\varepsilon(E,L) - \partial_E^2 T^0(E_{L^*}^{\min 0}, L^*)| < \delta$.*

Here, $\partial_E T^0(E_{L^*}^{\min 0}, L^*)$ and $\partial_E^2 T^0(E_{L^*}^{\min 0}, L^*)$ denote the continuous extensions of $\partial_E T^0$ and $\partial_E^2 T^0$, respectively, onto $(E_{L^*}^{\min 0}, L^*)$ for $L^* > 0$. By Lemma 6.2.5, these extensions are given by

$$\partial_E T^0(E_{L^*}^{\min 0}, L^*) = 6\pi \frac{(L^*)^{\frac{5}{2}}}{M^4}, \quad \partial_E^2 T^0(E_{L^*}^{\min 0}, L^*) = 30\pi \frac{(L^*)^{\frac{7}{2}}}{M^6}, \qquad L^* > 0. \tag{6.2.67}$$

Proof. First notice that Lemmas 6.2.11 and 6.2.12 allow us to always assume $[r_-^\varepsilon(E,L), r_+^\varepsilon(E,L)] \subset]R_{\min}^\varepsilon, R_{\max}^\varepsilon[$ for (ε, E, L) as above by choosing $\varepsilon_0 > 0$ and $\eta > 0$ sufficiently small. In particular, U_0^ε is infinitely differentiable on the relevant domains of integration.

The proof now proceeds in two steps: First, we apply the (extended) mean value theorem as in the proofs of Lemmas A.4.6 and A.4.9 to study the limits of

$$\int_{r_-^\varepsilon(E,L)}^{r_+^\varepsilon(E,L)} \frac{(G_{1,L}^\varepsilon)'(r)}{\sqrt{2E - 2\Psi_L^\varepsilon(r)}}\,\mathrm{d}r \tag{6.2.68}$$

and

$$\frac{1}{2}\int_{r_-^\varepsilon(E,L)}^{r_+^\varepsilon(E,L)} \frac{(G_{3,L}^\varepsilon)'(r)}{\sqrt{2E - 2\Psi_L^\varepsilon(r)}}\,\mathrm{d}r \tag{6.2.69}$$

instead of $\partial_E T^\varepsilon(E,L)$ and $\partial_E^2 T^\varepsilon(E,L)$, respectively. Here, $(G_{1,L}^\varepsilon)'$ and $(G_{3,L}^\varepsilon)'$ are given by (A.3.75) and (A.4.36)–(A.4.37), respectively, on the radial interval $]R_{\min}^\varepsilon, R_{\max}^\varepsilon[$ for $L > 0$ and $\varepsilon \geq 0$.

The second step is then to proceed as in the proof of Lemma A.4.1 and show that (6.2.68) and (6.2.69) converge to $\pi \frac{(G_{1,L^*}^0)'(r_{L^*}^0)}{\sqrt{(\Psi_{L^*}^0)''(r_{L^*}^0)}}$ and $\frac{\pi}{2} \frac{(G_{3,L^*}^0)'(r_{L^*}^0)}{\sqrt{(\Psi_{L^*}^0)''(r_{L^*}^0)}}$, respectively. Using Lemma 6.2.5,

[160] The assumptions on $r_{L_1}^0$ and $r_{L_2}^0$ are only necessary to prove the statements regarding $\partial_E^2 T^\varepsilon$.

it is straight-forward to verify that the latter two values are equal to the extensions given by (6.2.67). The proof mainly relies on the bound

$$\left| \frac{(G^{\varepsilon}_{i,L})'(r)}{\sqrt{(\Psi^{\varepsilon}_{L})''(s)}} - \frac{(G^{0}_{i,L^*})'(r^0_{L^*})}{\sqrt{(\Psi^{0}_{L^*})''(r^0_{L^*})}} \right| < \frac{\delta}{\pi} \tag{6.2.70}$$

for $i \in \{1,3\}$, $0 \leq \varepsilon < \varepsilon_0$, $L_1 \leq L^* \leq L_2$, and $L > 0$ with $|L - L^*| < \varepsilon_0$ as well as $E_L^{\min\varepsilon} < E < E_L^{\min\varepsilon} + \eta$ and $r, s \in [r^{\varepsilon}_{-}(E,L), r^{\varepsilon}_{+}(E,L)]$. This holds for sufficiently small $\varepsilon_0 > 0$ and $\eta > 0$, which can be verified by Taylor expanding $(G^{\varepsilon}_{i,L})'$ as in the proofs of Lemmas A.3.18 and A.4.9 and then applying Lemma 6.2.16. □

The next step is to establish the pointwise convergence of $\partial_E T^{\varepsilon}$ and $\partial_E^2 T^{\varepsilon}$ similar to Lemma 6.2.18. This is based on [61, Lemmas A.13 and A.16].

Lemma 6.2.24. *Let $L_2 > L_1 > 0$ be s.t. $R^0_{\min} < r^0_{L_1} < r^0_{L_2} < R^0_{\max}$. Then the mappings $\mathcal{A}_0 \ni (\varepsilon, E, L) \mapsto \partial_E T^{\varepsilon}(E,L)$ and $\mathcal{A}_0 \cap \{L_1 \leq L \leq L_2\} \ni (\varepsilon, E, L) \mapsto \partial_E^2 T^{\varepsilon}(E,L)$ are both continuous at $\varepsilon = 0$. More precisely, for any $\delta > 0$ and $(E^*, L^*) \in \mathbb{A}^0_0$ there exists $\varepsilon_0 > 0$ s.t. for all $0 \leq \varepsilon < \varepsilon_0$ and $(E,L) \in \mathbb{A}^{\varepsilon}_0$ with $|(E,L) - (E^*,L^*)| < \varepsilon_0$ there holds $|\partial_E T^{\varepsilon}(E,L) - \partial_E T^0(E^*,L^*)| < \delta$ and, provided $L_1 \leq L^* \leq L_2$, also $|\partial_E^2 T^{\varepsilon}(E,L) - \partial_E^2 T^0(E^*,L^*)| < \delta$.*

Proof. The proof proceeds similarly to the one of Lemma 6.2.18, which is in turn based on the proof of Lemma A.3.1. We show the claimed convergences via Lebesgue's dominated convergence theorem: For this, we first rewrite the integral representations (A.3.32) and (A.3.84) of $\partial_E T^{\varepsilon}$ and $\partial_E^2 T^{\varepsilon}$, respectively, using the affine change of variables $r \mapsto s = \frac{r - r^{\varepsilon}_{-}(E,L)}{r^{\varepsilon}_{+}(E,L) - r^{\varepsilon}_{-}(E,L)}$. The pointwise convergence of the resulting integrand of (A.3.32) then follows by the convergences established in Lemmas 6.2.8 and 6.2.10 together with the continuity of $[0,\infty[\times]0,\infty[^2 \ni (\varepsilon, L, r) \mapsto G^{\varepsilon}_L(r)$ at $\varepsilon = 0$; the latter is due to Lemmas 6.2.8 and 6.2.16. Similar arguments also yield the continuity of $[0,\infty[\times [L_1, L_2] \times]0,\infty[\ni (\varepsilon, L, r) \mapsto (G^{\varepsilon}_{1,L})'(r)$ at $\varepsilon = 0$. We hence obtain the pointwise convergence of the integrand resulting from (A.3.84). Together with the concavity bound (2.2.73), we further deduce that the integrands are bounded by an integrable function locally uniformly in (ε, E, L). □

Identical arguments as in the proof of Lemma 6.2.19 show that these continuities are uniform on compact (E,L)-sets. Together with Lemma 6.2.23 we hence conclude the desired uniform convergences of $\partial_E T^{\varepsilon}$ and $\partial_E^2 T^{\varepsilon}$ as $\varepsilon \to 0$.

Lemma 6.2.25. *The mappings $\mathcal{A}_0 \ni (\varepsilon, E, L) \mapsto \partial_E T^{\varepsilon}(E,L)$ and $\mathcal{A}_0 \ni (\varepsilon, E, L) \mapsto \partial_E^2 T^{\varepsilon}(E,L)$ are both continuous at $\varepsilon = 0$ uniformly on suitably bounded (E,L)-sets. More precisely, for any $\delta > 0$, $E_1 < 0$, and $L_2 > L_1 > 0$ with $R^0_{\min} < r^0_{L_1} < r^0_{L_2} < R^0_{\max}$ there exists $\varepsilon_0 > 0$ s.t. for all $0 \leq \varepsilon < \varepsilon_0$, $L_1 \leq L^* \leq L_2$, and $E^{\min 0}_{L^*} < E^* < E_1$ as well as $L > 0$ and $E_L^{\min\varepsilon} < E < E_1$ with $|(E,L) - (E^*,L^*)| < \varepsilon_0$ there holds $|\partial_E T^{\varepsilon}(E,L) - \partial_E T^0(E^*,L^*)| < \delta$ and $|\partial_E^2 T^{\varepsilon}(E,L) - \partial_E^2 T^0(E^*,L^*)| < \delta$.*

Proof. The claims follow by combining Lemmas 6.2.23 and 6.2.24; see Lemma 6.2.20 for a similar proof. □

Since $R^0_{\min} < r^0_{L_0} < r^0_{L^0_{\max}} < R^0_{\max}$, the above lemma does, in particular, show the uniform convergences of $\partial_E T^{\varepsilon}$ and $\partial_E^2 T^{\varepsilon}$ on $\mathbb{D}^{\varepsilon}_0$. We hence conclude the convergences of the minimal and maximal values of $\partial_E T^{\varepsilon}$ and $\partial_E^2 T^{\varepsilon}$ on $\mathbb{D}^{\varepsilon}_0$; recall (6.2.47) and (6.2.48) for the definitions of these values. The lemma is based on [61, Lemma A.14 and A.17].

Lemma 6.2.26. *It holds that* $\lim_{\varepsilon\to 0}\partial_E T^\varepsilon_{\min} = \partial_E T^0_{\min}$, $\lim_{\varepsilon\to 0}\partial_E T^\varepsilon_{\max} = \partial_E T^0_{\max}$, $\lim_{\varepsilon\to 0}\partial_E^2 T^\varepsilon_{\min} = \partial_E^2 T^0_{\min}$, *and* $\lim_{\varepsilon\to 0}\partial_E^2 T^\varepsilon_{\max} = \partial_E^2 T^0_{\max}$, *where*

$$0 < \partial_E T^0_{\min} = \partial_E T^0(E^{\min 0}_{L_0}, L_0) = 6\pi\frac{L_0^{\frac{5}{2}}}{M^4} < \frac{3\pi}{2\sqrt{2}}\frac{M}{(-\kappa)^{\frac{5}{2}}} = \partial_E T^0(\kappa, L_0) = \partial_E T^0_{\max} < \infty, \tag{6.2.71}$$

$$0 < \partial_E^2 T^0_{\min} = \partial_E^2 T^0(E^{\min 0}_{L_0}, L_0) = 30\pi\frac{L_0^{\frac{7}{2}}}{M^6} < \frac{15\pi}{4\sqrt{2}}\frac{M}{(-\kappa)^{\frac{7}{2}}} = \partial_E^2 T^0(\kappa, L_0) = \partial_E^2 T^0_{\max} < \infty, \tag{6.2.72}$$

by (6.2.16)*, Lemma 6.2.5, and* (6.2.67)*.*

Proof. The claimed convergences follow by Lemma 6.2.25 in the same way as in the proof of Lemma 6.2.21. □

6.3 Linearisation and the Operators

The aim of this section is to linearise the system from Section 6.1 around a steady state surrounding a point mass and introduce and analyse the occurring operators. This will turn out to work very much similar to Chapters 3–5, which is why we will keep the presentation here rather short. We advise the reader to first familiarise him or herself with these chapters before reading the following part.

Let f_0 be a fixed steady state of the radial Vlasov-Poisson system around a point mass as constructed in Proposition 6.2.2. Following the arguments in Chapter 3, including the Antonov trick, we arrive at the following second-order equation for the odd-in-v part f of the linear perturbation:

$$\partial_t^2 f + \mathcal{L} f = 0. \tag{6.3.1}$$

Again, $\mathcal{L}$ is the linearised operator associated to the steady state given by

$$\mathcal{L} = -\mathcal{T}^2 - \mathcal{R}, \tag{6.3.2}$$

where

$$\mathcal{T} = v\cdot\partial_x - \left(\partial_x U_0(x) + M\frac{x}{|x|^3}\right)\cdot\partial_v = w\,\partial_r - \Psi_L'(r)\,\partial_w \tag{6.3.3}$$

is the transport operator and $\mathcal{R}$ is the gravitational response operator defined as in (3.1.13). The equation (6.3.1) is the *linearised Vlasov-Poisson system around a point mass in second-order formulation.*

The behaviour of its solutions is determined by the (spectral) properties of $\mathcal{L}$. To analyse them, we again rigorously define $\mathcal{L}$ on a suitable (subspace of a) Hilbert space. This is achieved in the same way as in Chapter 4: The underlying Hilbert space H is the spherically symmetric L^2-space over Ω_0 with weight $|\varphi'(E,L)|^{-1}$ defined as in Definition 4.2.3. As before, $\varphi' \coloneqq \partial_E\varphi$, and this function is negative on the interior of the steady state support because $k > 0$, recall (6.2.6)–(6.2.7). We define $\mathcal{L}$ on the domain $\mathrm{D}(\mathcal{L})$, which is contained in the odd-in-v subspace $\mathcal{H}$ of H, similarly to Definition 4.2.9. The two parts $\mathcal{T}^2$ and $\mathcal{R}$ of $\mathcal{L}$ are defined as in Definitions 4.2.5 and 4.2.8, respectively. Using these definitions, it turns out that the operators have the identical properties as in the case without a point mass for a steady state with $L_0 > 0$. This is due to the fact the relevant relations like (6.2.1) as well as the structure of the effective potential, cf. Lemma 6.2.4, are preserved by adding the

point mass. The only difference compared to Chapter 4 is that one has to add the central point mass to the local mass of the steady state in certain arguments, i.e., one has to replace $m_0(r) = r^2 U_0'(r)$ with $m_0(r) + M$. For instance, Antonov's coercivity bound (4.5.13) in the case of a point mass becomes

$$\langle \mathcal{L} f, f \rangle_H \geq \int_{\Omega_0} \frac{1}{|\varphi'(E,L)|} \left(\frac{U_0'(r)}{r} + \frac{M}{r^3} \right) |f(x,v)|^2 \,\mathrm{d}(x,v), \qquad f \in \mathrm{D}(\mathcal{T}) \cap \mathcal{H}. \tag{6.3.4}$$

Furthermore, the same analysis as in Chapter 5 yields an analogue of the Birman-Schwinger-Mathur principle, i.e., analogous versions of the criteria from Section 5.3 in the case of a point mass. From now on, we hence use the definitions and results from Chapters 4 and 5 in the present setting without further comments.

As a preparation for the following analysis, we now establish some further lemmas. The first one gives us control on the behaviour of the (change to) action-angle type variables close to minimal energies. It is based on [61, Lemma 3.5].

Lemma 6.3.1. *For $(E,L) \in \mathbb{A}_0$, let $R(\cdot,E,L)\colon \mathbb{R} \to]0,\infty[$ be the unique maximal solution of $\ddot{R} = -\Psi_L'(R)$ satisfying the initial condition $R(0,E,L) = r_-(E,L)$, i.e., R is defined as in Definition 2.2.16. Furthermore, let*

$$r\colon \mathbb{S}^1 \times \mathbb{A}_0 \to]0,\infty[,\ r(\theta,E,L) \coloneqq R(\theta\, T(E,L),E,L); \tag{6.3.5}$$

this functions gives the radial component of the change to action-angle type variables, cf. Definition 4.3.1. Then $r \in C^2(\mathbb{S}^1 \times \mathbb{A}_0)$ and there exists a constant $C > 0$ s.t. for all $(\theta,E,L) \in \mathbb{S}^1 \times \mathbb{D}_0$ the estimates

$$|r(\theta,E,L) - r_L| + |\partial_\theta r(\theta,E,L)| \leq C\sqrt{E - E_L^{\min}} \tag{6.3.6}$$

and

$$|\partial_E r(\theta,E,L)| \leq \frac{C}{\sqrt{E - E_L^{\min}}} \tag{6.3.7}$$

hold. The constant C can be bounded in terms of $T_{\max}$, $\partial_E T_{\max}$, $L_{\max}$, and $\|U_0''\|_{L^\infty([R_{\min},R_{\max}])}$ as well as M and the steady state parameters L_0, k, ℓ, and κ.[161]

Proof. In the same way as in Lemma A.3.2, the claimed regularity of r follows by basic ODE theory since $U_0 \in C^3([0,\infty[)$ by Proposition 6.2.2 (e); further recall $T \in C^2(\mathbb{A}_0)$.

For $(E,L) \in \overline{\mathbb{D}}_0$ let $\alpha(\cdot,E,L)\colon \mathbb{R} \to \mathbb{R}$ be the unique global solution of the linear ODE

$$\ddot{\alpha} = -\Psi_L''(R(\cdot,E,L))\,\alpha, \qquad \alpha(0) = 1,\ \dot{\alpha}(0) = 0; \tag{6.3.8}$$

in the case $E = E_L^{\min}$ we set $R(\cdot,E_L^{\min},L) \equiv r_L$. Note that this defines a continuous extension of R because of $R(\mathbb{R},E,L) = [r_-(E,L), r_+(E,L)]$ and (2.2.66). Since

$$|\Psi_L''(r)| \leq C, \qquad r \in [R_{\min},R_{\max}],\ L \in [L_0,L_{\max}], \tag{6.3.9}$$

Grönwall's inequality implies $|\alpha(s,E,L)| \leq C$ for $(E,L) \in \overline{\mathbb{D}}_0$ and $s \in [0,T_{\max}]$. The constant $C > 0$ is allowed to change its value throughout this proof, but it can always be bounded by the quantities specified above. Moreover, similar to Lemma A.3.2, $\partial_E R(s,E,L) = \alpha(s,E,L)\,\partial_E r_-(E,L)$ for $s \in \mathbb{R}$ and $(E,L) \in \mathbb{A}_0$, which shows

$$\partial_E r(\theta,E,L) = \dot{R}(\theta\, T(E,L),E,L)\,\theta\,\partial_E T(E,L) + \alpha(\theta\, T(E,L),E,L)\,\partial_E r_-(E,L) \tag{6.3.10}$$

[161] C being *bounded in terms of these parameters* means that C is uniformly bounded if these parameters range in a compact set.

for $\theta \in \mathbb{S}^1$ and $(E,L) \in \mathbb{A}_0$. For the first term on the right-hand side the estimate

$$|\dot{R}(\theta\, T(E,L),E,L)| = \sqrt{2E - 2\Psi_L(r(\theta,E,L))} \leq \sqrt{2E - 2E_L^{\min}} \leq \frac{\sqrt{2}\,(\kappa + \frac{M}{R_{\min}^0})}{\sqrt{E - E_L^{\min}}} \tag{6.3.11}$$

holds for $\theta \in \mathbb{S}^1$ and $(E,L) \in \mathbb{D}_0$. It thus remains to show

$$|\partial_E r_-(E,L)| \leq \frac{C}{\sqrt{E - E_L^{\min}}}, \qquad (E,L) \in \mathbb{D}_0, \tag{6.3.12}$$

in order to deduce (6.3.7).

To prove (6.3.12), first observe that for $L \geq L_0$ and $s \in [R_{\min}, r_L]$,

$$\Psi_L''(s) = -2\frac{\Psi_L'(s)}{s} + \frac{L}{s^4} + 4\pi\rho_0(s) \geq \frac{L_0}{(R_{\max}^0)^4} = \frac{1}{C} \tag{6.3.13}$$

since $\Psi_L'(s) \leq 0$. Hence, by (2.2.65) and the mean value theorem,

$$|\partial_E r_-(E,L)| = \frac{-1}{\Psi_L'(r_-(E,L))} = \frac{1}{\Psi_L''(s)\,(r_L - r_-(E,L))} \leq \frac{C}{r_L - r_-(E,L)}, \quad (E,L) \in \mathbb{D}_0, \tag{6.3.14}$$

for some $s \in [R_{\min}, r_L]$. Applying the mean value theorem twice again shows

$$\frac{(r_L - r_-(E,L))^2}{E - E_L^{\min}} = 2(r_-(\eta,L) - r_L)\,\partial_E r_-(\eta,L) = \frac{2}{\Psi_L''(s)} \tag{6.3.15}$$

for $(E,L) \in \mathbb{D}_0$ as well as some $\eta \in\,]E_L^{\min}, E_0[$ and $s \in [R_{\min}, r_L]$. Inserting (6.3.9) and (6.3.13) into (6.3.15) hence yields

$$\frac{1}{C}\sqrt{E - E_L^{\min}} \leq r_L - r_-(E,L) \leq C\sqrt{E - E_L^{\min}}, \qquad (E,L) \in \mathbb{D}_0. \tag{6.3.16}$$

Together with (6.3.14) this shows (6.3.12), and we conclude (6.3.7).

Moreover, since

$$\partial_\theta r(\theta,E,L) = T(E,L)\,\dot{R}(\theta\, T(E,L),E,L) \tag{6.3.17}$$

and

$$|r(\theta,E,L) - r_L| \leq |\partial_\theta r(\tau,E,L)| + |r_-(E,L) - r_L| \tag{6.3.18}$$

by the mean value theorem for $(E,L) \in \mathbb{D}_0$ and some $\tau \in \mathbb{S}^1$, the inequalities (6.3.11) and (6.3.16) also imply (6.3.6). □

The second lemma extends the results from Lemmas 4.4.5 and 4.4.6 regarding the properties of gravitational potentials of the form $U_{\mathcal{T}f}$. It is based on [61, Lemma 3.9].

Lemma 6.3.2. *Let $f \in \mathrm{D}(\mathcal{T})$. In addition to the properties of $U_{\mathcal{T}f}$ which follow from Lemmas 4.4.5 and 4.4.6, in radial variables there holds $U_{\mathcal{T}f} \in H^2 \cap C^1([0,\infty[)$ with*

$$\|U_{\mathcal{T}f}\|_{H^2} + \|U_{\mathcal{T}f}\|_\infty + \|U_{\mathcal{T}f}'\|_\infty \leq C\,\|\mathcal{T}f\|_H \tag{6.3.19}$$

for some constant $C > 0$ which depends on the steady state parameters L_0, k, ℓ, κ, and ε and which is locally uniformly bounded in $\varepsilon \geq 0$. In action-angle type variables, i.e., $U_{\mathcal{T}f}(\theta,E,L) = U_{\mathcal{T}f}(r(\theta,E,L))$ with r defined as in Lemma 6.3.1, there holds $U_{\mathcal{T}f} \in C^1(\mathbb{S}^1 \times \mathbb{A}_0)$ with

$$|\partial_E U_{\mathcal{T}f}(\theta,E,L)| \leq \frac{C}{\sqrt{E - E_L^{\min}}}\,|U_{\mathcal{T}f}'(r(\theta,E,L))|, \qquad (\theta,E,L) \in \mathbb{S}^1 \times \mathbb{D}_0, \tag{6.3.20}$$

and

$$\int_{\mathbb{D}_0} |\varphi'(E,L)|\,|\widehat{U_{\mathcal{T}f}}(n,E,L)|^2\,\mathrm{d}(E,L) \leq \frac{C}{n^2}\,\varepsilon \int_{\mathbb{R}^3} |\partial_x U_{\mathcal{T}f}(x)|^2\,\mathrm{d}x, \qquad n \in \mathbb{Z}^*, \tag{6.3.21}$$

for a constant $C > 0$ as in Lemma 6.3.1. Here, $\widehat{U_{\mathcal{T}f}}$ denotes the Fourier transform of $\mathbb{S}^1 \times \mathbb{D}_0 \ni (\theta, E, L) \mapsto U_{\mathcal{T}f}(\theta, E, L)$ w.r.t. the angle variable θ, recall Remark 4.3.11, and we use the notation

$$\mathbb{Z}^* \coloneqq \mathbb{Z} \setminus \{0\}. \tag{6.3.22}$$

Proof. Since $R_{\min} = R^0_{\min} > 0$ and $U'_{\mathcal{T}f} = 0$ on $[0, R_{\min}]$ by (4.4.16), $U_{\mathcal{T}f} \in H^2(\mathbb{R}^3)$ implies $U_{\mathcal{T}f} \in H^2(]0,\infty[)$. In addition, the identity (4.4.19) shows $U'_{\mathcal{T}f} = 0$ on $[R_{\max}, \infty[$, from which we deduce $U_{\mathcal{T}f} = 0$ on $[R_{\max}, \infty[$ because $\lim_{r\to\infty} U_{\mathcal{T}f}(r) = 0$. Together with the embedding $H^2(]0, R^0_{\max}[) \hookrightarrow C^1([0, R^0_{\max}])$, we hence conclude $U_{\mathcal{T}f} \in C^1([0,\infty[)$. These arguments also yield the bound (6.3.19). In particular, going through the proofs of Lemmas 4.1.3, 4.4.1, 4.4.5, and 4.4.6 shows that all occurring constants can be bounded by the steady state parameters as claimed above; recall the bound (6.2.23) on $R_{\max}$.

The regularity of $U_{\mathcal{T}f}$ in action-angle type variables and the estimate (6.3.20) then follow by Lemma 6.3.1 since $\partial_E U_{\mathcal{T}f}(\theta, E, L) = U'_{\mathcal{T}f}(r(\theta, E, L))\,\partial_E r(\theta, E, L)$ for $\theta \in \mathbb{S}^1$ and $(E, L) \in \mathbb{D}_0$. For the Fourier coefficients $\widehat{U_{\mathcal{T}f}}$ there holds

$$2\pi i n\,\widehat{U_{\mathcal{T}f}}(n,E,L) = \widehat{\partial_\theta U_{\mathcal{T}f}}(n,E,L), \qquad n \in \mathbb{Z},\ (E,L) \in \mathbb{D}_0. \tag{6.3.23}$$

Together with Parseval's theorem as well as the identities $\partial_\theta U_{\mathcal{T}f} = U'_{\mathcal{T}f}\,\partial_\theta r$, (4.3.14), (6.3.17), and (4.1.8) we thus conclude

$$\begin{aligned}
\int_{\mathbb{D}_0} |\varphi'(E,L)|\,|\widehat{U_{\mathcal{T}f}}(n,E,L)|^2\,\mathrm{d}(E,L) &\leq \frac{C}{n^2}\int_{\mathbb{D}_0} |\varphi'(E,L)| \sum_{j\in\mathbb{Z}} |\widehat{\partial_\theta U_{\mathcal{T}f}}(j,E,L)|^2\,\mathrm{d}(E,L) = \\
&= \frac{C}{n^2}\int_{\mathbb{S}^1\times\mathbb{D}_0} |\varphi'(E,L)|\,|U'_{\mathcal{T}f}(r(\theta,E,L))|^2\,|\partial_\theta r(\theta,E,L)|^2\,\mathrm{d}(\theta,E,L) \leq \\
&\leq \frac{C}{n^2}\int_{R_{\min}}^{R_{\max}} |U'_{\mathcal{T}f}(r)|^2 \int_0^\infty \int_{\mathbb{R}} w^2 |\varphi'(E,L)|\,\mathrm{d}w\,\mathrm{d}L\,\mathrm{d}r = \\
&= \frac{C}{n^2}\int_{R_{\min}}^{R_{\max}} r^2 |U'_{\mathcal{T}f}(r)|^2 \rho_0(r)\,\mathrm{d}r \leq \frac{C}{n^2}\,\varepsilon\,\|\partial_x U_{\mathcal{T}f}\|_2^2
\end{aligned} \tag{6.3.24}$$

for $n \in \mathbb{Z}^*$ and C as specified above; in the last inequality we used (6.2.8) to estimate $\|\rho_0\|_\infty$. □

6.4 Absence of Eigenvalues in the Essential Gap

The aim of this section is to show that the linearised operator $\mathcal{L}\colon \mathrm{D}(\mathcal{L}) \to \mathcal{H}$ associated to certain "small" steady states does not possess an eigenvalue inside its essential gap. As in (1.2.21), the essential gap $\mathcal{G}$ is defined as

$$\mathcal{G} \coloneqq \left]0, \frac{4\pi^2}{(T_{\max})^2}\right[. \tag{6.4.1}$$

We fix the steady state parameters L_0, k, ℓ, and κ as specified in Proposition 6.2.2. For $\varepsilon > 0$, let f_0 be the steady state given by Proposition 6.2.2. The result is an application of the Birman-Schwinger-Mathur principle developed in Chapter 5; by the discussion above, it can also be applied in the present setting with a point mass. The result is inspired by [61, Thm. 5.4], and the techniques used in the proof are related to those used for Corollary 5.4.4.

Theorem 6.4.1 (Absence of Eigenvalues in $\mathcal{G}$ for $\varepsilon \ll 1$)**.** *In addition to* (6.2.7)*, assume that the polytropic exponent k satisfies*

$$k > 1. \tag{6.4.2}$$

Then there exists $\varepsilon_0 > 0$ s.t. for any $0 < \varepsilon < \varepsilon_0$ the linearised operator $\mathcal{L}$ has no eigenvalues in the essential gap $\mathcal{G}$.

Proof. By Theorem 5.3.3 it remains to show

$$32\pi^2 \sum_{n=1}^{\infty} \int_{\mathbb{D}_0} \frac{|\varphi'(E,L)|}{T(E,L)} \frac{1}{\frac{4\pi^2 n^2}{T(E,L)^2} - \frac{4\pi^2}{(T_{\max})^2}} \int_{r_-(E,L)}^{r_+(E,L)} \frac{\sin^2(2\pi n\, \theta(r,E,L))}{r^2} \,\mathrm{d}r \,\mathrm{d}(E,L) < 1. \tag{6.4.3}$$

The integral on the left-hand side can be estimated as follows:

$$\begin{aligned} 32\pi^2 \sum_{n=1}^{\infty} \int_{\mathbb{D}_0} \frac{|\varphi'(E,L)|}{T(E,L)} \frac{1}{\frac{4\pi^2 n^2}{T(E,L)^2} - \frac{4\pi^2}{(T_{\max})^2}} \int_{r_-(E,L)}^{r_+(E,L)} \frac{\sin^2(2\pi n\, \theta(r,E,L))}{r^2} \,\mathrm{d}r \,\mathrm{d}(E,L) \leq \\ \leq C \int_{\mathbb{D}_0} \frac{|\varphi'(E,L)|}{T_{\max} - T(E,L)} \,\mathrm{d}(E,L). \end{aligned} \tag{6.4.4}$$

Here, the constants $C > 0$ always depend on the fixed steady state parameters L_0, k, ℓ, and κ as well as on $\varepsilon_0 > 0$, but are independent of $\varepsilon \in]0, \varepsilon_0[$. We choose $\varepsilon_0 > 0$ sufficiently small in order to deduce the boundedness of $T_{\max}$ and $(T_{\min})^{-1}$ via Proposition 6.2.6 (e), and recall the uniform bounds on $R_{\min}$ and $R_{\max}$ derived in Proposition 6.2.2 (c). After possibly reducing $\varepsilon_0 > 0$, we apply (6.2.49) and the mean value theorem to obtain

$$T_{\max} - T(E,L) = T_{\max} - T(E_0,L) + T(E_0,L) - T(E,L) \geq \frac{1}{C}(E_0 - E) \tag{6.4.5}$$

for $(E,L) \in \mathbb{D}_0$; note $(E_0, L) \in \overline{\mathbb{D}}_0$, and thus $T(E_0,L) \leq T_{\max}$. Inserting this estimate together with (6.2.6) into the right-hand side of (6.4.4) leads to

$$\begin{aligned} \int_{\mathbb{D}_0} \frac{|\varphi'(E,L)|}{T_{\max} - T(E,L)} \,\mathrm{d}(E,L) &\leq C\varepsilon \int_{\mathbb{D}_0} (E_0 - E)^{k-2} (L - L_0)^{\ell} \,\mathrm{d}(E,L) = \\ &= C\varepsilon \int_{L_0}^{L_{\max}} (L - L_0)^{\ell} \int_{E_L^{\min}}^{E_0} (E_0 - E)^{k-2} \,\mathrm{d}E \,\mathrm{d}L = \\ &= C\varepsilon \int_{L_0}^{L_{\max}} (L - L_0)^{\ell} \, (E_0 - E_L^{\min})^{k-1} \,\mathrm{d}L; \end{aligned} \tag{6.4.6}$$

recall $k > 1$. Since $E_0 - E_L^{\min} < \kappa + \frac{M}{R_{\min}^0}$, $\ell > -1$, and $L_{\max}$ is uniformly bounded for $\varepsilon \in]0, \varepsilon_0[$ by Proposition 6.2.6 (c) (after possibly reducing $\varepsilon_0 > 0$ again), the integral in the latter expression is uniformly bounded for $\varepsilon \in]0, \varepsilon_0[$. Thus, with $\varepsilon_0 > 0$ sufficiently small, the right-hand side of (6.4.6) is indeed smaller than one, and we conclude (6.4.3). □

Notice that the assumption (6.4.2) on the regularity of the steady state is crucial for the above proof: If $0 < k \leq 1$, the integral in the second line of (6.4.6) would be infinite. In particular, we do not believe that the assumption (6.4.2) can be weakened without fundamentally changing/improving the strategy of the proof.

In the context of analysing the spectrum of $\mathcal{L}$ in $\mathcal{G}$, it is a natural question whether we can also prove the existence of eigenvalues in $\mathcal{G}$ for sufficiently small steady states surrounding a point mass which are less regular than the ones satisfying (6.4.2). Unfortunately, this turns out to be more complicated than showing the absence of such eigenvalues. To conclude this section, let us briefly discuss this issue.

Remark 6.4.2 (Existence of Eigenvalues in $\mathcal{G}$ for $\varepsilon \ll 1$?)**.** *In addition to* (6.2.7)*, assume that the polytropic exponents k and ℓ satisfy*

$$k + \ell \leq 0. \tag{6.4.7}$$

With Theorem 5.4.1 in mind, it seems promising that one can prove the existence of an eigenvalue in $\mathcal{G}$ by applying Theorem 5.3.1. More precisely, after deriving an estimate similar to (5.4.10)*, we would like to show that an integral of the form*

$$\int_{L_0}^{L_0+\iota} \int_{E_0-\iota}^{E_0} \frac{|\varphi'(E,L)|}{T_{\max} - T(E,L)} \,\mathrm{d}(E,L) \tag{6.4.8}$$

is large, where $\iota > 0$ is some (small) ε-independent number. By Proposition 6.2.6 and Lemma 6.2.20, we know that $T_{\max} - T(E_0, L_0) \to 0$ as $\varepsilon \to 0$, which yields

$$\int_{L_0}^{L_0+\iota} \int_{E_0-\iota}^{E_0} \frac{|\tilde{\varphi}'(E,L)|}{T_{\max} - T(E,L)} \,\mathrm{d}(E,L) \to \infty, \qquad \varepsilon \to 0, \tag{6.4.9}$$

by similar calculations as in the proof of Theorem 5.4.1. However, due to the ε-factor included in $\varphi = \varepsilon\tilde{\varphi}$, recall (6.2.6)*, we cannot infer from* (6.4.9) *that* (6.4.8) *gets large for $0 < \varepsilon \ll 1$.*

We would get around this problem if

$$T_{\max} = T(E_0, L_0). \tag{6.4.10}$$

If this were true, we would be in the same situation as in Theorem 5.4.1 and the integral (6.4.8) *would be infinite for any $\varepsilon > 0$. By Proposition 6.2.6 (e) and the shape of $\mathbb{D}_0$, for all sufficiently small $\varepsilon > 0$ there exists $L^* \in [L_0, L_{\max}]$ s.t. $T_{\max} = T(E_0, L^*)$. Proving $L^* = L_0$ requires knowledge of the L-monotonicity of T. However, the period function T^0 is constant in L in the limiting case $\varepsilon = 0$, cf. Lemma 6.2.5. Hence, the L-monotonicity of T for $0 < \varepsilon \ll 1$ is harder to analyse compared to the arguments in Section 6.2.1. We will later discuss a way of studying this L-monotonicity, cf. Chapter 9.*

6.5 Absence of Embedded Eigenvalues

The aim of this section is to show that the linearised operator $\mathcal{L}\colon \mathrm{D}(\mathcal{L}) \to \mathcal{H}$ associated to certain "small" steady states does not possess any eigenvalues embedded into its essential spectrum; recall that $\sigma_{\mathrm{ess}}(\mathcal{L})$ is given by (4.5.3). Let L_0, k, ℓ, and κ be fixed as specified in Proposition 6.2.2. For $\varepsilon > 0$, let f_0 be the steady state given by Proposition 6.2.2. This whole section is based on [61, Sc. 4]; here, we "generalise" the results to steady states with an L-dependency.

As a preparation, we first derive additional properties of the period function in the regime $0 < \varepsilon \ll 1$ and introduce some notation.

Lemma 6.5.1. *There exists $\varepsilon_0 > 0$ s.t. the following assertions hold for any $0 < \varepsilon < \varepsilon_0$: For any $L \in [L_0, L_{\max}]$, the mapping*

$$T(\cdot, L)\colon [E_L^{\min}, E_0] \to [T_{\min}(L), T_{\max}(L)],\ E \mapsto T(E,L) \tag{6.5.1}$$

is one-to-one and strictly increasing, where

$$T_{\min}(L) \coloneqq T(E_L^{\min}, L), \qquad T_{\max}(L) \coloneqq T(E_0, L); \tag{6.5.2}$$

the former value refers to the continuous extension of the period function to minimal energies defined by (A.4.11)*. We denote the inverse of* (6.5.1) *by*

$$E(\cdot, L)\colon [T_{\min}(L), T_{\max}(L)] \to [E_L^{\min}, E_0], \tag{6.5.3}$$

i.e., $E(t, L)$ is defined via

$$T(E(t, L), L) = t, \qquad L \in [L_0, L_{\max}],\ t \in [T_{\min}(L), T_{\max}(L)]. \tag{6.5.4}$$

Moreover, the mapping $[L_0, L_{\max}] \ni L \mapsto T_{\min}(L)$ is strictly increasing, and thus $T_{\min} = T_{\min}(L_0)$.

Proof. The claimed monotonicity of $T(\cdot, L)$ follows by Proposition 6.2.6 (e). By Proposition 6.2.2 (e) and Lemma 6.2.4, $L \mapsto \Psi_L''(r_L) = 4\pi\,\rho_0(r_L) + \frac{L}{r_L^4}$ is continuously differentiable with

$$\partial_L\big[\Psi_L''(r_L)\big] = \frac{4\pi\rho_0'(r_L) - \frac{4L}{r_L^5}}{4\pi r_L^3\rho_0(r_L) + M + m_0(r_L)} + \frac{1}{r_L^4}, \qquad L > 0. \tag{6.5.5}$$

By Proposition 6.2.6 and (6.2.36), the latter expression tends to $-\frac{3}{(r_L^0)^4} < 0$ as $\varepsilon \to 0$ uniformly on compact L-sets. Together with Proposition 6.2.6 (c) we hence conclude the claimed monotonicity of $[L_0, L_{\max}] \ni L \mapsto T_{\min}(L)$. □

In order to show the absence of embedded eigenvalues of $\mathcal{L}$, we first translate the eigenvalue equation into a first-order Fourier setting. This is based on [61, Lemma 4.1].

Lemma 6.5.2. *Suppose that $\mathcal{L}\colon \mathrm{D}(\mathcal{L}) \to \mathcal{H}$ possesses the eigenvalue $\frac{4\pi^2 m^2}{T_m^2}$ for some $m \in \mathbb{N} = \mathbb{N}\setminus\{0\}$ and $T_m \in [T_{\min}, T_{\max}]$ with eigenfunction $g \in \mathrm{D}(\mathcal{L})$. In addition, let $0 < \varepsilon < \varepsilon_0$ with sufficiently small $\varepsilon_0 > 0$. Then the function*[162] *$f = g + \frac{T_m}{2\pi i m}\mathcal{T}g$ enjoys the regularity $f \in \mathrm{D}(\mathcal{T})$ and the equation*

$$\hat{f}(n, E, L) = -T_m \frac{|\varphi'(E, L)|\,\widehat{U_f}(n, E, L)}{T_m - \frac{m}{n}T(E, L)}, \qquad n \in \mathbb{Z}^*,\ \text{a.e. } (E, L) \in \mathbb{D}_0, \tag{6.5.6}$$

holds. Moreover, $U_f = \frac{T_m}{2\pi i m}U_{\mathcal{T}g}$, so that the statements of Lemmas 4.4.6 and 6.3.2 apply to U_f, and $U_f' \not\equiv 0$.

Proof. First observe $U_g = 0$ since g is odd in v. Using (4.4.23), it is then easy to check that f is an eigenfunction of the operator

$$\tilde{\mathcal{L}}\colon \mathrm{D}(\mathcal{T}) \to H,\ \tilde{\mathcal{L}}h \coloneqq \mathcal{T}\big(h + |\varphi'(E, L)|\,U_h\big) \tag{6.5.7}$$

to the eigenvalue $\frac{2\pi i m}{T_m}$. Notice that $U_h' \in L^2([0, \infty[)$ for $h \in H$ by Lemma 4.4.5. Hence, by Lemmas 4.1.3 and 4.3.9, $|\varphi'(E, L)|\,U_h \in \mathrm{D}(\mathcal{T})$, which shows that $\tilde{\mathcal{L}}$ is well-defined. Writing the eigenvalue equation for f in action-angle type variables via Lemma 4.3.9 leads to

$$\frac{1}{T(E, L)}\,\partial_\theta\big(f + |\varphi'(E, L)|\,U_f\big) = \frac{2\pi i m}{T_m}\,f \qquad \text{a.e. on } \mathbb{S}^1 \times \mathbb{D}_0. \tag{6.5.8}$$

We then apply the Fourier transform w.r.t. θ onto this equation, cf. Remark 4.3.11 and Lemma 4.3.12, to obtain

$$\frac{n}{T(E, L)}\Big(\hat{f}(n, E, L) + |\varphi'(E, L)|\,\widehat{U_f}(n, E, L)\Big) = \frac{m}{T_m}\,\hat{f}(n, E, L), \quad n \in \mathbb{Z}^*,\ \text{a.e. } (E, L) \in \mathbb{D}_0; \tag{6.5.9}$$

[162] Obviously, f is complex-valued. Operators acting on such a function is to be understood in the sense of Remark 4.2.4 (f).

recall the regularity of $U_f = \frac{T_m}{2\pi i m} U_{\mathcal{T}g}$ in action-angle type variables shown in Lemma 6.3.2. It is convenient to rewrite this equation in the following form:

$$\Big(T_m - \frac{m}{n}\, T(E,L)\Big)\hat{f}(n,E,L) = -T_m|\varphi'(E,L)|\,\widehat{U_f}(n,E,L), \qquad n \in \mathbb{Z}^*, \text{ a.e. } (E,L) \in \mathbb{D}_0. \tag{6.5.10}$$

By Proposition 6.2.6 (e), the set of $(E,L) \in \mathbb{D}_0$ with $T_m - \frac{m}{n}\, T(E,L) = 0$ has zero measure for $n \in \mathbb{Z}^*$ provided $\varepsilon_0 > 0$ is sufficiently small. We thus conclude (6.5.6).

Lastly, assume that $U_f' = 0$. Then $U_f = 0$ by Lemma 4.4.5, and thus $f = 0$ a.e. by (6.5.9). By the definition of f, this means $\mathcal{T}g = -\frac{2\pi i m}{T_m} g$, which is impossible since $g \not\equiv 0$ is odd in v and $\mathcal{T}$ reverses v-parity, cf. Lemma 4.3.16. □

The above lemma suggests that the (n,E,L)-values where the denominator on the right-hand side of (6.5.6) vanishes play a distinguished role in the study of embedded eigenvalues. We call such frequency-action triples $(n,E,L) \in \mathbb{Z}^* \times \overline{\mathbb{D}}_0$ *resonant*. The next lemma provides quantitative bounds on the number of frequencies that are nearly resonant, i.e., on the amount of n-values where the denominator gets small. This is based on [61, Lemma 4.3 and Eqn. (4.7)].

Lemma 6.5.3 (δ-Resonant Set)**.** *For fixed $(m,T_m) \in \mathbb{N} \times [T_{\min}, T_{\max}]$ and $0 < \delta < \frac{1}{2}T_{\min}$ consider the δ-resonant set*

$$L_m^\delta := \Big\{ n \in \mathbb{Z}^* \mid \exists (E,L) \in \overline{\mathbb{D}}_0 \colon |T_m - \frac{m}{n} T(E,L)| < \delta \Big\}; \tag{6.5.11}$$

recall the continuous extension of T onto $\overline{\mathbb{D}}_0$ given by (A.4.11)*. Then $L_m^\delta \subset \mathbb{N}$ and there exists a constant $C > 0$, which can be bounded in terms of $T_{\min}$ and $T_{\max}$, s.t.*

$$\frac{n}{m} + \frac{m}{n} \le C, \qquad n \in L_m^\delta. \tag{6.5.12}$$

In addition, L_m^δ possesses the disjoint decomposition

$$L_m^\delta = \mathcal{R}_m \cup \mathcal{P}_m^\delta \cup \mathcal{N}_m^\delta, \tag{6.5.13}$$

where

$$\mathcal{R}_m := \{ n \in L_m^\delta \mid \exists (E,L) \in \overline{\mathbb{D}}_0 \colon T_m - \frac{m}{n} T(E,L) = 0 \}, \tag{6.5.14}$$

$$\mathcal{P}_m^\delta := \{ n \in L_m^\delta \mid \forall (E,L) \in \overline{\mathbb{D}}_0 \colon T_m - \frac{m}{n} T(E,L) > 0 \}, \tag{6.5.15}$$

$$\mathcal{N}_m^\delta := \{ n \in L_m^\delta \mid \forall (E,L) \in \overline{\mathbb{D}}_0 \colon T_m - \frac{m}{n} T(E,L) < 0 \}. \tag{6.5.16}$$

Proof. If $-\delta < T_m - \frac{m}{n} T(E,L) < \delta$ for some $n \in \mathbb{Z}^*$ and $(E,L) \in \overline{\mathbb{D}}_0$, clearly $\frac{m}{n} > 0$ since $\delta < \frac{1}{2}T_{\min}$, i.e., $n \in \mathbb{N}$. Furthermore,

$$\frac{1}{2}\frac{T_{\min}}{T_{\max}} < \frac{T_{\min} - \delta}{T_{\max}} \le \frac{T_m - \delta}{T(E,L)} < \frac{m}{n} < \frac{T_m + \delta}{T(E,L)} \le \frac{T_{\max} + \delta}{T_{\min}} < \frac{3}{2}\frac{T_{\max}}{T_{\min}}. \tag{6.5.17}$$

The decomposition identity (6.5.13) follows since T is continuous on $\overline{\mathbb{D}}_0$ and $\overline{\mathbb{D}}_0$ is path-connected. □

Another useful piece of notation for the proof of the absence of embedded eigenvalues is given in the following lemma. It is based on [61, Def. 4.4].

Lemma 6.5.4 (The Function $p_{m,n}$)**.** *Let $0 < \varepsilon < \varepsilon_0$ with sufficiently small $\varepsilon_0 > 0$, and let $(m, T_m) \in \mathbb{N} \times [T_{\min}, T_{\max}]$ and $0 < \delta < \frac{1}{2} T_{\min}$. For $n \in L_m^\delta$ define*

$$p_{m,n}(t) \coloneqq -\frac{n}{m} \log(T_m - \frac{m}{n} t) + C_p, \qquad t \in [T_{\min}, T_{\max}] \text{ with } t < \frac{n}{m} T_m. \tag{6.5.18}$$

Here, C_p is chosen independently of m, T_m, n, and ε s.t. $p_{m,n} \geq 0$ on its domain of definition. Obviously, $p_{m,n}$ is an antiderivative of the map $t \mapsto \frac{1}{T_m - \frac{m}{n} t}$, and $p_{m,n}(t) \to \infty$ as $T_m - \frac{m}{n} t \searrow 0$. Moreover, for any $\alpha > 0$ there exists a constant $C > 0$ s.t.

$$p_{m,n}(t) \leq C \, (T_m - \frac{m}{n} t)^{-\alpha}, \qquad t \in [T_{\min}, T_{\max}] \text{ with } t < \frac{n}{m} T_m; \tag{6.5.19}$$

besides its dependency on the exponent α, the constant C has the same properties as C_p.

Proof. The existence of C_p as specified above is due to Lemma 6.5.3 together with the fact that $T_{\max} = T_{\max}^\varepsilon$ is uniformly bounded for $\varepsilon \in]0, \varepsilon_0[$ by Proposition 6.2.6 (e). Similar arguments also show (6.5.19) since $s^\alpha \log(s) \to 0$ as $s \searrow 0$. □

We have now gathered all tools to prove the central result of this section, which is based on [61, Thm. 4.5].

Theorem 6.5.5. *In addition to* (6.2.7)*, assume that the polytropic exponent k satisfies*

$$k > 1. \tag{6.5.20}$$

Then there exists $\varepsilon_0 > 0$ s.t. for any $0 < \varepsilon < \varepsilon_0$ the linearised operator $\mathcal{L}$ has no embedded eigenvalues, i.e., no eigenvalues within its essential spectrum $\sigma_{\mathrm{ess}}(\mathcal{L})$.

Proof. By way of contradiction, we assume that there exists an eigenvalue of $\mathcal{L}$ inside its essential spectrum, which by (4.5.3) means that it is of the form $\frac{4\pi^2 m^2}{T_m^2}$ for some $m \in \mathbb{N}$ and $T_m \in [T_{\min}, T_{\max}]$. Let $f \in \mathrm{D}(\mathcal{T})$ be the associated function derived in Lemma 6.5.2, i.e., the relation (6.5.6) holds, the statements of Lemmas 4.4.6 and 6.3.2 apply to U_f, and $U_f' \not\equiv 0$.

Step 1: An Energy Type Identity. We multiply (6.5.6) with $-T(E,L) \, \overline{\widehat{U_f}(n, E, L)}$, sum over $n \in \mathbb{Z}^*$, and integrate over $\mathbb{D}_0$. By Parseval's theorem, the left-hand side of the resulting identity equals

$$\begin{aligned} -\int_{\mathbb{D}_0} T(E,L) \int_{\mathbb{S}^1} f(\theta, E, L) \, \overline{U_f(\theta, E, L)} \, \mathrm{d}\theta \, \mathrm{d}(E, L) &= -\int_{\Omega_0} f(r, w, L) \, \overline{U_f(r)} \, \mathrm{d}(r, w, L) = \\ &= \frac{1}{16\pi^3} \int_{\mathbb{R}^3} |\partial_x U_f(x)|^2 \, \mathrm{d}x; \end{aligned} \tag{6.5.21}$$

notice that $\hat{f}(0, \cdot)$ vanishes a.e. on $\mathbb{D}_0$ by (6.5.9). As a result, we obtain the energy type identity

$$\frac{1}{16\pi^3} \, \|\partial_x U_f\|_2^2 = T_m \sum_{n \in \mathbb{Z}^*} \int_{\mathbb{D}_0} \frac{|\varphi'(E,L)| \, T(E,L)}{T_m - \frac{m}{n} T(E,L)} \, |\widehat{U_f}(n, E, L)|^2 \, \mathrm{d}(E, L). \tag{6.5.22}$$

Choosing $\delta = \frac{1}{4} T_{\min}$, we use (6.5.13) to decompose the sum on the right-hand side as follows:

$$\begin{aligned} &\frac{\|\partial_x U_f\|_2^2}{16\pi^3} = \\ &= T_m \left(\sum_{n \in \mathbb{Z}^* \setminus L_m^\delta} + \sum_{n \in \mathcal{R}_m} + \sum_{n \in \mathcal{P}_m^\delta} + \sum_{n \in \mathcal{N}_m^\delta} \right) \int_{\mathbb{D}_0} \frac{|\varphi'(E,L)| \, T(E,L)}{T_m - \frac{m}{n} T(E,L)} \, |\widehat{U_f}(n, E, L)|^2 \, \mathrm{d}(E, L). \end{aligned} \tag{6.5.23}$$

Let us analyse and estimate the integral(s) in the last line of this calculation, starting with the terms where $n \notin L_m^\delta$. First note the obvious bound

$$\frac{1}{|T_m - \frac{m}{n}T(E,L)|} \leq \frac{1}{\delta} \leq C, \qquad (E,L) \in \mathbb{D}_0,\ n \in \mathbb{Z}^* \setminus L_m^\delta. \tag{6.5.24}$$

Throughout this proof, the constants $C > 0$ are always allowed to depend on the fixed steady state parameters L_0, k, ℓ, and κ as well as on $\varepsilon_0 > 0$, but are independent of m, T_m, n, and ε. Since $(T_{\min})^{-1}$ and $T_{\max}$ are bounded uniformly in $\varepsilon \in]0, \varepsilon_0[$ by Proposition 6.2.6 (e), we further obtain

$$\frac{1}{|T_m - \frac{m}{n}T(E,L)|} \leq C\frac{|n|}{m}, \qquad (E,L) \in \mathbb{D}_0,\ n \in \mathbb{Z}^* \setminus L_m^\delta. \tag{6.5.25}$$

Together with (6.3.21) we hence deduce we following estimate for the first sum on the right-hand side of (6.5.23):

$$\begin{aligned} T_m \sum_{n \in \mathbb{Z}^* \setminus L_m^\delta} \int_{\mathbb{D}_0} \frac{|\varphi'(E,L)|\, T(E,L)}{T_m - \frac{m}{n}T(E,L)} \, |\widehat{U_f}(n,E,L)|^2 \,\mathrm{d}(E,L) \leq \\ \leq C \sum_{n \in \mathbb{Z}^* \setminus L_m^\delta} \frac{\sqrt{|n|}}{\sqrt{m}} \int_{\mathbb{D}_0} |\varphi'(E,L)|\, |\widehat{U_f}(n,E,L)|^2 \,\mathrm{d}(E,L) \leq \\ \leq \frac{C}{\sqrt{m}}\, \varepsilon\, \|\partial_x U_f\|_2^2 \sum_{n \in \mathbb{Z}^* \setminus L_m^\delta} \frac{1}{|n|^{\frac{3}{2}}} \leq \frac{C}{\sqrt{m}}\, \varepsilon\, \|\partial_x U_f\|_2^2. \end{aligned} \tag{6.5.26}$$

For $n \in \mathcal{P}_m^\delta$, Lemma 6.5.4 and an integration by parts in the particle energy E yield

$$\begin{aligned} &\int_{\mathbb{D}_0} \frac{|\varphi'(E,L)|\, T(E,L)}{T_m - \frac{m}{n}T(E,L)} \, |\widehat{U_f}(n,E,L)|^2 \,\mathrm{d}(E,L) = \\ &\quad = \int_{\mathbb{D}_0} \frac{|\varphi'(E,L)|\, T(E,L)}{\partial_E T(E,L)} \, \partial_E[p_{m,n}(T(E,L))] \, |\widehat{U_f}(n,E,L)|^2 \,\mathrm{d}(E,L) = \\ &\quad = A_n + B_n + \int_{L_0}^{L_{\max}} \frac{|\varphi'(E,L)|\, T(E,L)}{\partial_E T(E,L)} \, p_{m,n}(T(E,L)) \, |\widehat{U_f}(n,E,L)|^2 \Big|_{E=E_L^{\min}}^{E=E_0} \mathrm{d}L \leq \\ &\quad \leq A_n + B_n, \end{aligned} \tag{6.5.27}$$

where for $n \in \mathcal{P}_m^\delta$,

$$A_n \coloneqq -2 \int_{\mathbb{D}_0} \frac{|\varphi'(E,L)|\, T(E,L)}{\partial_E T(E,L)} \, p_{m,n}(T(E,L)) \, \mathrm{Re}\Big(\partial_E \widehat{U_f}(n,E,L)\, \overline{\widehat{U_f}(n,E,L)}\Big) \,\mathrm{d}(E,L), \tag{6.5.28}$$

$$B_n \coloneqq -\int_{\mathbb{D}_0} \partial_E \left[\frac{|\varphi'(E,L)|\, T(E,L)}{\partial_E T(E,L)}\right] p_{m,n}(T(E,L)) \, |\widehat{U_f}(n,E,L)|^2 \,\mathrm{d}(E,L). \tag{6.5.29}$$

In the last line of (6.5.27), we used $k > 1$ to deduce $\varphi'(E_0, L) = 0$ for $L \geq L_0$, which shows that the boundary term at $E = E_0$ vanishes; note that $\widehat{U_f}(n,\cdot) \in C^1(\mathbb{A}_0)$ by Lemmas 6.3.2 and 6.5.2. By (6.2.49) and Lemma 6.5.4, the other boundary term is non-positive provided $\varepsilon_0 > 0$ is sufficiently small.

A little more caution is needed to perform the analogous arguments for $n \in \mathcal{R}_m$. By the definition of this set, cf. (6.5.14),

$$t_n \coloneqq \frac{n}{m} T_m \in [T_{\min}, T_{\max}]. \tag{6.5.30}$$

Let

$$L_+(t) \coloneqq \sup\{L \in [L_0, L_{\max}] \mid T_{\min}(L) \le t\}, \qquad t \in [T_{\min}, T_{\max}]; \tag{6.5.31}$$

recall (6.5.2) for the definition of $T_{\min}(L)$. For $L \in]L_+(t_n), L_{\max}]$ there holds $T(E,L) \ge T_{\min}(L) > t_n$ for $E_L^{\min} \le E \le E_0$ by Lemma 6.5.1 provided $\varepsilon_0 > 0$ is sufficiently small, i.e., $T_m - \frac{m}{n}T(E,L) < 0$. For $L \in [L_0, L_+(t_n)]$ we set

$$E_n(L) \coloneqq \begin{cases} E(t_n, L), & \text{if } t_n \le T_{\max}(L), \\ E_0, & \text{otherwise;} \end{cases} \tag{6.5.32}$$

recall (6.5.4) for the definition of $E(t,L)$. The quantities $L_+(t)$ and $E_n(L)$ are defined s.t.

$$\{(E,L) \in \mathbb{D}_0 \mid T_m - \frac{m}{n}T(E,L) > 0\} = \{(E,L) \mid L_0 < L < L_+(t_n),\ E_L^{\min} < E < E_n(L)\} \tag{6.5.33}$$

holds for $n \in \mathcal{R}_m$. Hence, for $n \in \mathcal{R}_m$, a calculation similar to (6.5.27) yields

$$\begin{aligned} &\int_{\mathbb{D}_0} \frac{|\varphi'(E,L)|\,T(E,L)}{T_m - \frac{m}{n}T(E,L)} \,|\widehat{U_f}(n,E,L)|^2 \,\mathrm{d}(E,L) = \\ &\quad \le \int_{L_0}^{L_+(t_n)} \int_{E_L^{\min}}^{E_n(L)} \frac{|\varphi'(E,L)|\,T(E,L)}{T_m - \frac{m}{n}T(E,L)} \,|\widehat{U_f}(n,E,L)|^2 \,\mathrm{d}E\,\mathrm{d}L = \\ &\quad = A_n + B_n + \int_{L_0}^{L_+(t_n)} \frac{|\varphi'(E,L)|\,T(E,L)}{\partial_E T(E,L)}\, p_{m,n}(T(E,L))\, |\widehat{U_f}(n,E,L)|^2 \Big|_{E=E_L^{\min}}^{E=E_n(L)} \mathrm{d}L \le \\ &\quad \le A_n + B_n, \end{aligned} \tag{6.5.34}$$

where for $n \in \mathcal{R}_m$,

$$\begin{aligned} A_n \coloneqq -2 \int_{L_0}^{L_+(t_n)} \int_{E_L^{\min}}^{E_n(L)} &\frac{|\varphi'(E,L)|\,T(E,L)}{\partial_E T(E,L)}\, p_{m,n}(T(E,L)) \cdot \\ &\cdot \mathrm{Re}\Big(\partial_E \widehat{U_f}(n,E,L)\, \overline{\widehat{U_f}(n,E,L)}\Big)\,\mathrm{d}E\,\mathrm{d}L, \end{aligned} \tag{6.5.35}$$

$$B_n \coloneqq -\int_{L_0}^{L_+(t_n)} \int_{E_L^{\min}}^{E_n(L)} \partial_E \left[\frac{|\varphi'(E,L)|\,T(E,L)}{\partial_E T(E,L)}\right] p_{m,n}(T(E,L))\, |\widehat{U_f}(n,E,L)|^2 \,\mathrm{d}E\,\mathrm{d}L. \tag{6.5.36}$$

In the last line of (6.5.34), we again used that the boundary term coming from $E = E_L^{\min}$ is non-positive. The other boundary term vanishes for every $L \in [L_0, L_+(t_n)[$. In the case $t_n > T_{\max}(L)$, this is due to $\varphi'(E_0, L) = 0$. If $t_n = T_{\max}(L)$, $E_n(L) = E_0$. Hence, $k > 1$ together with (6.5.19) again yields that the boundary term vanishes. Lastly, in the case $T_{\min}(L) < t_n < T_{\max}(L)$, first note that $\widehat{U_f}(n, E_n(L), L) = 0$ by (6.5.10). Since $\widehat{U_f}(n,\cdot,L)\colon]E_L^{\min}, 0[\to \mathbb{C}$ is continuously differentiable by Lemma 6.3.2, we again use (6.5.19) to infer that the boundary term vanishes.

Altogether, inserting (6.5.26), (6.5.27), and (6.5.34) into (6.5.23) and using that the terms with $n \in \mathcal{N}_m^\delta$ are non-positive yields

$$\|\partial_x U_f\|_2^2 \le \frac{C}{\sqrt{m}}\,\varepsilon\,\|\partial_x U_f\|_2^2 + T_m \sum_{n \in \mathcal{R}_m} (A_n + B_n) + T_m \sum_{n \in \mathcal{P}_m^\delta} (A_n + B_n). \tag{6.5.37}$$

Step 2: Estimating A_n for $n \in \mathcal{P}_m^\delta$ and $n \in \mathcal{R}_m$. To cope with the degeneracy of the action-angle type variables at minimal energies $E = E_L^{\min}$, we introduce powers of

$$\delta E_L \coloneqq E - E_L^{\min} \tag{6.5.38}$$

as weights in our estimates. Observe that

$$2\pi in\,\widehat{U_f}(n,E,L) = \widehat{\partial_\theta U_f}(n,E,L), \qquad n\in\mathbb{Z},\ (E,L)\in\mathbb{A}_0. \tag{6.5.39}$$

For any $n\in\mathcal{P}_m^\delta$ we insert this identity into (6.5.28) and apply (6.5.12) and the Cauchy-Schwarz inequality to deduce

$$\begin{aligned}|A_n|^2 &\le \frac{C}{n^2}\left|\int_{\mathbb{D}_0}\frac{|\varphi'(E,L)|T(E,L)}{\partial_E T(E,L)}p_{m,n}(T(E,L))|\partial_E\widehat{U_f}(n,E,L)|\,|\widehat{\partial_\theta U_f}(n,E,L)|\,\mathrm{d}(E,L)\right|^2 \le\\ &\le \frac{C}{m^2}\int_{\mathbb{D}_0}|\varphi'(E,L)|\,T(E,L)\,\delta E_L\,|\partial_E\widehat{U_f}(n,E,L)|^2\,\mathrm{d}(E,L)\cdot\\ &\qquad\cdot\int_{\mathbb{D}_0}\frac{|\varphi'(E,L)|\,T(E,L)}{\partial_E T(E,L)^2}\,p_{m,n}(T(E,L))^2\frac{|\widehat{\partial_\theta U_f}(n,E,L)|^2}{\delta E_L}\,\mathrm{d}(E,L).\end{aligned} \tag{6.5.40}$$

Applying Cauchy's inequality and summing over $n\in\mathcal{P}_m^\delta$ yields

$$\begin{aligned}\sum_{n\in\mathcal{P}_m^\delta}|A_n| &\le \frac{C}{\sqrt{m}}\sum_{n\in\mathcal{P}_m^\delta}\int_{\mathbb{D}_0}|\varphi'(E,L)|\,T(E,L)\,\delta E_L\,|\partial_E\widehat{U_f}(n,E,L)|^2\,\mathrm{d}(E,L)+\\ &+\frac{C}{m^{\frac32}}\sum_{n\in\mathcal{P}_m^\delta}\int_{\mathbb{D}_0}\frac{|\varphi'(E,L)|\,T(E,L)}{\partial_E T(E,L)^2}\,p_{m,n}(T(E,L))^2\frac{|\widehat{\partial_\theta U_f}(n,E,L)|^2}{\delta E_L}\,\mathrm{d}(E,L).\end{aligned} \tag{6.5.41}$$

By the same arguments we also obtain

$$\begin{aligned}\sum_{n\in\mathcal{R}_m}|A_n| &\le \frac{C}{\sqrt{m}}\sum_{n\in\mathcal{R}_m}\int_{\mathbb{D}_0}|\varphi'(E,L)|\,T(E,L)\,\delta E_L\,|\partial_E\widehat{U_f}(n,E,L)|^2\,\mathrm{d}(E,L)+\\ &+\frac{C}{m^{\frac32}}\sum_{n\in\mathcal{R}_m}\int_{L_0}^{L_+(t_n)}\int_{E_L^{\min}}^{E_n(L)}\frac{|\varphi'(E,L)|\,T(E,L)}{\partial_E T(E,L)^2}\,p_{m,n}(T(E,L))^2\frac{|\widehat{\partial_\theta U_f}(n,E,L)|^2}{\delta E_L}\,\mathrm{d}E\,\mathrm{d}L.\end{aligned} \tag{6.5.42}$$

The first sums on the right-hand sides of (6.5.41) and (6.5.42), respectively, combine to give

$$\begin{aligned}&\frac{C}{\sqrt{m}}\sum_{n\in\mathcal{P}_m^\delta\cup\mathcal{R}_m}\int_{\mathbb{D}_0}|\varphi'(E,L)|\,T(E,L)\,\delta E_L\,|\partial_E\widehat{U_f}(n,E,L)|^2\,\mathrm{d}(E,L)\le\\ &\qquad\le\frac{C}{\sqrt{m}}\sum_{n\in\mathbb{Z}}\int_{\mathbb{D}_0}|\varphi'(E,L)|\,T(E,L)\,\delta E_L\,|\partial_E\widehat{U_f}(n,E,L)|^2\,\mathrm{d}(E,L)=\\ &\qquad=\frac{C}{\sqrt{m}}\int_{\mathbb{D}_0}|\varphi'(E,L)|\,T(E,L)\,\delta E_L\int_{\mathbb{S}^1}|\partial_E U_f(\theta,E,L)|^2\,\mathrm{d}\theta\,\mathrm{d}(E,L),\end{aligned} \tag{6.5.43}$$

where we used the Plancherel identity in the last line; notice $\partial_E\widehat{U_f}(n,E,L)=\widehat{\partial_E U_f}(n,E,L)$ for $(E,L)\in\mathbb{A}_0$ and $n\in\mathbb{Z}$ since $U_f\in C^1(\mathbb{S}^1\times\mathbb{A}_0)$ by Lemmas 6.3.2 and 6.5.2. We continue the calculation (6.5.43) by using the bound (6.3.20) and applying the change of variables $\theta\mapsto r=r(\theta,E,L)$ defined by (4.3.9), note that $\partial_\theta r(\theta,E,L)=T(E,L)\sqrt{2E-2\Psi_L(r)}$:

$$\begin{aligned}&\frac{C}{\sqrt{m}}\int_{\mathbb{D}_0}|\varphi'(E,L)|\,T(E,L)\,\delta E_L\int_{\mathbb{S}^1}|\partial_E U_f(\theta,E,L)|^2\,\mathrm{d}\theta\,\mathrm{d}(E,L)\le\\ &\qquad\le\frac{C}{\sqrt{m}}\int_{\mathbb{D}_0}|\varphi'(E,L)|\,T(E,L)\int_{\mathbb{S}^1}|U_f'(r(\theta,E,L))|^2\,\mathrm{d}\theta\,\mathrm{d}(E,L)=\\ &\qquad=\frac{C}{\sqrt{m}}\int_{R_{\min}}^{R_{\max}}|U_f'(r)|^2\int_{\mathbb{D}_0(r)}\frac{|\varphi'(E,L)|}{\sqrt{2E-2\Psi_L(r)}}\,\mathrm{d}(E,L)\,\mathrm{d}r,\end{aligned} \tag{6.5.44}$$

where $\mathbb{D}_0(r)$ is defined in (5.2.18) for $r \in [R_{\min}, R_{\max}]$. In order to compute the (E,L)-integral on the right-hand side of (6.5.44) for fixed $r \in]R_{\min}, R_{\max}[$, let $L_{\max}(r) \in]L_0, L_{\max}]$ be defined as the unique solution of $\Psi_{L_{\max}(r)}(r) = E_0$; the same notation has been used in the proof of Proposition 5.2.12. Then

$$\begin{aligned}\int_{\mathbb{D}_0(r)} \frac{|\varphi'(E,L)|}{\sqrt{2E-2\Psi_L(r)}}\,\mathrm{d}(E,L) &= k\varepsilon \int_{L_0}^{L_{\max}(r)} \int_{\Psi_L(r)}^{E_0} \frac{(E_0-E)^{k-1}(L-L_0)^\ell}{\sqrt{2E-2\Psi_L(r)}}\,\mathrm{d}E\,\mathrm{d}L = \\ &= C\varepsilon \int_{L_0}^{L_{\max}(r)} (L-L_0)^\ell (E_0-\Psi_L(r))^{k-\frac{1}{2}}\,\mathrm{d}L \le C\varepsilon \end{aligned} \tag{6.5.45}$$

because $k > \frac{1}{2}$ and $\ell > -1$, where we used the standard integral identity (2.2.23) as well as the estimate $E_0 - \Psi_L(r) \le \kappa + \frac{M}{R_{\min}^0}$ and the uniform boundedness of $L_{\max} = L_{\max}^\varepsilon$ for $0 < \varepsilon \ll 1$, cf. Proposition 6.2.6 (c). Overall, (6.5.43), (6.5.44), and (6.5.45) yield

$$\frac{C}{\sqrt{m}} \sum_{n \in \mathcal{P}_m^\delta \cup \mathcal{R}_m} \int_{\mathbb{D}_0} |\varphi'(E,L)|\, T(E,L)\, \delta E_L\, |\partial_E \widehat{U_f}(n,E,L)|^2\,\mathrm{d}(E,L) \le \frac{C}{\sqrt{m}}\,\varepsilon\,\|\partial_x U_f\|_2^2. \tag{6.5.46}$$

It remains to estimate the second sums on the right-hand sides of (6.5.41) and (6.5.42), respectively. We start with the more challenging part, the resonant contribution from (6.5.42). Since $\partial_\theta U_f = U_f' \,\partial_\theta r$, changing variables via $\theta \mapsto r = r(\theta, E, L)$, applying Plancherel's theorem, and using the uniform-in-$\varepsilon \in]0, \varepsilon_0[$ bounds from Proposition 6.2.6 lead to

$$\begin{aligned}&\sum_{n\in\mathcal{R}_m} \int_{L_0}^{L_+(t_n)} \int_{E_L^{\min}}^{E_n(L)} \frac{|\varphi'(E,L)|\,T(E,L)}{\partial_E T(E,L)^2}\, p_{m,n}(T(E,L))^2 \frac{|\widehat{\partial_\theta U_f}(n,E,L)|^2}{\delta E_L}\,\mathrm{d}E\,\mathrm{d}L \le \\ &\le C \sum_{n\in\mathcal{R}_m} \int_{L_0}^{L_+(t_n)} \int_{E_L^{\min}}^{E_n(L)} \frac{|\varphi'|}{\delta E_L}\, p_{m,n}(T)^2 \int_{\mathbb{S}^1} |\partial_\theta U_f(\theta,E,L)|^2\,\mathrm{d}\theta\,\mathrm{d}E\,\mathrm{d}L = \\ &= C \sum_{n\in\mathcal{R}_m} \int_{L_0}^{L_+(t_n)} \int_{E_L^{\min}}^{E_n(L)} \frac{|\varphi'|\,T}{\delta E_L}\, p_{m,n}(T)^2 \int_{r_-(E,L)}^{r_+(E,L)} |U_f'(r)|^2 \sqrt{2E-2\Psi_L(r)}\,\mathrm{d}r\,\mathrm{d}E\,\mathrm{d}L \le \\ &\le C \sum_{n\in\mathcal{R}_m} \int_{R_{\min}}^{R_{\max}} |U_f'(r)|^2\,\mathrm{d}r \int_{L_0}^{L_+(t_n)} \int_{E_L^{\min}}^{E_n(L)} \frac{|\varphi'|}{\sqrt{\delta E_L}}\, p_{m,n}(T)^2\,\mathrm{d}E\,\mathrm{d}L. \end{aligned} \tag{6.5.47}$$

To estimate the latter expression we have to bound the action integrals

$$I_{n,m} \coloneqq \int_{L_0}^{L_+(t_n)} \int_{E_L^{\min}}^{E_n(L)} \frac{|\varphi'(E,L)|}{\sqrt{\delta E_L}}\, p_{m,n}(T(E,L))^2\,\mathrm{d}E\,\mathrm{d}L. \tag{6.5.48}$$

First note that for $n \in \mathcal{R}_m$, $L \in [L_0, L_+(t_n)]$, and $E \in [E_L^{\min}, E_n(L)[$,

$$T_m - \frac{m}{n}T(E,L) \ge \frac{m}{n}(T(E_n(L),L) - T(E,L)) \ge \frac{1}{C}(E_n(L) - E) \tag{6.5.49}$$

by (6.2.49) and Lemma 6.5.3; in particular, this estimate holds in both cases of the definition (6.5.32) of $E_n(L)$. Together with the bound (6.5.19) with exponent $\alpha = \frac{1}{4}$, we thus

obtain

$$\begin{aligned} I_{n,m} &\leq C \int_{L_0}^{L_+(t_n)} \int_{E_L^{\min}}^{E_n(L)} \frac{|\varphi'(E,L)|}{\sqrt{\delta E_L}} \Big(T_m - \frac{m}{n} T(E,L)\Big)^{-\frac{1}{2}} \,\mathrm{d}E \,\mathrm{d}L \leq \\ &\leq C\varepsilon \int_{L_0}^{L_+(t_n)} (L-L_0)^\ell \int_{E_L^{\min}}^{E_n(L)} \frac{(E_0-E)^{k-1}}{\sqrt{E-E_L^{\min}}} \,(E_n(L)-E)^{-\frac{1}{2}} \,\mathrm{d}E \,\mathrm{d}L \leq \\ &\leq C\varepsilon \int_{L_0}^{L_{\max}} (L-L_0)^\ell (E_0 - E_L^{\min})^{k-1} \leq C\varepsilon, \end{aligned} \tag{6.5.50}$$

where we again used the integral identity (2.2.23) and $k > 1$. Inserting (6.5.50) into (6.5.47) and using the bound $\#\mathcal{R}_m \leq \#L_m^\delta \leq Cm$, which is due to Lemma 6.5.3, yields

$$\begin{aligned} \frac{C}{m^{\frac{3}{2}}} \sum_{n\in\mathcal{R}_m} \int_{L_0}^{L_+(t_n)} \int_{E_L^{\min}}^{E_n(L)} \frac{|\varphi'(E,L)|\,T(E,L)}{\partial_E T(E,L)^2} \, p_{m,n}(T(E,L))^2 \frac{|\widehat{\partial_\theta U_f}(n,E,L)|^2}{\delta E_L} \,\mathrm{d}E \,\mathrm{d}L \leq \\ \leq \frac{C}{m^{\frac{3}{2}}} \,\varepsilon \,\|\partial_x U_f\|_2^2 \,\#\mathcal{R}_m \leq \frac{C}{\sqrt{m}} \,\varepsilon \,\|\partial_x U_f\|_2^2. \end{aligned} \tag{6.5.51}$$

In an analogous, but simpler way we also obtain

$$\frac{C}{m^{\frac{3}{2}}} \sum_{n\in\mathcal{P}_m^\delta} \int_{\mathbb{D}_0} \frac{|\varphi'(E,L)|\,T(E,L)}{\partial_E T(E,L)^2} \, p_{m,n}(T(E,L))^2 \frac{|\widehat{\partial_\theta U_f}(n,E,L)|^2}{\delta E_L} \,\mathrm{d}(E,L) \leq \frac{C}{\sqrt{m}} \,\varepsilon \,\|\partial_x U_f\|_2^2; \tag{6.5.52}$$

just replace $L_+(t_n)$ and $E_n(L)$ with $L_{\max}$ and E_0, respectively, in the above arguments. Altogether, we have thus proven

$$\sum_{n\in\mathcal{R}_m\cup\mathcal{P}_m^\delta} |A_n| \leq \frac{C}{\sqrt{m}} \,\varepsilon \,\|\partial_x U_f\|_2^2. \tag{6.5.53}$$

Step 3: Estimating B_n for $n \in \mathcal{P}_m^\delta$ and $n \in \mathcal{R}_m$. Estimating B_n, recall (6.5.29) and (6.5.36) for the definitions of these integrals, works similarly to estimating the second sums on the right-hand sides of (6.5.41) and (6.5.42), respectively. In order to estimate $|\widehat{U_f}|$, we use (6.5.39) and (6.5.12) to obtain

$$|\widehat{U_f}(n,E,L)|^2 \leq \frac{C}{n^2} \,|\widehat{\partial_\theta U_f}(n,E,L)|^2 \leq \frac{C}{m^2} \,|\widehat{\partial_\theta U_f}(n,E,L)|^2 \tag{6.5.54}$$

for $n \in \mathcal{R}_m \cup \mathcal{P}_m^\delta$ and $(E,L) \in \mathbb{A}_0$. An additional information that needs to be used is the uniform-in-$\varepsilon \in \,]0,\varepsilon_0[$ boundedness of $\partial_E^2 T_{\max}$, cf. Proposition 6.2.6 (e). Besides these points, the only argument which one has to modify is the derivation of an analogue of the estimate (6.5.50) in the case where φ' is replaced with $\varphi'' \coloneqq \partial_E^2 \varphi$. Let us outline how this can be done: For $n \in \mathcal{R}_m$, applying (2.2.23), (6.5.49), and the estimate (6.5.19) with fixed exponent $0 < \alpha < \min\{1, k-1\}$ yields

$$\begin{aligned} \int_{L_0}^{L_+(t_n)} \int_{E_L^{\min}}^{E_n(L)} |\varphi''(E,L)| \,\big(E - E_L^{\min}\big)^{\frac{1}{2}} \, p_{m,n}(T(E,L)) \,\mathrm{d}E \,\mathrm{d}L \leq \\ \leq C\varepsilon \int_{L_0}^{L_+(t_n)} (L-L_0)^\ell \int_{E_L^{\min}}^{E_n(L)} (E_0-E)^{k-2} \frac{\big(E-E_L^{\min}\big)^{\frac{1}{2}}}{(E_n(L)-E)^\alpha} \,\mathrm{d}E \,\mathrm{d}L \leq \\ \leq C\varepsilon \int_{L_0}^{L_+(t_n)} (L-L_0)^\ell (E_0 - E_L^{\min})^{k-\alpha-\frac{1}{2}} \,\mathrm{d}L \leq C\varepsilon; \end{aligned} \tag{6.5.55}$$

note that there is no $(\delta E_L)^{-1}$-weight in the integrals B_n. Overall, we obtain

$$\sum_{n\in\mathcal{R}_m\cup\mathcal{P}_m^\delta} |B_n| \leq \frac{C}{m}\,\varepsilon\,\|\partial_x U_f\|_2^2. \tag{6.5.56}$$

Step 4: The Finale. Inserting the estimates (6.5.53) and (6.5.56) into (6.5.37) yields

$$\|\partial_x U_f\|_2^2 \leq \frac{C_{\text{final}}}{\sqrt{m}}\,\varepsilon\,\|\partial_x U_f\|_2^2. \tag{6.5.57}$$

With $\varepsilon_0 > 0$ small enough this gives the desired contradiction for $0 < \varepsilon < \varepsilon_0$, recall $\partial_x U_f \not\equiv 0$ by Lemma 6.5.2. □

The strategy of the above proof can also be used to show the absence of embedded eigenvalues in more general situations. The following remarks regarding this matter are based on [61, Rems. 4.6 and 4.8 and Cor. 4.7].

Remark 6.5.6 (A Criterion for the Absence of Embedded Eigenvalues)**.** *The above proof shows that a sufficient condition for the absence of embedded eigenvalues is $C_{\text{final}}\varepsilon < 1$, where $C_{\text{final}} > 0$ is the constant appearing in the final estimate* (6.5.57)*. In principle, the constant $C_{\text{final}} > 0$ is explicitly computable; it depends on the underlying steady state through quantities like k, ℓ, L_0, κ, $R_{\min}$, $R_{\max}$, $T_{\min}$, $T_{\max}$, $\partial_E T_{\min}$, $\partial_E T_{\max}$, and $\partial_E^2 T_{\max}$. As long as the relevant properties of the period function – most importantly, those from Lemma 6.5.1 – as well as appropriate regularity properties of the steady state – which are a suitable substitute for* (6.5.20) *– are present, the above proof also works in more general situations. For instance, this includes the steady states from Sections 2.2 and 4.1 without a central point mass. Hence, in the general case, the above proof shows that some (explicitly computable) constant being sufficiently small implies that no embedded eigenvalues occur.*

Remark 6.5.7 (No Embedded Eigenvalues at High Frequencies)**.** *In the above proof we have carefully tracked the dependence of the constants on $m \in \mathbb{N}$. This fixed number correspond to the frequency of the embedded eigenvalue; recall that, by the proof of Proposition 4.3.19, an element of the essential spectrum of the form $\frac{4\pi^2 m^2}{T(E_m,L_m)}$ corresponds to the eigendistribution $\mathbb{S}^1 \times \mathbb{D}_0 \ni (\theta, E, L) \mapsto \sin(2\pi m\theta)\,\delta_{(E_m,L_m)}(E,L)$.*[163,164] *It is evident that one could also obtain a contradiction from* (6.5.57) *by choosing m sufficiently large (instead of choosing ε sufficiently small). For instance, in the case of a steady state as above with $\varepsilon = 1$, i.e.,*

$$f_0(x,v) = (E_0 - E(x,v))_+^k\,(L(x,v) - L_0)_+^\ell, \tag{6.5.58}$$

with polytropic exponents satisfying (6.2.7) *and* (6.5.20)*, the above proof shows that there is no embedded eigenvalue of form $\frac{4\pi^2 m^2}{T_m^2}$ with $T_m \in [T_{\min}, T_{\max}]$ and sufficiently large frequency $m \gg 1$. As discussed in the previous remark, this does, however, require that certain properties of the period function are also valid in the case $\varepsilon = 1$.*[165] *Provided that this was true, we hence conclude that there exists a constant $C_0 > 0$ depending on the steady state (in an explicitly computable way) s.t. there are no embedded eigenvalues larger than C_0.*

As discussed in the previous remark, this also holds in more general settings (under suitable assumptions), including the case without a point mass.

[163] Note, however, that the frequency number m associated to some $\lambda \in \sigma_{\text{ess}}(\mathcal{L}) = \sigma(-\mathcal{T}^2\big|_{\mathcal{H}})$ is not unique in general.

[164] By Proposition 4.5.4, the essential spectra of $\mathcal{L}$ and $-\mathcal{T}^2\big|_{\mathcal{H}}$ are identical. The same proof – which is based on the relative compactness established in Lemma 4.5.3 – also shows that the associated eigendistributions for $-\mathcal{T}^2\big|_{\mathcal{H}}$ are also eigendistributions for $\mathcal{L}$, cf. [69, Proof of Thm. 14.6].

[165] The proof of Lemma 6.5.1 uses $0 < \varepsilon \ll 1$ in a crucial way; concretely, the smallness of ε is used to infer $\partial_E T_{\min} > 0$. To show that $(T_{\min})^{-1}$, $T_{\max}$, $\partial_E T_{\max}$, and $\partial_E^2 T_{\max}$ are finite (for the fixed choice of $\varepsilon = 1$), one can proceed as in Section A.4 and continuously extend the partial derivatives onto $\partial\mathbb{D}_0$.

6.6 Damping for Small Shells Surrounding a Point Mass

In this section we collect the results of the present chapter (and Appendix C) to conclude that the linearised dynamics around certain equilibria are indeed damped. This result is based on [61, Thm. 1.2 (b)].

Theorem 6.6.1 (Damping for Small Shells Surrounding a Point Mass)**.** *For fixed $M > 0$, let f_0 be a polytropic steady state around the point mass M as constructed in Proposition 6.2.2 with the following parameters: Let k and ℓ be polytropic exponents satisfying* (6.2.7) *and*

$$k > 1. \tag{6.6.1}$$

Moreover, let $L_0 > 0$ and we further restrict the range (6.2.16) *of the parameter κ by requiring*

$$-2^{-\frac{2}{3}}\frac{M^2}{2L_0} < \kappa < 0. \tag{6.6.2}$$

Then there exists $\varepsilon_0 > 0$ s.t. for any choice $0 < \varepsilon < \varepsilon_0$ of the smallness parameter ε of the steady state the following holds: For any $(\mathring{f}, \mathring{g}) \in \mathrm{D}(\mathcal{L}) \times (\mathrm{D}(\mathcal{T}) \cap \mathcal{H})$, the solution $\mathbb{R} \ni t \mapsto f(t) \in \mathrm{D}(\mathcal{L})$ of the linearised system (6.3.1) *launched by the initial condition $(f(0), \partial_t f(0)) = (\mathring{f}, \mathring{g})$ is damped in the following way:*

$$\lim_{T\to\infty} \frac{1}{T} \int_0^T \|\partial_x U_{\mathcal{T}f(t)}\|^2_{L^2(\mathbb{R}^3)} \,\mathrm{d}t = 0, \tag{6.6.3}$$

where $U_{\mathcal{T}f(t)}$ is the gravitational potential induced by $\mathcal{T}f(t)$, cf. Definition 4.4.5.

Proof. From (6.2.66) and (6.6.2) we obtain

$$\frac{T^0_{\max}}{T^0_{\min}} > 2. \tag{6.6.4}$$

Hence, Proposition 6.2.6 (e) yields

$$\frac{T_{\max}}{T_{\min}} > 2 \tag{6.6.5}$$

upon choosing $\varepsilon_0 > 0$ sufficiently small. The essential spectrum of the linearised operator, which is given by (4.5.3), thus contains no gaps (besides the essential gap $\mathcal{G}$), more precisely,

$$\sigma_{\mathrm{ess}}(\mathcal{L}) = \left[\frac{4\pi^2}{T^2_{\max}}, \infty\right[; \tag{6.6.6}$$

recall the discussion in Remark 4.3.20.

By Proposition 4.5.11, the spectrum of $\mathcal{L}$ can only contain positive elements. Theorem 6.4.1 shows that $\mathcal{L}$ does not possess eigenvalues in the essential gap $\mathcal{G} =]0, \infty[\backslash \sigma_{\mathrm{ess}}(\mathcal{L})$, and Theorem 6.5.5 implies that there are no (embedded) eigenvalues of $\mathcal{L}$ in $\sigma_{\mathrm{ess}}(\mathcal{L})$. To apply the latter two results, we have to potentially shrink $\varepsilon_0 > 0$ again. Altogether, we conclude that $\mathcal{L}$ possesses no eigenvalues.

The damping property (6.6.3) is then due to Lemma C.0.7; in particular, the discussion in Appendix C shows that (6.3.1) is equivalent to the first-order system (C.0.2) and that this system is well-posed. Notice that all the results from Appendix C remain true in the present setting with a point mass; the results are based only on the properties of the operators derived in Chapter 4, which also hold in the present setting, cf. Section 6.3. □

The additional assumption (6.6.2) on the range of κ ensures that the spectrum of the linearised operator is of the "single gap structure" (6.6.6) for $0 < \varepsilon \ll 1$. For this reason, the assumption (6.6.2) is called the *single gap condition* in [61]. It seems possible to get rid of this assumption (and replace it with (6.2.16)) by extending the methods from Section 6.5 so that they also yield the absence of eigenvalues of $\mathcal{L}$ in the gaps of $\sigma_{\mathrm{ess}}(\mathcal{L})$.

As discussed in Appendix C, the damping property (6.6.3) is, admittedly, rather weak. It is an interesting problem to prove a stronger type of damping in the situation of the above theorem, cf. Chapter 9.

Chapter 7

Similar Methods in Related Situations

In this chapter we demonstrate that the methods presented above can also be applied in related situations. The settings in Sections 7.1 and 7.2 are simplifications of the above situation(s), and we can thus derive improved results there. In Sections 7.3 and 7.4 we (briefly) discuss how to extend the methods to relativistic settings. The latter project is still in its infancy and we mainly outline the difficulties that must be overcome in the future.

Throughout this chapter we focus on the differences to the previous setting(s) and do not repeat arguments known from above. Therefore, the reader should already be familiar with the previous chapters and Appendix A.

7.1 The Vlasov-Poisson System in Plane Symmetry

So far, we have always assumed that both the steady state and the (linear) perturbation are spherically symmetric; recall Definition 2.1.1 for the definition of this symmetry class. We now present another symmetry class. The definition is based on [62, Sc. 1.2], and we generally follow [62] in this section.

Definition 7.1.1 (Plane Symmetry)**.** *(a) A function $f\colon \mathbb{R}^3 \to \mathbb{R}$ is* plane symmetric *(on $\mathbb{R}^3$) if there exists $\tilde{f}\colon \mathbb{R} \to \mathbb{R}$ s.t.*

$$f(x) = \tilde{f}(x_1) = \tilde{f}(-x_1), \qquad x = (x_1, x_2, x_3) \in \mathbb{R}^3. \tag{7.1.1}$$

(b) A function $f\colon \mathbb{R}^3 \times \mathbb{R}^3 \to \mathbb{R}$ is plane symmetric *(on $\mathbb{R}^3 \times \mathbb{R}^3$) if there exists $\tilde{f}\colon \mathbb{R} \times \mathbb{R}^3 \to \mathbb{R}$ s.t.*

$$f(x,v) = \tilde{f}(x_1, v) = \tilde{f}(-x_1, -v_1, \bar{v}), \qquad x = (x_1, x_2, x_3) \in \mathbb{R}^3,\ v = (v_1, \bar{v}) \in \mathbb{R}^3. \tag{7.1.2}$$

Throughout this section we write $v = (v_1, \bar{v})$ for $v \in \mathbb{R}^3$.

From a physics point of view, the mass density of a configuration (like a galaxy) being plane symmetric means that the density is constant in the (x_2, x_3)-plane. On a particle level, this corresponds to a system of space-homogeneous, gravitating planes passing freely through each other. In addition, we require reflection symmetry in the x_1-direction in (a) and in the (x_1, v_1)-direction in (b).[166] Plane symmetry is surely not as natural as spherical

[166] The reflection symmetry imposed in Definition 7.1.1 is of mathematical nature rather than being motivated physically. Nonetheless, we shall see later that any suitable (x_2, x_3)-independent steady state of the Vlasov-Poisson system is reflection symmetric in the x_1-direction.

symmetry, but configurations with this symmetry (or one-dimensional configurations which are related/equivalent to it) are nonetheless studied in the astrophysics literature [84, 100, 108, 111, 179]. In particular, we refer to [43, Ch. I] for further discussions regarding the physical relevance of this setting.

The Vlasov-Poisson System in Plane Symmetry

Similar as before we again identify $\tilde{f}$ with f in the situation of Definition 7.1.1 (a) or (b) by slight abuse of notation. Moreover, we will occasionally write x instead of x_1 for the remaining one-dimensional space variable. With these notational conventions, in plane symmetry the Vlasov-Poisson system (1.1.2)–(1.1.4) becomes

$$\partial_t f + v_1 \, \partial_{x_1} f - U' \, \partial_{v_1} f = 0, \tag{7.1.3}$$

$$U'' = 4\pi\rho, \tag{7.1.4}$$

$$\rho(t, x_1) = \int_{\mathbb{R}^3} f(t, x_1, v) \, \mathrm{d}v, \tag{7.1.5}$$

where $f = f(t, x_1, v)$, $\rho = \rho(t, x_1)$, and $U = U(t, x_1)$ are all assumed to be plane symmetric in the above sense. A prime $'$ now denotes a derivative w.r.t. x_1. Notice that the reflection symmetry imposed in Definition 7.1.1 behaves well with these equations. This system is not yet complete without a suitable boundary condition (at spatial infinity). Due to the homogeneity in the (x_2, x_3)-direction, the boundary condition (1.1.5) is no longer appropriate.[167] Instead, we require that U is explicitly given by

$$U(t, x_1) = 2\pi \int_{\mathbb{R}} |x_1 - y| \, \rho(t, y) \, \mathrm{d}y, \qquad x_1 \in \mathbb{R}. \tag{7.1.6}$$

Note that $U(t)$ is plane symmetric if $\rho(t)$ is. In addition, if $\rho(t)$ is sufficiently regular, $U(t)$ solves the equation (7.1.4) and there holds

$$U'(t, x_1) = 2\pi \int_{\mathbb{R}} \operatorname{sign}(x_1 - y) \, \rho(t, y) \, \mathrm{d}y = 4\pi \int_0^{x_1} \rho(t, y) \, \mathrm{d}y, \qquad x_1 \in \mathbb{R}; \tag{7.1.7}$$

the latter equation again requires $\rho(t)$ to be reflection symmetric. In this case, we further deduce

$$\lim_{x_1 \to \infty} U'(t, x_1) = - \lim_{x_1 \to -\infty} U'(t, x_1), \tag{7.1.8}$$

which is a natural substitute for (1.1.5).[168] It states that the forces at positive and negative infinity are equally strong and point in opposite directions. We refer to the system (7.1.3), (7.1.5), and (7.1.6) as the *Vlasov-Poisson system in plane symmetry*. It should be noted that this system is, in fact, equivalent to the one-dimensional Vlasov-Poisson system since one can simply integrate out the $\bar{v}$-dependency of f. However, we prefer to keep the system in the above form since it is closer to the astrophysics literature and we think that the analogies to the spherically symmetric case are more clear.

[167] The boundary condition $\lim_{x_1 \to \pm\infty} U(t, x_1) = 0$ is also inappropriate. To see this, consider the (physically natural) situation where ρ is non-negative and possesses a compact support in x_1, say $\operatorname{supp}(\rho) \subset [-R, R]$. Any solution U of (7.1.4) is then linear on $\mathbb{R} \setminus [-R, R]$. If U also satisfies the boundary condition $\lim_{x_1 \to \pm\infty} U(x_1) = 0$, it thus has to vanish outside $[-R, R]$. But since the second derivative of U is non-negative, this would imply that U vanishes identically.

[168] From a mathematics point of view, solutions of (7.1.4) and (7.1.8) are only uniquely determined up to the addition of a constant. However, such a translation of $U(t)$ does not affect the solutions of the Vlasov equation (7.1.3). By imposing that U is of the explicit form (7.1.6), we fix this additive constant.

Plane Symmetric Steady States

We now construct suitable steady states of the above system by proceeding in the same way as in the spherically symmetric case in Section 2.2. This is based on [62, Sc. 2.2].

In the case of a time-independent, plane symmetric potential $U_0 = U_0(x_1)$, the characteristic system associated to the Vlasov equation (7.1.3) is

$$\dot{x}_1 = v_1, \qquad \dot{v}_1 = -U_0'(x_1). \tag{7.1.9}$$

We leave out the trivial equations for $\bar{v}$ as it is simply conserved along the characteristic flow. This illustrates that the "effective dimension" of the phase space is now 2, parametrised by the variables (x_1, v_1), compared to the three-dimensional phase space with variables (r, w, L) in spherical symmetry.[169] Another conserved quantity is the particle energy given by

$$E(x_1, v_1) \coloneqq \frac{1}{2}v_1^2 + U_0(x_1), \qquad x_1, v_1 \in \mathbb{R}. \tag{7.1.10}$$

Similar to Definition 2.2.2, we search for stationary solutions which only depend on the phase space variables (x_1, v) through these conserved quantities, i.e.,

$$f_0(x_1, v) = \varphi(E(x_1, v_1), \bar{v}), \qquad (x_1, v) \in \mathbb{R} \times \mathbb{R}^3, \tag{7.1.11}$$

for a suitable ansatz function φ. Such f_0 is a *plane symmetric steady state* if f_0 and U_0 are related via (7.1.5)–(7.1.6).

Inspired by (2.2.12), we choose φ to be of the separated form

$$\varphi(E, \bar{v}) = \Phi(E_0 - E)\,\beta(\bar{v}), \qquad E \in \mathbb{R},\ \bar{v} \in \mathbb{R}^2. \tag{7.1.12}$$

Here, $\beta\colon \mathbb{R}^2 \to [0, \infty[$ is a continuous function with compact support which is normalised as follows:

$$\int_{\mathbb{R}^2} \beta(\bar{v})\,\mathrm{d}\bar{v} = 1. \tag{7.1.13}$$

As before, $E_0 \in \mathbb{R}$ is the cut-off energy which we determine below. For the *energy-dependency function* Φ we consider either the polytropic ansatz

$$\Phi(\eta) = \eta_+^k, \qquad \eta \in \mathbb{R}, \tag{7.1.14}$$

with polytropic exponent $k > \frac{1}{2}$ or the King ansatz

$$\Phi(\eta) = (e^\eta - 1)_+, \qquad \eta \in \mathbb{R}; \tag{7.1.15}$$

recall that $(\ldots)_+$ denotes the positive part of an expression. All of the following also works for more general steady states. However, in order to understand the basic concepts, including the differences to the spherically symmetric case, we focus on this class of steady states here. As discussed in the spherically symmetric setting, (7.1.14) and (7.1.15) are the most common ansatz functions.

Inserting (7.1.11)–(7.1.13) into (7.1.5) yields the following equation for the stationary mass density ρ_0:

$$\begin{aligned}\rho_0(x_1) \coloneqq \int_{\mathbb{R}^3} f_0(x, v)\,\mathrm{d}v = \int_{\mathbb{R}} \Phi(E_0 - \frac{1}{2}v_1^2 - U_0(x_1))\,\mathrm{d}v_1 = \\ = \sqrt{2}\int_0^{E_0 - U_0(x_1)} \frac{\Phi(\eta)}{\sqrt{E_0 - U_0(x_1) - \eta}}\,\mathrm{d}\eta, \qquad x_1 \in \mathbb{R};\end{aligned} \tag{7.1.16}$$

[169] Although L is conserved along the characteristic flow of spherically symmetric equilibria, the remaining system (2.2.93) for (r, w) depends on L. This is different from the role of $\bar{v}$ in the plane symmetric setting because the system (7.1.9) is independent of the conserved value of $\bar{v}$.

the latter integral is meant to vanish if $U_0(x_1) \geq E_0$. The relation between ρ_0 and U_0 is hence given by the function

$$g\colon \mathbb{R} \to \mathbb{R},\ g(z) \coloneqq \begin{cases} \sqrt{2}\int_0^z \frac{\Phi(\eta)}{\sqrt{z-\eta}}\,\mathrm{d}\eta, & \text{if } z > 0, \\ 0, & \text{if } z \leq 0; \end{cases} \tag{7.1.17}$$

more precisely,

$$\rho_0(x_1) = g(E_0 - U_0(x_1)), \qquad x_1 \in \mathbb{R}. \tag{7.1.18}$$

To study the regularity of g, we integrate by parts to obtain

$$g(z) = -2^{\frac{3}{2}} \int_0^z \Phi(\eta)\, \partial_\eta \big[\sqrt{z-\eta}\big]\,\mathrm{d}\eta = 2^{\frac{3}{2}} \int_0^z \Phi'(\eta)\,\sqrt{z-\eta}\,\mathrm{d}\eta, \qquad z > 0; \tag{7.1.19}$$

notice that $\Phi(0) = 0$. Hence, g is of a similar form as the respective function in the radial case, recall (2.2.25), with $\ell = 0$ and Φ being replaced by Φ'. Similar to Lemma 2.2.6, we thus obtain that g is continuously differentiable on $\mathbb{R}$ with $g' > 0$ on $]0,\infty[$; note that $k > \frac{1}{2}$ in the polytropic ansatz (7.1.14). Furthermore, in the polytropic case we can again apply the integral identity (2.2.23) to derive the following explicit representation of g:

$$g(z) = c_k\, z_+^{k+\frac{1}{2}}, \qquad z \in \mathbb{R}, \tag{7.1.20}$$

for some constant $c_k > 0$ depending on the polytropic exponent k. To construct plane symmetric steady states, we again consider

$$y \coloneqq E_0 - U_0 \tag{7.1.21}$$

instead of U_0. Since U_0 shall solve the one-dimensional Poisson equation (7.1.4) with right-hand side $4\pi\rho_0$, we arrive at the following equation for $y = y(x_1)$:

$$y'' = -4\pi\, g(y). \tag{7.1.22}$$

This equation is fundamentally simpler than the respective equation (2.2.35) in the spherically symmetric setting. It is a simple autonomous ODE for y with conserved quantity

$$\frac{1}{2}\big(y'\big)^2 + h(y), \tag{7.1.23}$$

where

$$h(z) \coloneqq 4\pi \int_0^z g(y)\,\mathrm{d}y, \qquad z \in \mathbb{R}. \tag{7.1.24}$$

Analysing the level sets of (7.1.23) in the (y, y')-plane shows that any maximal solution of (7.1.22) is global in x_1. In addition, for every non-constant solution $y \in C^2(\mathbb{R})$ there exists a unique $x^* \in \mathbb{R}$ s.t. $y'(x^*) = 0 < y(x^*)$. By shifting the x_1-variable of such solution, we can always assume $x^* = 0$. Then the resulting solutions are indeed plane symmetric in the sense of Definition 7.1.1 (a). Moreover, for any such solution there holds $\lim_{x_1\to\pm\infty} y(x_1) = -\infty$, while the limits $\lim_{x_1\to\infty} y'(x_1) = -\lim_{x_1\to-\infty} y'(x_1)$ exist and are explicitly given by

$$\lim_{x_1\to\infty} y'(x_1) = \int_0^\infty y''(\xi)\,\mathrm{d}\xi = -2\pi \int_{\mathbb{R}} \rho_0(\xi)\,\mathrm{d}\xi =: -2\pi M_0, \tag{7.1.25}$$

where ρ_0 is defined by y via

$$\rho_0(x_1) \coloneqq g(y(x_1)), \qquad x_1 \in \mathbb{R}, \tag{7.1.26}$$

and ρ_0 is obviously plane symmetric. This shows that the non-constant solutions of (7.1.22) can be parametrised by their total mass $M_0 > 0$. Equivalently, one can also use $\kappa = y(0) > 0$ to parametrise the solutions in a similar way as in the spherically symmetric setting; here, M_0 and κ are in one-to-one correspondence via[170]

$$2\pi^2 M_0^2 = \frac{1}{2}\left(\lim_{x_1\to\infty} y'(x_1)\right)^2 = h(y(0)), \tag{7.1.27}$$

recall our choice of x^* and that h is strictly increasing on $]0,\infty[$. For ρ_0 given by (7.1.26), we define U_0 via (7.1.6). By (7.1.7), $U_0'(x_1) = 4\pi\int_0^{x_1}\rho_0(\xi)\,\mathrm{d}\xi$ for $x_1 \in \mathbb{R}$, and thus

$$\lim_{x_1\to\infty} U'(t,x_1) = 2\pi M_0 = -\lim_{x_1\to-\infty} U'(t,x_1). \tag{7.1.28}$$

This shows $U_0 + y \equiv \text{const}$. In order to determine $E_0 \in \mathbb{R}$ s.t. (7.1.21) holds, let $R_0 > 0$ be the unique positive zero of y. Then $y(\pm R_0) = 0$ and $\operatorname{supp}(\rho_0) = [-R_0, R_0]$. Evaluating U_0 at $x_1 = R_0$ hence yields

$$E_0 \coloneqq U_0(R_0) + y(R_0) = U_0(R_0) = 2\pi\int_{-R_0}^{R_0}(R_0 - \xi)\,\rho_0(\xi)\,\mathrm{d}\xi = 2\pi R_0 M_0. \tag{7.1.29}$$

For any ansatz of the form (7.1.12) and any choice of $M_0 > 0$, the above procedure hence yields a plane symmetric steady state f_0 given by (7.1.11) which is compactly supported in $\mathbb{R}\times\mathbb{R}^3$ and has total mass M_0.[171]

The Period Function in Plane Symmetry

The particle motions within a plane symmetric steady state f_0 as constructed above are described by the characteristic system (7.1.9). Obviously, the potential U_0 is of "single-well structure" similar to Ψ_L in the spherically symmetric setting, cf. Lemma 2.2.12. More precisely, for any $E > U_0(0) = \min_{\mathbb{R}}(U_0)$ there exist unique $x_-(E) < 0 < x_+(E) = -x_-(E)$ s.t.

$$U_0(x_\pm(E)) = E. \tag{7.1.30}$$

In addition, for $x \in \mathbb{R}$, $U_0(x) < E$ is equivalent to $x_-(E) < x < x_+(E)$, and there holds $\lim_{E\searrow U_0(0)} x_\pm(E) = 0$. Next note that the particle energy E defined in (7.1.10) is a conserved quantity of the characteristic system (7.1.9). The constant solution $(x_1, v_1) \equiv (0,0)$ corresponds to the energy value $E = U_0(0)$. For every other solution there holds $E > U_0(0)$ and the solution is global and time-periodic with period

$$T(E) \coloneqq 2\int_{x_-(E)}^{x_+(E)} \frac{\mathrm{d}x}{\sqrt{2E - 2U_0(x)}} = 4\int_0^{x_+(E)} \frac{\mathrm{d}x}{\sqrt{2E - 2U_0(x)}}. \tag{7.1.31}$$

As in the spherically symmetric case, the properties of these periods are crucial to understand the behaviour of solutions of the plane symmetric Vlasov-Poisson system close to the fixed underlying steady state f_0. Fortunately, the properties of T are fundamentally easier to analyse in plane symmetry compared to the spherically symmetric case. The following lemma is based on [62, Lemma 2.6 and Props. 2.7 and 2.8].

[170] In the case of spherically symmetric steady states, the results from [131] show that $\kappa = y(0)$ and the total mass M_0 are not in a one-to-one correspondence in general.

[171] In particular, different from the spherically symmetric setting, we do not need an upper bound on the polytropic exponent k in order to arrive at a compactly supported steady state, recall Remark 2.2.5 (d).

Lemma 7.1.2 (Properties of the Period Function in Plane Symmetry)**.** *The* period function $T\colon]U_0(0),\infty[\to]0,\infty[$ *defined by* (7.1.31) *is continuously differentiable and strictly increasing with*

$$\lim_{E\searrow U_0(0)} T(E) = \frac{2\pi}{\sqrt{U_0''(0)}} = \frac{\sqrt{\pi}}{\sqrt{\rho_0(0)}} =: T(U_0(0)). \tag{7.1.32}$$

Proof. The same arguments as in Lemma A.3.9 show that T is differentiable with derivative given by

$$T'(E) = \frac{1}{E-U_0(0)} \int_{x_-(E)}^{x_+(E)} \frac{G(x)}{\sqrt{2E-2U_0(x)}}\,\mathrm{d}x = \frac{2}{E-U_0(0)} \int_{0}^{x_+(E)} \frac{G(x)}{\sqrt{2E-2U_0(x)}}\,\mathrm{d}x \tag{7.1.33}$$

for $E > U_0(0)$, where, in analogy to (A.3.33),

$$G\colon \mathbb{R}\to\mathbb{R},\ G(x) := \begin{cases} \frac{U_0'(x)^2 - 2(U_0(x)-U_0(0))\,U_0''(x)}{U_0'(x)^2}, & \text{if } x\neq 0,\\ 0, & \text{if } x = 0. \end{cases} \tag{7.1.34}$$

Similar to Lemma A.3.10, it follows that G is continuous; note $U_0 \in C^3(\mathbb{R})$ since g is continuously differentiable. Hence, the same arguments as in Lemma A.3.1 show that T' is continuous. Next observe that differentiating the numerator of G yields

$$\partial_x\big[U_0'(x)^2 - 2(U_0(x)-U_0(0))\,U_0''(x)\big] = -2(U_0(x)-U_0(0))\,U_0'''(x), \qquad x\in\mathbb{R}. \tag{7.1.35}$$

By (7.1.4), the third derivative of U_0 is given by $U_0'''(x) = 4\pi\rho_0'(x)$ for $x\in\mathbb{R}$, and this expression is negative for $x\in]0,R_0[$ by (7.1.18) since U_0' and g' are both positive on $]0,\infty[$. Because $G(0)=0$, we hence conclude $G>0$ on $]0,\infty[$ which shows the claimed monotonicity of T via (7.1.33). The identity (7.1.32) can be proven similarly to Lemma A.4.1. □

The reason why the monotonicity of T is so much easier to show here than in the spherically symmetric setting, cf. Section A.3.3, is that the radial Poisson equation $U_0'' + \frac{2}{r}U_0' = 4\pi\rho_0$ is replaced by the simpler one-dimensional Poisson equation $U_0'' = 4\pi\rho_0$ in plane symmetry. From a physics point of view, this corresponds to the fact that in plane symmetry, gravity only acts (effectively) in one space dimension.

Linearisation and the Operators

For a fixed steady state f_0 as above, we now linearise the plane symmetric Vlasov-Poisson system around f_0. This is based on [62, Sc. 3]. The same arguments as in Chapter 3 show that the linearised system can be written in the form

$$\partial_t^2 f + \mathcal{L} f = 0. \tag{7.1.36}$$

Here, f is the odd-in-v_1 part of the plane symmetric, linearised perturbation. More precisely, $g := f(t)\colon \mathbb{R}\times\mathbb{R}^3\to\mathbb{R}$ satisfies

$$g(x_1,v) = -g(x_1,-v_1,\bar{v}) = -g(-x_1,v), \qquad (x_1,v)\in\mathbb{R}\times\mathbb{R}^3; \tag{7.1.37}$$

notice that any function which is odd in v_1 and which satisfies the reflection symmetry (7.1.2) is also odd in x_1. In addition, $f(t)$ has its support inside

$$\Omega_0 := \{(x_1,v)\in\mathbb{R}\times\mathbb{R}^3 \mid f_0(x_1,v)>0\} = \{(x_1,v_1)\in\mathbb{R}\times\mathbb{R} \mid E(x_1,v_1)<E_0\}\times\{\beta>0\}. \tag{7.1.38}$$

The *linearised operator* $\mathcal{L}$ is, in analogy to (1.2.9), of the form

$$\mathcal{L} = -\mathcal{T}^2 - \mathcal{R}, \tag{7.1.39}$$

with *transport operator*

$$\mathcal{T} \coloneqq v_1\, \partial_{x_1} - U_0'(x_1)\, \partial_{v_1} \tag{7.1.40}$$

and *response operator* given by

$$\mathcal{R}g(x_1, v) \coloneqq 4\pi\, |\varphi'(E, \bar{v})|\, v_1\, j_g(x_1), \qquad (x_1, v) \in \Omega_0, \tag{7.1.41}$$

where

$$j_g(x_1) \coloneqq \int_{\mathbb{R}} v_1\, g(x_1, v)\, \mathrm{d}v, \qquad x_1 \in \mathbb{R}, \tag{7.1.42}$$

for suitable $g\colon \mathbb{R} \times \mathbb{R}^3 \to \mathbb{R}$. As before, we use the notation $\varphi' \coloneqq \partial_E \varphi$.

In order to study the behaviour of solutions of (7.1.36), we analyse the spectrum of the linearised operator $\mathcal{L}$ (which first has to be defined in a mathematical rigorous manner). For instance, a positive eigenvalue of $\mathcal{L}$ again corresponds to an oscillating solution of (7.1.36). Similar to Definition 4.2.3, the underlying function space for this spectral analysis is

$$H \coloneqq \{f\colon \Omega_0 \to \mathbb{R} \text{ measurable } \&\text{ plane symmetric a.e. } |\, \|f\|_H < \infty\}, \tag{7.1.43}$$

where

$$\|f\|_H^2 \coloneqq \int_{\Omega_0} \frac{1}{|\varphi'(E, \bar{v})|}\, |f(x_1, v)|^2\, \mathrm{d}(x_1, v), \tag{7.1.44}$$

and f being plane symmetric a.e. means that (7.1.2) holds a.e. on Ω_0. Moreover, note that by the choice of the energy-dependency function Φ of the steady state, $\varphi'(E, \bar{v}) < 0$ on Ω_0. With the canonical inner product H becomes a Hilbert space. Furthermore, in analogy to (4.2.6), we denote the odd-in-v_1 subspace of H by

$$\mathcal{H} \coloneqq \{f \in H \mid f \text{ is odd in } v_1 \text{ a.e.}\}; \tag{7.1.45}$$

this means that for any $f \in \mathcal{H}$, the equations (7.1.37) hold a.e. on Ω_0. Analogous to Definitions 4.2.5 and 4.2.8, the operators $\mathcal{T}$ and $\mathcal{T}^2$ can be defined in a suitable weak sense on dense subsets $\mathrm{D}(\mathcal{T})$ and $\mathrm{D}(\mathcal{T}^2)$ of H, respectively, while $\mathcal{R}$ can be defined on the entire space H. In particular, notice that $\mathcal{T}^2$ and $\mathcal{R}$ both map functions from $\mathcal{H}$ back into this space. Accordingly, the suitable domain of definition of $\mathcal{L}$ is $\mathrm{D}(\mathcal{L}) \coloneqq \mathrm{D}(\mathcal{T}^2) \cap \mathcal{H}$. The properties of $\mathcal{T}$, $\mathcal{T}^2$, $\mathcal{R}$, and $\mathcal{L}$ can be analysed using the same techniques as in the spherically symmetric case. Crucial for this is that we can again reparametrise $\Omega_0 \setminus (\{(0,0)\} \times \mathbb{R}^2)$ by introducing action-angle type variables $(\theta, E, \bar{v}) \in \mathbb{S}^1 \times \mathbb{I}_0 \times \{\beta \neq 0\}$, where

$$\mathbb{I}_0 \coloneqq]U_0(0), E_0[\tag{7.1.46}$$

denotes the energy support of the steady state. In particular, $\bar{v}$ is part of the action variables. As in Section 4.3, one can then prove that $-\mathcal{T}^2\big|_{\mathcal{H}}\colon \mathrm{D}(\mathcal{L}) \to \mathcal{H}$ is self-adjoint and possesses the spectrum

$$\sigma(-\mathcal{T}^2\big|_{\mathcal{H}}) = \sigma_{\mathrm{ess}}(-\mathcal{T}^2\big|_{\mathcal{H}}) = \left(\frac{4\pi\mathbb{N}}{T([U_0(0), E_0])}\right)^2; \tag{7.1.47}$$

the additional factor 4 (compared to the spherically symmetric case, cf. Proposition 4.3.19) comes from the fact that $\mathbb{S}^1 \times \mathbb{I}_0 \times \{\beta \neq 0\} \ni (\theta, E, \bar{v}) \mapsto \sin(2\pi n\theta)\, \delta_{(E^*, \bar{v}^*)}(E, \bar{v})$ (formally) satisfies the reflection symmetry (7.1.2) only for even $n \in \mathbb{N}$. The response operator

$\mathcal{R}\big|_{\mathcal{H}}\colon \mathcal{H} \to \mathcal{H}$ is bounded, symmetric, and relatively $(\mathcal{T}^2\big|_{\mathcal{H}})$-compact. Thus, the linearised operator $\mathcal{L}\colon \mathrm{D}(\mathcal{L}) \to \mathcal{H}$ is self-adjoint with essential spectrum given by

$$\sigma_{\mathrm{ess}}(\mathcal{L}) = \sigma(-\mathcal{T}^2\big|_{\mathcal{H}}) = \left(\frac{4\pi\mathbb{N}}{T([U_0(0), E_0])}\right)^2. \tag{7.1.48}$$

Moreover, a plane symmetric analogue of Antonov's coercivity bound holds, which implies $\sigma(\mathcal{L}) \subset]0, \infty[$, i.e., the underlying steady state is linearly stable. All these results (and further ones) are proven in more detail in [62, Scs. 4.2, 5.2, and 7.2].

A Birman-Schwinger-Mathur Principle

In order to study the existence of eigenvalues of $\mathcal{L}$ in the essential gap

$$\mathcal{G} \coloneqq \left]0, \frac{16\pi^2}{\sup_{\mathbb{I}_0}^2(T)}\right[=]0, \min(\sigma_{\mathrm{ess}}(\mathcal{L}))[, \tag{7.1.49}$$

one can derive a Birman-Schwinger-Mathur principle in plane symmetry by repeating the arguments from Chapter 5. More precisely, the plane symmetric analogue of the Mathur operator, cf. Definition 5.2.4 and Proposition 5.2.12, is

$$\mathcal{M}_\lambda\colon L^2([-R_0, R_0]) \to L^2([-R_0, R_0]),\ \mathcal{M}_\lambda F(x) \coloneqq \int_{-R_0}^{R_0} K_\lambda(x, y)\, F(y)\, \mathrm{d}y, \tag{7.1.50}$$

for $\lambda \in \mathcal{G}$, with integral kernel $K_\lambda\colon [-R_0, R_0]^2 \to \mathbb{R}$ defined by

$$K_\lambda(x, y) \coloneqq 32\pi \sum_{n=1}^{\infty} \int_{\mathbb{I}_0(x)\cap\mathbb{I}_0(y)} \frac{\Phi'(E_0 - E)}{T(E)} \frac{\sin(4\pi n\, \theta(r, E, L))\, \sin(4\pi n\, \theta(s, E, L))}{\frac{16\pi^2 n^2}{T(E)^2} - \lambda}\, \mathrm{d}E, \tag{7.1.51}$$

where

$$\mathbb{I}_0(x) \coloneqq \{E \in \mathbb{I}_0 \mid x_-(E) < x < x_+(E)\}, \qquad x \in \mathbb{R}. \tag{7.1.52}$$

We omit the calculations leading to this operator here; they can be found in [62, Sc. 8.1]. The number of eigenvalues of $\mathcal{L}$ in $\mathcal{G}$ is related to the Mathur operator in the same ways as in Theorems 5.3.1 and 5.3.3. Fortunately, the criterion from Theorem 5.3.1 is now easier to verify than in the spherically symmetric case. This leads to the following result, which is based on [62, Thm. 8.13].

Theorem 7.1.3 (Existence of Oscillatory Modes in Plane Symmetry)**.** *Let f_0 be a plane symmetric steady state as constructed above, with an energy dependency function Φ which is either polytropic* (7.1.14) *with polytropic exponent $\frac{1}{2} < k \leq 1$ or of King type* (7.1.15)*. Then the associated linearised operator $\mathcal{L}$ possesses an eigenvalue in the essential gap $\mathcal{G}$, corresponding to an oscillating solution of the linearised system* (7.1.36)*.*

Proof. The same arguments as in the proof of Theorem 5.4.1 yield

$$\mathfrak{M} \geq c \int_{E_0-\varepsilon}^{E_0} \frac{\Phi'(E_0 - E)}{\sup_{\mathbb{I}_0}(T) - T(E)}\, \mathrm{d}E \tag{7.1.53}$$

for sufficiently small $\varepsilon, c > 0$ depending on the steady state. The number $\mathfrak{M}$ is defined similarly to (5.3.1); as discussed above, $\mathfrak{M} > 1$ would imply the existence of an eigenvalue

of $\mathcal{L}$ in $\mathcal{G}$. By Lemma 7.1.2, $\sup_{\mathbb{I}_0}(T) = T(E_0)$ and T' is continuous on $]U_0(0), \infty[$. Hence, there exists a constant $C > 0$ s.t.

$$\sup_{\mathbb{I}_0}(T) - T(E) \leq C(E_0 - E), \qquad E \in [E_0 - \varepsilon, E_0]. \tag{7.1.54}$$

Inserting this estimate into (7.1.53) yields

$$\mathfrak{M} \geq c \int_{E_0-\varepsilon}^{E_0} \frac{\Phi'(E_0 - E)}{E_0 - E} \,\mathrm{d}E = c \begin{cases} k \int_0^\varepsilon \eta^{k-2} \,\mathrm{d}\eta, & \Phi \text{ polytropic with } \frac{1}{2} < k \leq 1 \\ \int_0^\varepsilon \frac{e^\eta}{\eta} \,\mathrm{d}\eta, & \Phi \text{ of King type} \end{cases} = \infty, \tag{7.1.55}$$

and we conclude. □

It is mainly due to two reasons why the criterion for the existence of oscillatory modes is easier to verify here than in the spherically symmetric case. Firstly, we know by Lemma 7.1.2 that the period function T attains it maximal value on $\bar{\mathbb{I}}_0$ at the largest energy value E_0. In Theorem 5.4.1, we have to assume the analogous property (5.4.2) in spherical symmetry. As already discussed above, this simplification in plane symmetry comes from the fact that gravity (effectively) acts in only one space dimension here. Secondly, the effective action space in plane symmetry is only one-dimensional, parametrised by the variable E, while it is two-dimensional in spherical symmetry with variables (E, L). This leads to the action integrals to be more singular in plane symmetry, more precisely, the integral on the right-hand side of (7.1.53) is infinite for a larger range of k compared to (5.4.10). Nonetheless, in the above theorem we also have to assume that the steady state is not too regular.

A natural next question in the plane symmetric setting is whether one can show the absence of eigenvalues of $\mathcal{L}$ for smoother steady states. This question is open. In order to proceed as in Sections 6.4 and 6.5, one always needs that certain constants given by the steady state are sufficiently small. This smallness does not seem to be much easier to establish in plane symmetry than it is in spherical symmetry.

7.2 The Vlasov-Poisson System With Single L Around a Point Mass

In this section we consider the radial Vlasov-Poisson system around a fixed point mass $M > 0$ from Section 6.1 with the additional assumption that all particles have the same L-value, i.e., the modulus of the angular momentum (vector) is the same for all particles. There is no physical motivation behind this assumption, but a mathematical one: Eliminating the L-dependency simplifies some parts of the analysis. Let $L > 0$ be the fixed L-value of all particles.[172] The *radial Vlasov-Poisson system with single L around a point mass* is

$$\partial_t f + w\,\partial_r f - \left(U' + \frac{M}{r^2} - \frac{L}{r^3}\right)\partial_w f = 0, \tag{7.2.1}$$

$$U'(t,r) = \frac{4\pi}{r^2}\int_0^r s^2 \rho(t,s)\,\mathrm{d}s, \qquad \lim_{r\to\infty} U(t,r) = 0, \tag{7.2.2}$$

$$\rho(t,r) = \frac{\pi}{r^2}\int_0^\infty \int_{\mathbb{R}} f(t,r,w)\,\mathrm{d}w. \tag{7.2.3}$$

[172] Due to the fixed point mass we have to exclude particles flying through the spatial origin. This is achieved by assuming L to be non-zero.

Here the phase space density function $f = f(t, r, w)$ no longer depends on L; the dimension of phase space is reduced from 3 to 2 by fixing L. Throughout this section we follow [61], where the same system was used to develop the methods presented in Chapter 6. As we saw in Chapter 6, methods from the situation with single L can indeed be generalised to the full spherically symmetric case. Nonetheless, fixing L is still a simplification because we no longer have to pay attention to the L-dependencies – allowing us to focus more on the key concepts. Moreover, fixing L yields a system which, in some aspects, is closer to the full radial system than the plane symmetric system introduced in the previous section. The reason for this is that gravity is still described by the (radial,) three-dimensional Poisson equation (7.2.2) instead of the one-dimensional equation (7.1.4). We further note that although we only consider the situation of a single L with a point mass here, it is also possible to make the same simplification without a point mass. In fact, the existence of radial steady states and their properties with the single L-value $L = 0$ (without a point mass) is analysed in [129, Kap. 5]. The particles in such steady states have pure radial motions, cf. Remark 2.2.17 (a).

Similar as in Section 6.2 we search for a steady state of the system (7.2.1)–(7.2.3) of the form

$$f_0(r, w) = \varphi(E(r, w)), \qquad (r, w) \in]0, \infty[\times \mathbb{R}, \tag{7.2.4}$$

where, as before,

$$E(r, w) \coloneqq \frac{1}{2}w^2 + U_0(r) + \frac{L}{2r^2} - \frac{M}{r} =: \frac{1}{2}w^2 + \Psi(r), \qquad (r, w) \in]0, \infty[\times \mathbb{R}, \tag{7.2.5}$$

is the particle energy. The function f_0 is a steady state provided U_0 is the gravitational potential induced by f_0 via (7.2.2)–(7.2.3). As in Section 6.2 we restrict the discussion to polytropic ansatz functions of the form

$$\varphi(E) \coloneqq \varepsilon\tilde{\varphi}(E) \coloneqq \varepsilon(E_0 - E)_+^k, \qquad E \in \mathbb{R}, \tag{7.2.6}$$

where $E_0 < 0$ is the cut-off energy, $\varepsilon > 0$ is a smallness parameter, and k is the polytropic exponent satisfying

$$k > \frac{1}{2}. \tag{7.2.7}$$

By the same arguments as in Proposition 6.2.2, it follows that for any value of the parameter

$$\kappa \in]-\frac{M^2}{2L}, 0[\tag{7.2.8}$$

there exists a steady state of the form (7.2.4) with $E_0 - U_0(0) = \kappa$ which has finite mass and compact support in phase space. In particular, the support is bounded uniformly in ε since the steady states are "trivially bounded" by the assumption $\kappa < 0$, recall Remark 6.2.1. Furthermore, for fixed k and κ the convergence statements analogous to Proposition 6.2.6 apply as $\varepsilon \to 0$. For a more detailed discussion of the existence of steady states and their properties we refer to [61, Scs. 3.1–3.3 and App. A].

Linearising the system (7.2.1)–(7.2.3) around a steady state f_0 as above leads to the following system for the odd-in-w part $f = f(r, w) = -f(r, -w)$ of the linearised perturbation:

$$\partial_t^2 + \mathcal{L}f = 0, \tag{7.2.9}$$

where the linearised operator $\mathcal{L}$ is again of the form

$$\mathcal{L} = -\mathcal{T}^2 - \mathcal{R}. \tag{7.2.10}$$

Here,

$$\mathcal{T} \coloneqq w\,\partial_r - \Psi'(r)\,\partial_w \tag{7.2.11}$$

is the transport operator and

$$\mathcal{R}g(r,w) \coloneqq 4\pi^2\,|\varphi'(E)|\,\frac{w}{r^2}\int_{\mathbb{R}} \tilde{w}\,g(r,\tilde{w})\,\mathrm{d}\tilde{w} \tag{7.2.12}$$

defines the gravitational response operator for suitable functions g on (the interior of) the steady state support

$$\Omega_0 \coloneqq \{(r,w)\in\,]0,\infty[\,\times\mathbb{R}\mid f_0(r,w)>0\} = \{(r,w)\in\,]0,\infty[\,\times\mathbb{R}\mid E(r,w)<E_0\}. \tag{7.2.13}$$

Similar as before, the underlying Hilbert space for the spectral analysis of $\mathcal{L}$ is

$$H \coloneqq \{f\colon \Omega_0\to\mathbb{R} \text{ measurable} \mid \|f\|_H<\infty\}, \tag{7.2.14}$$

where

$$\|f\|_H^2 \coloneqq 4\pi^2\int_{\Omega_0}\frac{1}{|\varphi'(E)|}\,|f(r,w)|^2\,\mathrm{d}(r,w). \tag{7.2.15}$$

The analysis of the operators $\mathcal{T}$, $\mathcal{T}^2$, $\mathcal{R}$, and $\mathcal{L}$ can be performed in the same way as in Section 6.3, which is in turn based on Chapters 4 and 5, and yields the analogous results as above. We do not elaborate on this here, but refer to [61, Scs. 3.4 and 5.1] for a (slightly) more detailed discussion. We will use the same notation as before for the objects occurring in this analysis.

Based on this we can now apply the methods from Sections 6.4 and 6.5 to study the absence/presence of eigenvalues of $\mathcal{L}$ for steady states in the regime $0<\varepsilon\ll 1$. This leads to the following result which originates from [61, Thm. 1.2].

Theorem 7.2.1 (Oscillations vs. Damping for Steady States With Single L Around a Point Mass)**.** *For fixed $M, L>0$ let f_0 be a steady state of the radial Vlasov-Poisson system with single L around a point mass as constructed above. We further require that the parameter κ satisfies*[173]

$$-2^{-\frac{2}{3}}\frac{M^2}{2L}<\kappa<0. \tag{7.2.16}$$

Then there exists $\varepsilon_0>0$, depending on κ and the polytropic exponent $k>\frac{1}{2}$, s.t. the following assertions hold if the smallness parameter $\varepsilon>0$ of the steady state satisfies $0<\varepsilon<\varepsilon_0$:

(a) If $\frac{1}{2}<k\leq 1$, there exists a positive eigenvalue of $\mathcal{L}$ in the essential gap corresponding to an oscillating solution of the linearised system (7.2.9)*.*

(b) If $k>1$, any solution $\mathbb{R}\ni t\mapsto f(t)\in \mathrm{D}(\mathcal{L})$ of the linearised system (7.2.9) *launched by initial data $(f(0),\partial_t f(0))\in \mathrm{D}(\mathcal{L})\times(\mathrm{D}(\mathcal{T})\cap\mathcal{H})$ is damped in the following way:*

$$\lim_{T\to\infty}\frac{1}{T}\int_0^T \|U'_{\mathcal{T}f(t)}\|_2^2\,\mathrm{d}t = 0. \tag{7.2.17}$$

[173] The additional assumption (7.2.16) on the range of the parameter κ is only used to show the damping result in part (b). For part (a) it suffices if κ satisfies (7.2.8).

Proof. The proof of part (a) is similar to the one of Theorem 7.1.3: We first proceed as in the proof of Theorem 5.4.1 to derive the following estimate on the number $\mathfrak{M}$ characterising the presence of an eigenvalue of $\mathcal{L}$ in the essential gap:

$$\mathfrak{M} \geq c \int_{E_0-\iota}^{E_0} \frac{|\varphi'(E)|}{T_{\max} - T(E)} \, \mathrm{d}E, \tag{7.2.18}$$

where $c, \iota > 0$ are (small) ε-independent constants and $T_{\max} \coloneqq \sup_{]\min(\Psi), E_0[}(T)$ denotes the maximal period in the steady state. Similar to Proposition 6.2.6 (e) it follows that $T_{\max} = T(E_0)$ for $0 < \varepsilon \ll 1$. Hence, together with the usual regularity of the period function T we obtain

$$\mathfrak{M} \geq c \int_{E_0-\iota}^{E_0} \frac{|\varphi'(E)|}{E_0 - E} \, \mathrm{d}E = ck\varepsilon \int_0^{\iota} \eta^{k-2} \, \mathrm{d}\eta = \infty, \tag{7.2.19}$$

which concludes the proof of part (a).

Part (b) follows by similar, but simpler arguments as in Theorem 6.6.1: We first use (7.2.16) to infer, for $0 < \varepsilon \ll 1$, that any isolated eigenvalue of $\mathcal{L}$ has to lie below the bottom of the essential spectrum of $\mathcal{L}$. Then, applying the Birman-Schwinger-Mathur principle once again shows that no such eigenvalue exists by estimating $\mathfrak{M}$ in the same way as in Theorem 6.4.1. Lastly, the absence of embedded eigenvalues of $\mathcal{L}$ follows in the same way as in Theorem 6.5.5. Note that in the proof of Theorem 6.5.5, all major steps – like integrating by parts – are always performed in the E-integral and can thus be adapted to the present setting. □

It should be emphasised that the above theorem shows a *sharp* dichotomy between oscillation(s) and damping for polytropic steady states. While increasing the polytropic exponent k, the transition from oscillation to damping takes places precisely at the point where the steady states (7.2.4) become continuously differentiable at the boundary $\partial\Omega_0$ of their phase space support.

To conclude this section, let us compare the above theorem to the results obtained in the full radial setting in Chapter 6. On the one hand, the class of steady states for which we can show damping is effectively the same. On the other hand, there are two main reasons why we can now prove the existence of oscillatory modes for "all" other polytropic steady states while this was more difficult in the full radial setting: Firstly, fixing L leads to the action space to be only one-dimensional here. As a consequence, the integral on the right-hand side of (7.2.18) gets infinite for a larger range of k compared to the respective integral (5.4.10) in the full radial case. The same mechanism was also present in the plane symmetric setting in the previous section. Secondly, fixing L allows us to conclude where the period function T attains its maximal value on the steady state support by using that T is energy-increasing for $0 < \varepsilon \ll 1$. In the full radial case, this is more difficult due to the additional L-dependency of the period function, recall Remark 6.4.2.

7.3 The Relativistic Vlasov-Poisson System

The *relativistic Vlasov-Poisson system* is

$$\partial_t f + \frac{v}{\sqrt{1+|v|^2}} \cdot \partial_x f - \partial_x U \cdot \partial_v f = 0, \tag{7.3.1}$$

$$\Delta U = 4\pi\rho, \tag{7.3.2}$$

$$\rho(t,x) = \int_{\mathbb{R}^3} f(t,x,v)\,\mathrm{d}v, \tag{7.3.3}$$

$$\lim_{|x|\to\infty} U(t,x) = 0. \tag{7.3.4}$$

Compared to the (non-relativistic) Vlasov-Poisson system (1.1.2)–(1.1.5), only the Vlasov equation (7.3.1) changed. It now corresponds to the characteristic system

$$\dot{x} = \frac{v}{\sqrt{1+|v|^2}}, \qquad \dot{v} = -\partial_x U(t,x). \tag{7.3.5}$$

In particular, the (modulus of the) velocity $\dot{x}$ of any particle is always smaller than the speed of light, which is normalised to unity here. It is this boundedness property that gives the system its name. It should be noted, however, that the system is not "purely relativistic" since gravity is still given by Newton's law (7.3.2). The relativistic Vlasov-Poisson system should hence be thought of as a "hybrid system". Even though the relativistic Vlasov-Poisson system is surely not as physically relevant as the pure Newtonian Vlasov-Poisson system or the fully relativistic Einstein-Vlasov system, it is still natural to first extend the methods from the Vlasov-Poisson system to the relativistic Vlasov-Poisson system. This can reveal general difficulties arising in relativistic settings.

For instance, the existence theory of (compactly supported, spherically symmetric) steady states is very much similar for the relativistic Vlasov-Poisson system than for the (non-relativistic) Vlasov-Poisson system, cf. [130], but the (non-linear) stability analysis is conceptionally more difficult in the former setting. We refer to [144, Sc. 4] for a recent review regarding this issue. Nonetheless, in [59] the non-linear stability of a large class of steady states of the relativistic Vlasov-Poisson system is proven. This stability result mainly relies on an analogue of Antonov's coercivity bound, cf. [59, Lemma 3.4].

To the author's knowledge, the linearisation of the relativistic Vlasov-Poisson system has not yet been analysed. We do not attempt to do so here, but simply refer to [102], where the linearised relativistic Vlasov-Poisson system will be studied in detail, culminating in an analogue of the Birman-Schwinger-Mathur principle which gives a criterion for the existence of oscillating modes. Let us just mention here that the linearised system in second-order formulation is again governed by an operator of the form (1.2.9) and that the structure of the particle orbits is the same as in the non-relativistic case.

7.4 The Einstein-Vlasov System

In this section we want to discuss a genuinely general relativistic setting, the *Einstein-Vlasov system*. This whole section is based on [49]. We further refer to [182] for an even more detailed discussion than in [49] as well as to [144] for a recent review which also covers most of the topics we will discuss below.

Using Schwarzschild coordinates to parametrise spacetime and assuming spherical symmetry, asymptotic flatness, and a regular centre, the Einstein-Vlasov system reads

$$\partial_t f + e^{\mu-\lambda}\frac{v}{\sqrt{1+|v|^2}}\cdot\partial_x f - \Big(\dot{\lambda}\frac{x\cdot v}{r} + e^{\mu-\lambda}\,\mu'\sqrt{1+|v|^2}\Big)\frac{x}{r}\cdot\partial_v f = 0, \tag{7.4.1}$$

$$e^{-2\lambda}(2r\lambda'-1)+1 = 8\pi r^2\rho_f, \tag{7.4.2}$$

$$e^{-2\lambda}(2r\mu'+1)-1 = 8\pi r^2 p_f, \tag{7.4.3}$$

$$\dot{\lambda} = -4\pi r e^{\lambda+\mu}\,j_f, \tag{7.4.4}$$

$$e^{-2\lambda}\Big(\mu'' + (\mu' - \lambda')(\mu' + \frac{1}{r})\Big) - e^{-2\mu}\Big(\ddot{\lambda} + \dot{\lambda}(\dot{\lambda} - \dot{\mu})\Big) = 8\pi q_f, \tag{7.4.5}$$

$$\rho_f(t,r) = \rho_f(t,x) = \int_{\mathbb{R}^3} \sqrt{1+|v|^2}\, f(t,x,v)\,\mathrm{d}v, \tag{7.4.6}$$

$$p_f(t,r) = p_f(t,x) = \int_{\mathbb{R}^3} \Big(\frac{x\cdot v}{r}\Big)^2 f(t,x,v)\,\frac{\mathrm{d}v}{\sqrt{1+|v|^2}}, \tag{7.4.7}$$

$$j_f(t,r) = j_f(t,x) = \int_{\mathbb{R}^3} \frac{x\cdot v}{r}\, f(t,x,v)\,\mathrm{d}v, \tag{7.4.8}$$

$$q_f(t,r) = q_f(t,x) = \frac{1}{2}\int_{\mathbb{R}^3} \left|\frac{x\times v}{r}\right|^2 f(t,x,v)\frac{\mathrm{d}v}{\sqrt{1+|v|^2}}, \tag{7.4.9}$$

$$\lim_{r\to\infty} \mu(t,r) = 0 = \lim_{r\to\infty} \lambda(t,r) = \lambda(t,0). \tag{7.4.10}$$

Here, $f = f(t,x,v) = f(t,r,w,L)$ is the spherically symmetric phase space density of the configuration under consideration; spherical symmetry and the radial coordinates (r,w,L) are defined as before, cf. Definition 2.1.1 and Remark 2.1.2. We always assume that $f(t)$ has compact support. The equation (7.4.1) for f is the *Vlasov equation*; a dot $\dot{}$ denotes a derivative w.r.t. t. Instead of a gravitational field as in the case of the Vlasov-Poisson system, gravity is now described by the metric coefficients $\mu = \mu(t,x) = \mu(t,r)$ and $\lambda = \lambda(t,x) = \lambda(t,r)$ solving the *field equations* (7.4.2)–(7.4.5). The source terms ρ_f, p_f, j_f, and q_f induced by f via (7.4.6)–(7.4.9) are the energy density, radial pressure, particle current, and tangential pressure, respectively. The boundary conditions (7.4.10) ensure asymptotic flatness and a regular centre. For (physical and mathematical) background on this system we refer to [4, 138, 144] and the references therein.

Steady States

In order to construct suitable steady states of the above system we make a similar ansatz as in (2.2.6):

$$f_0(x,v) = \varphi(E(x,v), L(x,v)) = \Phi\left(1 - \frac{E(x,v)}{E_0}\right)(L(x,v) - L_0)_+^\ell, \qquad (x,v)\in\mathbb{R}^3\times\mathbb{R}^3. \tag{7.4.11}$$

The particle energy E induced by the stationary metric coefficient μ_0 is now given by

$$E(x,v) = e^{\mu_0(x)}\sqrt{1+|v|^2}, \qquad (x,v)\in\mathbb{R}^3\times\mathbb{R}^3, \tag{7.4.12}$$

and $L = L(x,v)$ is defined as before. For the sake of simplicity, we assume the energy dependency function Φ to be of the polytropic form

$$\Phi(\eta) = \eta_+^k, \qquad \eta\in\mathbb{R}, \tag{7.4.13}$$

with polytropic exponent $0 < k < \ell + \frac{3}{2}$. Similar as before, $0 < E_0 < 1$ is the cut-off energy which is implicitly determined by other parameters. The L-dependency of the ansatz function is given by the parameter $L_0 \geq 0$ and the (other) polytropic exponent $\ell > -\frac{1}{2}$; recall our convention (2.2.13). Choosing $L_0 = 0 = \ell$ leads to the important isotropic steady states which only depend on the phase space coordinates through the particle energy E.

Similar, but more difficult arguments as in Section 2.2 show that any choice $\kappa > 0$ of the parameter

$$\kappa = \ln(E_0) - \mu_0(0) \tag{7.4.14}$$

results in a compactly supported steady state f_0 of the above system, cf. [130]. The parameter κ describes how relativistic the steady state is – larger values of κ correspond to more relativistic equilibria, see [50, Eqn. (2.11)].

Linearisation and the Operators

We again linearise the system (7.4.1)–(7.4.10) around a fixed steady state as constructed above. A second-order formulation of the linearised system analogous to (1.2.8) has first been derived in [71, Sc. IVd)], see also [58, Lemma 4.21]. It is of the form

$$\partial_t^2 f + \mathcal{L} f = 0, \tag{7.4.15}$$

where $f = f(t, x, v)$ is the odd-in-v part of the linearised perturbation which is again assumed to be spherically symmetric. The *linearised operator* is

$$\mathcal{L} := -\mathcal{B}^2 - \mathcal{R}, \tag{7.4.16}$$

where

$$\mathcal{B} := \mathcal{T} + \mathcal{S} \tag{7.4.17}$$

is referred to as the *essential operator*; this name is due to [182]. It consists of the *transport operator*

$$\mathcal{T} := -e^{-\lambda_0}(\partial_v E \cdot \partial_x - \partial_x E \cdot \partial_v) \tag{7.4.18}$$

as well as the non-local operator $\mathcal{S}$ defined by

$$\mathcal{S} f(r, w, L) := -4\pi r |\varphi'(E, L)|\, e^{2\mu_0 + \lambda_0} \left(w\, p_f - \frac{w^2}{\sqrt{1 + w^2 + \frac{L}{r^2}}}\, j_f \right) \tag{7.4.19}$$

for suitable spherically symmetric functions $f = f(x, v) = f(r, w, L)$ on the phase space support of f_0. We again use the notation $\varphi' = \partial_E \varphi$ here. Moreover, λ_0 is the metric coefficient of the steady state and p_f and j_f are defined as in (7.4.7) and (7.4.8), respectively. The remaining term on the right-hand side of (7.4.16) is the *gravitational response operator* $\mathcal{R}$ given by

$$\mathcal{R} f(r, w, L) := 4\pi |\varphi'(E, L)|\, e^{3\mu_0} \big(2r\mu_0' + 1\big) w\, j_f. \tag{7.4.20}$$

In order to analyse the behaviour of solutions of (7.4.15), we again study the (functional analytic and) spectral properties of the linearised operator $\mathcal{L}$. It turns out that the properties of the linearised operator $\mathcal{L}$ are more diverse here than for Vlasov-Poisson system. This is particularly evident in the fact that linear stability now depends on the parameter κ. More precisely, for a fixed isotropic ansatz $L_0 = 0 = \ell$ with polytropic exponent $0 < k < \frac{3}{2}$, there holds the following:

- [60, Thm. 5.1]: If $0 < \kappa \ll 1$, the steady state is linearly stable in the sense that a coercivity estimate similar to Antonov's coercivity bound (Lemma 4.5.6) holds.

- [58, Thm. 4.3]: If $\kappa \gg 1$, the steady state is linearly unstable in the sense that $\mathcal{L}$ possesses a negative eigenvalue corresponding to an exponentially growing solution of the linearised system (7.4.15).

Hence, in addition to the existence of positive eigenvalues corresponding to oscillating solutions of the linearised system (7.4.15), it is now necessary to (first) study the existence of negative eigenvalues of the linearised operator $\mathcal{L}$.[174]

To analyse the linearised operator $\mathcal{L}$, it is convenient to proceed as in Chapter 4 and start by studying the (only) unbounded part of $\mathcal{L}$, the squared transport operator $\mathcal{T}^2$. However, when trying to apply the methods from Section 4.3 to the transport operator in the relativistic setting, one immediately encounters a major obstacle: In general, it is unknown whether the (analogue of the) effective potential has the single-well structure that Ψ_L has in the Newtonian case, recall Lemma 2.2.12 and Remark 2.2.13. The single-well structure, in turn, is necessary to introduce action-angle type variables as in Section 4.3.1. For a detailed discussion of the presence of the single-well structure for steady states of the Einstein-Vlasov system, including a formal definition of the property, we refer to [49, Sc. 3.1]. In particular, it follows by [49, Lemma 3.2] and [60, Cor. 3.2] that the single-well structure is present for isotropic steady states which are not too relativistic, i.e., $L_0 = 0 = \ell$ and $0 < \kappa \ll 1$. Numerical simulations clearly indicate, however, that the single-well structure is also present for a much larger class of steady states, cf. [182, Sc. 2.4.2].

Under the assumption that the single-well structure is present, one can proceed as in Section 4.3 to prove that $\mathcal{T}^2$ is self-adjoint[175] and determine its essential spectrum, cf. [49, Prop. 5.1 and Remark 6.3] as well as [182, Thm. 4.3.18]. Here we always mean that $\mathcal{T}^2$ acts only on odd-in-v functions and require that it is defined on the "right" domain of definition. Using that the non-local operators $\mathcal{S}$ and $\mathcal{R}$ are both bounded and relatively compact w.r.t. the transport part, cf. [182, Lemmas 4.3.12, 4.3.14, and 4.3.15], it can then be deduced that $\mathcal{B}^2$ and $\mathcal{L}$ are self-adjoint with

$$\sigma_{\text{ess}}(\mathcal{L}) = \sigma_{\text{ess}}(-\mathcal{B}^2) \subset \sigma_{\text{ess}}(-\mathcal{T}^2), \tag{7.4.21}$$

again assuming that the operators act only on odd-in-v functions and are defined on a suitable domain of definition, cf. [49, Lemma 6.2 and Remark 6.3] as well as [182, Thm. 4.3.18].

Oscillating Solutions

Assume that (the spectrum of) $\mathcal{L}$ is positive. By the stability result cited above and [182, Thm. 5.1.4], this is, e.g., the case if the steady state is isotropic and $0 < \kappa \ll 1$. A natural question is whether one can derive an analogue of the Birman-Schwinger-Mathur principle to characterise the presence of eigenvalues below $\inf(\sigma_{\text{ess}}(\mathcal{L}))$. Such an eigenvalue would again correspond to an oscillating solution of the linearised system (7.4.15). However, when trying to adapt the methods from Chapter 5 to the present setting, a major difficulty arises: Instead of having to compute $(-\mathcal{T}^2 - \lambda)^{-1}$, which is rather easy using action-angle type variables, recall Lemma 4.3.18, we now have to compute $(-\mathcal{B}^2 - \lambda)^{-1}$. The latter is very challenging due to the additional non-local term $\mathcal{S}$ contained in $\mathcal{B}$, and it has not (yet) been achieved. One way to overcome this issue might be to introduce a wave operator relating $\mathcal{B}$ to $\mathcal{T}$. For now, showing the presence of oscillating solutions via a Birman-Schwinger-Mathur principle remains open.

Despite all the additional difficulties that the Einstein-Vlasov system brings with it compared to the Vlasov-Poisson system, there is a (recently developed) way of showing the existence of certain oscillating solutions which only works in the relativistic setting: For a

[174] We refer to [71, Sc. IVf)] for a discussion regarding the effects of a zero eigenvalue of $\mathcal{L}$ and otherwise neglect this aspect here.

[175] Proving the skew-adjointness of $\mathcal{T}$ and the self-adjointness of $\mathcal{T}^2$ can, in fact, also be done without using action-angle type variables or the single-well structure, cf. Remark 4.3.14 and [147].

fixed isotropic ansatz $L_0 = 0 = \ell$ with polytropic exponent $0 < k < \frac{3}{2}$, the linear stability results cited above imply $\inf(\sigma(\mathcal{L})) > 0$ for small $\kappa > 0$ and $\inf(\sigma(\mathcal{L})) < 0$ for large κ. Hence, assuming that the bottom of the spectrum of $\mathcal{L} = \mathcal{L}_\kappa$ changes continuous in κ, there exists $\kappa_0 > 0$ s.t. $\inf(\sigma(\mathcal{L}_{\kappa_0})) = 0$ as well as $\inf(\sigma(\mathcal{L}_\kappa)) > 0$ for $0 < \kappa < \kappa_0$. Under the additional assumption that $\inf(\sigma_{\text{ess}}(\mathcal{L}_\kappa))$ is always positive and continuous in κ, we deduce $0 < \inf(\sigma(\mathcal{L}_\kappa)) < \inf(\sigma_{\text{ess}}(\mathcal{L}_\kappa))$ for $\kappa < \kappa_0$ with $\kappa_0 - \kappa \ll 1$. For such κ, $\inf(\sigma(\mathcal{L}_\kappa))$ has to be an eigenvalue of $\mathcal{L} = \mathcal{L}_\kappa$ corresponding to an oscillating mode. These arguments originate from [182, Ch. 6]. In particular, the continuity assumptions on the spectra of $\mathcal{L}$ are verified in [182] for suitable families of equilibria.

Steady States Surrounding a Black Hole

In the above discussion, it became clear that the single-well structure is crucial for the spectral analysis of the linearised operator $\mathcal{L}$. One class of steady states where this property can be rigorously verified can be obtained in a perturbative regime similar to the one from Chapter 6. Concretely, we consider a shell of Vlasov matter surrounding a fixed Schwarzschild black hole. The system analogous to (7.4.1)–(7.4.10) including such a black hole is stated in [49, Sc. 1.1]. As in Section 6.2, one can construct compactly supported steady states of this system of the form (7.4.11) with sufficiently large[176] $L_0 > 0$ and an additional smallness parameter $\varepsilon > 0$. Choosing $0 < \varepsilon \ll 1$ leads to stationary shells which are small (compared to the fixed black hole) in a similar way as in Proposition 6.2.6 (a). In this regime, the single-well structure can be rigorously proven. We refer to [49, Scs. 2 and 3] for proofs of these properties. A different approach to construct small steady states surrounding a Schwarzschild black hole is pursued in [72].

A Birman-Schwinger-Mathur Principle for Linear Stability

As discussed above, it is unclear whether one can derive a version of the Birman-Schwinger-Mathur principle to characterise the presence of eigenvalues below $\inf(\sigma_{\text{ess}}(\mathcal{L})) > 0$. However, it is possible to derive such a principle for the existence of non-positive eigenvalues of $\mathcal{L}$. The latter is easier because instead of $(-\mathcal{B}^2 - \lambda)$ with $\lambda > 0$ one has to invert $\mathcal{B}^2$. This is possible in a semi-explicit way using action-angle type variables, cf. [49, Sc. 5.2.2]. In particular, we again have to assume the single-well structure of the effective potential. By proceeding similarly to Chapter 5, we can then translate the existence of non-negative eigenvalues of $\mathcal{L}$ into the existence of an eigenvalue ≥ 1 of a suitable Hilbert-Schmidt operator $\mathcal{M}\colon L^2([0,\infty[) \to L^2([0,\infty[)$, cf. [49, Prop. 6.20 and Thm. 6.22]. Moreover, there holds a Birman-Schwinger type bound similar to Theorem 5.3.3 bounding the number of negative eigenvalues by a suitable norm of the integral kernel associated to $\mathcal{M}$, cf. [49, Thm. 6.24].

The criterion for the absence of non-positive eigenvalues of $\mathcal{L}$ can be verified in the perturbative regime described above. We hence conclude the linear stability – in the sense of [49, Def. 4.4] – of sufficiently small stationary shells surrounding a Schwarzschild black hole, cf. [49, Thm. 7.1].

[176] More precisely, L_0 has to be larger than twelve times the squared mass of the fixed black hole to ensure that the steady state is bounded away from the event horizon of the black hole.

Chapter 8

Numerical Experiments

In this chapter we analyse and visualise several of the quantities we encountered in our mathematical studies via numerical simulations. We start with the steady states and the (radial) period functions associated to them in Sections 8.1 and 8.2. Subsequently, in Sections 8.3 and 8.4, we numerically simulate the linearised Vlasov-Poisson system and the (non-linearised) Vlasov-Poisson system. The general aim of this chapter is to get an impression of which statements about solutions of the Vlasov-Poisson system close to steady states are true and how the theory developed here can help to prove them rigorously.

Throughout this chapter, we only consider the setting from Chapters 2–5, i.e., spherical symmetry without a point mass, as it is the most relevant one from a physics point of view. Straight-forward modifications of our code yield simulations of the spherically symmetric setting with a point mass (cf. Section 6.1), the plane symmetric setting (cf. Section 7.1), the single-L setting with a point mass (cf. Section 7.2), or the relativistic Vlasov-Poisson system (cf. Section 7.3). More modifications would be necessary to obtain numerical simulations of the Einstein-Vlasov system (cf. Section 7.4).

The code we use here is newly written. It is based on the codes used in [48, 50] to simulate the Einstein-Vlasov system, which are in turn based on the codes used earlier in [5, 132]. We will briefly outline our numerical methods at the beginning of each of the following sections. We refrain from providing more detailed descriptions and instead make our code publicly available via the following link:

https://github.com/c-straub/radVP

The code is written in `C++` in an object-oriented way. We have tried to keep the code as simple as possible, and in particular have not used any specialised programming library, to make it understandable for less programming experienced readers as well. The simulations – in particular, the numerically expensive ones in Sections 8.3 and 8.4 – were run on the supercomputers provided by the Keylab HPC of the University of Bayreuth. All figures in this chapter (as well as Figure 1.1.1) were created using gnuplot.[177]

We will state the main findings of this chapter not as theorems, propositions, or lemmas, but as *observations*. Any such observation is based on numerical simulations which we describe before stating the observation. As a caveat, we emphasise that each of the observations might be distorted by the numerical methods chosen, possible programming errors, our choices of numerical parameters, our choices of states/quantities/cases to consider, our interpretation of the data, or a combination of these factors. We sincerely hope that our extensive testing of the program during its development and a thorough analysis of the obtained data has minimised these effects.

[177] We further used the online tool https://www.iloveimg.com/compress-image to compress all images.

8.1 Numerics of Steady States

In this section we numerically analyse the steady states introduced in Section 2.2 and the (macroscopic) quantities associated to them. Here, the aim is not to gain new insights, but rather to reinforce our understanding of steady states by visualising them in various ways. We study the shapes of macroscopic quantities like the mass density ρ_0 and gravitational potential U_0 as well as "global" quantities like the total mass M_0 and maximal radius $R_{\max}$. Other steady state quantities which are more tied to the particle motions, like the effective potential Ψ_L or the (E, L)-support $\mathbb{D}_0$, will be analysed in Section 8.2.

The Numerical Method

For a prescribed ansatz of the general form (2.2.12) and a prescribed parameter $\kappa > 0$, we compute a steady state by solving the integro-differential equation (2.2.35) with initial condition (2.2.36). This is implemented numerically via the midpoint method with radial step size $\leq 10^{-6}$. The function g defined by (2.2.25) is evaluated by computing the integral via Simpson's rule. In the polytropic case, we instead use the explicit formula (2.2.29). Once a numerical solution y of (2.2.35)–(2.2.36) is found, the steady state and the (macroscopic) quantities associated to it are defined as described in Proposition 2.2.9. A similar algorithm for computing steady states of the Vlasov-Poisson system is used in the numerical study [132] and in the context of the Einstein-Vlasov system in [6, 48, 50].

Families of steady states are calculated by executing several calls of the above algorithm in parallel using the Pthreads API in `C++`.

The Isotropic Polytropic Steady State $k = 1 = R_{\max}$

We first consider a single steady state with isotropic polytropic equation of state (2.2.18). For the sake of simplicity, we choose the polytropic exponent $k = 1$ resulting in a(n affine) linear dependence of the phase space density f_0 on the particle energy E. The parameter κ is chosen s.t. the resulting steady state is radially supported on the unit interval, i.e., $R_{\max} = 1$. This is possible by the scaling laws from Appendix B. We denote this κ-value by κ^*; numerical computations yield $\kappa^* \approx 0.614$. Several macroscopic quantities associated to this steady state are depicted in Figure 8.1.1. In the course of this chapter, we will always use this steady state as a prototype for the numerical analysis.

Isotropic Polytropic Steady States

Let us next consider general isotropic polytropic steady states (1.2.3) with polytropic exponents $0 \leq k < \frac{7}{2}$. Because the steady states become more and more elongated as the polytropic exponent k approaches $\frac{7}{2}$, we always restrict ourselves here to $k \leq 3.2$. For every such ansatz, we again choose the parameter $\kappa > 0$ s.t. $R_{\max} = 1$; this is possible by Appendix B.[178] These values κ^* as well as the values of the total mass of the resulting steady states are depicted in Figure 8.1.2 as functions of the polytropic exponent k. The mass densities and gravitational potentials of a few of these steady states are plotted in Figure 8.1.3.

In Figure 8.1.4 we plot the (R, M)-diagrams for some selected isotropic polytropic ansatz functions, i.e., the values of $R_{\max}$ and M_0 for steady states with a fixed ansatz function and different values of $\kappa > 0$. The plots match the scaling law (B.0.11) to high accuracy. As

[178] We note that the scaling laws (B.0.8) and (B.0.10) for the maximal radius and the total mass of steady states, respectively, also hold in the case $k = 0$.

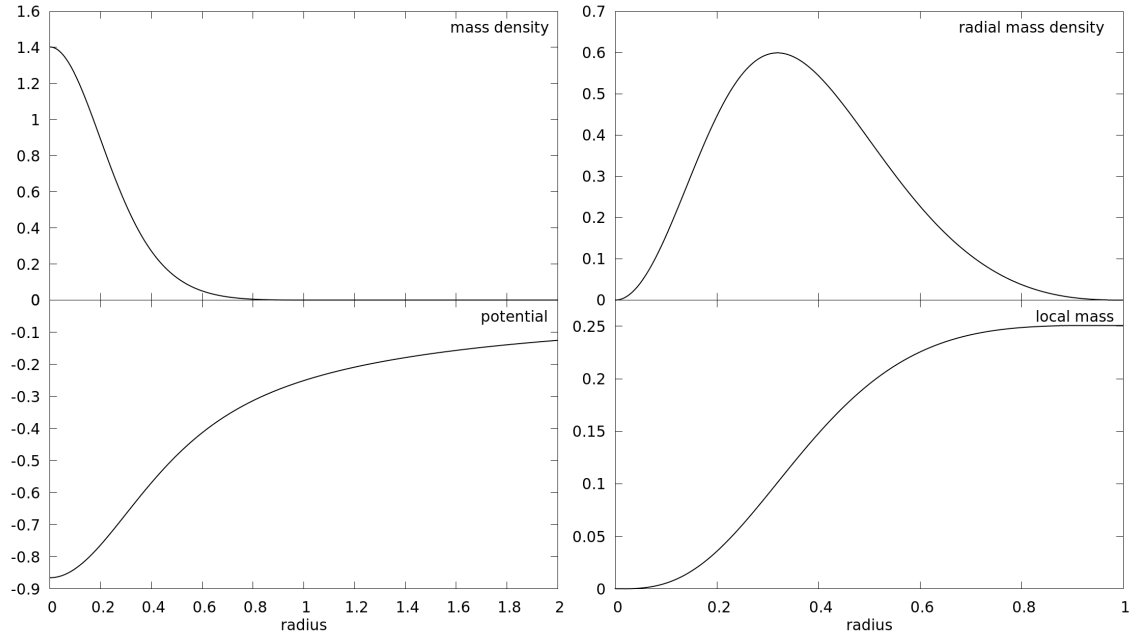

Figure 8.1.1: Macroscopic quantities associated to the isotropic polytropic steady state (1.2.3) with polytropic exponent $k = 1$ and $R_{\max} = 1$. The four panels show the mass density ρ_0, the radial mass density $r \mapsto 4\pi r^2 \rho_0(r)$, the gravitational potential U_0, and the local mass m_0, respectively.

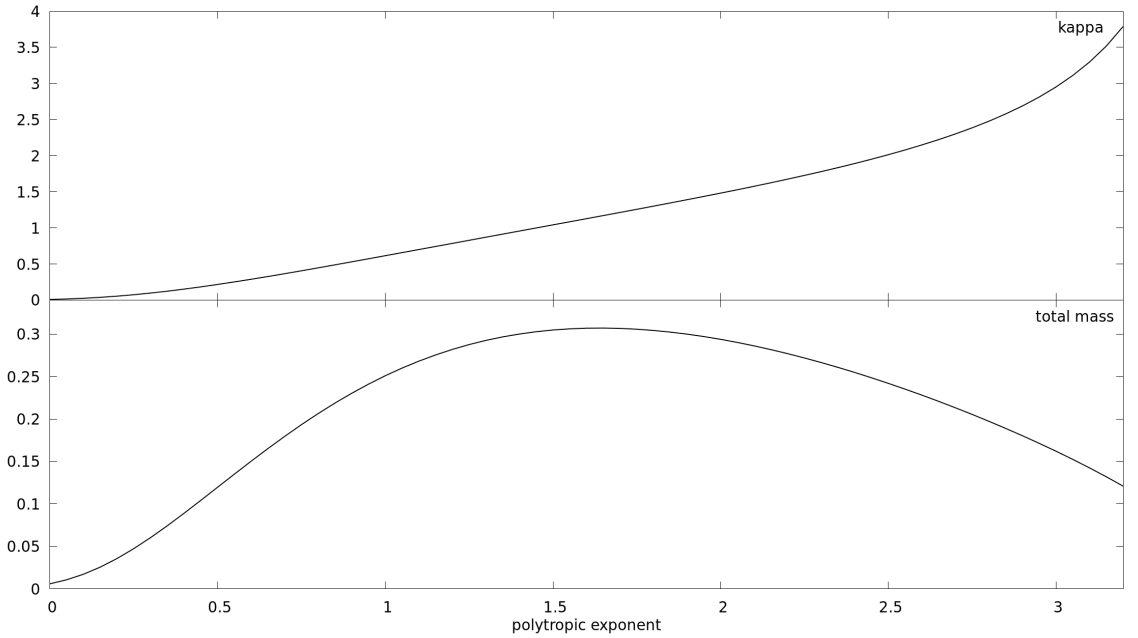

Figure 8.1.2: The top panel shows the values κ^* leading to $R_{\max} = 1$ for the isotropic polytropes as a function of k. The bottom panel shows the values of the total mass M_0 of the resulting steady states.

an aside, we note that we used κ-values of up to 200 in Figure 8.1.4. Steady states with large κ-values are generally more difficult to compute numerically because $g(y(r))$, and thus $\rho_0(r)$, cf. (2.2.27), attains large values for $r \approx 0$ in this case. Nonetheless, even for such

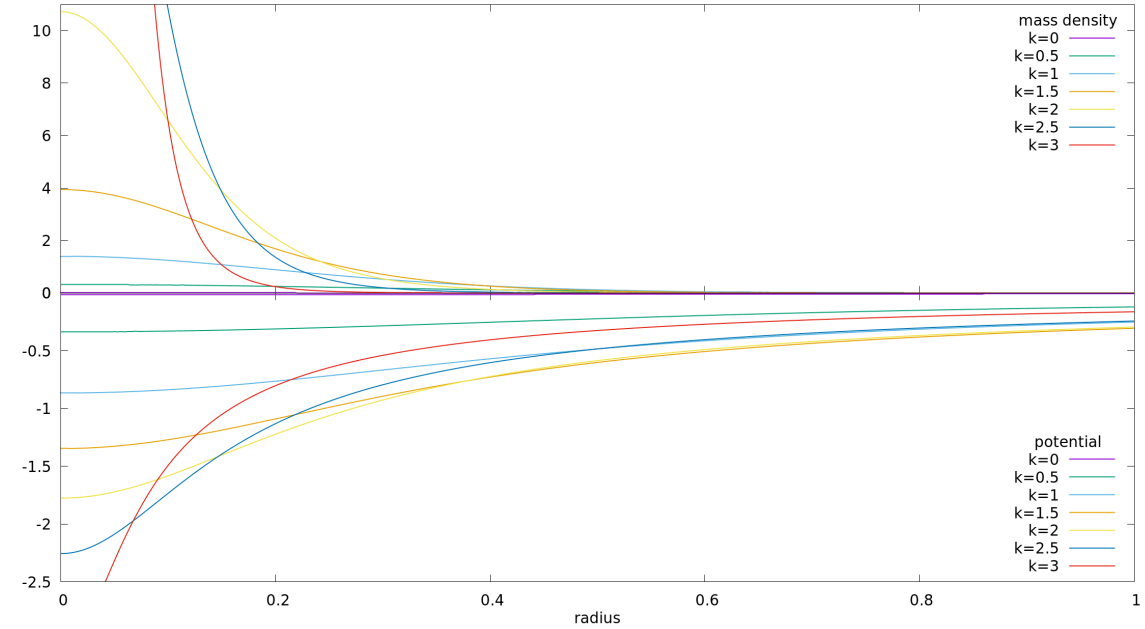

Figure 8.1.3: Macroscopic quantities associated to the isotropic polytropes (1.2.3) with polytropic exponents $k \in \{0, \frac{1}{2}, 1, \frac{3}{2}, 2, \frac{5}{2}, 3\}$ and $R_{\max} = 1$. The top panel shows the mass densities ρ_0 and the bottom panel the gravitational potentials U_0.

large values of κ, the numerics remain accurate.

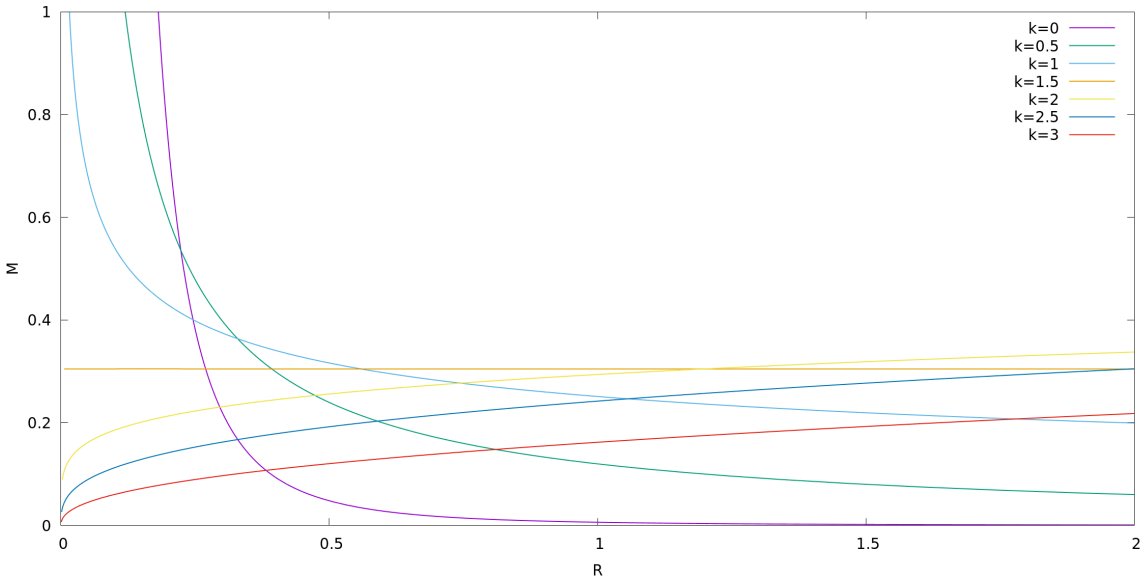

Figure 8.1.4: (R, M)-diagrams for the isotropic polytropes with polytropic exponents $k \in \{0, \frac{1}{2}, 1, \frac{3}{2}, 2, \frac{5}{2}, 3\}$, i.e., the values of the maximal radius $R_{\max}$ and the total mass M_0 of the steady states with fixed equation of state and different values of $\kappa > 0$. See [129, Abb. 3.2] for a related figure.

King Models

We next consider the King models (1.2.4) with different values of the parameter $\kappa > 0$. The mass densities and gravitational potentials of a few of these steady states are plotted in Figure 8.1.5. Notice, in particular, the very large values of ρ_0 close to the spatial origin $r = 0$ in the case of large κ. They are due to the exponential King ansatz function Φ, which leads to g defined by (2.2.25) to grow rather fast.

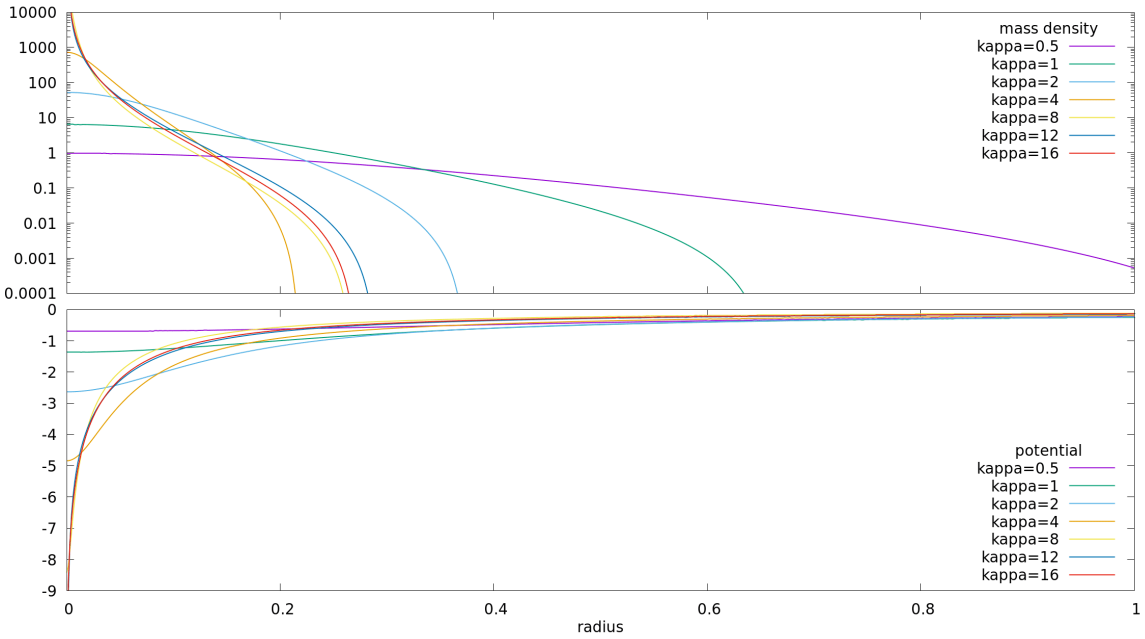

Figure 8.1.5: Macroscopic quantities for the King models (1.2.4) with parameter $\kappa \in \{\frac{1}{2}, 1, 2, 4, 8, 12, 16\}$. The top panel shows the mass densities ρ_0 in a logarithmic scale and the bottom panel the gravitational potentials U_0.

As mentioned several times before, in the case of King's equation of state (2.2.19), a scaling law like (B.0.11) does not hold. This qualitative difference between polytropes and King models can be seen quite clearly in the (R, M)-diagrams: Unlike the monotonic curves in the polytropic case, cf. Figure 8.1.4, the (R, M)-diagram is a spiral for King's equation of state, see Figure 8.1.6. This spiral structure is proven rigorously in [131] and accurately reproduced by our numerics. It should be noted again that large κ-values of up to 30 – leading to very large $\rho_0(0)$-values – are used in Figure 8.1.6. For the numerics to work accurately in this regime, we have (immensely) reduced the radial step size in the steady state computation for large κ.

Moreover, as an illustrative support of the discussion from Remark 2.2.10 (c), the dependence of the cut-off energy E_0 on the parameter κ in the case of King's equation of state is visualised in Figure 8.1.7. It is evident from this figure that the mapping $]0, \infty[\ni \kappa \mapsto E_0 \in]-\infty, 0[$ is neither injective nor surjective for King's equation of state.

Anisotropic Polytropic Steady States with $L_0 = 0$

Let us return to polytropic equations of state (2.2.17). Unlike before, however, we now consider anisotropic steady states. We start with the situation where there is no inner radial vacuum region, i.e., $L_0 = 0 = R_{\min}$. Note that, due to the assumption ($\varphi 4$), such steady states are not included in the analysis of Chapters 4–5. Nevertheless, they are interesting

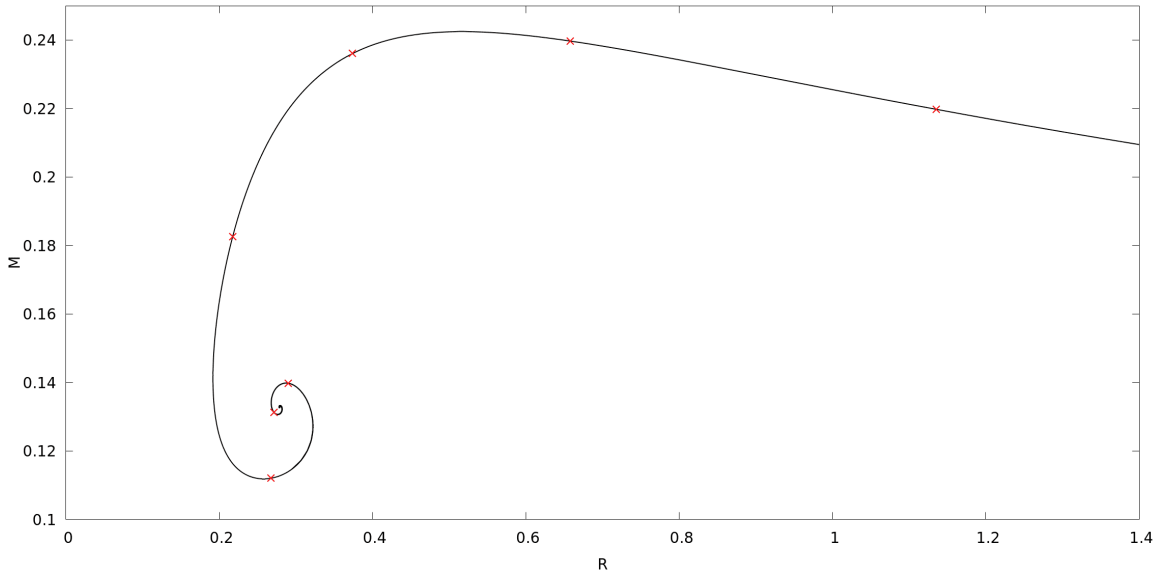

Figure 8.1.6: The black curve is the (R, M)-diagram of the King models, i.e., the values of the maximal radius $R_{\max}$ and the total mass M_0 of steady states with King's equation of state (2.2.19) and different values of $\kappa \in [\frac{1}{10}, 30]$. As κ increases, one moves into the spiral. The red crosses mark the positions of the κ-values $\{\frac{1}{2}, 1, 2, 4, 8, 12, 16\}$ used in Figure 8.1.5. Similar figures can be found in [129, Abb. 4.1] and [131, Fig. 1].

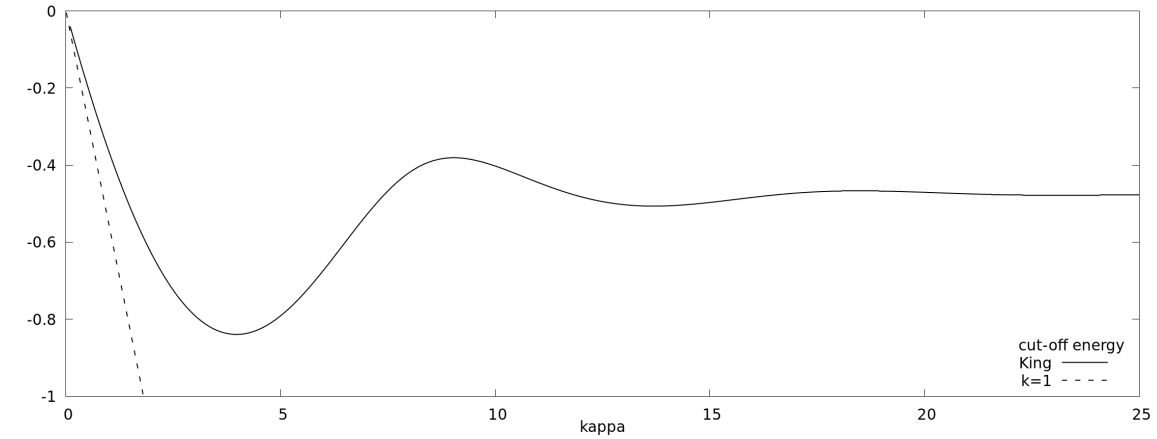

Figure 8.1.7: The cut-off energy E_0 as a function of the steady state parameter κ for King's equation of state (solid line) and the isotropic polytropes with $k = 1$ (dashed line).

to analyse numerically – in particular, because of the property discussed in Remark A.4.5, which we will address further in the following section.

The most striking difference of these steady states compared to isotropic ones is that the mass density vanishes at the spatial origin $r = 0$. This can be seen in Figure 8.1.8, where we plot the mass densities and gravitational potentials of some of these steady states. In this figure, we again chose all κ-values s.t. $R_{\max} = 1$. Note that the scaling laws from Appendix B apply to this class of steady states. The scaling law (B.0.11) for the (R, M)-diagrams is again accurately reproduced by our numerics, see Figure 8.1.9.

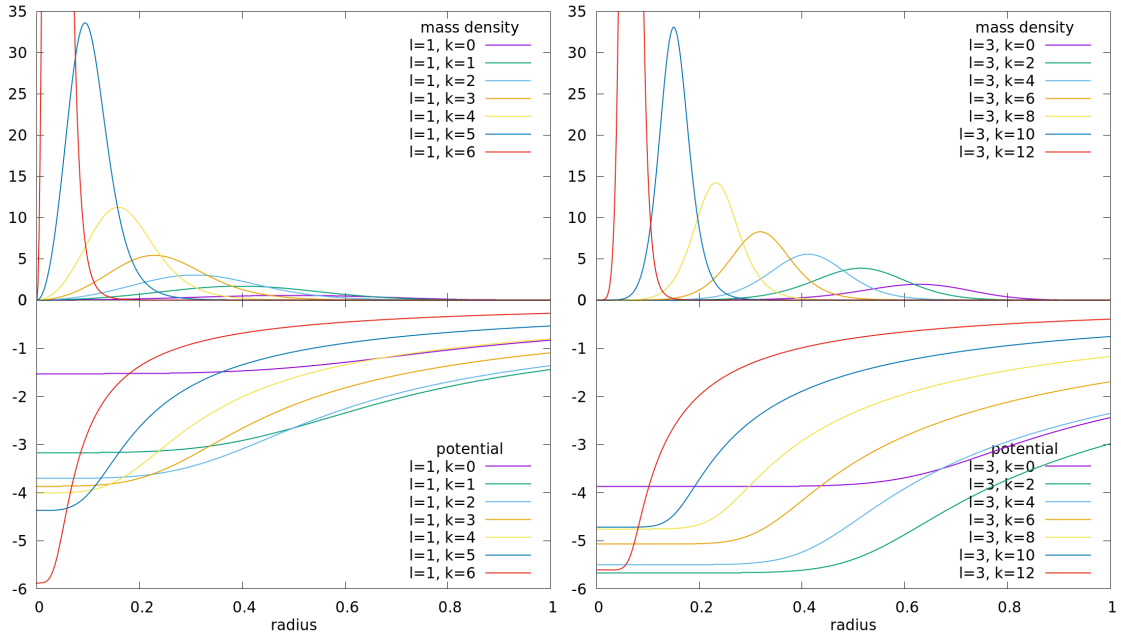

Figure 8.1.8: Macroscopic quantities associated to anisotropic polytropic steady states (2.2.17) with $L_0 = 0$ and κ chosen s.t. $R_{\max} = 1$. The top left panel shows the mass densities ρ_0 for the polytropic exponents $\ell = 1$ and $k \in \{0, 1, 2, 3, 4, 5, 6\}$, the bottom left panel the associated potentials U_0. The two panels on the right show the same quantities for polytropic exponents $\ell = 3$ and $k \in \{0, 2, 4, 6, 8, 10, 12\}$.

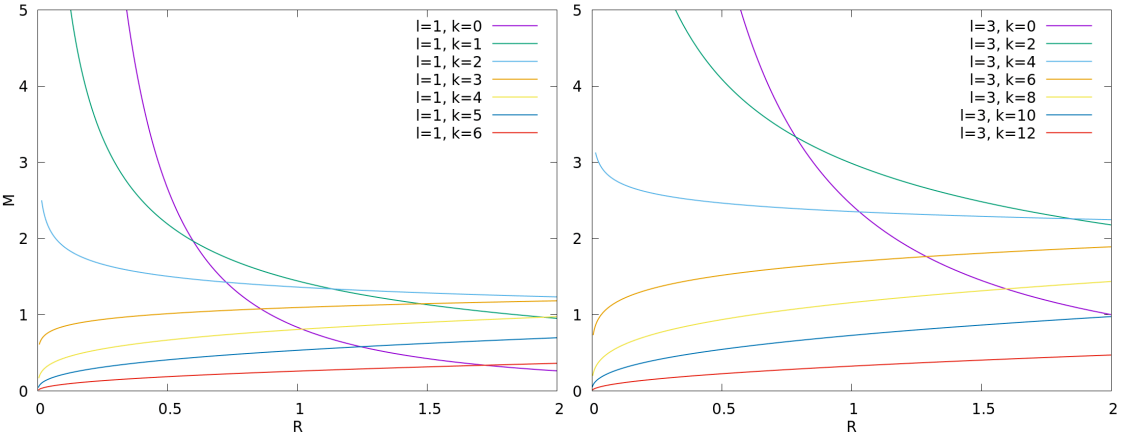

Figure 8.1.9: (R, M)-diagrams for some anisotropic polytropes with $L_0 = 0$, i.e., the values of the maximal radius $R_{\max}$ and total mass M_0 of steady states with fixed equation of state and different values of $\kappa > 0$. The left panel contains the (R, M)-diagrams for the polytropic exponents $\ell = 1$ and $k \in \{0, 1, 2, 3, 4, 5, 6\}$, the right panel the diagrams for $\ell = 3$ and $k \in \{0, 2, 4, 6, 8, 10, 12\}$. See [129, Abb. 3.3] for a figure related to the left panel.

Polytropic Shells

The last class of steady states which we discuss in this section are polytropes (1.2.5) with $L_0 > 0$. These steady states possess an inner radial vacuum region, i.e., $R_{\min} > 0$. The inner vacuum region is clearly visible in Figure 8.1.10, where we plot macroscopic quantities associated to a few of such steady states. As L_0 increases, the inner vacuum region gets larger by (2.2.42), while the steady states approach the respective configuration with $L_0 =$

$0 = R_{\min}$ (which we discussed and illustrated above) as $L_0 \searrow 0$.

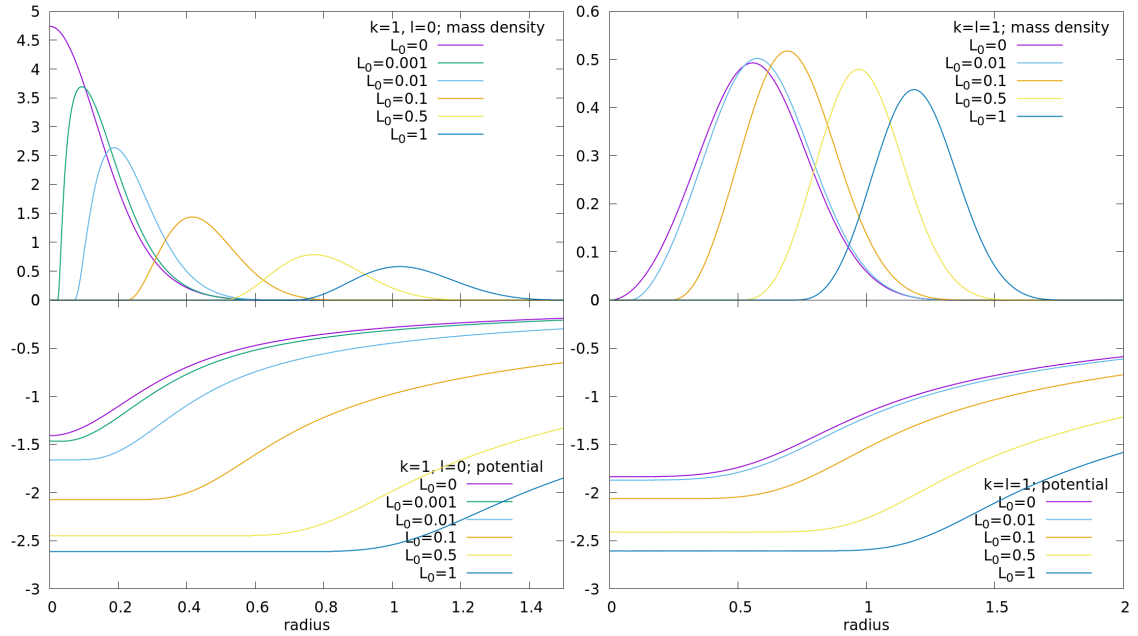

Figure 8.1.10: Macroscopic quantities associated to polytropic steady states (1.2.5) with $\kappa = 1$. The top left panel shows the mass densities ρ_0 for the polytropic exponents $(k, \ell) = (1, 0)$ and $L_0 \in \{0, \frac{1}{1000}, \frac{1}{100}, \frac{1}{10}, \frac{1}{2}, 1\}$, the bottom left panel the associated potentials U_0. The two panels on the right show the same quantities for polytropic exponents $(k, \ell) = (1, 1)$ and $L_0 \in \{0, \frac{1}{100}, \frac{1}{10}, \frac{1}{2}, 1\}$.

It should also be noted that the scaling laws from Appendix B get lost when choosing $L_0 > 0$ in the polytropic ansatz. Some (R, M)-diagrams for such polytropes are plotted in Figure 8.1.11. Qualitatively, however, they do not appear significantly different from the corresponding curves in the case $L_0 = 0$. We further observed that (R, M)-diagrams for polytropic equations of state with $\ell < 0$ and $L_0 > 0$ are qualitatively similar to the ones depicted in Figure 8.1.11.

8.2 Numerics of the Period Function

In this section we analyse the (radial) period function T associated to the steady states from Section 2.2; recall Definition 2.2.16 for the definition of the period function. The properties of the period function were essential at several places in this thesis. However, despite the detailed analysis in Appendix A, we have not yet succeeded in rigorously proving all the properties of T we need to conclude some desired statements regarding solutions of the linearised Vlasov-Poisson system. The numerical analysis presented below shall help us to understand which statements about T are true and which strategies might be helpful to prove them rigorously. A focus will be on the monotonicity of the period function w.r.t. its two variables E and L, as this property is particularly important for our applications.

To the author's knowledge, this is the first numerical analysis of the (radial) period function associated to steady states of the Vlasov-Poisson system. A related study in the context of the Einstein-Vlasov system is conducted in [182, Sc. 2.4.2].

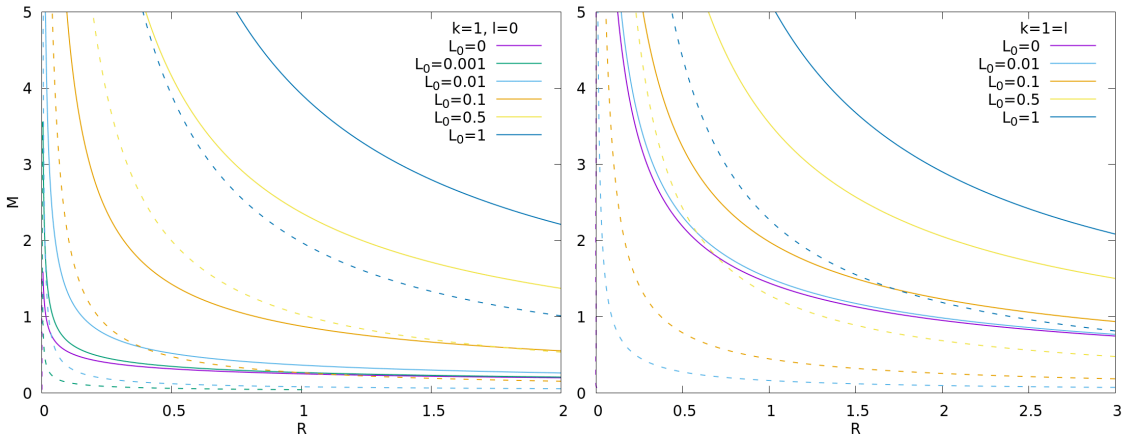

Figure 8.1.11: The solid lines are the (R, M)-diagrams for some polytropic equations of state, i.e., the values of the maximal radius $R_{\max}$ and the total mass M_0 of steady states with the fixed equation of state and different values of $\kappa > 0$. The dashed lines depict the respective values of the minimal radius $R_{\min}$. The left panel contains the (R, M)-diagrams for polytropes with $k = 1$, $\ell = 0$, and $L_0 \in \{0, \frac{1}{1000}, \frac{1}{100}, \frac{1}{10}, \frac{1}{2}, 1\}$, the right panel the (R, M)-diagrams for $k = 1$, $\ell = 1$, and $L_0 \in \{0, \frac{1}{100}, \frac{1}{10}, \frac{1}{2}, 1\}$.

The Numerical Method

We start with a fixed steady state f_0 computed numerically as described in the previous section. Our aim is to compute $T(E, L)$ for $(E, L) \in \mathbb{A}_0$. Due to the singular integrand, we do not use the integral representation (2.2.97) of the period function for this task. Instead, we compute (the relevant parts of) the solution $(\tilde{R}, \tilde{W})(\cdot, E, L) \colon \mathbb{R} \to]0, \infty[\times \mathbb{R}$ of the radial characteristic system (2.2.93) with parameter L satisfying the initial condition $(\tilde{R}, \tilde{W})(0, E, L) = (r_+(E, L), 0)$.[179,180] In order to determine $T(E, L)$, we just have to wait until the velocity component of the solution $(\tilde{R}, \tilde{W})(\cdot, E, L)$ becomes positive since

$$\frac{1}{2} T(E, L) = \inf\{s \geq 0 \mid \tilde{W}(s, E, L) > 0\}. \tag{8.2.1}$$

To compute $(\tilde{R}, \tilde{W})(\cdot, E, L)$, we actually do not solve (2.2.93) directly but instead transform (back) to Cartesian coordinates and solve (2.2.2). More precisely, for given radial coordinates (r, w, L), associated Cartesian coordinates s.t. (2.1.3) holds are, e.g., given by

$$x = (r, 0, 0), \quad v = (w, \frac{\sqrt{L}}{r}, 0). \tag{8.2.2}$$

Once the initial condition $(r_+(E, L), 0, L)$ is transformed to Cartesian coordinates in this way, we solve (2.2.2) until $x \cdot v = rw$ becomes positive and obtain the value of $T(E, L)$ via (8.2.1). The reason why it is more convenient to work in Cartesian coordinates is because this avoids difficulties arising close to the spatial origin $r = 0$. This will become even more important in the following section, where we have to solve the characteristic system with more general initial data. In addition, using Cartesian coordinates allows us

[179] Another reason why we do not calculate the integral (2.2.97) but instead compute the solutions of the characteristic system is because we have to numerically solve the characteristic system anyway when simulating the linearised Vlasov-Poisson system, cf. Section 8.3.

[180] The reason why we choose the initial condition $(r_+(E, L), 0)$ instead of $(r_-(E, L), 0)$ (as in Definition 2.2.16) is that the effective potential Ψ_L is rather steep at $r \approx 0$. This makes the calculation of $r_-(E, L)$ more difficult and prone to numerical errors compared to $r_+(E, L)$, in particular, for small values of L.

to compute $T(E, L)$ for $L = 0$ as well, recall Remark 2.2.17 (a). However, the price we pay is that the six-dimensional system (2.2.2) is, of course, numerically more expensive to solve than the planar system (2.2.93).

To solve (2.2.2) numerically, we use the classical Runge-Kutta method (henceforth abbreviated as "RK4") with time step size $\delta t \leq 10^{-6}$.

Furthermore, we extend the period function to points $(E_L^{\min}, L)$ lying on the minimal energy curve by using the extension formula (A.4.11). Extensive testing has shown that this indeed extends the values of $T(E, L)$ for $(E, L) \in \mathbb{A}_0$ in a continuous way with high accuracy. This demonstrates that our numerical computation of the period function $T(E, L)$ works accurately, even in the near circular regime $E \approx E_L^{\min}$.

For several aspects of the following analysis, e.g., to accurately compute the maximum of T on $\overline{\mathbb{D}}_0$, it is necessary to evaluate the period function on a very large set of (E, L)-pairs. This is realised by performing several evaluations of the period function in parallel using the Pthreads API in `C++` again.

The Isotropic Polytropic Steady State $k = 1 = R_{\max}$

As in Section 8.1, we start our analysis by considering in detail the isotropic polytrope (1.2.3) with polytropic exponent $k = 1$ and parameter $\kappa > 0$ chosen s.t. $R_{\max} = 1$. Because the radial particle motions are determined by the effective potential Ψ_L, we first depict this function for some values of $L \in \overline{\mathbb{L}}_0$ in Figure 8.2.1. Encouragingly, the shape of Ψ_L computed numerically is as described in Lemma 2.2.12, and the figure is consistent with the monotonicity and limiting properties proven in Lemma 2.2.14.

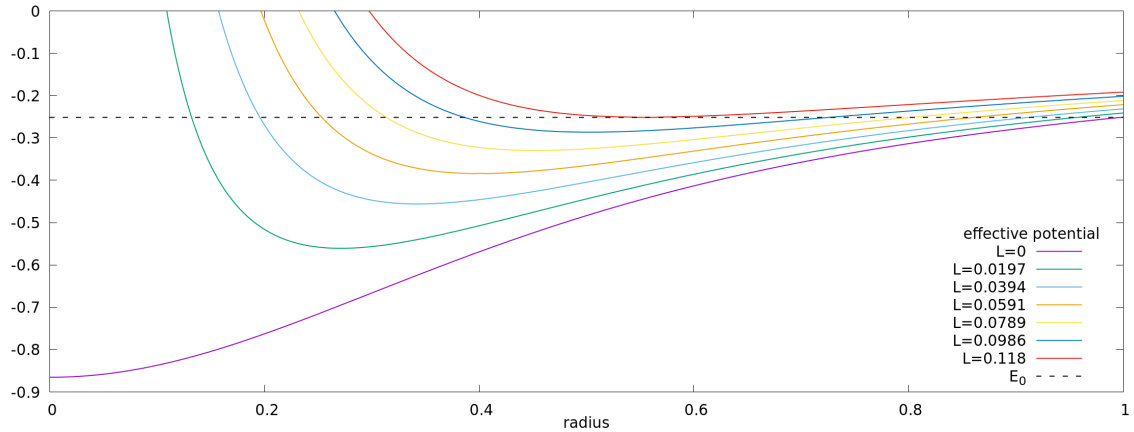

Figure 8.2.1: The effective potential Ψ_L for some values of L for the isotropic polytropic steady state $k = 1 = R_{\max}$. The L-value associated to the red line is $L_{\max}$ (up to numerical errors and rounding). The dashed black line shows the value of the cut-off energy E_0.

The associated period function T on (the closure of) the (E, L)-support $\mathbb{D}_0$ is visualised in Figure 8.2.2. Note that the shape of $\mathbb{D}_0$ obtained numerically is qualitatively identical to the one of the schematic visualisation in Figure 2.2.2.

Figure 8.2.2 reveals two important insights. Firstly, we see that the maximum of T on $\overline{\mathbb{D}}_0$ is attained at $(E_0, 0)$, i.e.,

$$\sup_{\mathbb{D}_0}(T) = T(E_0, 0). \tag{8.2.3}$$

The point $(E_0, 0)$ corresponds to the bottom right corner in Figure 8.2.2. The value of the period function attained there is given by $T(E_0, 0) \approx 4.727$. The fact that $T\big|_{\overline{\mathbb{D}}_0}$ indeed

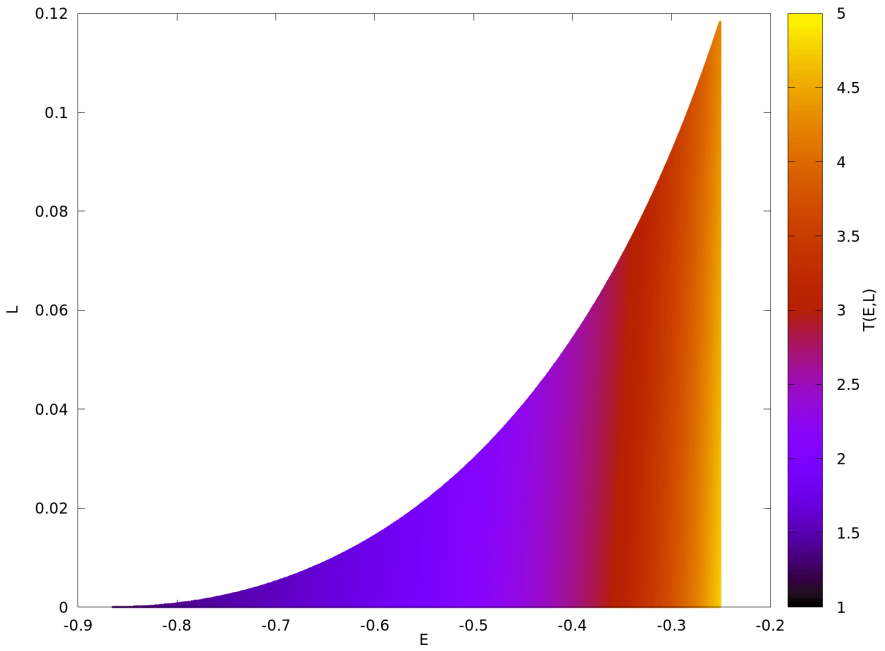

Figure 8.2.2: The (E, L)-support $\overline{\mathbb{D}}_0$ of the isotropic polytrope $k = 1 = R_{\max}$ and values of the period function T (colour gradient) attained on it.

attains its maximum at $(E_0, 0)$ has been checked by comparing $T(E_0, 0)$ to all the other (more than $5 \cdot 10^5$) T-values used in Figure 8.2.2. By the scaling laws derived in Appendix B, (8.2.3) holds for all $\kappa > 0$ if it holds for one value of κ. Let us summarise this finding.

Observation 8.2.1 (Maximum of T for the Isotropic Polytrope $k = 1$)**.** *In the case of an isotropic polytropic steady state* (1.2.3) *with polytropic exponent $k = 1$, the maximum of the period function T on the (E, L)-support $\overline{\mathbb{D}}_0$ of the steady state is attained at the maximal energy value E_0 and the minimal L-value $L_0 = 0$, i.e.,* (8.2.3) *holds. In addition, this is the only point where the maximal period is attained.*

Secondly, the period function T is even monotonic[181] w.r.t. both of its variables on $\mathbb{D}_0$. More precisely, T is increasing in E and decreasing in L on $\mathbb{D}_0$. This property can already be seen in Figure 8.2.2. It is even more clearly visible in Figure 8.2.3, where we depict $T(\cdot, L)$ and $T(E, \cdot)$ for some fixed values of L and E. We verified these monotonicities by analysing the functions $T(\cdot, L)$ and $T(E, \cdot)$ for more (than 1000) values of L and E. Up to an error of $5 \cdot 10^{-6}$, these functions are indeed monotonic. By Appendix B, these monotonicities hold for every $\kappa > 0$ if they hold for one κ.

Observation 8.2.2 (T-Monotonicity for the Isotropic Polytrope $k = 1$)**.** *In the case of an isotropic polytrope* (1.2.3) *with polytropic exponent $k = 1$, the period function T is increasing in E and decreasing in L on the (E, L)-support $\mathbb{D}_0$ of the steady state.*

As an aside, we note that the minimal value of the period function T on $\overline{\mathbb{D}}_0$ is attained at the minimal energy value $U_0(0) = \lim_{L \searrow 0} E_L^{\min}$ and the minimal L-value $L_0 = 0$, i.e., at $(U_0(0), 0)$. This point corresponds to the bottom left corner in Figure 8.2.2. The minimal T-value is given by $T(U_0(0), 0) \approx 1.296$. The fact that the T-minimum is attained at this point

[181] In this chapter, we generally do not distinguish between strict and non-strict monotonicity, as this difference is hard, if not impossible, to detect numerically. Similarly, we do not distinguish between positive and non-negative numbers.

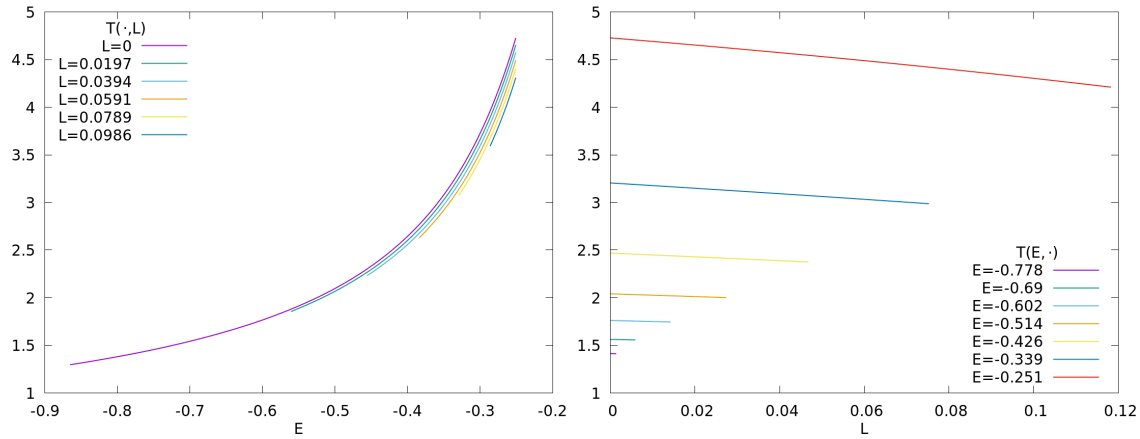

Figure 8.2.3: Values of the period function T for the isotropic polytropic steady state $k = 1 = R_{\max}$. The left panel shows the function $T(\cdot, L)$ on $[E_L^{\min}, E_0]$ for some values of $0 \leq L < L_{\max}$, the right panel the function $T(E, \cdot)$ on $[0, L_{\max}(E)]$ for some values of $U_0(0) < E \leq E_0$. Here, $L_{\max}(E) := \sup\{L > 0 \mid E_L^{\min} < E\}$ for $U_0(0) < E < 0$.

fits to the monotonicity observed above combined with the monotonicity of $L \mapsto T(E_L^{\min}, L)$ proven in Lemma A.4.3.

Although the discussion in Section A.3.3 mainly shows that it is rather difficult to prove the statements from Observation 8.2.2 rigorously, it also contains a useful criterion for these monotonicity properties: By Lemma A.3.22, the statements from Observation 8.2.2 follow if the two functions G_L^{ref} and H_L^{ref} are both positive on $]r_-(E_0, L), r_L[$ for every $0 < L < L_{\max}$. These two functions are essentially given by the effective potential and its derivatives up to second order. We plot these functions as well as G_L and H_L for some values of $L \gtrless 0$ in Figure 8.2.4.

As indicated by Lemma A.3.20 and (A.3.98), the functions G_L and H_L do not take only one sign on $]r_-(E_0, L), r_+(E_0, L)[$ for $0 < L < L_{\max}$. Nonetheless, the functions G_L^{ref} and H_L^{ref} are positive on $[r_-(E_0, L), r_L[$ for $L \in]0, L_{\max}[$. This is clearly visible in Figure 8.2.4, where it even looks like G_L^{ref} and H_L^{ref} are radially decreasing with $\lim_{r \searrow r_L} G_L^{\text{ref}}(r) = 0 = \lim_{r \searrow r_L} H_L^{\text{ref}}(r)$. The positivity of these functions has also been further checked by considering more L-values than in Figure 8.2.4 (50 equidistant $L \in]0, L_{\max}[$). Up to an error of 10^{-4}, G_L^{ref} and H_L^{ref} are always positive. Extending the scaling laws from Appendix B to G_L^{ref} and H_L^{ref} again allows us to generalise this finding to all values of $\kappa > 0$.

Observation 8.2.3 (Positivity of G_L^{ref} and H_L^{ref} for the Isotropic Polytrope $k = 1$)**.** *In the case of an isotropic polytrope* (1.2.3) *with polytropic exponent* $k = 1$*, the functions* G_L^{ref} *and* H_L^{ref} *defined in* (A.3.102) *and* (A.3.103)*, respectively, are positive on* $]r_-(E_0, L), r_L[$ *for* $0 < L < L_{\max}$*.*

As an aside, we note that we have also numerically analysed the limits of the partial derivatives $\partial_E T$ and $\partial_L T$ in the near circular regime, i.e., the limits of $\partial_E T(E, L)$ and $\partial_L T(E, L)$ as $(E, L) \to (E_{L^*}^{\min}, L^*)$ for $0 < L^* \leq L_{\max}$. These limits are explicitly given by the formulae (A.4.17) and (A.4.23) derived in Lemmas A.4.6 and A.4.8, respectively. It turned out that for each of the (more than 1000) values of L^* we considered, $\lim_{(E,L)\to(E_{L^*}^{\min}, L^*)} \partial_E T(E, L)$ is positive and $\lim_{(E,L)\to(E_{L^*}^{\min}, L^*)} \partial_L T(E, L)$ is negative. This behaviour is just as expected in the light of the above observation.

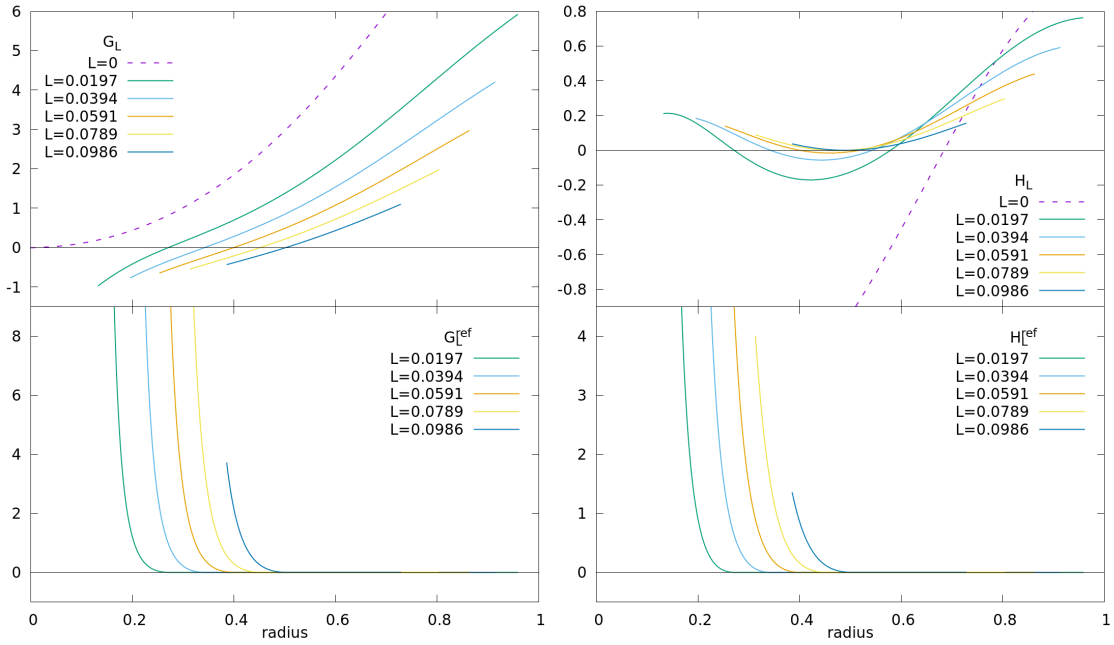

Figure 8.2.4: The two top panels show the functions G_L and H_L defined in (A.3.33) and (A.3.64), respectively, on $[r_-(E_0, L), r_+(E_0, L)]$ for some values of $L \in [0, L_{\max}[$ for the isotropic polytropic steady state $k = 1 = R_{\max}$. In the case $L = 0$ we replace Ψ_L with U_0 in the definitions of G_L and H_L; the resulting functions are depicted by the dashed lines. The bottom panels show the functions G_L^{ref} and H_L^{ref} defined in (A.3.102) and (A.3.103), respectively, on $[r_-(E_0, L), r_L[$ for some values of $L \in]0, L_{\max}[$.

Isotropic Polytropic Steady States

Let us next analyse the period function associated to general isotropic polytropes (1.2.3). As before, we consider the polytropic exponents $0 \leq k \leq 3.2$ and always choose the parameter $\kappa > 0$ s.t. $R_{\max} = 1$ for the resulting steady states. The values of the period function T on the (E, L)-support $\overline{\mathbb{D}}_0$ for a few isotropic polytropes are shown in Figure 8.2.5; recall Figure 8.2.2 for the same plot with polytropic exponent $k = 1$. At first glance, the shape of $\mathbb{D}_0$ and the behaviour of the period function on this set appears to be qualitatively the same for all isotropic polytropes. Nevertheless, let us discuss in detail the similarities and differences for different polytropic exponents k.

Firstly, the maximum of the period function is always attained at $(E_0, 0)$. This is already indicated by Figure 8.2.5, where the point $(E_0, 0)$ corresponds to the bottom right corner of each plot. We have also checked this finding by scanning through all the T-values computed and by considering more polytropic exponents than in Figure 8.2.5. Hence, Observation 8.2.1 seems to hold for general isotropic polytropes.

Observation 8.2.4 (Maximum of T for General Isotropic Polytropes)**.** *In the case of an isotropic polytrope* (1.2.3) *with polytropic exponent* $0 \leq k \leq 3.2$*, the maximum of the period function* T *on the* (E, L)*-support* $\overline{\mathbb{D}}_0$ *of the steady state is attained at the maximal energy* E_0 *and the minimal* L*-value* $L_0 = 0$*, i.e.,* (8.2.3) *holds. In addition, this always seems to be the only point where the maximal period is attained.*

The maximal and minimal values of T on $\overline{\mathbb{D}}_0$ for the different polytropic exponents are shown in Figure 8.2.6; they will become important in the following section.

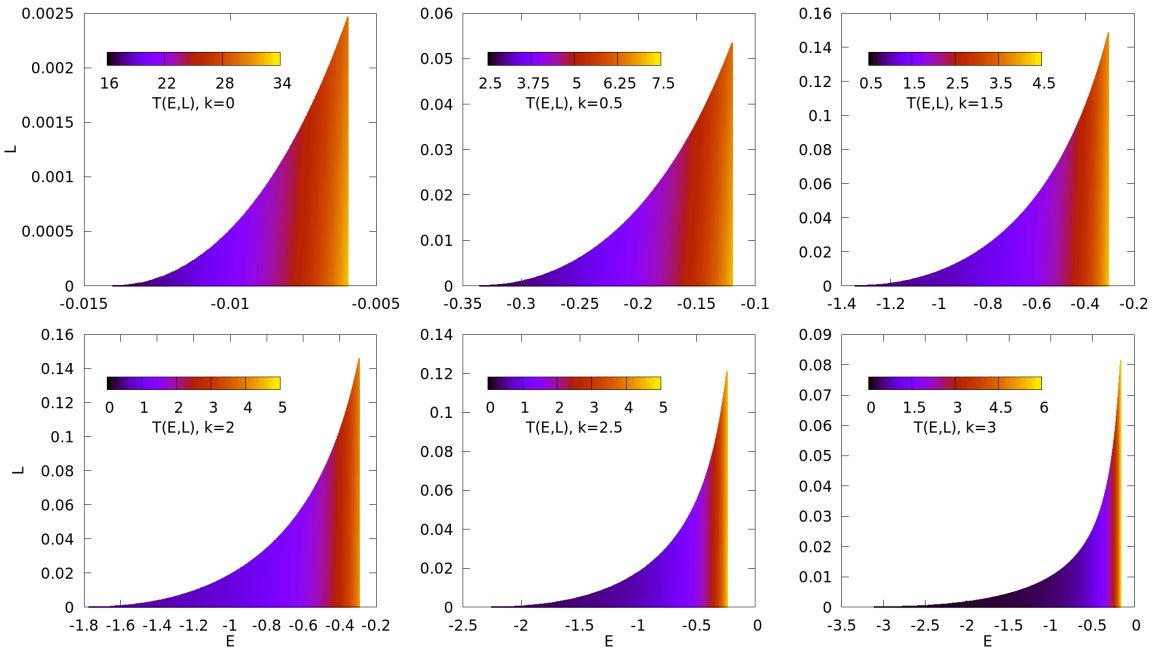

Figure 8.2.5: The (E, L)-supports $\overline{\mathbb{D}}_0$ of isotropic polytropes with polytropic exponents $k \in \{0, \frac{1}{2}, \frac{3}{2}, 2, \frac{5}{2}, 3\}$ and $R_{\max} = 1$ as well as values of the associated period functions T (colour gradient) attained on these sets.

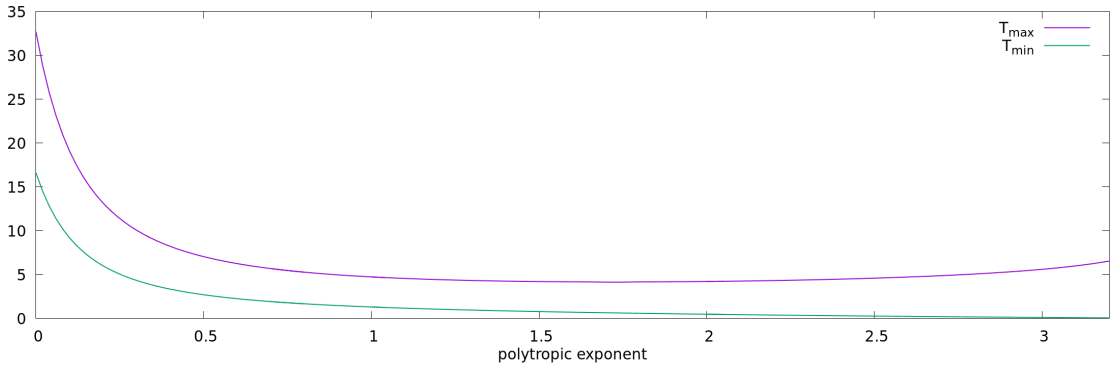

Figure 8.2.6: The maximal and minimal values of the period function T on the (E, L)-support $\mathbb{D}_0$, i.e., $T_{\max} = \sup_{\mathbb{D}_0}(T)$ and $T_{\min} = \inf_{\mathbb{D}_0}(T)$, for isotropic polytropes with $R_{\max} = 1$ as a function of the polytropic exponent $k \in [0, 3.2]$.

Secondly, regarding the monotonicity of the period function, we find that T is again always increasing in E, i.e., $T(\cdot, L)$ is increasing on $[E_L^{\min}, E_0]$ for any $0 \leq L < L_{\max}$. This can be seen quite clearly in Figure 8.2.5, but we have also checked it for several polytropic exponents $0 \leq k \leq 3.2$ in the same way as in the case $k = 1 = R_{\max}$ above. This monotonicity property is further supported by the observation that the function G_L^{ref} is always positive on $]r_-(E_0, L), r_L[$ for $0 < L < L_{\max}$. In the case of the polytropic exponent $k = 3$, this will be illustrated below in Figure 8.2.8 below. The monotonicity of the period function w.r.t. L is more diverse: For not too large values of the polytropic exponent k, up to about 2.35, the period function is decreasing in L, i.e., $T(E, \cdot)$ is decreasing on $[0, L_{\max}(E)]$ for $U_0(0) < E \leq E_0$. We have checked this finding in the same way as the E-monotonicity above, and also observed that the function H_L^{ref} is positive on $]r_-(E_0, L), r_L[$ for $0 < L < L_{\max}$. For larger polytropic exponents, however, the period function is no longer

monotonic w.r.t. L.[182] As this qualitative difference is not well visible in Figure 8.2.5, we depict $T(E_0, \cdot)$ in the case of the polytropic exponent $k = 3$ in Figure 8.2.7. This finding is

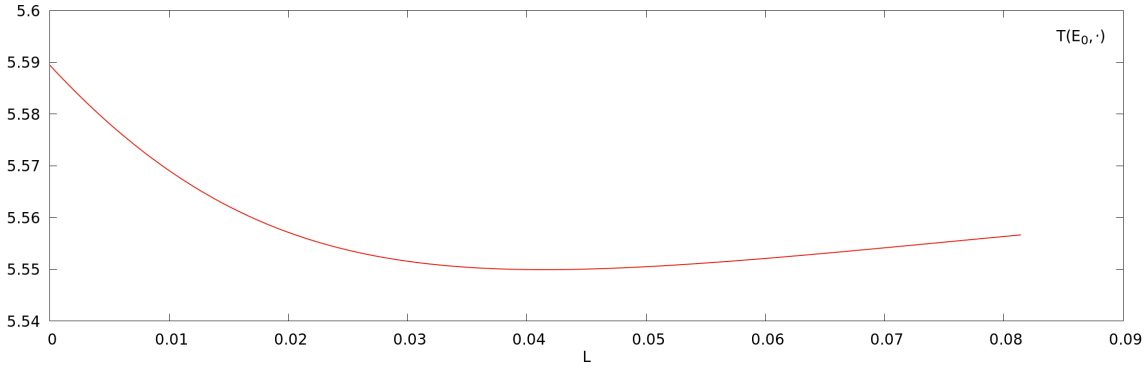

Figure 8.2.7: $T(E_0, \cdot)$ on $[0, L_{\max}]$ for the isotropic polytrope with $k = 3$ and $R_{\max} = 1$.

also supported by the observation that the function H_L^{ref} is no longer positive for all values of $0 < L < L_{\max}$. This can be seen from Figure 8.2.8, where we plot H_L^{ref} and G_L^{ref} for some values of L in the case of the polytropic exponent $k = 3$.

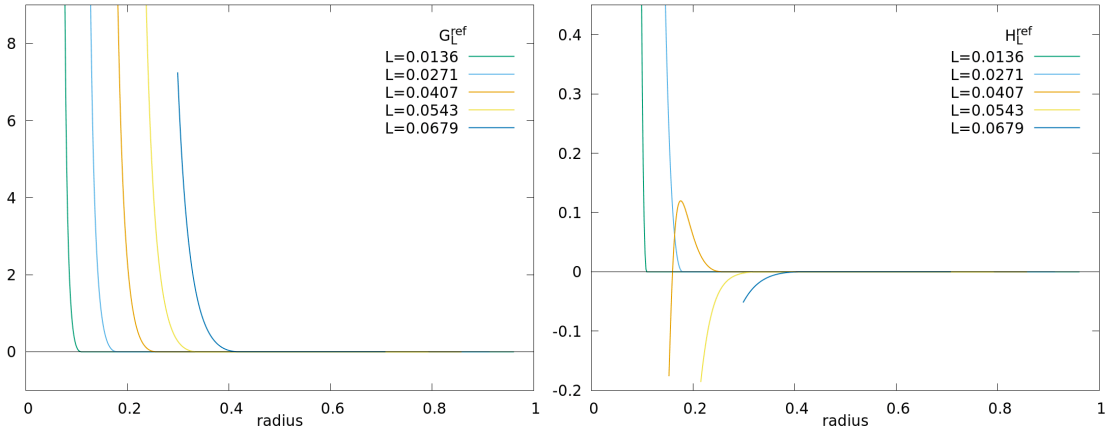

Figure 8.2.8: The functions G_L^{ref} and H_L^{ref} defined in (A.3.102) and (A.3.103), respectively, on $[r_-(E_0, L), r_L[$ for some $L \in]0, L_{\max}[$ for the isotropic polytrope with $k = 3$ and $R_{\max} = 1$.

Figure 8.2.8 also reveals two further insights: Firstly, we see that H_L^{ref} is negative on the entire radial domain $]r_-(E_0, L), r_L[$ for large[183] values of L. By Lemma A.3.22, this implies $\partial_L T(E, L) > 0$ for such values of L and every $E_L^{\min} < E < E_0$. Secondly, it should be noted that the positivity of H_L^{ref} gets lost only for not too small values of L. For small values of L, H_L^{ref} is positive. This is both consistent with Figure 8.2.7, where we see that $T(E_0, \cdot)$ is only non-decreasing for not too small values of L. The period function being decreasing in L for small values of L is also important for the fact that the maximum of T is attained at $(E_0, 0)$, recall Observation 8.2.4. Let us summarise our findings regarding the monotonicity of T.

[182] We have not invested much effort in precisely determining the threshold polytropic exponent at which the L-monotonicity of T gets lost. Our simulations merely show that the L-monotonicity holds for polytropic exponents $k \leq 2.35$, while it does not hold for $k \geq 2.4$.

[183] Here, an L-value being large refers to its relative position within the L-support $[0, L_{\max}]$ of the steady state.

Observation 8.2.5 (T-Monotonicity for General Isotropic Polytropes)**.** *In the case of an isotropic polytropic steady state* (1.2.3) *with polytropic exponent* $0 \leq k \leq 3.2$*, the period function* T *is increasing in* E *on the* (E, L)*-support* $\mathbb{D}_0$ *of the steady state. Moreover, the function* G_L^{ref} *defined in* (A.3.102) *is positive on* $]r_-(E_0, L), r_L[$ *for* $0 < L < L_{\max}$*.*

If the polytropic exponent is not too large (smaller than about 2.35*), the period function is decreasing in* L *on the* (E, L)*-support* $\mathbb{D}_0$ *of the steady state, and the function* H_L^{ref} *defined in* (A.3.103) *is positive on* $]r_-(E_0, L), r_L[$ *for* $0 < L < L_{\max}$*. For larger polytropic exponents, the period function is not monotonic in* L*.*

King Models

We next analyse the period function associated to the King models (1.2.4). Here, we choose the parameter κ in the range $0 < \kappa \leq 7.5$. The reason for this is that the mass density ρ_0 attains very large values near the radial origin $r = 0$ for large values of κ, recall Figure 8.1.5. This makes the computation of the particle motions rather difficult numerically. One way in which this problem manifests itself is as follows: By (A.4.4) and (A.4.11), large values of $\rho_0(0)$ lead to small values of the period function $T(E, L)$ in the near circular regime $E = E_L^{\min}$ for small L. Since $T(E, L)$ can only be determined numerically as a multiple of the time step size δt, computing such small periods is prone to numerical errors. In fact, we also applied our program to King models with larger values of κ, but some curious effects occur there. Whether these are real or due to these numerical difficulties, we do not feel able to confidently decide here.

Anyway, the values of the period function on the (E, L)-support $\overline{\mathbb{D}}_0$ for some values of $0 < \kappa \leq 7.5$ are depicted in Figure 8.2.9.

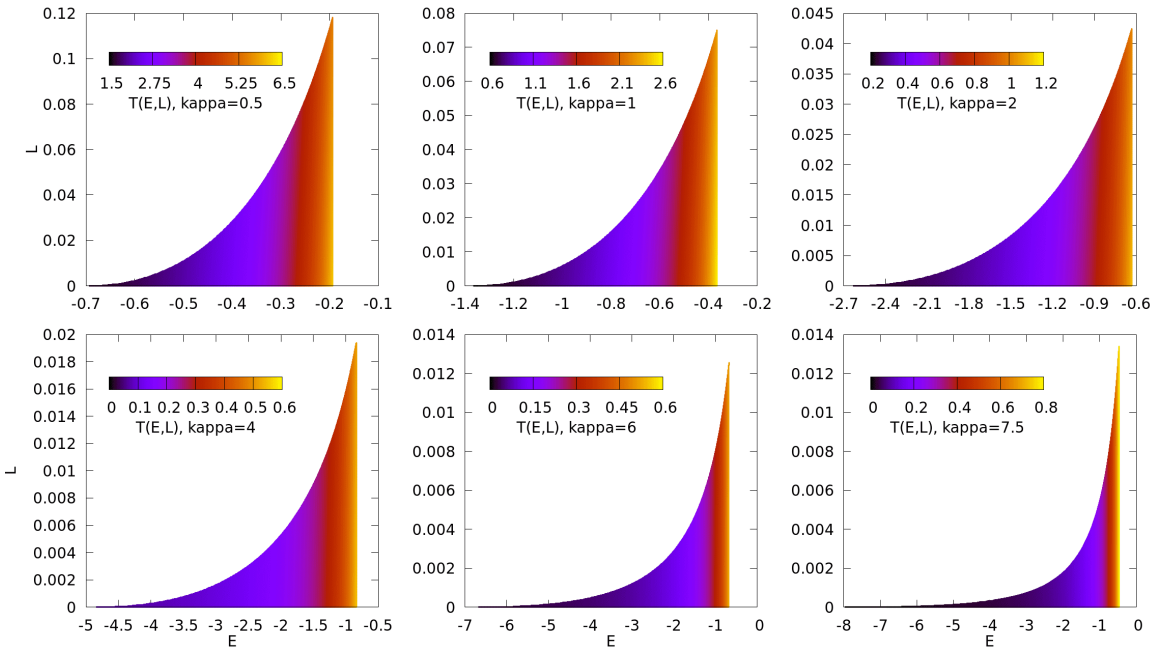

Figure 8.2.9: The (E, L)-supports $\overline{\mathbb{D}}_0$ of King models with $\kappa \in \{\frac{1}{2}, 1, 2, 4, 6, 7.5\}$ and values of the respective period functions T (colour gradient) attained on these sets.

The behaviour of the period function for the King models is, in fact, very similar to the isotropic polytropic case. We analysed King models with more than 100 κ-values $\in]0, 7.5]$ and observed the following.

Observation 8.2.6 (Properties of T for King Models)**.** *In the case of a King model* (1.2.4) *with parameter* $0 < \kappa \leq 7.5$*, the maximum of the period function* T *on the* (E, L)*-support* $\overline{\mathbb{D}}_0$ *of the steady state is always attained at* $(E_0, 0)$*, i.e.,* (8.2.3) *holds.*

Moreover, T *is increasing in* E *on* $\mathbb{D}_0$*, and the function* G_L^{ref} *defined in* (A.3.102) *is positive on* $]r_-(E_0, L), r_L[$ *for* $0 < L < L_{\max}$*.*

For not too large values of κ *(up to about* 5.5*), the period function is decreasing in* L *on the* (E, L)*-support* $\mathbb{D}_0$ *of the steady state, and the function* H_L^{ref} *defined in* (A.3.103) *is positive on* $]r_-(E_0, L), r_L[$ *for* $0 < L < L_{\max}$*. For larger values of* κ*, the period function is not monotonic in* L*.*

Anisotropic Polytropes Including Polytropic Shells

The next (and last) class of steady states examined in this section are anisotropic polytropes (1.2.5). We always choose $\kappa = 1$ here; recall that the scaling laws from Appendix B do not apply in the case $L_0 > 0$.

We first consider the polytropic exponents $k = 1 = \ell$. As shown in Remark A.4.5, the period function T is unbounded on $\mathbb{D}_0$ in the case $L_0 = 0$ since $\lim_{\mathbb{A}_0 \ni (E,L) \to (U_0(0),0)} T(E, L) = \infty$. This fact is indicated by the plot in the left panel of Figure 8.2.10, where $(U_0(0), 0)$ is the bottom left corner and bright colours correspond to large values of T. If we now choose a positive but very small value for L_0, the period function is bounded on $\mathbb{D}_0$ by Proposition A.0.1 (a), but its maximum on $\overline{\mathbb{D}}_0$ is still attained at $(E_{L_0}^{\min}, L_0)$. For instance, this is the case when choosing $L_0 = \frac{1}{1000}$; the values of the period function on $\overline{\mathbb{D}}_0$ in this situation are depicted in the right panel of Figure 8.2.10.

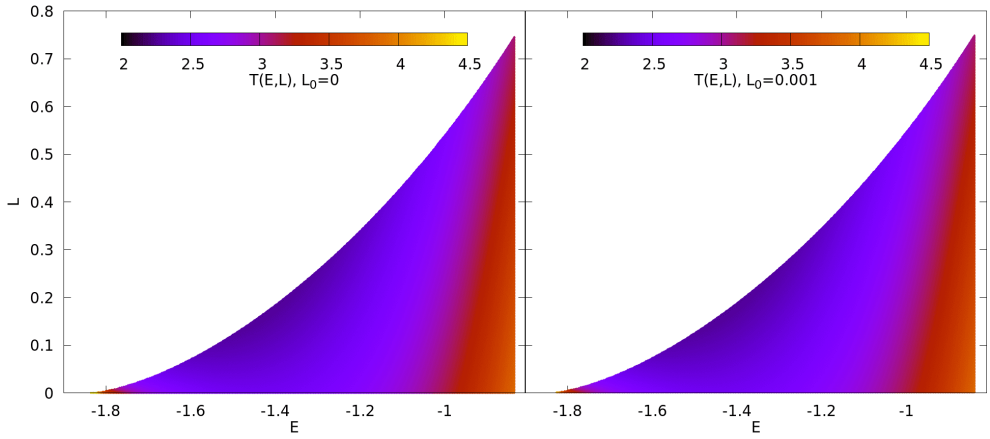

Figure 8.2.10: The (E, L)-supports $\mathbb{D}_0$ of polytropic steady states with polytropic exponents $k = 1 = \ell$ and parameters $\kappa = 1$ and $L_0 \in \{0, \frac{1}{1000}\}$. The colour gradients depict values of the respective period functions attained on these sets.

Although we have only studied this behaviour for one choice of polytropic exponents and one value of κ, it is very plausible that it occurs generally for polytropes with $\ell > 0$ since steady states ought to depend continuously on the parameter L_0.

Observation 8.2.7 (Polytropes with T-Maximum not at (E_0, L_0))**.** *For any polytrope* (1.2.5) *with polytropic exponents* $k, \ell > 0$ *satisfying* $k < 3\ell + \frac{7}{2}$ *and sufficiently small* $L_0 > 0$*, the maximum of the period function* T *on* $\overline{\mathbb{D}}_0$ *is not attained at* (E_0, L_0)*, but at* $(E_{L_0}^{\min}, L_0)$*.*

It should not be too hard to prove this statement rigorously by considering the limit $L_0 \to 0$ and arguing similarly to Section 6.2.1. Anyway, the take-home message of the above

observation is that we cannot expect the maximum of T on $\overline{\mathbb{D}}_0$ to be attained at (E_0, L_0) in general.

We next choose the polytropic exponents $k = \frac{1}{4}$ and $\ell = -\frac{1}{4}$. This case is qualitatively different from the one above because ℓ is now negative. Analysing where T attains its maximum on $\overline{\mathbb{D}}_0$ in this situation is important in the light of Theorem 5.4.1. When choosing the parameter L_0 within the set $\left\{10^{j/2} \mid j \in \{-10, \dots, 2\}\right\}$ (and again $\kappa = 1$), the behaviour of T is qualitatively the same as for isotropic polytropes. In particular, the maximum of the period function on $\mathbb{D}_0$ is always attained at (E_0, L_0). This observation is also (partially) included in [62, Rem. 8.16]. We have confirmed the same properties for more polytropes with $\ell < 0$, cf. below, and always verified it in the same way as described in the context of isotropic polytropes.

Observation 8.2.8 (Examples for Theorem 5.4.1)**.** *For any polytropic steady state with exponents* $(k, \ell) \in \{(\frac{1}{10}, -\frac{2}{5}), (\frac{1}{10}, -\frac{1}{4}), (\frac{1}{10}, -\frac{1}{10}), (\frac{1}{4}, -\frac{2}{5}), (\frac{1}{4}, -\frac{1}{4}), (\frac{2}{5}, -\frac{2}{5})\}$ *as well as parameters* $\kappa = 1$ *and* $L_0 \in \left\{10^{j/2} \mid j \in \{-10, \dots, 2\}\right\}$*, the period function attains its maximum on* $\overline{\mathbb{D}}_0$ *at* (E_0, L_0)*. Moreover, the period function is always increasing in* E*, but not always monotonic w.r.t.* L *on* $\mathbb{D}_0$*.*

This observation hence provides explicit examples of steady states satisfying the assumptions of Theorem 5.4.1, see also Remark 5.4.2 (a). It should be noted that the chosen polytropic exponents and values of L_0 and κ are not special, but serve only as exemplary choices. We expect that the properties from the observation above also hold for more general choices of $k > 0$, $\ell < 0$, $\kappa > 0$, and $L_0 > 0$ satisfying (5.4.1), since we have not yet encountered any such parameters were it is not satisfied.

Further General Observations

We now collect some additional, less central observations regarding the period function that we made for all steady states encountered during the above analysis. The first one concerns the position at which the period function attains its maximum on $\overline{\mathbb{D}}_0$. Although we have seen that this position is not necessarily (E_0, L_0), we still observed the following.

Observation 8.2.9 (T-Maximiser is Always on Boundary)**.** *For every steady state considered above, the maximum of the period function* T *on the steady state support* $\overline{\mathbb{D}}_0$ *is attained on the boundary of* $\mathbb{D}_0$*.*

We checked this property by scanning through all the T-values computed for each steady state. The above observation shows that it is indeed unclear whether the assumption of Corollary 5.4.3 holds for any steady state.

The second observation concerns the level sets of the period function on $\mathbb{D}_0$. We investigated these sets by analysing the plots of T on $\mathbb{D}_0$ from Figures 8.2.2, 8.2.5, 8.2.9, and 8.2.10. The level sets of $T\big|_{\mathbb{D}_0}$ always seem to be a curve in the (E, L)-plane or a finite union of such curves. In particular, we never saw any evidence that the period function is constant on some non-empty open subset of $\mathbb{D}_0$. On this basis, we feel confident enough to state the following observation, although it would of course be very difficult to numerically verify it in detail.

Observation 8.2.10 (Level Sets of T)**.** *For every steady state considered above, all level sets of the period function* T *on the steady state support* $\mathbb{D}_0$ *are sets of measure zero.*

By Lemma 4.3.22, this shows that the squared transport operator $-\mathcal{T}^2\big|_{\mathcal{H}} \colon \mathrm{D}(\mathcal{T}^2) \cap \mathcal{H} \to \mathcal{H}$ does not possess any eigenvalues for the steady states considered here.

Kunze's Criterion

As a prelude to the numerical analysis of the linearised Vlasov-Poisson system – which will be the subject of the following section – we now examine the validity of Kunze's criterion from Lemma 4.5.19 numerically. To check the criterion, the maximum of the period function T on $\overline{\mathbb{D}_0}$ must be compared with (the maximum of) a macroscopic function associated to the steady state. If Kunze's criterion was satisfied, we would conclude the presence of an oscillatory mode around the steady state. Since we always computed the maximal value of the period function on $\overline{\mathbb{D}_0}$ anyway, we checked the validity of Kunze's criterion for all steady states encountered above.

The pleasing result is that for some isotropic steady states, Kunze's criterion is indeed satisfied. This is illustrated in Figure 8.2.11, where we depict the left-hand and right-hand sides of Kunze's criterion (4.5.53) for isotropic polytropes with different polytropic exponents $k \geq 0$ and $R_{\max} = 1$.

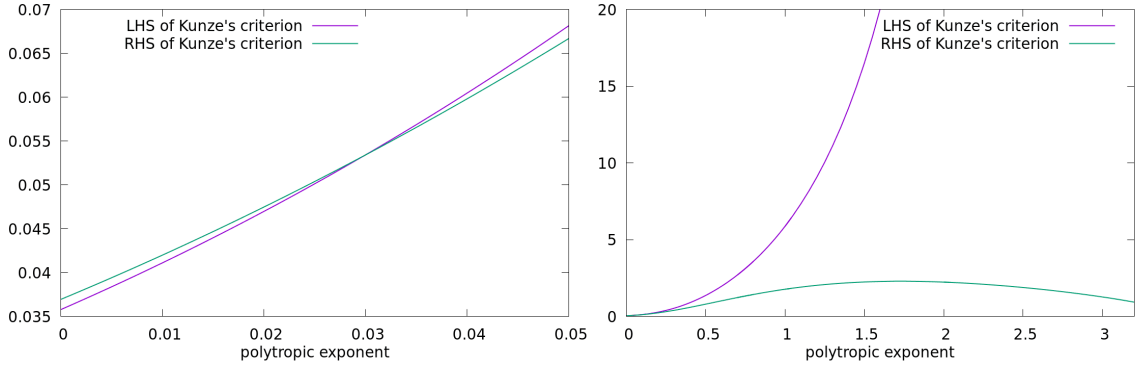

Figure 8.2.11: The left-hand ("LHS": $\sup_{r\in]0,1]} \frac{U_0'(r)}{r} = \frac{4\pi}{3}\rho_0(0)$) and right-hand ("RHS": $\frac{4\pi^2}{\sup^2_{\mathbb{D}_0}(T)}$) sides of Kunze's criterion (4.5.53) for the isotropic polytropes with different polytropic exponents k and parameter $\kappa > 0$ chosen s.t. $R_{\max} = 1$. For better visibility, the left panel shows the plot restricted to small values of k.

The criterion is satisfied if the left-hand side is smaller than the right-hand side, which is evidently the case for very small polytropic exponents. By Appendix B, we can generalise this finding to all values of $\kappa > 0$.

Observation 8.2.11 (Kunze's Criterion for Isotropic Polytropes)**.** *For isotropic polytropes* (1.2.3) *with very small polytropic exponents $k > 0$ (smaller than about* 0.03*), Kunze's criterion from Lemma 4.5.19 is satisfied.*

We will later discuss how this important observation could be proven, cf. Chapter 9.

For the King models, Kunze's criterion never seems to be satisfied.

For anisotropic polytropes (1.2.5), there are numerous examples of steady states satisfying Kunze's criterion. A natural first class to check the criterion are the polytropes with $L_0 > 0$ and $\ell < 0$ for which we have already shown the existence of oscillatory modes via Theorem 5.4.1 and Observation 8.2.8. Indeed, if $L_0 > 0$ is not too small, Kunze's criterion is satisfied for all of the steady states considered in Observation 8.2.8. For instance, for the polytropic exponents $k = \frac{1}{4}$ and $\ell = -\frac{1}{4}$ as well as $\kappa = 1$, the resulting steady states satisfy Kunze's criterion for $L_0 \geq \frac{1}{1000}$. More surprisingly, the same behaviour also occurs when choosing $(k, \ell) = (1, 0)$ or $(k, \ell) = (1, 1)$. For these exponents, Theorem 5.4.1 does not apply, but Kunze's criterion is nonetheless satisfied if $L_0 > 0$ is not too small large. More precisely, for both polytropic exponent pairs $(k, \ell) \in \{(1, 0), (1, 1)\}$, choosing $L_0 \geq \frac{1}{100}$

yields steady states satisfying Kunze's criterion. These polytropic exponents (and $\kappa = 1$) are not special but only used as examples. We expect that the same behaviour also occurs for more general polytropes.

Observation 8.2.12 (Kunze's Criterion for Anisotropic Polytropes)**.** *The polytropic steady states with parameter $\kappa = 1$ and polytropic exponents $(k, \ell) \in \{(1,0), (1,1), (\frac{1}{10}, -\frac{2}{5}), (\frac{1}{10}, -\frac{1}{4}), (\frac{1}{10}, -\frac{1}{10}), (\frac{1}{4}, -\frac{2}{5}), (\frac{1}{4}, -\frac{1}{4}), (\frac{2}{5}, -\frac{2}{5})\}$ satisfy Kunze's criterion if $L_0 > 0$ is not too small.*

8.3 Numerics of the Linearised Vlasov-Poisson System

In this section we numerically analyse the linearised Vlasov-Poisson system. The underlying steady states are the same as studied above, recall Sections 2.2 and 8.1. Let us emphasise that we are not considering the linearised system because it is easier to simulate numerically than the non-linearised system. Although one might hope so, it is not easier from a numerics point of view; this has already been noted in [93, Sc. 3.4] and we will also see it here. The reason for considering the linearised system is to align the observations made here with the mathematical results of this thesis, which (only) concern the linearised system. For instance, analysing solutions of the linearised Vlasov-Poisson system will allow us to draw conclusions about the central object of this thesis: The spectrum of the linearised operator $\mathcal{L}$. The question of what effects occur when transitioning from the linearised to the non-linearised system will be discussed in the next section.

The linearised Vlasov-Poisson system has rarely been investigated numerically in the literature before, with numerical analyses usually directly focused on the actual non-linearised system. Previous numerical investigation of the linearised system will be referenced below. Our numerical investigation is the first in spherical symmetry for the steady states from Section 2.2. Moreover, it is more comprehensive than previous investigations due to the availability of greater computational resources.

We will only consider here the Eulerian formulation of the linearised Vlasov-Poisson system derived in Section 3.1 because it is the one most commonly used in the literature. A numerical investigation of the linearised Vlasov-Poisson system in a Lagrangian formulation is conducted in [173].

The Numerical Method

For a fixed steady state f_0 as computed in Section 8.1, let us describe how to numerically solve the associated linearised Vlasov-Poisson system. We have adapted the numerical method from that used to simulate the non-linearised Vlasov-Poisson system, which we will discuss in the next section. In particular, the code used for the simulation of the linearised system is based on the ones used in [48, 50], although we have entirely rewritten the code in an object-oriented way. Later we discovered that (essentially) the same method had already been used in the astrophysics literature (albeit in different settings), cf. [93, 112].

In the Eulerian formulation, the linearised Vlasov-Poisson system is given by (3.1.1)–(3.1.3). It is convenient to first rewrite this system, which we will do below through formal calculations. The resulting reformulation will remain of first order, which is more practical for the numerics than the second-order formulation (1.2.8) of the linearised Vlasov-Poisson system.

As before, let (X, V) denote the characteristic flow of the steady state f_0, i.e.,

$(X,V)\colon \mathbb{R}\times\mathbb{R}^3\times\mathbb{R}^3 \to \mathbb{R}^3\times\mathbb{R}^3$ solves

$$\dot{X} = V, \quad \dot{V} = -\partial_x U_0(X), \qquad (X,V)(0,x,v) = (x,v). \tag{8.3.1}$$

By (3.1.1), for every spherically symmetric solution $f = f(t,x,v)$ of the linearised Vlasov-Poisson system we obtain

$$\begin{aligned}\partial_s[f(s,(X,V)(s,x,v))] &= \partial_t f(s,(X,V)(s,x,v)) + \mathcal{T} f(s,(X,V)(s,x,v)) = \\ &= \varphi'(E(x,v),L(x,v))\, W(s,x,v)\, U_f'(s,R(s,x,v)),\end{aligned} \tag{8.3.2}$$

where we have rewritten the response term as in Section 3.1 and used that E and L are constant along the characteristic flow, cf. Lemma 2.2.1. We also introduced the following notations, which are natural in the light of Remark 2.1.2 (b):

$$R(s,x,v) \coloneqq |X(s,x,v)|, \qquad W(s,x,v) \coloneqq \frac{X(s,x,v)\cdot V(s,x,v)}{R(s,x,v)}. \tag{8.3.3}$$

Integrating (8.3.2) w.r.t. the proper time s of the characteristic flow leads to

$$f(t,(X,V)(t,x,v)) = f(0,x,v) + \varphi'(E(x,v),L(x,v)) \int_0^t W(s,x,v)\, U_f'(s,R(s,x,v))\,\mathrm{d}s \tag{8.3.4}$$

for $(t,x,v)\in\mathbb{R}\times\mathbb{R}^3\times\mathbb{R}^3$. This equation can be interpreted as a new formulation of the linearised Vlasov-Poisson system. The existence theory for the system in this very form (for isotropic steady states) is studied in [15], and the same formulation is also used in [93, 112].

In order to solve (8.3.4) numerically, we have to compute the steady state characteristics (X,V). We have discussed in the previous section how this can be done. In order to cope with the second term on the right-hand side of (8.3.4), we use the following approximation of (8.3.4) for $0 < t \ll 1$:

$$f(t,(X,V)(t,x,v)) \approx f(0,x,v) + \varphi'(E(x,v),L(x,v)) \int_0^t W(s,x,v)\, U_f'(0,R(s,x,v))\,\mathrm{d}s. \tag{8.3.5}$$

Based on the steady state characteristics and $f(0)$, this approximation allows us to compute $f(t)$ for small values of t. Iterating this process yields an approximation of $f(T)$ also for larger $T > 0$.

We implement this procedure using a *particle-in-cell scheme*. As mentioned above and as we shall see in the following section, this method is commonly used to simulate the (non-linearised) Vlasov-Poisson system as well as related systems. The key idea is to split the phase space support of the steady state f_0 into finitely many distinct cells. We do this by first setting up an equidistant radial grid of step size δr. At each fixed radius, the momentum space is segmentated using an equidistant grid in each of the variables u and α, recall Remark 2.1.2 (f). Using (r,u,α)-coordinates for the initial setup of the cells has proven beneficial in previous numerical investigations.[184] We then place a *(numerical) particle* into the centre[185] of each cell as a representative of the contributions of its cell. For each particle we save its position in (r,w,L)-coordinates, the volume of its cell, and the value of the initial distribution $f(0,r,w,L)$. These particles represent the initial phase space density $f(0)$; note that $\operatorname{supp}(f(0)) \subset \operatorname{supp}(f_0)$. In order to compute the corresponding mass density $\rho_f(0)$,

[184] More precisely, using an equidistant (r,u,α)-grid for setting up the cells seems to yield a better approximation of a given initial distribution $f(0)$ compared to using (r,w,L)-coordinates (or other coordinates).

[185] The centre of the cell is again taken in (r,u,α)-coordinates, in which each cell is just a cuboid.

we sum over the contributions of all particles in the momentum variables and interpolate linearly in the radius. The associated local mass $m_f(0)$ and gravitational potential $U_f(0)$ can then be obtained by radial integration according to (2.1.10). When computing the local mass $m(0,r) = 4\pi \int_0^r s^2 \rho(0,s)\,\mathrm{d}s$, we use Simpson's rule to take into account the order of the integrand near the spatial origin $r = 0$. For these steps we use the same radial grid as for setting up the cells. Once these macroscopic quantities are computed,[186] we are ready to propagate the particles so that they represent the phase space distribution $f(\delta t)$ at the next time step $\delta t > 0$. The new positions of the particles are given by evolving the old positions via the characteristic flow of the steady state. The f-values are updated according to (8.3.5); the integral on the right-hand side containing $U_f'(0)$ is calculated during the computation of the characteristic flow of the steady state. In fact, we do not use (8.3.5) as it stands which would correspond to the Euler method – instead, we employ a suitable adaption of RK4 which is more accurate numerically. The volumes of the cells associated to the particles remain constant during the particle evolution as the characteristic flow of the steady state is measure preserving [143, Lemma 1.2]. Repeating this entire process results in a simulation of the linearised Vlasov-Poisson system.

For our numerical simulations we choose the radial step size δr in the order of magnitude 10^{-3} to 10^{-4} in the case of a steady state with $R_{\max} = 1$. The precise choice of this parameter depends on the underlying steady state; for instance, we use a finer grid for steady states with steeper mass densities ρ_0. The momentum step sizes for u and α are chosen s.t. we arrive at a total of 10^7 to 10^8 numerical particles; we always make sure to use at least 10^7 particles. Again, the suitable number of numerical particles depends on the underlying steady state (and the computational resources available). The time step size δt is chosen to be of a similar magnitude as δr. In total, simulating the linearised Vlasov-Poisson system with such parameters to a terminal time of, say, $t = 50$ requires more than a trillion individual particle propagation steps. To be able to perform such simulations within a reasonable computation time, we parallelised the particle propagation as well as various other parts of the algorithm like the computation of ρ. Fortunately, the particle-in-cell scheme fits very well with parallel computing. We use the Pthreads API in `C++` to implement a shared-memory parallelisation on a CPU based on [81]; a GPU-based parallelisation of a related particle-in-cell scheme was developed in [80].

In order to evaluate the accuracy of the simulation, we consider several conserved quantities of the linearised Vlasov-Poisson system and monitor whether/the degree to which they remain constant during the numerical simulation. The first conserved quantity is the *free energy*. For suitable $f\colon \Omega_0 \to \mathbb{R}$, it is given by

$$E^{\mathrm{free}}(f) \coloneqq E^{\mathrm{free}}_{\mathrm{kin}}(f) + E^{\mathrm{free}}_{\mathrm{pot}}(f), \tag{8.3.6}$$

where the kinetic and potential parts are defined as

$$E^{\mathrm{free}}_{\mathrm{kin}}(f) \coloneqq -\frac{1}{2}\int_{\Omega_0} \frac{f(x,v)^2}{\varphi'(E,L)}\,\mathrm{d}(x,v) = \frac{1}{2}\,\|f\|_H^2, \tag{8.3.7}$$

$$E^{\mathrm{free}}_{\mathrm{pot}}(f) \coloneqq \frac{1}{2}\int_{\Omega_0} U_f(x)\,f(x,v)\,\mathrm{d}(x,v) = -\frac{1}{8\pi}\,\|\partial_x U_f\|^2_{L^2(\mathbb{R}^3)}, \tag{8.3.8}$$

respectively. We refer to [15, Sc. 4] for a proof that E^{free} is constant along solutions of the linearised Vlasov-Poisson system. The second conserved quantity results from linearising

[186] We actually only need $U_f'(0,r) = \frac{m_f(0,r)}{r^2}$ to evolve the particles; the potential $U_f(0,r) = -\int_r^\infty U_f'(0,s)\,\mathrm{d}s$ is "only" computed to analyse the solution.

the total energy – which is a conserved quantity of the non-linearised Vlasov-Poisson system, cf. [143, Sc. 1.5] – in the same way as in (3.1.21)–(3.1.22). We refer to it as the *linearised energy*. For f as above, it is of the form

$$E^{\mathrm{lin}}(f) \coloneqq E^{\mathrm{lin}}_{\mathrm{kin}}(f) + E^{\mathrm{lin}}_{\mathrm{pot}}(f) = \int_{\Omega_0} E(x,v)\, f(x,v)\, \mathrm{d}(x,v), \tag{8.3.9}$$

with kinetic and potential parts given by

$$E^{\mathrm{lin}}_{\mathrm{kin}}(f) \coloneqq \frac{1}{2} \int_{\Omega_0} |v|^2 f(x,v)\, \mathrm{d}(x,v), \tag{8.3.10}$$

$$E^{\mathrm{lin}}_{\mathrm{pot}}(f) \coloneqq \int_{\Omega_0} U_0(x)\, f(x,v)\, \mathrm{d}(x,v), \tag{8.3.11}$$

respectively. The third conserved quantity is the *total mass* which is defined as usual:

$$M(f) \coloneqq \int_{\Omega_0} f(x,v)\, \mathrm{d}(x,v). \tag{8.3.12}$$

It is straight-forward to verify that E^{lin} and M are indeed conserved along solutions of the linearised Vlasov-Poisson system. To track the evolution of these quantities, the integrals (8.3.6)–(8.3.12) are computed numerically by adding up the contributions of all particles with the respective weights.

To study and illustrate the behaviour of a solution $t \mapsto f(t)$ of the linearised Vlasov-Poisson system, we track the evolution of each single energy component over time, i.e., we analyse $E^{\mathrm{free}}_{\mathrm{kin}}(f(t))$, $E^{\mathrm{free}}_{\mathrm{pot}}(f(t))$, $E^{\mathrm{lin}}_{\mathrm{kin}}(f(t))$, and $E^{\mathrm{lin}}_{\mathrm{pot}}(f(t))$. We also track the value of the gravitational potential at the spatial origin, i.e.,

$$U_f(t,0) = -\int_0^\infty U_f'(t,r)\, \mathrm{d}r = -\int_0^\infty \frac{m_f(t,r)}{r^2}\, \mathrm{d}r, \tag{8.3.13}$$

as it is a physically motivated indicator for the overall behaviour of f. In addition, we will analyse the values of the macroscopic functions $\rho_f(t)$, $m_f(t)$, and $U_f(t)$ on a fixed radial grid at selected times t.

The Isotropic Polytropic Steady State $k = 1 = R_{\max}$

As in the previous sections, we start the numerical analysis with the isotropic polytropic steady state with polytropic exponent $k = 1$ and parameter $\kappa > 0$ chosen s.t. $R_{\max} = 1$.

We first analyse the solution of the corresponding linearised Vlasov-Poisson system launched by the initial condition $f(0) = w\,\varphi'(E)$. The evolution of the total linearised energy E^{lin} as well as $E^{\mathrm{lin}}_{\mathrm{kin}}$ and $E^{\mathrm{lin}}_{\mathrm{pot}}$ is depicted in Figure 8.3.1.

We clearly observe that the solution $t \mapsto f(t)$ exhibits an oscillatory behaviour. More precisely, for a brief period at the beginning (i.e., at $t = 0$), the solution is partially damped in the sense that the amplitude decreases during the initial oscillations. Afterwards, the oscillation seems undamped. We will analyse quantitative aspects of this oscillation, like its period, in the context of more general isotropic polytropes later. We first want to illustrate that the oscillation is not only visible in the linearised energy components, but in all macroscopic quantities associated to the solution. To see this, we plot the evolutions of the kinetic and potential parts of the free energy as well as the value of the gravitational potential at the spatial origin in Figure 8.3.2. The time evolutions of the mass density ρ_f and the gravitational potential U_f are shown in Figure 8.3.3. In order to make clear that

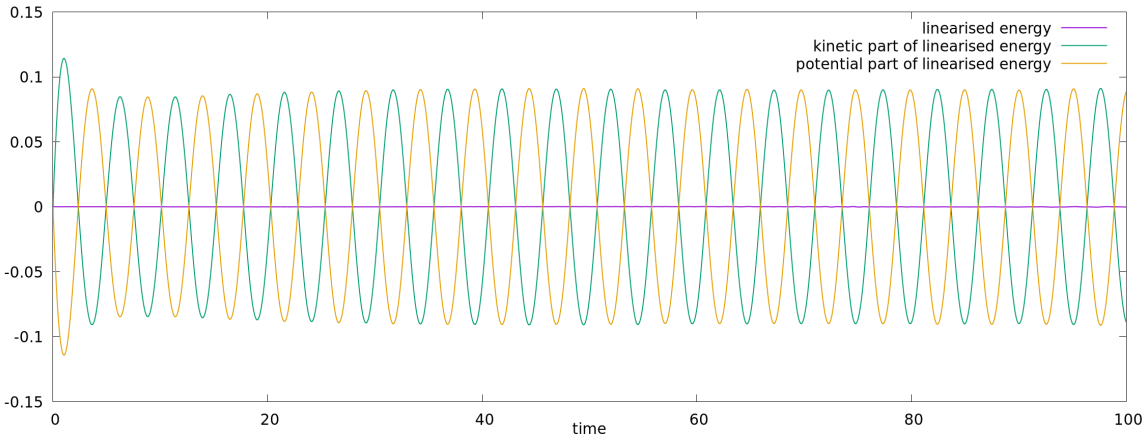

Figure 8.3.1: Evolution of the linearised energy E^{lin} and its kinetic and potential parts $E^{\mathrm{lin}}_{\mathrm{kin}}$ and $E^{\mathrm{lin}}_{\mathrm{pot}}$ (see (8.3.9)–(8.3.11) for the definitions of these quantities) for the solution of the linearised Vlasov-Poisson system launched by the initial condition $w\,\varphi'(E)$. The underlying steady state is the isotropic polytrope with $k = 1$ and $R_{\max} = 1$.

these two macroscopic functions are periodic in time (after the brief initial damping phase), we use an additional visualisation method from [132, Figs. 2 and 4] and plot $(t_1, t_2) \mapsto \|\rho_f(t_1) - \rho_f(t_2)\|_2$ and $(t_1, t_2) \mapsto \|U_f(t_1) - U_f(t_2)\|_2$ in Figure 8.3.4. We see that these differences vanish periodically, meaning that ρ_f and U_f are indeed time-periodic as a whole.

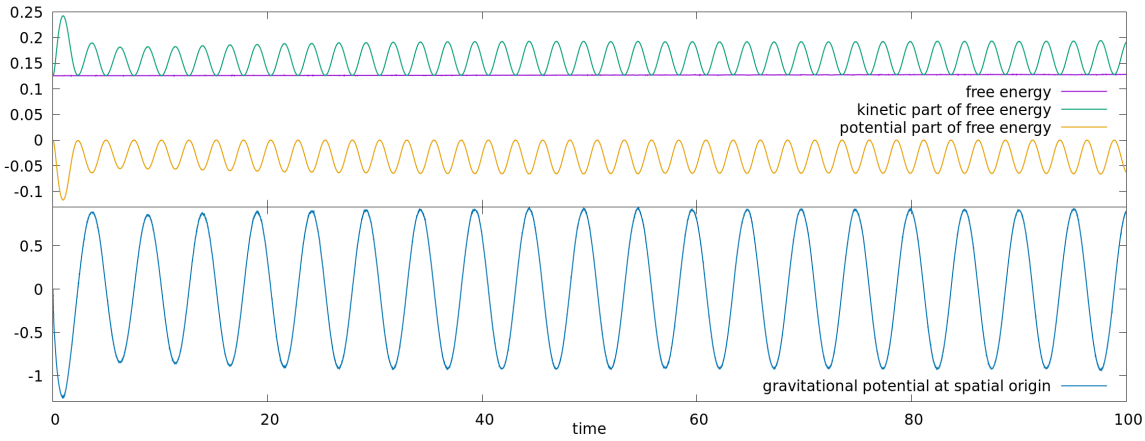

Figure 8.3.2: Evolution of the free energy E^{free} and its kinetic and potential parts $E^{\mathrm{free}}_{\mathrm{kin}}$ and $E^{\mathrm{free}}_{\mathrm{pot}}$ (top panel; see (8.3.6)–(8.3.8) for the definitions of these quantities) as well as the evolution of $U_f(\cdot, 0)$ (bottom panel) for the solution of the linearised Vlasov-Poisson system launched by the initial condition $f(0) = w\,\varphi'(E)$. The underlying steady state is the isotropic polytrope with $k = 1$ and $R_{\max} = 1$.

All these visualisations of the solution show the same qualitative behaviour. In particular, the oscillation period of all quantities is consistent, except for the kinetic and potential parts of the free energy which oscillate with twice the frequency as the other quantities. This phenomenon can be explained by the following two observations: On the one hand, it is suggested by Figure 8.3.3 that the solution changes its sign after half an oscillation period. On the other hand, both components of the free energy are sign-invariant, i.e., $E^{\mathrm{free}}_{\mathrm{kin}}(f) = E^{\mathrm{free}}_{\mathrm{kin}}(-f)$ and $E^{\mathrm{free}}_{\mathrm{pot}}(f) = E^{\mathrm{free}}_{\mathrm{pot}}(-f)$, thus resulting in the doubled frequency

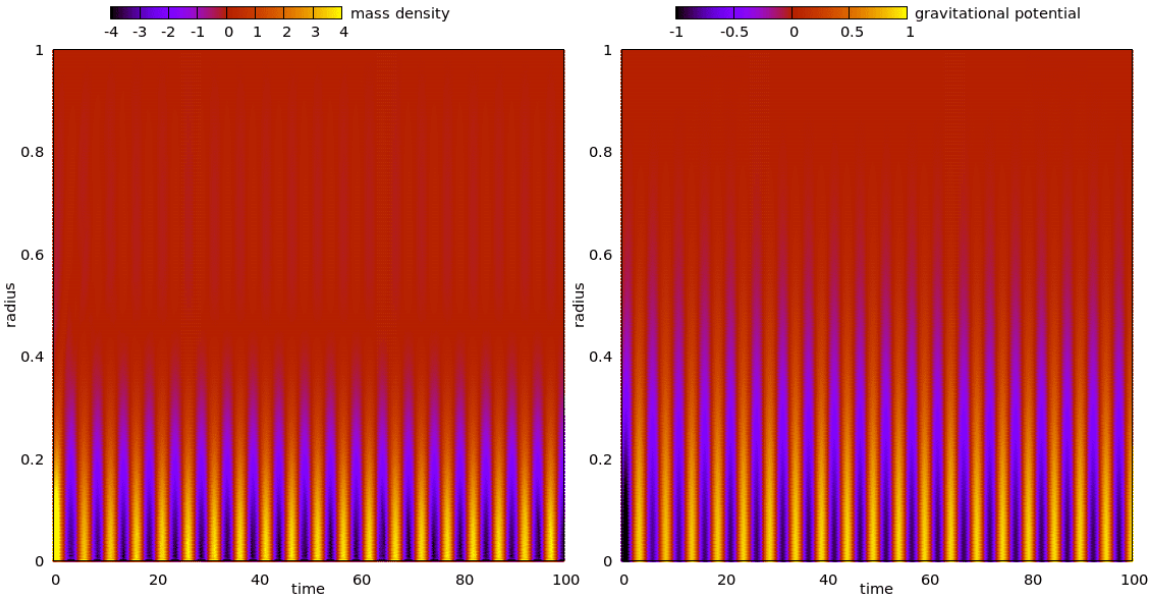

Figure 8.3.3: Values of the mass density $\rho_f = \rho_f(t,r)$ (left panel) and the gravitational potential $U_f = U_f(t,r)$ (right panel) at different time-radius pairs (t,r) for the solution f of the linearised Vlasov-Poisson system launched by the initial condition $f(0) = w\,\varphi'(E)$. The underlying steady state is the isotropic polytrope with $k = 1$ and $R_{\max} = 1$.

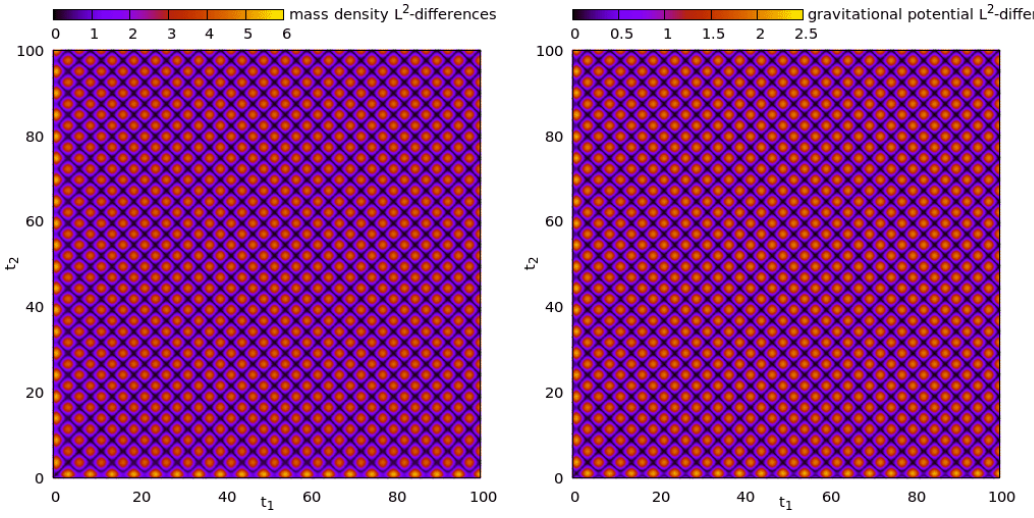

Figure 8.3.4: L^2-differences of the mass density ρ_f (left panel) and the gravitational potential U_f (right panel) at different times, i.e., $\|\rho_f(t_1) - \rho_f(t_2)\|_2$ and $\|U_f(t_1) - U_f(t_2)\|_2$ for different $t_1, t_2 \geq 0$, for the solution f of the linearised Vlasov-Poisson system launched by the initial condition $f(0) = w\,\varphi'(E)$. The underlying steady state is the isotropic polytrope with $k = 1$ and $R_{\max} = 1$.

of $E_{\text{kin}}^{\text{free}}$ and $E_{\text{pot}}^{\text{free}}$. We hence conclude the following.

Observation 8.3.1 (All Macroscopic Quantities Behave Equivalently)**.** *The qualitative behaviour of a solution of the linearised Vlasov-Poisson system can be observed alike in the evolutions of* $E_{\text{kin}}^{\text{lin}}$, $E_{\text{pot}}^{\text{lin}}$, $E_{\text{kin}}^{\text{free}}$, $E_{\text{pot}}^{\text{free}}$, *and* $U_f(\cdot,0)$, *as well as in the evolution of macroscopic functions like* ρ_f *and* U_f.

So far we have only discussed the fact that all quantities associated to a solution of the linearised Vlasov-Poisson system are equivalent in the case of a single solution. We have, however, consistently checked and confirmed this equivalency for all solutions considered throughout this section.

Before considering more general solutions, let us briefly discuss the numerical accuracy of the above simulation by analysing the degree to which the conserved quantities of the linearised Vlasov-Poisson system introduced above are conserved. It is already visible from Figures 8.3.1 and 8.3.2 that the linearised energy and the free energy remain rather unchanged during the evolution. Concretely, until the final time $T = 100$, the absolute value of E^{lin} is always smaller than $2 \cdot 10^{-4}$; notice that the linearised energy vanishes at $t = 0$ because $f(0)$ is odd in w. The relative error of the free energy, i.e., the absolute value of $\frac{E^{\text{free}}(f(t)) - E^{\text{free}}(f(0))}{E^{\text{free}}(f(0))}$, remains smaller than 1%. In addition, the absolute value of the total mass, which also vanishes at $t = 0$, stays smaller than 10^{-3}. We believe that these errors are small enough to allow us to claim that our numerical simulations indeed accurately describe the behaviour of the solutions of the linearised Vlasov-Poisson system. In the remainder of this section, we will not discuss the errors of the conserved quantities in each case, but have always ensured – by appropriately choosing the numerical parameters – that they are of the same order of magnitude as the error values mentioned above.

Let us next analyse solutions launched by other initial conditions. We consider eight different initial conditions which are stated in Table 8.3.1. For the sake of comparison, we have also included the initial condition already used above (Number 5 in Table 8.3.1). The behaviour of the solutions of the linearised Vlasov-Poisson system launched by these initial conditions is depicted in Figure 8.3.5.

Nr.	$f(0) = f(0, r, w, L)$	Nr.	$f(0) = f(0, r, w, L)$
1	$\varphi(E)$	5	$w\,\varphi'(E)$
2	$w\,\varphi(E)$	6	$w^2\,\varphi'(E)$
3	$w^2\,\varphi(E)$	7	$\sqrt{r^2 + w^2}\,\varphi'(E)$
4	$\varphi'(E)$	8	$\chi(E, L)\,\sqrt{r^2 + w^2}\,\varphi'(E)$

Table 8.3.1: Some initial conditions used for the linearised Vlasov-Poisson system. The function $\chi = \chi(E, L)$ contained in the eighth initial condition is a smooth cut-off function which vanishes iff $E - E_L^{\min} \leq \frac{\kappa}{4}$.

We can clearly see from Figure 8.3.5 that the qualitative behaviour of the solution is independent of the initial data. If we compare some solutions in pairs (e.g., Numbers 1 and 5), we see that they are shifted in their "oscillatory phase", i.e., after the initial damping phase. These shiftings are due to different behaviours at the beginning of the evolution, which are to be expected given the different initial conditions. Nonetheless, the oscillation period is identical for all solutions. However, there are differences in the strength of the initial damping phase, i.e., in the difference between the first local extremum of $E_{\text{kin}}^{\text{lin}}$ and the extrema attained later. Let us try to make this behaviour plausible: From a spectral analysis point of view, every initial condition $f(0)$ should be thought of as a sum of the following two parts: The first part is the orthogonal projection of $f(0)$ onto the space of eigenfunctions of the linearised operator, provided such eigenfunctions exist. As discussed earlier, this part causes the undamped oscillations of the solution. The remaining part of $f(0)$ is orthogonal to all eigenfunctions and should hence get damped by the dynamics (on the macroscopic level). How these two parts are weighted with respect to each other naturally depends on the specific initial condition $f(0)$. It should also be noted that, provided that eigenfunctions

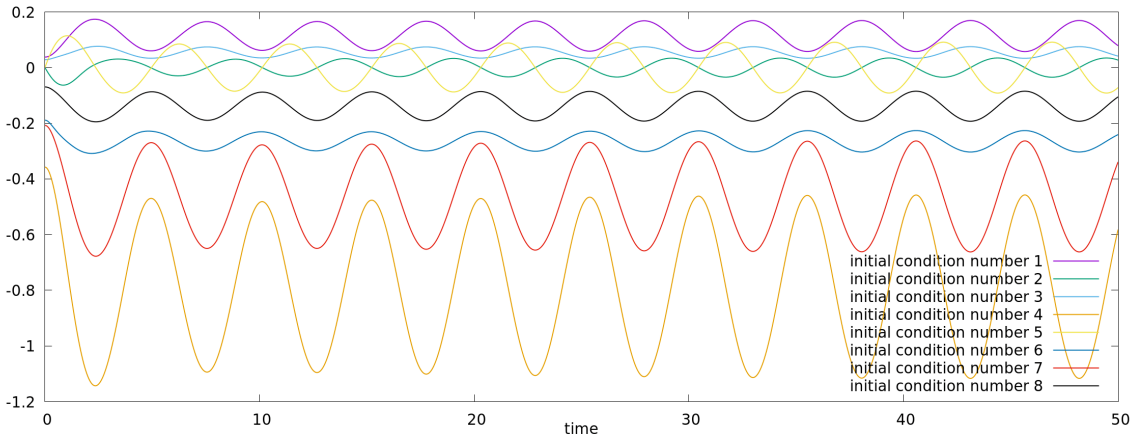

Figure 8.3.5: Evolutions of the kinetic parts of the linearised energy $E_{\text{kin}}^{\text{lin}}$ for the solutions of the linearised Vlasov-Poisson system launched by the initial conditions from Table 8.3.1. For better visibility, we have multiplied some of the initial conditions with a positive factor. The underlying steady state is the isotropic polytrope with $k = 1$ and $R_{\max} = 1$.

exist, we can always expect that both parts – the one causing the oscillation and the one getting damped – are present, in the sense that they have a non-zero weight. The reason for this is that it is not to be expected that initial data like the ones from Table 8.3.1, which we have chosen with total naïvety as simple examples, are a linear combination of, or orthogonal to, the (unknown) eigenfunctions.

Observation 8.3.2 (All Initial Data Lead to Equivalent Behaviours)**.** *The qualitative behaviour of solutions of the linearised Vlasov-Poisson system (for some fixed steady state) is qualitatively the same for all* generic *initial data. Here, an initial condition is referred to as* generic *if it (is non-trivial and) has been selected "arbitrarily", without specifically aiming to cause exclusively oscillatory or exclusively damped behaviour in the resulting solution. Explicit examples for such initial conditions are given in Table 8.3.1.*

In further internal analyses, we have tested several other generic initial data besides those from Table 8.3.1, but never found a qualitative difference in the behaviour of the resulting solution. In particular, we verified all of the following observations regarding the linearised Vlasov-Poisson system (with steady states different from the one considered so far) with more initial data than the ones we will present below.

We refer to Chapter 9 for a further discussion of (a potential application of) the aforementioned aspect that the damping phase of a solution varies in "strength" depending on the initial data. In the present section, we will not further elaborate on this aspect.

Isotropic Polytropic Steady States

We next analyse the solutions of the linearised Vlasov-Poisson system for general isotropic polytropes (1.2.3). As in Section 8.1, we consider the polytropic exponents $0 < k \leq 3.2$ and always choose the parameter $\kappa > 0$ s.t. $R_{\max} = 1$. It follows by the analysis from Appendix B that the solutions of the linearised Vlasov-Poisson system are simply rescaled when changing the parameter κ of the underlying isotropic polytropic steady state. We now exclude the case $k = 0$ because this steady state is not included in the mathematical analysis of the

linearised system, recall Section 4.1.[187] Moreover, in accordance with Observation 8.3.2, we only present here solutions launched by the initial distribution $f(0) = w\,\varphi'(E)$. The evolutions of the separate components of the linearised energy for these solutions are plotted in Figure 8.3.6 for a few isotropic polytropes.

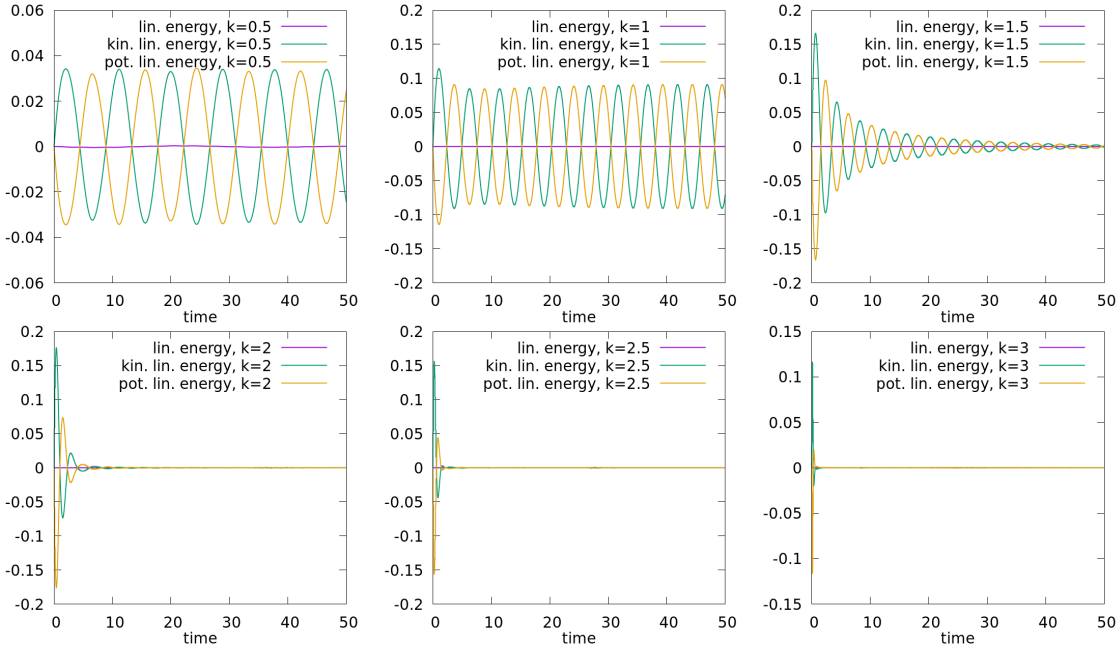

Figure 8.3.6: Evolution of the linearised energy E^{lin} and its kinetic and potential parts $E^{\mathrm{lin}}_{\mathrm{kin}}$ and $E^{\mathrm{lin}}_{\mathrm{pot}}$ for the solutions of the linearised Vlasov-Poisson systems for isotropic polytropes with $R_{\max} = 1$ and polytropic exponents $k \in \{\frac{1}{2}, 1, \frac{3}{2}, 2, \frac{5}{2}, 3\}$. The initial condition is $f(0) = w\,\varphi'(E)$ in all cases.

It is evident from Figure 8.3.6 that the qualitative behaviour of the solution depends on the polytropic exponent of the underlying steady state: As discussed above, in the case $k = 1$ the solution exhibits a (partially) undamped oscillatory behaviour, i.e., it oscillates undamped after a short initial damping period in which a part of the solution seems to get damped. The same behaviour can also be observed in the case $k = \frac{1}{2}$ as well as for other polytropic exponents $0 < k < 1$ which we have not included in this figure. In particular, we observe that solutions of the linearised Vlasov-Poisson system for isotropic polytropes with polytropic exponents $0 < k \ll 1$ – e.g., $k = 0.02$ – exhibit an undamped oscillatory behaviour, which is consistent with Observation 8.2.11. Furthermore, for smaller polytropic exponents, the damping at the beginning seems to be weaker; this can be seen in Figure 8.3.6 by comparing the solutions for $k = \frac{1}{2}$ and $k = 1$. In contrast, for $k \in \{\frac{3}{2}, 2, \frac{5}{2}, 3\}$ (and for other polytropic exponents $\frac{3}{2} \leq k \leq 3.2$ which we have not included in this figure), the solutions are (fully) damped, in the sense that $E^{\mathrm{lin}}_{\mathrm{kin}}(f(t))$ and $E^{\mathrm{lin}}_{\mathrm{pot}}(f(t))$ decay to zero as t gets larger. During this damping, the solutions nonetheless exhibit an oscillatory behaviour. Moreover, the damping seems to be stronger, i.e., faster, for larger polytropic exponents k. We will, however, not further investigate the damping rates here. As indicated by Observation 8.3.1, the damping cannot only be observed in the different

[187] In the case $k = 0$, it is very challenging to simulate the linearised Vlasov-Poisson system numerically due to the presence of the factor $\partial_v f_0$ in the response term of the linearised Vlasov equation (3.1.1). This factor is a delta distribution concentrated at the boundary of the steady state support.

components of the linearised energy, but also in all other macroscopic quantities. At this point we should emphasise that damping can only be present at the macroscopic level, i.e., "global" quantities like $E^{\mathrm{lin}}_{\mathrm{kin}}(f(t))$, $E^{\mathrm{lin}}_{\mathrm{pot}}(f(t))$, $E^{\mathrm{free}}_{\mathrm{kin}}(f(t))$, or $E^{\mathrm{free}}_{\mathrm{pot}}(f(t))$ may converge to fixed numbers or macroscopic functions like $\rho_f(t)$, $m_f(t)$, or $U_f(t)$ may converge to limiting functions as t gets larger. The phase space configuration $f(t)$ is not expected to approach a limiting configuration as $t \to \infty$ since the linearised Vlasov-Poisson system is conservative (meaning that it possesses the conserved quantities introduced above), i.e., there is no damping on the microscopic level. Anyway, to illustrate how the damping manifests itself at the level of the macroscopic functions ρ_f and U_f, we visualise the evolutions of these functions in Figures 8.3.7 and 8.3.8 in the case $k = \frac{3}{2}$. These figures should be compared to Figures 8.3.3 and 8.3.4, where the same quantities (on a different time scale) are plotted in the case $k = 1$. The qualitative differences between the fully damped behaviour ($k = \frac{3}{2}$) and the partially undamped oscillatory behaviour ($k = 1$) are clearly visible at the level of these functions as well.

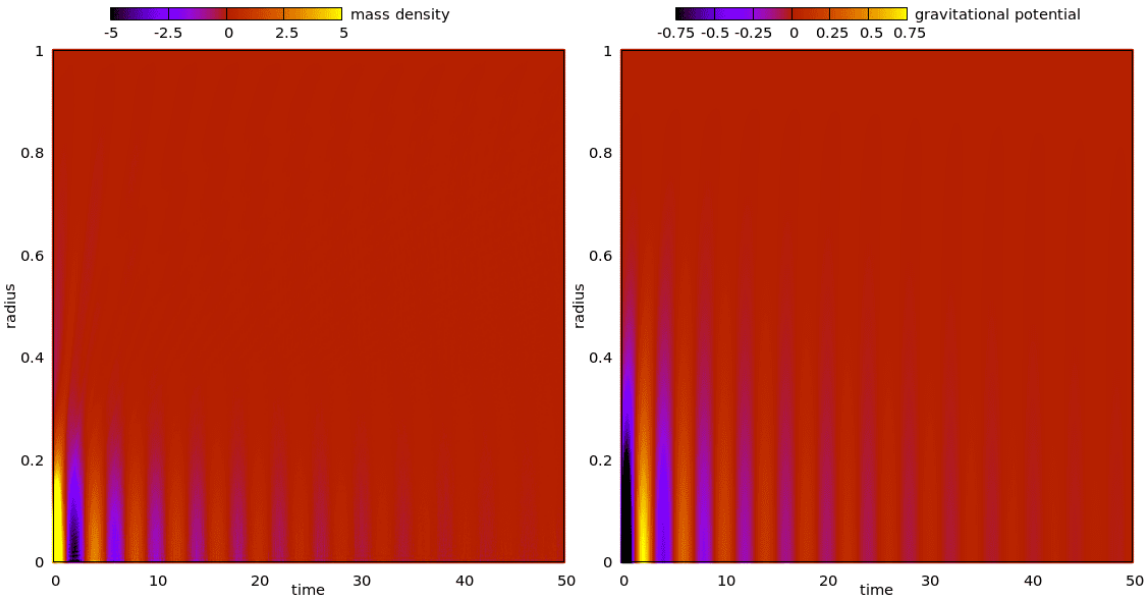

Figure 8.3.7: Values of the mass density $\rho_f = \rho_f(t,r)$ (left panel) and the gravitational potential $U_f = U_f(t,r)$ (right panel) at different time-radius pairs (t,r) for the solution f of the linearised Vlasov-Poisson system for the isotropic polytropic steady state with $R_{\max} = 1$ and $k = \frac{3}{2}$. The initial condition is $f(0) = w\,\varphi'(E)$.

To examine the transition from partially undamped to fully damped behaviour in more detail, we show the evolutions of similar solutions as before for the polytropic exponents $k \in \{1.2, 1.25, 1.3\}$ in Figure 8.3.9. In the case $k = 1.2$, the oscillations are clearly partially undamped. The slightly increasing amplitude of the oscillation for this solution – which could be interpreted as a sign of instability of the underlying steady state – is due to the numerics, which become slightly inaccurate after the large amount of oscillations. For $k = 1.3$, it is evident that the solution is fully damped. We do not dare to assign the case $k = 1.25$ clearly to one behaviour. The solution is probably fully damped in this case too, but the damping is rather slow, which could also be due to an undamped part of the solution.

Anyway, we feel confident to say that the transition from partially undamped oscillatory to fully damped behaviour when increasing the polytropic exponent k occurs between $k =$

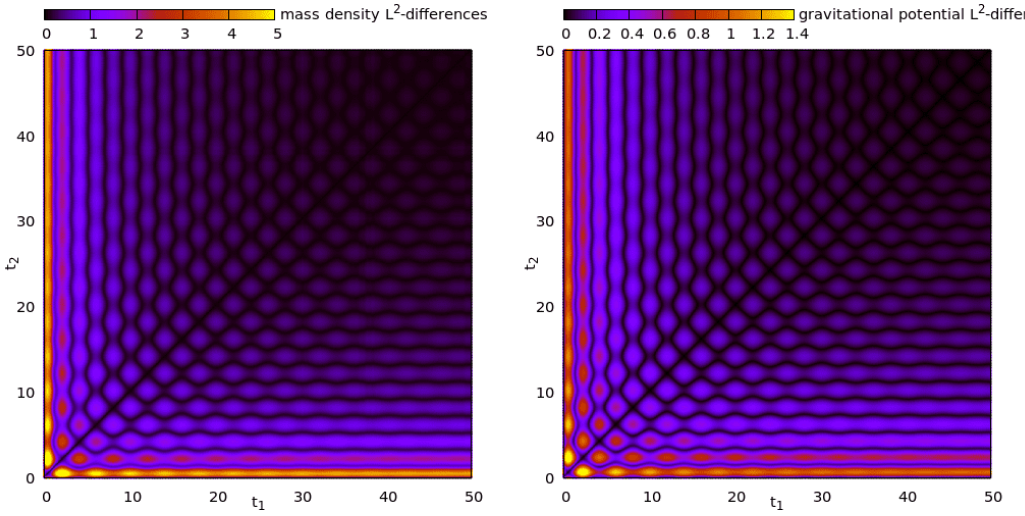

Figure 8.3.8: L^2-differences of the mass density ρ_f (left panel) and the gravitational potential U_f (right panel) at different time steps, i.e., $\|\rho_f(t_1)-\rho_f(t_2)\|_2$ and $\|U_f(t_1)-U_f(t_2)\|_2$ for different $t_1, t_2 \geq 0$, for the solution f of the linearised Vlasov-Poisson system for the isotropic polytropic steady state with $R_{\max} = 1$ and $k = \frac{3}{2}$. The initial condition is $f(0) = w\,\varphi'(E)$.

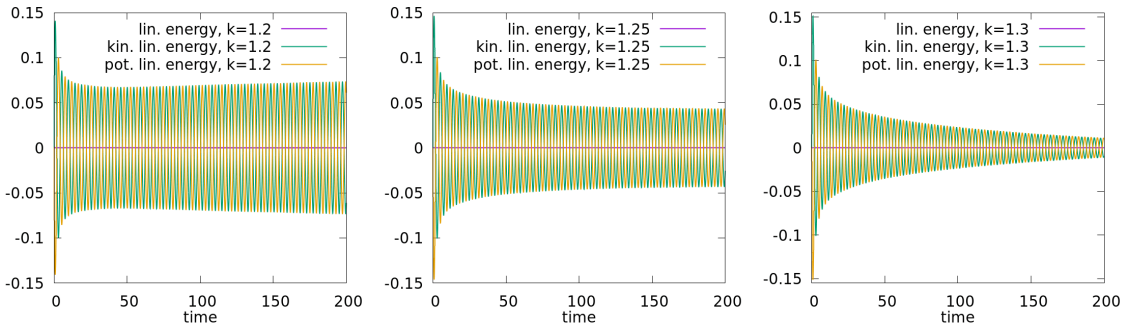

Figure 8.3.9: Evolution of the linearised energy E^{lin} and its kinetic and potential parts $E^{\text{lin}}_{\text{kin}}$ and $E^{\text{lin}}_{\text{pot}}$ for the solutions of the linearised Vlasov-Poisson systems for isotropic polytropes with $R_{\max} = 1$ and polytropic exponents $k \in \{1.2, 1.25, 1.3\}$. The initial condition is $f(0) = w\,\varphi'(E)$ in all cases.

1.2 and $k = 1.3$. In particular, the analysis of many more polytropic exponents $0 < k \leq 3.2$ than presented here has confirmed that there is only this one transition from undamped oscillations to damping. Let us state this finding.

Observation 8.3.3 (Oscillations vs. Damping for Isotropic Polytropes at the Linear Level)**.** *In the case of an isotropic polytrope with polytropic exponent* $0 < k \leq 1.2$*, any solution of the linearised Vlasov-Poisson system (launched by "generic" initial data, cf. Observation 8.3.2) exhibits a partially undamped oscillatory behaviour. In contrast, for polytropic exponents* $1.3 \leq k \leq 3.2$*, every solution of the linearised Vlasov-Poisson system is fully damped (on the macroscopic level).*

This observation shows that polytropic exponents $k \approx 1.25$ play a distinguished role as the threshold between undamped oscillations and damping. Unfortunately, we have not found any other specific features for such polytropic exponents. For instance, the isotropic polytropes with $R_{\max} = 1$ attain their maximal total mass at the polytropic exponent

$k \approx 1.65$, cf. Figure 8.1.2, which is already in the fully damped regime.

The above observation indicates that more regular steady states, corresponding to a larger value of k, lead to fully damped solutions, whilst less regular steady states, corresponding to smaller k, lead to undamped oscillations. This is consistent with the results derived in Chapter 6 – recall Remark 6.4.2 and Theorem 6.6.1 – and those from [61, Thm. 1.2]. However, we will see below that, in general, the presence of oscillating modes does not depend solely on the regularity of the steady state, cf. Observations 8.3.6 and 8.3.8.

The above observation is also consistent with Observation 8.2.11 which, together with Lemma 4.5.19, showed the presence of linear oscillations for isotropic polytropes with very small polytropic exponents $0 < k \ll 1$.

We next aim to draw conclusions about spectral properties of the linearised operator $\mathcal{L}$ by examining the (numerically computed) solutions of the linearised Vlasov-Poisson system. The connection between the behaviour of solutions and the spectrum we will establish is, however, purely formal and not based on rigorous arguments. This connection relies on the *fundamental oscillation period* of the oscillatory motion of the solutions, i.e., the period of the oscillation which is dominantly visible. We determine this period by analysing the zeros of $t \mapsto E_{\text{kin}}^{\text{lin}}(f(t))$ for the solution launched by the initial condition $f(0) = w\,\varphi'(E)$. More precisely, we take the average distance of all succeeding zeros of $t \mapsto E_{\text{kin}}^{\text{lin}}(f(t))$ and multiply this value by 2 to arrive at the fundamental oscillation period p. In fact, we omit the first few zeros for this computation as the solution's behaviour can be somewhat different at the beginning, e.g., as during the initial damping phase in the case $k = 1$. It should, nonetheless, be noted that the distances between succeeding zeros remain rather constant during the evolution. In the case $k = 1$, recall Figure 8.3.1, this method yields a fundamental oscillation period of $p \approx 5.07$. Let us mention that in some cases, e.g., $k = \frac{1}{2}$ in Figure 8.3.6, there may be a superposition of multiple oscillations.[188] We will, however, ignore this here and only focus on the fundamental period.

In the situation where the solution contains an undamped oscillatory part, the fundamental oscillation period p should correspond to an eigenvalue λ of the linearised operator $\mathcal{L}$; the relation of p and λ is given by (1.2.12). Otherwise, in the case of full damping, the solutions still exhibit periodic oscillations with a reasonably constant fundamental oscillating period p.[189] In this case, we also convert p into λ using (1.2.12); λ is still expected to be an element of the spectrum of $\mathcal{L}$, although it is not (expected to be) an eigenvalue. In both cases, we refer to λ as the *fundamental spectral element*.

As an aside, let us note that we have checked and confirmed the validity of the Eddington-Ritter type relation, cf. Appendix B, for the fundamental oscillation periods p and the associated fundamental spectral elements λ for the isotropic polytropes. More precisely, for several polytropic exponents $0 < k \leq 3.2$, the values of p and λ associated to steady states with different values of κ satisfy (B.0.22) and (B.0.23) to high accuracy. This has been observed before in [132, Sc. 4] for suitable solutions of the non-linearised Vlasov-Poisson system. On the linearised level, the validity of the Eddington-Ritter type relation is to be expected since, by (B.0.21), choosing different values of κ just corresponds to rescaling the linearised operator $\mathcal{L}$ appropriately. This can thus be interpreted as a further proof of

[188] We have implemented a discrete Fourier transform (henceforth abbreviated as "DFT") to detect the presence of multiple periodic motions in our data. In the case $k = \frac{1}{2}$ in Figure 8.3.6, the DFT shows that the fundamental oscillation period ≈ 8.84 is indeed more than four times stronger than the second strongest period ≈ 10.66 detected in the data; the "strength" of a period refers to its amplitude in the Fourier space.

[189] For strongly damped solutions, which arise in the case of large polytropic exponents, determining the fundamental oscillation period becomes inaccurate since it gets difficult to distinguish the oscillations from numerical noise.

the accuracy of the numerics.

It is now interesting to compare the fundamental spectral element λ to the essential spectrum of $\mathcal{L}$. The latter is determined by the minimum and maximum values of the period function T on the steady state support, recall Remark 4.3.20 and Proposition 4.5.4. For each (isotropic polytropic) steady state, the minimum and maximum value of T on the steady state support can be calculated numerically using the methods from the previous section; recall Figure 8.2.6 for a visualisation of these values for the isotropic polytropes. The essential spectra of the linearised operators calculated in this way as well as the fundamental spectral elements λ are shown in Figure 8.3.10 for various isotropic polytropes. What is not visible from the figure is that, for all isotropic polytropes shown, the essential spectrum of $\mathcal{L}$ has no further gaps besides the essential gap $\mathcal{G}$.

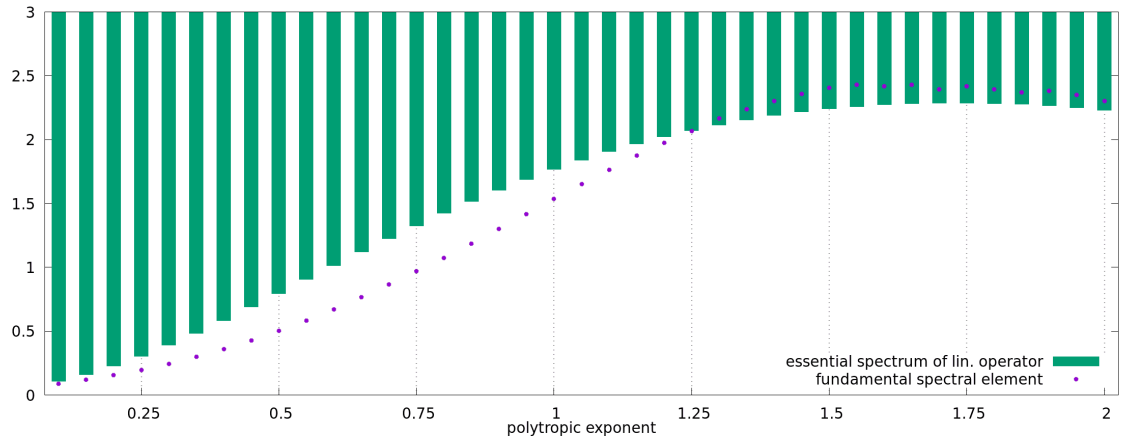

Figure 8.3.10: The green bars illustrate the essential spectra of the linearised operators $\mathcal{L}$ associated to isotropic polytropic steady states with $R_{\max} = 1$ and polytropic exponents $0.1 \leq k \leq 2$. The purple dots depict the fundamental spectral elements λ which correspond to the fundamental oscillation periods of the solutions of the linearised Vlasov-Poisson system. The computation of λ and $\sigma_{\text{ess}}(\mathcal{L})$ is describe in more detail in the text above.

We see in Figure 8.3.10 that the fundamental spectral element λ is always smaller than $\inf(\sigma_{\text{ess}}(\mathcal{L}))$ for isotropic polytropes with polytropic exponents $0.25 \leq k \leq 1.2$. In the case $k = 1.25$, the bottom of the essential spectrum coincides with λ (within the range of the numerical (in)accuracies), while for larger polytropic exponents, the fundamental spectral element lies inside the essential spectrum of $\mathcal{L}$. The same behaviour persists for all polytropic exponents $0 < k \leq 3.2$ and is not restricted to the range we have selected in the above figure for the sake of better visibility, i.e., $\lambda < \inf(\sigma_{\text{ess}}(\mathcal{L}))$ for $0 < k \leq 1.2$ and $\lambda \in \sigma_{\text{ess}}(\mathcal{L})$ for $1.3 \leq k \leq 3.2$.

This is remarkably consistent with Observation 8.3.3. More specifically, as previously discussed, the fundamental spectral element λ should be an eigenvalue of $\mathcal{L}$ in the case of a steady state that causes (partially) undamped oscillations of solutions of the linearised Vlasov-Poisson system. By Figure 8.3.10, these eigenvalues are always isolated and not embedded into the essential spectrum of $\mathcal{L}$. This fits to the result established in Theorem 6.5.5 which proves that no embedded eigenvalues can occur for steady states that are, admittedly, very different from the ones we are considering here. In other words, the fundamental oscillation period is larger than all individual (radial) particle periods within the steady state. In the case $k = \frac{1}{2}$, this observation has previously been made in [159, Fig. 2] on the non-linearised level. For larger polytropic exponents, all solutions of the linearised Vlasov-

Poisson system are damped by Observation 8.3.3 and the fundamental spectral elements always lie in the essential spectrum of the linearised operator. This means that, in every case where the solution is damped, the fundamental oscillation period or an integer multiple of it equals the (radial) periods of some particles within the steady state. It is argued in the physics literature that such "resonance" necessarily leads to damping, see [19, Sc. 5.3]. Let us summarise these findings.

Observation 8.3.4 (No Embedded Eigenvalues for Isotropic Polytropes)**.** *For all isotropic polytropes, there never seems to be an eigenvalue embedded into the essential spectrum of the linearised operator $\mathcal{L}$. More precisely, all eigenvalues seem to lie below the essential spectrum, i.e., inside the essential gap $\mathcal{G}$. In the fully damped cases, the fundamental oscillation periods correspond to elements of the essential spectrum of $\mathcal{L}$.*

As an aside, let us also mention that Observations 8.3.3 and 8.3.4 are remarkably consistent with the numerical results obtained in [182, Sc. 8.5]. Among other things, this thesis investigates the linearised Einstein-Vlasov system for isotropic polytropic steady states with small redshift values. Such steady states are close to the respective isotropic polytropes for the Vlasov-Poisson system, cf. [60], and it is to be expected that the solutions of the linearised Einstein-Vlasov system behave similarly to the ones of the linearised Vlasov-Poisson system. It is found in [182, Sc. 8.5] that the transition from oscillation to damping occurs close to the polytropic exponent $k = 1.2$ for isotropic polytropes with small redshifts. This is very close to the threshold value $k \approx 1.25$ observed here, despite the analysis of a different system in [182] and also despite the fact that in [182, Ch. 8], the spectrum of the linearised Einstein-Vlasov system is numerically studied using variational methods which differs conceptually from the particle-in-cell method employed here.

The Pure Transport Equation

In the current context of examining the isotropic polytropes, let us now address another aspect of the linearised Vlasov-Poisson system. It is sometimes argued that (in suitable settings) the response term has negligible influence on the behaviour of solutions, cf., e.g., [103, p. 280]. This means that instead of the linearised Vlasov-Poisson system (3.1.1)–(3.1.3), one considers the following simpler equation:

$$\partial_t f + \mathcal{T} f = 0. \tag{8.3.14}$$

This equation is commonly referred to as the *pure transport equation*. Solutions of this equation for various steady states and general prescribed potentials U_0 are, e.g., studied in [27, 103, 116, 148].

Let us (numerically) analyse the solutions of (8.3.14) for isotropic polytropic steady states and compare them to the solutions of the actual linearised Vlasov-Poisson system. It is, in fact, quite easy to modify our numerical methods to simulate the pure transport equation instead of the linearised Vlasov-Poisson system: On the right-hand side of (8.3.4), we just drop the second term. As this term caused most of the difficulties in the numerical implementation, it is conceptionally easier to simulate the pure transport equation than the linearised Vlasov-Poisson system. This manifests itself in the fact that the errors of the conserved quantities of (8.3.14) – which are given by $E^{\text{free}}_{\text{kin}}$, E^{lin}, and M defined in (8.3.7), (8.3.9), and (8.3.12), respectively – during a numerical simulation remain even smaller than for the linearised Vlasov-Poisson system (with the same initial configuration and numerical parameters). The evolution of the solution of the pure transport equation launched by the

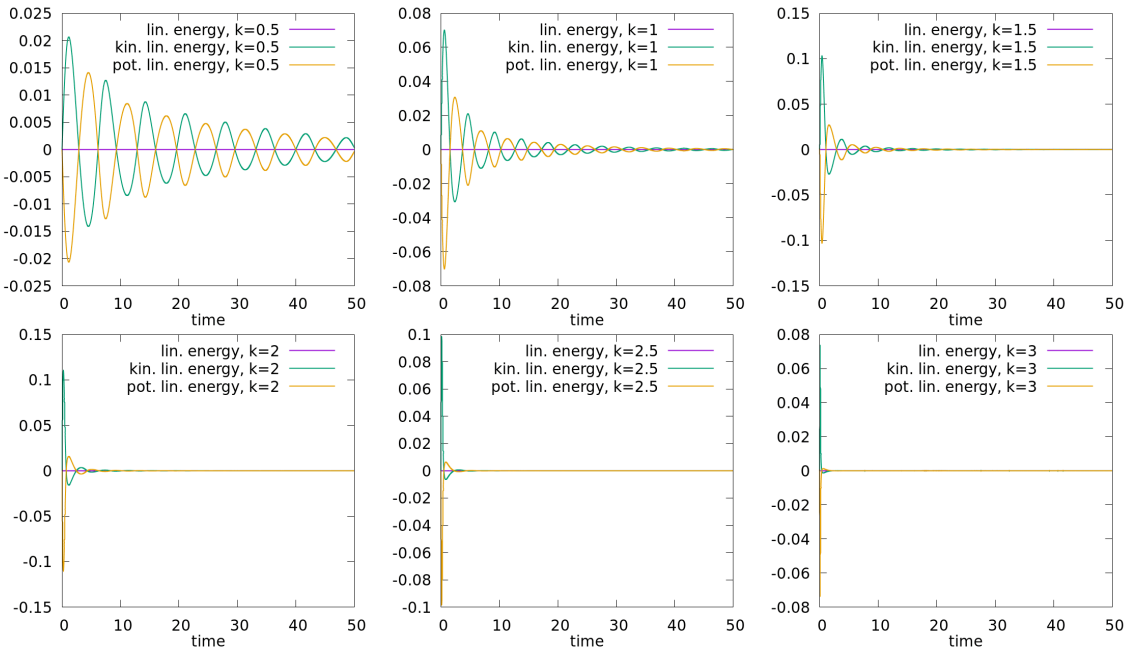

Figure 8.3.11: Evolution of the linearised energy E^{lin} and its kinetic and potential parts $E^{\text{lin}}_{\text{kin}}$ and $E^{\text{lin}}_{\text{pot}}$ (see (8.3.9)–(8.3.11) for the definitions of these quantities) for the solutions of the pure transport equation (8.3.14) for isotropic polytropes with $R_{\max} = 1$ and polytropic exponents $k \in \{\frac{1}{2}, 1, \frac{3}{2}, 2, \frac{5}{2}, 3\}$. The initial condition is $w\,\varphi'(E)$ in all cases.

initial distribution $w\,\varphi'(E)$ is shown in Figure 8.3.11 for the same isotropic polytropes as analysed above.

We clearly see that all the solutions of the pure transport equation shown in this figure are fully damped. This is to be expected in the light of Remark 4.3.30 and Observation 8.2.10 which imply that the transport operator $\mathcal{T}$ does not possess eigenvalues for the steady states considered here. Similar to Observation 8.3.1, the damping can be observed equivalently in all other (macroscopic) quantities. It should, however, be pointed out that, due to Proposition 4.3.23, all initial conditions depending only on E and L lead to constant-in-time solutions. Besides this restriction, all generic initial data also lead to full damping, e.g., the initial conditions 2, 3, 5, 6, 7, and 8 from Table 8.3.1. As an aside, we note that the strength of the damping seems to depend on the initial distribution for solutions of the pure transport equation. Nonetheless, the conclusions we draw below about the solutions of the pure transport equation apply to all initial data.

The behaviour of the solutions of the pure transport equation depicted in Figure 8.3.11 should now be compared to Figure 8.3.6, where similar solutions of the linearised Vlasov-Poisson system are shown. It becomes evident that the solutions of the pure transport equation behave very differently than the ones of the linearised Vlasov-Poisson system. The most striking difference is the absence of undamped oscillatory behaviour of solutions of the pure transport equation for polytropic exponents $k \leq 1.2$. For such steady states, the fundamental oscillation period of the solutions of the linearised Vlasov-Poisson system is always larger than the associated period for the pure transport equation. This is consistent with Observation 8.3.4 since the fundamental oscillation periods of solutions of the pure transport equation correspond to elements within the spectrum of the transport operator; recall that the essential spectrum of the linearised operator equals the spectrum of the transport part by Propositions 4.3.19 and 4.5.4.

For larger polytropic exponents, where both the linearised Vlasov-Poisson system's solutions and the pure transport equation's solutions are fully damped, the damping is stronger for the pure transport equation. This can be seen most clearly by comparing the plots in the case $k = \frac{3}{2}$ in Figures 8.3.6 and 8.3.11.

Observation 8.3.5 (Differences Between Linearised Vlasov-Poisson System and Pure Transport Equation)**.** *For an isotropic polytropic steady state, the behaviour of the solutions of the linearised Vlasov-Poisson system is qualitatively different from the pure transport equation* (8.3.14)*. Concretely, the solutions of the pure transport equation are always damped, even if the associated solutions of the linearised Vlasov-Poisson system partially oscillate undamped. The periods of these oscillations are different from the fundamental oscillation periods observed for solutions of the pure transport equation. For the steady states where all solutions of the linearised Vlasov-Poisson system are fully damped, the solutions of the pure transport equation are damped more strongly.*

We also observed similar differences between solutions of the pure transport equation and the linearised Vlasov-Poisson system for different steady states than the isotropic polytropes. We will, however, not further discuss the pure transport system in this section. We shall reveal in the next section whether the solutions of the pure transport equation or the linearised Vlasov-Poisson system actually reflect the behaviour of suitable solutions of the (non-linearised) Vlasov-Poisson system, cf. Observation 8.4.4.

King Models

Let us now consider the linearised Vlasov-Poisson system with a King model (1.2.4) as the underlying steady state. We keep this part shorter than the above analysis for the isotropic polytropes since the occurring effects are somewhat similar.

The evolutions of the kinetic and potential parts of the linearised energy of solutions of the linearised Vlasov-Poisson systems for King models with different values of κ are depicted in Figure 8.3.12. In accordance with Observation 8.3.1, other (macroscopic) quantities behave equivalently as $E^{\mathrm{lin}}_{\mathrm{kin}}$ and $E^{\mathrm{lin}}_{\mathrm{pot}}$. As the initial condition we have again always chosen $f(0) = w\,\varphi'(E)$, but point out that further testing suggests that different "generic" initial data lead to qualitatively similar behaviour.

It is clearly visible from Figure 8.3.12 that King models with small values of κ lead to partially undamped oscillatory solutions of the linearised Vlasov-Poisson system, while all solutions are fully damped for larger values of κ.[190] We have also tested and confirmed this behaviour for further King models than the ones shown in the figure. Let us attempt to explain, by means of (very) formal arguments, why we think that this is consistent with the above observations for the isotropic polytropes: First notice that a steady state with parameter $\kappa > 0$ is only affected by the values of the energy dependency function Φ on $]-\infty, \kappa]$. We also observe that the energy dependency function of the King models is linear to first order, more precisely, $\Phi(\eta) = (e^{\eta} - 1)_+ = \eta_+ + \mathcal{O}_{\eta\to 0}(\eta^2)$. Hence, for small values of κ, King models should be close to an isotropic polytrope with polytropic exponent $k = 1$. Since we have observed partially undamped oscillatory solutions in the case of this isotropic polytrope, cf. Observation 8.3.3, it is to be expected that solutions of the linearised Vlasov-Poisson system also oscillate undamped for King models with $0 < \kappa \ll 1$, as indeed they do. For larger values of κ, the higher-order terms in the series expansion of the energy dependency function $\Phi(\eta) = \sum_{i\in\mathbb{N}} \frac{\eta_+^i}{i!}$ become more important. Hence, the corresponding

[190] As in Figure 8.3.9, the slightly increasing amplitudes of the oscillations in the cases $\kappa = 1$ and $\kappa = \frac{3}{2}$ are due to numerical inaccuracies.

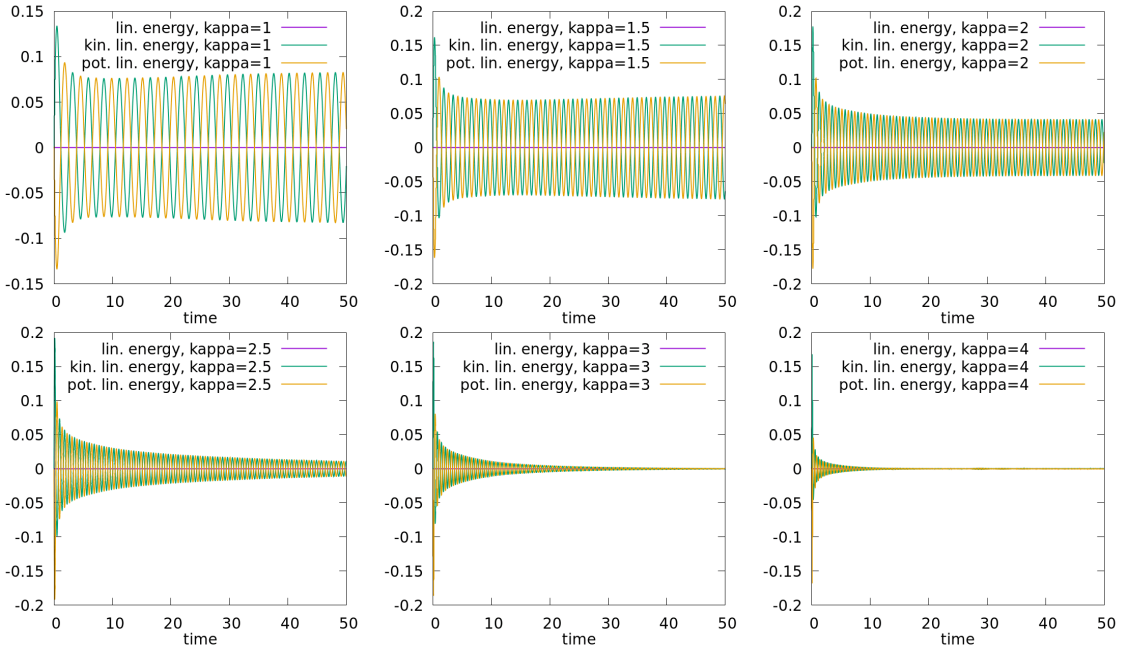

Figure 8.3.12: Evolution of the linearised energy E^{lin} and its kinetic and potential parts $E^{\text{lin}}_{\text{kin}}$ and $E^{\text{lin}}_{\text{pot}}$ for the solutions of the linearised Vlasov-Poisson systems for King models with parameters $\kappa \in \{1, \frac{3}{2}, 2, \frac{5}{2}, 3, 4\}$. The initial condition is $w\,\varphi'(E)$ in all cases.

King models are somewhat closer to isotropic polytropes with larger polytropic exponents, for which we have observed fully damped solutions. Notice, however, that all King models are equally regular. In particular, the King models are all linear in $(E - E_0)$ close to the vacuum boundary $\{E = E_0\}$ in phase space, even for large values of κ. Figure 8.3.12 hence yields the following insight:

Observation 8.3.6 (Steady State Regularity is not the Only Decisive Factor)**.** *Whether the solutions of the linearised Vlasov-Poisson system exhibit a partially undamped oscillatory behaviour or whether they are fully damped is* not *solely determined by the regularity of the underlying steady state.*

For the King models, it is, however, difficult to determine the threshold value for $\kappa > 0$ at which the transition from partially undamped oscillatory behaviour to fully damped behaviour occurs. Our impression is that this transition proceeds much more slowly for the King models when increasing κ compared to when increasing the polytropic exponent k for the isotropic polytropes. In fact, for a wide range of King models, the behaviour of the solutions of the linearised Vlasov-Poisson system is somewhat similar to the polytropic case $k = 1.25$, cf. Figure 8.3.9, which we cannot confidently classify as being fully damped or not. We are, nonetheless, certain that all King models with $0 < \kappa \leq \frac{3}{2}$ lead to partially undamped oscillatory solutions of the linearised Vlasov-Poisson system, while all solutions are fully damped for $\kappa \geq \frac{5}{2}$.

Furthermore, in contrast to the isotropic polytropic case, comparing the fundamental spectral element λ with the essential spectrum of the linearised operator $\mathcal{L}$ does not provide any further insights into the onset of fully damped behaviour for the King models when increasing κ. This is because, for all values of $\kappa > 1$ we analysed, the fundamental spectral elements λ are in such close proximity to $\inf(\sigma_{\text{ess}}(\mathcal{L}))$ that – given the inherent numerical inaccuracies – it is not possible to clearly say whether λ lies in the essential spectrum of $\mathcal{L}$

or just below it. On the non-linearised level, this phenomenon for one fixed King model has previously been observed in [159, Fig. 2]. For $0 < \kappa < 1$, the fundamental spectral elements always lie below $\inf(\sigma_{\mathrm{ess}}(\mathcal{L}))$. Let us emphasise that we have never clearly observed λ lying inside $\sigma_{\mathrm{ess}}(\mathcal{L})$ in a case where the solutions of the linearised Vlasov-Poisson system partially oscillate undamped or where we are uncertain of the occurring behaviour. This is again very similar to the isotropic polytropes, recall Observation 8.3.4.

Despite the uncertainties in the analysis of the linearised Vlasov-Poisson systems for the King models, we feel confident enough to conclude the following.

Observation 8.3.7 (Linearised Dynamics for the King Models)**.** *For King models with small values of the parameter κ (at least $0 < \kappa \leq \frac{3}{2}$), the solutions of the linearised Vlasov-Poisson system (launched by "generic" initial data, cf. Observation 8.3.2) all exhibit a partially undamped oscillatory behaviour. In contrast, for King models with larger values of κ (at least $\kappa \geq \frac{5}{2}$), all solutions of the linearised Vlasov-Poisson system are fully damped (on the macroscopic level).*

Moreover, we have never encountered an undamped oscillation clearly corresponding to an embedded eigenvalue of the linearised operator for any King model. For all King models with $1 \leq \kappa \leq 4$, the fundamental spectral element is rather close to the bottom of the essential spectrum of the linearised operator.

Anisotropic Polytropes with $L_0 = 0$

We now return to the polytropic steady states and consider the case of an equation of state of the form (2.2.17) with $L_0 = 0 < \ell$. The resulting steady states are anisotropic and have no inner radial vacuum region, i.e., $R_{\min} = 0$. Due to the assumption ($\varphi 4$), such steady states are not included in the analysis of Chapters 4 and 5 since their periods are unbounded, cf. Remarks 4.1.1 (a) and A.4.5. Nonetheless, we numerically study the linearised Vlasov-Poisson system here for such steady states in order to understand how the anisotropy of the steady states affects the linearised dynamics.

For several different polytropic exponents k and ℓ, Figure 8.3.13 displays whether the numerics indicate the presence of partially undamped oscillatory solutions of the linearised Vlasov-Poisson system or whether all solutions are fully damped. We have determined the qualitative behaviour in the same way as above, i.e., by analysing the evolution of $E_{\mathrm{kin}}^{\mathrm{lin}}$ up to a terminal time of about $t = 50$. In some cases, the behaviour is similar to the isotropic polytropic case $k = 1.25$, recall Figure 8.3.9; we do not dare to assign such cases clearly to one behaviour. For all steady states, we have chosen the parameter κ leading to $R_{\max} = 1$; note that, by Appendix B, the qualitative behaviour of solutions of the linearised Vlasov-Poisson system does not depend on κ. Furthermore, in accordance with Observations 8.3.1 and 8.3.2, the qualitative behaviour does not depend on the initial condition, nor on which macroscopic quantity we analyse. Figure 8.3.13 can be seen as an extension of (and homage to) [66, Fig. 5], where the stability of similar anisotropic polytropes is studied (on the non-linearised level). However, in [66] the focus lies more on anisotropic polytropes with non-positive polytropic exponents k and ℓ, which we do not consider here.

We clearly see from Figure 8.3.13 that undamped oscillatory behaviour exists for smaller values of the polytropic exponent k and for larger values of the polytropic exponent ℓ. Just like Observation 8.3.6, this shows that, in general, a less regular steady state does not lead to an undamped oscillatory behaviour – as one may have believed after analysing the isotropic polytropes – since a larger value of ℓ corresponds to a more regular steady state. Instead, it appears that a greater degree of anisotropy of the steady state, corresponding to a larger value of ℓ, increases the likelihood of undamped oscillations. The fact that larger ℓ lead to

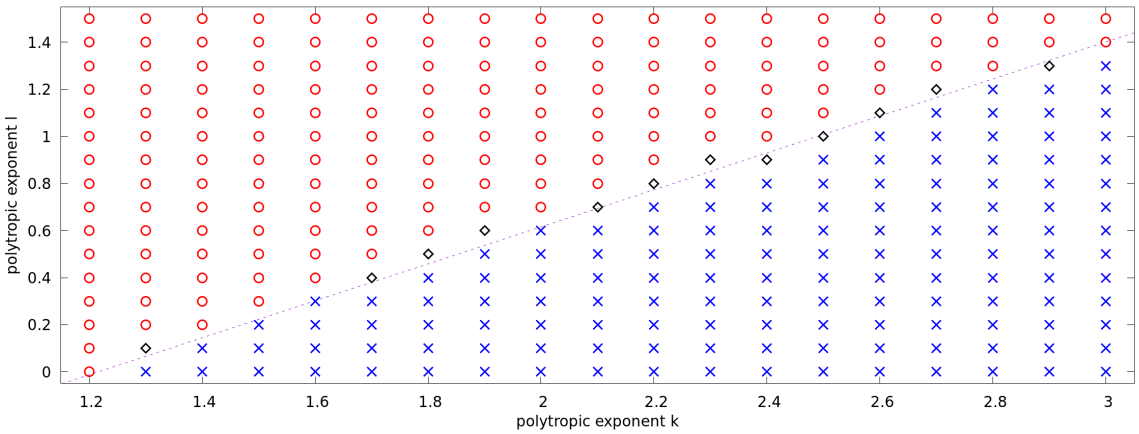

Figure 8.3.13: The qualitative behaviour of solutions of the linearised Vlasov-Poisson system for polytropes with $L_0 = 0$ and different polytropic exponents $k > 0$ and $\ell \geq 0$ satisfying $k < 3\ell + \frac{7}{2}$. Either there are parts of the solutions which oscillate undamped (red circles), or the solutions are fully damped (blue crosses), or we cannot say for sure which of these two cases is present (black squares). The dashed purple line corresponds to polytropic exponents satisfying $\frac{\pi^2}{12}k - \frac{\pi}{3}\ell = 1$.

undamped oscillatory behaviour has also been observed in [132] on the non-linearised level. There it is argued that steady states with small ℓ are somewhat more homogeneous which, in the light of the results known in the plasma physics case [120], ought to correspond to more damping.

The most remarkable observation from Figure 8.3.13 is that the presence of an undamped oscillation or damping seems to depend on the polytropic exponents k and ℓ in a linear way. To our knowledge, such observation has not been made before, not even on the non-linearised level. Concretely, the dashed line included into the figure seems to separate the two regimes quite well, despite the inherent inaccuracies of the numerics. We have fitted this line by manual trial and error and discovered, to our delight, that the coefficients can be expressed in a rather simple form. In the isotropic case $\ell = 0$, this line suggests that the transition from undamped oscillations to damping occurs at the polytropic exponent $k = \frac{12}{\pi^2} \approx 1.22$, which is consistent with Observation 8.3.3.

It should be also be noted that, given Observations 8.3.4 and 8.3.7, it is already surprising that there exist polytropic steady states with $L_0 = 0$ and positive ℓ leading to (partially) undamped oscillations of the linearised Vlasov-Poisson system. As noted above, the period function is unbounded on the support of such steady states. Although we have not proven it here, it is plausible by Proposition 4.5.4 that the essential spectrum of the linearised operator $\mathcal{L}$ is given by $\sigma_{\text{ess}}(\mathcal{L}) = [0, \infty[$. Hence, any undamped oscillation corresponds to an eigenvalue of $\mathcal{L}$ which is embedded into its essential spectrum. This shows that we cannot expect the absence of embedded eigenvalues for anisotropic steady states.

Observation 8.3.8 (Linearised Dynamics for Anisotropic Polytropes with $L_0 = 0$)**.** *An anisotropic polytropic steady state with $L_0 = 0$, i.e., an ansatz function of the form $\varphi(E, L) = (E_0 - E)_+^k L^\ell$ with $\ell \geq 0$ and $0 < k < 3\ell + \frac{7}{2}$, leads to partially undamped oscillatory solutions of the linearised Vlasov-Poisson system if k is small and ℓ is large. More precisely, the following linear relation between the polytropic exponents k and ℓ of the steady state and the qualitative behaviour of the solutions of the linearised Vlasov-Poisson system applies to high accuracy: There exist partially undamped oscillatory solutions if and*

only if

$$\frac{\pi^2}{12}k - \frac{\pi}{3}\ell < 1. \tag{8.3.15}$$

For $\ell > 0$, these oscillations correspond to eigenvalues which are embedded into the essential spectrum of the linearised operator, i.e., the oscillation period of the whole solution is in resonance with the periods of individual particles within the steady state.

Polytropic Shells

We next consider the case of a polytropic shell, i.e., a steady state with microscopic equation of state of the form (2.2.17) with $L_0 > 0$. We only consider the case $\kappa = 1$ here, but are certain that a similar behaviour can also be observed for general values of κ.

Let us first analyse the alteration in the linearised Vlasov-Poisson system when slowly increasing L_0 from 0. As to be expected, for $0 < L_0 \ll 1$, the solutions of the linearised system are somewhat close to the respective solutions in the case $L_0 = 0$. For instance, the solutions exhibit a partially undamped oscillatory behaviour for the polytrope with $k = 1 = \ell = \kappa$ and $L_0 = 0$, and a similar behaviour can also be observed for polytropes with the same polytropic exponents and $0 < L_0 \ll 1 = \kappa$. In addition, the oscillation periods in these cases are close to each other, as are the values of the period function. Since $\sup_{\mathbb{D}_0}(T) = \infty$ in the case $L_0 = 0$, we also observe that for small values of $L_0 > 0$, the fundamental oscillation period of the entire solution is in resonance with the periods of individual particles. Concretely, this is the case for $0 \leq L_0 \leq 0.0003$, while the fundamental oscillation periods of the entire solutions are larger than $\sup_{\mathbb{D}_0}(T)$ for $L_0 \geq 0.0005$; in particular, we have observed a partially undamped oscillation for all polytropes we analysed with $L_0 \geq 0$ and $k = 1 = \ell = \kappa$. As explained before, the former corresponds to an eigenvalue that is embedded into the essential spectrum of the linearised operator. This shows that the absence of embedded eigenvalues cannot be expected for polytropes with $L_0 > 0$, even though these steady states are admissible for the analysis in Chapters 4–5 provided that k and ℓ are suitably chosen. Further recall that the absence of embedded eigenvalues was proven in Section 6.5 for polytropic shells which are small and which surround a point mass. The above discussion hence shows that the presence of the point mass is crucial for the results in Section 6.5. We have only explicitly analysed this phenomenon for one choice of polytropic exponents $k, \ell > 0$, but consider it very plausible that there generally exists an embedded eigenvalue for polytropes with $0 < L_0 \ll 1$ and polytropic exponents which correspond to partially undamped oscillations in the case $L_0 = 0$, cf. Figure 8.3.13.

For polytropic exponents corresponding to fully damped solutions in the case $L_0 = 0$, cf. Figure 8.3.13, we observe a similar behaviour for $0 < L_0 \ll 1$ as well. For instance, for the polytropes with $k = 2$, $\ell = \frac{1}{4}$, and $\kappa = 1$, we observe that all solutions of the linearised Vlasov-Poisson system are fully damped for $0 \leq L_0 \leq 0.01$.

When increasing the parameter $L_0 > 0$, we actually never observe such fully damped solutions. For instance, for all polytropes with $L_0 = 1 = \kappa$ and polytropic exponents k and ℓ contained in Figure 8.3.13, the solutions of the linearised Vlasov-Poisson system are oscillating partially undamped. The associated oscillation periods are always smaller than all particle periods, corresponding to an eigenvalue of the linearised operator in the essential gap. This is consistent with Observation 8.2.12 which also indicated that polytropic shells with not too small $L_0 > 0$ possess an eigenvalue in the essential gap.

Lastly, let us discuss the behaviour of solutions of the linearised Vlasov-Poisson system for polytropic shells with parameters satisfying the conditions (5.4.1) of Theorem 5.4.1. Such solutions are, in fact, harder to study from a numerics point of view and we encounter

larger numerical errors than for other steady states. This is due to the fact that all steady states satisfying (5.4.1) are not smooth at the boundary of their support because of $\ell < 0$. Nonetheless, for all the steady states mentioned in Observation 8.2.8, we clearly found that the solutions of the linearised Vlasov-Poisson system possess an undamped oscillatory part. This is consistent with the statement from Theorem 5.4.1; recall that Observation 8.2.8 indicates that the assumption (5.4.2) is satisfied for these steady states.

Let us summarise our findings regarding the polytropic shells.

Observation 8.3.9 (Linearised Dynamics for Polytropic Shells)**.** *For all polytropic shells with polytropic exponents $k, \ell > 0$ and $0 < L_0 \ll 1$, the solutions of the linearised Vlasov-Poisson system are similar to the respective solutions in the case $L_0 = 0$. If the solutions are partially oscillating undamped, the oscillation periods correspond to an eigenvalue which is embedded into the essential spectrum of the linearised operator.*

If $L_0 > 0$ is not too small, the solutions of the linearised Vlasov-Poisson system always seem to possess an undamped oscillatory part, regardless of the polytropic exponents k and ℓ.

Undamped oscillatory behaviour can also be observed for all polytropic shells satisfying the conditions (5.4.1) *of Theorem 5.4.1.*

8.4 Numerics of the (Non-Linearised) Vlasov-Poisson System

In this section we numerically analyse solutions of the (non-linearised) Vlasov-Poisson system close to steady states. The main purpose is to investigate whether the behaviour of such solutions can indeed be explained by the behaviour of suitable solutions of the linearised Vlasov-Poisson system. Since the theoretical parts of this thesis have dealt solely with the linearised Vlasov-Poisson system, we refrain here from studying the properties of the non-linearised system itself in more detail. In addition, numerous works have already numerically investigated different aspects of the Vlasov-Poisson system. A (most likely incomplete) list of previous numerical investigations that are not too far away from the setting considered here – spherically symmetric solutions close to compactly supported steady states – is [13, 66, 82, 93, 100, 115, 124, 127, 132, 159, 168, 177, 180]. However, the transition from the linearised to the non-linearised Vlasov-Poisson system has, to our knowledge, not yet been numerically analysed.

The Numerical Method

Let us describe how we simulate the radial Vlasov-Poisson system (2.1.9)–(2.1.11). Similar as for the linearised Vlasov-Poisson system, cf. Section 8.3, we simulate the Vlasov-Poisson system using a *particle-in-cell scheme*. The same method has also been used in [132] to numerically analyse the presence of undamped oscillations or damping close to similar steady states as the ones considered here. Furthermore, the particle-in-cell method is commonly used to simulate the Vlasov-Poisson system in a plasma physics context [20] as well as to simulate the Einstein-Vlasov system in spherical symmetry [5, 48, 50, 182] and in other symmetries [2, 3]. The code we use here is based on the ones used in [5, 48, 50, 132], although we have entirely rewritten the code in an object-oriented way. Compared to the code used in [132], we have included some improvements which we will describe below. For instance, the spatial origin $r = 0$ is handled more carefully and we employ an RK4 scheme instead of a Euler scheme for evolving the particles. In the astrophysics literature – see the references above – the Vlasov-Poisson system has also been analysed numerically, but with

different numerical methods. In fact, most of these numerical investigations are based on N-body simulations in one form or another. The particle-in-cell scheme is more adapted to the Vlasov-Poisson system. In particular, it is proven in [153] that a particle-in-cell simulation actually converges to the true solution of the Vlasov-Poisson system when increasing the accuracy of the discretisation. Furthermore, in the context of plasma physics, numerous techniques have been developed to further improve the numerical methods presented here, see [122, 123] and the references therein.

The key idea of the particle-in-cell scheme is to split the phase space support of the initial distribution $f(0)$ into finitely many distinct cells. This phase space separation proceeds in the same way as in the linearised case, cf. above. In particular, we again use the (r, u, α)-coordinates from Remark 2.1.2 (f) for this step; note that these coordinates are also used in [153]. Each of the resulting cells is represented by a *(numerical) particle* placed into its centre. Again, each particle stores its position in phase space in (r, w, L)-coordinates, the volume of its cell, and the value of the initial distribution $f(0, r, w, L)$. These particles represent the initial phase space distribution $f(0)$, and the evolution of f governed by the Vlasov-Poisson system is given through the evolution of the particles. The particle trajectories are governed by the ODE

$$\dot{x} = v, \qquad \dot{v} = -\partial_x U_f(t, x), \tag{8.4.1}$$

where $U_f(t)$ is the gravitational potential generated by f at time t. However, since f is only (yet) known at time $t = 0$, we use the following approximation of (8.4.1):

$$\dot{x} = v, \qquad \dot{v} = -\partial_x U_f(0, x). \tag{8.4.2}$$

The right-hand side of this ODE is computed using the formula $\partial_x U_f(0, x) = m_f(0, |x|)\frac{x}{|x|^3}$, where $m_f(0, r)$ is obtained from the particles as described in the context of the linearised system. In particular, we again take into account the order of the integrand of $m(0, r)$ close to the radial origin $r = 0$ by employing Simpson's rule to compute the integral. Note that the assumption of spherical symmetry significantly simplifies this step since we only have to compute a one-dimensional integral to compute the right-hand side of (8.4.2) instead of solving the three-dimensional Poisson equation. When evolving the particles, we deliberately avoid using radial coordinates and instead change to Cartesian (x, v)-coordinates when solving the characteristic system. This prevents numerical errors arising from the (artificial) singularity at $r = 0$ in radial coordinates and has been developed in [48, 132]. Evolving the particles via (8.4.2) gives a good approximation of their position at time $\delta t > 0$ provided that the time step size δt is sufficiently small. In fact, for the particle propagation, we do not use (8.4.2) directly, which would correspond to the Euler method, but instead employ a suitable adaptation of RK4 similar to [50]. Also note that the value of f and the cell size associated to each numerical particle remain constant during the particle evolution since the phase space density f is constant along the characteristic flow of the Vlasov equation and this flow is measure-preserving, cf. [143, Lemmas 1.2 and 1.3]. Hence, the particles represent the phase space distribution $f(\delta t)$ at the next time step δt after updating their positions. Iterating this entire process results in a simulation of the Vlasov-Poisson system.

We choose similar numerical parameters as for the simulation of the linearised Vlasov-Poisson system. In particular, we always use a total of 10^7–10^8 numerical particles. To be able to run the program within reasonable time, we employ a shared-memory parallelisation similar to [48, 50, 81, 132], which is again implement using the Pthreads API in `C++`. We refer to [80] for a GPU-based parallelisation scheme in a related context.

Similar to the linearised case, we evaluate the accuracy of the simulation by monitoring the conserved quantities of the Vlasov-Poisson system, see [143, Sc. 1.5] for an overview over such conserved quantities. The first one is the *total energy*

$$E_{\mathrm{tot}}(f) \coloneqq E_{\mathrm{kin}}(f) + E_{\mathrm{pot}}(f), \tag{8.4.3}$$

with kinetic and potential parts given by (3.1.19) and (3.1.20), respectively. The other conserved quantity we consider here is the total mass of f given by (8.3.12). It is straightforward to numerically compute these quantities by adding up the contributions of all particles with suitable weights.

In order to analyse the solution $f = f(t)$, we consider the evolutions of $E_{\mathrm{kin}}(f(t))$, $E_{\mathrm{pot}}(f(t))$, and $U_f(t,0)$; the latter quantity can be computed from the local mass $m_f(t,r)$ via (8.3.13). Furthermore, we analyse the evolution of the support of the solution by considering the minimal and maximal radius of the solution given by

$$R_{\mathrm{min}}(t) \coloneqq \inf\{r > 0 \mid \exists (w,L)\colon f(t,r,w,L) > 0\}, \tag{8.4.4}$$

$$R_{\mathrm{max}}(t) \coloneqq \sup\{r > 0 \mid \exists (w,L)\colon f(t,r,w,L) > 0\}, \tag{8.4.5}$$

as well as the minimal and maximal w-values of the solution which are defined similarly. In addition, we study the behaviour of the macroscopic functions $\rho_f(t)$, $m_f(t)$, and $U_f(t)$.

In order to analyse the dynamics of the Vlasov-Poisson system close to a fixed steady state f_0, we consider solutions launched by initial data of the form

$$f(0) = \alpha\, f_0, \tag{8.4.6}$$

which should be viewed as a perturbation of the steady state. The strength of the perturbation is determined by the difference of the *perturbation amplitude* α and 1. We choose this type of perturbation here for the sake of simplicity and because its strength is directly determined by the parameter α. It should, however, be emphasised that it was found in [132] that different perturbations, including dynamically accessible ones, always lead to qualitatively similar behaviour of the resulting solutions.

The Isotropic Polytropic Steady State $k = 1 = R_{\mathrm{max}}$

We again start by considering the isotropic polytrope (1.2.3) with polytropic exponent $k = 1$ and parameter $\kappa > 0$ chosen s.t. $R_{\mathrm{max}} = 1$; such κ exists by Appendix B.

We first analyse the solution of the Vlasov-Poisson system launched by the initial condition (8.4.6) with perturbation amplitude $\alpha = 1.01$. The evolutions of the kinetic, potential, and total energy for this solution are shown in Figure 8.4.1.

We clearly see that the solution exhibits an undamped oscillatory behaviour. More precisely, it seems like the solution travels to a state close to the original equilibrium at the beginning (i.e., for small t) and then oscillates around this new state undamped. Given the oscillatory behaviour of the solutions of the linearised Vlasov-Poisson system for this steady state and the arguments from Section 3.1, such oscillations are to be expected. We will analyse this oscillation, and how similar it is to the oscillations observed on the linearised level, below in more detail in the context of general isotropic polytropes. Before doing so, we want to discuss further aspects of the above solution.

Firstly, we note that the oscillatory behaviour is visible in all macroscopic quantities associated to the solution. Figure 8.4.2 shows the behaviour of the value of the gravitational potential at the spatial origin – recall (8.3.13) for a formula for this quantity – as well as

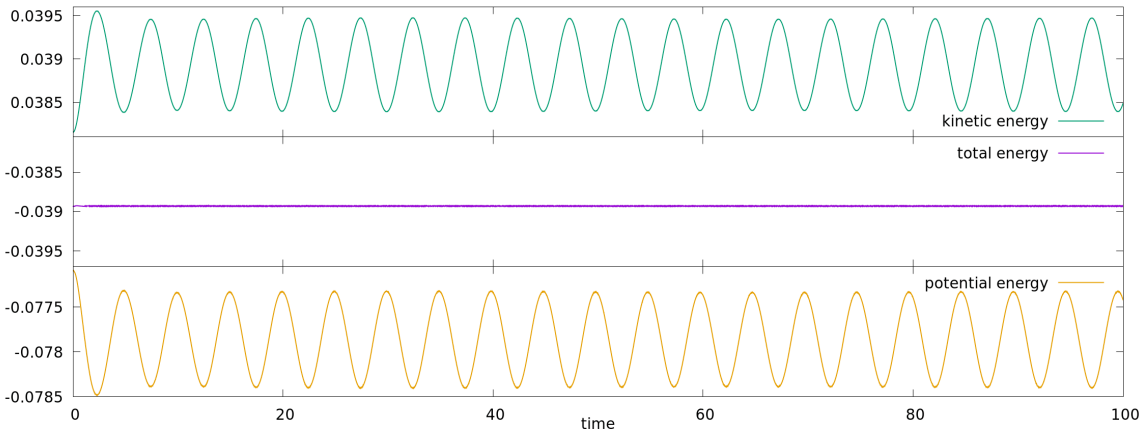

Figure 8.4.1: Evolution of the total energy E_{tot} and its kinetic and potential parts E_{kin} and E_{pot} (see (3.1.19), (3.1.20), and (8.4.3) for the definitions of these quantities) for the solution of the Vlasov-Poisson system launched by the initial condition $1.01\, f_0$, where f_0 is the isotropic polytrope with $k = 1$ and $R_{\max} = 1$.

the behaviour of the maximal radius $R_{\max}(t)$.[191] The former evidently behaves similarly to the kinetic and potential energies. The time evolution of the maximal radius looks significantly more chaotic than the other plots. This is because this quantity can be affected by the behaviour of a small number of numerical particles (out of the $\approx 4 \cdot 10^7$ numerical particles used for the simulation) and is hence vulnerable to even the slightest numerical inaccuracies. Nonetheless, we see that the maximal radius also exhibits an undamped oscillatory behaviour. This is consistent with the pulsation motivated by Sections 3.2–3.3 in the case of an eigenvalue of the linearised operator.

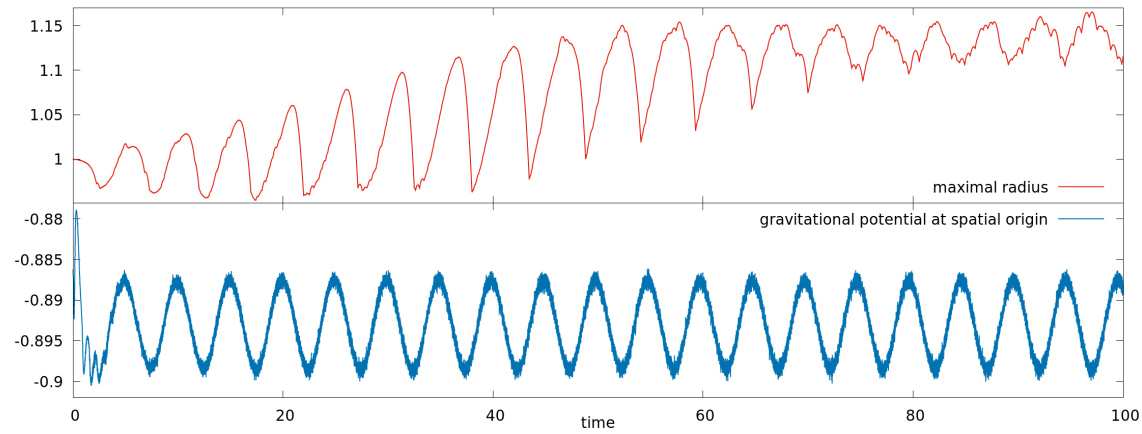

Figure 8.4.2: Evolutions of the maximal radius $R_{\max}(t)$ (top panel, recall (8.4.5) for the definition of this quantity) and $U_f(t, 0)$ (bottom panel) for the solution of the Vlasov-Poisson system launched by the initial condition $1.01\, f_0$, where f_0 is the isotropic polytrope with $k = 1$ and $R_{\max} = 1$.

The pulsating nature is even better visible in the macroscopic functions associated to the solution. In Figure 8.4.3, the time evolutions of several such functions are shown. Recall

[191] The minimal radius $R_{\min}(t)$ always remains (very close to) 0. This means that the solution preserves the ball-like structure of the steady state.

Figure 8.1.1 for plots of the same macroscopic functions for the unperturbed steady state.

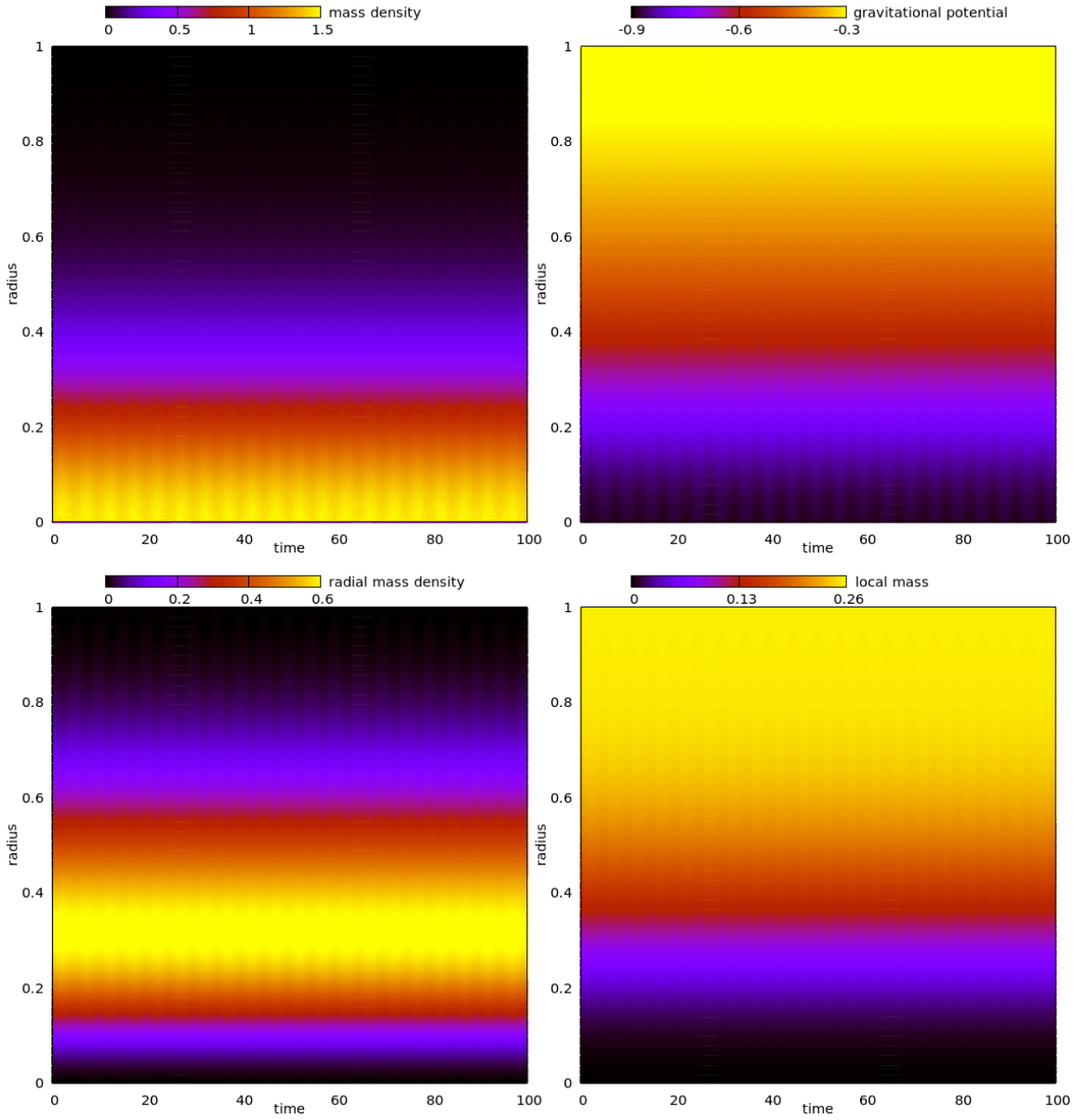

Figure 8.4.3: Values of the mass density $\rho_f = \rho_f(t,r)$ (top left panel), gravitational potential $U_f = U_f(t,r)$ (top right panel), radial mass density $4\pi r^2 \rho_f(t,r)$ (bottom left panel), and local mass $m_f = m_f(t,r)$ (bottom right panel) at different time-radius pairs (t,r) for the solution f of the Vlasov-Poisson system launched by the initial condition $1.01\, f_0$, where f_0 is the isotropic polytrope with $k = 1$ and $R_{\max} = 1$.

To see that these functions as a whole are indeed time-periodic, we plot $(t_1, t_2) \mapsto \|\rho_f(t_1) - \rho_f(t_2)\|_2$ and $(t_1, t_2) \mapsto \|U_f(t_1) - U_f(t_2)\|_2$ in Figure 8.4.4. The behaviour of these differences is very similar to [132, Figs. 2 and 4]. These figures were the inspiration for Figure 8.4.4, although different solutions are considered there. In the left panel of Figure 8.4.4, we see that $\|\rho_f(t_1) - \rho_f(t_2)\|_2$ does not become zero (black colour) for $t_1 \neq t_2$, but at most close to zero (violet colour). This is due to numerical noise in the mass density ρ_f. The figure nonetheless clearly shows that $t \mapsto \rho_f(t)$ is time periodic. In the

right panel of Figure 8.4.4, we see that $\|U_f(t_1) - U_f(t_2)\|_2$ indeed vanishes periodically for $t_1, t_2 > 0$. This is because the numerical noise contained in the mass density ρ_f cancels out during the two radial integrations in the computation of the gravitational potential U_f.

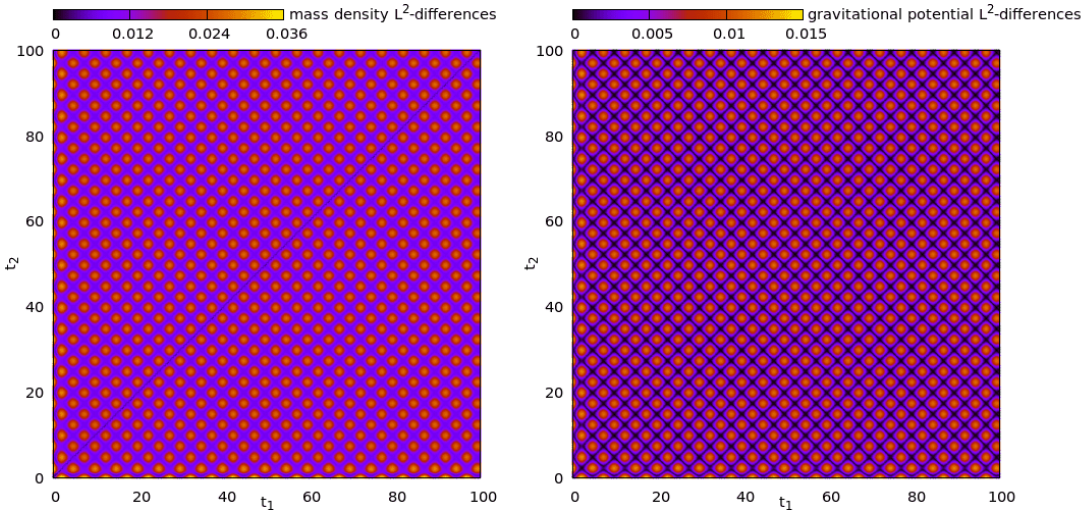

Figure 8.4.4: L^2-differences of the mass density ρ_f (left panel) and the gravitational potential U_f (right panel) at different time steps, i.e., $\|\rho_f(t_1) - \rho_f(t_2)\|_2$ and $\|U_f(t_1) - U_f(t_2)\|_2$ for different $t_1, t_2 \geq 0$, for the solution f of the Vlasov-Poisson system launched by the initial condition $1.01\, f_0$, where f_0 is the isotropic polytrope with $k = 1$ and $R_{\max} = 1$.

Although we will not further illustrate this here, we note that the minimal and maximal values of the radial velocity w in the support of the solution exhibit a similar evolution as the maximal radius $R_{\max}(t)$, see Figure 8.4.2: These quantities also behave quite chaotic, but an oscillatory motion is nonetheless clearly visible. This is consistent with the arguments from Section 3.3 which explain that the whole phase space support of the solution oscillates in the case of an oscillation on the linearised level.

Altogether, we conclude that the oscillation is indeed visible in all macroscopic quantities associated to the solution. The same is also true for other solutions which we will analyse below. This is similar to the linearised level, recall Observation 8.3.1.

Observation 8.4.1 (All Macroscopic Quantities Behave Equivalently)**.** *The qualitative behaviour of a solution of the Vlasov-Poisson system can be observed alike in the evolutions of E_{kin}, E_{pot}, $R_{\max}(t)$, and $U_f(t, 0)$, as well as in macroscopic functions like ρ_f and U_f. In particular, an oscillatory behaviour indeed occurs as a pulsation, i.e., the spatial support of the solution expands and contracts in a time-periodic way.*

Secondly, let us briefly discuss the numerical accuracy of the simulation. As already visible in Figure 8.4.1, the total energy is preserved to high accuracy during the evolution. Concretely, until the final time $T = 100$, the relative error of the total energy, i.e., the absolute value of $\frac{E_{\text{tot}}(f(t)) - E_{\text{tot}}(f(0))}{E_{\text{tot}}(f(0))}$, remains smaller than 0.01%. The relative error of the total mass even remains smaller than 0.002%.[192] Comparing these errors to the ones which occurred for the simulations of the linearised Vlasov-Poisson system, we come to the (surprising) conclusion that we can, in fact, simulate the non-linearised Vlasov-Poisson more

[192] It is to be expected that the error of the total mass is smaller than the errors of other conserved quantities, like the total energy, because the conservation of the total mass is somewhat build into the particle-in-cell scheme, cf. [153].

accurately than the linearised system. The reason for this is probably that the particle-in-cell method which we use to simulate both systems is more adapted to the non-linearised system. Anyway, the small error values give us great confidence that our numerical simulations of the Vlasov-Poisson system are indeed accurate. In the remaining parts of this section we will not further discuss the numerical accuracy, but note that the errors are always of a similar order of magnitude as those of the above simulation.

Thirdly, as already mentioned above, the oscillation takes place around a state which is different from the original steady state. This is, for instance, well visible in Figure 8.4.1: The oscillation of the kinetic energy takes place around a value which is larger than the initial value, which is in turn larger than the kinetic energy of the steady state. This phenomenon is also visible in Figures 8.4.2– 8.4.4. Given that the steady state is (non-linearly) stable, this behaviour might be surprising. However, it is only due to the strength of the perturbation used above. If one decreases the strength of the perturbation by choosing the perturbation amplitude α closer to 1, the oscillation of the solution takes place closer to the original steady state. This is well visible in Figure 8.4.5, where solutions launched by different perturbation amplitudes are depicted. Let us note that the same effect – i.e., oscillations taking place around a state different from the original equilibrium – has also been observed in [132] for different perturbations, including dynamically accessible ones. This shows that this effect is not only due to the naïve perturbation type chosen here.

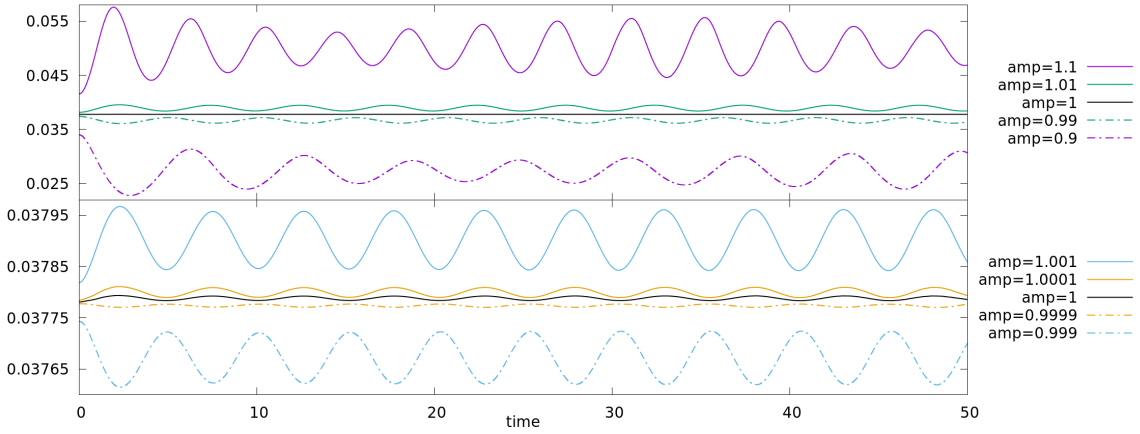

Figure 8.4.5: Evolution of the kinetic energy E_{kin} for the solutions of the Vlasov-Poisson system launched by the initial conditions αf_0 with perturbation amplitudes $\alpha \in \{1.1, 1.01, 1.001, 1.0001, 1, 0.9999, 0.999, 0.99, 0.9\}$, where f_0 is the isotropic polytrope with $k = 1$ and $R_{\max} = 1$.

Let us further analyse Figure 8.4.5. We see that stronger perturbations not only lead to the oscillations to take place further away from the original steady state, but also to different oscillation periods. For instance, the (fundamental) oscillation periods of the solutions launched by the perturbation amplitudes $\alpha = 1.1$, $\alpha = 1.01$, and $\alpha = 1.001$ are all different from one another. In the cases $\alpha = 1.001$, $\alpha = 1.0001$, and $\alpha = 1$, the oscillation periods seem quite identical to one another. Notice that in the case $\alpha = 1$, the slight oscillation of the solution is due to numerical errors acting in the same way as a perturbation. The same effects are also visible for perturbation amplitudes $\alpha \leq 1$, more precisely, the (fundamental) oscillation periods are different for $\alpha = 0.9$, $\alpha = 0.99$ and $\alpha \in \{0.999, 0.9999, 1\}$. This behaviour also occurs for all other steady state which we will investigate throughout this section.

Observation 8.4.2 (Oscillations for Different Perturbations)**.** *Consider a steady state for which the solutions of the Vlasov-Poisson system close to it exhibit an undamped oscillatory behaviour. Such oscillations take place closer to the steady state if the strength of the perturbation is reduced. In addition, the fundamental oscillation periods converge to a fixed value as the strengths of the perturbations tend to zero.*

A similar observation has previously been made in [132, Fig. 5]. There, it is further concluded that the limiting oscillation period is independent of the perturbation type.

As an aside, let us briefly discuss another aspect of the solutions shown in Figure 8.4.5. In the case of a stronger perturbation, the solutions exhibit a second oscillatory motion in addition to the fundamental oscillation. Concretely, the solution launched by the perturbation amplitude $\alpha = 1.1$ has a fundamental oscillation period of ≈ 4.2 and shows another oscillation with a larger period of ≈ 35.4.[193] An explanation for this behaviour may be that the strong perturbation carries parts of the solution to different steady states, around which they oscillate with different periods. The presence of multiple oscillations for solutions which are perturbed rather strongly has also been observed in [132, Figs. 7 and 8]. Here, we will not discuss this phenomenon further and instead focus on solutions which are closer to a steady state, as only such solutions are related to suitable solutions of the linearised Vlasov-Poisson system.

Isotropic Polytropic Steady States

We next consider solutions of the Vlasov-Poisson system close to general isotropic polytropes (1.2.3). As before, we always choose the parameter $\kappa > 0$ s.t. $R_{\max} = 1$ for the resulting steady states, cf. Appendix B. The evolutions of the kinetic energies for different such solutions are shown in Figure 8.4.6.

We see that the solutions close to isotropic polytropes with polytropic exponents $k \in \{\frac{1}{2}, 1\}$ exhibit an undamped oscillatory behaviour. As stated in Observation 8.4.1, these oscillations are of pulsating nature. For larger polytropic exponents $k \in \{\frac{3}{2}, 2, \frac{5}{2}, 3\}$, the solutions also exhibit an oscillatory behaviour, but the oscillation fully damps out over time. This damping seems to be stronger, i.e., faster, for larger polytropic exponents. Similar to the oscillatory case, cf. Observation 8.4.2, the solutions do not converge to the original steady state, but to a state close by. Reducing the perturbation strength again leads to the limiting configuration to be closer to the original equilibrium. Let us also note that the "noise" which is visible in the cases $k \in \{\frac{5}{2}, 3\}$ seems to be of pure numerical nature; increasing the numerical accuracy reduces it. Furthermore, the damping is also visible in the evolution of other macroscopic quantities associated to the solution. In Figures 8.4.7 and 8.4.8, the evolutions of several macroscopic functions of a solution close to the isotropic polytrope $k = \frac{3}{2}$ are visualised. These figures should be compared to Figures 8.4.3 and 8.4.4, where the same quantities of a similar solution in the case $k = 1$ are plotted. Let us note that, despite the damping, the differences $\|\rho_f(t_1) - \rho_f(t_2)\|_2$ in the left panel of Figure 8.4.8 do not seem to become zero (black colour) for large $t_1 \neq t_2$, but only close to zero (violet colour). This is again due to numerical noise being present on the level of the mass density ρ_f. In the right panel of Figure 8.4.8, we see that $\|U_f(t_1) - U_f(t_2)\|_2$ indeed becomes zero for sufficiently large $t_1, t_2 > 0$, which illustrates the damping quite nicely.

To study where the transition from undamped oscillatory behaviour to full damping takes place, we depict the behaviour of solutions close to the isotropic polytropes with

[193] These oscillation periods have been determined by applying the discrete Fourier transform to $E_{\text{kin}}(f(t))$.

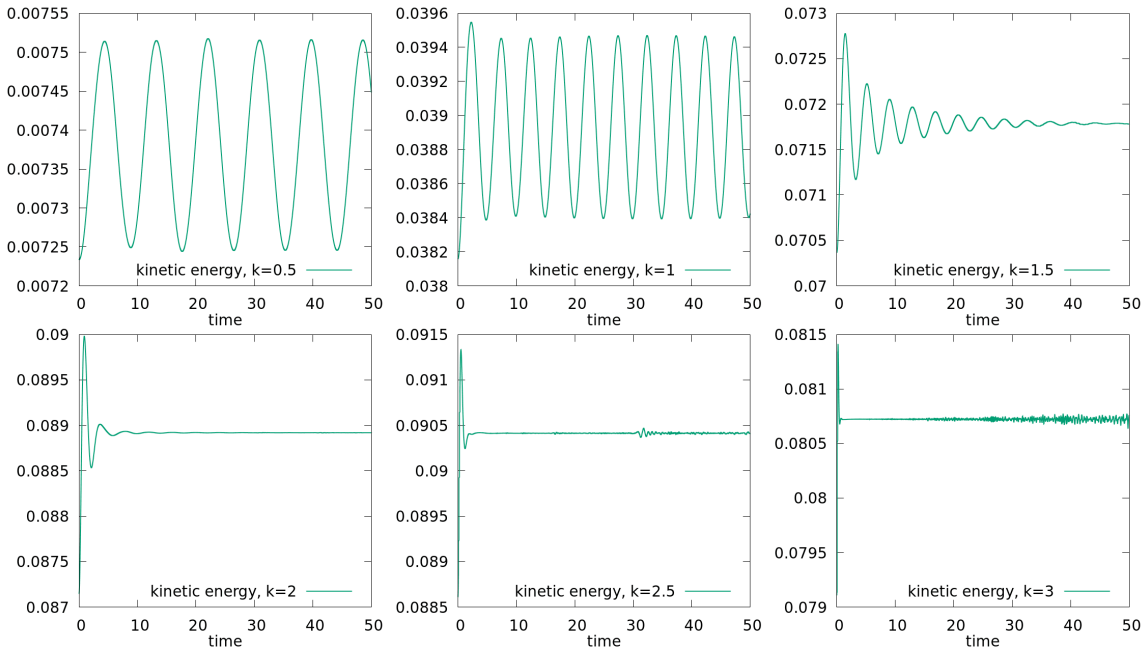

Figure 8.4.6: Evolution of the kinetic energy E_{kin} for the solutions of the Vlasov-Poisson system launched by the initial conditions $1.01\, f_0$ for the isotropic polytropes f_0 with $k \in \{\frac{1}{2}, 1, \frac{3}{2}, 2, \frac{5}{2}, 3\}$ and $R_{\max} = 1$.

polytropic exponents $k \in \{1.2, 1.25, 1.3\}$ in Figure 8.4.9. We use a weaker perturbation than above to be sure that the effects are indeed determined by the respective steady state.

In Figure 8.4.9, the solution close to the isotropic polytrope with polytropic exponent $k = 1.2$ oscillates and the oscillation does not seem to fully damp out, i.e., a part of the solution oscillates undamped. In contrast, in the case $k = 1.3$, the oscillation gets fully damped. For the polytropic exponent $k = 1.25$, we are not quite sure which of these two behaviours is present – the solution might be fully damped as well, but the damping proceeds too slowly to be certain. Anyway, we have observed only this one transition from undamped oscillatory to fully damped behaviour. More precisely, considering further solutions has shown that solutions close to isotropic polytropes with polytropic exponents $0 < k \leq 1.2$ exhibit an undamped oscillatory behaviour, while the solutions close isotropic polytropes with $1.2 \leq k \leq 3.2$ are fully damped; for the same reasons as in Section 8.1, we do not choose $k > 3.2$ here. In particular, Figure 1.1.1 shows the time evolutions of solutions close to the isotropic polytropes with $k = \frac{1}{2}$ (left panel) and $k = \frac{7}{4}$ (right panel). We have chosen a rather strong perturbation ($\alpha = 1.1$) there so that the qualitatively different behaviours of the solutions are clearly visible.

Observation 8.4.3 (Oscillations vs. Damping for Isotropic Polytropes at the Non–Linearised Level)**.** *The solutions of the (non-linearised) Vlasov-Poisson system close to isotropic polytropes with polytropic exponents* $0 < k \leq 1.2$ *exhibit a partially undamped oscillatory behaviour. In contrast, any solution close to an isotropic polytrope with polytropic exponent* $1.3 \leq k \leq 3.2$ *is fully damped (on the macroscopic level), in the sense that its macroscopic quantities are convergent.*

This observation is consistent with previous numerical investigations of the isotropic polytropes, which we review now: In [115], it was observed that the kinetic and potential energies of solutions close to the isotropic polytrope $k = \frac{3}{2}$ exhibit an oscillatory behaviour.

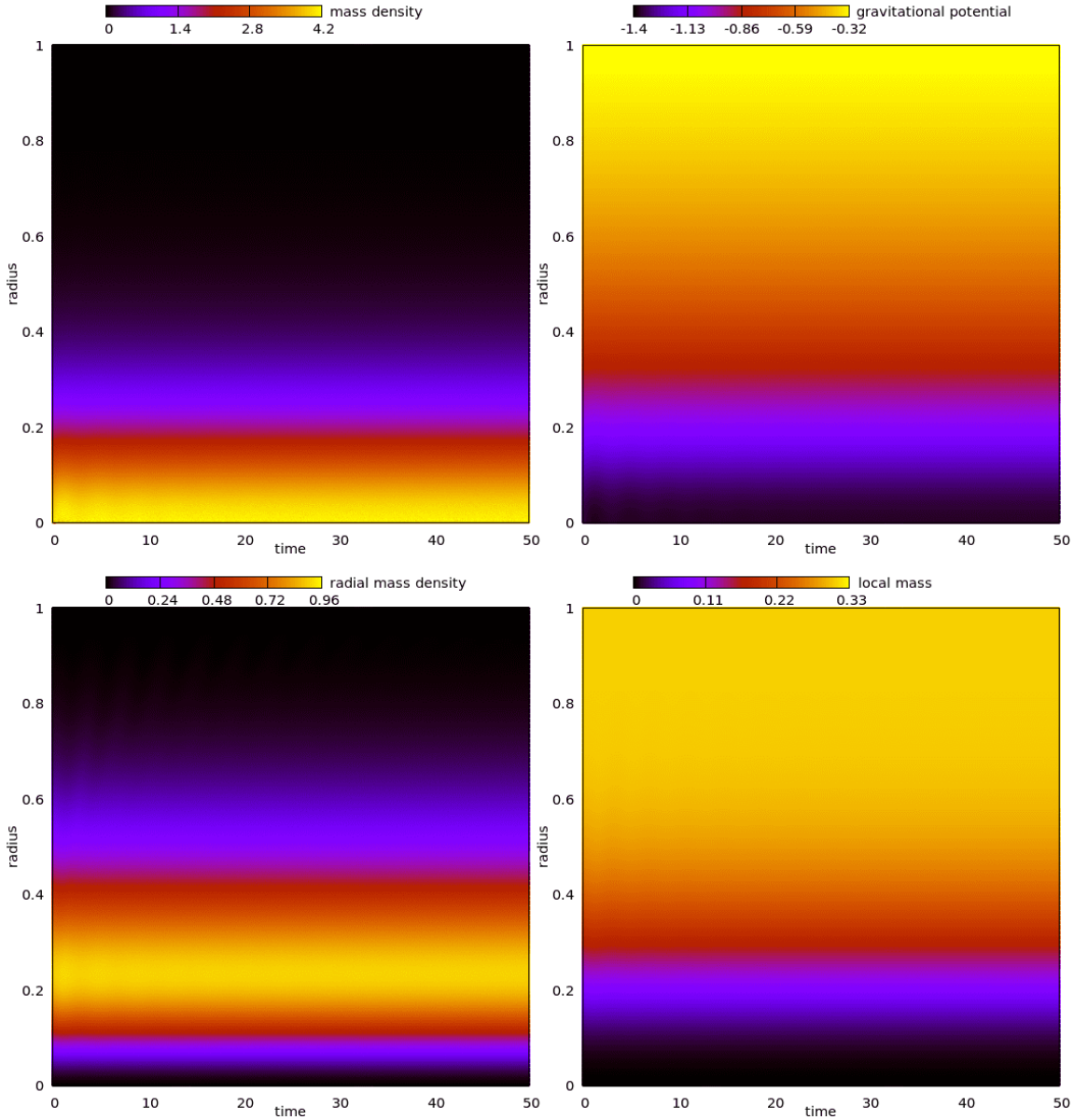

Figure 8.4.7: Values of the mass density $\rho_f = \rho_f(t,r)$ (top left panel), gravitational potential $U_f = U_f(t,r)$ (top right panel), radial mass density $4\pi r^2 \rho_f(t,r)$ (bottom left panel), and local mass $m_f = m_f(t,r)$ (bottom right panel) at different time-radius pairs (t,r) for the solution f of the Vlasov-Poisson system launched by the initial condition $1.01\, f_0$, where f_0 is the isotropic polytrope with $k = \frac{3}{2}$ and $R_{\max} = 1$.

In accordance with Observation 8.4.3, these oscillations seem to be damped. These findings were verified in [176] with a different numerical method which is more adapted to the Vlasov-Poisson system than the N-body code used in [115]. In [168], somewhat damped pulsations were observed for solutions close to the Plummer sphere which corresponds to the polytropic exponent $k = \frac{7}{2}$. In [159], it was found that perturbing an isotropic polytrope with polytropic exponent $k \leq 1$ leads to "very weakly decaying modes"; we even go so far here as to call these modes undamped. Again, these oscillations were also observed for the supports of the solutions. It is also stated in [159] that the oscillations are "strongly

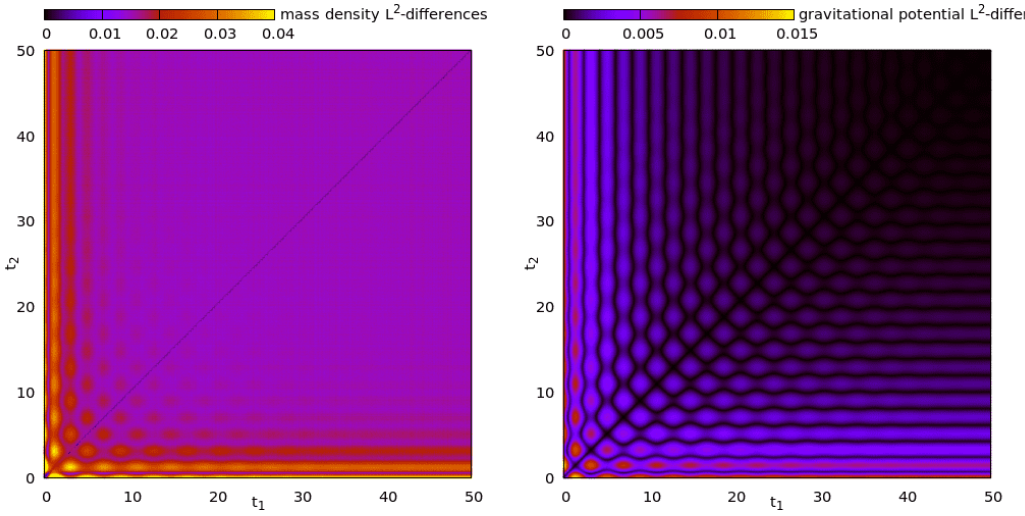

Figure 8.4.8: L^2-differences of the mass density ρ_f (left panel) and the gravitational potential U_f (right panel) at different time steps, i.e., $\|\rho_f(t_1) - \rho_f(t_2)\|_2$ and $\|U_f(t_1) - U_f(t_2)\|_2$ for different $t_1, t_2 \geq 0$, for the solution f of the Vlasov-Poisson system launched by the initial condition $1.01\, f_0$, where f_0 is the isotropic polytrope with $k = \frac{3}{2}$ and $R_{\max} = 1$.

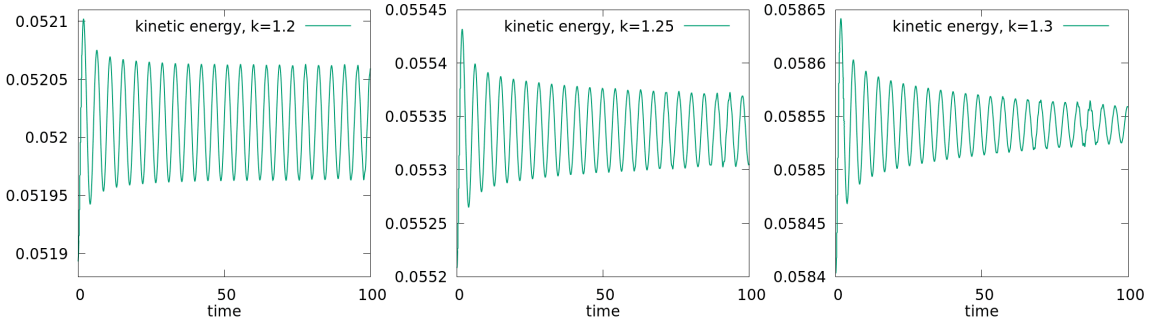

Figure 8.4.9: Evolution of the kinetic energy E_{kin} for the solutions of the Vlasov-Poisson system launched by the initial conditions $1.001\, f_0$ for the isotropic polytropes f_0 with $k \in \{1.2, 1.25, 1.3\}$ and $R_{\max} = 1$.

damped" for the isotropic polytropes with polytropic exponents $k \geq 1.2$. Given that the findings from [159] are based on N-body simulations (which were probably not as accurate as the simulations here due to the lower availability of computational resources 25 years ago), this is nonetheless quite consistent with Observation 8.4.3. In [124], solutions close to isotropic polytropes with polytropic exponents $k \in \{\frac{1}{2}, \frac{3}{2}, \frac{5}{2}, \frac{7}{2}\}$ (as well as $k \in \{-\frac{3}{2}, -\frac{1}{2}\}$) were studied. It was found that the kinetic energy oscillates undamped in the cases $k \leq \frac{1}{2}$, and that the behaviour is qualitatively different for $k \geq \frac{3}{2}$. The most recent numerical study of the isotropic polytropes was conducted in [132]. It is clearly visible in [132, Fig. 6] that perturbing the isotropic polytrope with $k = \frac{1}{2}$ leads to an undamped oscillatory behaviour, while perturbing the isotropic polytrope with $k = 1.6$ leads to a fully damped solution. For the solution close to the isotropic polytrope $k = 1.2$ shown in [132, Fig. 6], it is unclear whether the oscillation damps out entirely; the behaviour of this solution is very much similar to the one shown in the left panel of Figure 8.4.9.

Let us now turn to the primary aspect of this section: Comparing the solutions of the non-linearised Vlasov-Poisson system to the solutions of the linearised system. The

reader has probably already noticed that the solutions discussed in this section behave very similarly to the ones discussed in the previous section. Concretely, the partially undamped oscillatory behaviour of the solution of the non-linearised Vlasov-Poisson close to the isotropic polytrope with polytropic exponent $k = 1$ visualised in Figures 8.4.1–8.4.4 is similar to the behaviour of the solutions of the linearised Vlasov-Poisson for the same steady state, recall Figures 8.3.1–8.3.5. Likewise, the fully damped behaviour close to the isotropic polytrope $k = \frac{3}{2}$ is similar to the behaviour of the solutions of the respective linearised Vlasov-Poisson system, cf. Figures 8.4.6–8.4.8 and Figures 8.3.6–8.3.8. To further illustrate these similarities, the solutions on the linearised and non-linearised levels for these steady states are shown together in Figure 8.4.10.

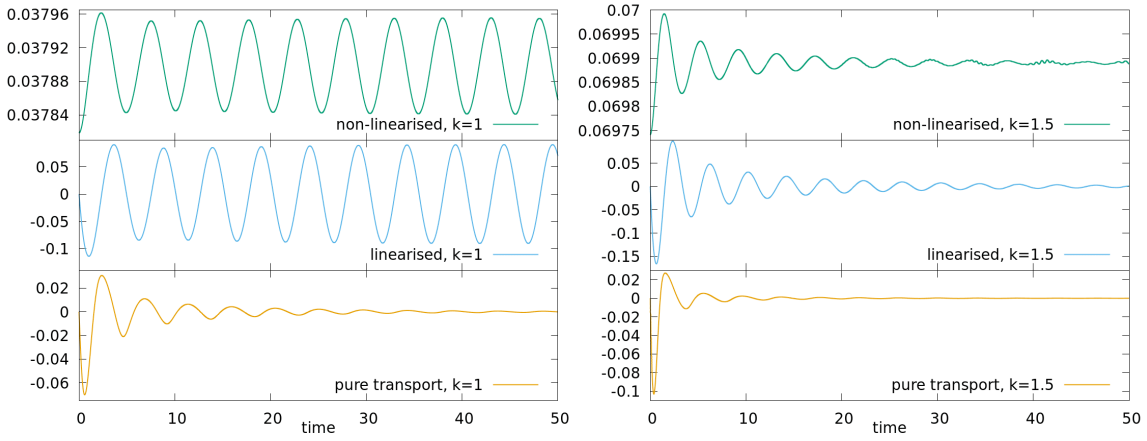

Figure 8.4.10: The top panels show the evolutions of the kinetic energy E_{kin} for the solutions of the Vlasov-Poisson system launched by the initial conditions $1.001\, f_0$ for the isotropic polytropes f_0 with polytropic exponents $k \in \{1, \frac{3}{2}\}$ and $R_{\max} = 1$. Below are the evolutions of the linearised kinetic energy (8.3.10) of the solutions of the linearised Vlasov-Poisson system (middle) and the pure transport equation (8.3.14) (bottom) launched by the initial condition $w\,|\varphi'(E)|$ for the same two steady states.

We can see in Figure 8.4.10 that the oscillations in the case $k = 1$ on the non-linearised and linearised level are both partially undamped and have the same oscillation period. The oscillations are, however, slightly shifted due to the different behaviours at the beginning of the simulations; this is to be expected in the light of Figure 8.3.5. Further note that we have chosen a rather weak perturbation for the solution of the non-linearised system; if we would have chosen a stronger perturbation, the oscillation period would be sightly different from the one on the linearised level, recall Observation 8.4.2. For the polytropic exponent $k = \frac{3}{2}$, we can also see that the fundamental oscillation periods are identical on the non-linearised and on the linearised levels, and that the damping seems to be equally strong, i.e., fast, on both levels.

In Figure 8.4.10, we also depicted the behaviour of the respective solutions of the pure transport equation. As noted in Observation 8.3.5, these solutions behave in a qualitatively different way to the ones of the linearised Vlasov-Poisson system. We can now conclude that the solutions of the pure transport equation behave in a qualitatively different way to the solutions of the actual non-linearised system: In the case $k = 1$, the solution of the pure transport equation is fully damped, while there is an undamped oscillation on the non-linearised level. Moreover, the fundamental oscillation periods are different from one another. In the case $k = \frac{3}{2}$, the solution is damped on the non-linearised and on the pure

transport level, but the damping is significantly stronger, i.e., faster, on the latter.

The same relations between the solutions of the non-linearised and linearised Vlasov-Poisson system (as well as the pure transport equation) are also present for general isotropic polytropes. This can be seen by comparing Figures 8.3.6, 8.3.11, and 8.4.6 to one another; we have also verified these relations for further polytropic exponents than the ones considered in these figures. Furthermore, by Observations 8.3.3 and 8.4.3, the solutions of the non-linearised Vlasov-Poisson system close to an isotropic polytrope are fully damped if, and only if, the solutions of the respective linearised system are fully damped.

Even though we only discussed the isotropic polytropes with κ-values s.t. $R_{\max} = 1$ thus far, further testing showed that the same relations also hold true for general $\kappa > 0$. In particular, this shows that the Eddington-Ritter type relation (B.0.23) between the parameter κ and the (fundamental) oscillation period p also holds on the non-linearised level. This was previously observed in [132, Sc. 4].

In addition, we will see below that the same relations also hold for all steady states we consider. Let us summarise these illuminating findings.

Observation 8.4.4 (Linearised and Non-Linearised Dynamics)**.** *The solutions of the non-linearised Vlasov-Poisson system close to a steady state behave similarly to the solutions of the respective linearised system. More precisely, if the solutions of the linearised Vlasov-Poisson system oscillate partially undamped for some steady state, the solutions of the non-linearised system close to the same steady state do so as well, and the oscillation periods are similar. If the solutions of the linearised system are fully damped, so are the solutions of the non-linearised Vlasov-Poisson system close to the respective steady state, and the damping seems to be equally strong. All these statements require that the solution of the non-linearised system is sufficiently close to the respective steady state, i.e., the perturbation is sufficiently weak.*

In contrast, the solutions of the pure transport equation (8.3.14) *behave in a qualitatively different way to the solutions of the non-linearised Vlasov-Poisson system.*

Although the arguments from Chapter 3 make it quite plausible that the behaviour of solutions of the non-linearised Vlasov-Poisson system close to a steady state can be described qualitatively by the linearised system, this should not be taken for granted. For other systems, there are time-periodic solutions on the linearised level, but the solutions on the non-linearised level are nonetheless damped, cf. [164].

King Models

Let us next consider the solutions of the Vlasov-Poisson system close to King models (1.2.4) with different values of $\kappa > 0$. As for the isotropic polytropes, we again observed that such solutions behave qualitatively similar to the solutions of the linearised Vlasov-Poisson system, i.e., Observation 8.4.4 also holds for the King models. Concretely, as summarised in Observation 8.3.7, solutions close to King models with small κ-values exhibit a partially undamped oscillatory behaviour, while the solutions are fully damped for larger values of κ. These two qualitatively different behaviours were also observed in previous numerical investigations, although the explicit dependence on the parameter κ found here is, to the author's knowledge, new. More precisely, it was observed in [132] that perturbing a King model may lead to undamped oscillations similar to the isotropic polytropic case. In [159, Sc. 2], it was found that the solution close to a (different) King model is fully damped.

Anisotropic Polytropes

Lastly, we consider the solutions of the Vlasov-Poisson system close to general polytropes (1.2.5). As in Section 8.3, we study polytropes with $L_0 = 0$ as well as the polytropic shells corresponding to $L_0 > 0$. For both of these types of steady states, the solutions close to them behave in a qualitatively similar way as the solutions of the respective linearised Vlasov-Poisson system, i.e., Observation 8.4.4 also holds for the anisotropic polytropes. Concretely, as stated in Observation 8.3.8, whether solutions close to a polytropic steady state with $L_0 = 0$ are damped depends linearly on the polytropic exponents k and ℓ. This is consistent with [132, Fig. 6 (d)], where it was observed that a solution close to a polytrope with $k = 3$, $\ell = 5$, $L_0 = 0$ oscillates undamped; notice that $\frac{\pi^2}{12}\,3 - \frac{\pi}{3}\,5 < 1$. In addition, it was observed in [132, Sc. 4] that the Eddington-Ritter relation (B.0.23) also holds for the (fundamental) oscillation periods of the solutions of the non-linearised system close to polytropes with $L_0 = 0$. Our simulations verify this finding. Similar to Observation 8.3.9, the behaviour of solutions of the non-linearised system close to polytropes with $k, \ell > 0$ and $0 < L_0 \ll 1$ is similar to the case $L_0 = 0$. When choosing $L_0 > 0$ not too small, the solutions close to the resulting polytrope oscillate undamped. The latter is in agreement with [132, Sc. 5], where it is stated that solutions of the non-linearised Vlasov-Poisson system close to all polytropic shells are undamped – probably only not too small values of $L_0 > 0$ were considered there. Any such oscillation is again of pulsating nature which can now also be observed in the oscillation of the inner radius $R_{\min}(t) > 0$. A similar behaviour was also observed in [132, Fig. 4].

Overall, we hence conclude that the behaviour of solutions of the Vlasov-Poisson system close to all the steady states we considered here are indeed accurately described by the linearised Vlasov-Poisson system.

Chapter 9

Outlook

As our joint journey comes to its close, let us recall the metaphor from the end of the introduction. Our odyssey through the mathematical landscape has often taken us down thorny paths – think of the 118 lemmas we have overcome in this thesis. Nevertheless, we hope that our faithful reader will remember the journey as a rewarding one, and has found pleasure in the 15 propositions and eight theorems that we have encountered. But on the distant horizon, veiled in the mist of the yet unproven, we have caught glimpses of even more beautiful results: Some of them are mentioned in the 58 remarks in this thesis, but mainly they are found in the 25 numerical observations in Chapter 8. We wish to gather here our thoughts on some of these results, in the deep hope that future endeavours will reveal the paths to their proofs.

Thus, let us now leave the metaphors behind and turn to the discussion of some open questions and approaches for proving them. The presented topics are of course subjectively chosen; the list could be much longer and completely different. For instance, a similar list with (partly) different topics can be found in [86, Sc. 11]. Our focus is on the issues we consider particularly important and enlightening, while it also seems realistic that they are solvable. More general issues like extending the analysis to a larger class of steady states, dropping the assumption of spherical symmetry, or transferring the results to the non-linearised regime are left for another day.

I. Properties of the Period Function

Despite the extensive analysis of the (radial) period function T in Appendix A, we saw at several places in this thesis that certain aspects of the linearised system depend on properties of T that we cannot rigorously prove (yet). For instance, if we knew which particles within the steady state support correspond to the largest periods, we could deduce the existence of an oscillatory mode in some situations, cf. Theorem 5.4.1 and Corollary 5.4.3. For this purpose, it would be beneficial if T were monotonic. Such monotonicity would also be crucial to show statements towards damping with the methods from Chapter 6 in further situations.

The numerical analysis from Section 8.2 shows that, for certain equilibria, the period function T is indeed monotonic on the steady state support. In particular, T always seems to be increasing in the particle energy E for isotropic steady states, cf. Observations 8.2.5 and 8.2.6. We discussed several possible approaches towards proving such monotonicity in Section A.3.3. We believe that the most promising one is to prove that G_L^{ref} (and/or H_L^{ref}) is positive on a suitable radial domain, cf. Lemma A.3.22. Notice that the numerics even indicate that G_L^{ref} is monotonic in the case of an isotropic steady state, cf. Figures 8.2.4

and 8.2.8, which would simplify proving its positivity.

In any case, any further knowledge of the properties of the radial period function would certainly expand our understanding of the linearised Vlasov-Poisson system.

II. Pulsations Around Isotropic Polytropes with Exponents $0 < k \ll 1$

Of all isotropic steady states which we considered here, it seems most promising to prove the presence of oscillatory modes for isotropic polytropes (1.2.3) with very small polytropic exponents $k > 0$. The reason for this is that the numerics indicate the applicability of Kunze's criterion for the existence of eigenvalues of $\mathcal{L}$ only for these isotropic steady states, i.e., the inequality (4.5.53) from Lemma 4.5.19 holds for these steady states, cf. Observation 8.2.11. In addition, the numerical simulations from Sections 8.3 and 8.4 show the occurrence of pulsating behaviour around these steady states on the linearised and non-linearised level.

One strategy to rigorously establish the existence of an eigenvalue of the linearised operator $\mathcal{L}$ for these steady states is to first verify Kunze's criterion in the case $k = 0$. Although isotropic polytropes with $k = 0$ are not permitted for the analysis of the linearised operator in Chapters 4 and 5 due to the assumption ($\varphi 5$), the simple form of their energy profile function $\Phi = \mathbb{1}_{]0,\infty[}$ makes them likely easier to be studied compared to isotropic polytropes with positive polytropic exponents k. If the inequality (4.5.53) holds for the polytropic exponent $k = 0$, continuity arguments show that it also holds for $0 < k \ll 1$. Indeed, the continuous dependence of the left-hand side of (4.5.53) on the polytropic exponent k (for some fixed $\kappa > 0$) follows trivially by (2.2.29), (2.2.48), and (4.5.54). The continuity of the right-hand side of (4.5.53) can be established with similar techniques as in Section 6.2.1, see [16, Sc. 7] for related arguments.

Concretely, for the isotropic polytrope with polytropic exponent $k = 0$ and parameter $\kappa = 1$, the left-hand side of Kunze's criterion (4.5.53) is approximately 49.63. This value can be computed explicitly using (2.2.29), (2.2.48), and (4.5.54). The right-hand side of Kunze's criterion is approximately 51.24 for this steady state; this value is based on a numerical computation of the maximum of the period function on the steady state support as described in Section 8.2. For a rigorous proof, all that remains to show is that the latter value is indeed larger than the former one. This requires establishing an upper bound on the values of the period function T on the steady state support which is as sharp as possible. As an alternative or as a tool for this, the use of interval arithmetic could be helpful.

III. Pulsations Around Polytropic Shells with $L_0 \gg 1$

Another class of steady states for which we consider the derivation of a rigorous proof of the existence of pulsating modes to be particularly promising are polytropes (1.2.5) with not too small values of $L_0 > 0$. For instance, the numerical analyses in Sections 8.2–8.4 indicate the presence of pulsating behaviour close to polytropes with $L_0 = 1 = \kappa$ and all polytropic exponents k and ℓ we considered.

In the case $k + \ell \leq 0$, Theorem 5.4.1 gives a criterion for the presence of pulsating modes which only requires knowledge of the period function T and works for all $L_0, \kappa > 0$. For general polytropic exponents, considering the limit $L_0 \to \infty$ could be helpful. More precisely, for fixed k, ℓ, and κ, one could study the limiting behaviour of both sides of Kunze's criterion (4.5.53) from Lemma 4.5.19 as $L_0 \to \infty$; recall that the numerics indicate that the criterion is satisfied for the polytropes considered here, cf. Observation 8.2.12. To determine the limit of the left-hand side of (4.5.53), it could be helpful to observe that $R_{\min} \to \infty$ as $L_0 \to \infty$ by (2.2.42). A lower bound on the limit of the right-hand side

of (4.5.53) could be established by using the estimate from Lemma A.1.1. An alternative approach would be to analyse the limit of the number $\mathfrak{M}$ from Theorem 5.3.1 as $L_0 \to \infty$.

IV. Eigenfunctions of $\mathcal{L}$

Although we have put a lot of effort into characterising the presence of eigenvalues of the linearised operator, our knowledge of the properties of the associated eigenfunctions is still rather limited. Obviously, by the definition of $\mathrm{D}(\mathcal{L})$ and Lemma 4.3.10, every eigenfunction is continuously differentiable w.r.t. the angle variable θ. The structure of the Fourier series w.r.t. θ of an eigenfunction is analysed in Remark 5.3.2. Further knowledge of the properties of eigenfunctions – e.g., their regularity w.r.t. (E, L) – is likely necessary in order to be able to prove the presence of pulsating behaviour at the non-linearised level. Furthermore, recall that the discussion in Chapter 3 shows that the properties of the eigenfunction determine the qualitative aspects of the oscillatory behaviour on the non-linearised level, e.g., which portions of the solution take part in the pulsation.

As demonstrated in Chapter 5, it can be helpful for our purposes to adopt certain techniques from quantum mechanics, more precisely, from the theory regarding the solutions of the (time-independent) Schrödinger equation. In this context, the regularity of solutions is, e.g., studied in [98, Thm. 11.7].

Unfortunately, the numerical methods from Chapter 8 are not particularly well suited for determining the eigenfunctions of $\mathcal{L}$. Nonetheless, one method to do so is outlined in Section 8.3: In the case of an oscillatory solution of the linearised Vlasov-Poisson system, we always observed that one part of the solution is damped. If one chooses an eigenfunction (or a linear combination of them) as the initial distribution, such damping cannot occur. Hence, by analysing whether this partial damping is present, one can test whether a given function is a linear combination of eigenfunctions. Alternatively, one can try to construct initial distributions which get fully damped to determine the orthogonal complement of the eigenfunctions.

In order to numerically study the properties of eigenfunctions, it would probably be more convenient to search for eigenvalues/eigenfunctions of the linearised operator via variational methods. Concretely, one could numerically determine the function(s) $f \in \mathrm{D}(\mathcal{L})$ with $\|f\|_H = 1$ which minimise(s) $\langle \mathcal{L}f, f\rangle_H$. By the usual variational principles (recall Lemma 4.5.16), these minimisers are eigenfunctions of $\mathcal{L}$ if the quadratic form gets smaller than the bottom of the essential spectrum. Such variational methods are implemented numerically in [161, 162] and, in context of the Einstein-Vlasov system, in [70] and [182, Ch. 8].

V. Further Techniques from Quantum Mechanics

The analysis of the eigenvalues of the linearised operator in Chapter 5 was based on the well-developed eigenvalue theory for Schrödinger operators. To gain further insights into our problem, it would certainly be helpful to study and transfer further results from this context. For instance, it seems possible to derive bounds on the sum of eigenvalues of $\mathcal{L}$ in the essential gap $\mathcal{G}$ similar to the Lieb-Thirring Inequalities [99, Ch. 4].

One step in this direction is taken in [117], where a bound on the number of eigenvalues of $\mathcal{L}$ in $\mathcal{G}$ is derived in a way qualitatively different to Theorem 5.3.3, recall Remark 5.3.4. Furthermore, the methods and results from [85, Ch. 4] – in particular, the statements regarding the dependence of the Mathur operator $\mathcal{M}_\lambda$ on λ, recall Remark 5.2.16 – could be valuable for deriving further results in this direction.

VI. Further Applications of the Criteria

One aim for future research is to develop applications of the criteria for the existence of oscillatory modes from Lemma 4.5.19 and Section 5.3 in addition to those already presented in Sections 5.4 and 6.4. For instance, being able to prove that the number $\mathfrak{M}$ from Theorem 5.3.1 is greater than one for steady states where $\mathfrak{M}$ is not infinite would expand the applications of Theorem 5.3.1.

Another application of Theorem 5.3.1 could be to prove that the presence of an oscillatory mode (in the essential gap) is "monotonic" along certain steady state families. For instance, Observation 8.3.3 indicates that all isotropic polytropic steady states with polytropic exponent $k > 0$ below some threshold exponent $k^* \approx 1.25$ possess an oscillatory mode, while no such oscillatory mode exists for $k > k^*$. It is hence possible that the number $\mathfrak{M}$ is non-increasing w.r.t. the polytropic exponent k along the isotropic polytropes (for a fixed value of κ or $R_{\max}$). By Observation 8.3.7, $\mathfrak{M}$ could also be monotonic w.r.t. the parameter κ in the case of the King models. Proving such monotonicity could be easier than actually determining whether $\mathfrak{M}$ is > 1 or ≤ 1 for a fixed steady state.

VII. Numerical Analysis of the Mathur Operator

To identify further applications of the criteria from Section 5.3, it would certainly be helpful to be able to numerically analyse the Mathur operator $\mathcal{M}_\lambda$ and the number $\mathfrak{M}$.

VIII. Existence of Pulsations for Small Shells Around a Point Mass

As discussed in Remark 6.4.2, it seems promising to prove the existence of oscillatory modes for polytropic steady states surrounding a point mass which are sufficiently small – i.e., $0 < \varepsilon \ll 1$ for a steady state as constructed in Proposition 6.2.2 – with polytropic exponents k and ℓ satisfying $k+\ell \leq 0$. The only statement that is left to be proven for this is that the period function T of a steady state with $0 < \varepsilon \ll 1$ is non-increasing w.r.t. L on $\mathbb{D}_0$. By Lemma 6.2.5, the period function is constant in L in the limiting case $\varepsilon = 0$, which is why the L-monotonicity of T for steady states with $0 < \varepsilon \ll 1$ cannot be established with the methods from Section 6.2.1. Instead, one would have to analyse the limit $\varepsilon \to 0$ to higher order. More precisely, the desired L-monotonicity would follow if $\partial_\varepsilon\big|_{\varepsilon=0}\partial_L T^\varepsilon \leq 0$ on a suitable domain.[194] Given that the proofs of the limiting statements in Section 6.2.1 were already a bit technical, it is to be expected that computing the derivative $\partial_\varepsilon\big|_{\varepsilon=0}\partial_L T^\varepsilon$ will also be technically quite involved. Nonetheless, $\partial_\varepsilon\big|_{\varepsilon=0}\partial_L T^\varepsilon$ should just be an expression containing the parameters M, L_0, k, ℓ, and κ, whose sign one can analyse.

IX. Damping in a Non-Perturbative Regime

So far, Theorem 6.6.1 is the only statement – besides [61, Thm. 1.2 (b)], on which it is based – showing damping around/towards a non-trivial steady state of the Vlasov-Poisson system (in the gravitational case). For the proof of Theorem 6.6.1, it is, however, essential to be in the perturbative regime of a small steady state surrounding a point mass. A natural aim is to establish a damping result in a non-perturbative regime too.

The numerics from Sections 8.3–8.4 indicate that there occurs damping for a large class of the steady states considered here, including the isotropic polytropes (1.2.3) with polytropic exponents $k \geq 1.3$. Hence, a natural steady state for proving damping is the

[194] It would, in fact, suffice to show $\partial_\varepsilon\big|_{\varepsilon=0}\partial_L T^\varepsilon \leq 0$ on a neighbourhood of $\{E = \kappa\}$ since, by Proposition 6.2.6, $\partial_E T^\varepsilon < 0$ on $\mathbb{D}_0^\varepsilon$ for $0 < \varepsilon \ll 1$ and $E_0^\varepsilon \to \kappa$ as $\varepsilon \to 0$.

Plummer sphere, cf. [19, Scs. 2.2.2(c) and 4.3.3(a)], which is just an isotropic polytrope with polytropic exponent $k = \frac{7}{2}$. This steady state is commonly studied in the astrophysics literature; see, e.g., [124, 168] for numerical investigations of solutions of the Vlasov-Poisson system close to the Plummer sphere. The potential of the Plummer sphere is explicitly known and thus all other quantities associated to the steady state are explicitly computable as well. However, the Plummer sphere is not compactly supported, which is why many of our arguments cannot be directly applied to it. In particular, the particle periods are unbounded within the Plummer sphere, which ought to result in the essential spectrum of the linearised operator to cover all non-negative numbers, i.e., $\sigma_{\mathrm{ess}}(\mathcal{L}) = [0, \infty[$. The linearised operator is again expected to be non-negative, which is why it remains to show the absence of embedded eigenvalues in order to arrive at a damping result similar to Theorem 6.6.1. It is an interesting open problem whether the strategies from the proof of Theorem 6.5.5 can be adapted to the situation of the Plummer sphere.

Another class of steady states for which one could try to establish damping are the *isochrone models*, cf. [64, 65] and [19, Scs. 2.2.2(d), 3.1(c), and 4.3.1(a)]. In particular, as reviewed in [18], (astro)physical considerations suggest that configurations close to an ischrone model evolve towards this steady state. Like the Plummer sphere, the isochrone models are explicitly computable, but have an unbounded supported. The mathematical basis for studying the linearised Vlasov-Poisson system around an isochrone model is established in [7].

X. Quantitative Damping

In the case where the linearised operator $\mathcal{L}$ of a steady state possesses no eigenvalues, we have proven in Lemma C.0.7 that the linearised dynamics are damped via the RAGE theorem. This is, however, a rather weak form of damping. It is hence desirable to prove stronger types of damping, for instance, the decay of suitable norms of macroscopic functions like $\partial_x U_{\mathcal{T}f}$. The numerics in Section 8.3 clearly indicate that such behaviour indeed holds. The numerics further indicate that the strength of the damping depends on the steady state, which is why it would also be interesting to study the decay rates. These issues will be addressed in future work.

The End.

Appendix A

The Period Function

This appendix is devoted to the analysis of the (radial) period function $T\colon \mathbb{A}_0 \to \mathbb{R}$ associated to a steady state. Recall Definition 2.2.16 for the definition of this function:

$$T(E,L) = 2\int_{r_-(E,L)}^{r_+(E,L)} \frac{\mathrm{d}r}{\sqrt{2E - 2\Psi_L(r)}}, \qquad (E,L) \in \mathbb{A}_0, \tag{A.0.1}$$

where the effective potential Ψ_L is defined in Definition 2.2.11, while the radii $r_\pm$ and the set of all admissible (E,L)-pairs $\mathbb{A}_0$ are introduced in Lemma 2.2.12 (b).

Throughout Appendix A, we consider the situation where the underlying steady state f_0 is given by Proposition 2.2.9. In addition to the conditions (φ1)–(φ3) imposed in Section 2.2, we further assume that the conditions (φ4)–(φ5) from Section 4.1 are satisfied.

In this setting, we prove the following properties of T.

Proposition A.0.1 (Main Properties of the Period Function)**.** *(a) The period function T is bounded and bounded away from zero on the (E,L)-support $\mathbb{D}_0$ of the steady state; recall* (2.2.88) *and Lemma 4.1.5 for the structure of this set. More precisely,*

$$\inf_{\mathbb{D}_0} T > 0 \qquad \textit{and} \qquad \sup_{\mathbb{D}_0} T < \infty. \tag{A.0.2}$$

(b) The period function is continuously differentiable on $\mathbb{A}_0$.

Proof. Part (a) is proven in Sections A.1 and A.2, while part (b) is due to Lemma A.3.3 or Proposition A.3.17. In particular, note that $\mathbb{A}_0$ is open by Lemma 2.2.14 (b). □

Apart from proving this crucial result, we also study further properties of the period function in this appendix, e.g., several formulae for the partial derivatives of T, cf. Section A.3, and the behaviour of the period function at a certain part of the boundary of $\mathbb{A}_0$, cf. Section A.4. A numerical study of the properties of T is the subject of Section 8.2. In particular, see Figures 8.2.2, 8.2.5, 8.2.9, and 8.2.10 for numerical plots of the values of the period function on the (E,L)-triangle $\mathbb{D}_0$ for different steady states.

Most parts of this appendix originate from [62, App. B]. Another detailed analysis of the period function is conducted in [85, Ch. 3], from which we also adopt some results and techniques. Related analyses in different settings can be found in [49, Sc. 3.2], [61, App. A.2], and [148, Apps. B and C].

A.1 An Upper Bound on the Period Function

The aim of this section is to show that the period function T is bounded from above on the (E, L)-support $\mathbb{D}_0$, i.e.,

$$\sup_{\mathbb{D}_0} T < \infty. \tag{A.1.1}$$

We mainly follow the arguments from [62, App. B.1] to establish this result.

The first upper bound on the period function is based on the concavity estimate (2.2.73) on the effective potential. The result originates from [147, Eqn. (16)] and [165, Rem. 3.19], see also [62, Eqn. (2.12)]. A similar bound is also proven in [57, Lemma 3.2].

Lemma A.1.1. *For $(E, L) \in \mathbb{A}_0$ there holds the estimate*

$$T(E, L) \leq 2\pi \frac{M_0^2}{\sqrt{L}\, E^2}, \tag{A.1.2}$$

where $M_0 \in]0, \infty[$ is the total mass of the steady state defined in (2.2.11).

Proof. The concavity estimate from Lemma 2.2.14 (f) yields

$$\begin{aligned} T(E, L) &\leq 2 \int_{r_-(E,L)}^{r_+(E,L)} \frac{r \sqrt{r_-(E, L)\, r_+(E, L)}}{\sqrt{L}\, \sqrt{(r_+(E, L) - r)\, (r - r_-(E, L))}}\, \mathrm{d}r \leq \\ &\leq 2\, \frac{r_+^2(E, L)}{\sqrt{L}} \int_0^1 \frac{\mathrm{d}s}{\sqrt{s\,(1-s)}} = 2\pi\, \frac{r_+^2(E, L)}{\sqrt{L}} \leq 2\pi\, \frac{M_0^2}{\sqrt{L}\, E^2}, \end{aligned} \tag{A.1.3}$$

where we changed variables via $r = r_-(E, L) + s\,(r_+(E, L) - r_-(E, L))$, inserted the integral identity (2.2.23), and used Lemma 2.2.14 (e) to estimate $r_+(E, L)$. □

In the case of an anisotropic steady state, there holds $L_0 > 0$ by (φ4). Hence, in this situation the desired estimate (A.1.1) is an immediate consequence of Lemma A.1.1; recall that the (E, L)-triangle $\mathbb{D}_0$ contains only energy values below the cut-off energy $E_0 < 0$ and L-values larger than L_0.

In the remainder of this section it thus remains to analyse the boundedness of the period function in the case of an isotropic steady state, i.e., $L_0 = 0 = \ell$. One way of showing the boundedness of the period function in this situation is given by Lemma 4.5.13. However, we prefer to present the proof of this result based on [62, App. B.1] here, since it can be generalised more directly to related systems – see, e.g., [49, Lemma 3.7].

Recall that the radial support of the steady state is of the form $\operatorname{supp}(\rho_0) = [0, R_{\max}]$ by Proposition 2.2.9 (c) in the isotropic situation. Furthermore, Remark 2.2.10 (a) implies $\rho_0(0) > 0$ and that ρ_0 is radially non-increasing. For (E, L)-pairs corresponding to a radial range where ρ_0 is bounded away from 0, the maximum principle can be applied to establish an upper bound on T. This result originates from [62, Lemma B.2].

Lemma A.1.2. *Consider an isotropic steady state, i.e., $L_0 = 0 = \ell$, and suppose that $(E, L) \in \mathbb{A}_0$ and $c > 0$ satisfy*

$$\rho_0 \geq c \text{ on } [r_-(E, L), r_+(E, L)]. \tag{A.1.4}$$

Then there holds the estimate

$$T(E, L) \leq \sqrt{\frac{3\pi}{c}}. \tag{A.1.5}$$

Proof. For fixed $(E, L) \in \mathbb{A}_0$ and $c > 0$ as in the statement of the lemma let $U_c \colon [r_-(E,L), r_+(E,L)] \to \mathbb{R}$ be defined by

$$\begin{aligned} U_c(r) &:= -\frac{2\pi}{3} c \frac{(r_+ - r)(r - r_-)(r + r_+ + r_-)}{r} \\ &= \frac{2\pi}{3} c \left(r^2 - (r_+ + r_-)^2 + r_- r_+ + \frac{1}{r} r_- r_+ (r_+ + r_-) \right) \end{aligned} \tag{A.1.6}$$

for $r \in [r_-, r_+]$, where we use the abbreviations $r_\pm = r_\pm(E, L)$. Obviously, $U_c(r_\pm) = 0 = E - \Psi_L(r_\pm)$. Applying the (radial) Laplacian $\Delta = \left(\partial_r^2 + \frac{2}{r}\partial_r\right)$ yields

$$\Delta U_c(r) = 4\pi c, \tag{A.1.7}$$

$$\Delta \Psi_L(r) = \Delta U_0(r) + \frac{L}{r^4} = 4\pi \rho_0(r) + \frac{L}{r^4} \tag{A.1.8}$$

for $r \in [r_-, r_+]$. Thus, (A.1.4) and the positivity of L imply

$$\Delta(U_c + E - \Psi_L) < 0 \text{ on } [r_-, r_+]. \tag{A.1.9}$$

By the maximum principle[195] we therefore conclude

$$U_c + E - \Psi_L > 0 \text{ on }]r_-, r_+[. \tag{A.1.10}$$

Inserting this estimate into the definition of the period function (2.2.97) and using the integral identity (2.2.23) then yields

$$T(E, L) = \sqrt{2} \int_{r_-}^{r_+} \frac{\mathrm{d}r}{\sqrt{E - \Psi_L(r)}} \leq \sqrt{\frac{3}{c\pi}} \int_{r_-}^{r_+} \frac{\mathrm{d}r}{\sqrt{(r_+ - r)(r - r_-)}} = \sqrt{\frac{3\pi}{c}}. \tag{A.1.11}$$

□

Let us recapitulate the implications of the above two lemmas in the case of an isotropic steady state. The bound (A.1.2) from Lemma A.1.1 implies that for any choice of $L_1 > 0 = L_0$ the period function T is bounded (from above) on $\{(E, L) \in \mathbb{D}_0 \mid L \geq L_1\}$; recall $E < E_0 < 0$ for $(E, L) \in \mathbb{D}_0$. Furthermore, for any choice of $E_1 \in]U_0(0), E_0[$, orbits corresponding to $(E, L) \in \mathbb{A}_0$ with $E \leq E_1$ are radially restricted to a compact subset of $\{\rho_0 > 0\}$, more precisely, $[r_-(E,L), r_+(E,L)] \subset]0, r_+(E_1, 0)] \subset]0, R_{\max}[$ by Lemma 2.2.14 and (2.2.82). Due to the properties of ρ_0 discussed above, ρ_0 is bounded away from zero on the interval $[0, r_+(E_1, 0)]$. Thus, Lemma A.1.2 shows that the period function T is bounded on $\{(E, L) \in \mathbb{D}_0 \mid E \leq E_1\} = \{(E, L) \in \mathbb{A}_0 \mid E \leq E_1\}$. The next lemma – which originates from [62, Lemma B.3] – closes the remaining gap.

Lemma A.1.3. *Consider an isotropic steady state, i.e., $L_0 = 0 = \ell$. Then there exist $E_1 \in]U_0(0), E_0[$ and $L_1 > 0$ as well as a constant $C > 0$ s.t.*

$$[E_1, E_0] \times]0, L_1] \subset \mathbb{A}_0 \tag{A.1.12}$$

and

$$T \leq C \text{ on } [E_1, E_0] \times]0, L_1]. \tag{A.1.13}$$

[195] More precisely, we apply the strong maximum principle for elliptic operators as, e.g., stated in [41, Sc. 6.4, Thm. 3] for the domain $B_{r_+} \setminus \bar{B}_{r_-}(0)$.

Proof. We consider fixed $L > 0$, $E \in]E_L^{\min}, E_0]$, and $\varepsilon > 0$ s.t. $E - \varepsilon > E_L^{\min}$; ε will be specified more precisely below. By Lemma 2.2.14 (c),

$$r_-(E,L) < r_-(E-\varepsilon,L) < r_+(E-\varepsilon,L) < r_+(E,L). \tag{A.1.14}$$

Our strategy is to separately estimate the times required for a particle with energy E and squared modulus of angular momentum L to travel between these radii, where the particle movement is determined by the steady state flow. Mathematically, this means that we split the integral (2.2.97) into the three parts

$$T(E,L) = 2\left(\int_{r_-(E,L)}^{r_-(E-\varepsilon,L)} + \int_{r_-(E-\varepsilon,L)}^{r_+(E-\varepsilon,L)} + \int_{r_+(E-\varepsilon,L)}^{r_+(E,L)}\right) \frac{\mathrm{d}r}{\sqrt{2E - 2\Psi_L(r)}} \tag{A.1.15}$$

and estimate each term separately in the following steps:

1) We first estimate the time a particle takes to travel from $r_-(E,L)$ to $r_-(E-\varepsilon,L)$. To do so, recall

$$\Psi_L'(r) = U_0'(r) - \frac{L}{r^3} \leq 0, \qquad r \in]0, r_L], \tag{A.1.16}$$

by the definition of r_L, cf. Lemma 2.2.12. Together with the (radial) Poisson equation $U_0'' + \frac{2}{r}U_0' = 4\pi\rho_0$ we thus obtain

$$\Psi_L''(r) = U_0''(r) + \frac{3L}{r^4} = 4\pi\rho_0(r) - \frac{2}{r}U_0'(r) + \frac{3L}{r^4} \geq 4\pi\rho_0(r) + \frac{L}{r^4} > 0 \tag{A.1.17}$$

for $r \in]0, r_L]$. Hence, the effective potential Ψ_L is convex on the interval $]0, r_L]$, which contains the radii $r_-(E,L)$ and $r_-(E-\varepsilon,L)$. For $r \in [r_-(E,L), r_-(E-\varepsilon,L)]$ we introduce the shorthand

$$\alpha(r) \coloneqq \frac{r - r_-(E,L)}{r_-(E-\varepsilon,L) - r_-(E,L)} \in [0,1] \tag{A.1.18}$$

and deduce

$$\Psi_L(r) \leq (1-\alpha(r))\Psi_L(r_-(E,L)) + \alpha(r)\Psi_L(r_-(E-\varepsilon,L)) = E - \alpha(r)\varepsilon \tag{A.1.19}$$

by the convexity of Ψ_L. Inserting this bound into the first term on the right-hand side of (A.1.15) then shows

$$\begin{aligned}\int_{r_-(E,L)}^{r_-(E-\varepsilon,L)} \frac{\mathrm{d}r}{\sqrt{2E - 2\Psi_L(r)}} &\leq \\ &\leq \frac{\sqrt{r_-(E-\varepsilon,L) - r_-(E,L)}}{\sqrt{2\varepsilon}} \int_{r_-(E,L)}^{r_-(E-\varepsilon,L)} \frac{\mathrm{d}r}{\sqrt{r - r_-(E,L)}} = \\ &= \sqrt{\frac{2}{\varepsilon}}\,(r_-(E-\varepsilon,L) - r_-(E,L)).\end{aligned} \tag{A.1.20}$$

2) We next estimate the time a particle takes to travel from $r_-(E-\varepsilon,L)$ to $r_+(E-\varepsilon,L)$. On this interval, $\Psi_L \leq E - \varepsilon$ by Lemma 2.2.12, and hence

$$\int_{r_-(E-\varepsilon,L)}^{r_+(E-\varepsilon,L)} \frac{\mathrm{d}r}{\sqrt{2E - 2\Psi_L(r)}} \leq \frac{r_+(E-\varepsilon,L) - r_-(E-\varepsilon,L)}{\sqrt{2\varepsilon}}. \tag{A.1.21}$$

3) Lastly, we estimate the time a particle takes to travel from $r_+(E-\varepsilon,L)$ to $r_+(E,L)$, which turns out to be the crucial part. Let

$$\mu \coloneqq \min\{\Psi_L'(r) \mid r \in [r_+(E-\varepsilon,L), r_+(E,L)]\}. \tag{A.1.22}$$

Obviously, $\mu > 0$ by Lemma 2.2.12 since $r_+(E-\varepsilon,L) > r_L$, but μ depends on (E,L). Anyway, the mean value theorem implies $\Psi_L(r) \leq E - \mu\,(r_+(E,L) - r)$ for $r \in [r_+(E-\varepsilon,L), r_+(E,L)]$, from which we deduce the inequality

$$\int_{r_+(E-\varepsilon,L)}^{r_+(E,L)} \frac{\mathrm{d}r}{\sqrt{2E-2\Psi_L(r)}} \leq \int_{r_+(E-\varepsilon,L)}^{r_+(E,L)} \frac{\mathrm{d}r}{\sqrt{2\mu\,(r_+(E,L)-r)}} = \\ = \sqrt{2}\frac{\sqrt{r_+(E,L)-r_+(E-\varepsilon,L)}}{\sqrt{\mu}}. \tag{A.1.23}$$

It thus remains to bound μ away from 0 independently of E and L for $(E,L) \in [E_1,E_0] \times]0,L_1]$ by choosing E_1 and L_1 suitably.

We recall $E_L^{\min} \to U_0(0)$ and $r_L \to R_{\min} = 0$ as $L \to 0$ and $r_+(E,L) \to r_+(E_0,0) = R_{\max}$ as $(E,L) \to (E_0,0)$ in the present, isotropic case by Lemma 2.2.14 and (2.2.82). Hence, there exist $\tilde{E}_1 \in]U_0(0),E_0[$ and $L_1 > 0$ s.t. $E_L^{\min} < \tilde{E}_1$ as well as

$$r_+(E,L) > r_{2L_1} > r_{L_1} \geq r_L \tag{A.1.24}$$

for $\tilde{E}_1 \leq E \leq E_0$ and $0 < L \leq L_1$. In particular, $[\tilde{E}_1,E_0] \times]0,L_1] \subset \mathbb{A}_0$. We now define

$$\varepsilon \coloneqq \frac{E_0 - \tilde{E}_1}{2}, \qquad E_1 \coloneqq \frac{E_0 + \tilde{E}_1}{2}. \tag{A.1.25}$$

For any $E \in [E_1,E_0]$ and $L \in]0,L_1]$ we then obtain $E - \varepsilon \geq \tilde{E}_1 > E_L^{\min}$, and hence $r_+(E-\varepsilon,L) > r_{2L_1}$. For $r \in [r_+(E-\varepsilon,L), r_+(E,L)] \subset [r_{2L_1}, R_{\max}]$ we thus conclude

$$\Psi_L'(r) = U_0'(r) - \frac{L}{r^3} \geq U_0'(r) - \frac{L_1}{r^3} = \Psi_{L_1}'(r) \geq \min\{\Psi_{L_1}'(s) \mid s \in [r_{2L_1}, R_{\max}]\} > 0; \tag{A.1.26}$$

note that the latter quantity does not depend on (E,L). Minimising over all such radii r provides the desired bound on μ.

We then deduce the claimed statement by combining the three steps from above as follows: First, choose $E_1 \in]U_0(0),E_0[$, $L_1 > 0$, and $\varepsilon > 0$ as described in Step 3). Then split the integral $T(E,L)$ for $(E,L) \in [E_1,E_0] \times]0,L_1]$ as in (A.1.15) and use the bounds from Steps 1), 2), and 3) to estimate the three integrals independently of (E,L); note $0 < r_\pm(E,L) \leq R_{\max}$. □

Combining Lemmas A.1.1, A.1.2, and A.1.3 as described above then shows the desired upper boundedness (A.1.1) of the period function on $\mathbb{D}_0$.

Alternative arguments to bound the period function on $\mathbb{D}_0$ in the case of an isotropic steady state[196] are presented in [85, Sc. 3.1]. However, we feel that these arguments are not significantly simpler than the ones shown above.

[196] The assumptions on the underlying steady state imposed in [85, Sc. 1.3] slightly differ from our conditions (φ1)–(φ5); most notably, the analysis in [85] is restricted to isotropic steady states. However, the arguments presented in [85, Ch. 3] regarding the properties of the period function can be carried over to all isotropic steady states considered in the present thesis.

Another way of establishing an upper bound on the period function T on the (E,L)-triangle $\mathbb{D}_0$ is to extend T continuously onto the boundary of $\mathbb{D}_0$. This approach is pursued in [85, Thm. 3.13] and is also mentioned in [62, Rem. B.6]. We will discuss this approach in more detail in Remark A.4.4, but already note that the arguments are also not simpler than the ones presented above, in particular, in the case of an isotropic steady state.

A.2 A Lower Bound on the Period Function

The aim of this section is to show that the period function T is bounded away from 0 on the (E,L)-support $\mathbb{D}_0$, i.e.,

$$\inf_{\mathbb{D}_0} T > 0. \tag{A.2.1}$$

We mainly follow the arguments from [62, App. B.2] but also include some improvements which have been developed in [49, Lemma 3.7] in a different context.

The main observation is that suitable applications of Taylor expansions and the mean value theorem yield a lower bound on T. The result originates from [62, Lemma B.4].

Lemma A.2.1. *For $(E,L) \in \mathbb{A}_0$, the inequality*

$$T(E,L) \geq 2\left(4\pi\|\rho_0\|_\infty + \frac{3L}{r_L^4}\right)^{-\frac{1}{2}} \tag{A.2.2}$$

holds; recall that ρ_0 is bounded as a compactly supported and continuous function, cf. Proposition 2.2.9.[197,198]

Proof. Naïvely estimating the integral (2.2.97) gives the inequality

$$T(E,L) \geq \sqrt{2}\,\frac{r_+(E,L) - r_-(E,L)}{\sqrt{E - \Psi_L(r_L)}} \geq \sqrt{2}\,\frac{r_+(E,L) - r_L}{\sqrt{E - \Psi_L(r_L)}}. \tag{A.2.3}$$

A second-order Taylor expansion yields

$$E = \Psi_L(r_+(E,L)) = \Psi_L(r_L) + \frac{1}{2}\,\Psi_L''(s)\,(r_+(E,L) - r_L)^2 \tag{A.2.4}$$

for some $s \in [r_L, r_+(E,L)]$ because $\Psi_L'(r_L) = 0$, recall Lemma 2.2.12. In particular, note $\Psi_L''(s) > 0$ since $E - \Psi_L(r_L) > 0$. Inserting this Taylor expansion into (A.2.3) implies[199]

$$T(E,L) \geq \frac{2}{\sqrt{\Psi_L''(s)}}. \tag{A.2.5}$$

Using the radial Poisson equation $U_0'' + \frac{2}{r}U_0' = 4\pi\rho_0$ and $U_0'(r) = \frac{m_0(r)}{r^2} \geq 0$ further shows

$$\Psi_L''(s) = 4\pi\rho_0(s) - \frac{2}{s}U_0'(s) + \frac{3L}{s^4} \leq 4\pi\|\rho_0\|_\infty + \frac{3L}{r_L^4}, \tag{A.2.6}$$

which concludes the proof of the lemma. □

[197] Note that the condition ($\varphi 4$) implies that the regularity properties of ρ_0 on $\mathbb{R}^3$ stated in Proposition 2.2.9 (e) hold true for the present steady state.

[198] Here it is important that ρ_0 is bounded, in particular, $\rho_0(0) < \infty$. Physically speaking, the latter means that the steady state has a smooth core, and we note that it is explicitly stated in [19, Sc. 5.5.3] that this property corresponds to $\frac{1}{T}$ being bounded on the steady state support.

[199] In the proof of [62, Lemma B.4], the expression $E - \Psi_L(r_L)$ is estimated by applying the (extended) mean value theorem twice. In this way, one obtains the estimate $T(E,L) \geq (\Psi_L''(\tilde{s}))^{-\frac{1}{2}}$ for some $\tilde{s} \in [r_L, r_+(E,L)]$. Hence, applying a Taylor expansion instead not only clarifies the proof, but also results in the superior estimate (A.2.5). This leads to the additional factor 2 on the right-hand side of the lower bound (A.2.2) compared to [62, Lemma B.4].

In the case of an anisotropic steady state, we have $L_0 > 0$ by (φ4). Inserting the bounds $L \leq L_{\max} < \infty$ and $r_L \geq r_{L_0} > 0$ for $(E, L) \in \mathbb{D}_0$, cf. (2.2.90) and Lemmas 2.2.14 and 2.2.15, into the estimate (A.2.2) thus shows the desired bound (A.2.1).

In the case of isotropic steady states we cannot directly infer (A.2.1) because arbitrary small L-values are contained in $\mathbb{D}_0$ and $r_L \to R_{\min} = 0$ as $L \to 0$ by Lemma 2.2.14. We thus have to analyse the behaviour of $\frac{L}{r_L^4}$ in more detail, in particular as $L \to 0$. In [62, Lemma B.5], this is done by applying l'Hospital's rule and using the formula (2.2.61) for the derivative of r_L. We instead present a simpler argument which originates from [49, Eqn. (3.11)] (where it is used in a different context).

Lemma A.2.2. *For $L > 0$ there holds the estimate*

$$\frac{L}{r_L^4} \leq \frac{4\pi}{3} \|\rho_0\|_\infty. \tag{A.2.7}$$

Proof. For $L > 0$ the definition of r_L implies $0 = \Psi_L'(r_L) = U_0'(r_L) - \frac{L}{r_L^3}$, cf. Lemma 2.2.12. Together with (2.2.32) we thus obtain

$$\frac{L}{r_L^4} = \frac{U_0'(r_L)}{r_L} = \frac{4\pi}{r_L^3} \int_0^{r_L} s^2 \rho_0(s)\,\mathrm{d}s \leq \frac{4\pi}{r_L^3} \|\rho_0\|_\infty \int_0^{r_L} s^2\,\mathrm{d}s = \frac{4\pi}{3} \|\rho_0\|_\infty. \tag{A.2.8}$$

□

Obviously, Lemmas A.2.1 and A.2.2 conclude the proof of the desired lower bound (A.2.1) on T.

In the case of an isotropic steady state, an alternative way of showing that the period function is bounded away from 0 on $\mathbb{D}_0$ can be found in [85, Sc. 3.2]. The main idea of that proof is to re-express the integral (2.2.97) by defining T as an integral with fixed limits of integration.

Furthermore, as noted in Section A.1, another way of obtaining a positive, lower bound on the period function T on the (E, L)-triangle $\mathbb{D}_0$ is to extend T continuously onto the boundary of $\mathbb{D}_0$ and verify that this extension is positive. We will comment on this approach in more detail in Remark A.4.4.

A.3 Regularity & Derivatives of the Period Function

In this section we discuss the regularity properties of the period function T on the set of admissible (E, L)-pairs $\mathbb{A}_0$, recall (2.2.55) for the definition of this set. We shall see that the period function is differentiable. As it is of interest to understand whether the period function is monotone w.r.t. to one of its variables, we further derive explicit formulae for the partial derivatives of T. We mainly follow [62, App. B.3] and [85, Sc. 3.3] in this section; similar arguments are also used in [61, App. A.2] in a different context.

The first result shows the continuity of integrals of the form (2.2.97). In particular, it implies that the period function T is continuous on $\mathbb{A}_0$, but we provide a more general result which will be useful later. The proof is based on the concavity bound from Lemma 2.2.14 (f) on the effective potential and originates from [62, Lemma B.7]; a variation of it can also be found in [61, Lemma A.7].

Lemma A.3.1. *Let $m > 0$ and $]0, \infty[^2 \ni (L, r) \mapsto F_L(r) \in \mathbb{R}$ be continuous. Then the mapping*

$$J\colon \mathbb{A}_0 \to \mathbb{R},\ J(E, L) \coloneqq \int_{r_-(E,L)}^{r_+(E,L)} \frac{F_L(r)}{(E - \Psi_L(r))^{1-m}}\,\mathrm{d}r \tag{A.3.1}$$

is continuous.

Proof. First note that similar arguments as in the proof of Lemma 2.2.16 show that the integral $J(E,L)$ exists for $(E,L) \in \mathbb{A}_0$. The affine change of variables $r = r_-(E,L) + (r_+(E,L) - r_-(E,L))s$ leads to

$$J(E,L) = (r_+(E,L) - r_-(E,L)) \int_0^1 \frac{F_L(r_-(E,L) + (r_+(E,L) - r_-(E,L))s)}{(E - \Psi_L(r_-(E,L) + (r_+(E,L) - r_-(E,L))s))^{1-m}} \,\mathrm{d}s. \tag{A.3.2}$$

For fixed $s \in]0,1[$, the integrand of the integral on the right-hand side of (A.3.2) is continuous in (E,L) since $r_\pm$ is continuous on $\mathbb{A}_0$ by Lemma 2.2.14. Moreover, in the case $0 < m < 1$ the concavity bound (2.2.73) yields

$$\begin{aligned}\frac{r_+(E,L) - r_-(E,L)}{(E - \Psi_L(r))^{1-m}} &\leq \frac{(r_+(E,L) - r_-(E,L))\,(2r^2\, r_-(E,L)\, r_+(E,L))^{1-m}}{L^{1-m}\,((r_+(E,L) - r)(r - r_-(E,L)))^{1-m}} = \\ &= \frac{(r_+(E,L) - r_-(E,L))^{2m-1}}{L^{1-m}} \frac{(2r^2\, r_-(E,L)\, r_+(E,L))^{1-m}}{(s(1-s))^{1-m}} \leq \\ &\leq (r_+(E,L) - r_-(E,L))^{2m-1} \left(\frac{2M_0^4}{E^4 L}\right)^{1-m} \frac{1}{(s(1-s))^{1-m}} \end{aligned} \tag{A.3.3}$$

for $s \in]0,1[$ and $r = r_-(E,L) + (r_+(E,L) - r_-(E,L))s$, where we have estimated $r_+(E,L)$ in the last step using Lemma 2.2.14 (e). Since $\int_0^1 (s(1-s))^{m-1}\,\mathrm{d}s < \infty$,[200] we have thus bounded the integrand of the integral on the right-hand side of (A.3.2) by an integrable function which can be chosen locally uniformly in $(E,L) \in \mathbb{A}_0$. In the case $m \geq 1$ there holds the estimate

$$\frac{r_+(E,L) - r_-(E,L)}{(E - \Psi_L(r))^{1-m}} \leq (r_+(E,L) - r_-(E,L))\,(E - E_L^{\min})^{m-1} \tag{A.3.4}$$

for r as above. For all $m > 0$, Lebesgue's dominated convergence theorem hence implies the desired continuity statement. □

Obviously, setting $m = \frac{1}{2}$ and $F_L(r) \equiv 1$ in the above lemma implies that $T\colon \mathbb{A}_0 \to]0,\infty[$ is continuous.

In order to show that the period function is (continuously) differentiable, there are two qualitatively different approaches:

The first one uses that T is the period of solutions of the characteristic system associated to the steady state. Differentiating these solutions w.r.t. suitable parameters or initial conditions then shows that T is differentiable. This – quite elegant – approach is pursued in [85, Sc. 3.3 & App. A.3].

The second way just uses the integral representation (2.2.97) of the period function. Differentiating such integrals is a somewhat technical task, but provides explicit integral formulae for the partial derivatives of the period function. Such integral representations then provide simple criteria for the monotonicity of the period function w.r.t. one of its variables. This approach is inspired by [31, Thm. 2.1] and has been used in the context of the Vlasov-Poisson system in [62, App. B.3], [148, App. C], and [61, App. A.2].

As both approaches have their advantages and provide different ways to analyse the partial derivatives of the period function, we present both of them in the succeeding sections.

[200] The (finite) value of the integral $\int_0^1 (s(1-s))^{m-1}\,\mathrm{d}s$ can be computed explicitly using the integral identity (2.2.23).

A.3.1 Derivatives via Characteristics

In this section – which is based[201] on [85, Sc. 3.3 & App. A.3] – we relate the regularity and the derivatives of the period function to the ones of the solutions of the characteristic system associated to the steady state. To this end, let $(R,W)\colon \mathbb{R}\times\mathbb{A}_0\to\,]0,\infty[\,\times\mathbb{R}$ be as in Definition 2.2.16, i.e., for $(E,L)\in\mathbb{A}_0$, $(R,W)(\cdot,E,L)\colon\mathbb{R}\to\,]0,\infty[\,\times\mathbb{R}$ is the maximal solution of[202]

$$\dot R = W,\quad \dot W = -\Psi_L'(R),\qquad (R,W)(0,E,L) = (r_-(E,L),0). \tag{A.3.5}$$

We first analyse the regularity of (R,W) similar to [85, Lemma A.11] and [61, Lemma 3.4].

Lemma A.3.2 (Regularity of Characteristics)**.** *It holds that $(R,W)\in C^2(\mathbb{R}\times\mathbb{A}_0)$. Moreover, for fixed $(E,L)\in\mathbb{A}_0$, $\alpha\coloneqq\partial_E R(\cdot,E,L)$ is given as the (unique) solution of*

$$\ddot\alpha = -\Psi_L''(R(s,E,L))\,\alpha,\qquad \alpha(0)=\partial_E r_-(E,L),\quad \dot\alpha(0)=0, \tag{A.3.6}$$

while $\beta\coloneqq\partial_L R(\cdot,E,L)$ is the solution of

$$\ddot\beta = -\Psi_L''(R(s,E,L))\,\beta + \frac{1}{R(s,E,L)^3},\qquad \beta(0)=\partial_L r_-(E,L),\quad \dot\beta(0)=0; \tag{A.3.7}$$

in particular, the derivatives $\partial_E\ddot R$ and $\partial_L\ddot R$ exist on $\mathbb{R}\times\mathbb{A}_0$ and are continuous. Recall Lemma 2.2.14 (c) for explicit formulae for $\partial_E r_-$ and $\partial_L r_-$.

Proof. First observe that $(L,r)\mapsto\Psi_L(r)$ defines a $C^3(]0,\infty[^2)$-function by Proposition 2.2.9 (e). Thus, further differentiating (2.2.65) shows $r_\pm\in C^3(\mathbb{A}_0)$. The claimed regularity of the characteristics (R,W) together with (A.3.6) and (A.3.7) then follows by basic ODE theory, see, e.g., [12, Sc. 32.6]. □

Because $T(E,L)$ is the period of $(R,W)(\cdot,E,L)$ for $(E,L)\in\mathbb{A}_0$, one can deduce the regularity of T from the regularity of the characteristics by applying the implicit function theorem suitably. This method is due to[203] [85, Thm. 3.6, Rem. 3.7, and Lemma A.12] and it is also used in [61, Lemma 3.4].

Lemma A.3.3 (Regularity of the Period Function)**.** *It holds that $T\in C^2(\mathbb{A}_0)$ with*

$$\partial_E T(E,L) = \frac{\partial_E W(T(E,L),E,L)}{\Psi_L'(r_-(E,L))} = 2\frac{\partial_E W\big(\frac12 T(E,L),E,L\big)}{\Psi_L'(r_+(E,L))}, \tag{A.3.8}$$

$$\partial_L T(E,L) = \frac{\partial_L W(T(E,L),E,L)}{\Psi_L'(r_-(E,L))} = 2\frac{\partial_L W\big(\frac12 T(E,L),E,L\big)}{\Psi_L'(r_+(E,L))}, \tag{A.3.9}$$

for $(E,L)\in\mathbb{A}_0$.

Proof. We follow [85, Proof of Thm. 3.6] and first recall that for any fixed $(E^*,L^*)\in\mathbb{A}_0$, by the discussion from Section 2.2.2, $(R,W)(\cdot,E^*,L^*)$ is time-periodic with period $T(E^*,L^*)$. Moreover, for $s\in\mathbb{R}$ there holds

$$W(s,E^*,L^*)=0\qquad\Leftrightarrow\qquad s\in\frac{\mathbb{Z}}{2}\,T(E^*,L^*). \tag{A.3.10}$$

[201] We again note that the assumptions imposed on the steady state here differ from the ones in [85], where only isotropic steady states are considered. Nonetheless, all arguments from [85] regarding the regularity of the period function also work for our class of equilibria.

[202] As before, a dot denotes the derivative w.r.t. to the proper time variable s of $(R,W)=(R,W)(s,E,L)$.

[203] It is, however, stated in [85, Proof of Thm. 3.6] that such methods were already known before.

Now set $s^* := T(E^*, L^*)$, so that $W(s^*, E^*, L^*) = 0$ with

$$\dot{W}(s^*, E^*, L^*) = -\Psi'_{L^*}(R(s^*, E^*, L^*)) = -\Psi'_{L^*}(r_-(E^*, L^*)) > 0. \tag{A.3.11}$$

Together with the regularity of W derived in Lemma A.3.2, the implicit function theorem yields the existence of a continuously differentiable mapping $s\colon U \to \mathbb{R}$ defined on an open neighbourhood $U \subset \mathbb{A}_0$ of (E^*, L^*) s.t. $W(s(E,L), E, L) = 0$ for $(E, L) \in U$ and $s(E^*, L^*) = s^* = T(E^*, L^*)$; recall that $\mathbb{A}_0$ is open by Lemma 2.2.14 (b). The smoothness of s together with (A.3.10) and the continuity of $T > 0$ established in Lemma A.3.1 then imply $s(E, L) = T(E, L)$ for $(E, L) \in U$, in particular, $T \in C^1(U)$. As $(E^*, L^*) \in \mathbb{A}_0$ is arbitrary, we conclude $T \in C^1(\mathbb{A}_0)$.

Similar to [85, Lemma A.12], differentiating the identities

$$0 = W(T(E,L), E, L) = W\left(\frac{1}{2}T(E,L), E, L\right), \qquad (E, L) \in \mathbb{A}_0, \tag{A.3.12}$$

w.r.t. E and L then yields (A.3.8) and (A.3.9); recall $R(T(E,L), E, L) = r_-(E, L)$ and $R\big(\frac{1}{2}T(E,L), E, L\big) = r_+(E, L)$. Lastly, Lemma A.3.2 shows that the right-hand sides of (A.3.8) and (A.3.9) are again continuously differentiable on $\mathbb{A}_0$, which implies that T is indeed twice continuously differentiable. □

The identities (A.3.8) and (A.3.9) show that we can not only conclude the regularity of T from the regularities of the characteristics, but we can also relate the values of the partial derivatives $\partial_E T$ and $\partial_L T$ to the behaviour of $\partial_E W = \partial_E \dot{R}$ and $\partial_L W = \partial_L \dot{R}$. Let us thus briefly discuss the properties of the ODEs determining $\partial_E R$ and $\partial_L R$.

Remark A.3.4. *Let $(E, L) \in \mathbb{A}_0$ be fixed. By Lemma A.3.2, $\partial_E R(\cdot, E, L)$ is a solution of*

$$\ddot{\alpha} = -\Psi''_L(R(s, E, L))\,\alpha. \tag{A.3.13}$$

If we consider $R(\cdot, E, L)$ as given, this equation is a linear, homogeneous, non-autonomous, second-order ODE. Moreover, the coefficient of this linear equation is $T(E, L)$-periodic. An ODE of the specific structure (A.3.13) *is known as* Hill's equation*, see [106] and [183] for thorough analyses of its solutions. The study of (more general) linear ODEs with periodic coefficients is the subject of* Floquet theory*, cf. [29, Sc. 2.4] or [170, Sc. 3.6] and see also [12, Sc. 28] for a related discussion.*

A further observation, which is due to [85, Lemma A.12 (a)], is that $W(\cdot, E, L)$ also solves (A.3.13)*. However, $\partial_E R(\cdot, E, L)$ and $W(\cdot, E, L)$ satisfy different initial conditions:*

$$\partial_E R(0, E, L) = \frac{1}{\Psi'_L(r_-(E, L))}, \qquad \partial_E \dot{R}(0, E, L) = 0, \tag{A.3.14}$$

$$W(0, E, L) = 0, \qquad \dot{W}(0, E, L) = -\Psi'_L(r_-(E, L)) \tag{A.3.15}$$

by (A.3.6) *and* (2.2.65)*. In fact, the two solutions $W(\cdot, E, L)$ and $\partial_E R(\cdot, E, L)$ form a fundamental system of the linear ODE* (A.3.13) *because* (A.3.14) *and* (A.3.15) *imply that the Wronskian determinant of these solutions equals* 1*, cf. [85, Lemma A.12 (a)].*

In order to see another difference of these solutions, we differentiate the identity

$$R(s, E, L) = R(s + jT(E, L), E, L) \tag{A.3.16}$$

for fixed $s \in \mathbb{R}$ and $j \in \mathbb{Z}$ w.r.t. E to deduce

$$\partial_E R(s, E, L) = W(s, E, L)\, j\, \partial_E T(E, L) + \partial_E R(s + jT(E, L), E, L) \tag{A.3.17}$$

by the $T(E,L)$-periodicity of $W(\cdot,E,L)$. Recalling (A.3.10)*, we thus see that $\partial_E R(\cdot,E,L)$ is periodic iff $\partial_E T(E,L)=0$, which will not be the case in general. Nonetheless, inserting $s=0$ and $s=\frac{1}{2}T(E,L)$ into* (A.3.17) *shows*

$$\frac{1}{\Psi_L'(r_-(E,L))} = \partial_E R(0,E,L) = \partial_E R(jT(E,L),E,L), \tag{A.3.18}$$

$$\frac{1}{\Psi_L'(r_+(E,L))} = \partial_E R\Big(\frac{1}{2}T(E,L),E,L\Big) = \partial_E R\Big(\Big(\frac{1}{2}+j\Big)T(E,L),E,L\Big), \tag{A.3.19}$$

for $j\in\mathbb{Z}$. Most of these observations are also stated in [85, Lemma A.11 (b)].

Furthermore, Lemma A.3.2 implies that $\partial_L R(\cdot,E,L)$ solves

$$\ddot{\beta} = -\Psi_L''(R(s,E,L))\,\beta + \frac{1}{R(s,E,L)^3}. \tag{A.3.20}$$

Compared to (A.3.13)*, this ODE contains an inhomogeneous term which is again $T(E,L)$-periodic.*

The techniques of the present section can also be used to study how a more regular steady state translates into higher-order regularity of the associated period function. This is based on [85, Rem. 3.17].

Remark A.3.5 (Higher-Order Regularities)**.** *Let us assume $\rho_0\in C^j(]0,\infty[)$ for some $j\in\mathbb{N}$; up to now, this was satisfied with $j=1$, recall Proposition 2.2.9 (e). For instance, this is the case if $g\in C^j(\mathbb{R})$, where g is the function relating ρ_0 and U_0 via* (2.2.27)*.*[204] *This regularity of g is in turn present if, e.g., the steady state is polytropic* (1.2.5) *with exponents k and ℓ satisfying $k+\ell+\frac{3}{2}>j$, recall Remark 2.2.7. If the steady is non-polytropic, similar conditions on the energy dependency function Φ also ensure the regularity of g.*[205]

In this situation, the radial Poisson equation (2.2.32) *yields $U_0\in C^{j+2}(]0,\infty[)$, which then implies that $(L,r)\mapsto\Psi_L(r)$ defines a $C^{j+2}(]0,\infty[^2)$ function. Further differentiating* (2.2.65) *thus shows $r_\pm\in C^{j+2}(\mathbb{A}_0)$. Hence, applying the same arguments as in the proof of Lemma A.3.2 yields $(R,W)\in C^{j+1}(\mathbb{R}\times\mathbb{A}_0)$. Due to the identities* (A.3.8) *and* (A.3.9)*, we thus conclude $T\in C^{j+1}(\mathbb{A}_0)$.*

A.3.2 Derivatives via the Integral Representation

In this section we differentiate the integral representation of the period function T. Alternative integral expressions of T are derived in [85, Lemmas 3.3 and 3.10] and [148, Eqn. (B3)] among others, but we prefer to stick to the classical formula (2.2.97).

In order to differentiate (2.2.97), we first introduce a new function which is useful when studying T.

Definition A.3.6 (The Area Function)**.** *For $(E,L)\in\mathbb{A}_0$ let*

$$A(E,L) \coloneqq 2\int_{r_-(E,L)}^{r_+(E,L)} \sqrt{2E-2\Psi_L(r)}\,\mathrm{d}r. \tag{A.3.21}$$

The induced function $A\colon\mathbb{A}_0\to]0,\infty[$ is called the area function *of the steady state.*[206]

[204] This can be verified by iteratively differentiating the relations (2.2.27) and (2.2.32) between U_0 and ρ_0.
[205] For instance, similar arguments as in Lemma 2.2.6 show $g\in C^j(\mathbb{R})$ if $\Phi\in C^{j-1}(\mathbb{R})$.
[206] The name *area function* is due to [148].

The area function occurs naturally in the context of planar Hamiltonian systems like the characteristic system (2.2.93), cf. [11, Sc. 50.B] and see also Remark 4.3.2. In the context of the Vlasov-Poisson system this function appears in [85, Eqn. (A.11)], [96, Eqn. (1.27)], and [148, Eqn. (18)] among others. Let us add some comments on the physical interpretation of the area function, which will explain its name.

Remark A.3.7. *For $(E,L) \in \mathbb{A}_0$ let $(R,W)(\cdot,E,L)$ be as specified in Section A.3.1. As discussed in Section 2.2.2, the solution is time-periodic and its orbit (in the (r,w)-plane) is closed, see Figure 2.2.3. The area enclosed by this solution, i.e., the area of*[207]

$$\{(r,w) \in]0,\infty[\times \mathbb{R} \mid E(r,w,L) < E\}, \tag{A.3.22}$$

is given by $A(E,L)$.

The following result establishes a connection between the area function and the period function.

Lemma A.3.8. *Let $m > 0$ and $F\colon]0,\infty[\to \mathbb{R}$ be continuous. Then the function*

$$I\colon \mathbb{A}_0 \to \mathbb{R},\ I(E,L) \coloneqq \int_{r_-(E,L)}^{r_+(E,L)} F(r)\,(2E - 2\Psi_L(r))^m \,\mathrm{d}r \tag{A.3.23}$$

is partially differentiable w.r.t. E with

$$\partial_E I(E,L) = 2m \int_{r_-(E,L)}^{r_+(E,L)} F(r)\,(2E - 2\Psi_L(r))^{m-1} \,\mathrm{d}r \tag{A.3.24}$$

for $(E,L) \in \mathbb{A}_0$.[208]

Proof. The proof is inspired by the proof of Lemma 2.2.6 (which we have not presented here). First observe that the integrals in (A.3.23) and (A.3.24) exist since F is locally bounded, $\Psi_L'(r_\pm(E,L)) \neq 0$, and $m > 0$. In order to verify that $I(\cdot,L)\colon]E_L^{\min},0[\to \mathbb{R}$ is differentiable for fixed $L > 0$, we start by computing the right-derivative $\partial_E^+ I(\cdot,L)$. Let $E \in]E_L^{\min},0[$ and $\eta > 0$ be s.t. $E + 2\eta < 0$. Then there holds the estimate

$$\begin{aligned}
&\left| \frac{I(E+\eta,L) - I(E,L)}{\eta} - 2m \int_{r_-(E,L)}^{r_+(E,L)} F(r)\,(2E - 2\Psi_L(r))^{m-1} \,\mathrm{d}r \right| \leq \\
&\leq 2^m \int_{r_-(E,L)}^{r_+(E,L)} |F(r)| \left| \frac{(E+\eta-\Psi_L(r))^m - (E-\Psi_L(r))^m}{\eta} - m\,(E-\Psi_L(r))^{m-1} \right| \mathrm{d}r + \\
&\quad + \frac{1}{\eta} \left(\int_{r_-(E+\eta,L)}^{r_-(E,L)} + \int_{r_+(E,L)}^{r_+(E+\eta,L)} \right) |F(r)|\,(2E + 2\eta - 2\Psi_L(r))^m \,\mathrm{d}r,
\end{aligned} \tag{A.3.25}$$

recall $r_-(E+\eta,L) < r_-(E,L) < r_+(E,L) < r_+(E+\eta,L)$ by Lemma 2.2.14 (c). For fixed $r \in]r_-(E,L), r_+(E,L)[$, the integrand of the first term on the right-rand side of (A.3.25) tends to 0 as $\eta \searrow 0$. In addition, by the mean value theorem there exists $\tilde{\eta} \in]0,\eta[$ s.t.

$$\begin{aligned}
&\left| \frac{(E+\eta-\Psi_L(r))^m - (E-\Psi_L(r))^m}{m\,\eta} - (E-\Psi_L(r))^{m-1} \right| = \\
&\qquad = \left| (E+\tilde{\eta}-\Psi_L(r))^{m-1} - (E-\Psi_L(r))^{m-1} \right|,
\end{aligned} \tag{A.3.26}$$

[207] Recall that the orbit $(R,W)(\mathbb{R},E,L)$ equals the energy level set $\{(r,w) \in]0,\infty[\times\mathbb{R} \mid E(r,w,L) = E\}$ and that smaller energy values correspond to "inner" orbits since $r_-(E,L) < r_-(\tilde{E},L) < r_L$ for $E_L^{\min} < \tilde{E} < E$ by Lemma 2.2.14 (c).

[208] Obviously, the same result holds if the function F also depends on L because all statements in this lemma only concern $I(\cdot,L)$ for a fixed value of L.

and the latter expression can be bounded independently of η by a function which is integrable in $r \in]r_-(E,L), r_+(E,L)[$. As F is bounded on $[r_-(E,L), r_+(E,L)]$, we thus obtain that the first integral on the right-rand side of (A.3.25) tends to 0 as $\eta \searrow 0$ by Lebesgue's dominated convergence theorem. In order to see that the remaining integrals on the right-rand side of (A.3.25) exhibit the same limiting behaviour as $\eta \searrow 0$, we use the structure of Ψ_L, recall Lemma 2.2.12, to infer the estimate

$$(2E + 2\eta - 2\Psi_L(r))^m \leq (2\eta)^m, \qquad r \in]r_-(E+\eta, L), r_+(E+\eta, L)[\setminus]r_-(E,L), r_+(E,L)[, \tag{A.3.27}$$

which yields

$$\begin{aligned} \frac{1}{\eta}\left(\int_{r_-(E+\eta,L)}^{r_-(E,L)} + \int_{r_+(E,L)}^{r_+(E+\eta,L)}\right) |F(r)|\,(2E + 2\eta - 2\Psi_L(r))^m \,\mathrm{d}r \leq \\ \leq \frac{r_-(E,L) - r_-(E+\eta,L) + r_+(E+\eta,L) - r_+(E,L)}{\eta}\, C\,(2\eta)^m, \end{aligned} \tag{A.3.28}$$

where

$$C \coloneqq \max\left\{ |F(r)| \mid r \in [r_-(\frac{1}{2}E, L), r_+(\frac{1}{2}E, L)] \right\}; \tag{A.3.29}$$

recall $\eta < -\frac{1}{2}E$. Because $r_\pm$ are differentiable by Lemma 2.2.14 (c), the right-hand side of (A.3.28) indeed converges to 0 as $\eta \searrow 0$. We thus conclude that $I(\cdot, L)$ is right-differentiable with

$$\partial_E^+ I(E,L) = 2m \int_{r_-(E,L)}^{r_+(E,L)} F(r)\,(2E - 2\Psi_L(r))^{m-1}\,\mathrm{d}r, \qquad E_L^{\min} < E < 0. \tag{A.3.30}$$

By Lemma A.3.1, this right-derivative $\partial_E^+ I(\cdot, L)\colon]E_L^{\min}, 0[\to \mathbb{R}$ is continuous. We hence conclude that $I(\cdot, L)$ is indeed differentiable with $\partial_E I = \partial_E^+ I$, see, e.g., [68, Ex. (17.24)]. □

Obviously, setting $m = \frac{1}{2}$ and $F \equiv 1$ in the above lemma yields[209]

$$\partial_E A = T \quad \text{ on } \mathbb{A}_0. \tag{A.3.31}$$

We note that this connection between the area function and the period function is known for general (planar) Hamiltonian systems, cf. [11, p. 20]. In the context of the Vlasov-Poisson system it is, e.g., stated in [148, Eqn. (33)].

Unfortunately, the energy derivative of the period function cannot be computed as in Lemma A.3.8 because differentiating the integrand of $T(E,L)$ w.r.t. E results in the non-integrable term $(2E - 2\Psi_L(r))^{-\frac{3}{2}}$. However, we can get around this problem with a clever calculation due to [31, Thm. 2.1], which has been applied in the context of the Vlasov-Poisson system in [62, Lemma 2.6] and [61, Lemma A.10]. An alternative method of differentiating (2.2.97) is presented in [148, App. B].

Lemma A.3.9 (The Energy Derivative of the Period Function)**.** *The period function $T\colon \mathbb{A}_0 \to]0, \infty[$ defined by* (2.2.97) *is partially differentiable w.r.t. E with*

$$\partial_E T(E,L) = \frac{1}{E - E_L^{\min}} \int_{r_-(E,L)}^{r_+(E,L)} G_L(r)\, \frac{\mathrm{d}r}{\sqrt{2E - 2\Psi_L(r)}}, \qquad (E,L) \in \mathbb{A}_0, \tag{A.3.32}$$

[209] We cannot help but notice the following pun: The area function A not only gives the *area* enclosed by solutions of the characteristic system, cf. Remark A.3.7, but can also be used to compute the *area* under the graph of $T(\cdot, L)$ by (A.3.31) and the main theorem of calculus.

where

$$G_L\colon]0,\infty[\to \mathbb{R},\ G_L(r) \coloneqq \begin{cases} \frac{\Psi_L'(r)^2 - 2(\Psi_L(r) - E_L^{\min})\Psi_L''(r)}{\Psi_L'(r)^2}, & r \neq r_L, \\ 0, & r = r_L, \end{cases} \tag{A.3.33}$$

for $L > 0$. The function G_L is continuous on $]0,\infty[$ for $L > 0$ and thus the integral on the right-hand side of (A.3.32) *exists.*

Proof. The continuity of G_L follows by a more general result which we will show below, cf. Lemma A.3.10. Given this continuity, the existence of the integral on the right-hand side of (A.3.32) is evident from the structure of the effective potential Ψ_L.

In order to establish the relation (A.3.32), we follow [31, Proof of Thm. 2.1] and define

$$I(E,L) \coloneqq \int_{r_-(E,L)}^{r_+(E,L)} \left(2E_L^{\min} - 2\Psi_L(r)\right) \sqrt{2E - 2\Psi_L(r)}\,\mathrm{d}r, \qquad (E,L) \in \mathbb{A}_0. \tag{A.3.34}$$

Lemma A.3.8 implies that $I\colon \mathbb{A}_0 \to \mathbb{R}$ is partially differentiable w.r.t. E with

$$\partial_E I(E,L) = \int_{r_-(E,L)}^{r_+(E,L)} \frac{2E_L^{\min} - 2\Psi_L(r)}{\sqrt{2E - 2\Psi_L(r)}}\,\mathrm{d}r = \frac{1}{2}A(E,L) - \left(E - E_L^{\min}\right) T(E,L) \tag{A.3.35}$$

for $(E,L) \in \mathbb{A}_0$. On the other hand,

$$I(E,L) = \frac{2}{3}\int_{r_-(E,L)}^{r_+(E,L)} \frac{\Psi_L(r) - E_L^{\min}}{\Psi_L'(r)}\,\partial_r\left[(2E - 2\Psi_L(r))^{\frac{3}{2}}\right]\mathrm{d}r. \tag{A.3.36}$$

Evidently, it is our intention to integrate by parts in (A.3.36). To see that the necessary conditions for this step are satisfied, first observe[210]

$$\Psi_L(r) - E_L^{\min} = \frac{1}{2}\Psi_L''(r_L)\,(r - r_L)^2 + o((r - r_L)^2), \tag{A.3.37}$$

$$\Psi_L'(r) = \Psi_L''(r_L)\,(r - r_L) + o(r - r_L), \tag{A.3.38}$$

$$\Psi_L''(r) = \Psi_L''(r_L) + o(1), \tag{A.3.39}$$

for $r, L > 0$ by Taylor's theorem; recall $\Psi_L \in C^3(]0,\infty[)$ with $\Psi_L'(r_L) = 0$. Hence, for any $L > 0$, the mapping $]0,\infty[\ni r \mapsto \frac{\Psi_L(r) - E_L^{\min}}{\Psi_L'(r)}$ is continuous with

$$\frac{\Psi_L(r) - E_L^{\min}}{\Psi_L'(r)}\Big|_{r=r_L} =: \lim_{r \to r_L} \frac{\Psi_L(r) - E_L^{\min}}{\Psi_L'(r)} = 0. \tag{A.3.40}$$

Moreover,

$$\partial_r\left[\frac{\Psi_L(r) - E_L^{\min}}{\Psi_L'(r)}\right] = \frac{\Psi_L'(r)^2 - (\Psi_L(r) - E_L^{\min})\,\Psi_L''(r)}{\Psi_L'(r)^2} \tag{A.3.41}$$

for $r \in]0,\infty[\setminus \{r_L\}$, and (A.3.37)–(A.3.39) show that defining

$$\frac{\Psi_L'(r)^2 - (\Psi_L(r) - E_L^{\min})\,\Psi_L''(r)}{\Psi_L'(r)^2}\Big|_{r=r_L} \coloneqq \frac{1}{2} \tag{A.3.42}$$

[210] Here we employ the standard Landau notation, i.e., for $n \in \mathbb{N}_0$, the expression $o((r - r_L)^n)$ represents a continuous function $\alpha\colon]0,\infty[\to \mathbb{R}$ s.t. $\lim_{r \to r_L} \frac{\alpha(r)}{(r - r_L)^n} = 0$.

extends $\partial_r \left[\frac{\Psi_L(r) - E_L^{\min}}{\Psi_L'(r)} \right]$ continuously onto $]0,\infty[$; note that $\Psi_L''(r_L) = 4\pi\rho_0(r_L) + \frac{L}{r_L^4} > 0$ by (2.2.32). Hence, we can indeed integrate by parts in (A.3.36), which yields

$$I(E,L) = -\frac{2}{3} \int_{r_-(E,L)}^{r_+(E,L)} \frac{\Psi_L'(r)^2 - (\Psi_L(r) - E_L^{\min})\, \Psi_L''(r)}{\Psi_L'(r)^2} \, (2E - 2\Psi_L(r))^{\frac{3}{2}} \, \mathrm{d}r \tag{A.3.43}$$

for $(E,L) \in \mathbb{A}_0$. Applying Lemma A.3.8 twice then implies that I is twice partially differentiable w.r.t. E with

$$\partial_E^2 I(E,L) = -2 \int_{r_-(E,L)}^{r_+(E,L)} \frac{\Psi_L'(r)^2 - (\Psi_L(r) - E_L^{\min})\, \Psi_L''(r)}{\Psi_L'(r)^2} \, \frac{\mathrm{d}r}{\sqrt{2E - 2\Psi_L(r)}} \tag{A.3.44}$$

for $(E,L) \in \mathbb{A}_0$. By (A.3.31) and (A.3.35), T is thus partially differentiable w.r.t. E with

$$\partial_E^2 I = \frac{1}{2} \partial_E A - T - \left(E - E_L^{\min}\right) \partial_E T \tag{A.3.45}$$

on $\mathbb{A}_0$. Inserting (2.2.97), (A.3.31), and (A.3.44) into this identity and solving for $\partial_E T$ then yields (A.3.32). □

In order to show that $\partial_E T$ is continuous, we further analyse G_L.

Lemma A.3.10. *The function* $]0,\infty[^2 \ni (L,r) \mapsto G_L(r)$ *defined by* (A.3.33) *is continuous.*

Proof. The continuity on the set $\{(L,r) \in]0,\infty[^2 \mid r \neq r_L\}$ follows by the regularity of U_0 established in Proposition 2.2.9 (e); note that this set is open by Lemma 2.2.14 (a).

It thus remains to show the continuity in (L^*, r_{L^*}) for $L^* > 0$. To do so, we apply Taylor's theorem to infer that for any $L > 0$ and $r > 0$ there exist $\xi_1, \xi_2, \xi_3, \xi_4 > 0$ with $|\xi_i - r_L| \leq |r - r_L|$ for $i \in \{1,2,3,4\}$ s.t.

$$\Psi_L(r) - E_L^{\min} = \frac{1}{2} \Psi_L''(r_L)\, (r - r_L)^2 + \frac{1}{6} \Psi_L'''(\xi_1)\, (r - r_L)^3, \tag{A.3.46}$$

$$\Psi_L'(r) = \Psi_L''(\xi_2)\, (r - r_L) = \Psi_L''(r_L)\, (r - r_L) + \frac{1}{2} \Psi_L'''(\xi_3)\, (r - r_L)^2, \tag{A.3.47}$$

$$\Psi_L''(r) = \Psi_L''(r_L) + \Psi_L'''(\xi_4)\, (r - r_L). \tag{A.3.48}$$

Inserting these expansions into the definition of G_L yields

$$G_L(r) = \frac{r - r_L}{\Psi_L''(\xi_2)^2} \Bigg(\Psi_L''(r_L) \left(\Psi_L'''(\xi_3) - \Psi_L'''(\xi_4) - \frac{1}{3} \Psi_L'''(\xi_1) \right) + \\ + \frac{r - r_L}{4} \Psi_L'''(\xi_3)^2 - \frac{r - r_L}{3} \Psi_L'''(\xi_1)\, \Psi_L'''(\xi_4) \Bigg) \tag{A.3.49}$$

for $L > 0$ and $r > 0$ with $r \neq r_L$. Because $]0,\infty[^2 \ni (L,r) \mapsto \Psi_L^{(j)}(r)$ is continuous for $j \in \{0,1,2,3\}$ by Proposition 2.2.9 (e), all terms containing some ξ_i are locally bounded in (L,r). Moreover, since $\Psi_{L^*}''(r_{L^*}) > 0$, the expression $\Psi_L''(\xi_2)$ is bounded away from zero for all (L,r) in a sufficiently small neighbourhood of (L^*, r_{L^*}); notice that ξ_i depends on (L,r). Hence, (A.3.49) shows that $G_L(r) \to 0$ as $(L,r) \to (L^*, r_{L^*})$. □

The above lemma now allows us to conclude that the energy derivative of the period function is continuous.

Corollary A.3.11. *The function* $\partial_E T \colon \mathbb{A}_0 \to \mathbb{R}$ *is continuous.*

Proof. Combine Lemmas A.3.1, A.3.9, and A.3.10. □

Our next aim is to compute the L-derivative of the period function T. We shall not do this by directly differentiating (2.2.97) w.r.t. L, as this would require somewhat new (and technical) arguments. Instead, we follow a different strategy in which we can recycle the above arguments used to compute $\partial_E T$: We first differentiate the area function A w.r.t. L, which is rather straight-forward. The resulting expression $\partial_L A$ is qualitatively similar to T. We can therefore differentiate it w.r.t. E using the same methods as in Lemma A.3.9, and obtain a representation for $\partial_L T = \partial_L \partial_E A$ by commuting the partial derivatives. Let us proceed with the first step of this strategy.

Lemma A.3.12. *The area function $A\colon \mathbb{A}_0 \to \mathbb{R}$ introduced in Definition A.3.6 is partially differentiable w.r.t. L with*

$$\partial_L A(E,L) = -\int_{r_-(E,L)}^{r_+(E,L)} \frac{\mathrm{d}r}{r^2\sqrt{2E - 2\Psi_L(r)}}, \qquad (E,L) \in \mathbb{A}_0. \tag{A.3.50}$$

Proof. The statement can be shown similarly to Lemma A.3.8. More precisely, we first show that (A.3.50) holds if one replaces the partial derivative ∂_L with the left-derivative ∂_L^-. We then conclude the claimed statement because the integral on the right-hand side of (A.3.50) is continuous as a function of $(E,L) \in \mathbb{A}_0$ by Lemma A.3.1. □

Except for the $\frac{1}{r^2}$-weight, the integral representation (A.3.50) of $\partial_L A$ looks similar to the one of the period function T. In fact, it is possible to interpret $\partial_L A$ as the period function associated to another, suitably chosen potential. This observation is due to [85, Rem. 3.17].

Lemma A.3.13. *For $L > 0$ let*

$$\tilde{\Psi}_L\colon]0,\infty[\to \mathbb{R},\ \tilde{\Psi}_L(\sigma) \coloneqq \Psi_L\Big(\frac{\sqrt{L}}{\sigma}\Big) = U_0\Big(\frac{\sqrt{L}}{\sigma}\Big) + \frac{\sigma^2}{2}. \tag{A.3.51}$$

Then the function $\tilde{\Psi}_L$ has similar properties as the ones stated in Lemma 2.2.12 for the effective potential Ψ_L.[211] *Concretely,*

$$\min_{]0,\infty[} \tilde{\Psi}_L = \min_{]0,\infty[} \Psi_L = E_L^{\min}, \tag{A.3.52}$$

and the unique minimiser of $\tilde{\Psi}_L$ is

$$\sigma_L \coloneqq \frac{\sqrt{L}}{r_L}. \tag{A.3.53}$$

In addition, for every $E \in]E_L^{\min}, 0[$, the unique values $0 < \sigma_-(E,L) < \sigma_+(E,L) < \infty$ satisfying

$$\tilde{\Psi}_L(\sigma_\pm(E,L)) = E \tag{A.3.54}$$

are given by

$$\sigma_\pm(E,L) \coloneqq \frac{\sqrt{L}}{r_\mp(E,L)}. \tag{A.3.55}$$

Furthermore, solutions of the system

$$\dot{\sigma} = w, \tag{A.3.56a}$$

$$\dot{w} = -\tilde{\Psi}_L'(\sigma), \tag{A.3.56b}$$

[211] One difference to the effective potential is the limiting behaviour of $\tilde{\Psi}_L(\sigma)$ as $\sigma \to 0$ and as $\sigma \to \infty$ because $\lim_{\sigma\to 0} \tilde{\Psi}_L(\sigma) = 0 = \lim_{r\to\infty} \Psi_L(r)$ and $\lim_{\sigma\to\infty} \tilde{\Psi}_L(\sigma) = \infty = \lim_{r\to 0} \Psi_L(r)$.

behave similarly to the ones of (2.2.93)*. In particular, the energy defined by*

$$\tilde{E}(\sigma, w, L) \coloneqq \frac{1}{2}w^2 + \tilde{\Psi}_L(\sigma), \qquad (\sigma, w, L) \in]0, \infty[\times \mathbb{R} \times]0, \infty[, \tag{A.3.57}$$

is a conserved quantity of (A.3.56)*, and every solution of* (A.3.56) *with parameter* $L > 0$ *and conserved energy value* $E = \tilde{E} \in]E_L^{\min}, 0[$ *is time-periodic with period*

$$\tilde{T}(E, L) \coloneqq 2 \int_{\sigma_-(E,L)}^{\sigma_+(E,L)} \frac{\mathrm{d}\sigma}{\sqrt{2E - 2\tilde{\Psi}_L(\sigma)}}. \tag{A.3.58}$$

There holds the relation

$$\partial_L A(E, L) = -\frac{1}{2\sqrt{L}} \tilde{T}(E, L), \qquad (E, L) \in \mathbb{A}_0. \tag{A.3.59}$$

Proof. The properties of the function $\tilde{\Psi}_L$ easily follow by the ones of the effective potential Ψ_L derived in Lemma 2.2.12. Similar as in Section 2.2.2, one can then verify the claimed behaviour of the solutions of (A.3.56).

In order to establish (A.3.59), we change variables via $\sigma = \frac{\sqrt{L}}{r}$ in (A.3.50) to conclude

$$\partial_L A(E, L) = -\frac{1}{\sqrt{L}} \int_{\sigma_-(E,L)}^{\sigma_+(E,L)} \frac{\mathrm{d}\sigma}{\sqrt{2E - 2\tilde{\Psi}_L(\sigma)}} = -\frac{1}{2\sqrt{L}} \tilde{T}(E, L) \tag{A.3.60}$$

for $(E, L) \in \mathbb{A}_0$. □

Let us briefly discuss the physical meaning of $\tilde{T}$.

Remark A.3.14. *As shown above, applying the change of variables* $\sigma = \frac{\sqrt{L}}{r}$ *to* (A.3.58) *yields*

$$\tilde{T}(E, L) = 2\sqrt{L} \int_{r_-(E,L)}^{r_+(E,L)} \frac{\mathrm{d}r}{r^2\sqrt{2E - 2\Psi_L(r)}} \tag{A.3.61}$$

for $(E, L) \in \mathbb{A}_0$*. Following [19, Sc. 3.1], this quantity is related to the particle motions as follows: Consider a solution of the characteristic system* (2.2.2) *of the steady state in Cartesian* (x, v)*-coordinates with conserved quantities* $(E, L) \in \mathbb{A}_0$*. The solution moves in the orbital plane, i.e., the plane perpendicular to the (conserved) angular momentum vector, around the centre of symmetry* $r = 0$*. As discussed in Section 2.2.2, the radial period of this solution, i.e., the time needed for the spatial radius of the solution to move from its minimal value* $r_-(E, L)$ *to its maximal value* $r_+(E, L)$ *and back to* $r_-(E, L)$*, is given by* $T(E, L)$*. During one such radial period, the azimuthal angle of the solution in the orbital plane increases by* $\tilde{T}(E, L)$*, cf. [19, Eqn. (3.18b)]. The mean angular speed of the solution in the orbital plane is thus given by the ratio*

$$\frac{\tilde{T}(E, L)}{T(E, L)}. \tag{A.3.62}$$

Using the relation (A.3.59) from Lemma A.3.13 and applying the techniques from Lemma A.3.9 allows us to compute the energy derivative of $\partial_L A$.

Lemma A.3.15. *The function $\partial_L A\colon \mathbb{A}_0 \to \mathbb{R}$ is partially differentiable w.r.t. E with*

$$\partial_E \partial_L A(E,L) = -\frac{1}{2(E-E_L^{\min})} \int_{r_-(E,L)}^{r_+(E,L)} H_L(r)\, \frac{\mathrm{d}r}{r^2\sqrt{2E-2\Psi_L(r)}}, \qquad (E,L)\in\mathbb{A}_0, \tag{A.3.63}$$

where

$$H_L\colon]0,\infty[\to\mathbb{R},\ H_L(r) \coloneqq \begin{cases} \frac{\Psi_L'(r)^2 - 2(\Psi_L(r)-E_L^{\min})\,(\Psi_L''(r)+\frac{2}{r}\Psi_L'(r))}{\Psi_L'(r)^2}, & r\neq r_L, \\ 0, & r = r_L. \end{cases} \tag{A.3.64}$$

The function $]0,\infty[^2\ni (L,r)\mapsto H_L(r)$ is continuous and the integral on the right-hand side of (A.3.63) *exists.*

Proof. Mimicking the proof of Lemma A.3.9 shows that $\tilde{T}\colon \mathbb{A}_0 \to \mathbb{R}$ defined in Lemma A.3.13 is partially differentiable w.r.t. E with

$$\partial_E \tilde{T}(E,L) = \frac{1}{E-E_L^{\min}} \int_{\sigma_-(E,L)}^{\sigma_+(E,L)} \tilde{G}_L(\sigma)\, \frac{\mathrm{d}\sigma}{\sqrt{2E-2\tilde{\Psi}_L(\sigma)}}, \tag{A.3.65}$$

where

$$\tilde{G}_L\colon]0,\infty[\to\mathbb{R},\ \tilde{G}_L(\sigma) \coloneqq \begin{cases} \frac{\tilde{\Psi}_L'(\sigma)^2 - 2(\tilde{\Psi}_L(\sigma)-E_L^{\min})\tilde{\Psi}_L''(\sigma)}{\tilde{\Psi}_L'(\sigma)^2}, & \sigma\neq\sigma_L, \\ 0, & \sigma=\sigma_L. \end{cases} \tag{A.3.66}$$

Similar arguments as in the proof of Lemma A.3.10 yield that $]0,\infty[^2\ni (L,\sigma)\mapsto \tilde{G}_L(\sigma)$ is continuous because $\tilde{\Psi}_L$ has the same properties as the effective potential Ψ_L; in particular, the calculation (A.3.68) below will show $\tilde{\Psi}_L''(\sigma_L)>0$.

In order to change to the variable $r=\frac{\sqrt{L}}{\sigma}$ in the integral on the right-hand side of (A.3.65), first observe that differentiating (A.3.51) and using the radial Poisson equation (2.2.32) yields

$$\tilde{\Psi}_L'(\sigma) = -\frac{r^2}{\sqrt{L}}\,\Psi_L'(r), \tag{A.3.67}$$

$$\tilde{\Psi}_L''(\sigma) = \frac{r^4}{L}\,\Psi_L''(r) + 2\frac{r^3}{L}\,\Psi_L'(r) = \frac{r^4}{L}\,\Delta\Psi_L(r) = \frac{r^4}{L}\left(4\pi\rho_0(r)+\frac{L}{r^4}\right), \tag{A.3.68}$$

for $L>0$, $\sigma>0$, and $r=\frac{\sqrt{L}}{\sigma}$. Hence,

$$\tilde{G}_L\Big(\frac{\sqrt{L}}{r}\Big) = \frac{\Psi_L'(r)^2 - 2(\Psi_L(r)-E_L^{\min})\,(\Psi_L''(r)+\frac{2}{r}\,\Psi_L'(r))}{\Psi_L'(r)^2} = H_L(r) \tag{A.3.69}$$

for $L,r>0$ with $r\neq r_L$, and the continuity of $]0,\infty[^2\ni (L,\sigma)\mapsto\tilde{G}_L(\sigma)$ implies the claimed continuity of $]0,\infty[^2\ni (L,r)\mapsto H_L(r)$. Changing variables via $r=\frac{\sqrt{L}}{\sigma}$ in (A.3.65) thus yields

$$\partial_E \tilde{T}(E,L) = \frac{\sqrt{L}}{E-E_L^{\min}} \int_{r_-(E,L)}^{r_+(E,L)} H_L(r)\, \frac{\mathrm{d}r}{r^2\sqrt{2E-2\Psi_L(r)}}, \qquad (E,L)\in\mathbb{A}_0. \tag{A.3.70}$$

Inserting this identity into (A.3.59) concludes the proof of (A.3.63). □

Lemmas A.3.12 and A.3.15 now allow us to compute the L-derivative of the period function by commuting derivatives w.r.t. E and L.

Lemma A.3.16 (The L-Derivative of the Period Function)**.** *The period function* $T\colon \mathbb{A}_0 \to]0,\infty[$ *defined by* (2.2.97) *is partially differentiable w.r.t. L with*

$$\partial_L T(E,L) = \partial_E \partial_L A(E,L) = -\frac{1}{2(E-E_L^{\min})} \int_{r_-(E,L)}^{r_+(E,L)} H_L(r)\, \frac{\mathrm{d}r}{r^2\sqrt{2E-2\Psi_L(r)}} \tag{A.3.71}$$

for $(E,L) \in \mathbb{A}_0$, where H_L is defined in (A.3.64)*.*

Proof. Lemmas A.3.8 and A.3.12 imply that $\partial_E A$ and $\partial_L A$ exist on $\mathbb{A}_0$. In addition, $\partial_E \partial_L A$ exists by Lemma A.3.15 and applying Lemma A.3.1 to (A.3.63) shows that $\partial_E \partial_L A$ is continuous on $\mathbb{A}_0$. Hence, $\partial_E A$ is partially differentiable w.r.t. L with

$$\partial_L \partial_E A = \partial_E \partial_L A \qquad \text{on } \mathbb{A}_0 \tag{A.3.72}$$

by Schwarz's theorem. Recalling (A.3.31), we conclude that T is partially differentiable w.r.t. L and that (A.3.71) holds. □

Let us summarise the findings of the present section so far.

Proposition A.3.17. *The period function* $T\colon \mathbb{A}_0 \to]0,\infty[$ *defined by* (2.2.97) *is continuously differentiable and its partial derivatives are given by* (A.3.32) *and* (A.3.71)*. Moreover,*

$$\partial_L T(E,L) = -\frac{1}{2\sqrt{L}}\, \partial_E \tilde{T}(E,L), \qquad (E,L) \in \mathbb{A}_0, \tag{A.3.73}$$

where $\tilde{T}$ is defined in Lemma A.3.13.

We (again) note that an alternative way of computing the second-order derivatives of the area function A is presented in [148, App. C]. In particular, the integral representations of $\partial_E^2 A$ and $\partial_E \partial_L A = \partial_L \partial_E A$ from [148, Eqns. (C.11) and (C.12)] are identical to the expressions derived above.

Although it is not necessary for the proof of Proposition A.0.1, it is useful (for the analysis in Chapter 6) to derive integral representations for the higher-order partial derivatives of T as well; recall $T \in C^2(\mathbb{A}_0)$ by Lemma A.3.3. We illustrate how this works for $\partial_E^2 T$. Other second-order partial derivates can be computed in the same way using (A.3.73). In order to differentiate the integral representation of $\partial_E T$ derived in Lemma A.3.9 by applying the general result from Lemma A.3.8, we first rewrite (A.3.32). This is based on [61, Eqn. (A.21)].

Lemma A.3.18. *For $L > 0$ let*

$$G_{1,L}\colon]0,\infty[\to \mathbb{R},\ G_{1,L}(r) \coloneqq \begin{cases} \frac{G_L(r)}{\Psi_L'(r)}, & r \neq r_L, \\ -\frac{1}{3}\,\frac{\Psi_L'''(r_L)}{\Psi_L''(r_L)^2}, & r = r_L, \end{cases} \tag{A.3.74}$$

where G_L is defined in (A.3.33)*. Assume that the underlying steady state satisfies $U_0 \in C^4(I)$ for some open interval I.*[212] *For $L > 0$ with $r_L \in I$, $G_{1,L}$ is differentiable on $]0,\infty[$ with*

$$G_{1,L}'(r) = \begin{cases} \frac{6(\Psi_L(r)-E_L^{\min})\,\Psi_L''(r)^2 - 3\Psi_L'(r)^2\,\Psi_L''(r) - 2(\Psi_L(r)-E_L^{\min})\,\Psi_L'(r)\,\Psi_L'''(r)}{\Psi_L'(r)^4}, & r \neq r_L, \\ \frac{5}{12}\,\frac{\Psi_L'''(r_L)^2}{\Psi_L''(r_L)^3} - \frac{1}{4}\,\frac{\Psi_L^{(4)}(r_L)}{\Psi_L''(r_L)^2}, & r = r_L, \end{cases} \tag{A.3.75}$$

[212] We will comment on this regularity assumption in Remark A.4.7.

for $r > 0$. The functions $]0,\infty[^2 \ni (L,r) \mapsto G_{1,L}(r)$ and $\{\tilde{L} > 0 \mid r_{\tilde{L}} \in I\} \times]0,\infty[\ni (L,r) \mapsto G'_{1,L}(r)$ are both continuous. Furthermore, for all $(E,L) \in \mathbb{A}_0$ with $r_L \in I$ there holds the identity

$$\int_{r_-(E,L)}^{r_+(E,L)} \frac{G_L(r)}{\sqrt{2E - 2\Psi_L(r)}}\,\mathrm{d}r = \int_{r_-(E,L)}^{r_+(E,L)} G'_{1,L}(r)\,\sqrt{2E - 2\Psi_L(r)}\,\mathrm{d}r. \tag{A.3.76}$$

Proof. We first verify the claimed properties of $G_{1,L}$. Taylor expanding G_L with quantitative control of the rest terms, see (A.3.49) in the proof of Lemma A.3.10, shows that $]0,\infty[^2 \ni (L,r) \mapsto G_{1,L}(r)$ is continuous. The formula (A.3.75) for $G'_{1,L}(r)$ in the case $r \neq r_L$ follows by direct computation. In order to analyse $G'_{1,L}(r)$ at $r = r_L$, we Taylor expand all terms to fourth order, i.e., we write

$$\Psi_L(r) = E_L^{\min} + \frac{\Psi''_L(r_L)}{2}\,(r - r_L)^2 + \frac{\Psi'''_L(r_L)}{6}\,(r - r_L)^3 + \frac{\Psi^{(4)}_L(\xi_1)}{24}\,(r - r_L)^4, \tag{A.3.77}$$

$$\Psi'_L(r) = \Psi''_L(\xi_2)\,(r - r_L) = \Psi''_L(r_L)\,(r - r_L) + \frac{\Psi'''_L(r_L)}{2}\,(r - r_L)^2 + \frac{\Psi^{(4)}_L(\xi_3)}{6}\,(r - r_L)^3, \tag{A.3.78}$$

$$\Psi''_L(r) = \Psi''_L(r_L) + \Psi'''_L(r_L)\,(r - r_L) + \frac{\Psi^{(4)}_L(\xi_4)}{2}\,(r - r_L)^2, \tag{A.3.79}$$

$$\Psi'''_L(r) = \Psi'''_L(r_L) + \Psi^{(4)}_L(\xi_5)\,(r - r_L), \tag{A.3.80}$$

for $r \in I$ and $L > 0$ with $r \neq r_L \in I$ and some $\xi_1, \xi_2, \xi_3, \xi_4, \xi_5 \in I$ with $|\xi_i - r_L| \leq |r - r_L|$ for $i \in \{1,2,3,4,5\}$. Recall that we assume that U_0 is four times continuously differentiable on I. Inserting these expansions into the numerator of $G'_{1,L}(r)$ yields

$$\begin{aligned}\frac{\Psi'_L(r)^4\,G'_{1,L}(r)}{(r - r_L)^4} &= \frac{1}{4}\,\Psi''_L(r_L)^2\,\Psi^{(4)}_L(\xi_1) - \Psi''_L(r_L)^2\,\Psi^{(4)}_L(\xi_3) + \\ &\quad + \frac{3}{2}\,\Psi''_L(r_L)^2\,\Psi^{(4)}_L(\xi_4) - \Psi''_L(r_L)^2\,\Psi^{(4)}_L(\xi_5) + \frac{5}{12}\,\Psi''_L(r_L)\,\Psi'''_L(r_L)^2 + o(1),\end{aligned} \tag{A.3.81}$$

while the denominator can be written as

$$\frac{\Psi'_L(r)^4}{(r - r_L)^4} = \Psi''_L(\xi_2)^4. \tag{A.3.82}$$

Here, the $o(1)$-terms are sums of products of the expansion terms from the right-hand sides of (A.3.77)–(A.3.80) containing some positive power of $(r - r_L)$. Since $]0,\infty[\times I \ni (L,r) \mapsto \Psi^{(j)}_L(r)$ is continuous for $0 \leq j \leq 4$, the $o(1)$-terms converge to 0 as $r \to r_L$ locally uniformly in L. Considering the limit $r \to r_L$ in (A.3.81) and (A.3.82) hence shows that $G_{1,L}$ is indeed differentiable with (A.3.75) and that $(L,r) \mapsto G'_{1,L}(r)$ is continuous on $\{(L,r_L) \mid L > 0 \text{ with } r_L \in I\}$; recall $\Psi''_L(r_L) > 0$.

The identity (A.3.76) is then obtained by integrating by parts:

$$\begin{aligned}\int_{r_-(E,L)}^{r_+(E,L)} \frac{G_L(r)}{\sqrt{2E - 2\Psi_L(r)}}\,\mathrm{d}r &= -\int_{r_-(E,L)}^{r_+(E,L)} G_{1,L}(r)\,\partial_r\Big[\sqrt{2E - 2\Psi_L(r)}\Big]\,\mathrm{d}r = \\ &= \int_{r_-(E,L)}^{r_+(E,L)} G'_{1,L}(r)\,\sqrt{2E - 2\Psi_L(r)}\,\mathrm{d}r\end{aligned} \tag{A.3.83}$$

for $(E,L) \in \mathbb{A}_0$ as specified in the statement of the lemma. □

We can now directly apply Lemma A.3.8 to the right-hand side of (A.3.76) to obtain an integral representation of $\partial_E^2 T$. This is based on [61, Eqn. (A.28)].

Lemma A.3.19 (The Second-Order Energy Derivative of the Period Function)**.** *Assume $U_0 \in C^4(I)$ for some open interval I, and consider $(E, L) \in \mathbb{A}_0$ with $r_L \in I$. Then $\partial_E T$ is partially differentiable in (E, L) w.r.t. E with*

$$\partial_E^2 T(E,L) = \frac{1}{(E - E_L^{\min})^2} \int_{r_-(E,L)}^{r_+(E,L)} G'_{1,L}(r) \left(\frac{\Psi_L(r) - E_L^{\min}}{\sqrt{2E - 2\Psi_L(r)}} - \frac{1}{2}\sqrt{2E - 2\Psi_L(r)} \right) \mathrm{d}r; \tag{A.3.84}$$

recall that $G'_{1,L}$ is given by (A.3.75)*.*

Proof. Combining (A.3.32) and (A.3.76) shows

$$\partial_E T(E,L) = \frac{1}{E - E_L^{\min}} \int_{r_-(E,L)}^{r_+(E,L)} G'_{1,L}(r) \sqrt{2E - 2\Psi_L(r)}\, \mathrm{d}r. \tag{A.3.85}$$

Differentiating this expression w.r.t. E using Lemma A.3.8 yields

$$\partial_E^2 T(E,L) = \frac{1}{(E - E_L^{\min})^2} \int_{r_-(E,L)}^{r_+(E,L)} G'_{1,L}(r) \left(\frac{E - E_L^{\min}}{\sqrt{2E - 2\Psi_L(r)}} - \sqrt{2E - 2\Psi_L(r)} \right) \mathrm{d}r. \tag{A.3.86}$$

We then conclude (A.3.84) by rewriting the integrand. □

A.3.3 Monotonicity of the Period Function ?

When studying the presence of oscillatory modes, we see that it is crucial to understand where the period function T attains its maximal and minimal values on the (closure of the) (E, L)-triangle $\mathbb{D}_0$. In fact, the numerical simulations indicate that T is monotonic in at least one of its variables for many steady states, cf. Section 8.2. In this section, we thus use the identities for the partial derivatives of T derived above to investigate the monotonicity of the period function w.r.t. one of its variables. As a caveat, however, we shall say in advance that we are not able to prove the monotonicity of the period function for any steady state from Section 2.2 mathematically. We rather limit ourselves here to collecting criteria for the monotonicity of T, which can then be checked numerically – and hopefully also mathematically in future work.

Further criteria for the monotonicity of a period function, as well as examples where they are satisfied, are, e.g., derived in [23, 28, 30, 31, 45, 125, 148, 152]. We present some of the ideas from these references below, but also admit that we may not have understood well enough some arguments from the rich literature leading to the monotonicity of T w.r.t. one of its variables.

Monotonicity via Characteristics ?

Lemma A.3.3 shows[213]

$$\operatorname{sign}(\partial_E T(E,L)) = -\operatorname{sign}(\partial_E W(T(E,L),E,L)) = \operatorname{sign}\Big(\partial_E W\Big(\frac{1}{2}T(E,L),E,L\Big)\Big), \tag{A.3.87}$$

$$\operatorname{sign}(\partial_L T(E,L)) = -\operatorname{sign}(\partial_L W(T(E,L),E,L)) = \operatorname{sign}\Big(\partial_L W\Big(\frac{1}{2}T(E,L),E,L\Big)\Big), \tag{A.3.88}$$

for $(E,L) \in \mathbb{A}_0$, where (R,W) is the characteristic flow of the steady state as specified in Section A.3.1. For instance, in order to understand whether T is monotonic in E, one has to analyse the sign of $\partial_E W(\frac{1}{2}T(E,L),E,L)$ for $(E,L) \in \mathbb{A}_0$. Recall $\partial_E W = \partial_E \dot{R} = \partial_s \partial_E R$ and that $\partial_E R(\cdot,E,L)$ is the unique solution of the linear second-order ODE (A.3.13) satisfying the initial condition

$$\partial_E R(0,E,L) = \frac{1}{\Psi_L'(r_-(E,L))} < 0, \qquad \partial_E \dot{R}(0,E,L) = 0, \tag{A.3.89}$$

cf. Remark A.3.4. Another solution of the ODE (A.3.13) is given by $W(\cdot,E,L)$, and the latter solution is $T(E,L)$-periodic with

$$W(0,E,L) = 0 = W\Big(\frac{1}{2}T(E,L),E,L\Big), \tag{A.3.90}$$

$$\dot{W}(0,E,L) = -\Psi_L'(r_-(E,L)) > 0 > -\Psi_L'(r_+(E,L)) = \dot{W}\Big(\frac{1}{2}T(E,L),E,L\Big). \tag{A.3.91}$$

If we imagine this solution in the $(\alpha,\dot{\alpha})$-plane, $W(\cdot,E,L)$ completes "half a round" at time $s = \frac{1}{2}T(E,L)$. The sign of $\partial_E W(\frac{1}{2}T(E,L),E,L)$ is determined by whether $\partial_E R(\cdot,E,L)$ is faster than $W(\cdot,E,L)$, more precisely, whether it has already completed half a round after the same time ($\partial_E \dot{R}(\frac{1}{2}T(E,L),E,L) < 0 = \partial_E \dot{R}(0,E,L)$), or not ($\partial_E \dot{R}(\frac{1}{2}T(E,L),E,L) > 0$).[214] A suitable comparison statement could provide insight into issues of this type.

Another observation from Remark A.3.4 is that $\partial_E T(E,L) = 0$ is equivalent to $\partial_E R(\cdot,E,L)$ being periodic; this is due to (A.3.17). In this case, the period of $\partial_E R(\cdot,E,L)$ is $T(E,L)$, i.e., the period equals the one of $W(\cdot,E,L)$. Hence, as $\partial_E R(\cdot,E,L)$ and $W(\cdot,E,L)$ form a fundamental system of (A.3.13), every solution of this ODE is $T(E,L)$-periodic. This is referred to as an instance of *coexistence*, and in the context of a Hill equation like (A.3.13) its presence is analysed in [106, Ch. 7] for some special cases. Moreover, by (A.3.17), $\partial_E T(E,L) = 0$ is equivalent to 0 being a stable equilibrium of (A.3.13). Relations between this stability and properties of the coefficient $\Psi_L''(R(\cdot,E,L))$ of the equation (A.3.13) are, e.g., studied in [106, Sc. 2.6 & Ch. 5] and [183, Sc. II.4].

Similar characterisations can also be derived for the L-derivative of T. Recall that $\partial_L R(\cdot,E,L)$ solves the ODE (A.3.20), which arises from (A.3.13) by adding an inhomogeneous term.

Monotonicity via the Integral Representations ?

Another way of checking whether the period function is monotonic w.r.t. one of its variables is provided by the integral representations of the partial derivatives $\partial_E T$ and $\partial_L T$, recall

[213] Here we employ the convention $\operatorname{sign}(0) := 0$.

[214] One should, however, be careful with this description as the angle of the solution $\partial_E R(\cdot,E,L)$ in the $(\alpha,\dot{\alpha})$-plane need not be monotonic in general.

Lemmas A.3.9 and A.3.16. A particularly naïve approach is to deduce the sign of $\partial_E T$ or $\partial_L T$ by showing that the integrand of the respective integral only attains one sign on the whole domain of integration. Unfortunately, the following lemma shows that this is not to be expected in general.

Lemma A.3.20. *Assume that the underlying steady state is isotropic, i.e., $L_0 = 0 = \ell$. Then, for any fixed $L > 0$, the function $G_L\colon]0,\infty[\to \mathbb{R}$ defined in* (A.3.33) *switches its sign at $r = r_L$. More precisely, for any $L > 0$ there exists some $\delta > 0$ s.t.*

$$G_L < 0 \text{ on }]r_L - \delta, r_L[, \qquad G_L > 0 \text{ on }]r_L, r_L + \delta[. \tag{A.3.92}$$

Proof. The continuity of $G_{1,L}$ shown in Lemma A.3.18 implies

$$\lim_{r\to r_L} \frac{G_L(r)}{\Psi_L'(r)} = -\frac{1}{3}\,\frac{\Psi_L'''(r_L)}{\Psi_L''(r_L)^2}. \tag{A.3.93}$$

By the radial Poisson equation (2.2.32) we obtain

$$\Psi_L'''(r) = 4\pi\rho_0'(r) - \frac{8\pi}{r}\,\rho_0(r) + \frac{6}{r^4}\,m_0(r) - 12\frac{L}{r^5}, \qquad r > 0. \tag{A.3.94}$$

Inserting $0 = \Psi_L'(r_L) = \frac{m_0(r_L)}{r_L^2} - \frac{L}{r_L^3}$ into (A.3.94) thus yields

$$\Psi_L'''(r_L) = 4\pi\rho_0'(r_L) - \frac{8\pi}{r_L}\,\rho_0(r_L) - 6\frac{L}{r_L^5}. \tag{A.3.95}$$

Now recall that ρ_0 is non-increasing in the case of an isotropic steady state by Remark 2.2.10 (a). Hence,

$$\Psi_L'''(r_L) < 0 \tag{A.3.96}$$

in the present, isotropic situation. Together with (A.3.93) we thus conclude that there exists some $\delta > 0$ s.t.

$$\frac{G_L}{\Psi_L'} > 0 \text{ on }]r_L - \delta, r_L + \delta[, \tag{A.3.97}$$

which implies (A.3.92) by recalling the structure of the effective potential Ψ_L derived in Lemma 2.2.12. □

Because the sign of the integrand in the integral representation (A.3.32) of $\partial_E T(E,L)$ is determined by the sign of G_L, the above lemma shows that we cannot hope to prove the energy monotonicity of T by the naïve approach described above,[215] at least in the case of an isotropic equilibrium. In the situation of a general steady state, the above arguments show that G_L switches its sign at r_L as long as $\Psi_L'''(r_L)$ does not vanish, which is expected to be the case in general.[216]

Similar statements also hold for the L-derivative of the period function. In fact, Taylor expanding the numerator of the function H_L defined in (A.3.64) shows

$$\lim_{r\to r_L} \frac{H_L(r)}{\Psi_L'(r)} = \lim_{r\to r_L} \frac{G_L(r)}{\Psi_L'(r)} \tag{A.3.98}$$

[215] In particular, note that the radius r_L, where the integrand switches its sign, is always contained in the domain of integration.

[216] Using the same techniques as above, one can, e.g., show that G_L always switches its sign at $r = r_L$ provided that $r_L > R_{\max}$. However, as L-values satisfying this condition cannot be found inside the support of the steady state, this observation is not too enlightening.

for fixed $L > 0$, i.e., H_L behaves similarly to G_L at $r = r_L$.

One possibility to get around this issue is to suitably reflect the integrand at $r = r_L$ in order to compare radii to the left and to the right of r_L with one another. We discuss this idea next; a similar approach is pursued in [23, Sc. 2].

Definition A.3.21 (A Radial Reflection Mapping)**.** *For $L > 0$ let*

$$\zeta_L \colon \{r > 0 \mid r < r_L \ \&\ \Psi_L(r) < 0\} \to]r_L, \infty[,\ \zeta_L(r) \coloneqq r_+(\Psi_L(r), L). \tag{A.3.99}$$

We call ζ_L a radial reflection mapping.

The mapping ζ_L operates as follows: Each radius $r > 0$ to the left of r_L is mapped to the right of r_L s.t. the value of the effective potential Ψ_L is preserved, i.e.,

$$\Psi_L(r) = \Psi_L(\zeta_L(r)), \qquad r \in]0, r_L[\text{ with } \Psi_L(r) < 0. \tag{A.3.100}$$

For this to be possible, we have to assume $\Psi_L(r) < 0$; recall the structure of the effective potential derived in Lemma 2.2.12, in particular, $\lim_{r\to 0} \Psi_L(r) = \infty$ and $\lim_{r\to\infty} \Psi_L(r) = 0$. Further note that Lemma 2.2.14 (c) implies that ζ_L is differentiable with

$$\zeta_L'(r) = \frac{\Psi_L'(r)}{\Psi_L'(\zeta_L(r))} \tag{A.3.101}$$

for $0 < r < r_L$ with $\Psi_L(r) < 0$. An illustration of the reflection mapping is provided in Figure A.3.1.

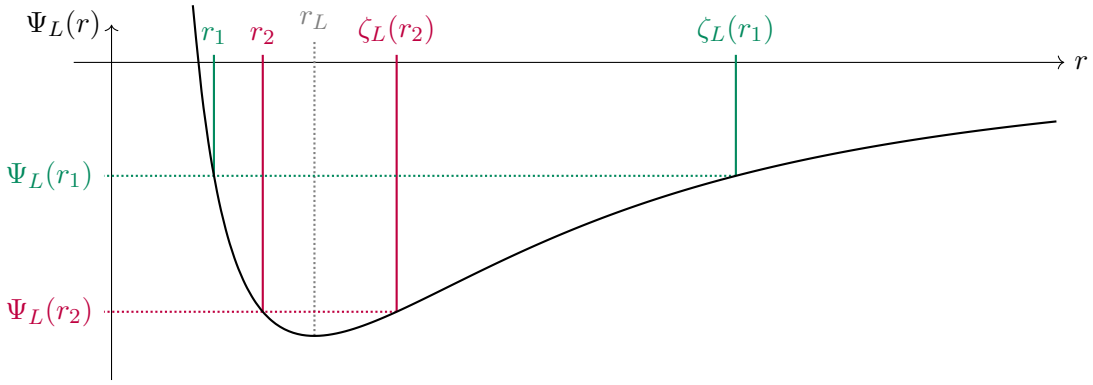

Figure A.3.1: A schematic visualisation of the radial reflection mapping ζ_L for $L > 0$.

We can use the radial reflection mapping ζ_L to rewrite the integral representations of $\partial_E T$ and $\partial_L T$.

Lemma A.3.22. *For $L > 0$ let*

$$G_L^{\mathrm{ref}} \colon \{r > 0 \mid r < r_L \ \&\ \Psi_L(r) < 0\} \to \mathbb{R},\ G_L^{\mathrm{ref}}(r) \coloneqq G_L(r) - G_L(\zeta_L(r))\,\zeta_L'(r), \tag{A.3.102}$$

$$H_L^{\mathrm{ref}} \colon \{r > 0 \mid r < r_L \ \&\ \Psi_L(r) < 0\} \to \mathbb{R},\ H_L^{\mathrm{ref}}(r) \coloneqq \frac{H_L(r)}{r^2} - \frac{H_L(\zeta_L(r))}{\zeta_L(r)^2}\,\zeta_L'(r), \tag{A.3.103}$$

where G_L and H_L are defined in (A.3.33) *and* (A.3.64)*, respectively. Then, for $(E, L) \in \mathbb{A}_0$,*

$$\partial_E T(E, L) = \frac{1}{E - E_L^{\min}} \int_{r_-(E,L)}^{r_L} \frac{G_L^{\mathrm{ref}}(r)}{\sqrt{2E - 2\Psi_L(r)}}\,\mathrm{d}r, \tag{A.3.104}$$

$$\partial_L T(E, L) = -\frac{1}{2(E - E_L^{\min})} \int_{r_-(E,L)}^{r_L} \frac{H_L^{\mathrm{ref}}(r)}{\sqrt{2E - 2\Psi_L(r)}}\,\mathrm{d}r. \tag{A.3.105}$$

Proof. We first rewrite the formula for $\partial_E T$ from Lemma A.3.9 as follows:

$$\big(E - E_L^{\min}\big)\,\partial_E T(E,L) = \int_{r_-(E,L)}^{r_L} \frac{G_L(r)}{\sqrt{2E - 2\Psi_L(r)}}\,\mathrm{d}r + \int_{r_L}^{r_+(E,L)} \frac{G_L(r)}{\sqrt{2E - 2\Psi_L(r)}}\,\mathrm{d}r \tag{A.3.106}$$

for $(E,L) \in \mathbb{A}_0$. Changing variables via $r = \zeta_L(\tilde{r})$ in the second integral on the right-hand side of (A.3.106) – observe that $\zeta_L\colon [r_-(E,L), r_L[\to]r_L, r_+(E,L)]$ is one-to-one – and using (A.3.100) then yields (A.3.104). The identity (A.3.105) follows similarly using Lemma A.3.16. □

Showing that the integrands on the right-hand sides of (A.3.104) and (A.3.105) take only one sign is more likely to succeed. Concretely, if $G_L^{\mathrm{ref}} > 0$ and $H_L^{\mathrm{ref}} > 0$ on $]r_-(E,L), r_L[$ for some $(E,L) \in \mathbb{A}_0$, we obtain $\partial_E T(E,L) > 0$ and $\partial_L T(E,L) > 0$. We analyse this criterion for the monotonicity of T numerically in Section 8.2. As a slight preview, we note that the numerics indicate that G_L^{ref} and H_L^{ref} are indeed positive on suitable radial domains for certain steady states, cf. Observations 8.2.3, 8.2.5, and 8.2.6. Hence, the above lemma might be helpful to rigorously prove the monotonicity of T in future work.

Monotonicity at the Boundary

The above discussion is only concerned with the monotonicity of the period function inside $\mathbb{A}_0$. In order to understand where T attains its maximal/minimal values on the (E,L)-support $\mathbb{D}_0 = \mathbb{A}_0 \cap \{E < E_0 \ \&\ L > L_0\}$ of the steady state, it is also useful to analyse the monotonicity of (a suitable extension of) T on the boundary of $\mathbb{A}_0$. Of particular interest is the behaviour of T on the following two parts of the boundary of $\mathbb{A}_0$:[217]

$$\{(E_L, L) \mid L > 0\} \subset \partial\mathbb{A}_0, \tag{A.3.107}$$

$$\{(E,0) \mid U_0(0) \le E < 0\} \subset \partial\mathbb{A}_0; \tag{A.3.108}$$

it follows by Lemma 2.2.14 that these two sets are indeed part of the boundary of $\mathbb{A}_0$.

We will not yet study the behaviour of T on (A.3.107), but will analyse it in Section A.4. In particular, a monotonicity statement of the period function on this part of the boundary will be proven in Lemma A.4.3.

As to the second part (A.3.108) of the boundary, recall Remark 2.2.17 (a), where it is argued that (2.2.99) defines a natural extension of the period function onto $\{(E,0) \mid U_0(0) < E < 0\}$. A detailed proof that this extension is indeed continuous is provided in [85, Lemma 3.12]. Moreover, the behaviour of $T(E,L)$ in the limit $(E,L) \to (U_0(0),0)$ will be briefly discussed in Remark A.4.4.

It is observed in [85, Lemma 3.15] that the (extension of the) period function is indeed monotonic on $\{(E,0) \mid U_0(0) < E < 0\}$ under suitable assumptions on the steady state. Since the proof of this statement could be helpful for further monotonicity proofs, we include it here.

Lemma A.3.23. *Assume that the underlying steady state is isotropic, i.e., $L_0 = 0 = \ell$. Then the function*

$$T(\cdot,0)\colon]U_0(0), 0[\to]0,\infty[,\ T(E,0) \coloneqq 2\int_0^{r_+(E,0)} \frac{\mathrm{d}r}{\sqrt{2E - 2U_0(r)}} \tag{A.3.109}$$

is strictly increasing.

[217] The remaining part of $\partial\mathbb{A}_0$ is $\{(0,L) \mid L \ge 0\}$. However, this set is not of interest when studying the behaviour of T on $\mathbb{D}_0$, because the energy values inside $\mathbb{D}_0$ are bounded from above by $E_0 < 0$.

Proof. We follow the proof from [85, Lemma 3.15], which is in turn based on [125]. Consider the mapping

$$\hat{T}\colon]0,\infty[\to]0,\infty[,\ \hat{T}(\hat{r}) \coloneqq 2\int_0^{\hat{r}} \frac{\mathrm{d}r}{\sqrt{2U_0(\hat{r})-2U_0(r)}}, \tag{A.3.110}$$

which is well-defined since $U_0' < 0$ on $]0,\infty[$ by the radial Poisson equation (2.2.32) and Proposition 2.2.9 (c). Recalling the definition of $r_+(\cdot,0)$ from Lemma 2.2.14 (c), there obviously holds

$$T(E,0) = \hat{T}(r_+(E,0)), \qquad E \in]U_0(0),0[. \tag{A.3.111}$$

Moreover, since $r_+(\cdot,0)\colon]U_0(0),0[\to]0,\infty[$ is strictly increasing, the claimed monotonicity of $T(\cdot,0)$ is equivalent to $\hat{T}$ being strictly increasing on $]0,\infty[$.

To prove the latter, we first use the radial Poisson equation (2.2.32) together with the fact that, in the case of an isotropic steady state, ρ_0 is strictly decreasing on $[0,R_{\max}]$ by Remark 2.2.10 (a) to infer

$$U_0''(r)-\frac{U_0'(r)}{r} = 4\pi\rho_0(r)-\frac{12\pi}{r^3}\int_0^r s^2\rho_0(s)\,\mathrm{d}s < 4\pi\rho_0(r)-\frac{12\pi}{r^3}\,\rho_0(r)\int_0^r s^2\,\mathrm{d}s = 0 \tag{A.3.112}$$

for $r>0$. Hence, $]0,\infty[\ni r \mapsto \frac{U_0'(r)}{r}$ is strictly decreasing, which implies

$$\frac{U_0'(p\,r)}{p} < U_0'(r), \qquad r>0,\ p>1. \tag{A.3.113}$$

Coming back to $\hat{T}$, we change variables via $r = p\,s$ to deduce

$$\hat{T}(p\,\hat{r}) = 2\int_0^{p\,\hat{r}} \frac{\mathrm{d}r}{\sqrt{2U_0(p\,\hat{r})-2U_0(r)}} = 2p\int_0^{\hat{r}} \frac{\mathrm{d}s}{\sqrt{2U_0(p\,\hat{r})-2U_0(p\,s)}} \tag{A.3.114}$$

for $\hat{r}>0$ and $p>1$. Applying the main theorem of calculus and (A.3.113) shows that for any $s \in]0,\hat{r}[$ there holds

$$U_0(p\,\hat{r})-U_0(p\,s) = p\int_s^{\hat{r}} U_0'(p\,\sigma)\,\mathrm{d}\sigma < p^2\int_s^{\hat{r}} U_0'(\sigma)\,\mathrm{d}\sigma = p^2(U_0(\hat{r})-U_0(s)). \tag{A.3.115}$$

Inserting this estimate into (A.3.114) then yields

$$\hat{T}(p\,\hat{r}) > 2\int_0^{\hat{r}} \frac{\mathrm{d}s}{\sqrt{2U_0(\hat{r})-2U_0(s)}} = \hat{T}(\hat{r}) \tag{A.3.116}$$

for $\hat{r}>0$ and $p>1$, which concludes the proof. □

The above arguments crucially rely on the fact that the domain of integration for the integral $T(E,0)$ starts at $r=0$. All attempts of the author to show the monotonicity of $T(\cdot,L)$ for $L>0$ with the above ideas have failed so far. Furthermore, using Lemmas A.3.13, A.3.15, and A.3.16 allows us to relate the L-monotonicity of the function T to the E-monotonicity of $\tilde{T}$ from Lemma A.3.13. However, using the above ideas to show that $\tilde{T}(\cdot,L)$ is monotonic has not succeeded so far either. Nonetheless, we refer to the discussion in [85, Rem. 3.17] for some evidence why proving the L-monotonicity of T in this way seems rather promising.

A.4 Extending the Period Function to Minimal Energies

In this section we analyse the behaviour of the period function close to the *minimal energy curve*

$$\{(E_L^{\min}, L) \mid L > 0\}. \tag{A.4.1}$$

In [61], this region is called the *near circular regime* because solutions of the characteristic system with squared modulus of angular momentum $L > 0$ and energy $E = E_L^{\min}$ are radially constant, i.e., $r \equiv r_L$, which corresponds to a circular motion in Cartesian (x, v)-coordinates.

More precisely, we study the limiting behaviour of $T(E, L)$ and of its partial derivatives $\partial_E T(E, L)$ and $\partial_L T(E, L)$ as $(E, L) \to (E_{L^*}^{\min}, L^*)$ for $L^* > 0$; note that the set (A.4.1) is contained in $\partial\mathbb{A}_0$. We shall solely work with the integral representations of T and its partial derivatives. For this, we first prove the following general result which is based on [61, Lemmas A.11 and A.12].

Lemma A.4.1. *Let* $]0, \infty[^2 \ni (L, r) \mapsto F_L(r) \in \mathbb{R}$ *be continuous.*[218] *Then, for* $L^* > 0$*,*

$$\lim_{\mathbb{A}_0 \ni (E,L) \to (E_{L^*}^{\min}, L^*)} \int_{r_-(E,L)}^{r_+(E,L)} F_L(r) \sqrt{2E - 2\Psi_L(r)}\, \mathrm{d}r = 0, \tag{A.4.2}$$

$$\lim_{\mathbb{A}_0 \ni (E,L) \to (E_{L^*}^{\min}, L^*)} \int_{r_-(E,L)}^{r_+(E,L)} \frac{F_L(r)}{\sqrt{2E - 2\Psi_L(r)}}\, \mathrm{d}r = \pi \frac{F_{L^*}(r_{L^*})}{\sqrt{\Psi''_{L^*}(r_{L^*})}}, \tag{A.4.3}$$

where we recall

$$\Psi''_{L^*}(r_{L^*}) = 4\pi\rho_0(r_{L^*}) + \frac{L^*}{r_{L^*}^4} = 4\pi\rho_0(r_{L^*}) + \frac{U_0'(r_{L^*})}{r_{L^*}} > 0. \tag{A.4.4}$$

Proof. By Lemma 2.2.14 (c) we have $r_\pm(E, L) \to r_{L^*}$ as $(E, L) \to (E_{L^*}^{\min}, L^*)$. Since $F_L(r)$ is locally bounded, we thus trivially conclude (A.4.2).

Showing (A.4.3) is harder due to the singular integrand. For fixed $(E, L) \in \mathbb{A}_0$ we obtain

$$\begin{aligned}\int_{r_-(E,L)}^{r_+(E,L)} \frac{F_L(r)}{\sqrt{2E - 2\Psi_L(r)}}\, \mathrm{d}r &= \left(\int_{r_-(E,L)}^{r_L} + \int_{r_L}^{r_+(E,L)}\right) \frac{F_L(r)}{\sqrt{2E - 2\Psi_L(r)}}\, \mathrm{d}r = \\ &= \int_{E_L^{\min}}^{E} \frac{F_L(r_-(\eta, L))}{\sqrt{2(E-\eta)\, \Psi_L'(r_-(\eta, L))^2}}\, \mathrm{d}\eta + \int_{E_L^{\min}}^{E} \frac{F_L(r_+(\eta, L))}{\sqrt{2(E-\eta)\, \Psi_L'(r_+(\eta, L))^2}}\, \mathrm{d}\eta \end{aligned} \tag{A.4.5}$$

by changing variables via $\eta = \Psi_L(r)$, $r = r_\pm(\eta, L)$ in both integrals; note the different signs of the Ψ_L'-terms. We focus on the first integral on the right-hand side of this calculation; the arguments for the second integral are similar.

The extended mean value theorem yields that for every $\eta \in]E_L^{\min}, E[$ there exists some $s \in]r_-(\eta, L), r_L[\subset]r_-(E, L), r_L[$ s.t.

$$\frac{\Psi_L'(r_-(\eta, L))^2}{\eta - E_L^{\min}} = \frac{\Psi_L'(r_-(\eta, L))^2}{\eta - \Psi_L(r_L)} = \frac{2\Psi_L'(s)\, \Psi_L''(s)}{\Psi_L'(s)} = 2\Psi_L''(s); \tag{A.4.6}$$

recall $\Psi_L'(r_L) = 0$. Hence, the integrand of the integral under consideration can be rewritten as

$$\frac{F_L(r_-(\eta, L))}{\sqrt{2(E-\eta)\, \Psi_L'(r_-(\eta, L))^2}} = \frac{F_L(r_-(\eta, L))}{2\sqrt{(E-\eta)(\eta - E_L^{\min})\, \Psi_L''(s)}}. \tag{A.4.7}$$

[218] Obviously, the continuity of $(L, r) \mapsto F_L(r)$ is only necessary in a neighbourhood of (L^*, r_{L^*}) for the statements of Lemma A.4.1 to hold.

Next observe that (A.4.4), which is due to the radial Poisson equation (2.2.32) and $\Psi'_{L^*}(r_{L^*}) = 0$, combined with the limiting behaviour of $r_\pm$ from Lemma 2.2.14 (c) and the continuities of $(L,r) \mapsto F_L(r)$ and $(L,r) \mapsto \Psi''_L(r)$ imply

$$\forall \varepsilon > 0\, \exists \delta > 0\, \forall (E,L) \in \mathbb{A}_0 \text{ with } |(E,L) - (E^{\min}_{L^*}, L^*)| < \delta\colon \\ \left| \frac{F_L(r)}{\sqrt{\Psi''_L(s)}} - \frac{F_{L^*}(r_{L^*})}{\sqrt{\Psi''_{L^*}(r_{L^*})}} \right| < \frac{2\varepsilon}{\pi} \text{ for } r,s \in [r_-(E,L), r_+(E,L)]. \quad \text{(A.4.8)}$$

For arbitrary $\varepsilon > 0$, choosing $\delta > 0$ as above and inserting (A.4.7) hence yields

$$\begin{aligned} &\left| \int_{E^{\min}_L}^E \frac{F_L(r_-(\eta,L))}{\sqrt{2(E-\eta)\,\Psi'_L(r_-(\eta,L))^2}}\,\mathrm{d}\eta - \frac{\pi}{2}\,\frac{F_{L^*}(r_{L^*})}{\sqrt{\Psi''_{L^*}(r_{L^*})}} \right| = \\ &= \left| \int_{E^{\min}_L}^E \frac{F_L(r_-(\eta,L))}{\sqrt{2(E-\eta)\,\Psi'_L(r_-(\eta,L))^2}}\,\mathrm{d}\eta - \frac{F_{L^*}(r_{L^*})}{2\sqrt{\Psi''_{L^*}(r_{L^*})}} \int_{E^{\min}_L}^E \frac{\mathrm{d}\eta}{\sqrt{(E-\eta)(\eta - E^{\min}_L)}} \right| < \\ &< \frac{\varepsilon}{\pi} \int_{E^{\min}_L}^E \frac{\mathrm{d}\eta}{\sqrt{(E-\eta)(\eta - E^{\min}_L)}} = \varepsilon, \end{aligned} \quad \text{(A.4.9)}$$

for $(E,L) \in \mathbb{A}_0$ with $|(E,L) - (E^{\min}_{L^*}, L^*)| < \delta$, where we again used the integral identity (2.2.23). This shows the desired convergence for the integral under consideration. □

As a direct consequence of the above lemma we obtain the following limiting behaviour of the period function T and the area function A defined in Definitions 2.2.16 and A.3.6, respectively.

Corollary A.4.2. *For $L^* > 0$ it holds that*

$$\lim_{\mathbb{A}_0 \ni (E,L) \to (E^{\min}_{L^*}, L^*)} A(E,L) = 0, \quad \text{(A.4.10)}$$

$$\lim_{\mathbb{A}_0 \ni (E,L) \to (E^{\min}_{L^*}, L^*)} T(E,L) = \frac{2\pi}{\sqrt{\Psi''_{L^*}(r_{L^*})}} =: T(E^{\min}_{L^*}, L^*). \quad \text{(A.4.11)}$$

Proof. Apply Lemma A.4.1 with $F_L(r) \equiv 1$. □

Similar limiting properties of a period function also hold in a more general setting, cf. [11, p. 20]. In the context of the Vlasov-Poisson system, (A.4.11) is also proven in [85, Lemma 3.8] and [148, Eqn. (B4)] (in ways different from the above).

In the light of Section A.3.3, it is interesting to analyse the monotonicity of the continuous extension (A.4.11) of the period function. We do this next for suitable steady states; the same result is also contained in [85, Lemma 3.14].

Lemma A.4.3. *Assume that the underlying steady state is isotropic, i.e., $L_0 = 0 = \ell$. Then the function $]0,\infty[\ni L \mapsto T(E^{\min}_L, L)$ defined by* (A.4.11) *is strictly increasing.*

Proof. The isotropy of the steady state implies that ρ_0 is non-increasing, cf. Remark 2.2.10 (a), which yields that $]0,\infty[\ni r \mapsto \frac{U_0'(r)}{r}$ is strictly decreasing by a straightforward calculation; recall (A.3.112). Hence, the mapping $]0,\infty[\ni L \mapsto \Psi''_L(r_L)$ given by (A.4.4) is strictly decreasing; recall that $]0,\infty[\ni L \mapsto r_L$ is strictly increasing by Lemma 2.2.14 (a). □

Analysing the limiting behaviour of the period function T at the boundary of its domain of definition particularly yields an alternative way of showing that T is bounded on the (E,L)-support $\mathbb{D}_0$ defined in (2.2.88). Let us briefly discuss this approach next.

Remark A.4.4. *The boundary of the (E,L)-support $\mathbb{D}_0$ is of the form*

$$\partial\mathbb{D}_0 = \{(E_L^{\min}, L) \mid L_0 < L < L_{\max}\} \cup (\{E_0\} \times [L_0, L_{\max}]) \cup \big([E_{L_0}^{\min}, E_0] \times \{L_0\}\big), \quad \text{(A.4.12)}$$

where $L_{\max}$ is defined in Lemma 2.2.15 and we set $E_L^{\min}\big|_{L=0} := U_0(0)$; the latter is in accordance with Lemma 2.2.14 (b).

In the case of an anisotropic steady state we have $L_0 > 0$ by (φ4). Hence, (A.4.11) *fully shows how to continuously extend the period function T onto $\overline{\mathbb{D}}_0$. Since $T(E_L^{\min}, L)$ is bounded and bounded away from zero for $L \in [L_0, L_{\max}]$, we have thus discovered an alternative proof of Proposition A.0.1 (a).*

In the case of an isotropic steady state $L_0 = 0 = \ell$, we further have to suitably extend the period function to $L = 0$. It is discussed in Remark 2.2.17 (a) how to continuously extend T onto $]U_0(0), E_0] \times \{0\}$. Moreover, since

$$\frac{U_0'(r)}{r} = \frac{4\pi}{r^3}\int_0^r s^2\rho_0(s)\,\mathrm{d}s \to \frac{4\pi}{3}\,\rho_0(0) \text{ as } r \to 0 \quad \text{(A.4.13)}$$

and $r_L \to 0$ as $L \to 0$ by Lemma 2.2.14 (a), (A.4.4) *and* (A.4.11) *indicate*

$$\lim_{\mathbb{A}_0 \ni (E,L) \to (U_0(0),0)} T(E,L) = \frac{\sqrt{3\pi}}{2\sqrt{\rho_0(0)}}; \quad \text{(A.4.14)}$$

recall $\rho_0(0) > 0$ by Remark 2.2.10 (a). Proving this limit requires particularly careful and technical arguments, which is why we omit a proof here and instead refer the interested reader to [85, Lemma 3.11]. Hence, also in the isotropic case, the continuous extension of T onto $\partial\mathbb{D}_0$ is positive and finite, which provides an alternative proof of Proposition A.0.1 (a).

For a much more thorough analysis of the limiting behaviour of the period function at $\partial\mathbb{D}_0$ see [85, Thm. 3.13].

The identity (A.4.14) indicates that the period function $T(E,L)$ is unbounded as $(E,L) \to (U_0(0),0)$ if $\rho_0(0) = 0$. Indeed, it is. We comment on this phenomenon in the following remark.

Remark A.4.5 (Compactly Supported Equilibria with Unbounded Periods)**.** *The limit* (A.4.11) *holds for all steady states from Section 2.2, i.e., the conditions (φ4) and (φ5) have not been used in its proof. In particular, we can choose $L_0 = 0 < \ell$ in* (2.2.12)*, i.e., we consider a steady state of the form*

$$f_0(x,v) = \Phi(E_0 - E(x,v))\,L(x,v)^\ell, \qquad (x,v) \in \mathbb{R}^3 \times \mathbb{R}^3, \qquad \text{with } \ell > 0. \quad \text{(A.4.15)}$$

In this case, $\rho_0(0) = 0$ by (2.2.27)*, but still $0 = R_{\min} \in \operatorname{supp}(\rho_0)$ by Proposition 2.2.9 (c) as well as $(U_0(0),0) \in \partial\mathbb{D}_0$. Similar arguments as in Remark A.4.4 hence show $\Psi_L''(r_L) \to 0$ as $L \to 0$, which implies*

$$\sup_{\mathbb{D}_0} T = \infty \quad \text{(A.4.16)}$$

by (A.4.11) *for such steady states. In particular, since T tends to infinity at the minimal energy value $U_0(0) = \lim_{L \searrow 0} E_L^{\min}$, the period function cannot be energy-increasing on $\mathbb{D}_0$ in this case.*

It is, in fact, the main purpose of the assumption (φ4) to exclude steady states with the property (A.4.16) *from our analysis. Recall that the period function T is bounded on $\mathbb{D}_0$ for all steady states satisfying (φ1)–(φ5) by Proposition A.0.1 (a), and this property enters our analysis crucially.*

Let us note that this finding contradicts a statement in [19, Sc. 5.5.3], where it is claimed that the particle periods within a spherically symmetric equilibrium with finite extent are bounded.

Our next goal is to determine the limiting behaviour of the partial derivatives $\partial_E T$ and $\partial_L T$ of the period function as well. We start with the energy derivative of T; the arguments for the L-derivative are similar due to the relation (A.3.73).

Considering the integral representation (A.3.32) of $\partial_E T$ from Lemma A.3.9, we see that it contains an integral which behaves similarly to the integral (2.2.97) defining the period function. However, there is the additional factor $(E - E_L^{\min})^{-1}$ on the right-hand side of (A.3.32), which becomes singular in the near circular regime. To deal with this factor, we proceed as in [61, Eqn. (A.21) and (A.24)] and rewrite the integral using the identity (A.3.76). This will allow us to explicitly compute the limit of $\partial_E T(E, L)$ as $(E, L) \to (E_{L^*}^{\min}, L^*)$. A similar result is also stated in [61, Rem. A.18] in a slightly different context.

Lemma A.4.6. *Let $L^* > 0$ and assume that U_0 is four times continuously differentiable in a neighbourhood of r_{L^*}. Then there holds*

$$\lim_{\mathbb{A}_0 \ni (E,L) \to (E_{L^*}^{\min}, L^*)} \partial_E T(E, L) = \pi \frac{G'_{1,L^*}(r_{L^*})}{\sqrt{\Psi''_{L^*}(r_{L^*})}} = \frac{5\pi}{12} \frac{\Psi'''_{L^*}(r_{L^*})^2}{\Psi''_{L^*}(r_{L^*})^{\frac{7}{2}}} - \frac{\pi}{4} \frac{\Psi^{(4)}_{L^*}(r_{L^*})}{\Psi''_{L^*}(r_{L^*})^{\frac{5}{2}}}; \quad \text{(A.4.17)}$$

recall that $G'_{1,L}$ is given by (A.3.75) *and $\Psi''_{L^*}(r_{L^*}) > 0$ by* (A.4.4).

Proof. We follow the strategy from [61, Eqn. (A.24)] and define

$$J(E, L) \coloneqq \int_{r_-(E,L)}^{r_+(E,L)} \frac{G_L(r)}{\sqrt{2E - 2\Psi_L(r)}} \, \mathrm{d}r = \int_{r_-(E,L)}^{r_+(E,L)} G'_{1,L}(r) \sqrt{2E - 2\Psi_L(r)} \, \mathrm{d}r \quad \text{(A.4.18)}$$

for $(E, L) \in \mathbb{A}_0$ close to $(E_{L^*}^{\min}, L^*)$. The second identity is due to (A.3.76); notice that, for L close to L^*, the assumptions for (A.3.76) are satisfied by Lemma 2.2.14 (a). By Lemma A.3.9,

$$\partial_E T(E, L) = \frac{J(E, L)}{E - E_L^{\min}} \quad \text{(A.4.19)}$$

for such (E, L). The regularity of $G'_{1,L}$ established in Lemma A.3.18 implies that J is partially differentiable w.r.t. E in $(E, L) \in \mathbb{A}_0$ close to $(E_{L^*}^{\min}, L^*)$ with

$$\partial_E J(E, L) = \int_{r_-(E,L)}^{r_+(E,L)} \frac{G'_{1,L}(r)}{\sqrt{2E - 2\Psi_L(r)}} \, \mathrm{d}r \quad \text{(A.4.20)}$$

by Lemma A.3.8. Furthermore, Lemma A.4.1 shows that $J(E_L^{\min}, L) \coloneqq 0$ for L close to L^* defines a continuous extension of J. Hence, by applying the mean value theorem in the energy variable, we obtain that for any $(E, L) \in \mathbb{A}_0$ close to $(E_{L^*}^{\min}, L^*)$ there exists some $\eta \in]E_L^{\min}, E[$ s.t.

$$\partial_E T(E, L) = \frac{J(E, L)}{E - E_L^{\min}} = \partial_E J(\eta, L) = \int_{r_-(\eta,L)}^{r_+(\eta,L)} \frac{G'_{1,L}(r)}{\sqrt{2\eta - 2\Psi_L(r)}} \, \mathrm{d}r. \quad \text{(A.4.21)}$$

Together with (A.4.3) we thus conclude

$$\lim_{\mathbb{A}_0 \ni (E,L) \to (E^{\min}_{L^*}, L^*)} \partial_E T(E,L) = \lim_{\mathbb{A}_0 \ni (E,L) \to (E^{\min}_{L^*}, L^*)} \partial_E J(E,L) = \pi \, \frac{G'_{1,L^*}(r_{L^*})}{\sqrt{\Psi''_{L^*}(r_{L^*})}}. \quad \text{(A.4.22)}$$

□

In order to establish this limiting behaviour of $\partial_E T$, we had to impose an additional regularity assumption on the steady state. It is evident that such an assumption is mandatory because the fourth-order derivative of the effective potential appears on the right-hand side of (A.4.17). Let us briefly comment on this regularity assumption.

Remark A.4.7. *As discussed in Remark A.3.5, U_0 is four times continuously differentiable on $]0,\infty[$ if $\rho_0 \in C^2(]0,\infty[)$, which is in turn the case if the microscopic equation of state φ is sufficiently smooth.*

If one is only interested in the limiting behaviour of $\partial_E T$ at $\{(E^{\min}_L, L) \mid L > 0\} \cap \partial\mathbb{D}_0$, which is the relevant part of the minimal energy curve, it suffices to assume $U_0 \in C^4(]R_{\min}, R_{\max}[)$ because $r_L \in]R_{\min}, R_{\max}[$ for $L \in \overline{\mathbb{L}}_0 \setminus \{0\}$; recall (2.2.90)*. This regularity of U_0 on $]R_{\min}, R_{\max}[$ holds, e.g., if the function g relating U_0 and ρ_0 via* (2.2.27) *satisfies $g \in C^2(]0,\infty[)$. The latter is, e.g., the case for the King models* (2.2.19) *and for every polytropic ansatz* (2.2.17)*, independent of the polytropic exponents. In the polytropic case there even holds $\rho_0, U_0 \in C^\infty(]0,\infty[\setminus \{R_{\min}, R_{\max}\})$.*

Using the relation (A.3.73) between the L-derivative of the period function T and the energy derivative of $\tilde{T}$ allows us to conclude the limiting behaviour of $\partial_L T(E,L)$ as (E,L) approaches the minimal energy curve.

Lemma A.4.8. *Let $L^* > 0$ and assume that U_0 is four times continuously differentiable in a neighbourhood of r_{L^*}. Then*

$$\lim_{\mathbb{A}_0 \ni (E,L) \to (E^{\min}_{L^*}, L^*)} \partial_L T(E,L) = -\frac{\pi}{r^4_{L^*} \, \Psi''_{L^*}(r_{L^*})^{\frac{7}{2}}} \Big(3\Psi''_{L^*}(r_{L^*})^2 + \\ + r_{L^*} \, \Psi''_{L^*}(r_{L^*}) \, \Psi'''_{L^*}(r_{L^*}) - \frac{r^2_{L^*}}{8} \, \Psi''_{L^*}(r_{L^*}) \, \Psi^{(4)}_{L^*}(r_{L^*}) + \frac{5}{24} \, r^2_{L^*} \, \Psi'''_{L^*}(r_{L^*})^2 \Big) \quad \text{(A.4.23)}$$

holds for $L^* > 0$.

Proof. As discussed in Lemma A.3.13, the potential $\tilde{\Psi}_L$ associated to $\tilde{T}$ has the same properties as Ψ_L. Hence, the same arguments as in Lemma A.4.6 yield

$$\lim_{\mathbb{A}_0 \ni (E,L) \to (E^{\min}_{L^*}, L^*)} \partial_E \tilde{T}(E,L) = \frac{5\pi}{12} \frac{\tilde{\Psi}'''_{L^*}(\sigma_{L^*})^2}{\tilde{\Psi}''_{L^*}(\sigma_{L^*})^{\frac{7}{2}}} - \frac{\pi}{4} \frac{\tilde{\Psi}^{(4)}_{L^*}(\sigma_{L^*})}{\tilde{\Psi}''_{L^*}(\sigma_{L^*})^{\frac{5}{2}}}. \quad \text{(A.4.24)}$$

Differentiating the relation (A.3.51) between $\tilde{\Psi}_L$ and Ψ_L and inserting $\sigma_L = \frac{\sqrt{L}}{r_L}$ implies

$$\tilde{\Psi}''_L(\sigma_L) = \frac{r^4_L}{L} \, \Psi''_L(r_L), \quad \text{(A.4.25)}$$

$$\tilde{\Psi}'''_L(\sigma_L) = -6\frac{r^5_L}{L^{\frac{3}{2}}} \, \Psi''_L(r_L) - \frac{r^6_L}{L^{\frac{3}{2}}} \, \Psi'''_L(r_L), \quad \text{(A.4.26)}$$

$$\tilde{\Psi}^{(4)}_L(\sigma_L) = 36\frac{r^6_L}{L^2} \, \Psi''_L(r_L) + 12\frac{r^7_L}{L^2} \, \Psi'''_L(r_L) + \frac{r^8_L}{L^2} \, \Psi^{(4)}_L(r_L). \quad \text{(A.4.27)}$$

Inserting these formulae into (A.4.24) and using (A.3.73) then shows (A.4.23). □

In the light of Section A.3.3, it would of course be interesting to analyse the signs of the limits (A.4.17) and (A.4.23), as this would imply monotonicity properties of the period function in the near circular regime. However, both of these expressions contain a fourth-order derivative of the effective potential evaluated at $r = r_L$, which is of the form

$$\Psi_L^{(4)}(r_L) = 4\pi\rho_0''(r_L) - \frac{8\pi}{r_L}\,\rho_0'(r_L) + \frac{32\pi}{r_L^2}\,\rho_0(r_L) + \frac{36L}{r_L^6}, \qquad L > 0. \tag{A.4.28}$$

Since the sign of ρ_0'' is unclear – even in the case of an isotropic steady state – we refrain from analysing the signs of (A.4.17) and (A.4.23) mathematically. In Section 8.2, we briefly study these expressions numerically.

The arguments above can also be extended to compute the limiting behaviour of higher-order partial derivatives of the period function in the near circular regime. To conclude this section, let us show how this works for $\partial_E^2 T$. Also, this limiting behaviour of $\partial_E^2 T$ is useful for the analysis in Chapter 6. The lemma is based on [61, Lemma A.15].

Lemma A.4.9. *Let $L^* > 0$ and assume that U_0 is six times continuously differentiable in a neighbourhood of r_{L^*}. Then there holds*

$$\begin{aligned}\lim_{\mathbb{A}_0 \ni (E,L) \to (E_{L^*}^{\min}, L^*)} \partial_E^2 T(E,L) = &-\frac{\pi}{24}\frac{\Psi_{L^*}^{(6)}(r_{L^*})}{\Psi_{L^*}''(r_{L^*})^{\frac{7}{2}}} + \frac{7\pi}{24}\frac{\Psi_{L^*}'''(r_{L^*})\,\Psi_{L^*}^{(5)}(r_{L^*})}{\Psi_{L^*}''(r_{L^*})^{\frac{9}{2}}} + \\ &+ \frac{35\pi}{192}\frac{\Psi_{L^*}^{(4)}(r_{L^*})^2}{\Psi_{L^*}''(r_{L^*})^{\frac{9}{2}}} - \frac{35\pi}{32}\frac{\Psi_{L^*}'''(r_{L^*})^2\,\Psi_{L^*}^{(4)}(r_{L^*})}{\Psi_{L^*}''(r_{L^*})^{\frac{11}{2}}} + \frac{385\pi}{576}\frac{\Psi_{L^*}'''(r_{L^*})^4}{\Psi_{L^*}''(r_{L^*})^{\frac{13}{2}}}.\end{aligned} \tag{A.4.29}$$

Proof. First recall the integral representation (A.3.84) of $\partial_E^2 T(E,L)$, which, by Lemma 2.2.14 (a), holds for $(E,L) \in \mathbb{A}_0$ close to $(E_{L^*}^{\min}, L^*)$. In order to take the limit $(E,L) \to (E_{L^*}^{\min}, L^*)$ in this identity, we have to get rid of the $(E - E_L^{\min})^{-2}$ factor in front of the integral. This is achieved similarly to the proof of Lemma A.4.6: Let I be an open interval containing r_{L^*} s.t. $U_0 \in C^6(I)$. For $L > 0$ define

$$G_{2,L}\colon I \to \mathbb{R},\ G_{2,L}(r) \coloneqq \begin{cases} G_{1,L}'(r)\,\frac{\Psi_L(r) - E_L^{\min}}{\Psi_L'(r)} - \frac{1}{2}G_{1,L}(r), & r \neq r_L, \\ \frac{1}{6}\,\frac{\Psi_L'''(r_L)}{\Psi_L''(r_L)^2}, & r = r_L; \end{cases} \tag{A.4.30}$$

recall that $G_{1,L}$ and $G_{1,L}'$ are given by (A.3.74) and (A.3.75), respectively. For $L > 0$ and $r \in I \setminus \{r_L\}$, direct computation yields

$$\begin{aligned}G_{2,L}'(r) = \frac{1}{\Psi_L'(r)^6}\Big(&-\frac{3}{2}\Psi_L'(r)^4\,\Psi_L''(r) - 2(\Psi_L(r) - E_L^{\min})^2\,\Psi_L'(r)^2\,\Psi_L^{(4)}(r) + \\ &+ 20(\Psi_L(r) - E_L^{\min})^2\,\Psi_L'(r)\,\Psi_L''(r)\,\Psi_L'''(r) - 30(\Psi_L(r) - E_L^{\min})^2\,\Psi_L''(r)^3 + \\ &- 6(\Psi_L(r) - E_L^{\min})\,\Psi_L'(r)^3\,\Psi_L'''(r) + 18(\Psi_L(r) - E_L^{\min})\,\Psi_L'(r)^2\,\Psi_L''(r)^2\Big).\end{aligned} \tag{A.4.31}$$

Taylor expanding Ψ_L and its derivatives to fifth order similarly to the proof of Lemma A.3.18 shows that $]0,\infty[\times I \ni (L,r) \mapsto G_{2,L}'(r)$ is continuous with $G_{2,L}'(r_L) = 0$.[219] In addition,

[219] We have verified the continuity of $G_{2,L}'$ with the aid of a computer algebra software, and highly recommend doing so.

for fixed $L > 0$, $G_{2,L}$ is continuous on I. Radially integrating by parts then allows us to rewrite (A.3.84) as follows:

$$\partial_E^2 T(E,L) = \frac{1}{(E-E_L^{\min})^2} \int_{r_-(E,L)}^{r_+(E,L)} G'_{2,L}(r)\,\sqrt{2E-2\Psi_L(r)}\,\mathrm{d}r =: \frac{J_1(E,L)}{(E-E_L^{\min})^2} \tag{A.4.32}$$

for $(E,L) \in \mathbb{A}_0$ close to $(E_{L^*}^{\min}, L^*)$. By Lemma A.3.8, J_1 is partially differentiable w.r.t. E in such (E,L) with

$$\partial_E J_1(E,L) = \int_{r_-(E,L)}^{r_+(E,L)} \frac{G'_{2,L}(r)}{\sqrt{2E-2\Psi_L(r)}}\,\mathrm{d}r. \tag{A.4.33}$$

Furthermore, Lemma A.4.1 shows that $J_1(E_L^{\min}, L) \coloneqq 0$ for L close to L^* defines a continuous extension of J_1. Hence, by the extended mean value theorem, for any $(E,L) \in \mathbb{A}_0$ close to $(E_{L^*}^{\min}, L^*)$ there exists some $\tilde{\eta} \in \,]E_L^{\min}, E[$ s.t.

$$\partial_E^2 T(E,L) = \frac{1}{2(\tilde{\eta}-E_L^{\min})} \int_{r_-(\tilde{\eta},L)}^{r_+(\tilde{\eta},L)} \frac{G'_{2,L}(r)}{\sqrt{2\tilde{\eta}-2\Psi_L(r)}}\,\mathrm{d}r. \tag{A.4.34}$$

In order to analyse the limit $(E,L) \to (E_{L^*}^{\min}, L^*)$ in this expression, we analyse the limit $(\tilde{\eta}, L) \to (E_{L^*}^{\min}, L^*)$ of the right-hand side by applying the same methods again to get rid of the $(\tilde{\eta} - E_L^{\min})^{-1}$ factor in front of the integral.

For this sake let

$$G_{3,L}\colon I \to \mathbb{R},\ G_{3,L}(r) \coloneqq \begin{cases} \frac{G'_{2,L}(r)}{\Psi'_L(r)}, & r \neq r_L, \\ -\frac{1}{10}\frac{\Psi_L^{(5)}(r_L)}{\Psi''_L(r_L)^3} + \frac{1}{2}\frac{\Psi'''_L(r_L)\,\Psi_L^{(4)}(r_L)}{\Psi''_L(r_L)^4} - \frac{4}{9}\frac{\Psi'''_L(r_L)^3}{\Psi''_L(r_L)^5}, & r = r_L, \end{cases} \tag{A.4.35}$$

for $L > 0$. The same Taylor expansion as above shows that $]0,\infty[\times I \ni (L,r) \mapsto G_{3,L}(r)$ is continuous. Obviously, $G_{3,L}$ is continuously differentiable on $I \setminus \{r_L\}$, and a straight-forward computation based on (A.4.31) shows

$$\begin{aligned} G'_{3,L}(r) =& \frac{1}{\Psi'_L(r)^8}\Big(-2(\Psi_L(r)-E_L^{\min})^2\,\Psi'_L(r)^3\,\Psi_L^{(5)}(r) + \\ &+ 30(\Psi_L(r)-E_L^{\min})^2\,\Psi'_L(r)^2\,\Psi''_L(r)\,\Psi_L^{(4)}(r) + 20(\Psi_L(r)-E_L^{\min})^2\,\Psi'_L(r)^2\,\Psi'''_L(r)^2 + \\ &- 210(\Psi_L(r)-E_L^{\min})^2\,\Psi'_L(r)\,\Psi''_L(r)^2\,\Psi'''_L(r) + 210(\Psi_L(r)-E_L^{\min})^2\,\Psi''_L(r)^4 + \\ &- 10(\Psi_L(r)-E_L^{\min})\,\Psi'_L(r)^4\,\Psi_L^{(4)}(r) + 100(\Psi_L(r)-E_L^{\min})\,\Psi'_L(r)^3\,\Psi''_L(r)\,\Psi'''_L(r) + \\ &- 150(\Psi_L(r)-E_L^{\min})\,\Psi'_L(r)^2\,\Psi''_L(r)^3 - \frac{15}{2}\,\Psi'_L(r)^5\,\Psi'''_L(r) + \frac{45}{2}\,\Psi'_L(r)^4\,\Psi''_L(r)^2\Big) \end{aligned} \tag{A.4.36}$$

for $L > 0$ and $r \in I \setminus \{r_L\}$. With the extension

$$\begin{aligned} G'_{3,L}(r_L) = &-\frac{1}{12}\frac{\Psi_L^{(6)}(r_L)}{\Psi''_L(r_L)^3} + \frac{7}{12}\frac{\Psi'''_L(r_L)\,\Psi_L^{(5)}(r_L)}{\Psi''_L(r_L)^4} + \frac{35}{96}\frac{\Psi_L^{(4)}(r_L)^2}{\Psi''_L(r_L)^4} + \\ &- \frac{35}{16}\frac{\Psi'''_L(r_L)^2\,\Psi_L^{(4)}(r_L)}{\Psi''_L(r_L)^5} + \frac{385}{288}\frac{\Psi'''_L(r_L)^4}{\Psi''_L(r_L)^6} \end{aligned} \tag{A.4.37}$$

for $L > 0$ with $r_L \in I$, the mapping $]0,\infty[\times I \ni (L,r) \mapsto G'_{3,L}(r)$ becomes continuous. This can be verified by a Taylor expansion similar to the one above; here, the effective potential

has to be expanded to sixth order.[220] For $(E,L) \in \mathbb{A}_0$ close to $(E^{\min}_{L^*}, L^*)$, we radially integrate by parts to rewrite the integral on the right-hand side of (A.4.34) as follows:

$$\int_{r_-(E,L)}^{r_+(E,L)} \frac{G'_{2,L}(r)}{\sqrt{2E-2\Psi_L(r)}}\,\mathrm{d}r = -\int_{r_-(E,L)}^{r_+(E,L)} G_{3,L}(r)\,\partial_r\Big[\sqrt{2E-2\Psi_L(r)}\Big]\,\mathrm{d}r = \\ = \int_{r_-(E,L)}^{r_+(E,L)} G'_{3,L}(r)\,\sqrt{2E-2\Psi_L(r)}\,\mathrm{d}r =: J_2(E,L). \quad \text{(A.4.38)}$$

The properties of $G_{3,L}$ established above imply that $J_2(E^{\min}_L, L) \coloneqq 0$ for L close to L^* defines a continuous extension of J_2, cf. Lemma A.4.1, and that J_2 is partially differentiable w.r.t. E in $(E,L) \in \mathbb{A}_0$ close to $(E^{\min}_{L^*}, L^*)$ with

$$\partial_E J_2(E,L) = \int_{r_-(E,L)}^{r_+(E,L)} \frac{G'_{3,L}(r)}{\sqrt{2E-2\Psi_L(r)}}\,\mathrm{d}r. \quad \text{(A.4.39)}$$

Hence, continuing the calculation (A.4.34) by applying the mean value theorem shows that for any $(E,L) \in \mathbb{A}_0$ close to $(E^{\min}_{L^*}, L^*)$ there exists some $\eta \in]E^{\min}_L, E[$ s.t.

$$\partial_E^2 T(E,L) = \frac{1}{2}\int_{r_-(\eta,L)}^{r_+(\eta,L)} \frac{G'_{3,L}(r)}{\sqrt{2\eta-2\Psi_L(r)}}\,\mathrm{d}r. \quad \text{(A.4.40)}$$

By Lemma A.4.1, we thus conclude

$$\lim_{\mathbb{A}_0 \ni (E,L) \to (E^{\min}_{L^*}, L^*)} \partial_E^2 T(E,L) = \lim_{\mathbb{A}_0 \ni (E,L) \to (E^{\min}_{L^*}, L^*)} \frac{1}{2}\int_{r_-(E,L)}^{r_+(E,L)} \frac{G'_{3,L}(r)}{\sqrt{2E-2\Psi_L(r)}}\,\mathrm{d}r = \\ = \frac{\pi}{2}\frac{G'_{3,L^*}(r_{L^*})}{\sqrt{\Psi''_{L^*}(r_{L^*})}}, \quad \text{(A.4.41)}$$

which, by (A.4.37), is precisely the claimed identity (A.4.29). □

Let us briefly present an alternative way of determining the limits of T and its partial derivatives in the near circular regime. This approach was recently pointed out to the author by Thomas Kriecherbauer, and it is also pursued in [148, App. C].

Remark A.4.10. *In the integral representation* (2.2.97) *of T, we change variables via*

$$z = \operatorname{sign}(r - r_L)\sqrt{\Psi_L(r) - E^{\min}_L}. \quad \text{(A.4.42)}$$

In other words, we set $z^2 = \Psi_L(r) - E^{\min}_L$, which illustrates that we are essentially transforming the effective potential into the potential associated to the harmonic oscillator. On the relevant domain of integration, (A.4.42) *is invertible. Let $h_L = h_L(z)$ denote the inverse of* (A.4.42)*. The change of variables then leads to*

$$T(E,L) = \sqrt{2}\int_{-\sqrt{E-E^{\min}_L}}^{\sqrt{E-E^{\min}_L}} \frac{h'_L(z)}{\sqrt{E-E^{\min}_L-z^2}}\,\mathrm{d}z = \sqrt{2}\int_{-1}^{1} \frac{h'_L(y\sqrt{E-E^{\min}_L})}{\sqrt{1-y^2}}\,\mathrm{d}y. \quad \text{(A.4.43)}$$

[220] We again recommend using a computer algebra software for this calculation. If the reader chooses not to do so, we are either honoured to be trusted with (A.4.37) or wish the reader the best of luck in verifying this identity purely by hand.

The E-dependency of the latter integral is easier than that of the original integral (2.2.97)*, allowing us to determine the near circular limits more directly. More precisely, it is straightforward to verify that*

$$\lim_{\mathbb{A}_0 \ni (E,L) \to (E^{\min}_{L^*}, L^*)} T(E,L) = \sqrt{2}\pi\, h'_{L^*}(0) = \frac{2\pi}{\sqrt{\Psi''_{L^*}(r_{L^*})}}; \tag{A.4.44}$$

the value of $h'_{L^*}(0)$ *can, e.g., be computed by Taylor expanding* Ψ_L *and* h_L *in the identity* $z^2 = \Psi_L(h_L(z)) - E^{\min}_L$ *and equating the coefficients of different powers of* z*. In the same way, one can compute higher order derivatives of* h_{L^*} *in* $z = 0$ *as well, provided that* Ψ_L *is sufficiently smooth. After differentiating* (A.4.43) *w.r.t.* E*, this leads to*

$$\lim_{\mathbb{A}_0 \ni (E,L) \to (E^{\min}_{L^*}, L^*)} \partial_E T(E,L) = \frac{\pi}{2\sqrt{2}}\, h'''_{L^*}(0) = \frac{5\pi}{12} \frac{\Psi'''_{L^*}(r_{L^*})^2}{\Psi''_{L^*}(r_{L^*})^{\frac{7}{2}}} - \frac{\pi}{4} \frac{\Psi^{(4)}_{L^*}(r_{L^*})}{\Psi''_{L^*}(r_{L^*})^{\frac{5}{2}}}. \tag{A.4.45}$$

Notice that (A.4.44) *and* (A.4.45) *are consistent with* (A.4.11) *and* (A.4.17)*, respectively. Further differentiating* (A.4.43) *provides an alternative way of establishing* (A.4.29)*.*

Appendix B

An Eddington-Ritter Type Relation

In this chapter we consider a polytropic steady state with $L_0 = 0$, i.e., the microscopic equation of state φ is of the form

$$\varphi(E, L) = (E_0 - E)_+^k \, L^\ell, \qquad E \in \mathbb{R},\ L \geq 0, \tag{B.0.1}$$

with polytropic exponents $\ell \geq 0$ and $k \in]0, 3\ell + \frac{7}{2}[$. In particular, choosing $\ell = 0$ leads to the isotropic polytropic ansatz (2.2.18). The ansatz function (B.0.1) obviously satisfies the conditions (φ1)–(φ3) (and also (φ5)). Let f_0^κ be the steady state associated to this ansatz given by Proposition 2.2.9 with parameter $\kappa > 0$. The subject of this chapter is to study how f_0^κ depends on κ (for a fixed ansatz of the form (B.0.1)). More precisely, we consider the period function T^κ, the linearised operator $\mathcal{L}^\kappa$, and other quantities associated to the steady state; we add a superscript κ to all quantities here to highlight the κ-dependency. The primary goal of this analysis is to derive a relation between the parameter $\kappa > 0$ and the periods of (possible) linear oscillations around f_0^κ. In the context of isotropic equilibria of the Euler-Poisson system, such a relation is known as the *Eddington-Ritter relation*, see, e.g., [39, Sc. 8], [107, p. 555], or [149, p. 235].[221] For the Vlasov-Poisson system, such a relation was first stated (and numerically checked) in [132, Sc. 4].[222] The first rigorous derivations were then given in [62, Sc. 3.3] and, in the isotropic case $\ell = 0$, in [85, Ch. 6]. For general scaling properties of solutions of the Vlasov-Poisson system we refer to [35].

We use the quantities introduced in Chapters 2, 4, and 5 here without further reference. Moreover, we will refrain here from presenting lengthy calculations, but only present their results. We follow [62, Sc. 3.3].

Let $y^* := y^1 \in C^2([0, \infty[)$ be the unique solution of (2.2.35) satisfying the boundary/initial conditions (2.2.36) with $\kappa = 1$, i.e.,

$$y^*(0) = 1, \qquad (y^*)'(0) = 0. \tag{B.0.2}$$

All quantities associated to y^* will be denoted by a superscript $*$. Due to the specific ansatz (B.0.1) chosen here and Remark 2.2.7, the integro-differential equation (2.2.35) can

[221] More precisely, the Eddington-Ritter relation states a connection between the linear oscillation period(s) and the central density $\rho_0(0)$ of the steady state. By Remark 2.2.10 (a), the central density $\rho_0(0)$ is in one-to-one correspondence with the parameter κ used here.

[222] It should be noted that the numerics in [132] analyse the oscillation period(s) of solutions close to steady states of the form (B.0.1) on the *non-linearised* level.

be written as

$$y'(r) = -\frac{4\pi c_{k,\ell}}{r^2} \int_0^r s^{2\ell+2}\, y(s)_+^{k+\ell+\frac{3}{2}}\, \mathrm{d}s, \qquad r > 0, \tag{B.0.3}$$

where $c_{k,\ell}$ is some constant depending on the polytropic exponents via (2.2.30). Hence, y^* is related to the solution $y^\kappa \in C^2([0,\infty[)$ of (2.2.35)–(2.2.36) for general $\kappa > 0$ as follows:

$$y^\kappa(r) = \kappa\, y^*(\kappa^{\frac{2k+2\ell+1}{4\ell+4}} r), \qquad r > 0. \tag{B.0.4}$$

For the associated mass densities, cut-off energies, and gravitational potentials, we thus obtain

$$\rho_0^\kappa(r) = \kappa^{\frac{2k+4\ell+3}{2\ell+2}} \rho_0^*(\kappa^{\frac{2k+2\ell+1}{4\ell+4}} r), \quad E_0^\kappa = \kappa\, E_0^*, \quad U_0^\kappa(r) = \kappa\, U_0^*(\kappa^{\frac{2k+2\ell+1}{4\ell+4}} r), \qquad r > 0. \tag{B.0.5}$$

The steady state induced by y^κ is hence given by

$$f_0^\kappa(r, w, L) = \kappa^{\frac{2k+\ell}{2\ell+2}} f_0^*(\kappa^{\frac{2k+2\ell+1}{4\ell+4}} r, \kappa^{-\frac{1}{2}} w, \kappa^{\frac{2k-1}{2\ell+2}} L), \tag{B.0.6}$$

where we used that for the particle energy there holds

$$E^\kappa(r, w, L) = \kappa\, E^*(\kappa^{\frac{2k+2\ell+1}{4\ell+4}} r, \kappa^{-\frac{1}{2}} w, \kappa^{\frac{2k-1}{2\ell+2}} L) \tag{B.0.7}$$

for $r > 0$, $w \in \mathbb{R}$, and $L \geq 0$. Furthermore, $R_{\min}^\kappa = 0 = R_{\min}^*$ since $L_0 = 0$, and

$$R_{\max}^\kappa = \kappa^{-\frac{2k+2\ell+1}{4\ell+4}} R_{\max}^*. \tag{B.0.8}$$

Moreover, for the local mass there holds

$$m^\kappa(r) = \kappa^{\frac{-2k+2\ell+3}{4\ell+4}} m^*(\kappa^{\frac{2k+2\ell+1}{4\ell+4}} r), \qquad r > 0. \tag{B.0.9}$$

In particular, for the total mass we thus obtain

$$M_0^\kappa = \kappa^{\frac{-2k+2\ell+3}{4\ell+4}} M_0^*. \tag{B.0.10}$$

The identities (B.0.8) and (B.0.10) are also established in [129, Satz 3.2]. In particular, (B.0.8) and (B.0.10) show that the (R, M)-diagram of the steady state family $(f_0^\kappa)_{\kappa>0}$ equals the graph of $]0,\infty[\ni \sigma \mapsto \sigma^{\frac{2k-2\ell+3}{2k+2\ell+1}}$ up to the multiplication by some positive constant, more precisely,

$$\{(R_{\max}^\kappa, M_0^\kappa) \mid \kappa > 0\} = \left\{ (\sigma, M_0^* \left(\frac{\sigma}{R_{\max}^*} \right)^{\frac{2k-2\ell-3}{2k+2\ell+1}}) \mid \sigma > 0 \right\}. \tag{B.0.11}$$

Visualisations of this set for several choices of the polytropic exponents k and ℓ are contained in Section 8.1, see Figures 8.1.4 and 8.1.9, as well as in [129, p. 41]. In contrast, we note that the analogous (R, M)-diagram for the steady state family associated to the King ansatz function (2.2.19) is a spiral, cf. [131]. This shows that the specific form of the ansatz function (B.0.1) is crucial for the arguments in this chapter.

For the (E, L)-support of the steady state there holds

$$(E, L) \in \mathbb{D}_0^\kappa \qquad \Leftrightarrow \qquad (\kappa^{-1} E, \kappa^{\frac{2k-1}{2\ell+2}} L) \in \mathbb{D}_0^*; \tag{B.0.12}$$

the analogous relation also holds for the set of admissible (E,L)-pairs $\mathbb{A}_0^\kappa$. Moreover, if $x^*\colon I\to\mathbb{R}^3$ is a solution of $\ddot{x}=-\partial_x U_0^*(x)$,

$$x^\kappa(s) \coloneqq \kappa^{-\frac{2k+2\ell+1}{4\ell+4}}\, x^*(\kappa^{\frac{2k+4\ell+3}{4\ell+4}}\, s) \tag{B.0.13}$$

defines a solution of $\ddot{x}=-\partial_x U_0^\kappa(x)$. The conserved quantities (E^κ,L^κ) associated to x^κ are related to the respective quantities (E^*,L^*) of x^* as follows:

$$E^\kappa=\kappa\, E^*, \qquad L^\kappa=\kappa^{-\frac{2k-1}{2\ell+2}}\, L^*. \tag{B.0.14}$$

For the radial periods we thus obtain

$$T^\kappa(E,L)=\kappa^{-\frac{2k+4\ell+3}{4\ell+4}}\, T^*(\kappa^{-1}E,\kappa^{\frac{2k-1}{2\ell+2}}L), \qquad (E,L)\in\mathbb{A}_0^\kappa. \tag{B.0.15}$$

Together with (B.0.12) this shows

$$T^\kappa(\mathbb{D}_0^\kappa)=\kappa^{-\frac{2k+4\ell+3}{4\ell+4}}\, T^*(\mathbb{D}_0^*), \qquad \sup_{\mathbb{D}_0^\kappa} T^\kappa=\kappa^{-\frac{2k+4\ell+3}{4\ell+4}}\sup_{\mathbb{D}_0^*} T^*. \tag{B.0.16}$$

Next, we study the κ-dependency of the operators defined in Section 4.2. It should be noted that in the case $\ell>0$, the ansatz (B.0.1) does not satisfy the condition $(\varphi 4)$. However, for the definitions of the operators and the succeeding arguments, this condition is not needed. Let the spherically symmetric functions $f^\kappa\colon\Omega_0^\kappa\to\mathbb{R}$ and $f^*\colon\Omega_0^*\to\mathbb{R}$ be related via

$$f^\kappa(r,w,L)=f^*(\kappa^{\frac{2k+2\ell+1}{4\ell+4}}r,\kappa^{-\frac{1}{2}}w,\kappa^{\frac{2k-1}{2\ell+2}}L). \tag{B.0.17}$$

Then $f^\kappa\in H^\kappa$ is equivalent to $f^*\in H^*$. For the transport operator and its square there hold the relations

$$\mathcal{T}^\kappa f^\kappa(r,w,L)=\kappa^{\frac{2k+4\ell+3}{4\ell+4}}\,\mathcal{T}^* f^*(\kappa^{\frac{2k+2\ell+1}{4\ell+4}}r,\kappa^{-\frac{1}{2}}w,\kappa^{\frac{2k-1}{2\ell+2}}L), \tag{B.0.18}$$

$$(\mathcal{T}^\kappa)^2 f^\kappa(r,w,L)=\kappa^{\frac{2k+4\ell+3}{2\ell+2}}\,(\mathcal{T}^*)^2 f^*(\kappa^{\frac{2k+2\ell+1}{4\ell+4}}r,\kappa^{-\frac{1}{2}}w,\kappa^{\frac{2k-1}{2\ell+2}}L); \tag{B.0.19}$$

in particular, $f^\kappa\in\mathrm{D}(\mathcal{T}^\kappa)$ or $f^\kappa\in\mathrm{D}((\mathcal{T}^\kappa)^2)$ is equivalent to $f^*\in\mathrm{D}(\mathcal{T}^*)$ or $f^*\in\mathrm{D}((\mathcal{T}^*)^2)$, respectively. Recalling the connection between $T^\kappa(\mathbb{D}_0^\kappa)$ and the spectrum of $-(\mathcal{T}^\kappa)^2\big|_{\mathcal{H}^\kappa}$ established in Proposition 4.3.19, we see that (B.0.16) and (B.0.19) are consistent. For the response operator there holds

$$\mathcal{R}^\kappa f^\kappa(r,w,L)=\kappa^{\frac{2k+4\ell+3}{2\ell+2}}\,\mathcal{R}^* f^*(\kappa^{\frac{2k+2\ell+1}{4\ell+4}}r,\kappa^{-\frac{1}{2}}w,\kappa^{\frac{2k-1}{2\ell+2}}L), \tag{B.0.20}$$

i.e., the scaling behaviour of $\mathcal{R}^\kappa$ is similar to the one of $(\mathcal{T}^\kappa)^2$. For the linearised operator we thus deduce

$$\mathcal{L}^\kappa f^\kappa(r,w,L)=\kappa^{\frac{2k+4\ell+3}{2\ell+2}}\,\mathcal{L}^* f^*(\kappa^{\frac{2k+2\ell+1}{4\ell+4}}r,\kappa^{-\frac{1}{2}}w,\kappa^{\frac{2k-1}{2\ell+2}}L). \tag{B.0.21}$$

Hence, if $\mathcal{L}^*$ possesses some eigenvalue $\lambda^*>0$,

$$\lambda^\kappa\coloneqq\kappa^{\frac{2k+4\ell+3}{2\ell+2}}\lambda^* \tag{B.0.22}$$

is an eigenvalue of $\mathcal{L}^\kappa$ and vice versa. The associated eigenfunctions are related via (B.0.17). A similar scaling also applies to the essential spectrum and to the infimum of the whole spectrum of the linearised operator. Furthermore, the periods p^κ, p^* of the linear oscillations/pulsations associated to the eigenvalues λ^κ, λ^* via (1.2.12) satisfy

$$p^\kappa=\kappa^{-\frac{2k+4\ell+3}{4\ell+4}}\, p^*. \tag{B.0.23}$$

In other words,

$$p^\kappa \, \kappa^{\frac{2k+4\ell+3}{4\ell+4}} \equiv \text{const.}, \tag{B.0.24}$$

i.e., the quantity on the left-hand side is independent of $\kappa > 0$. This is the desired relation between κ and the linear oscillation period p^κ. We refer to the identity (B.0.24) as an *Eddington-Ritter type relation*. In the isotropic polytropic case $\ell = 0$, (B.0.5) implies $\rho_0^\kappa(0) = \kappa^{k+\frac{3}{2}} \, \rho_0^*(0)$, and hence

$$p^\kappa \, \sqrt{\rho_0^\kappa(0)} \equiv \text{const.} \tag{B.0.25}$$

This is precisely the Eddington-Ritter relation known from the Euler-Poisson system.

Similar calculations as the ones above further yield the following scaling properties for the operators from Chapter 5: If $\lambda^* < \inf(\sigma(-(\mathcal{T}^*)^2\big|_{\mathcal{H}^*}))$ and λ^κ is given by (B.0.22),

$$Q^\kappa_{\lambda^\kappa} f^\kappa(r, w, L) = Q^*_{\lambda^*} f^*(\kappa^{\frac{2k+2\ell+1}{4\ell+4}} r, \kappa^{-\frac{1}{2}} w, \kappa^{\frac{2k-1}{2\ell+2}} L), \tag{B.0.26}$$

where f^* and f^κ are again related via (B.0.17). The same scaling identity also holds for the Mathur operator. In particular, the number $\mathfrak{M}$ introduced in Theorem 5.3.1 is independent of κ.

Appendix C

The Evolution of the Linearised Vlasov-Poisson System

The aim of this appendix is to establish a rigorous well-posedness theory for the linearised Vlasov-Poisson system (in second-order formulation). We do this by applying the general results from semigroup theory [40] to our specific setting. We follow [61, Sc. 6] here, where the same is done in a slightly different setting. A more direct approach is pursued in [15]. In addition, we relate the (long-term) behaviour of solutions of the linearised Vlasov-Poisson system to the spectral properties of the linearised operator $\mathcal{L}$.

Throughout this appendix, let f_0 be a fixed steady state satisfying the conditions (φ1)–(φ5) stated in Sections 2.2 and 4.1. As derived in Chapter 3, the linearised Vlasov-Poisson system around this steady state in second-order formulation is

$$\partial_t^2 f + \mathcal{L} f = 0, \tag{C.0.1}$$

where $\mathcal{L}$ is the linearised operator defined in Definition 4.2.9. In the following discussion we will use the quantities introduced in Chapter 4 without giving a reference each time; the reader is advised to familiarise him or herself with Chapter 4 first. The above equation can be rewritten into the following two-dimensional system of first order:

$$\partial_t \psi = \mathcal{A}\psi, \tag{C.0.2}$$

where $\psi = (\psi_1(t), \psi_2(t))$ and[223]

$$\mathcal{A} \coloneqq \begin{pmatrix} 0 & \mathrm{id} \\ -\mathcal{L} & 0 \end{pmatrix}. \tag{C.0.3}$$

The equivalence of (C.0.1) and (C.0.2) is straight-forward to see via the identifications

$$\psi = (f, \partial_t f), \qquad f = \psi_1. \tag{C.0.4}$$

It should be noted that the first-order system (C.0.2) is conceptionally different from – but still equivalent to – the linearised Vlasov-Poisson in the first-order formulation (3.1.1)–(3.1.3) since (C.0.2) contains the second-order derivative operator $\mathcal{L}$. To apply the methods from semigroup theory, it is more convenient to work with the system (C.0.2) rather than (C.0.1). Nevertheless, all results regarding (the solutions of) (C.0.2) carry over to (C.0.1).

[223] The "matrix representation" (C.0.3) of the operator $\mathcal{A}$ means $\mathcal{A}(\psi_1, \psi_2) = (\psi_2, -\mathcal{L}\psi_1)$. By slight abuse of notation, we identify a vector (ψ_1, ψ_2) with its transpose $(\psi_1, \psi_2)^T$.

Following [40, Sc. VI.3], we consider the system (C.0.2) on the space

$$\mathcal{X} \coloneqq (\mathrm{D}(\mathcal{T}) \cap \mathcal{H}) \times \mathcal{H} \tag{C.0.5}$$

with

$$\langle (f,F),(g,G)\rangle_{\mathcal{X}} \coloneqq \langle \mathcal{L}f, g\rangle_H + \langle F, G\rangle_H \tag{C.0.6}$$

for $(f,F),(g,G) \in \mathcal{X}$. The first term on the right-hand side of (C.0.6) is to be understood as a generalisation of Definition 4.5.7, i.e.,

$$\langle \mathcal{L}f, g\rangle_H \coloneqq \langle \mathcal{T}f, \mathcal{T}g\rangle_H - \langle \mathcal{R}f, g\rangle_H = \langle \mathcal{T}f, \mathcal{T}g\rangle_H - \frac{1}{4\pi}\langle \partial_x U_{\mathcal{T}f}, \partial_x U_{\mathcal{T}g}\rangle_2, \quad f,g \in \mathrm{D}(\mathcal{T}) \cap \mathcal{H}. \tag{C.0.7}$$

Again, this definition is consistent with the usual definition of the scalar product if $f \in \mathrm{D}(\mathcal{L})$ or $g \in \mathrm{D}(\mathcal{L})$. In the latter case, $\langle \mathcal{L}f, g\rangle_H = \langle f, \mathcal{L}g\rangle_H$; recall that $\mathcal{L}$ is symmetric. In the definition (C.0.5) of $\mathcal{X}$, we do include complex-valued functions, cf. Remark 4.2.4 (f), in order to be able to apply the results from the general semigroup theory. Before applying these results, let us first analyse the basic structure of the space $(\mathcal{X}, \langle\cdot,\cdot\rangle_{\mathcal{X}})$.

Lemma C.0.1. *$(\mathcal{X}, \langle\cdot,\cdot\rangle_{\mathcal{X}})$ is a Hilbert space.*

Proof. The positivity of $\mathcal{L}$ established in Proposition 4.5.11 shows that $\langle\cdot,\cdot\rangle_{\mathcal{X}}$ defines a positive definite inner product on $\mathcal{X}$. In order to verify that $(\mathcal{X}, \langle\cdot,\cdot\rangle_{\mathcal{X}})$ is complete, let $(f_j, F_j)_{j\in\mathbb{N}} \subset \mathcal{X}$ be a Cauchy sequence. Since $\mathcal{L} \geq 0$, the sequence $(F_j)_{j\in\mathbb{N}}$ is obviously (strongly) convergent in $\mathcal{H}$. Moreover, by Lemma 4.5.14 and Proposition 4.5.11, there exist $f \in \mathcal{H}$ and $g \in H$ s.t. $f_j \to f$ and $\mathcal{T}f_j \to g$ in H as $j \to \infty$. By the weak definition of the transport operator, it is then easy to verify that $f \in \mathrm{D}(\mathcal{T})$ with $\mathcal{T}f = g$. Thus, $(f,F) \in \mathcal{X}$, and since the response operator is bounded there holds $(f_j, F_j) \to (f,F)$ in $\mathcal{X}$ as $j \to \infty$. □

The natural domain of definition for the operator $\mathcal{A}$ is given by

$$\mathrm{D}(\mathcal{A}) \coloneqq \mathrm{D}(\mathcal{L}) \times (\mathrm{D}(\mathcal{T}) \cap \mathcal{H}). \tag{C.0.8}$$

With this domain of definition, the key functional analytic and spectral properties of $\mathcal{L}$ carry over to $\mathcal{A}$.

Lemma C.0.2. *The operator $\mathcal{A}\colon \mathrm{D}(\mathcal{A}) \to \mathcal{X}$ is skew-adjoint as a densely defined operator on $\mathcal{X}$, i.e., $\mathcal{A}^* = -\mathcal{A}$. Furthermore, any $\lambda \in \mathbb{C}$ is an eigenvalue of $\mathcal{A}$ if and only if $-\lambda^2$ is an eigenvalue of $\mathcal{L}$.*

Proof. First note that $\mathrm{D}(\mathcal{A})$ is a dense subspace of $\mathcal{X}$ since $\big(C^\infty_{c,r}(\Omega_0) \cap \mathcal{H}\big)^2$ is densely contained in $\mathcal{X}$ by Lemma 4.3.31.

To verify the skew-adjointness of $\mathcal{A}$, consider $(f,F) \in \mathrm{D}(\mathcal{A}^*)$ and let $(h,H) \coloneqq \mathcal{A}^*(f,F) \in \mathcal{X}$. By the definition of $\mathcal{A}^*$, see [136, Sc. VIII.1], this means that for every $(g,G) \in \mathrm{D}(\mathcal{A})$ there holds

$$\langle \mathcal{L}G, f\rangle_H - \langle \mathcal{L}g, F\rangle_H = \langle \mathcal{A}(g,G),(f,F)\rangle_{\mathcal{X}} = \langle (g,G),(h,H)\rangle_{\mathcal{X}} = \langle \mathcal{L}g, h\rangle_H + \langle G, H\rangle_H. \tag{C.0.9}$$

Inserting $(g,0)$ and $(0,G)$ for $g \in \mathrm{D}(\mathcal{L})$ and $G \in \mathrm{D}(\mathcal{T}) \cap \mathcal{H}$ into this equation yields the two identities

$$-\langle \mathcal{L}g, F\rangle_H = \langle \mathcal{L}g, h\rangle_H, \tag{C.0.10}$$

$$\langle \mathcal{L}G, f\rangle_H = \langle G, H\rangle_H. \tag{C.0.11}$$

Inserting $g = \mathcal{L}^{-1}\xi$ for arbitrary $\xi \in \mathcal{H}$ into (C.0.10) yields $-F = h \in \mathrm{D}(\mathcal{T}) \cap \mathcal{H}$; recall that $\mathcal{L}\colon \mathrm{D}(\mathcal{L}) \to \mathcal{H}$ is invertible by Proposition 4.5.11. The equation (C.0.11) holds for any $G \in \mathrm{D}(\mathcal{L})$, which means $f \in \mathrm{D}(\mathcal{L}^*)$ with $\mathcal{L}^* f = H$. Since $\mathcal{L}$ is self-adjoint by Lemma 4.5.2, we hence deduce $f \in \mathrm{D}(\mathcal{L})$ with $\mathcal{L}f = H$. Overall, $(f, F) \in \mathrm{D}(\mathcal{A})$ with $\mathcal{A}(f, F) = -(h, H) = -\mathcal{A}^*(f, F)$.

To conclude the skew-adjointness of $\mathcal{A}$, it remains to show that $\mathcal{A}$ is skew-symmetric. This follows by the symmetry of $\mathcal{L}$ since, for every $(f, F), (g, G) \in \mathrm{D}(\mathcal{A})$,

$$\begin{aligned}\langle \mathcal{A}(f, F), (g, G)\rangle_{\mathcal{X}} &= \langle \mathcal{L}F, g\rangle_H - \langle \mathcal{L}f, G\rangle_H = \\ &= -\langle \mathcal{L}f, G\rangle_H + \langle F, \mathcal{L}g\rangle_H = -\langle (f, F), \mathcal{A}(g, G)\rangle_{\mathcal{X}}. \end{aligned} \tag{C.0.12}$$

For the relation between the eigenvalues of $\mathcal{A}$ and $\mathcal{L}$ let $\lambda \in \mathbb{C}$ be an eigenvalue of $\mathcal{A}$ with eigenvector $(f, F) \in \mathrm{D}(\mathcal{A})$. Then $\mathcal{L}f = -\lambda F = -\lambda^2 f$. Conversely, if $-\lambda^2$ is an eigenvalue of $\mathcal{L}$ with eigenfunction $f \in \mathrm{D}(\mathcal{L})$, there holds $\mathcal{A}(f, \lambda f) = \lambda(f, \lambda f)$. □

By Stone's theorem [40, Thm. II.3.24], $\mathcal{A}$ thus generates the unitary C^0-group $(e^{t\mathcal{A}})_{t\in\mathbb{R}}$ on $\mathcal{X}$. The unique solution of (C.0.2) satisfying the initial condition

$$\psi(0) = (\mathring{f}, \mathring{F}) \tag{C.0.13}$$

for $(\mathring{f}, \mathring{F}) \in \mathrm{D}(\mathcal{A})$ is hence given by $\mathbb{R} \ni t \mapsto \psi(t) \coloneqq e^{t\mathcal{A}}(\mathring{f}, \mathring{F})$. More precisely, the initial value problem (C.0.2) & (C.0.13) is solved in the sense that $\psi \in C^1(\mathbb{R}; \mathcal{X})$ with $\psi(t) \in \mathrm{D}(\mathcal{A})$ for $t \in \mathbb{R}$ and the equations (C.0.2) and (C.0.13) hold. In particular, the initial value problem (C.0.2) & (C.0.13) is well-posed, see the discussion in [40, Sc. II.6]. From this solution of (C.0.2), a solution of (C.0.1) can then be obtained via (C.0.4) which solves (C.0.1) in a similar way, see [40, Sc. VI.3].

Let us now analyse the long-term behaviour of solutions of (C.0.2). The first simple observation is the stability of the stationary point $(0, 0)$.

Lemma C.0.3. *The norm $\|\cdot\|_{\mathcal{X}}$ is conserved along solutions of* (C.0.2)*, i.e., for any $(\mathring{f}, \mathring{F}) \in \mathrm{D}(\mathcal{A})$ and $t \in \mathbb{R}$ there holds $\|e^{t\mathcal{A}}(\mathring{f}, \mathring{F})\|_{\mathcal{X}} = \|(\mathring{f}, \mathring{F})\|_{\mathcal{X}}$. Hence, the stationary point $(0, 0)$ of* (C.0.2) *is stable w.r.t. the norm $\|\cdot\|_{\mathcal{X}}$.*

Proof. The statements follow by the fact that the group $(e^{t\mathcal{A}})_{t\in\mathbb{R}}$ is unitary. □

Remark C.0.4. *We have claimed several times that the positivity of $\mathcal{L}$ corresponds to the linear stability of the underlying steady state. In order to prove the above stability statement, the positivity of $\mathcal{L}$ was, in fact, necessary for various arguments – most notably to show that $\langle\cdot,\cdot\rangle_{\mathcal{X}}$ is positive definite.*

The further qualitative behaviour of the solutions of (C.0.2) depends on the spectrum of $\mathcal{L}$. Let us first formalise the statement that (positive) eigenvalues of $\mathcal{L}$ yield time-periodic solutions of the linearised system.

Lemma C.0.5. *Suppose that $\mathcal{L}$ possesses the eigenvalue $\lambda > 0$ with eigenfunction $f \in \mathrm{D}(\mathcal{L})$. Then*

$$\mathbb{R} \ni t \mapsto e^{i\sqrt{\lambda}\, t}(f, i\sqrt{\lambda}\, f) \tag{C.0.14}$$

solves (C.0.2)*. Obviously, this solution is time-periodic with period $\frac{2\pi}{\sqrt{\lambda}}$.*

Proof. Lemma C.0.2 (and its proof) show that $i\sqrt{\lambda}$ is an eigenvalue of $\mathcal{A}$ with eigenfunction $(f, i\sqrt{\lambda} f)$. Thus, (C.0.14) solves (C.0.2). □

Remark C.0.6. *If the eigenfunction $f \in \mathrm{D}(\mathcal{L})$ of $\mathcal{L}$ in Lemma C.0.5 is real-valued, the real and imaginary parts of* (C.0.14) *are*

$$\mathbb{R} \ni t \mapsto (\cos(\sqrt{\lambda}\, t) f, -\sqrt{\lambda}\, \sin(\sqrt{\lambda}\, t) f), \tag{C.0.15}$$

$$\mathbb{R} \ni t \mapsto (\sin(\sqrt{\lambda}\, t) f, \sqrt{\lambda}\, \cos(\sqrt{\lambda}\, t) f). \tag{C.0.16}$$

Obviously, these two functions and any linear combinations of them are real-valued solutions of (C.0.2)*, which are again time-periodic.*

We next consider the converse situation where $\mathcal{L}$ does not possess an eigenvalue.

Lemma C.0.7. *Suppose that $\mathcal{L}$ does not possess an eigenvalue. Then for any solution $\mathbb{R} \ni t \mapsto \psi(t) = (f(t), F(t))$ of* (C.0.2) *with $(f(0), F(0)) \in \mathrm{D}(\mathcal{A})$ there holds*

$$\lim_{T\to\infty} \frac{1}{T} \int_0^T \|\partial_x U_{\mathcal{T} f(t)}\|_{L^2(\mathbb{R}^3)}^2 \,\mathrm{d}t = 0. \tag{C.0.17}$$

Proof. We follow [61, Sc. 6] and first consider the operator

$$K \colon \mathcal{X} \to \mathcal{X},\ K(f, F) \coloneqq (0, |\varphi'(E, L)|\, U_{\mathcal{T} f}). \tag{C.0.18}$$

This operator is well-defined and bounded by Lemmas 4.1.3, 4.4.6, and 4.5.14 since

$$\|K(f,F)\|_{\mathcal{X}} = \||\varphi'(E,L)|\, U_{\mathcal{T}f}\|_H \le C\|U_{\mathcal{T}f}\|_2 \le C\|\mathcal{T}f\|_H \le C\langle \mathcal{L}f, f\rangle_H \le C\|(f,F)\|_{\mathcal{X}} \tag{C.0.19}$$

for $(f, F) \in \mathcal{X}$. Similar arguments as in the proof of Lemma 4.5.3 further show that K is compact. More precisely, let $(f_j, F_j)_{j\in\mathbb{N}} \subset \mathcal{X}$ be bounded. By Lemma 4.5.14, $(\mathcal{T} f_j)_{j\in\mathbb{N}} \subset H$ is bounded, which, by Lemma 4.4.6, implies that $(U_{\mathcal{T} f_j})_{j\in\mathbb{N}}$ is bounded in $H^2(\mathbb{R}^3)$. In addition, $U'_{\mathcal{T} f_j}$ is given by (4.4.16). Since $\int_0^{R_{\max}} s^2 \rho_{\mathcal{T} f_j}(s)\,\mathrm{d}s = 0$ by the arguments from the proof of Lemma 4.4.6, there holds $\operatorname{supp}(\partial_x U_{\mathcal{T} f_j}) \subset \overline{B}_{R_{\max}}(0)$, from which we conclude $\operatorname{supp}(U_{\mathcal{T} f_j}) \subset \overline{B}_{R_{\max}}(0)$ because of $\lim_{r\to\infty} U_{\mathcal{T} f_j}(r) = 0$ for $j \in \mathbb{N}$. Thus, by the compact embedding $H^2(B_{R_{\max}}(0)) \Subset L^2(B_{R_{\max}}(0))$, a subsequence of $(U_{\mathcal{T} f_j})_{j\in\mathbb{N}}$ is (strongly) convergent in $L^2(\mathbb{R}^3)$. By the estimate (C.0.19), there hence exists a subsequence of $(K(f_j, F_j))_{j\in\mathbb{N}}$ which is (strongly) convergent in $\mathcal{X}$.

Because we assume that $\mathcal{L}$ has no eigenvalues, Lemma C.0.2 implies that $\mathcal{A}$ has no eigenvalues. By the RAGE theorem [135, Thm. XI.115], we thus obtain

$$0 = \lim_{T\to\infty} \frac{1}{T} \int_0^T \|K(f(t), F(t))\|_{\mathcal{X}}^2 \,\mathrm{d}t = \lim_{T\to\infty} \frac{1}{T} \int_0^T \||\varphi'(E,L)|\, U_{\mathcal{T} f(t)}\|_H^2 \,\mathrm{d}t; \tag{C.0.20}$$

note that $(f(t), F(t)) = e^{t\mathcal{A}}(f(0), F(0))$ for $t \in \mathbb{R}$ by the above uniqueness statement for the initial value problem (C.0.2) & (C.0.13). Furthermore, for $t \in \mathbb{R}$, integrating by parts and applying the Cauchy-Schwarz inequality yields

$$\frac{1}{4\pi}\|\partial_x U_{\mathcal{T} f(t)}\|_2^2 = -\int_{\Omega_0} U_{\mathcal{T} f(t)}(x)\, \mathcal{T} f(t,x,v)\,\mathrm{d}(x,v) \le \||\varphi'(E,L)|\, U_{\mathcal{T} f(t)}\|_H\, \|\mathcal{T} f(t)\|_H, \tag{C.0.21}$$

and Lemmas 4.5.14 and C.0.3 imply

$$\|\mathcal{T} f(t)\|_H^2 \le C\langle \mathcal{L} f(t), f(t)\rangle_H \le C\|(f(t), F(t))\|_{\mathcal{X}}^2 = C\|(f(0), F(0))\|_{\mathcal{X}}^2 = C; \tag{C.0.22}$$

the constants $C > 0$ are always t-independent. Thus, by applying the Cauchy-Schwarz inequality once again we arrive at

$$\frac{1}{T}\int_0^T \|\partial_x U_{\mathcal{T}f(t)}\|_2^2 \,\mathrm{d}t \leq \frac{C}{T}\int_0^T \||\varphi'(E,L)|\, U_{\mathcal{T}f(t)}\|_H \,\mathrm{d}t \leq$$
$$\leq C\left(\frac{1}{T}\int_0^T \||\varphi'(E,L)|\, U_{\mathcal{T}f(t)}\|_H^2 \,\mathrm{d}t\right)^{\frac{1}{2}} \tag{C.0.23}$$

for $T > 0$, from which we conclude (C.0.17) via (C.0.20). □

It should be noted, however, that (C.0.17) is a rather weak form of damping, because it merely states that the mean of the norm of the macroscopic quantity $\partial_x U_{\mathcal{T}f}$ decays as the time interval gets larger. In order to show the actual decay of suitable norms of this macroscopic quantity (or related ones), one has to refine the above arguments. This can hopefully be achieved in future work.

Bibliography

[1] Ambrosio, L., Colombo, M., Figalli, A.: On the Lagrangian structure of transport equations: The Vlasov-Poisson system. *Duke Math. J.* **166**, 3505–3568 (2017).

[2] Ames, E., Andréasson, H., Rinne, O.: Dynamics of gravitational collapse in the axisymmetric Einstein-Vlasov system. *Classical Quantum Gravity* **38**, 105003 (2021).

[3] Ames, E., Andréasson, H., Rinne, O.: Hoop and weak cosmic censorship conjectures for the axisymmetric Einstein-Vlasov system. *Phys. Rev. D* **108**, 064054 (2023).

[4] Andréasson, H.: The Einstein-Vlasov System/Kinetic Theory. *Living Rev. Relativ.* **14**, 4 (2011).

[5] Andréasson, H., Rein, G.: A numerical investigation of the stability of steady states and critical phenomena for the spherically symmetric Einstein-Vlasov system. *Classical Quantum Gravity* **23**, 3659–3677 (2006).

[6] Andréasson, H., Rein, G.: On the steady states of the spherically symmetric Einstein-Vlasov system. *Classical Quantum Gravity* **24**, 1809–1832 (2007).

[7] Ansorge, N.: *Stability of isochrone steady states of the Vlasov-Poisson system*, Master thesis, Universität Bayreuth 2024. *In Progress.*

[8] Antonov, V. A.: Remarks on the problems of stability in stellar dynamics. *Soviet Astronom. AJ* **4**, 859–867 (1960).

[9] Antonov, V. A.: *Solution of the Problem of Stability of a Stellar System with Emden's Density Law and a Spherical Distribution of Velocities*, Vestnik Leningradskogo Universiteta, Leningrad 1962.

[10] Antonov, V. A.: Solution of the Problem of Stability of a Stellar System with Emden's Density Law and a Spherical Distribution of Velocities. *Proc. IAU Symposium* **127**, 531–548 (1987).

[11] Arnold, V. I.: *Mathematical Methods of Classical Mechanics* (second edition), Grad. Texts in Math. **60**, Springer-Verlag, New York 1989.

[12] Arnold, V. I.: *Ordinary Differential Equations*, Springer Textbook, Springer-Verlag, Berlin 1992.

[13] Barnes, J., Goodman, J., Hut, P.: Dynamical Instabilities in Spherical Stellar Systems. *Astrophys. J.* **300**, 112–131 (1986).

[14] Batt, J., Faltenbacher, W., Horst, E.: Stationary Spherically Symmetric Models in Stellar Dynamics. *Arch. Rational Mech. Anal.* **93**, 159–183 (1986).

[15] Batt, J., Morrison, P. J., Rein, G.: Linear stability of stationary solutions of the Vlasov-Poisson system in three dimensions. *Arch. Rational Mech. Anal.* **130**, 163–182 (1995).

[16] Batt, J., Pfaffelmoser, K.: On the radius continuity of the models of polytropic gas spheres which correspond to the positive solutions of the generalized Emden-Fowler equation. *Math. Methods Appl. Sci.* **10**, 499–516 (1988).

[17] Bedrossian, J.: A brief introduction to the mathematics of Landau damping. *Preprint arXiv:2211.13707v1*, 38pp. (2022).

[18] Binney, J.: Hénon's Isochrone Model, in *Une vie dédiée aux systèmes dynamiques*, Hermann, Paris, 99–109 (2016).

[19] Binney, J., Tremaine, S.: *Galactic Dynamics* (second edition), Princeton Series in Astrophysics **13**, Princeton University Press 2008.

[20] Birdsall, C. K., Langdon, A. B.: *Plasma Physics via Computer Simulation*, CRC Press, Boca Raton 1991.

[21] Birman, M. Š.: On the spectrum of singular boundary-value problems. *Mat. Sb. (N.S.)* **55**, 125–174 (1961).

[22] Bognár, J.: *Indefinite Inner Product Spaces*, Ergeb. Math. Grenzgeb. **78**, Springer-Verlag, New York-Heidelberg 1974.

[23] Bonorino, L. P., Brietzke, E. H. M., Lukaszczyk, J. P., Taschetto, C. A.: Properties of the period function for some Hamiltonian systems and homogeneous solutions of a semilinear elliptic equation. *J. Differential Equations* **214**, 156–175 (2005).

[24] Brezis, H.: *Functional Analysis, Sobolev Spaces and Partial Differential Equations*, Universitext, Springer, New York 2011.

[25] Camm, G. L.: Self-Gravitating Star Systems. II. *Mon. Notices Royal Astron. Soc.* **112**, 155–176 (1952).

[26] Chandrasekhar, S., Elbert, D. D.: Some Elementary Applications of the Virial Theorem to Stellar Dynamics. *Mon. Notices Royal Astron. Soc.* **155**, 435–447 (1972).

[27] Chaturvedi, S., Luk, J.: Phase mixing for solutions to 1D transport equation in a confining potential. *Kinet. Relat. Models* **15**, 403–416 (2022).

[28] Chicone, C.: The Monotonicity of the Period Function for Planar Hamiltonian Vector Fields. *J. Differential Equations* **69**, 310–321 (1987).

[29] Chicone, C.: *Ordinary Differential Equations with Applications*, Texts Appl. Math. **34**, Springer, New York 1999.

[30] Chouikha, R., Kelfa, A.: Monotonicity conditions for the period function of some planar Hamiltonian systems. *Comm. Appl. Nonlinear Anal.* **3**, 99–120 (1996).

[31] Chow, S.-N., Wang, D.: On the monotonicity of the period function of some second order equations. *Časopis Pěst. Mat.* **111**, 14–25 (1986).

[32] Courant, R., Hilbert, D.: *Methods of Mathematical Physics. I.*, Interscience Publishers, Inc., New York 1953.

[33] David, M., Theuns, T.: Numerical experiments on radial virial oscillations in N-body systems. *Mon. Notices Royal Astron. Soc.* **240**, 957–974 (1989).

[34] De Branges, L.: Perturbations of Self-Adjoint Transformations. *Amer. J. Math.* **84**, 543–560 (1962).

[35] Dolbeault, J., Rein, G.: Time-dependent rescalings and Lyapunov functionals for the Vlasov-Poisson and Euler-Poisson systems, and for related models of kinetic equations, fluid dynamics and quantum physics. *Math. Models Methods Appl. Sci.* **11**, 407–432 (2001).

[36] Doremus, J.-P., Feix, M. R., Baumann, G.: Stability of Encounterless Spherical Stellar Systems. *Phys. Rev. Lett.* **26**, 725–728 (1971).

[37] Doremus, J.-P., Feix, M. R., Baumann, G.: Stability of a Self Gravitating System with Phase Space Density Function of Energy and Angular Momentum. *Astron. Astrophys.* **29**, 401–407 (1973).

[38] Ebin, D. G., Marsden, J.: Groups of diffeomorphisms and the motion of an incompressible fluid. *Ann. of Math.* **92**, 102–163 (1970).

[39] Eddington, A. S.: On the Pulsations of a Gaseous Star and the Problem of the Cepheid Variables. Part I. *Mon. Not. R. Astr. Soc.* **79**, 2–22 (1918).

[40] Engel, K.-J., Nagel, R.: *One-Parameter Semigroups for Linear Evolution Equations*, Grad. Texts in Math. **194**, Springer-Verlag, New York 2000.

[41] Evans, L. C.: *Partial Differential Equations* (second edition), Grad. Stud. Math. **19**, American Mathematical Society, Providence 2010.

[42] Ferreira, J. C., Menegatto, V. A.: Eigenvalues of Integral Operators Defined by Smooth Positive Definite Kernels. *Integral Equations Operator Theory* **64**, 61–81 (2009).

[43] Fridman, A. M., Polyachenko, V. L.: *Physics of Gravitating Systems I*, Springer Berlin, Heidelberg 1984.

[44] Fridman, A. M., Polyachenko, V. L.: *Physics of Gravitating Systems II*, Springer Berlin, Heidelberg 1984.

[45] Gasull, A., Guillamon, A., Villadelprat, J.: The Period Function for Second-Order Quadratic ODEs is Monotone. *Qual. Theory Dyn. Syst.* **4**, 329–352 (2004).

[46] Gidas, B., Ni, W.-M., Nirenberg, L.: Symmetry and Related Properties via the Maximum Principle. *Comm. Math. Phys.* **68**, 209–243 (1979).

[47] Glassey, R. T.: *The Cauchy Problem in Kinetic Theory*, SIAM, Philadelphia 1996.

[48] Günther, S., Körner, J., Lebeda, T., Pötzl, B., Rein, G., Straub, C., Weber, J.: A numerical stability analysis for the Einstein-Vlasov system. *Classical Quantum Gravity* **38**, 035003 (2021).

[49] Günther, S., Rein, G., Straub, C.: A Birman-Schwinger Principle in General Relativity: Linearly Stable Shells of Collisionless Matter Surrounding a Black Hole. *Preprint arXiv:2204.10620v1*, 58pp. (2022).

[50] Günther, S., Straub, C., Rein, G.: Collisionless Equilibria in General Relativity: Stable Configurations beyond the First Binding Energy Maximum. *Astrophys. J.* **918**, 48 (2021).

[51] Guo, Y.: Variational Method for Stable Polytropic Galaxies. *Arch. Ration. Mech. Anal.* **150**, 209–224 (1999).

[52] Guo, Y.: On the generalized Antonov's stability criterion. *Contemp. Math.* **263**, 85–107 (2000).

[53] Guo, Y., Lin, Z.: Unstable and Stable Galaxy Models. *Comm. Math. Phys.* **279**, 789–813 (2008).

[54] Guo, Y., Rein, G.: Stable Steady States in Stellar Dynamics. *Arch. Ration. Mech. Anal.* **147**, 225–243 (1999).

[55] Guo, Y., Rein, G.: Existence and Stability of Camm Type Steady States in Galactic Dynamics. *Indiana Univ. Math. J.* **48**, 1237–1255 (1999).

[56] Guo, Y., Rein, G.: Isotropic Steady States in Galactic Dynamics. *Comm. Math. Phys.* **219**, 607–629 (2001).

[57] Guo, Y., Rein, G.: A Non-Variational Approach to Nonlinear Stability in Stellar Dynamics Applied to the King Model. *Comm. Math. Phys.* **271**, 489–509 (2007).

[58] Hadžić, M., Lin, Z., Rein, G.: Stability and Instability of Self-Gravitating Relativistic Matter Distributions. *Arch. Ration. Mech. Anal.* **241**, 1–89 (2021).

[59] Hadžić, M., Rein, G.: Global Existence and Nonlinear Stability for the Relativistic Vlasov-Poisson System in the Gravitational Case. *Indiana Univ. Math. J.* **56**, 2453–2488 (2007).

[60] Hadžić, M., Rein, G.: On the small redshift limit of steady states of the spherically symmetric Einstein-Vlasov system and their stability. *Math. Proc. Cambridge Philos. Soc.* **159**, 529–546 (2015).

[61] Hadžić, M., Rein, G., Schrecker, M., Straub, C.: Damping versus oscillations for a gravitational Vlasov-Poisson system. *Preprint arXiv:2301.07662v1*, 49pp. (2023).

[62] Hadžić, M., Rein, G., Straub, C.: On the Existence of Linearly Oscillating Galaxies. *Arch. Ration. Mech. Anal.* **243**, 611–696 (2022).

[63] Heinzle, J. M., Rendall, A. D., Uggla, C.: Theory of Newtonian self-gravitating stationary spherically symmetric systems. *Math. Proc. Cambridge Philos. Soc.* **140**, 177-192 (2006).

[64] Hénon, M.: L'amas isochrone. I. *Annales d'Astrophysique* **22**, 126–139 (1959).

[65] Hénon, M.: L'amas isochrone. III. – Fonction de distribution. *Annales d'Astrophysique* **23**, 474–477 (1960).

[66] Hénon, M.: Numerical Experiments on the Stability of Spherical Stellar Systems. *Astron. Astrophys.* **24**, 229–238 (1973).

[67] Hénon, M.: Vlasov Equation? *Astron. Astrophys.* **114**, 211–212 (1982).

[68] Hewitt, E., Stromberg, K.: *Real and Abstract Analysis. A Modern Treatment of the Theory of Functions of a Real Variable*, Springer-Verlag, New York 1965.

[69] Hislop, P. D., Sigal, I. M.: *Introduction to Spectral Theory*, Appl. Math. Sci. **113**, Springer-Verlag, New York 1996.

[70] Ipser, J. R.: Relativistic, Spherically Symmetric Star Clusters. III. Stability of Compact Isotropic Models. *Astrophys. J.* **158**, 17–43 (1969).

[71] Ipser, J. R., Thorne, K. S.: Relativistic, Spherically Symmetric Star Clusters. I. Stability Theory for Radial Perturbations. *Astrophys. J.* **154**, 251–270 (1968).

[72] Jabiri, F. E.: Static Spherically Symmetric Einstein-Vlasov Bifurcations of the Schwarzschild Spacetime. *Ann. Henri Poincaré* **22**, 2355–2406 (2021).

[73] Jabiri, F. E.: Stationary axisymmetric Einstein-Vlasov bifurcations of the Kerr spacetime. *Preprint arXiv:2202.10245v1*, 239pp. (2022).

[74] Jang, J.: Time-periodic approximations of the Euler-Poisson system near Lane-Emden stars. *Anal. PDE* **9**, 1043–1078 (2016).

[75] Jang, J., Masmoudi, N.: Well-Posedness for Compressible Euler Equations with Physical Vacuum Singularity. *Comm. Pure Appl. Math.* **62**, 1327–1385 (2009).

[76] Jeans, J. H.: On the Theory of Star-Streaming and the Structure of the Universe. *Mon. Notices Royal Astron. Soc.* **76**, 70–84 (1915).

[77] Kandrup, H. E., Sygnet, J. F.: A simple proof of dynamical stability for a class of spherical clusters. *Astrophys. J.* **298**, 27–33 (1985).

[78] King, I. R.: The Structure of Star Clusters. III. Some Simple Dynamical Models. *Astron. J.* **71**, 64–75 (1966).

[79] King, I. R.: The Dynamics of Globular Clusters. *Q. J. R. Astron. Soc.* **22**, 227–243 (1981).

[80] Korch, M., Raithel, P., Werner, T.: Implementation and Optimization of a 1D2V PIC Method for Nonlinear Kinetic Models on GPUs, in *2020 28th Euromicro International Conference on Parallel, Distributed and Network-Based Processing (PDP)*, 30–37 (2020).

[81] Korch, M., Ramming, R., Rein, G.: Parallelization of Particle-in-Cell Codes for Nonlinear Kinetic Models from Mathematical Physics, in *2013 42nd International Conference on Parallel Processing (ICPP)*, IEEE Computer Society, 523–529 (2013).

[82] Körner, J.: *The spherically symmetric Vlasov-Poisson system*, Master thesis, Universität Bayreuth 2020.

[83] Körner, J., Rein, G.: Strong Lagrangian Solutions of the (Relativistic) Vlasov-Poisson System for NonSmooth, Spherically Symmetric Data. *SIAM J. Math. Anal.* **53**, 4985–4996 (2021).

[84] Kulsrud, R. M., Mark, J. W.-K.: Collective Instabilities and Waves for Inhomogeneous Stellar Systems. I. The Necessary and Sufficient Energy Principle. *Astrophys. J.* **160**, 471–483 (1970).

[85] Kunze, M.: *A Birman-Schwinger Principle in Galactic Dynamics*, Prog. Math. Phys. **77**, Birkhäuser/Springer, Cham 2021.

[86] Kunze, M.: A Birman–Schwinger principle in galactic dynamics: ESI, Vienna, 07–11 February 2022. *Classical Quantum Gravity* **39**, 244001 (2022).

[87] Kunze, M.: A second look at the Kurth solution in galactic dynamics. *Kinet. Relat. Models* **15**, 651–662 (2022).

[88] Kuroda, S. T.: Perturbation of continuous spectra by unbounded operators, I. *J. Math. Soc. Japan* **11**, 246–262 (1959).

[89] Kuroda, S. T.: Perturbation of continuous spectra by unbounded operators, II. *J. Math. Soc. Japan* **12**, 243–257 (1960).

[90] Kurth, R.: A global particular solution to the initial-value problems of stellar dynamics. *Quart. Appl. Math.* **36**, 325–329 (1978).

[91] Landau, L. D.: On the vibrations of the electronic plasma. *Akad. Nauk SSSR. Zhurnal Eksper. Teoret. Fiz.* **16**, 574–586 (1946).

[92] Landau, L. D., Lifshitz, E. M.: *Mechanics* (third edition), Course of Theoretical Physics **1**, Butterworth-Heinemann 1982.

[93] Leeuwin, F., Combes, F., Binney, J.: N-body simulations with perturbation particles – I. Method and tests. *Mon. Not. R. Astr. Soc.* **262**, 1013–1022 (1993).

[94] Lemou, M., Méhats, F., Raphaël, P.: The Orbital Stability of the Ground States and the Singularity Formation for the Gravitational Vlasov Poisson System. *Arch. Ration. Mech. Anal.* **189**, 425–468 (2008).

[95] Lemou, M., Méhats, F., Raphaël, P.: Structure of the Linearized Gravitational Vlasov-Poisson System Close to a Polytropic Ground State. *SIAM J. Math. Anal.* **39**, 1711–1739 (2008).

[96] Lemou, M., Méhats, F., Raphaël, P.: A new variational approach to the stability of gravitational systems. *Comm. Math. Phys.* **302**, 161–224 (2011).

[97] Lemou, M., Méhats, F., Raphaël, P.: Orbital stability of spherical galactic models. *Invent. Math.* **187**, 145–194 (2012).

[98] Lieb, E. H., Loss, M.: *Analysis* (second edition), Grad. Stud. Math. **14**, American Mathematical Society, Providence, RI 2001.

[99] Lieb, E. H., Seiringer, R.: *The Stability of Matter in Quantum Mechanics*, Cambridge University Press, Cambridge 2010.

[100] Louis, P. D.: Discrete oscillation modes and damped stationary density waves in one-dimensional collisionless systems. *Mon. Not. R. Astr. Soc.* **258**, 552–570 (1992).

[101] Louis, P. D., Gerhard, O. E.: Can galaxies oscillate? A self-consistent model of a non-stationary stellar system. *Mon. Not. R. Astr. Soc.* **233**, 337–365 (1988).

[102] Lunk, Y.: *Oscillating solutions of the relativistic Vlasov-Poisson system*, Master thesis, Universität Bayreuth 2024. *In Progress.*

[103] Lynden-Bell, D.: The stability and vibrations of a gas of stars. *Mon. Not. R. Astr. Soc.* **124**, 279–296 (1962).

[104] Lynden-Bell, D.: Statistical Mechanics of Violent Relaxation in Stellar Systems. *Mon. Not. R. Astr. Soc.* **136**, 101–121 (1967).

[105] Lynden-Bell, D.: Lectures on Stellar Dynamics, in *Galactic dynamics and N-body simulations*, Lecture Notes in Physics **433**, Springer, Berlin, 3–31 (1994).

[106] Magnus, W., Winkler, S.: *Hill's Equation* (corrected reprint of the 1966 edition), Dover Publications, Inc., New York 1979.

[107] Makino, T.: On spherically symmetric motions of a gaseous star governed by the Euler-Poisson equations. *Osaka J. Math.* **52**, 545–580 (2015).

[108] Mark, J. W.-K.: Collective Instabilities and Waves for Inhomogeneous Stellar Systems. II. The Normal-Modes Problem of the Self-Consistent Plane-Parallel Slab. *Astrophys. J.* **169**, 455–475 (1971).

[109] Marsden, J. E.: A group theoretic approach to the equations of plasma physics. *Canad. Math. Bull.* **25**, 129–142 (1982).

[110] Mathur, S. D.: Irreversibility due to mixing in collisionless systems. *Mon. Not. R. Astr. Soc.* **231**, 367–378 (1988).

[111] Mathur, S. D.: Existence of oscillation modes in collisionless gravitating systems. *Mon. Not. R. Astr. Soc.* **243**, 529–536 (1990).

[112] Merritt, D.: Stability of Elliptical Galaxies. Numerical Experiments, in *Structure and Dynamics of Elliptical Galaxies*, IAU Symposium **127**, 315–330 (1987).

[113] Michie, R. W.: On the Distribution of High Energy Stars in Spherical Stellar Systems. *Mon. Notices Royal Astron. Soc.* **125**, 127–139 (1962).

[114] Michie, R. W., Bodenheimer, P. H.: The Dynamics of Spherical Stellar Systems: II.—Theoretical Models. *Mon. Notices Royal Astron. Soc.* **126**, 269–281 (1963).

[115] Miller, R. H., Smith, B. F.: Galactic oscillations. *Celest. Mech. Dyn. Astron.* **59**, 161–199 (1994).

[116] Moreno, M., Rioseco, P., Van Den Bosch, H.: Mixing in anharmonic potential well. *J. Math. Phys.* **63**, 071502 (2022).

[117] Moreno, M., Rioseco, P., Van Den Bosch, H.: Spectrum of the linearized Vlasov–Poisson equation around steady states from galactic dynamics. *Preprint arXiv:2305.05749v2*, 18pp. (2023).

[118] Morrison, P. J.: Hamiltonian description of the ideal fluid. *Rev. Mod. Phys.* **70**, 467–521 (1998).

[119] Mouhot, C.: Stabilité orbitale pour le système de Vlasov-Poisson gravitationnel (d'après Lemou-Méhats-Raphaël, Guo, Lin, Rein et al.). *Astérisque* **352**, 35–82 (2013).

[120] Mouhot, C., Villani, C.: On Landau damping. *Acta Math.* **207**, 29–201 (2011).

[121] Müller, J.: *Non-linear stability of matter shells surrounding a point mass*, Master thesis, Universität Bayreuth 2024. *In Progress.*

[122] Muralikrishnan, S., Cerfon. A. J., Frey, M., Ricketson, L. F., Adelmann, A.: Sparse grid-based adaptive noise reduction strategy for particle-in-cell schemes. *J. Comput. Phys. X* **11**, 100094 (2021).

[123] Myers, A., Colella, P., Van Straalen, B.: A 4th-Order Particle-in-Cell Method with Phase-Space Remapping for the Vlasov–Poisson Equation. *SIAM J. Sci. Comput.* **39**, B467–B485 (2017).

[124] Namboodiri, P. M. S.: Oscillations in Galaxies. *Celest. Mech. Dyn. Astron.* **76**, 69–77 (2000).

[125] Opial, Z.: Sur les périodes des solutions de l'équation différentielle $x'' + g(x) = 0$. *Ann. Polon. Math.* **10**, 49–72 (1961).

[126] Pausader, B., Widmayer, K.: Stability of a Point Charge for the Vlasov–Poisson System: The Radial Case. *Comm. Math. Phys.* **385**, 1741–1769 (2021).

[127] Perez, J., Alimi, J.-M., Aly, J.-J., Scholl, H.: Stability of spherical stellar systems – II. Numerical results. *Mon. Notices Royal Astron. Soc.* **280**, 700–710 (1996).

[128] Perez, J., Aly, J.-J.: Stability of spherical stellar systems – I. Analytical results. *Mon. Notices Royal Astron. Soc.* **280**, 689–699 (1996).

[129] Ramming, T.: *Über Familien sphärisch symmetrischer stationärer Lösungen des Vlasov-Poisson-Systems*, Doctoral thesis, Hut, München 2012.

[130] Ramming, T., Rein, G.: Spherically Symmetric Equilibria for Self-Gravitating Kinetic or Fluid Models in the Nonrelativistic and Relativistic Case—A Simple Proof for Finite Extension. *SIAM J. Math. Anal.* **45**, 900–914 (2013).

[131] Ramming, T., Rein, G.: Mass-Radius Spirals for Steady State Families of the Vlasov-Poisson System. *Arch. Ration. Mech. Anal.* **224**, 1127–1159 (2017).

[132] Ramming, T., Rein, G.: Oscillating solutions of the Vlasov-Poisson system—A numerical investigation. *Phys. D* **365**, 72–79 (2018).

[133] Reed, M., Simon, B.: *Methods of Modern Mathematical Physics. II. Fourier Analysis, Self-Adjointness*, Academic Press, New York – London 1975.

[134] Reed, M., Simon, B.: *Methods of Modern Mathematical Physics. IV. Analysis of Operators*, Academic Press, New York – London 1978.

[135] Reed, M., Simon, B.: *Methods of Modern Mathematical Physics. III. Scattering Theory*, Academic Press, New York – London 1979.

[136] Reed, M., Simon, B.: *Methods of Modern Mathematical Physics. I. Functional analysis* (second edition), Academic Press, Inc., New York 1980.

[137] Rein, G.: Static solutions of the spherically symmetric Vlasov-Einstein system. *Math. Proc. Cambridge Philos. Soc.* **115**, 559–570 (1994).

[138] Rein, G.: *The Vlasov-Einstein System with Surface Symmetry*, Habilitation thesis, Ludwig-Maximilians-Universität München 1995.

[139] Rein, G.: Flat Steady States in Stellar Dynamics—Existence and Stability. *Comm. Math. Phys.* **205**, 229–247 (1999).

[140] Rein, G.: Static Shells for the Vlasov-Poisson and Vlasov-Einstein Systems. *Indiana Univ. Math. J.* **48**, 335–346 (1999).

[141] Rein, G.: Stationary and static stellar dynamic models with axial symmetry. *Nonlinear Anal.* **41**, 313–344 (2000).

[142] Rein, G.: Stability of Spherically Symmetric Steady States in Galactic Dynamics against General Perturbations. *Arch. Ration. Mech. Anal.* **161**, 27–42 (2002).

[143] Rein, G.: Collisionless Kinetic Equations from Astrophysics—The Vlasov-Poisson System, in *Handb. of Differ. Equ.: Evolutionary Equations* **3**, Elsevier/North-Holland, Amsterdam, 383–476 (2007).

[144] Rein, G.: Stability and instability results for equilibria of a (relativistic) self-gravitating collisionless gas—a review. *Classical Quantum Gravity* **40**, 193001 (2023).

[145] Rein, G., Guo, Y.: Stable models of elliptical galaxies. *Mon. Notices Royal Astron. Soc.* **344**, 1296–1306 (2003).

[146] Rein, G., Rendall, A. D.: Compact support of spherically symmetric equilibria in non-relativistic and relativistic galactic dynamics. *Math. Proc. Cambridge Philos. Soc.* **128**, 363–380 (2000).

[147] Rein, G., Straub, C.: On the transport operators arising from linearizing the Vlasov-Poisson or Einstein-Vlasov system about isotropic steady states. *Kinet. Relat. Models* **13**, 933–949 (2020).

[148] Rioseco, P., Sarbach, O.: Phase space mixing in an external gravitational central potential. *Classical Quantum Gravity* **37**, 195027 (2020).

[149] Rosseland, S.: The Pulsation Theory of Cepheid Variables (George Darwin Lecture). *Mon. Not. R. Astr. Soc.* **103**, 233–238 (1943).

[150] Sánchez, Ó., Soler, J.: Orbital stability for polytropic galaxies. *Ann. Inst. H. Poincaré C Anal. Non Linéaire* **23**, 781–802 (2006).

[151] Sansone, G.: Sulle soluzioni di Emden dell'equazione di Fowler. *Univ. Roma Ist. Naz. Alta Mat. Rend. Mat. e Appl.* **1**, 163–176 (1940).

[152] Schaaf, R.: A class of Hamiltonian systems with increasing periods. *J. Reine Angew. Math.* **363**, 96–109 (1985).

[153] Schaeffer, J.: Discrete approximation of the Poisson-Vlasov system. *Quart. Appl. Math.* **45**, 59–73 (1987).

[154] Schaeffer, J.: A Class of Counterexamples to Jeans' Theorem for the Vlasov-Einstein System. *Comm. Math. Phys.* **204**, 313–327 (1999).

[155] Schulze, A.: Existence and stability of static shells for the Vlasov-Poisson system. *Analysis (Munich)* **26**, 527–543 (2006).

[156] Schulze, A.: Existence of axially symmetric solutions to the Vlasov-Poisson system depending on Jacobi's integral. *Commun. Math. Sci.* **6**, 711–727 (2008).

[157] Schulze, A.: Existence and stability of static shells for the Vlasov-Poisson system with a fixed central point mass. *Math. Proc. Cambridge Philos. Soc.* **146**, 489–511 (2009).

[158] Schwinger, J.: On the Bound States of a Given Potential. *Proc. Nat. Acad. Sci. U.S.A.* **47**, 122–129 (1961).

[159] Sellwood, J. A., Pryor, C.: Pulsation Modes of Spherical Stellar Systems, in *Highlights of Astronomy. International Astronomical Union* **11**, Springer, Dordrecht, 638–642 (1998).

[160] Simon, B.: *Quantum Mechanics for Hamiltonians Defined as Quadratic Forms*, Princeton Ser. Phys. **1**, Princeton University Press, Princeton, NJ 1971.

[161] Sobouti, Y.: Linear oscillations of isotropic stellar systems. I. Basic theoretical considerations. *Astron. Astrophys.* **140**, 82–90 (1984).

[162] Sobouti, Y.: Linear oscillations of isotropic stellar systems. II. Radial modes of energy-truncated models. *Astron. Astrophys.* **147**, 61–66 (1985).

[163] Sobouti, Y.: Linear oscillations of isotropic stellar systems. III. A classification of non-radial modes. *Astron. Astrophys.* **169**, 95–110 (1986).

[164] Soffer, A., Weinstein, M. I.: Resonances, radiation damping and instability in Hamiltonian nonlinear wave equations. *Invent. Math.* **136**, 9–74 (1999).

[165] Straub, C.: *Stability of the King model – a coercivity-based approach*, Master thesis, Universität Bayreuth 2019. Available at DOI:10.15495/EPub_UBT_00005033

[166] Straub, C., Wolfschmidt, S.: EVStabilityNet: Predicting the Stability of Star Clusters in General Relativity. *Preprint arXiv:2310.08253v1*, 16pp. (2023).

[167] Strauss, W. A., Wu, Y.: Steady States of Rotating Stars and Galaxies. *SIAM J. Math. Anal.* **49**, 4865–4914 (2017).

[168] Sweatman, W. L.: A study of Lagrangian radii oscillations and core-wandering using N-body simulations. *Mon. Not. R. Astr. Soc.* **261**, 497–512 (1993).

[169] Sygnet, J. F., Des Forets, G., Lachieze-Rey, M., Pellat, R.: Stability of gravitational systems and gravothermal catastrophe in astrophysics. *Astrophys. J.* **276**, 737–745 (1984).

[170] Teschl, G.: *Ordinary Differential Equations and Dynamical Systems*, Grad. Stud. Math. **140**, American Mathematical Society, Providence, RI 2012.

[171] Tremaine, S., Hénon, M., Lynden-Bell, D.: H-functions and mixing in violent relaxation. *Mon. Not. R. Astr. Soc.* **219**, 285–297 (1986).

[172] Vandervoort, P. O.: On the oscillations and the stability of stellar systems. *Astrophys. J.* **273**, 511–529 (1983).

[173] Vandervoort, P. O.: On an example of an N-body method for the study of small perturbations in galaxies. *Mon. Not. R. Astr. Soc.* **303**, 393–410 (1999).

[174] Vandervoort, P. O.: On stationary oscillations of galaxies. *Mon. Not. R. Astr. Soc.* **339**, 537–555 (2003).

[175] Vandervoort, P. O.: On a matrix method for the study of small perturbations in galaxies. *Mon. Not. R. Astr. Soc.* **348**, 482–514 (2004).

[176] Wachlin, F. C., Muzzio, J. C.: Testing Galactic Oscillations. *Celest. Mech. Dyn. Astron.* **67**, 225–235 (1997).

[177] Wachlin, F. C., Rybicki, G. B., Muzzio, J. C.: A perturbation particle method for stability studies of stellar systems. *Mon. Not. R. Astr. Soc.* **262**, 1007–1012 (1993).

[178] Wang, Z., Guo, Y., Lin, Z., Zhang, P.: Unstable galaxy models. *Kinet. Relat. Models* **6**, 701–714 (2013).

[179] Weinberg, M. D.: Vertical Oscillation of the Galactic Disk. *Astrophys. J.* **373**, 391–404 (1991).

[180] Weinberg, M. D.: Weakly damped modes in star clusters and galaxies. *Astrophys. J.* **421**, 481–490 (1994).

[181] Wolansky, G.: On nonlinear stability of polytropic galaxies. *Ann. Inst. H. Poincaré C Anal. Non Linéaire* **16**, 15–48 (1999).

[182] Wolfschmidt, S.: *Stability and Oscillations of Star Clusters in General Relativity.* Doctoral thesis, Universität Bayreuth 2023.

[183] Yakubovich, V. A., Starzhinskii, V. M.: *Linear Differential Equations with Periodic Coefficients 1*, Halsted Press (John Wiley & Sons), New York-Toronto 1975.

[184] Zel'dovich, Y. B., Novikov, I. D.: *Relativistic Astrophysics. Vol. 1: Stars and Relativity*, University of Chicago Press, Chicago 1971.

Publications

The author has contributed to the following publications and preprints:

[48] Günther, S., Körner, J., Lebeda, T., Pötzl, B., Rein, G., Straub, C., Weber, J.: A numerical stability analysis for the Einstein-Vlasov system. *Classical Quantum Gravity* **38**, 035003 (2021).

[49] Günther, S., Rein, G., Straub, C.: A Birman-Schwinger Principle in General Relativity: Linearly Stable Shells of Collisionless Matter Surrounding a Black Hole. *Preprint arXiv:2204.10620v1*, 58pp. (2022).

[50] Günther, S., Straub, C., Rein, G.: Collisionless Equilibria in General Relativity: Stable Configurations beyond the First Binding Energy Maximum. *Astrophys. J.* **918**, 48 (2021).

[61] Hadžić, M., Rein, G., Schrecker, M., Straub, C.: Damping versus oscillations for a gravitational Vlasov-Poisson system. *Preprint arXiv:2301.07662v1*, 49pp. (2023).

[62] Hadžić, M., Rein, G., Straub, C.: On the Existence of Linearly Oscillating Galaxies. *Arch. Ration. Mech. Anal.* **243**, 611–696 (2022).

[147] Rein, G., Straub, C.: On the transport operators arising from linearizing the Vlasov-Poisson or Einstein-Vlasov system about isotropic steady states. *Kinet. Relat. Models* **13**, 933–949 (2020).

[166] Straub, C., Wolfschmidt, S.: EVStabilityNet: Predicting the Stability of Star Clusters in General Relativity. *Preprint arXiv:2310.08253v1*, 16pp. (2023).

This thesis is mainly based on [62]. The definition of the transport operator, cf. Definition 4.2.5, and the proofs of some of its properties are based on [147], which is in turn based on the author's master thesis:

[165] Straub, C.: *Stability of the King model – a coercivity-based approach*, Master thesis, Universität Bayreuth 2019. Available at DOI:10.15495/EPub_UBT_00005033

Several improvements and extension of the Birman-Schwinger-Mathur principle from [62, Sc. 8], which were developed in [49], have been incorporated in Chapter 5. Chapter 6, Appendix C, and some parts of Appendix A are based on [61]. The settings used in [49, 61, 62] are the basis of the discussions in Sections 7.1, 7.2, and 7.4. The code we have used for the numerical analysis in Chapter 8 is (partially) based on the codes used in [48, 50]; otherwise, the observations from [48, 50] have not been used here.

The methods and results developed in the recent preprint [166] are independent of this thesis.